frontiers | Research Topics

The advances of endoscopic skull base tumor surgery: From basic to clinical research

Edited by
Peng Zhao, Yazhuo Zhang, Songbai Gui and Luigi Maria Cavallo

Published in
Frontiers in Surgery
Frontiers in Oncology

ISSN 1664-8714
ISBN 978-2-8325-3877-7
DOI 10.3389/978-2-8325-3877-7

About Frontiers

Frontiers is more than just an open access publisher of scholarly articles: it is a pioneering approach to the world of academia, radically improving the way scholarly research is managed. The grand vision of Frontiers is a world where all people have an equal opportunity to seek, share and generate knowledge. Frontiers provides immediate and permanent online open access to all its publications, but this alone is not enough to realize our grand goals.

Frontiers journal series

The Frontiers journal series is a multi-tier and interdisciplinary set of open-access, online journals, promising a paradigm shift from the current review, selection and dissemination processes in academic publishing. All Frontiers journals are driven by researchers for researchers; therefore, they constitute a service to the scholarly community. At the same time, the *Frontiers journal series* operates on a revolutionary invention, the tiered publishing system, initially addressing specific communities of scholars, and gradually climbing up to broader public understanding, thus serving the interests of the lay society, too.

Dedication to quality

Each Frontiers article is a landmark of the highest quality, thanks to genuinely collaborative interactions between authors and review editors, who include some of the world's best academicians. Research must be certified by peers before entering a stream of knowledge that may eventually reach the public - and shape society; therefore, Frontiers only applies the most rigorous and unbiased reviews. Frontiers revolutionizes research publishing by freely delivering the most outstanding research, evaluated with no bias from both the academic and social point of view. By applying the most advanced information technologies, Frontiers is catapulting scholarly publishing into a new generation.

What are Frontiers Research Topics?

Frontiers Research Topics are very popular trademarks of the *Frontiers journals series*: they are collections of at least ten articles, all centered on a particular subject. With their unique mix of varied contributions from Original Research to Review Articles, Frontiers Research Topics unify the most influential researchers, the latest key findings and historical advances in a hot research area.

Find out more on how to host your own Frontiers Research Topic or contribute to one as an author by contacting the Frontiers editorial office: frontiersin.org/about/contact

The advances of endoscopic skull base tumor surgery: From basic to clinical research

Topic editors

Peng Zhao — Capital Medical University, China
Yazhuo Zhang — Capital Medical University, China
Songbai Gui — Capital Medical University, China
Luigi Maria Cavallo — University of Naples Federico II, Italy

Citation

Zhao, P., Zhang, Y., Gui, S., Cavallo, L. M., eds. (2023). *The advances of endoscopic skull base tumor surgery: From basic to clinical research*. Lausanne: Frontiers Media SA. doi: 10.3389/978-2-8325-3877-7

Table of contents

frontiers | Frontiers in Surgery

ORIGINAL RESEARCH
published: 21 June 2022
doi: 10.3389/fsurg.2022.923143

Identification and Verification of SLC27A1, PTBP1 and EIF5A With Significantly Altered Expression in Aggressive Pituitary Adenomas

*Jianhua Cheng[2†], Ruya Sun[3†], Ding Nie[2], Bin Li[2], Song Bai Gui[1], Chu Zhong Li[2], Ya Zhuo Zhang[2] and Peng Zhao[1]**

[1]Neurosurgical Department, Beijing Tiantan Hospital, Capital Medical University, Beijing, China, [2]Department of Cell and Biology, Beijing Neurosurgical Institute, Capital Medical University, Beijing, China, [3]Department of Biomedical Informatics, Department of Physiology and Pathophysiology, Center for Noncoding RNA Medicine, MOE Key Lab of Cardiovascular Sciences, School of Basic Medical Sciences, Peking University, Beijing, China

OPEN ACCESS

Edited by:
Wai Sang Poon, The Chinese University of Hong Kong, China

Reviewed by:
Hong Xue, Hong Kong University of Science and Technology, Hong Kong, SAR China
Danny T.M. Chan, The Chinese University of Hong Kong, China

****Correspondence:***
Peng Zhao
zhaopeng@ccmu.edu.cn

[†]These authors have contributed equally to this work

Specialty section:
This article was submitted to Neurosurgery, a section of the journal Frontiers in Surgery

Received: *19 April 2022*
Accepted: *06 June 2022*
Published: *21 June 2022*

Citation:
Cheng J, Sun R, Nie D, Li B, Gui SB, Li CZ, Zhang YZ and Zhao P (2022) Identification and Verification of SLC27A1, PTBP1 and EIF5A With Significantly Altered Expression in Aggressive Pituitary Adenomas. Front. Surg. 9:923143. doi: 10.3389/fsurg.2022.923143

Background: Aggressive pituitary adenoma encircling the internal carotid artery has a poor clinical prognosis because of a high surgical risk and a high recurrence rate. This seriously affects patients' quality of life and yet there is no effective medical treatment. The European Diagnostic Guidelines have recommended the use of temozolomide (TMZ) for these aggressive pituitary adenomas, but the treatment remission rate has been less than 50%.

Methods: In this study, transcriptome sequencing of pituitary tumour tissues and TMZ-treated pituitary tumour cell lines were employed to explore the significance gene expressions affecting the efficacy of TMZ treatment for pituitary tumours. To clarify the roles of these gene expressions, six adult patients with pituitary adenomas treated in Tiantan Hospital from 2015 to 2020 and a pituitary adenoma cell line (Att20 sensitive to TMZ treatment) were analyzed by mRNA transcriptome sequencing. The differentially expressed genes were assayed by analyzing the sequencing results, and the expression level of these genes was further verified by immunohistochemistry. In addition, Ki67, VEGF, and p53 of the tumour tissues were also verified by immunohistochemistry.

Results: In tumour tissues, mRNA sequencing showed that PTBP1 and EIF5A were significantly overexpressed in primary pituitary adenomas and SLC27A1 was significantly overexpressed in aggressive pituitary adenomas. Also in the pituitary adenoma cell line (AtT20), SLC27A1 expression levels were suppressed by TMZ treatment. Subsequent immunohistochemistry confirmed the sequencing results.

Conclusion: High expression of SLC27A1 and low expression of EIF5A and PTBP1 may be potential indicators to predict the progression of aggressive pituitary adenomas, and patients with high SLC27A1 subtype may be sensitive to TMZ in clinical treatments.

Keywords: aggressive pituitary adenom, TMZ, SLC27A1, PTBP1, recurrent pituitary adenoma, primary pituitary adenoma

INTRODUCTION

Pituitary adenomas, one of the most common intracranial tumors, account for about 17% of intracranial tumors (1), non-functional pituitary adenomas account for nearly half of pituitary adenomas (2). Most pituitary adenomas show the growth characteristics of benign tumors, and most patients can be cured by surgery or drug treatments (2, 3). However, about 35% of pituitary adenomas show aggressive growth in imaging (4). These tumors grow rapidly and are resistant to conventional treatments such as surgery, medication and radiotherapy. This kind of tumor tends to relapse or regrowth in the early stage after operation (5, 6). We define this kind of tumor as aggressive pituitary adenoma. Non-functional pituitary adenoma recurred after operation is also a kind of aggressive pituitary adenoma (7). The literature reported that the postoperative recurrence rate of nonfunctional pituitary adenomas was 7.9%–46% (8, 9).

Temozolomide (TMZ) is a new alkylating agent, which interferes with gene transcription by methylation of DNA guanine and induces DNA damage. Temozolomide has broad-spectrum anti-tumor activity. Temozolomide is a first-line chemotherapy drug after the failure of the standard treatment of aggressive pituitary tumors. Patients who do not respond to TMZ treatment show resistance to TMZ. Therefore, there is no clear conclusion on the adaptation of temozolomide treatment. Blind use of TMZ treatment may waste resources, and may even affect the treatment of patients. Therefore, it is of great significance to explore the star gene of TMZ in patients with sensitive and aggressive pituitary adenomas.

Aggressive pituitary adenomas proliferate actively, oppress the optic nerve, and are not separated from the surrounding tissues, and are easy to invade the dura mater, cavernous sinus, bone, and other tissues, which brings difficulties to surgical treatment and affects the prognosis of patients (10). Therefore, it is of great significance to explore the factors affecting aggressive pituitary adenomas. Previous studies have shown that the Ki67 index, tumor invasion, and the extent of tumor resection are the factors affecting tumor progression (11, 12). According to the definition of WHO, the Ki67 index >3% in pituitary adenomas indicates active tumor proliferation (13, 14). Interestingly, some patients did not have a high Ki67 index but also showed tumor recurrence. On the contrary, some patients had a Ki67 index of more than 3%, but no tumor recurrence was found during long-term follow-up (11, 15, 16). Some studies have shown that p53 and VEGF are related to tumor invasiveness, but the relationship between p53 and tumor recurrence is still unclear. Therefore, these indicators are not accurate. It is particularly important to find the key genes to predict tumor progression from molecular biology.

METHODS AND MATERIALS

Patients and Tumor Specimens

All the patient information is preliminarily determined through the database of Beijing Tiantan Hospital. The patients with primary pituitary adenomas were followed up for more than 5 years without recurrence (9). Patients with postoperative recurrence were defined as the aggressive pituitary adenomas group. All patients finished the examination of cranial contrast MRI and hormone levels before the operation. The clinical data of the research included clinical symptoms, radiographic examination, surgical results, immunohistochemical results, and follow-up results collected by reviewing clinical case information and telephone follow-up. The tumor specimens of each patient were preserved in two parts, and one of them was fixed with formalin immediately after the operation and embedded in paraffin blocks, the other part is sub-packed into a frozen tube and immediately stored in nitrogen liquid for mRNA analysis. Six tumor samples stored in liquid nitrogen were randomly selected for further transcriptional sequencing, including 3 patients with primary pituitary adenomas and 3 patients with aggressive pituitary adenomas. The wax blocks of 10 patients with primary pituitary adenomas and 10 patients with aggressive pituitary adenomas were randomly selected and stained for immunohistochemistry to verify gene expression.

This research was approved by the Ethics Committee of Beijing Tiantan Hospital. The procedures involving experiments on human subjects met the ethical standards of the Helsinki Declaration in 1975. All patients and their families signed up to participate in this study.

Cell Culture and IC50 of TMZ

The mouse pituitary adenoma cell line GT1-1 (ATCC, USA) was cultured in Dulbecco's modified Eagle medium (DMEM) containing 10% fetal bovine serum (FBS, Gibco, USA) and the mouse pituitary tumor cell line ATt20 (ATCC, USA) were cultured in 12K Medium (F-12K) supplemented with 15% horse serum and 2.5% FBS. Both GT1-1 and ATt20 cells were cultured at 37°C in a 5% CO_2 humidified incubator.

Two types of cells were treated with different doses of TMZ (ranged from100 to 500 nM). The IC50 results for ATT20 cells are shown in **Supplementary Material 1**.

RNA Sequencing and Bioinformatics Analysis

Primary and aggressive pituitary adenomas were chosen for RNA-seq according to intraoperative pathological diagnosis, Imaging diagnosis, and clinical diagnosis, each with 3 replicates. The clinical information of the tumor is shown in (**Table 1**). AtT20 cells treated with TMZ and mock-treated were tested for RNA-seq. (each with 3 replicates) RNA was extracted using TRIzol (Invitrogen, 15596-026, Grand Island, NY) according to the manufacturer's protocol. Total RNA was reverse transcribed using an RT-PCR kit (Tiangen, KR103-03, Beijing, China) The sequencing readings are generated using the BGISEQ-500 platform as recommended by the manufacturer. Use tophat v2.0.12 to compare the paired-end clean reading with the reference human genome (UCSC version of hg19). The readings of each gene were calculated by HTSeq v0.6.1 and the gene expression level was calculated by RSEM v1.2.31. We use an MA map, volcano map, scatter map, and heatmap to express the distribution of different genes. The corrected *P*-value of Holm is 0.005 and the multiplier log2 (doubling) is 1 as the threshold for significant differential expression. Then the functional enrichment analysis of the gene was carried out.

Differential Expression Gene Identification

The raw count expression matrix was normalized to RPM first. Identification of differential expression genes (DEGs) between TMZ with and without TMZ as well as DEGs between recurrent and primary pituitary adenoma patients was then completed using the limma R package (version 3.40.6) (https://bioconductor.org/packages/limma/). DEGs of the above experiment groups were extracted using eBayes method of limma with $P < 0.05$ as a cutoff value for a Benjamini-Hochberg adjusted *P*-value.

Immunohistochemistry and Correlation Analyze

SLC27A1 (Solarbio, China, dilution:1:200), PTBP1 (Solarbio, China, dilution:1:100), EIF5A (Solarbio, China, dilution:1:50), Ki67 (Solarbio, China, dilution:1:100), VEGF (Solarbio, China, dilution:1:100), and P53 (Solarbio, China, dilution:1:200) were evaluated by immunohistochemistry. The paraffin-embedded specimens were cut into 4 μm thick sections. According to the manufacturer's instructions, an antibody immunohistochemical analysis was performed on all sections using Leica Bond-III's automatic, random, and continuous slide staining system (Leica Biosystems, Germany). Images were obtained using a whole-slide scanner (3DHISTECH Ltd, Budapest, Hungary) and the immunohistochemical expression was scored by two observers using the CaseViewer software. The criterion of immunohistochemistry was that there were obvious brown granules in the cytoplasm or nucleus. The H score (range 0–300) was obtained by multiplying the staining intensity (0–3) by the percentage of positive cells (0%–100%), and the expression of tumor cells was scored semi-quantitatively.

TABLE 1 | Clinical characteristics of patients whose tumor was detected by Transcriptome sequencing.

Patient ID	Gender	Age	Tumor location	Tumor size (cm)	Ki67 index (%)
P1	Male	27	Intrasellar	2.2	1
P2	Male	39	Intrasellar	1.7	1
P3	Female	56	Intrasellar + Suprasellar	1.2	3
R1	Male	53	Intrasellar + Suprasellar	3.4	3
R2	Female	45	Intrasellar + Cavernous sinus	3.6	3
R3	Male	39	Intrasellar	2.9	5
P-value	1.0	0.621	0.414	0.083	0.101

P1–P3, Primary pituitary adenomas; R1–R3, Recurrent pituitary adenomas.

Statistical Analysis

The clinical and imaging data of all patients diagnosed with pituitary adenoma were mainly collected from the case and imaging system, as well as telephone follow-up. The follow-up period ranged from 4 to 168 months (mean 67 months). The descriptive statistics of the immunohistochemical results were expressed by the median and quartile range (IQR). The tumor size and Ki67 index between groups were compared by independent sample t-test. SPSS statistical software was used for the analysis. All statistical tests were two-tailed exact tests with a $P < 0.05$ considered significant.

RESULTS

Differential Expression Gene Identification

The aggressive and primary pituitary adenomas and the ATt20 cells treated with TMZ were sequenced and analyzed with the normal control group (**Figure 1**). The differentially expressed genes were found by transcriptome sequencing analysis in aggressive and primary pituitary adenomas, and we selected the

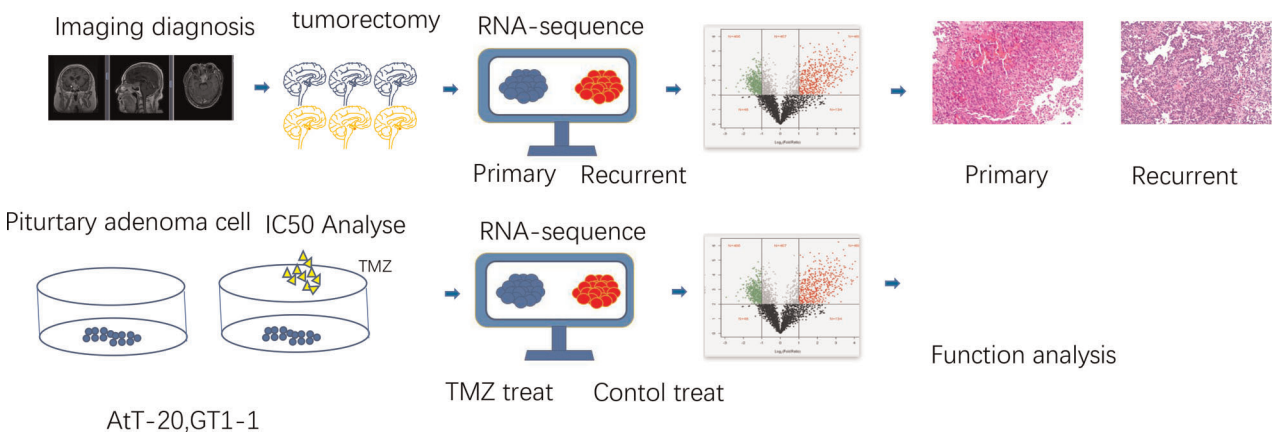

FIGURE 1 | The process design of the experiment. At the tissue level, aggressive pituitary adenomas and primary pituitary adenomas were selected by clinical information and imaging data, and then pituitary adenomas were taken for transcriptional sequencing to screen the differentially expressed genes, and then the expression of differential genes was verified by immunohistochemistry. At the cellular level, pituitary adenoma cells were treated with TMZ to screen drug-sensitive cell lines, and then transcriptional sequencing was performed to screen differentially expressed genes for analysis.

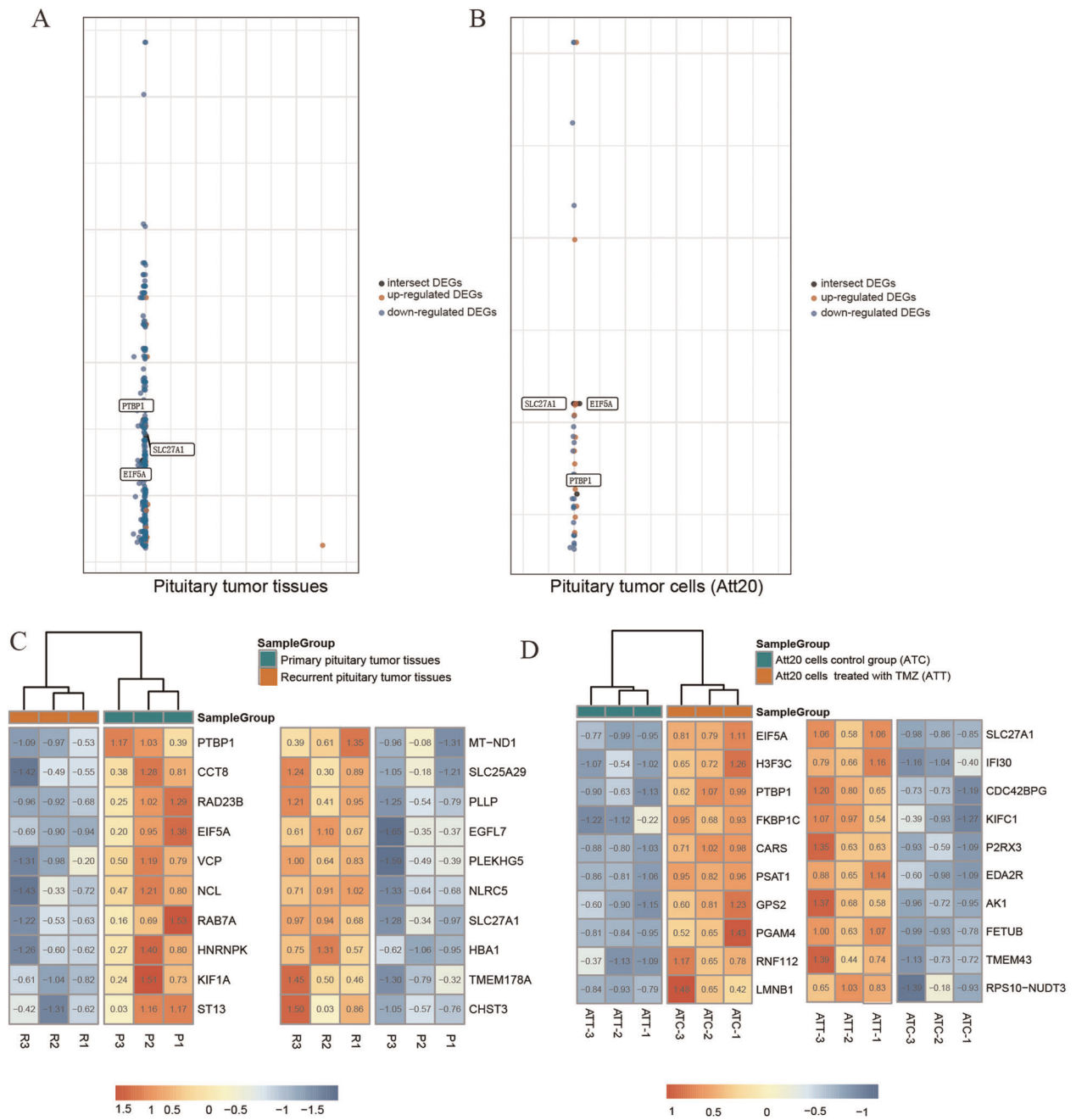

FIGURE 2 | The graph shows the distribution of datasets with statistically significant mRNA overexpression (Brown) or down-regulated expression (blue) of the target gene. Genes intersecting tumor tissue (**A**) with cell sequencing (**B**) are labeled in black. The threshold was designed with the following parameters: *P*-value <0.001, fold change >1.5 (**A**,**B**). Sequencing heat map results of pituitary tumor tissues and cells are presented (**C**,**D**). Among the differentially expressed genes, the top 10 genes in the high expression ranking were each selected for heat map plotting with the top 10 genes in the low expression ranking. SLC27A1, eIF5A, and PTBP1 were expressed in both tumor tissues and cells.

first 10 genes with the most significant differences between high expression and low expression (**Figures 2A,C**). After analysis, it is found that PTBP1, CCTB, RAD23B, EIF5A, VCP, NCL, RAB7A, HNRNPK, KIF1A, and ST13 is in the original. High expression in pituitary adenomas. And MT-ND1, SLC25A29, PLLP, EGFL7, PLEKHG5, NLRC5, SLC27A1, HBA1, TMEM178A, and CHST3 was highly expressed in aggressive pituitary adenomas. Pituitary adenoma cells Att20 were treated by TMZ and normal control cells were sequenced and analyzed by EIF5A, H3F3C, PTBP1, FKBP1C, CARS, PSAT1, GPS2,

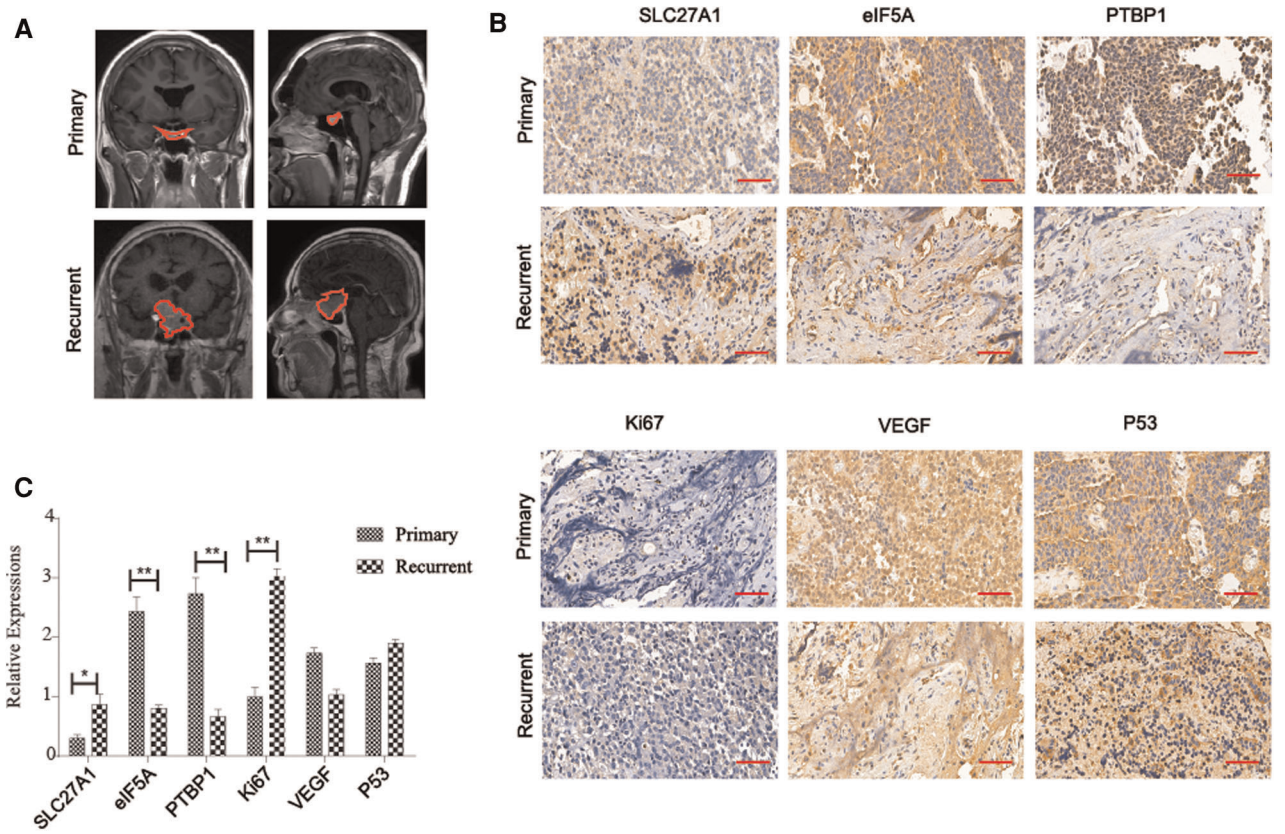

FIGURE 3 | (**A**) Imaging information of primary and aggressive pituitary adenomas, the outline of the tumor is depicted with a red dotted line. (**B**) Immunohistochemical assay to verify the expression of SLC27A1, eIF5A, PTBP1, Ki67, VEGF, and p53 in recurrent and primary pituitary adenomas (**C**) Statistical analysis of immunohistochemical results

PGAM4, RNF112, LMNB1 was highly expressed in sensitive cell lines treated with TMZ, while SLC27A1, IFI30, CDC42BPG, KIFC1, P2RX3, EDA2R, AK1, FETUB, TMEM43, RPS10-NUDT3 was highly expressed in control cells (**Figures 2B,D**). After the data of the two groups were overlapped, it was found that PTBP1 and EIF5A were highly expressed in the primary pituitary adenomas and normal control pituitary tumor cells, and SLC27A1 was highly expressed in aggressive pituitary adenomas and TMZ-treated ATt20 cells.

Immunohistochemical Analysis

Immunohistochemical examination was performed in 10 patients with aggressive pituitary adenomas and 10 patients with primary pituitary adenomas. The results of representative immunohistochemical staining are shown in **Figure 3**. SLC27A1 was highly expressed in aggressive pituitary adenomas. Compared with aggressive pituitary adenomas, PTBP1 and eIF5A were highly expressed in primary pituitary adenomas. Ki67 was highly expressed in aggressive pituitary adenomas compared with primary pituitary adenomas. There was no significant difference between the expression of p53 and VEGF in aggressive pituitary adenomas and primary pituitary adenomas.

DISCUSSION

Recurrent nonfunctional pituitary adenomas account for more than half of aggressive pituitary adenomas. 57% of recurrent pituitary adenomas show invasive biological characteristics, which are more likely to invade the dura mater and bone, invade the cavernous sinus and enclose the internal carotid artery, which brings difficulties to surgical treatment and affects the prognosis of patients (17). Therefore, the study to predict the related factors of pituitary tumor recurrence is of great significance to improve the prognosis of patients. It is well known that clinicians should weigh a variety of factors to make individual treatment decisions. The purpose of this study was to explore the factors affecting the recurrence of pituitary adenomas from a genetic point of view.

Many clinical factors are affecting the recurrence of non-functional pituitary adenomas. In Brochier's research, it was found that tumor invasiveness was one of the prognostic factors affecting tumor recurrence (18). In our study, after a systematic analysis of patients, it was also found that tumors invading suprasellar, cavernous sinus and internal carotid artery were more likely to recur, and the difference was statistically significant. Similarly, the size of the tumor was

also included in our study, and it was also found that tumors with a maximum diameter larger than 3cm were more likely to relapse. However, in the study of Lelotte et al, no correlation was found between the size of nonfunctional pituitary adenomas and tumor recurrence (10). Based on the results of our data analysis, we consider that invasive pituitary adenomas grow rapidly, invade surrounding tissues, and their tumors are larger in diameter because of their invasive growth characteristics. Of course, this requires more samples to verify its relevance.

The accuracy of predicting the recurrence of pituitary adenomas by the clinical characteristics of patients is poor. To improve the diagnosis rate, we further analyze the abnormally expressed genes in patients with aggressive pituitary adenomas from the perspective of genetics. It has been found that the expression of Ki67, P53, and VEGF is significantly increased in malignant tumors such as gastric cancer, bladder cancer renal cell carcinoma, and glioma (19–22). We speculate they are also abnormally expressed in aggressive pituitary adenomas. The features described as atypical adenomas in World Health Organization (WHO)'s classification in 2004 included Ki67 > 3%, increased mitosis, and extensive or strong expression of p53 (23). But these standards are quite controversial. Some resear ches have shown that the Ki67 index has a significant independent value in predicting recurrence (18), which is consistent with our results. But other studies have shown that this criterion is usually proved to be of predictive value only in the case of invasive tumors or residual tumors after surgery (10). No significant difference was found in the expression of p53 and VEGF in our study.

Therefore, the accuracy of the current molecules for predicting the recurrence of pituitary adenomas is poor, so it is more important to further look for abnormally expressed genes in aggressive pituitary adenomas.

Temozolomide is a new alkylating agent, which interferes with gene transcription by methylation of DNA guanine and induces DNA damage (24). Temozolomide has broad-spectrum anti-tumor activity and good permeability to the blood-brain barrier (25). At present, the clinical and basic research of TMZ in the treatment of aggressive pituitary adenomas is a hot spot, and scholars at home and abroad have carried out a series of studies on it. Losa et al reported a study of patients with aggressive pituitary adenomas treated with TMZ. During the treatment, 25 patients (80.6%) had pituitary adenomas under control and 6 patients (19.4%) had tumor progression. There is no definite conclusion on the indication of TMZ in the treatment of pituitary adenomas. Therefore, in order to find the sensitive genes which are effective in the treatment of TMZ, we carried out drug sensitivity test and sequencing analysis through the Att20 cell line.

Through a comprehensive analysis of the results of histological and cytological experiments, we found that the expression of SLC27A1 was significantly high in aggressive pituitary adenomas and TMZ therapy sensitive cell lines, while the expression of PTBP1 and EIF5A was significantly decreased. Studies have shown that SLC27A1 is involved in the regulation of lipid metabolism through the brain-liver axis (26), but the research in the field of oncology is still blank, so it is likely to be a new star molecule involved in the regulation of tumorigenesis and development. PTBP1 gene is involved in the regulation of glioma, multiple myeloma, and hepatocellular carcinoma (27–29), but its role in pituitary adenoma is still unknown. EIF5A was found to be abnormally expressed in thyroid carcinoma and breast cancer (30, 31). In pituitary adenomas, the subsequent immunohistochemical results confirmed the differential expression of SLC27A1, PTBP1, and EIF5A genes in aggressive pituitary adenomas and primary pituitary adenomas, and the difference was statistically significant. Therefore, SLC27A1, PTBP1, and EIF5A may be important molecular markers for predicting the recurrence of pituitary adenomas. Similarly, the results of cytological sequencing showed that the high expression of SLC27A1 suggested that TMZ treatment was effective, while the high expression of PTBP1 and EIF5A indicated that the therapeutic effect of TMZ was not good.

In summary, our study demonstrates that the high expression of SLC27A1 and the low expressions of PTBP1 and EIF5A predict the progression of an aggressive pituitary adenoma. Data from murine pituitary adenoma cell lines AtT20 together with TMZ-sensitivity tests suggest that aggressive pituitary adenomas with this molecular pattern may be responsive to TMZ treatment.

DATA AVAILABILITY STATEMENT

The datasets presented in this study can be found in online repositories. The names of the repository/repositories and accession number(s) can be found in the article/ **Supplementary Material**.

ETHICS STATEMENT

The studies involving human participants were reviewed and approved by Ethics Committee of Beijing Tiantan Hospital, Capital Medical University (Beijing, China). The patients/ participants provided their written informed consent to participate in this study.

SUPPLEMENTARY MATERIAL

The Supplementary Material for this article can be found online at: https://www.frontiersin.org/articles/10.3389/fsurg.2022.923143/full#supplementary-material.

REFERENCES

1. Mahajan A, Bronen R, Mian A, Omay S, Spencer D, Inzucchi S. Diagnosis and management of pituitary disease with focus on the role of Magnetic Resonance Imaging. *Endocrine*. (2020) 68:489–501. doi: 10.1007/s12020-020-02242-3
2. Molitch ME. Diagnosis and treatment of pituitary adenomas: a review. *JAMA*. (2017) 317:516–24. doi: 10.1001/jama.2016.19699
3. Freda P, Beckers A, Katznelson L, Molitch M, Montori V, Post K, et al. Pituitary incidentaloma: an endocrine society clinical practice guideline. *J Clin Endocrinol Metab*. (2011) 96:894–904. doi: 10.1210/jc.2010-1048
4. Kasuki L, Raverot G. Definition and diagnosis of aggressive pituitary tumors. *Rev Endocr Metab Disord*. (2020) 21:203–8. doi: 10.1007/s11154-019-09531-x
5. Di Ieva A, Rotondo F, Syro LV, Cusimano MD, Kovacs K. Aggressive pituitary adenomas—diagnosis and emerging treatments. *Nat Rev Endocrinol*. (2014) 10:423. doi: 10.1038/nrendo.2014.64
6. Donoho DA, Bose N, Zada G, Carmichael JD. Management of aggressive growth hormone secreting pituitary adenomas. *Pituitary*. (2017) 20:169–78. doi: 10.1007/s11102-016-0781-7
7. Fleseriu M, Popovic V. The journey in diagnosis and treatment, from pituitary adenoma to aggressive pituitary tumors. *Rev Endocr Metab Disord*. (2020) 21:201–2. doi: 10.1007/s11154-020-09561-w
8. Chang EF, Zada G, Kim S, Lamborn KR, Quinones-Hinojosa A, Tyrrell JB, et al. Long-term recurrence and mortality after surgery and adjuvant radiotherapy for nonfunctional pituitary adenomas. *J Neurosurg*. (2008) 108:736–45. doi: 10.3171/JNS/2008/108/4/0736
9. Seltzer J, Wedemeyer MA, Bonney PA, Carmichael JD, Weiss M, Zada G. Outcomes following transsphenoidal surgical management of incidental pituitary adenomas: a series of 52 patients over a 17-year period. *J Neurosurg*. (2018) 130:1584–92. doi: 10.3171/2017.11.JNS171485
10. Lelotte J, Mourin A, Fomekong E, Michotte A, Raftopoulos C, Maiter D. Both invasiveness and proliferation criteria predict recurrence of non-functioning pituitary macroadenomas after surgery: a retrospective analysis of a monocentric cohort of 120 patients. *Eur J Endocrinol*. (2018) 178:237–46. doi: 10.1530/eje-17-0965
11. Ghadir M, Khamseh M, Panahi-Shamsabad M, Ghorbani M, Akbari H, Mehrjardi A, et al. Cell proliferation, apoptosis, and angiogenesis in non-functional pituitary adenoma: association with tumor invasiveness. *Endocrine*. (2020) 69:596–603. doi: 10.1007/s12020-020-02366-6
12. Yao X, Gao H, Li C, Wu L, Bai J, Wang J, et al. Analysis of Ki67, HMGA1, MDM2, and RB expression in nonfunctioning pituitary adenomas. *J Neurooncol*. (2017) 132:199–206. doi: 10.1007/s11060-016-2365-9
13. Figarella-Branger D, Trouillas J. The new WHO classification of human pituitary tumors: comments. *Acta Neuropathol*. (2006) 111:71–2. doi: 10.1007/s00401-005-1099-0
14. Trouillas J, Roy P, Sturm N, Dantony E, Cortet-Rudelli C, Viennet G, et al. A new prognostic clinicopathological classification of pituitary adenomas: a multicentric case–control study of 410 patients with 8 years post-operative follow-up. *Acta Neuropathol*. (2013) 126:123–35. doi: 10.1007/s00401-013-1084-y
15. Trouillas J, Jaffrain-Rea M, Vasiljevic A, Dekkers O, Popovic V, Wierinckx A, et al. Are aggressive pituitary tumors and carcinomas two sides of the same coin? Pathologists reply to clinician's questions. *Rev Endocr Metab Disord*. (2020) 21:243–51. doi: 10.1007/s11154-020-09562-9
16. Miermeister C, Petersenn S, Buchfelder M, Fahlbusch R, Lüdecke D, Hölsken A, et al. Histological criteria for atypical pituitary adenomas - data from the German pituitary adenoma registry suggests modifications. *Acta Neuropathol Commun*. (2015) 3:50. doi: 10.1186/s40478-015-0229-8
17. Ntali G, Capatina C, Fazal-Sanderson V, Byrne J, Cudlip S, Grossman A, et al. Mortality in patients with non-functioning pituitary adenoma is increased: systematic analysis of 546 cases with long follow-up. *Eur J Endocrinol*. (2016) 174:137–45. doi: 10.1530/eje-15-0967
18. Brochier S, Galland F, Kujas M, Parker F, Gaillard S, Raftopoulos C, et al. Factors predicting relapse of nonfunctioning pituitary macroadenomas after neurosurgery: a study of 142 patients. *Eur J Endocrinol*. (2010) 163:193–200. doi: 10.1530/EJE-10-0255
19. Almiron Bonnin D, Havrda M, Lee M, Liu H, Zhang Z, Nguyen L, et al. Secretion-mediated STAT3 activation promotes self-renewal of glioma stem-like cells during hypoxia. *Oncogene*. (2018) 37:1107–18. doi: 10.1038/onc.2017.404
20. Graziano F, Fischer N, Bagaloni I, Di Bartolomeo M, Lonardi S, Vincenzi B, et al. TP53 mutation analysis in gastric cancer and clinical outcomes of patients with metastatic disease treated with ramucirumab/paclitaxel or standard chemotherapy. *Cancers*. (2020) 12:2049. doi: 10.3390/cancers12082049
21. Garcia P, Seiva F, Carniato A, de Mello Júnior W, Duran N, Macedo A, et al. Increased toll-like receptors and p53 levels regulate apoptosis and angiogenesis in non-muscle invasive bladder cancer: mechanism of action of P-MAPA biological response modifier. *BMC cancer*. (2016) 16:422. doi: 10.1186/s12885-016-2474-z
22. Lee S, Kang J, Ha J, Lee J, Oh S, Choi H, et al. Transglutaminase 2-Mediated p53 depletion promotes angiogenesis by increasing HIF-1α-p300 binding in renal cell carcinoma. *Int J Mol Sci*. (2020) 21(14):5042. doi: 10.3390/ijms21145042
23. Travis WD, Brambilla E, Muller-Hermelink HK, Harris CC. World Health Organization classification of tumours. In: *Pathology and genetics of tumours of the lung, pleura, thymus and heart*. Vol. 10 (2004). p. 179–84.
24. Moshkin O, Syro L, Scheithauer B, Ortiz L, Fadul C, Uribe H, et al. Aggressive silent corticotroph adenoma progressing to pituitary carcinoma: the role of temozolomide therapy. *Hormones (Athens)*. (2011) 10:162–7. doi: 10.14310/horm.2002.1307
25. Lim S, Shahinian H, Maya M, Yong W, Heaney A. Temozolomide: a novel treatment for pituitary carcinoma. *Lancet Oncol*. (2006) 7:518–20. doi: 10.1016/s1470-2045(06)70728-8
26. Zhao B, Cui Y, Fan X, Qi P, Liu C, Zhou X, et al. Anti-obesity effects of Spirulina platensis protein hydrolysate by modulating brain-liver axis in high-fat diet fed mice. *PLoS One*. (2019) 14:e0218543. doi: 10.1371/journal.pone.0218543
27. Shen L, Lei S, Zhang B, Li S, Huang L, Czachor A, et al. AxlSkipping of exon 10 in pre-mRNA regulated by PTBP1 mediates invasion and metastasis process of liver cancer cells. *Theranostics*. (2020) 10:5719–35. doi: 10.7150/thno.42010
28. He X, Sheng J, Yu W, Wang K, Zhu S, Liu Q. LncRNA MIR155HG promotes temozolomide resistance by activating the Wnt/β-catenin pathway via binding to PTBP1 in glioma. *Cell Mol Neurobiol*. (2020) 41:1271–84. doi: 10.1007/s10571-020-00898-z
29. Bai H, Chen B. Abnormal PTBP1 expression sustains the disease progression of multiple myeloma. *Dis Markers*. (2020) 2020:4013658. doi: 10.1155/2020/4013658
30. Pagaza-Straffon C, Marchat L, Herrera L, Díaz-Chávez J, Avante M, Rodríguez Y, et al. Evaluation of a panel of tumor-associated antigens in breast cancer. *Cancer Biomark*. (2020) 27:207–11. doi: 10.3233/cbm-190708
31. Hao F, Zhu Q, Lu L, Sun S, Huang Y, Zhang J, et al. EIF5A2 is highly expressed in anaplastic thyroid carcinoma and is associated with tumor growth by modulating TGF- signals. *Oncol Res*. (2020) 28:345–55. doi: 10.3727/096504020x15834065061807

Conflict of Interest: The authors declare that the research was conducted in the absence of any commercial or financial relationships that could be construed as a potential conflict of interest.

frontiers | Frontiers in Surgery

TYPE Original Research
PUBLISHED 26 July 2022
DOI 10.3389/fsurg.2022.922626

OPEN ACCESS

EDITED BY
Adib Abla,
University of California, United States

REVIEWED BY
Shousen Wang,
Fujian Medical University, China
İhsan Anık,
Kocaeli University, Turkey

*CORRESPONDENCE
Yazhuo Zhang
zyz2004520@yeah.net
Lei Cao
caolei_163@163.com

†These authors have contributed equally to this work and share the first authorship

SPECIALTY SECTION
This article was submitted to Neurosurgery, a section of the journal Frontiers in Surgery

RECEIVED 18 April 2022
ACCEPTED 08 July 2022
PUBLISHED 26 July 2022

CITATION
Nie D, Zhao P, Li C, Liu C, Zhu H, Gui S, Zhang Y and Cao L (2022) Application of "mosiac sign" on T2-WI in predicting the consistency of pituitary neuroendocrine tumors.
Front. Surg. 9:922626.
doi: 10.3389/fsurg.2022.922626

Application of "mosiac sign" on T2-WI in predicting the consistency of pituitary neuroendocrine tumors

Ding Nie[1†], Peng Zhao[2†], Chuzhong Li[1], Chunhui Liu[2], Haibo Zhu[2], Songbai Gui[2], Yazhuo Zhang[1*] and Lei Cao[2*]

[1]Beijing Neurosurgical Institute, Capital Medical University, Beijing, China, [2]Department of Neurosurgery, Beijing Tiantan Hospital, Capital Medical University, Beijing, China

Purpose: Tumor consistency is important for pituitary neuroendocrine tumors (PitNETs) resection to improve surgical outcomes. In this study, we evaluated the T2-WI of PitNETs and defined a specific T2-WI signaling manifestation, the "Mosaic sign," to predict tumor consistency and resection of PitNETs.
Design: A retrospective review of MRI and tumor histology of 137 consecutive patients who underwent endoscopic endonasal resection for PitNETs was performed.
Methods: The "Mosaic sign" was defined by the ratio of the tumor itself T2-WI signals, and characterized by multiple intratumor hyperintense dots. The degree of tumor resection was an assessment by postoperative MRI examination. The presence of the "Mosaic sign" was compared with patients' basic information, tumor consistency, tumor pathological staining, and surgical result. To determine whether the presence or absence of "Mosaic sign" could predict tumor consistency and guide surgical resection of tumors.
Results: Statistical analysis showed that the consistency of the tumor and the degree of resection were correlated with the "Mosaic sign". In the 137 cases of T2-WI, 43 had "Mosaic sign", 39 cases had soft tumor consistency, and 4 were classified as fibrous, of which 42 were completely resected and 1 was subtotal resected. Of the 94 patients without "Mosaic sign", the consistency of tumor of 54 cases were classified as soft, the remaining 40 cases were fibrous, 80 cases were completely resected, and 14 cases were subtotal resected. Postoperative cerebrospinal fluid leakage occurred in 1 patient. The number of corticotroph adenomas in the group of "Mosaic sign" was higher, with the statistical difference between the two groups ($P = 0.0343$).
Conclusions: The presence of the "Mosaic sign" in T2-WI may provide preoperative information for pituitary adenomas consistency and effectively guide surgical approaches.

KEYWORDS

T2-weighted imaging, mosaic sign, consistency, surgical approaches, magnetic resonance imaging, PitNETs

Introduction

PitNET is a kind of common benign intracranial tumor (1). The transsphenoidal approach has been the preferred treatment for the vast majority of PitNETs. However, for 1%–4% of these tumors, a transcranial approach is still required (2). The choice of surgical approach remains a problem for tumors with extensive suprasellar and lateral extension (3). However, if tumor consistency can be predicted preoperatively, the choice of surgical approach in the face of these complex types of adenomas may no longer bother the surgeon (4–6). When the tumor is soft, it can be fully removed by aspiration and curettage *via* the transsphenoidal approach. However, when the tumor is fibrous, it is difficult to be completely resected. Sometimes, craniotomy is even necessary to achieve a satisfactory resected effect (4, 7). Magnetic resonance imaging (MRI) is an important means of preoperative examination for PitNETs, which can provide information including tumor location, size, and aggressiveness (8, 9). The predictive value of MRI in PitNET consistency is being continuously explored (10). Conventional MRI methods such as T1-WI and T2-WI as well as CE-FIESTA and DWI have been shown to predict tumor consistency in PitNETs (11–14). However, the reliability of the forecasts is controversial (15). The purpose of our study was to determine whether preoperative MRI features might be associated with tumor consistency. Specifically, we analyzed the relationship between the "Mosaic sign" in T2-WI and tumor consistency and surgical outcome to test whether it could effectively predict tumor consistency to provide guidelines for surgeons in planning operations.

Materials and methods

Patients

This retrospective study included all patients with histopathologically proven PitNETs who underwent transsphenoidal resection of tumors at our hospital between January 2020 and February 2021, and who underwent MRI before and after surgery. A total of 137 patients met the inclusion criteria. All patients were followed up until now. The study was approved by our hospital's Institutional Review Board.

Clinical setting

All patients were operated on by the same team of neurosurgeons. Tumor consistency, classified as soft or fibrous, was assessed in blinded double-check by the two surgeons according to the lesions' inner surgical features after reviewing their surgical notes and video records. In detail, tumors easily removable with conventional maneuvers of curettage and suction were defined as soft. More resistant ones, difficult to remove and thus requiring more complex maneuvers such as extracapsular dissection, were classified as fibrous (11). Although this definition is quite subjective, it is widely used and does make sense to surgeons (16).

Imaging

The scans were performed using a 3.0-Tesla MRI scanner (Magnetom Avanto). All patients underwent MRI before and after surgery, and T2-WI (TR 4000 ms, TE 89 ms, layer thickness 4 mm, layer spacing 1 mm, FOV 30 cm × 30 cm, matrix size, 240 × 320) were included in each examination. The MRI was examined by two neuroradiologists who were unaware of the patient's identity or response to treatment. The extent of resection was determined by postoperative MRI. Total resection indicated the absence of residual tumor; subtotal resection indicated resection of ≥90% of the tumor.

Definition of "mosaic sign"

"Mosaic sign" was defined as a lesion containing small multiple hyperintense dots (ranging in size from 0.5 mm to <2 mm), or cystic changes that are predicted to be a soft-tissue compartment of the adenoma. However, if the tumor presented with a homogenous hypointense signal without a mosaic sign, it predicted the tumor compartment to be fibrous (**Figure 1**) (14).

Histopathological examination

All surgical specimens were treated as usual. Tissues were fixed in 10% formalin buffer and embedded in paraffin. 4 μm tissue sections were prepared for immunohistochemical analysis.

The tumors were classified according to the fourth edition of the WHO Classification of Pituitary Tumors (17).

Statistical analysis

Statistical analyses were performed using SPSS version 21.0. Categorical variables were defined by frequency and percentage rate, and numeric variables with mean ± standard deviation (SD). In triple independent group comparisons, ANOVA tests were used for normally distributed numeric variables, and Kruskal–Wallis tests were used for non-normally distributed data. Categorical variables were compared using a Chi-square test. Statistically significant results were defined with a *P*-value of <0.05.

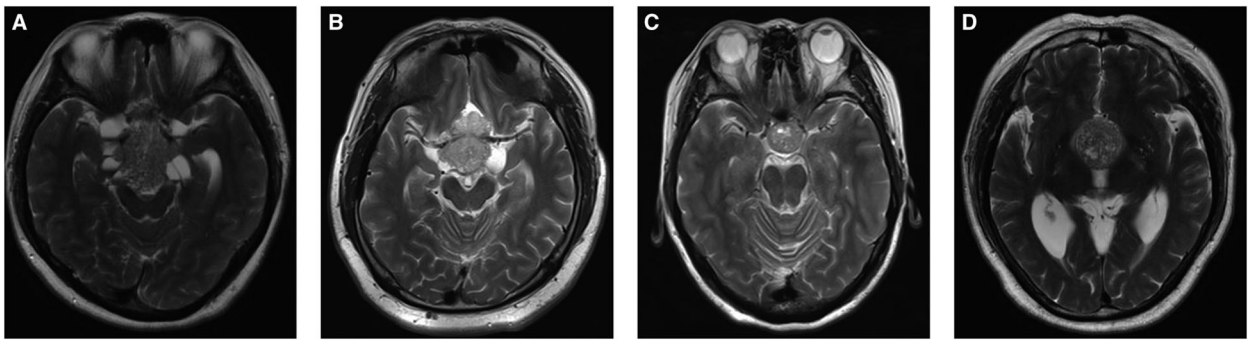

FIGURE 1
Radiological features of "Mosaic Sign". (A–D) Sagittal T2-WI in 4 patients showed intratumoral hyperintense dots within the tumor.

Results

Findings of basic data

A population of 137 patients was enrolled in this cohort, including 63 (46.0%) males and 74 (54.0%) females. The average age of surgery was 55.3 ± 16.9 years. According to the T2-WI manifestation and the classification of Knosp or Hardy (Table 1). However, we found a statistically significant difference in BMI values between the two groups. Patients without the "Mosaic sign" were higher than patients with the "Mosaic sign" ($P = 0.0280$).

Findings of surgery

Intraoperatively, all of the 43 (100%) patients had tumors that were classified as soft in the group of patients with the "Mosaic sign". In addition, 54 (57.4%) patients had tumors that were classified as soft, and 40 (42.6%) patients were found to have fibrous tumors in the other group. The difference was statistically significant between the two groups ($P < 0.0001$). The ROC curve and the area under the ROC curve (AUC) were generated to evaluate the "Mosaic sign" potential use as a predictor of tumor consistency with a sensitivity and specificity of 70.7% and 100%, respectively (Figure 2). The group of "Mosaic sign" gross total resection was achieved in 42 (97.6%) patients, subtotal resection (>90% of tumor) in 1 (2.4%) patient. Among patients without the "Mosaic sign", 80 cases (85.1%) had a gross total resection, and 14 cases (24.9%) had subtotal resections (estimated resection of >90%). This difference was statistically significant ($P = 0.0288$). (Table 1). In the "Mosaic sign" group, 22 cases had Knosp grade ≥3, and 19 cases had Hardy grade ≥C (This type of tumor is considered invasive (18, 19)). Only subtotal resection was performed in 1 patient because the tumor enveloped the internal carotid artery and the adhesion was tight. By contrast, in the other group, subtotal resection was performed in 14 of 49 PitNETs of Knosp grades 3 and 4 (28.5%), and 11 cases (29.7%)were subtotal resections in PitNETs of Hardy grade ≥C (Table 2).

Findings of pathologic analyses

16 cases (37.2%) in the group of "Mosaic sign" were corticotroph tumors, which was higher than that in the non-Mosaic group19 cases (20.2%), which ($P = 0.0343$). There was no statistical difference among other types (Somatotroph adenomas, $P = 0.0785$; Lactotroph tumors, $P = 0.2199$; Gonadotroph tumors, $P = 0.6774$; Plurihormonal tumors, $P = 0.7800$; Null cell tumors, $P = 0.5421$) (Table 1).

Illustrative cases

Case 1 was a 39-year-old female patient who presented with vision loss. Pre-op. A huge invasive tumor located in the sellar and suprasellar region was found on MRI. The tumor presented a "Mosaic sign" on T2-WI, hence it was predicted to be a soft tumor. So, we chose an EEA to remove the tumors, which were confirmed to be soft (Supplementary Figure S1). Post-op. No complications such as CSF leakage, intra-cranial infection, or hypopituitarism occurred after surgery (Figure 3). The immunohistochemical result proved to be a silent ACTHoma (Supplementary Figure S2). (GH (−), PRL (−), LH (−), TSH (−), FSH (−), ACTH (+), Ki-67 (1–3%), PIT-1 (−), SF-1 (+), T-PIT (+)).

Case 2 was a 47-year-old male patient who presented with vision loss and headache. Pre-op. The neoplasm showed uniform hyposensitivity on T2-WI and was therefore predicted to be a fibrous tumor. Because the tumor growth

TABLE 1 Clinical features, imaging, surgical, and pathological details of 137 patients with PitNETs.

	Patients with the "Mosaic sign" ($n = 43$)	Patients without the "Mosaic sign" ($n = 94$)	*P*
Age ± STD	53.4 ± 16.9	56.6 ± 15.9	0.2749
Gender (male/female)	20/23	43/51	0.9334
BMI (kg/m^2)	24.9 ± 3.5	26.3 ± 3.3	0.0280*
Primary surgery	30 (69.8%)	66 (70.2%)	0.8864
Knosp			
1	8	13	0.4716
2	13	32	0.6595
3	16	39	0.6353
4	6	10	0.5750
Hardy			
A	11	34	0.2207
B	13	25	0.6590
C	7	20	0.4950
D	10	12	0.1207
E	2	5	0.8691
Tumor types			
Somatotroph tumors (*n*)	6 (14.0%)	26 (27.7%)	0.0785
Lactotroph tumors (*n*)	5 (11.6%)	19 (20.2%)	0.2199
Corticotroph tumors (*n*)	16 (37.2%)	19 (20.2%)	0.0343*
Gonadotroph tumors (*n*)	11 (25.6%)	21 (22.3%)	0.6774
Plurihormonal tumors (*n*)	1 (2.3%)	3 (3.2%)	0.7800
Null cell tumors(*n*)	4 (9.3%)	6 (4.2%)	0.5421
Tumor consistency			<0.0001*
Fibrous (*n*)	0 (0%)	40 (42.6%)	
Soft (*n*)	43 (100%)	54 (57.4%)	
Resection range			0.0288
Total (*n*)	42 (97.6%)	80 (85.1%)	
Subtotal (*n*)	1 (2.4%)	14 (24.9%)	
CSF leakage (*n*)	0 (0%)	1 (1.1%)	0.4972
Hospitalization days	8.5 ± 3.7	7.5 ± 4.0	0.0799

The symbol * represents $p < 0.05$.

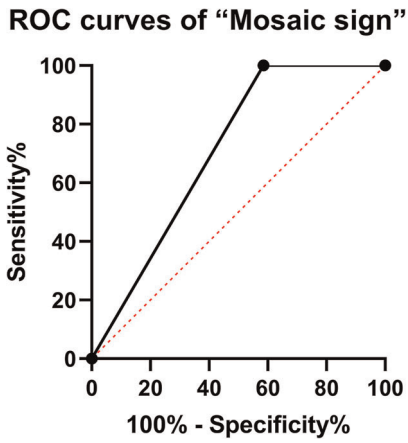

FIGURE 2
ROC curves of "Mosaic sign". Sensitivity and specificity of 70.7% and 100%, respectively.

TABLE 2 Invasion and degree of tumor resection.

	Total Resection (*n*)	Subtotal Resection (*n*)
"Mosaic sign"		
Knosp ≥3	22	0
Hardy ≥C	18	1
CSF leakage (*n*)	0	0
Non-"Mosaic sign"		
Knosp ≥3	35	14
Hardy ≥C	26	11
CSF leakage(*n*)	1	0

was relatively regular, we chose EEA to remove the tumor, which was proved to be fibrous (**Supplementary Figure S1**). Post-op. No complications such as CSF leakage, intra-cranial infection, or hypopituitarism occurred after surgery (**Figure 4**). The immunohistochemical result proved to be a nonfunction tumor (**Supplementary Figure S2**). (GH (−), PRL (−), LH (−), TSH (−), FSH (+), ACTH (−), Ki-67 (2–4%), PIT-1 (−), SF-1 (−), T-PIT (−)).

Discussion

Prediction of tumor consistency

The preoperative consistency prediction of PITnet is controversial, and different imaging has its unique value. For example, Wan et al. made consistent predictions based on a radiomic model of multi-parameter magnetic resonance imaging (mpMRI), while Cohen-Cohen et al. argued that MRE was a reliable tool compared to other sequences (20, 21). As far as we know, currently, studies on preoperative prediction of tumor consistency have focused on imaging findings on T2-WI (11, 22). Although there are controversies, it seems that T2-WI strongly indicates tumor consistency (23). Some studies have shown that a low signal on T2-weighted images corresponds to fibrotic tumors. Some people believe that a signal of equal intensity is more likely to predict fibrotic

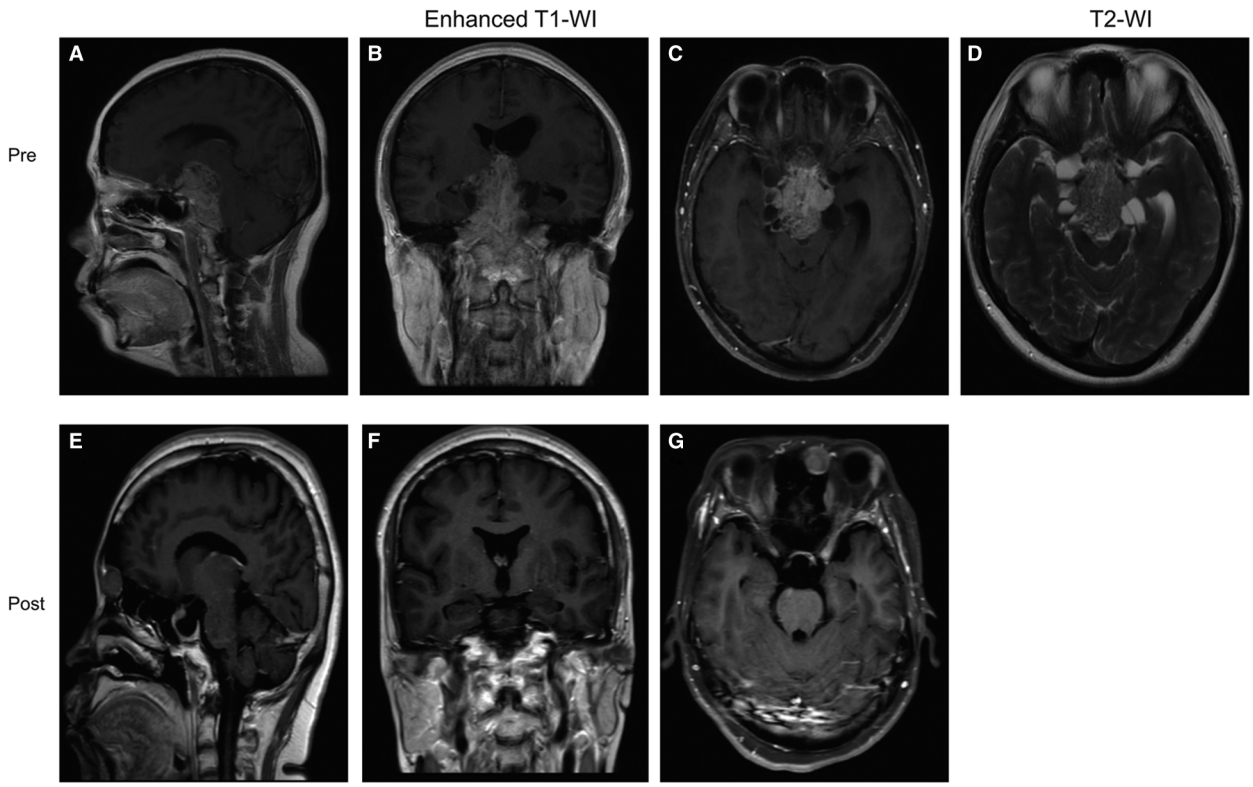

FIGURE 3
Preoperative and postoperative MRI images of a patient in the "Mosaic sign" group. (**A–C**) Preoperative coronal, axial, and sagittal enhanced MRI, Knosp = 3, Hardy = D; (**D**) Preoperative sagittal T2-WI with "Mosaic Sign"; (**E–G**) The tumor was completely resected on coronal, axial, sagittal enhanced MRI 1 month postoperatively.

tumors. Finally, some researchers believe that there is no significant relationship between tumor consistency and MRI (10, 16, 24). One study showed that tumors may be fibrous if showing low signal strength and homogeneous enhancement on T2-WI (10). Smith et al. suggested that tumor-to-cerebellar peduncle ratios could predict tumor consistency. Ratios >1.8 have a high predictive value for soft consistency tumors; ratios <1.5 have a high predictive value for firm consistency tumors (16). However, some studies have concluded that relative signal strength values do not correspond to tumor consistency (15, 25). The main reason may be that the factors influencing T2-WI signal strength are independent of the histological results (26). Based on existing reports, we found that PitNETs with mixed signals of high and low intensity present in T2-WI which we called "Mosaic sign" usually indicates that the tumor is soft and easy to remove. The judgment of signal level is only the comparison of the signal inside the tumor and has nothing to do with the factors outside the tumor, avoiding the error brought by comparing the gray matter or other tissues with the tumor tissue. In this study, all the tumors with "Mosaic sign" had a soft consistency. The causes of such imaging are complex, uneven tumor cell density, or uneven free water, fiber, and collagen content in different parts of the tumor, or the presence of multimicrocystic. There is evidence that tumors with more collagen show lower signal intensity on T2-weighted images (10). From our point of view, when tumor components are mixed, that is, collagen and free water are mixed and dispersed between tumors, there will be "Mosaic" markers, which may be related to tumor growth rate and growth mode, which needs to be further explored. Furthermore, there is a special case, that is, scattered small cystic changes within the tumor.

"Mosaic sign" for surgical selection

At present, the surgical approach for the giant tumor is still controversial. For larger lesions, the consistency of the tumor may be a factor in determining the need for craniotomy (27). If the tumor consistency is soft, endoscopic transnasal surgery can achieve satisfactory results (28). Meanwhile, the consistency of PitNET is an important intraoperative characteristic that may dictate operative dissection techniques and/or instruments used for tumor removal during endoscopic endonasal approaches (6, 29). Furthermore, preoperative determination of tumor consistency can

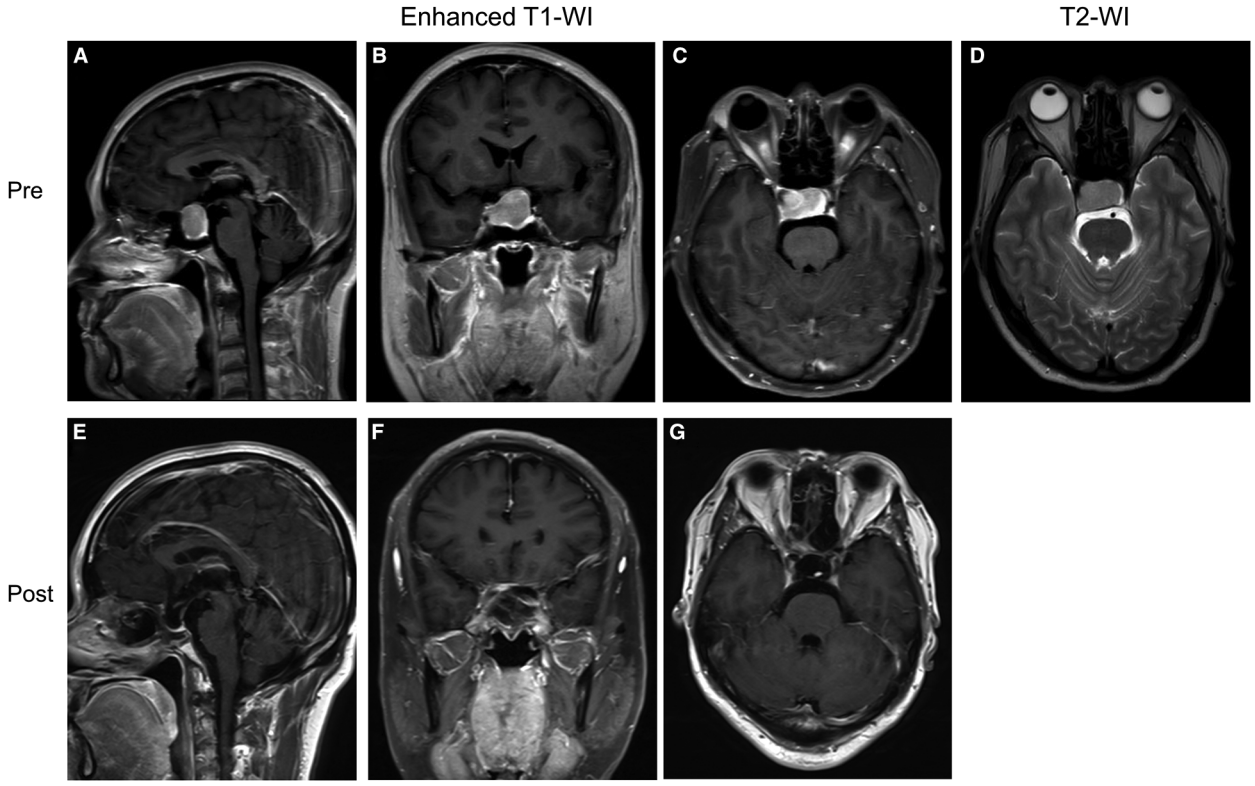

FIGURE 4
Preoperative and postoperative MRI images of a patient in the group without "Mosaic sign". (**A–C**) Preoperative coronal, axial, and sagittal enhanced MRI, Knosp = 2, Hardy = B; (**D**) Preoperative sagittal T2-WI without "Mosaic Sign"; (**E–G**) The tumor was completely resected on coronal, axial, sagittal enhanced MRI 1 month postoperatively.

minimize the chance of postoperative complications and residual tumors (17). Tumors with soft consistency are easy to be sucked out/curetted intraoperatively, and the effect of resection is better. Secondly, if there is a suprasellar extension of the tumor, after intraoperative resection of the lower part of the tumor, the saddle of the tumor is easy to descend, and the complete resection of the tumor can be completed at one time, avoiding the secondary operation or even craniotomy. Finally, the soft tumors are more likely to separate from the surrounding tissue and proper intraoperative use of aspirators can help the surgeon remove the tumor adequately, causing less damage to the surrounding tissue. Fibrous tumors are more difficult to remove with a transsphenoidal approach. Internal debulking can be difficult even with the use of an ultrasound aspirator, and the fragmentation cannot be easily accomplished without adequate mobilization (28). Moreover, it is difficult to peel off such tumors that adhere to the surrounding tissues with ordinary instruments, which is easy to cause damage to the surrounding tissues. At this time, transcranial approaches or combined transcranial and endoscopic approaches are necessary (30). Therefore, preoperative assessment and prediction of tumor consistency are particularly important. The improved preoperative prediction may better guide patients on risks and benefits. In our study cohort, it is not difficult to find that for giant tumors, transnasal endoscopic surgery in the "Mosaic sign" group of cases is more likely to achieve satisfactory results, and there are no significant complications. One of the main reasons is that tumors with the "Mosaic sign" tend to be softer and easier to remove during surgery. There is no denying that the surgeon's skill and experience can also affect the outcome. In conclusion, endoscopic transsphenoidal surgery can be selected even if the pituitary tumor is large if there is a "Mosaic" sign on T2-weighted images before surgery, and better surgical results can be achieved.

"Mosaic sign" and tumor types

Notably, the pathological type of the tumor was correlated with the "Mosaic sign", that is, corticotroph tumors (Including SCAs) were more prone to the "Mosaic sign", suggesting soft tumor consistency, consistent with what has been reported in the literature (31). Microcyst patterns on T2-WI have been considered radiological features of SCAs in several studies (32, 33). Laure et al. found multiple microcysts

in most SCAs and pseudopapillary artefactual dehiscences and perivascular pseudorosettes in SCAs on pathological examination. They considered that a dissociated tissue with pseudopapillary dehiscences could explain the small hyperintense foci in T2-WI (34). The radiographic appearance of this microcyst coincides with our definition of a "Mosaic sign". However, the mechanism needs further research.

Limitation

Our study has several limitations. Firstly, this study was a retrospective analysis with a relatively small number of patients. Secondly, the quantitative description of the "Mosaic sign" was not included in our study. In future work, we can quantitatively describe such imaging findings by reviewing more case data. Third and finally, we did not quantitatively analyze the degree of fibrosis in histopathological specimens, and we will verify this in the future.

Conclusions

The "Mosaic sign" on T2-WI in patients with PitNET may indicate a soft tumor texture, and a satisfactory resection can be achieved by endoscopic transnasal surgery, even for large, aggressive tumors. But further large-scale studies are needed to confirm and improve this approach.

Data availability statement

Some or all datasets generated during and analyzed during the current study are not publicly available but are available from the corresponding author on reasonable request.

Ethics statement

Written informed consent was obtained from the individual(s) for the publication of any potentially identifiable images or data included in this article.

Author contributions

DN and PZ drafted the manuscript. CL, CL, HZ, and SG helped to revise the manuscript. YZ and LC read and approved the final manuscript. All authors contributed to the article and approved the submitted version.

Funding

This study was supported by the Capital's Funds for Health Improvement and Research (2020-4-1077).

Conflict of interest

The authors declare that the research was conducted in the absence of any commercial or financial relationships that could be construed as a potential conflict of interest.

Supplementary material

The Supplementary Material for this article can be found online at: https://www.frontiersin.org/articles/10.3389/fsurg.2022.922626/full#supplementary-material.

SUPPLEMENTARY FIGURE 1
Intraoperative conditions. (A-B) The texture of the tumor is soft; (C) The texture of the tumor is fibrous.

SUPPLEMENTARY FIGURE 2
Hematoxylin-eosin staining. (A) Case 1; (B) Case 2.

Publisher's note

All claims expressed in this article are solely those of the authors and do not necessarily represent those of their affiliated organizations, or those of the publisher, the editors and the reviewers. Any product that may be evaluated in this article, or claim that may be made by its manufacturer, is not guaranteed or endorsed by the publisher.

References

1. Budan RM, Georgescu CE. Multiple pituitary adenomas: a systematic review. *Front Endocrinol (Lausanne)*. (2016) 7:1. doi: 10.3389/fendo.2016.00001

2. Wilson CB. A decade of pituitary microsurgery: the Herbert Olivecrona lecture. *J Neurosurg*. (1984) 61(5):814–33. doi: 10.3171/jns.1984.61.5.0814

3. Mortini P, Barzaghi R, Losa M, Boari N, Giovanelli M. Surgical treatment of giant pituitary adenomas: strategies and results in a series of 95 consecutive patients. *Neurosurgery*. (2007) 60(6):993–1004. doi: 10.1227/01.NEU.0000255459.14764.BA

4. Buchfelder M, Kreutzer J. Transcranial surgery for pituitary adenomas. *Pituitary*. (2008) 11(4):375–84. doi: 10.1007/s11102-008-0120-8

5. Youssef AS, Agazzi S, van Loveren HR. Transcranial surgery for pituitary adenomas. *Neurosurgery*. (2005) 57(1 Suppl):168–75; discussion 168–75. doi: 10.1227/01.neu.0000163602.05663.86

6. Couldwell WT. Transsphenoidal and transcranial surgery for pituitary adenomas. *J Neurooncol*. (2004) 69(1-3):237–56. doi: 10.1023/B:NEON.0000041886.61149.ab

7. D'Haens J, Van Rompaey K, Stadnik T, Haentjens P, Poppe K, Velkeniers B. Fully endoscopic transsphenoidal surgery for functioning pituitary adenomas: a retrospective comparison with traditional transsphenoidal microsurgery in the same institution. *Surg Neurol.* (2009) 72(4):336–40. doi: 10.1016/j.surneu.2009.04.012

8. Bashari WA, Senanayake R, Fernández-Pombo A, Gillett D, Koulouri O, Powlson AS, et al. Modern imaging of pituitary adenomas. *Best Pract Res Clin Endocrinol Metab.* (2019) 33(2):101278. doi: 10.1016/j.beem.2019.05.002

9. Gao A, Bai J, Cheng J, Cheng X, Li S, Zhang Z, et al. Differentiating skull base chordomas and invasive pituitary adenomas with conventional MRI. *Acta Radiol.* (2018) 59(11):1358–64. doi: 10.1177/0284185118757576

10. Iuchi T, Saeki N, Tanaka M, Sunami K, Yamaura A. MRI prediction of fibrous pituitary adenomas. *Acta Neurochir.* (1998) 140(8):779–86. doi: 10.1007/s007010050179

11. Cuocolo R, Ugga L, Solari D, Corvino S, D'Amico A, Russo D, et al. Prediction of pituitary adenoma surgical consistency: radiomic data mining and machine learning on T2-weighted MRI. *Neuroradiology.* (2020) 62(12):1649–56. doi: 10.1007/s00234-020-02502-z

12. Suzuki C, Maeda M, Hori K, Kozuka Y, Sakuma H, Taki W, et al. Apparent diffusion coefficient of pituitary macroadenoma evaluated with line-scan diffusion-weighted imaging. *J Neuroradiol.* (2007) 34(4):228–35. doi: 10.1016/j.neurad.2007.06.007

13. Lagerstrand K, Gaedes N, Eriksson S, Farahmand D, De Coursey E, Johansson G, et al. Virtual magnetic resonance elastography has the feasibility to evaluate preoperative pituitary adenoma consistency. *Pituitary.* (2021) 24(4):530–41. doi: 10.1007/s11102-021-01129-4

14. Yamamoto J, Kakeda S, Shimajiri S, Takahashi M, Watanabe K, Kai Y, et al. Tumor consistency of pituitary macroadenomas: predictive analysis on the basis of imaging features with contrast-enhanced 3D FIESTA at 3 T. *AJNR Am J Neuroradiol.* (2014) 35(2):297–303. doi: 10.3174/ajnr.A3667

15. Bahuleyan B, Raghuram L, Rajshekhar V, Chacko AG. To assess the ability of MRI to predict consistency of pituitary macroadenomas. *Br J Neurosurg.* (2006) 20(5):324–6. doi: 10.1080/02688690601000717

16. Smith KA, Leever JD, Chamoun RB. Prediction of consistency of pituitary adenomas by magnetic resonance imaging. *J Neurol Surg B Skull Base.* (2015) 76(5):340–3. doi: 10.1055/s-0035-1549005

17. Mete O, Lopes MB. Overview of the 2017 WHO classification of pituitary tumors. *Endocr Pathol.* (2017) 28(3):228–43. doi: 10.1007/s12022-017-9498-z

18. Basaran R, Gundogan D, Senol M, Bozdogan C, Gezen F, Sav A. The expression of stem cell markers (CD133, Nestin, OCT4, SOX2) in invasive pituitary adenomas. *Acta Endocrinol (Buchar).* (2020) 16(3):303–10. doi: 10.4183/aeb.2020.303

19. Wu X, Xie SH, Tang B, Yang YQ, Yang L, Ding H, et al. Pituitary adenoma with posterior area invasion of cavernous sinus: surgical anatomy, approach, and outcomes. *Neurosurg Rev.* (2020) 44(4):2229–37. doi: 10.1007/s10143-020-01404-1

20. Wan T, Wu C, Meng M, Liu T, Li C, Ma J, et al. Radiomic features on multiparametric MRI for preoperative evaluation of pituitary macroadenomas consistency: preliminary findings. *J Magn Reson Imaging.* (2022) 55(5):1491–503. doi: 10.1002/jmri.27930

21. Cohen-Cohen S, Helal A, Yin Z, Ball MK, Ehman RL, Van Gompel JJ, et al. Predicting pituitary adenoma consistency with preoperative magnetic resonance elastography. *J Neurosurg.* (2021):1–8. doi: 10.3171/2020.10.JNS201642. [Epub ahead of print]

22. Boxerman JL, Rogg JM, Donahue JE, Machan JT, Goldman MA, Doberstein CE. Preoperative MRI evaluation of pituitary macroadenoma: imaging features predictive of successful transsphenoidal surgery. *AJR Am J Roentgenol.* (2010) 195(3):720–8. doi: 10.2214/AJR.09.4128

23. Chen XY, Ding CY, You HH, Chen JY, Jiang CZ, Yan XR, et al. Relationship between pituitary adenoma consistency and extent of resection based on tumor/cerebellar peduncle T2-weighted imaging intensity (TCTI) ratio of the point on preoperative magnetic resonance imaging (MRI) corresponding to the residual point on postoperative MRI. *Med Sci Monit.* (2020) 26:e919565. doi: 10.12659/MSM.919565

24. Theodros D, Patel M, Ruzevick J, Lim M, Bettegowda C. Pituitary adenomas: historical perspective, surgical management and future directions. *CNS Oncol.* (2015) 4(6):411–29. doi: 10.2217/cns.15.21

25. Thotakura AK, Patibandla MR, Panigrahi MK, Mahadevan A. Is it really possible to predict the consistency of a pituitary adenoma preoperatively? *Neurochirurgie.* (2017) 63(6):453–7. doi: 10.1016/j.neuchi.2017.06.003

26. Hagiwara A, Inoue Y, Wakasa K, Haba T, Tashiro T, Miyamoto T. Comparison of growth hormone–producing and non–growth hormone–producing pituitary adenomas: imaging characteristics and pathologic correlation. *Radiology.* (2003) 228(2):533–8. doi: 10.1148/radiol.2282020695

27. Snow RB, Lavyne MH, Lee BC, Morgello S, Patterson RH Jr. Craniotomy versus transsphenoidal excision of large pituitary tumors: the usefulness of magnetic resonance imaging in guiding the operative approach. *Neurosurgery.* (1986) 19(1):59–64. doi: 10.1227/00006123-198607000-00008

28. Cappelletti M, Ruggeri AG, Spizzichino L, D'Amico A, D'avella E, Delfini R. Fibrous pituitary macroadenomas: predictive role of preoperative radiologic investigations for proper surgical planning in a cohort of 66 patients. *World Neurosurg.* (2019) 121:e449–57. doi: 10.1016/j.wneu.2018.09.137

29. Rutkowski MJ, Chang KE, Cardinal T, Du R, Tafreshi AR, Donoho DA, et al. Development and clinical validation of a grading system for pituitary adenoma consistency. *J Neurosurg.* (2020):1–8. doi: 10.3171/2020.4.JNS193288

30. Pratheesh R, Rajaratnam S, Prabhu K, Mani SE, Chacko G, Chacko AG. The current role of transcranial surgery in the management of pituitary adenomas. *Pituitary.* (2013) 16(4):419–34. doi: 10.1007/s11102-012-0439-z

31. Jiang S, Zhu J, Feng M, Yao Y, Deng K, Xing B, et al. Clinical profiles of silent corticotroph adenomas compared with silent gonadotroph adenomas after adopting the 2017 WHO pituitary classification system. *Pituitary.* (2021) 24(4):564–73. doi: 10.1007/s11102-021-01133-8

32. Kasuki L, Antunes X, Coelho M, Lamback EB, Galvão S, Silva Camacho AH, et al. Accuracy of microcystic aspect on T2-weighted MRI for the diagnosis of silent corticotroph adenomas. *Clin Endocrinol (Oxf).* (2020) 92(2):145–9. doi: 10.1111/cen.14133

33. Cazabat L, Dupuy M, Boulin A, Bernier M, Baussart B, Foubert L, et al. Silent, but not unseen: multimicrocystic aspect on T2-weighted MRI in silent corticotroph adenomas. *Clin Endocrinol (Oxf).* (2014) 81(4):566–72. doi: 10.1111/cen.12443

34. Langlois F, Lim D, Yedinak CG, Cetas I, McCartney S, Cetas J, et al. Predictors of silent corticotroph adenoma recurrence; a large retrospective single center study and systematic literature review. *Pituitary.* (2018) 21(1):32–40. doi: 10.1007/s11102-017-0844-4

frontiers | Frontiers in Surgery

TYPE Original Research
PUBLISHED 02 August 2022
DOI 10.3389/fsurg.2022.959440

OPEN ACCESS

EDITED BY
Peng Zhao,
Capital Medical University, China

REVIEWED BY
Fabio Ferreli,
Humanitas University, Italy
Jose Landeiro,
Fluminense Federal University, Brazil

*CORRESPONDENCE
Julien Boetto
j-boetto@chu-montpellier.fr

SPECIALTY SECTION
This article was submitted to Neurosurgery, a section of the journal Frontiers in Surgery

RECEIVED 01 June 2022
ACCEPTED 15 July 2022
PUBLISHED 02 August 2022

CITATION
Boetto J, Joitescu I, Raingeard I, Ng S, Le Corre M, Lonjon N, Crampette L and Favier V (2022) Endoscopic transsphenoidal surgery for non-functioning pituitary adenoma: Learning curve and surgical results in a prospective series during initial experience.
Front. Surg. 9:959440.
doi: 10.3389/fsurg.2022.959440

Endoscopic transsphenoidal surgery for non-functioning pituitary adenoma: Learning curve and surgical results in a prospective series during initial experience

Julien Boetto[1,2]*, Irina Joitescu[1], Isabelle Raingeard[3], Sam Ng[1,2], Marine Le Corre[1], Nicolas Lonjon[1], Louis Crampette[4] and Valentin Favier[4]

[1]Department of Neurosurgery, Gui de Chauliac Hospital, Montpellier University Medical Center, Montpellier, France, [2]IGF, Université de Montpellier, CNRS, INSERM, Montpellier, France, [3]Department of Endocrinology, Lapeyronie Hospital, Montpellier University Medical Center, Montpellier, France, [4]Department of ENT Surgery, Gui de Chauliac Hospital, Montpellier University Medical Center, Montpellier, France

Background: To report the initial experience of surgery for non-functioning pituitary adenoma (NFPA) from a neurosurgeon in a dedicated residency training endoscopic transsphenoidal (ETS) program, and detail the surgical and clinical outcomes during this period.
Methods: A prospective series of all patients operated for NFPA, using an ETS approach, during the three first years of experience of a newly board-certified neurosurgeon was analysed. Clinical, radiological and peri-operative data were collected. Extent of resection (EOR) was determined by formal volumetric analysis. Impact of the learning curve and predictive factors of gross total resection (GTR) were determined.
Results: Fifty-three patients with NFPA were included in this prospective cohort which was divided in two periods of time ("First period": 30 first cases, and "second period": 23 following cases). Baseline characteristics of the patients in the two periods were similar. Overall occurrence of complication was 22% and was not significantly different in the two periods of time. No patient had severe neurological complication. Gross total resection was achieved in 70% of patients. Mean Extent of resection was 96%. In a multiple linear regression model, a higher EOR was positively correlated with experience ($p = 0.018$) and negatively correlated with Knosp Score equal to 4 ($p < 0.001$). Predictive factors for GTR were Higher Knosp grade ($p = 0,01$), higher pre-operative volume ($p = 0.03$), and second period of time ($p = 0.01$).
Conclusion: NFPA surgery can be safe and efficient during the learning period. Dedicated intensive learning, careful patient selection and multidisciplinary work are key to shorten the learning curve and achieve satisfactory results.

KEYWORDS

Pituitary, learning curve, skull base surgery, endoscopic endonasal approach, pituitary adenama

Introduction

The endoscopic endonasal approach to the sella has been widely used since the late 1990s for pituitary adenoma surgery (1). First described by R. Jankowski in 1992 (2), endoscopic guided transsphenoidal surgery was standardized in clinical practice by Jho and Carrau (3, 4) and Capabianca (5). Though it allows similar gross total resection rates as microscopic approaches (6), the enhanced illumination and visualization of both anatomical elements and the pituitary lesion provided by the endoscope has led most pituitary surgeons to turn to purely endoscopic procedures (1). However, a key factor in the use of the endoscope is the significant learning curve associated with its safe and effective use (7, 8). It is often considered to be less intuitive than the microscope because of a potential decreased ability to use instruments under the direct vision of the operating surgeon. As a result, several studies report a steep learning curve before proficiency is achieved when converting to this challenging method. However, there are conflicting reports and no clear consensus as to the endpoint of the learning curve in order to achieve satisfactory results, with published reports varying between 15 and 100 procedures as being necessary (8–10). Indeed, recent publications show that the effect of the learning curve is still visible even after extensive experience of endoscopic surgery (11).

Studies focusing on this topic generally describe very experienced pituitary surgeons who have turned from microscopic to endoscopic surgery. The next generations of pituitary surgeons will undoubtedly commence their experience with fully endoscopic procedures after a residency period and a dedicated training period marked by the predominance of the endoscope. The possibility of transposing learning curve results from surgeons who are experienced in microscopic vision and gestures who have converted to endoscopic surgery, to surgeons who are fully trained in endoscopy is uncertain: very few studies have focused on surgical results during the initial training period in endoscopic surgery for less experienced surgeons who have no previous experience with microscopic pituitary surgery.

In this study, we report an initial experience of fully endoscopic non-functioning pituitary adenoma (NFPA) surgery from a neurosurgeon who had a dedicated endonasal endoscopic training during residency, and without any experience of previous microscopic pituitary surgery. The main objective was to assess the impact of experience on surgical results and to characterize a potential learning curve. The secondary objective was to examine predictive factors of gross total resection and surgical complications.

Material and methods

Patient population and study design

A prospective cohort study including all patients undergoing endoscopic endonasal surgery between November 2017 and November 2020 by a single neurosurgeon (JB) was established. At the beginning of the study, the neurosurgeon (JB) was starting his experience as a board-certified neurosurgeon. Patients who fulfilled the following criteria were included in this study: patients with non-functioning pituitary adenomas (NFPA), operated through endoscopic non-extended approach (no parasellar or transplanar resection). Patient's medical history was prospectively recorded, including demographics, tumor type, visual status, endocrine status, operative data (approach, total operative time, cerebro-spinal fluid (CSF) leak, closure), post-operative complications, need for revision surgery, quality of resection with volumetric assessment, and length of hospital stay (LOS).

All patients provided informed consent for the prospective or retrospective analysis of their clinical and radiological information. The study received the approval of the Institutional Review Board (n°2019 IRB_MTP_12-02) of the University Hospital of Montpellier.

Radiological evaluation

All patients underwent magnetic resonance imaging (MRI) with 1.5-Tesla T2-weighted and T1-weighted imaging, with and without gadolinium enhancement. Pituitary adenomas were classified according to the maximum tumor diameter into microadenomas (<10 mm), macroadenomas (between 10 and 40 mm), and giant adenomas (>40 mm). Tumor extension was radiologically defined in the prospective group using the modified Knosp Score (12). "Invasion" represents a composite criterion based on radiological findings (cavernous sinus or sphenoidal sinus invasion), intraoperative examination and histopathological findings, as defined by the Hypopronos score (13).

Patients underwent a systematic postoperative CT-scan in the first 24 h following surgery and a 6-month follow-up MRI. A volumetric assessment was performed using HOROS software (Nimble Co LLC d/b/a Purview in Annapolis, MD, USA) based on presurgical MRI and 6-month post-operative MRI.

Ophthalmologic evaluation

All patients underwent pre-operative and post-operative ophthalmological examinations at 3 months and 12 months follow-up. Visual acuity and Goldman visual field were tested

for both eyes. Ophthalmologic results were divided into four groups: worsened when visual acuity or visual field decreased; unchanged when no post-operative change occurred; partial recovery; and complete recovery (visual acuity and visual field both returned to normal).

Hormonal assessments

All patients underwent pre-operative static endocrinological examination including measurement of serum levels of prolactin, luteinizing hormone, follicle-stimulating hormone, testosterone (in men) and estradiol (in women), 8:00 am adrenocorticotropic hormone and cortisol, insulin-like growth factor-I, thyroid stimulating hormone and free T3 and T4. These measurements were repeated at 1 month, 3 months and 1 year after surgery. The results were classified as "worsened" when at least one new pituitary deficit occurred, as "partial recovery" when at least one pituitary deficit recovered, as "complete recovery" when all pituitary deficits recovered, and as "unchanged" when no change occurred. Post-operative diabetes insipidus (DI) was defined as daily diuresis over 3L with urinary osmolarity <1005 mOsmol/kg. Endocrine deficits were considered as permanent when found to be persistent at 1 year after surgery.

Operative technique

Procedures were performed with a 30° endoscope, using a unilateral right nostril transseptal fully endoscopic approach, as described previously (14). The nasal phase was generally performed by an ENT, and the sellar phase was performed systematically by the neurosurgeon. Neuronavigation was used in selected cases (particularly in surgery for recurrence). A large anterior sphenoidotomy was performed. A bone resection of the sellar floor was performed with conservation of the inferior margin to facilitate closure at the end of the procedure. The sellar dura was incised and the tumor was removed according to classical microsurgery methods, using cottonoids, curettes, microspatula and suction devices. The chopsticks technique (15) was generally used and no endoscope-holder was used. A Vasalva manoeuvre was generally performed at the end of the resection to confirm the absence of CSF leak or in case of insufficient prolapse of the suprasellar extension of the lesion. After resection, haemostasis was achieved using warm saline irrigation and compression with cottonoids. A solution of thrombin (SURGIFLO Thombin, Ethicon, Somerville, New jersey, USA) was generally used to secure the intrasellar hemostasis. In case of CSF leak, an abdominal fat graft was used with a fibrinogen sealant (Tisseel, Baxter, Deerfield, Illinois, USA) to fill the sella. No cases required the use of a naso-septal flap.

Post-operative complications

Post-operative complications were recorded and categorized as follows: surgical complications (CSF leak, meningitis, sino-nasal complications, neurological complications, visual impairment), endocrine complications (permanent anterior pituitary deficiency, permanent diabetes insipidus), and medical complications (venous thrombosis, infection …). Evaluation of sino-nasal morbidity was done by in-office endoscopy examination, performed by an ENT physician 10 to 15 days after the surgery.

Extent of resection

The extent of resection (EOR) was evaluated on the basis of the pre- and 6 months post-operative MRI with volumetric assessment. EOR was judged as gross total resection (GTR) when no residual tumor was present. When the residual tumor was calculated to be less than 10%, the resection was judged as subtotal resection (STR). Partial resection (PR) was defined as residual tumor that was greater than 10%. Partial and subtotal resection were grouped as "incomplete resection".

Learning curve assessment

To assess the impact of the learning curve, two strategies were used. First, patients were numbered in a chronologic fashion and correlations were established with the increasing number of cases. Second, the cohort was arbitrarily divided into a "first period" (first 30 patients, corresponding to the two first years of experience) and a "second period" (23 following patients, corresponding to the last year of experience).

Statistical analysis

Categorical variables were compared using Fisher's exact test or Chi-Square test, while continuous variables were compared using either a paired Student t-test or the Mann-Whitney test, depending on normal distribution of the data, or one-way ANOVA when more than two groups were compared. Statistical analysis performed in a sequential fashion delineated a learning curve for operative time, length of hospital stays, EOR or tumor residual volume using Pearson correlations (with r defined as the correlation coefficient). To study factors correlated with extent of resection, a multiple linear regression model was build including all factors potentially affecting the quality of resection (based on univariate correlation tests). For all statistical analyses, tests were two-sided and $p < 0.05$ was

considered statistically significant. Statistical tests were performed using RStudio 1.3.1093 software.

Results

Participants

Among the 86 patients operated for skull base lesions through ETS during the prospective inclusion period (2017–2020), 53 patients had NFPA and were included in the present study.

Demographic and radiological assessment

Main baseline demographics and radiological characteristics of the cohort are summarized in Table 1. As expected for NFPA, no patient had microadenoma. 45% of lesions were "invasive" as defined in the Hypopronos Score. Mean pre-operative volume was 7.37 ± 7 cm^3. 19% of cases were recurrence surgeries. There was no significant difference between the population or the radiological appearance (size, invasiveness) between the two periods of time (Supplementary Table S1).

TABLE 1 Demographics and tumor type.

Demographics	General cohort ($N = 53$)
Sex	
Female, *n* (%)	23 (43)
Male, *n* (%)	30 (57)
Mean age (SD)	59 (15.1)
Symptoms at diagnosis	
Mass effect, *n* (%)	34 (64)
Endocrine, *n* (%)	10 (19)
Apoplexy, *n* (%)	2 (4)
Incidental, *n* (%)	7 (13)
MRI characteristics	
Macroadenoma, *n* (%)	46 (87)
Giant adenoma, *n* (%)	7 (13)
Mean maximum diameter (mm) (SD)	27.5 (10.8)
Mean Preoperative Volume (cm^3) (SD)	7.37 (7.03)
Invasion, *n* (%)	24 (45)
Knosp Score, *n* (%)	
0	5 (9.4)
1	12 (23)
2	16 (30)
3a	8 (15)
3b	3 (5.7)
4	9 (17)
Procedure	
First surgery	43 (81)
Recurrence surgery	10 (19)

Operative course and post-operative complications

Results concerning the operative course and post-operative complications are summarized in Table 2. Mean operative time was 121 min. No patient died from a complication of the surgery, had an internal carotid artery injury, a post-operative neurologic deficit, or a visual deterioration. Overall, the occurrence of complications was 22%: 5 patients (9%) had a surgical complication and 7 patients (13%) an endocrine complication (defined as a permanent diabetus insipidus or a worsened hypopituitarism). 3 patients needed a revision surgery (one for a hematoma of the sella and two for a post-

TABLE 2 Intra-operative course and post-operative complications.

	General Cohort ($N = 53$)
Mean Total Operative time[a], min (SD)	121 (29)
Mean length of stay, days (SD)	7.6 (2.3)
Quality of resection	
Complete resection, *n* (%)	37 (70)
Incomplete resection, *n* (%)	16 (30)
STR, *n* (%)	8 (15)
PR, *n* (%)	8 (15)
Mean extent of resection (%), (SD)	96 (8)
Visual outcome	
Complete recovery, *n* (%)	9 (28)
Partial recovery, *n* (%)	9 (30)
Stabilization, *n* (%)	10 (31)
Worsening, *n* (%)	0 (0)
Surgical complication	
Meningitis, *n* (%)	1 (1.8)
Hematoma of the sella, *n* (%)	1 (3)
Permanent CSF leak, *n* (%)	2 (3.7)
Internal carotid injury, *n* (%)	0 (0)
Neurological deficit, *n* (%)	0 (0)
Nasal complication	
Epistaxis, *n* (%)	0 (0)
Anosmia, *n* (%)	1 (1.8)
Endocrine complication	
Permanent DI, *n* (%)	2 (3.7)
Worsened hypopituitarism, *n* (%)	5 (9.4)
Need for reintervention, *n* (%)	3 (5.6)
Death, *n* (%)	0 (0)

[a]Total operative time includes both nasal and sellar phase.

operative CSF leakage). Occurrence of complication depending on the period of time are summarized in **Supplementary Table 2**.

Extent of resection

The mean pre-operative volume was 6.65 ± 7 cm^3 (Range 1.2—39.5 cm^3) and the mean residual tumor volume was 0.62 ± 1.4 cm^3 (Range 0–7.22 cm^3). The mean extent of resection (EOR) was 96%. GTR rate was 70%, STR rate was 15% and PR rate was 15% (**Table 2**). A higher EOR was positively correlated with a lower pre-operative volume ($r = -0.37$, $p = 0.006$), increasing surgical experience ($r = 0.29$, $p = 0.029$), and was associated with a lower invasiveness (Mann-Whitney Test, $p = 0.003$) and a lower Knosp Score (One-way ANOVA, $p = 5.69e\text{-}07$). Results are illustrated **Figure 1**. In a multiple linear regression model, Knosp grade 4 ($p < 0.001$) and starting the surgical experience ($p = 0.019$) were independently correlated with a lower EOR (**Figure 2**).

Predictive factors of GTR

Results of the univariate analysis of factors associated with a GTR are summarized in **Table 3**. Incomplete resection was associated with higher tumor volumes, invasiveness and a higher Knosp Score. Among NFPA patients with Knosp Scores of 0, 1 or 2, the GTR rate was 90%, whereas GTR rate was 35% in those patients harbouring NFPA with a Knosp score of 3 or more. Recurrence surgery had no clear impact on the rate of GTR.

Effect of the learning curve

Increasing surgical experience was correlated with a higher EOR ($r = 0.29$, $p = 0.029$), and a diminution of the operating time and the LOS ($r = -0.31$, $p = 0.021$ and $r = -0.25$, $p = 0.02$, respectively). The rates of resection depending on Knosp grade and Period of time are illustrated **Figure 3**. The occurrence of complication was not correlated with the period of time (**Supplementary Table S2**). All patients who needed a revision surgery were operated during the second period of time (**Supplementary Table S2**).

Discussion

In this prospective cohort of patients operated on using an endoscopic endonasal approach for a NFPA during the three first years of experience, we report that (1) these procedures can be performed with relatively low complication rates and satisfactory results during the learning period; (2) the effect of the learning curve was clearly visible on the EOR but not on the complication rate; (3) Starting the surgical experience and a Knosp score equal to 4 were the main independent factors correlated to lower EOR.

As in other specialities, a clear relationship between the level of the surgeon's experience and outcomes has been demonstrated in pituitary surgery, often described as the "learning curve" (16). It is supposed that patients treated by more experienced surgeons experience fewer complications, have a lower mortality rate, and lower hospital charges. Based on the assumption that technical performance improves with experience, learning curve analyses in surgical specialties have aimed to define the number of cases required to perform a certain procedure until outcomes reach an average rate or

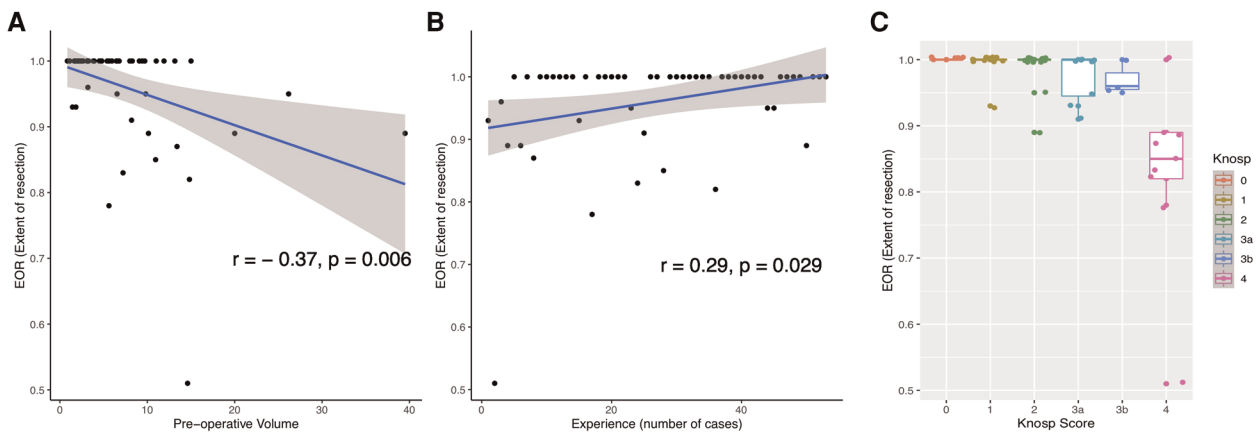

FIGURE 1
Representation of factors correlated with EOR (Extent of resection). (**A**) Scatterplot showing the correlation of EOR with pre-operative volume. (**B**) Scatterplot showing the correlation of surgical experience with EOR. (**C**) Boxplot showing the EOR depending on Knosp Scores.

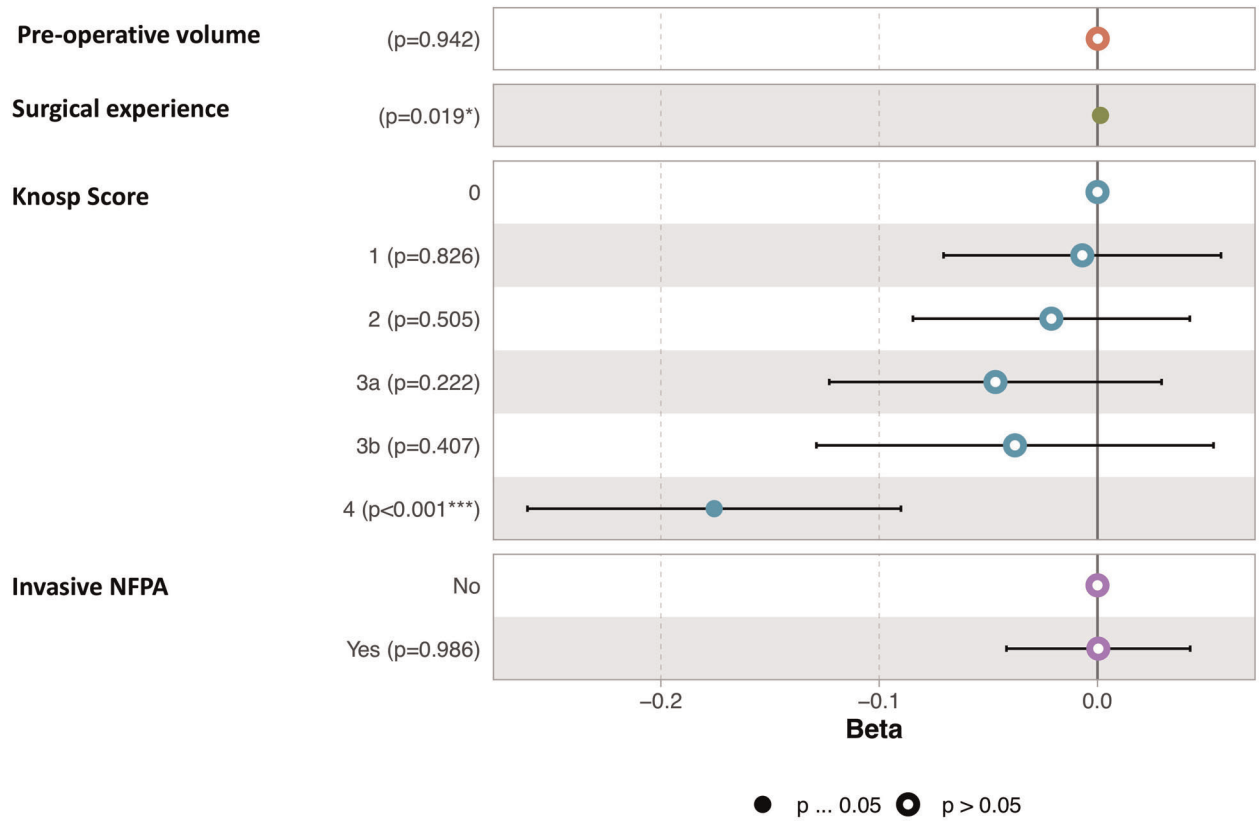

FIGURE 2
Graphic representation of the multiple linear regression model of factors correlated to EOR. The term "invasive" refers to the Hypopronos classification.

plateau. While cumulative sum analyses have been sometimes used to assess the improvement in surgical technical skills, they are not easy to construct in the case of complex procedures like tumoral resections, where an extremely complex array of variables is involved in intra-operative decision-making, and binary criteria of surgical "success" versus "failure" are not possible to identify (17, 18).

The endoscopic transsphenoidal approach is widely performed in pituitary surgery nowadays, with increasing evidence supporting its use for the gradual replacement of microsurgical techniques (6). The transition between these two techniques is the subject of several studies which aimed to define the learning curve (7, 8, 10, 19). Rates of GTR, the rate of hormonal remission (for hormone secreting adenomas) and operative times are generally markers of surgical efficiency, while complication rates are markers of surgical safety/skills. Among the latter, post-operative CSF leak is the most frequent complication and is generally defined as a pertinent marker reflecting the learning curve. Nevertheless, results from the literature are contradictory, with the required number of procedures estimated to reach a plateau ranging from 15 to more than 100, depending on the endpoint selected. In a recent study, Shikary *et al* reported a number of 120 procedures required for a team to reach a plateau of 125 min for mean operative length, and 100 procedures to stabilize CSF leak rates below 5% (10). However, the authors acknowledged that the pattern of the learning curve was difficult to analyse due to multiple factors affecting the quality of the surgery (e.g. size of the lesion, expansion of exposure, reconstruction technique, patients' morphological characteristics, aggressiveness of surgery…). Other studies have emphasised that the pattern of the learning curve is not so simple: a potential "rebound effect" with a "second learning curve effect" is defined as an increase in complication rates explained by the surgeon adopting a more aggressive resection approach after becoming more comfortable performing the procedure, or selecting more challenging cases (19). On the other hand, recent studies showed that contrary to popular belief, the surgical learning curve does not plateau but continues for several years after hundreds of cases (11, 20).

The introduction of endoscopy provided a new tool for these procedures which carries its own learning curve,

TABLE 3 Factors associated with GTR during initial experience.

	Incomplete resection ($n = 16$)	Complete resection ($n = 37$)	p-value
Demographics			
Mean Age	67 (14)	57 (13)	0.021[b]
Sex (female)	7 (44)	16 (43)	1[c]
MRI Characteristics			
Mean Preoperative Volume (cm^3) (SD)	12.1 (9.8)	5.3 (3.6)	0.004[b]
Invasion, *n* (%)	12 (74)	12 (32.4)	0.004[a]
Knosp Score, *n* (%)			
0	0 (0)	5 (14)	<0.001[c]
1	1 (6.2)	11 (30)	
2	2 (12)	14 (38)	
3a	3 (19)	5 (14)	
3b	2 (12)	1 (2.7)	
4	8 (50)	1 (2.7)	
Procedure			
First surgery, *n* (%)	13 (81)	30 (81)	1[c]
Recurrence surgery, *n* (%)	3 (19)	7 (19)	
Learning curve			
First period ($n = 30$), *n* (%)	12 (75)	18 (49)	0.07[a]
Second period ($n = 23$), *n* (%)	4 (25)	19 (51)	

[a]χ^2 test.
[b]Mann-Whitney test.
[c]Fisher's exact test.

explaining why the vast majority of studies have been dedicated to the learning curve for a transition between microscopic and endoscopic techniques for experienced operators (8–10, 19, 21–23). However, new generations of pituitary surgeons will undoubtedly commence their experience using fully endoscopic procedures, after a residency period and dedicated training period marked by the predominance of the endoscope. Whether it is possible to translate learning curve results from surgeons experienced in the microscopic technique who retrain in endoscopy, to surgeons solely trained in endoscopy is uncertain. A recent study comparing surgical results of two surgeons raised the provocative question of whether certain advantages of endoscopic surgery may help a less-experienced surgeon to achieve outcomes similar to those of more experienced surgeons for non-functioning adenomas (24). However, the junior neurosurgeon in this study already had experience of more than 100 cases, illustrating that no study in the literature has focused on surgical results during the actual beginning of the surgical experience.

In order to address this question, we studied the early surgical results of a newly board-certified neurosurgeon who undertook a dedicated training program during his residency. This training program consisted of obtaining a comprehensive knowledge of skull base anatomy, a dedicated learning of surgical gestures through weekly cadaveric dissections in the laboratory, participation in a specific course (360 degree skull base course (4 days), IRCAD, Strasbourg, France), a clinical fellowship in a high caseload volume reference center for endoscopic endonasal surgery, and active participation in pituitary surgeries involving a multidisciplinary team including ENT surgeons during his residency.

Our results suggest that the classical drawbacks of endoscopy at the beginning of the surgical experience (e.g. lack of adaptation to endoscopic visualisation, narrow operational space, bleeding or damage to the mucosa caused by movements of the endoscope or instruments) may have been overcome by this dedicated training and the benefits obtained from a multidisciplinary surgical team, leading to a shortening of the learning curve in terms of operative time and occurrence of complications Our mean operative time was 121 min and decreased with surgical experience. It was quite similar to operative times published by other groups (10, 21, 22, 25). Besides, there was no clear effect of the learning curve demonstrated in terms of occurrence of complications : our complication rate was quite similar to those described in the literature from more experienced operators (25–28). Although intraoperative CSF leak was frequent in our series (37%), a meticulous closing strategy enabled the post-operative CSF leak rate to be limited to less than 5%, corresponding to that seen in the more advanced period of experience reported in other series (10, 21, 23). Patients who needed revision surgery for surgical complications were actually operated during the second period of this study. This suggests that the increasing of confidence in order to achieve more extensive resection (**Figure 3**) led to more complication during this second period of time, classically described as "the rebound effect". In addition, no patient showed severe surgery-related complications such as carotid artery injury or neurological deficit, confirming that this procedure can be performed with an acceptable degree of safety during an initial experience course, with the only condition being an intense dedicated training program and a multidisciplinary working environment.

Results on the extent of resection showed 70% of GTR, and a mean EOR of 96%. Though EOR results could be improved in comparison to those published by very experienced teams (1, 6, 28), we demonstrated a clear impact of the learning curve that led to acceptable results during the second period of time (**Figure 3**): every patient having NFPA with Knosp score <3 had GTR after the 30 first patients operated and the mean volume of residual tumor was 0.6 cm^3 for the whole cohort. Main Predictive factors of higher EOR were the Knosp Score and the surgical experience. The invasiveness, as defined by the Hypopronos Score was also associated with decreased

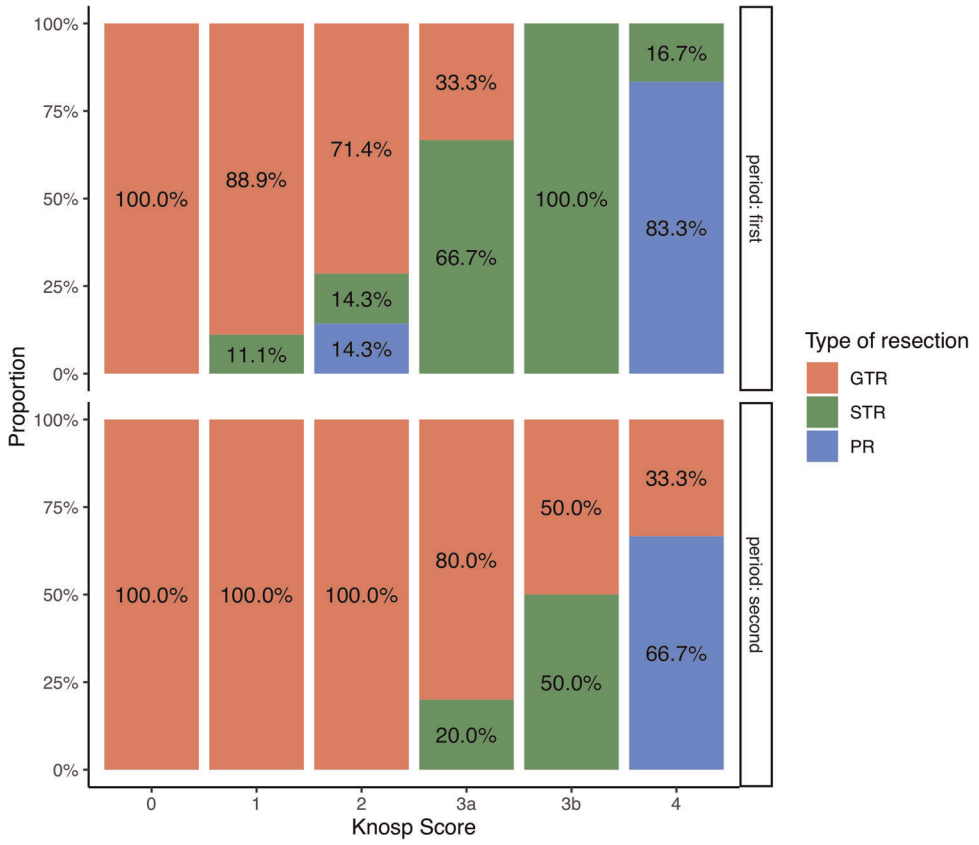

FIGURE 3
Bar-plot representation of the resection rates depending on the Knosp score during the first and the second period of time.

rates of GTR. These results are similar to those that have been published by expert teams. (6, 24, 29, 30).

Our results also confirm that NFPA are ideal cases for initial experience in pituitary surgery. While GTR is not always the goal of surgery in NFPA, surgical resection of hormone secreting adenomas is often a more complex procedure associated with higher complication rates, as well as having a strict necessity of gross total resection. As recommended by expert teams and master surgeons in this field, we chose to focus our initial experience on NFPA before attempting surgical resection of hormone secreting adenomas. Though our results could largely be improved, we demonstrated that in the era of fully endoscopic procedures, an intensive dedicated training program enables surgical resection of NFPA to be performed with an acceptable safety/efficiency profile from the very early experience period. We describe the complication rates and EOR during this early period using a strong methodology, and suggest that the use of the endoscope starting at the very beginning of the experience period may be associated with a shortening of the learning curve. These findings may have useful implications for surgical education, future studies on the learning curve in pituitary surgery and development of patient safety measures in the early surgical experience period.

Limitations

Firstly, the prospective cohort in our study is relatively small (53 patients), and a more extensive series would be necessary to better assess the impact of the learning curve. Secondly, our series concerned only NFPA and we believe that our conclusions cannot be translated to surgery for other types of pituitary lesions.

Conclusion

The acquisition of expertise in endoscopic endonasal surgery requires engaging in a dedicated training program. Provided that the prerequisite skills (perfect knowledge of nasal cavities and anatomy of the sellar region learned from dissection practice in the laboratory, endoscopic manipulation techniques, understanding of preoperative imaging) have been

appropriately mastered, resection of NFPA carries an acceptable complication rate and produces satisfactory outcomes even during the very early experience period of the surgeon. Meticulous patient selection and a multidisciplinary work environment are also key in achieving good results.

Data availability statement

The raw data supporting the conclusions of this article will be made available by the authors, without undue reservation.

Ethics statement

The studies involving human participants were reviewed and approved by The study received the approval of the Institutional Review Board (n°2019 IRB_MTP_12-02) of the University Hospital of Montpellier. The patients/participants provided their written informed consent to participate in this study.

Author contributions

Study design: JB, VF. Data collection: JB, IJ, VF, MLC. Data analysis: JB. Manuscript drafting: JB, IR, SNG, LC, NL, VF. Supervision of the study: JB. All authors contributed to the article and approved the submitted version.

Conflict of interest

The authors declare that the research was conducted in the absence of any commercial or financial relationships that could be construed as a potential conflict of interest.

Publisher's note

All claims expressed in this article are solely those of the authors and do not necessarily represent those of their affiliated organizations, or those of the publisher, the editors and the reviewers. Any product that may be evaluated in this article, or claim that may be made by its manufacturer, is not guaranteed or endorsed by the publisher.

Supplementary material

The Supplementary Material for this article can be found online at: https://www.frontiersin.org/articles/10.3389/fsurg.2022.959440/full#supplementary-material.

References

1. Goudakos JK, Markou KD, Georgalas C. Endoscopic versus microscopic trans-sphenoidal pituitary surgery: a systematic review and meta-analysis. *Clin Otolaryngol*. (2011) 36(3):212–20. doi: 10.1111/j.1749-4486.2011.02331.x

2. Jankowski R, Auque J, Simon C, Marchal JC, Hepner H, Wayoff M. Endoscopic pituitary tumor surgery. *Laryngoscope*. (1992) 102(2):198–202. doi: 10.1288/00005537-199202000-00016

3. Carrau RL, Jho HD, Ko Y. Transnasal-transsphenoidal endoscopic surgery of the pituitary gland. *Laryngoscope*. (1996) 106(7):914–8. doi: 10.1097/00005537-199607000-00025

4. Jho HD, Carrau RL. Endoscopic endonasal transsphenoidal surgery: experience with 50 patients. *J Neurosurg*. (1997) 87(1):44–51. doi: 10.3171/jns.1997.87.1.0044

5. Cappabianca P, Cavallo LM, de Divitiis E. Endoscopic endonasal transsphenoidal surgery. *Neurosurgery*. (2004) 55(4):933–40. discussion 940-941. doi: 10.1227/01.NEU.0000137330.02549.0D

6. Almutairi RD, Muskens IS, Cote DJ, Dijkman MD, Kavouridis VK, Crocker E, et al. Gross total resection of pituitary adenomas after endoscopic vs. microscopic transsphenoidal surgery: a meta-analysis. *Acta Neurochir (Wien)*. (2018) 160(5):1005–21. doi: 10.1007/s00701-017-3438-z

7. Sonnenburg RE, White D, Ewend MG, Senior B. The learning curve in minimally invasive pituitary surgery. *Am J Rhinol*. (2004) 18(4):259–63. doi: 10.1177/194589240401800412

8. Leach P, Abou-Zeid AH, Kearney T, Davis J, Trainer PJ, Gnanalingham KK. Endoscopic transsphenoidal pituitary surgery: evidence of an operative learning curve. *Neurosurgery*. (2010) 67(5):1205–12. doi: 10.1227/NEU.0b013e3181ef25c5

9. Robins JMW, Alavi SA, Tyagi AK, Nix PA, Wilson TM, Phillips NI. The learning curve for endoscopic trans-sphenoidal resection of pituitary macroadenomas. A single institution experience, Leeds, UK. *Acta Neurochir (Wien)*. (2018) 160(1):39–47. doi: 10.1007/s00701-017-3355-1

10. Shikary T, Andaluz N, Meinzen-Derr J, Edwards C, Theodosopoulos P, Zimmer LA. Operative learning curve after transition to endoscopic transsphenoidal pituitary surgery. *World Neurosurg*. (2017) 102:608–12. doi: 10.1016/j.wneu.2017.03.008

11. Younus I, Gerges MM, Uribe-Cardenas R, Morgenstern PF, Eljalby M, Tabaee A, et al. How long is the tail end of the learning curve? Results from 1000 consecutive endoscopic endonasal skull base cases following the initial 200 cases. *J Neurosurg*. (2020) 7:1–11. doi: 10.3171/2019.12.JNS192600

12. Micko ASG, Wöhrer A, Wolfsberger S, Knosp E. Invasion of the cavernous sinus space in pituitary adenomas: endoscopic verification and its correlation with an MRI-based classification. *J Neurosurg*. (2015) 122(4):803–11. doi: 10.3171/2014.12.JNS141083

13. Trouillas J, Roy P, Sturm N, Dantony E, Cortet-Rudelli C, Viennet G, et al. A new prognostic clinicopathological classification of pituitary adenomas: a multicentric case-control study of 410 patients with 8 years post-operative follow-up. *Acta Neuropathol*. (2013) 126(1):123–35. doi: 10.1007/s00401-013-1084-y

14. Favier V, Boetto J, Cartier C, Segnarbieux F, Crampette L. Endoscopic transnasal transseptal pituitary surgery. *Eur Ann Otorhinolaryngol Head Neck Dis*. (2019) 136(2):131–4. doi: 10.1016/j.anorl.2018.10.005

15. Labidi M, Watanabe K, Hanakita S, Park HH, Bouazza S, Bernat AL, et al. The chopsticks technique for endoscopic endonasal surgery-improving surgical efficiency and reducing the surgical footprint. *World Neurosurg*. (2018) 117:208–20. doi: 10.1016/j.wneu.2018.05.229

16. Hopper AN, Jamison MH, Lewis WG. Learning curves in surgical practice. *Postgrad Med J*. (2007) 83(986):777–9. doi: 10.1136/pgmj.2007.057190

17. McCarter FD, Luchette FA, Molloy M, Hurst JM, Davis K, Johannigman JA, et al. Institutional and individual learning curves for focused abdominal ultrasound for trauma. *Ann Surg*. (2000) 231(5):689–700. doi: 10.1097/00000658-200005000-00009

18. Cho SY, Choo MS, Jung JH, Jeong CW, Oh S, Lee SB, et al. Cumulative sum analysis for experiences of a single-session retrograde intrarenal stone surgery and analysis of predictors for stone-free status. *PLoS One*. (2014) 9(1):e84878. doi: 10.1371/journal.pone.0084878

19. Chi F, Wang Y, Lin Y, Ge J, Qiu Y, Guo L. A learning curve of endoscopic transsphenoidal surgery for pituitary adenoma. *J Craniofac Surg*. (2013) 24 (6):2064–7. doi: 10.1097/SCS.0b013e3182a24328

20. Younus I, Gerges MM, Uribe-Cardenas R, Morgenstern P, Kacker A, Tabaee A, et al. The slope of the learning curve in 600 consecutive endoscopic transsphenoidal pituitary surgeries. *Acta Neurochir (Wien)*. (2020) 162 (10):2361–70. doi: 10.1007/s00701-020-04471-x

21. Bokhari AR, Davies MA, Diamond T. Endoscopic transsphenoidal pituitary surgery: a single surgeon experience and the learning curve. *Br J Neurosurg*. (2013) 27(1):44–9. doi: 10.3109/02688697.2012.709554

22. Lofrese G, Vigo V, Rigante M, Grieco DL, Maresca M, Anile C, et al. Learning curve of endoscopic pituitary surgery: experience of a neurosurgery/ ENT collaboration. *J Clin Neurosci*. (2018) 47:299–303. doi: 10.1016/j.jocn.2017.09.011

23. Kim JH, Lee JH, Lee JH, Hong AR, Kim YJ, Kim YH. Endoscopic transsphenoidal surgery outcomes in 331 nonfunctioning pituitary adenoma cases after a single surgeon learning curve. *World Neurosurg*. (2018) 109: e409–16. doi: 10.1016/j.wneu.2017.09.194

24. Zaidi HA, Awad AW, Bohl MA, Chapple K, Knecht L, Jahnke H, et al. Comparison of outcomes between a less experienced surgeon using a fully endoscopic technique and a very experienced surgeon using a microscopic transsphenoidal technique for pituitary adenoma. *J Neurosurg*. (2016) 124 (3):596–604. doi: 10.3171/2015.4.JNS15102

25. Magro E, Graillon T, Lassave J, Castinetti F, Boissonneau S, Tabouret E, et al. Complications related to the endoscopic endonasal transsphenoidal approach for nonfunctioning pituitary macroadenomas in 300 consecutive patients. *World Neurosurg*. (2016) 89:442–53. doi: 10.1016/j.wneu.2016.02.059

26. Berker M, Hazer DB, Yücel T, Gürlek A, Cila A, Aldur M, et al. Complications of endoscopic surgery of the pituitary adenomas: analysis of 570 patients and review of the literature. *Pituitary*. (2012) 15(3):288–300. doi: 10.1007/s11102-011-0368-2

27. Gaillard S. The transition from microscopic to endoscopic transsphenoidal surgery in high-caseload neurosurgical centers: the experience of Foch Hospital. *World Neurosurg*. (2014) 82(6 Suppl):S116–20. doi: 10.1016/j.wneu.2014.07.033

28. Wang F, Zhou T, Wei S, Meng X, Zhang J, Hou Y, et al. Endoscopic endonasal transsphenoidal surgery of 1,166 pituitary adenomas. *Surg Endosc*. (2015) 29(6):1270–80. doi: 10.1007/s00464-014-3815-0

29. Paluzzi A, Fernandez-Miranda JC, Tonya Stefko S, Challinor S, Snyderman CH, Gardner PA. Endoscopic endonasal approach for pituitary adenomas: a series of 555 patients. *Pituitary*. (2014) 17(4):307–19. doi: 10.1007/s11102-013-0502-4

30. Ferreli F, Turri-Zanoni M, Canevari FR, Battaglia P, Bignami M, Castelnuovo P, et al. Endoscopic endonasal management of non-functioning pituitary adenomas with cavernous sinus invasion: a 10- year experience. *Rhinology*. (2015) 53(4):308–16. doi: 10.4193/Rhino14.309

frontiers | Frontiers in Surgery

TYPE Original Research
PUBLISHED 11 August 2022
DOI 10.3389/fsurg.2022.956345

OPEN ACCESS

EDITED BY
Peng Zhao,
Capital Medical University, China

REVIEWED BY
Jiwei Bai,
Capital Medical University, China
Mohamed Reda Mohamed Rady,
Cairo University, Egypt
Zhijun Yang,
Capital Medical University, China
Yazhuo Zhang,
Capital Medical University, China

*CORRESPONDENCE
Zhiquan Jiang
bbjiangzhq@163.com

SPECIALTY SECTION
This article was submitted to Neurosurgery, a section of the journal Frontiers in Surgery

RECEIVED 30 May 2022
ACCEPTED 01 August 2022
PUBLISHED 11 August 2022

CITATION
Wu J, Zhang B, Shao D, Ji S, Li Y, Xie S and Jiang Z (2022) Analysis of neuroendoscopy for the treatment of macroadenomas and giant pituitary adenomas.
Front. Surg. 9:956345.
doi: 10.3389/fsurg.2022.956345

Analysis of neuroendoscopy for the treatment of macroadenomas and giant pituitary adenomas

Junyong Wu[1,2], Binbin Zhang[1,2], Dongqi Shao[1,2], Shuxin Ji[1,2], Yu Li[1,2], Shan Xie[1,2] and Zhiquan Jiang[1,2]*

[1]Department of Neurosurgery, The First Affiliated Hospital of Bengbu Medical College, Bengbu, China, [2]Shandong University of Traditional Chinese Medicine, Jinan, China

Objective: This study investigated the use and effectiveness of endoscopic transnasal, transsphenoidal surgery, a minimally invasive method for the treatment of macroadenomas and giant pituitary a denomas, in a medical setting. The surgical results of 429 patients who received neuroendoscopic treatment of macroadenomas or giant pituitary adenomas were evaluated, and the experiences and lessons learned from treatment complications were assessed.

Patients and methods: From January 2012 to December 2021, 429 patients with macroadenomas or giant pituitary adenomas, including 60 patients with giant adenomas (diameter ≥4 cm) and 369 patients with macroadenomas (diameter 1–4 cm), received a 3D head CT, a MRI with contrast enhancement, and an endocrinology examination prior to surgery. Preoperative clinical and radiological features, visual measurements, hormone levels, length of stay, length of surgery, postoperative stay, visual and hormone outcomes, resection range, complication and recurrence rates, and routine patient information were recorded. The patients were followed up for 6–72 months (median = 40 months).

Results: Of 429 patients with macroadenomas or giant pituitary adenomas who received neuroendoscopic treatment, 348 (81.12%) had gross-total resections (GTR), 53 (12.35%) had near-total resections (NTR), and 28 (6.53%) had subtotal resections. There were 138 cases of post-operative diabetes insipidus (32.17%), including 7 cases of permanent diabetes insipidus (1.63%), 16 cases of nasal hemorrhage (3.73%), 39 cases of intraoperative cerebrospinal fluid leakage (9.09%), 4 cases of intracranial infection (0.9%), 16 cases of hypophysis (3.7%), and 15 cases of anosmia (3.50%). The clinical symptoms and endocrinology indices of the patients improved after surgery, and all patients were discharged 5–18 days (8.36 ± 2.65) postop.

Conclusion: Neuroendoscopy is a safe operation with a short recovery period and hospital stay and is thus an effective method to treat macroadenomas and giant pituitary adenomas. Preoperative evaluation and prediction can help to accurately address possible intraoperative situations and improve GTR.

KEYWORDS

neuroendoscopy, transnasal butterfly approach, giant pituitary adenoma, pituitary surgery, macroadenoma

Introduction

Pituitary adenomas are benign tumors of the anterior pituitary that lack classical oncogenic mutations. Disrupted cell cycle control and growth factor signaling may play a role in their pathogenesis and natural history (1). These adenomas represent approximately 15% of all intracranial adenomas, having the third highest incidence rate (2). A recent study also indicates that the prevalence rate of pituitary adenomas has increased from 7.5–15 to 77.6 per 100,000 persons (2). Pituitary adenomas can cause serious health issues among patients.

Medical, surgical, and/or radiosurgical treatments are used for pituitary adenomas, depending on the clinical status and size of the adenoma at the time of presentation (3). In pituitary adenoma patients experiencing clinical symptoms, surgical resection remains the most used clinical treatment. However, because of the irregular shape of some adenomas and important neurovascular involvement, the total resection rate of pituitary adenomas is low and recurrence is common (4). Surgery can be particularly challenging if the pituitary adenoma is a macroadenoma or giant pituitary adenoma. The traditional treatment for these adenomas is craniotomy and, if the adenoma has broken through the diaphragmatic sellae and the microscopic field of view is limited, brain tissue retraction is required (5). Postoperatively, patients are at risk for severe reactions, complications, and long hospital stays.

Neuroendoscopy, a technology that has developed rapidly over the past two decades, has been increasingly used for the treatment of pituitary adenomas (6, 7). While the efficacy of endoscopic intranasal sphenoidal surgery for macroadenomas and giant pituitary adenomas has been widely reported, the surgical cases and time spans explored by these studies have some important limitations (8–10).

The current study analyzes retrospective data from 429 pituitary adenoma patients who were treated at the Department of Neurosurgery of the First Affiliated Hospital of Bengbu Medical College, China from January 2012 to December 2021. A total of 429 patients met the criteria for butterfly macroadenoma and giant pituitary adenoma surgery, using a neuroendoscopic transnasal approach. The relationships between the surgical resection rate, Knosp classification, adenoma size, operation time, and adenoma-related complications were assessed. The advantages of transsphenoidal endoscopic resection of macroadenomas and giant pituitary adenomas were analyzed and discussed.

Materials and methods

Clinical materials

This study was approved by the Ethics Committee of the First Affiliated Hospital of Bengbu Medical College. The patients were treated in the Neurosurgery Department of the First Affiliated Hospital of Bengbu Medical College, China, from January 2012 to December 2021. 3D CT, MRI with contrast enhancement, and endocrine examinations were performed before surgery, and preoperative clinical and radiological characteristics, visual and hormonal outcomes, resection range, operation duration, postoperative discharge time, complications, recurrence rate and patient routine information were recorded and analyzed. Histopathological and immunohistochemical analyses were used to confirm the diagnosis of pituitary adenomas and assess multiple pituitary hormone levels. During data compilation, 429 patients met the radiological definitions of macroadenomas ($1 \leq D < 4$ cm) and giant adenomas (≥ 4 cm) in addition to the criteria required for the neuroendoscopic transnasal surgical approach for butterfly macroadenoma and giant pituitary adenoma surgeries (11). Medical and nursing conditions remained consistent for all patients. Those patients with an adenoma diameter <1 cm or with incomplete follow-up records were excluded from the final analysis. All included cases were followed up for at least 6 months. Patient and adenoma characteristics are summarized in **Table 1**.

Surgical methods

A neurosurgeon with >15 years of experience performed neuroendoscopy on all patients. The surgical objectives were to (1) achieve maximal resection and remission of symptoms with the least disturbance to neural and vascular structures and (2) maintain or reinstate endocrine function.

A transsphenoidal neuroendoscopic procedure was used to remove pituitary adenomas from a single (usually the right) nostril. During the procedure patients were supine with the head tilted posteriorly at 15°. Following induction of general anesthesia, the nasal mucosa and skin of the surgical site were disinfected, and a middle turbinate and septum approach was taken with the endoscope angled at 30°. After covering the nasal mucosa with an epinephrine-soaked cotton pad, the nasal turbinates were lateralized to expand the surgical space. The right pedicled nasoseptal flap was partially resected, stored inferior to the surgical channel, and fully harvested if an intraoperative cerebrospinal (CSF) leak occurred. A high-speed drill or osteotome was used to open the sphenoid sinus, and the sellar floor was removed so that the full floor could be observed in the sphenoid sinus (**Figure 1A**). The diameter of the sellar bottom bone window was ground to 1–2 cm (**Figure 1B**), the intrasellar aneurysm was treated by puncture, and the adenoma was removed using a pituitary curette and attractor. The field was intermittently flushed with saline, and any residual adenoma was observed in real-time during endoscopic resection. Residual lesions in the cavernous sinus were removed under direct observation. Intrasellar and

TABLE 1 Patient demographics and adenoma characteristics ($N = 429$).

Demographics	N	%
Male	195	45.45%
Female	234	54.55%
Mean age (years)	50.72 (8–78)	
LOS (length of stay)	16.9 (8–32)	
Postoperative hospital stay	8.4 (4–24)	
Diameter (average ± SD) (mm)	(26.57 ± 10.28)	
10–19	128	29.84%
20–29	131	30.54%
30–39	110	25.64%
>40	60	13.98%
Knosp classification		
Grade 0	129	30.1%
Grade 1	116	27.1%
Grade 2	96	22.4%
Grade 3A	51	11.8%
Grade 3B	27	6.3%
Grade 4	10	2.3%
Preoperative clinical signs and symptoms		
Visual field defects	278	64.80%
Anterior pituitary insufficiency	85	19.81%
Headache	159	37.06%
Drowsiness	5	1.17%
Treatment		
Endoscopic transnasal transsphenoidal surgery	429	100%
Surgical complications		
CSF leak	39	9.09%
Intracranial infection	4	0.93%
Loss of smell	15	3.50%
Diabetes insipidus	138	32.17%
Hypopituitarism	16	3.70%
Epistaxis	16	3.70%
Proliferation		
Nonproliferative	359	83.68%
Proliferative	70	16.32%

suprasellar adenomas were completely resected, and the endoscope was extended into the adenoma cavity to explore and remove any residual adenoma (Figure 1C). After hemostasis, the skull base was reconstructed using autologous tissue and artificial materials.

Data analysis

Continuous variables are presented as the mean, range, and median, and categorical data are presented as total counts and proportions. Demographic, clinical, radiological, and intraoperative adenoma characteristics of the resection range were analyzed using the Chi-square test. All statistical analyses were performed using SPSS version 22.0 (IBM Corporation), and a p-value of <0.05 was considered statistically significant.

Results

Patient characteristics

The male-to-female ratio of the 429 patients included in this study was 0.83:1. The median age was 53 years (range 8–78 years), and most cases were nonfunctional pituitary adenomas (NFPA) ($n = 277$). The majority of functional pituitary adenoma (FPA; $n = 152$) cases were those induced by the overproduction of growth hormone ($n = 34$; 7.92%) and prolactin ($n = 110$; 25.64%), followed by those induced by corticotropin ($n = 6$; 1.40%) or thyrotropin ($n = 2$; 0.47%). The Ki-67 labeling index was ≥5% in 31 patients (7.13%), <3% in 325 patients (75.76%), and 3%–5% in 74 patients (17.11%). P53 staining was positive in 51 patients (11.89%), negative in 359 patients (83.68%), and weak in 19 patients (4.43%) (Table 2). The most common symptoms before surgery included impaired visual acuity and visual field defects ($n = 278$; 64.8%), headache ($n = 159$; 37.06%), and endocrine-related indications ($n = 85$; 19.81%).

Imaging classification

The revised Knosp classification for "invasion of cavernous sinus space in pituitary adenoma", devised by Micko et al. (12), was used for all cases. Most patients ($n = 129$; 30.1%) received a Knosp Grade of 0. Adenomas in 116 patients (27.1%) were classified as Grade 1, 92 (21.4%) classified as Grade 2, 35 (8.16%) classified as Grade 3A, 17 (3.9%) classified as Grade 3B, and 10 (2.3%) classified as Grade 4. All cases were either macroadenomas (diameter >1 cm) or giant pituitary adenomas (>4 cm), with a mean diameter of 2.66 ± 0.51 cm.

Results of excision range

A total resection was performed for 348 cases (81.12%), had available preoperative and postoperative MRI studies (Figure 2) a near total resection was performed for 53 cases (12.35%), and a major resection was performed for 28 cases (6.53%). All of them had available preoperative and postoperative MRI studies (Figure 2). There were 138 cases of postoperative diabetes insipidus (DI) (8.86%), including 7 cases of permanent DI (1.63%), 16 cases of nasal hemorrhage (3.73%), 39 cases of intraoperative CSF leakage (9.09%), 4 cases of intracranial infection (0.9%), 16 cases of hypophysis (3.7%), and 15 cases of anosmia (3.50%). Patient clinical symptoms

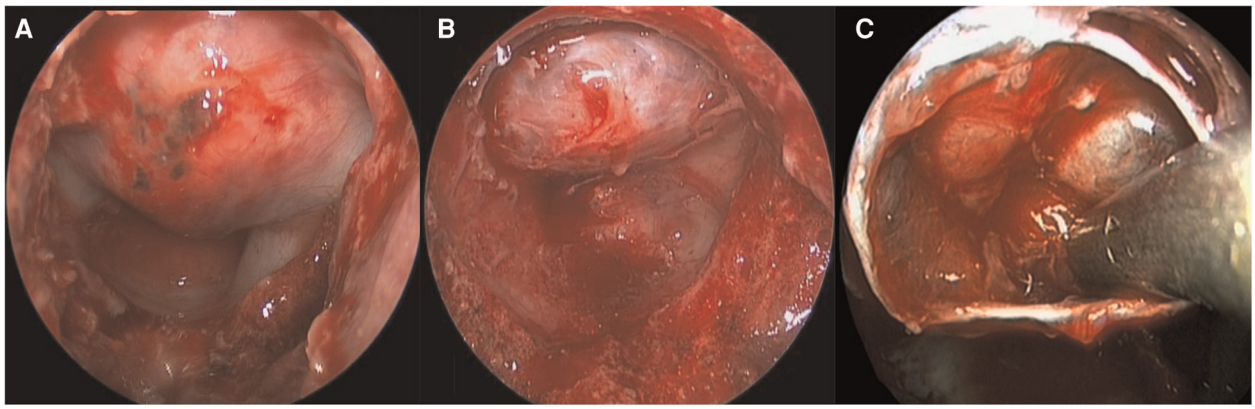

FIGURE 1
(A–C) Neuroendoscopy for the treatment of macroadenomas and giant pituitary adenomas. the full floor could be observed in the sphenoid sinus (A), The diameter of the sellar bottom bone window was ground to 1–2 cm (B), the endoscope was extended into the adenoma cavity to explore and remove the residual adenoma (C).

TABLE 2 Pathological characteristics.

Cell types	*N* (%)
Non-functioning	277 (64.57)
Prl	110 (25.64)
GH	34 (7.92)
ACTH	6 (1.40)
TSH	2 (0.47)
Ki-67	
<3%	325 (75.76)
3%–5%	74 (17.11)
>5%	31 (7.13)
P53	
Negative	359 (83.68)
Positive	51 (11.89)
Weak	19 (4.43)

and endocrinological indicators improved during the follow-up period (Table 3).

Factors for the extent of resection

The factors influencing adenoma resection are summarized in Table 4. The nature and shape of the adenoma significantly affected the resection range ($p < 0.01$). For example, GTR was easier to obtain for giant pituitary adenomas with a Knosp Grade of 0–1.

Discussion

A pituitary adenoma is a prevalent brain tumor that often invades the peripheral nerves, blood vessels, and cavernous sinus or suprasellar or paracellar regions. GTR of pituitary adenomas is technically challenging, even for highly experienced neurosurgeons (13). Macroadenomas are defined as adenomas that are >1 cm in diameter, and giant pituitary adenomas are defined as those with a diameter >4 cm (3). Giant pituitary adenomas are estimated to account for 5%–10% of all pituitary adenomas (14). Surgical resection, which is used to restore normal pituitary function, decompresses nerves and blood vessels with minimal damage to surrounding tissues and is considered the first-line treatment for pituitary adenoma. Since 1990, transsphenoidal neuroendoscopic surgery has been widely used because of its ability to enlarge and improve visual clarity of the surgical field.

Both transcranial and transsphenoidal approaches can be used to remove macroadenomas and giant pituitary adenomas, but the transsphenoidal approach is the preferred choice for resection (15). In recent years, the use of endoscopic surgery for pituitary adenomas has significantly increased in the United States (16), and the use of microsurgery has decreased. Møller et al. (17) found that patients undergoing endoscopic surgery for pituitary adenomas had better surgical outcomes and fewer complications than those undergoing a microsurgical approach. This is partially due to the better light sources and high-definition cameras used in endoscopic technology, which have improved visualization and provided a panoramic view of the sellar, paracellar and suprasellar areas. Many studies have demonstrated the possible superiority of endoscopy over traditional microscopy for both functional and nonfunctional pituitary adenomas.

For giant pituitary adenomas, especially those that are nonfunctional, total resection remains difficult. This may be because nonfunctional pituitary adenomas are difficult to detect until they become large enough to compress

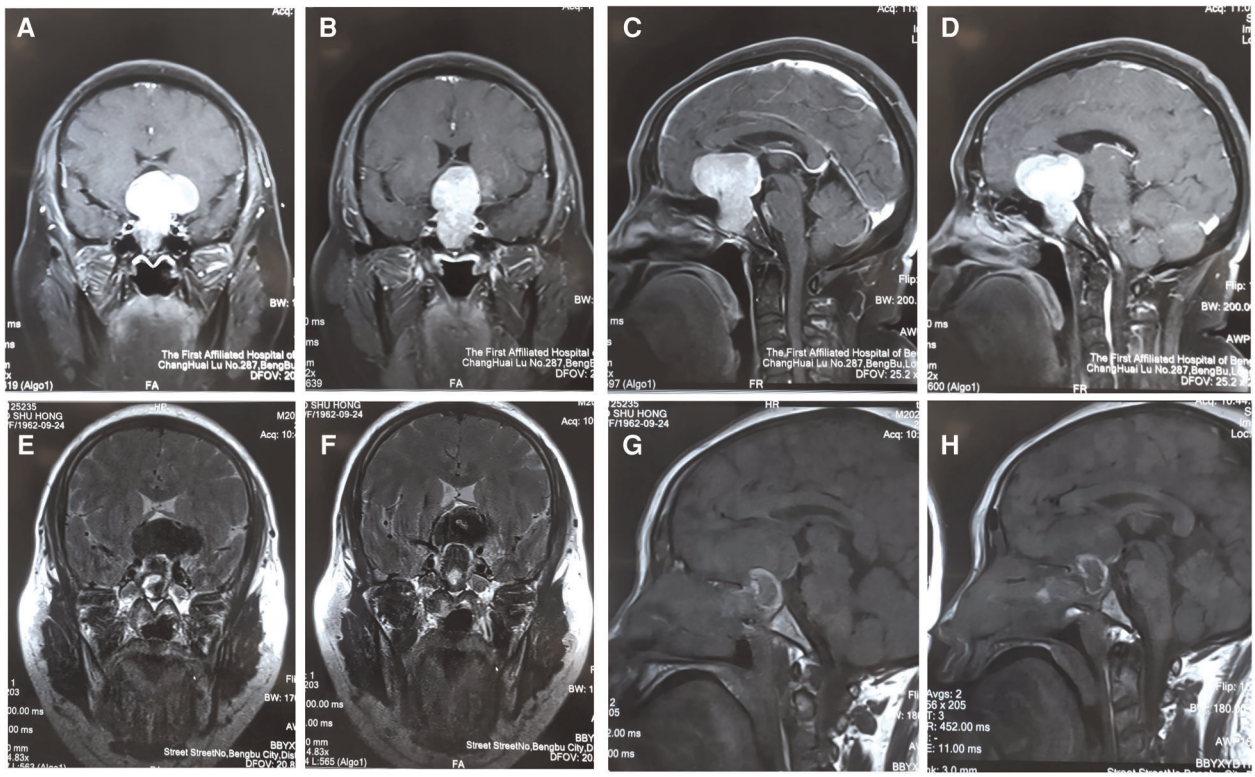

FIGURE 2
(A–H): This was a 50-year-old female patient who was admitted to hospital after the discovery of a pituitary tumor due to clinical manifestation. Preoperative MRI of a special giant pituitary adenoma (A–D). Postoperative MRI (E–H).

TABLE 3 Preoperative symptoms that improved after surgery.

Symptoms	Improved/Total (%)
Preoperative symptoms	
Visual field defects	277/278 (99.6)
Anterior pituitary insufficiency	44/85 (51.8)
Headache	131/159 (82.4)
Drowsiness	5/5 (100)
Syndrome	
CSF leak	39/39 (100)
Intracranial infection	4/4 (100)
Loss of smell	10/15 (66.7)
Diabetes insipidus	131/138 (94.9)
Hypopituitarism	9/16 (56.3)
Epistaxis	16/16 (100)

surrounding tissues (18). However, there has been success with endoscopic transsphenoidal and endoscopic combined resection of giant pituitary adenomas protruding into the third ventricle, as well as with endoscopy combined with a transsphenoidal suprasellar keyhole approach for the treatment of complex paraselellar pituitary adenomas (19, 20). Thus, some researchers believe that endoscopic transsphenoidal resection of giant pituitary adenomas is superior to microsurgery. During the resection of a giant adenoma, the order of surgical procedures is critical to prevent the premature decline of the sella turcica diaphragm, which can affect the adenoma resection, puncture the sella turcica diaphragm and cause CSF leakage. In general, it is advised to begin by removing the lower adenoma and cut both sides before removing the upper adenoma. The adenoma should be removed gently with a pituitary curette to prevent the rupture of the sellar diaphragm and potential CSF leakage. In addition, the adenoma should be removed *in situ* using an adenoma suction apparatus or a curette. The use of forceps should be avoided, as this can lead to intracranial hemorrhage or vision changes. Patients with partial resection of the pituitary adenoma are at risk of postoperative adenoma residual bleeding; thus, intraoperative hemostasis should be accurate, and patients should be watched closely after surgery. If a patient shows symptoms of vision loss or increased intracranial pressure, the head CT should be reviewed in a timely manner to ensure an accurate diagnosis, and an emergency craniotomy should be performed if necessary.

As a result of its optical lighting characteristics, the endoscopy angle, and the fisheye effect, neuroendoscopy conveniently reveals lesions at a closer range and higher

TABLE 4 Factors influencing adenoma resection.

Tumor type	GTR (%)	NGTR* (%)	*p*-value
Knosp classification			
Grade 0	114 (88.37)	15 (11.63)	<0.01
Grade 1	103 (88.79)	13 (11.21)	
Grade 2	75 (79.79)	19 (20.21)	
Grade 3A	35 (68.64)	18 (31.37)	
Grade 3B	17 (62.96)	10 (37.04)	
Grade 4	4 (40)	6 (60)	
Diameter (mm)			
10–19	114 (89.06)	14 (10.94)	<0.01
20–29	117 (89.31)	14 (10.69)	
30–39	80 (76.19)	25 (23.81)	
>40	37 (56.92)	28 (43.08)	
Hormone secretion			
NFPA	221 (82.85)	46 (17.25)	0.261
FPA	127 (78.43)	35 (21.67)	
Operative history			
Primary	339 (87.59)	48 (12.41)	<0.01
Recurrent	9 (21.92)	33 (78.18)	
Tumor shape			
Rounded	289 (92.04)	25 (7.96)	<0.01
Dumbbell	35 (53.03)	31 (46.97)	
Multilobular	24 (48.98)	25 (51.02)	

*Not total resection, including near total resection and a major resection.

exposure than the traditional transsphenoidal approach. While poor sphenoidal sinus gasification and giant pituitary adenomas, including the dumbbell type, fiber type, protrusion into the third ventricle, and invasion into the cavernous sinus, were previously considered contraindications of transsphenoidal surgery, this is no longer the case. A safe endoscopic resection can be accomplished for cases of sphenoid sinus gasification and poor pituitary adenoma because the retractor does not have to be used for full exposure and the eye shot is open, allowing enough space in the nose to use a high-speed grinding drill. Bone grinding can be conducted in all directions, and the depth and direction can be adjusted to identify the sphenoid sinus by various anatomical landmarks to ensure that the surgery proceeds in the correct direction. For macroadenomas and multilobular, fibrous, and dumbbell giant pituitary adenomas that are difficult to resect, invasion of the instrument into the subarachnoid space may cause CSF leakage and damage to the optic nervous system and adjacent blood vessels that complicate the operation. Existing surgical options include combined or staged transsphenoidal-transcranial approaches and staged transsphenoidal resections after the residual adenoma descends into the sella (21). Lumbar infusions or air injection to encourage descent of the suprasellar adenoma component have also been used (22). For the special pituitary adenoma described earlier, bone and dura resection at the sella plane were used in addition to opening the sella to provide a double surgical corridor. First, an endosellar, extraarachnoidal corridor was created to debulk the sellar component of the adenoma. Second, a suprasellar transarachnoidal corridor was created to debulk the suprasellar component of the lesion and sharp dissect the adenoma capsule from the overlying parasellar cisterns and optic apparatus under direct visualization. This was performed to avoid adenoma residue and brain tissue damage.

Thus, for macroadenomas and giant pituitary adenomas with a special shape, endoscopic surgery has obvious advantages over microsurgery or craniotomy. This technique may provide a greater resection area and prevent blind curettage of the suprasellar components, significantly reducing the risk of neurovascular injury. Prolonging the intranasal approach can also help to expose large lesions behind the dural opening, helping surgeons to avoid retraction of neurovascular structures. This ensures that all dissection is performed on the surface of the adenoma, without risking brain damage or traction of the olfactory tract.

Recent reports of surgical complications are consistent with those described in the current study (23–29). CSF leakage, for example, is a common complication of transsphenoidal neuroendoscopic resection (30), and there were 39 such cases in this series (9.1%). This complication is usually the result of surgical injury and adenoma invasion, especially for giant pituitary adenomas with anterior cranial fossa dilation (31). In the current study, most CSF leakage occurred during adenoma resection. This can be prevented by removing macroadenomas and giant adenomas along the edge of the sellar septum to prevent them from collapsing prematurely and damaging the arachnoid of the suprasellar cistern. If the diaphragmatic sella is ruptured intraoperatively, three layers of sellar bottom repair is often required. First, the adenoma cavity is filled with fat taken from the patient's outer thighs or lower abdomen. Then, artificial dura matter is used to cover the bottom of the sella turcica. This artificial dura matter is covered with autologous muscle and surrounded with medical adhesive to bind it. Finally, the artificial dura and muscle layer is covered, and the periphery is glued with medical adhesive to prevent additional leakage after the repair. If the sella turcica diaphragm is not damaged during the operation, it is not usually necessary to repair the bottom with fat and muscle. Rather, a gelatin sponge, quick gauze, and artificial dura mater can be used. Prior studies have reported a significant correlation between CSF leakage and postoperative intracranial infection, a common cause of death for patients with neuroendoscopic pituitary adenomas (32). Perioperative use of antibiotics and avoiding an excessively long operation time are important measures to reduce intracranial infection.

Indeed, the probability of intracranial infection doubles when the operation time exceeds 3–4 h (33).

DI was the most common surgical complication of endoscopic resection of macroadenomas and giant pituitary adenomas in this study; however, only 7 cases eventually developed permanent DI (5.07%). The type and location of pituitary adenomas are related to the occurrence of DI after surgery (34). For postoperative DI, treatment is focused on reducing urine output, replacing fluid loss, maintaining normal plasma osmotic pressure, and reducing or stopping the use of osmotic diuretics. For patients with mild DI with a urine volume of 3,000–5,000 ml in 24 h, oral camassia equine should be given to observe the curative effect. For those with moderate DI with a urine volume of 5,000–6,000 ml within 24 h, intramuscular injection of 6U pituitrin should be initiated and repeated after 12 h, with the amount being adjusted based on changes in urine volume. For those with severe DI with a 24 h urine volume >6,000 ml, 6U pituitrin should be tried first, and repeated at an interval of 8–12 h if the effect is not obvious. The times of pituitrin administration can be increased or the vasopressin tannate can be changed. The initial dose is 0.2 ml, and blood electrolytes can be monitored to prevent electrolyte disorder.

MRI is the most important method for follow-up after surgical treatment of pituitary adenomas. The primary use of postoperative MRI is to evaluate the effectiveness of surgery. However, even after the removal of the pituitary adenoma, the mass may not initially appear smaller on an MRI as a result of fillings, postoperative debris, mucosal thickening, and blood accumulation. These postoperative features begin to disappear and the adenoma volume gradually decreases over several months (35). Thus, it is generally recommended that patients have a second MRI within 6 months after surgery, and approximately every 6 months thereafter. Follow-up after surgical treatment of pituitary macroadenoma should also include postoperative ophthalmologic evaluation after 1–2 weeks, and follow-up evaluation at 1 and 2 years to evaluate the final effect of surgical treatment on visual functioning (36). An ophthalmologist at our hospital usually provides visual acuity and visual field examinations before and after surgery and at 3, 6, 12, and 24 months of follow-up. If the patient's visual acuity improves and stays the same during follow-up, the prognosis is good. For patients with extrasellar residues, actively administering radiotherapy to reduce the incidence of recurrence or closely observing patients and only administering radiotherapy to those who do develop recurrence remains controversial (37). The potential side effects of radiation therapy and the development of hypopituitarism need to be balanced against the risk of adenoma growth and vision loss. We believe that, under the guarantee of strict postoperative follow-up, the appropriate patients can be treated conservatively if there are no obvious postoperative symptoms of compression. If clinical symptoms develop, radiation therapy or reoperation may be required.

GTR is the optimal surgical outcome for macroadenoma and giant pituitary adenomas. We identified independent risk factors for resection scope to aid in the development of an appropriate surgical strategy. The size of the adenoma and the invasiveness of the giant pituitary adenoma into surrounding structures are key factors limiting the scope of resection. The current study found that an increase in adenoma diameter and Knosp grade decreased GTR opportunities. Therefore, both maximum diameter and Knosp grading were independent factors for the extent of resection. Sanmillan et al. (38) found that in 294 patients with pituitary adenoma, adenoma volume and Knosp grade were considered independent risk factors for resection scope, with Knosp grade having a greater impact. Similarly, we found that some giant pituitary adenomas with a low Knosp grade could be satisfactorily removed despite their large size. Thus, determining whether the pituitary adenoma invades the cavernous sinus is critical for surgical planning, and adenoma size can provide supplementary information. Additional improvements in surgical instruments, computer simulations, and endoscopes may further improve surgical resection rates and reduce the incidence of complications.

Limitations

The limitations of this study are primarily related to its retrospective design, lack of randomization, and the surgeon's assessment of the results. The results only present the experience provided from a single center with specific surgical techniques and protocols. In addition, this study only focused on patients undergoing endoscopic transnasal transsphenoidal surgery, which may lead to some epidemiological biases.

Conclusion

This study showed that the resection rate of pituitary adenomas under endoscopy was proportional to the size and Knosp grade of the pituitary adenoma. Preoperative evaluation of the Knosp grade helps identify situations where endoscopic approaches may be inadequate, allowing for more accurate treatment and preparation for possible serious complications. The findings shown here illustrate that neuroendoscopic transsphenoidal resection of pituitary adenomas is a safe and effective surgical method for pituitary adenomas with a clear surgical field, wide exposure range, and high adenoma resection rate and result in a lower rate of postoperative complications, quick postoperative recovery, and a short hospital stay.

Data availability statement

The raw data supporting the conclusions of this article will be made available by the authors, without undue reservation.

Ethics statement

The studies involving human participants were reviewed and approved by the EC of the First Affiliated Hospital of Bengbu Medical College(No.KJ2022A030). Written informed consent to participate in this study was provided by the participants' legal guardian/next of kin.

Author contributions

JW, and ZJ designed the study. DS, SJand SX analyzed the data. JW, BZ, and YL wrote the manuscript. ZJ revised the manuscript and supervised the study. All authors contributed to the article and approved the submitted version.

Funding

This study was supported by grants from the 10.13039/501100003995 Natural Science Foundation of Anhui Province (No. KJ2021ZD0078). 512 Talent Cultivation Program (by51202206).

Conflict of interest

The authors declare that the research was conducted in the absence of any commercial or financial relationships that could be construed as a potential conflict of interest.

Publisher's note

All claims expressed in this article are solely those of the authors and do not necessarily represent those of their affiliated organizations, or those of the publisher, the editors and the reviewers. Any product that may be evaluated in this article, or claim that may be made by its manufacturer, is not guaranteed or endorsed by the publisher.

References

1. Melmed S. Pituitary-tumor endocrinopathies. *N Engl J Med*. (2020) 382 (10):937–50. doi: 10.1056/NEJMra1810772

2. Fernandez A, Karavitaki N, Wass JA. Prevalence of pituitary adenomas: a community-based, cross-sectional study in Banbury (Oxfordshire, UK). *Clin Endocrinol*. (2010) 72(3):377–82. doi: 10.1111/j.1365-2265.2009.03667.x

3. Tritos NA, Biller BM, Swearingen B. Management of Cushing disease. *Nat Rev Endocrinol*. (2011) 7(5):279–89. doi: 10.1038/nrendo.2011.12

4. Mehta GU, Lonser RR. Management of hormone-secreting pituitary adenomas. *Neuro Oncol*. (2017) 19(6):762–73. doi: 10.1093/neuonc/now130

5. Juraschka K, Khan OH, Godoy BL, Monsalves E, Kilian A, Krischek B, et al. Endoscopic endonasal transsphenoidal approach to large and giant pituitary adenomas: institutional experience and predictors of extent of resection. *J Neurosurg*. (2014) 121(1):75–83. doi: 10.3171/2014.3.jns131679

6. Iglesias P, Rodríguez Berrocal V, Díez JJ. Giant pituitary adenoma: histological types, clinical features and therapeutic approaches. *Endocrine*. (2018) 61(3):407–21. doi: 10.1007/s12020-018-1645-x

7. Hlaváč M, Knoll A, Mayer B, Braun M, Karpel-Massler G, Etzrodt-Walter G, et al. Ten years' experience with intraoperative MRI-assisted transsphenoidal pituitary surgery. *Neurosurg Focus*. (2020) 48(6):E14. doi: 10.3171/2020.3.focus2072

8. Micko A, Agam MS, Brunswick A, Strickland BA, Rutkowski MJ, Carmichael JD, et al. Treatment strategies for giant pituitary adenomas in the era of endoscopic transsphenoidal surgery: amulticenter series. *J Neurosurg*. (2022) 136(3):776–85. doi: 10.3171/2021.1.jns203982

9. Marigil Sanchez M, Karekezi C, Almeida JP, Kalyvas A, Castro V, Velasquez C, et al. Management of giant pituitary adenomas: role and outcome of the endoscopic endonasal surgical approach. *Neurosurg Clin N Am*. (2019) 30 (4):433–44. doi: 10.1016/j.nec.2019.05.004

10. Elshazly K, Kshettry VR, Farrell CJ, Nyquist G, Rosen M, Evans JJ. Clinical outcomes after endoscopic endonasal resection of giant pituitary adenomas. *World Neurosurg*. (2018) 114:e447–56. doi: 10.1016/j.wneu.2018.03.006

11. Chen Y, Cai F, Cao J, Gao F, Lv Y, Tang Y, et al. Analysis of related factors of tumor recurrence or progression after transnasal sphenoidal surgical treatment of large and giant pituitary adenomas and establish a nomogram to predict tumor prognosis. *Front Endocrinol (Lausanne)*. (2021) 12:793337. doi: 10.3389/fendo.2021.793337

12. Micko A, Oberndorfer J, Weninger WJ, Vila G, Höftberger R, Wolfsberger S, et al. Challenging Knosp high-grade pituitary adenomas. *J Neurosurg*. (2019) 132(6):1739–46. doi: 10.3171/2019.3.jns19367

13. Tang OY, Hsueh WD, Eloy JA, Liu JK. Giant pituitary adenoma - special considerations. *Otolaryngol Clin North Am*. (2022) 55(2):351–79. doi: 10.1016/j.otc.2021.12.008

14. Trouillas J, Roy P, Sturm N, Dantony E, Cortet-Rudelli C, Viennet G, et al. A new prognostic clinicopathological classification of pituitary adenomas: amulticentric case-control study of 410 patients with 8 years post-operative follow-up. *Acta Neuropathol*. (2013) 126(1):123–35. doi: 10.1007/s00401-013-1084-y

15. Nakao N, Itakura T. Surgical outcome of the endoscopic endonasal approach for non-functioning giant pituitary adenoma. *J Clin Neurosci*. (2011) 18(1):71–5. doi: 10.1016/j.jocn.2010.04.049

16. Rolston JD, Han SJ, Aghi MK. Nationwide shift from microscopic to endoscopic transsphenoidal pituitary surgery. *Pituitary*. (2016) 19(3):248–50. doi: 10.1007/s11102-015-0685-y

17. Møller MW, Andersen MS, Glintborg D, Pedersen CB, Halle B, Kristensen BW, et al. Endoscopic vs. Microscopic transsphenoidal pituitary surgery: asingle centre study. *Sci Rep-UK*. (2020) 10(1):21942. doi: 10.1038/s41598-020-78823-z. Ceylan S, Sen HE, Ozsoy B, et al. Endoscopic approach for giant pituitary adenoma: clinical outcomes of 205 patients and comparison of two proposed classification systems for preoperative prediction of extent of resection. *J Neurosurg*. (2022) **136**(3):786–800. doi: 10.3171/2021.3.jns204116.

18. Cho HY, Cho SW, Kim SW, Shin CS, Park KS, Kim SY. Silent corticotroph adenomas have unique recurrence characteristics compared with other nonfunctioning pituitary adenomas. *Clin Endocrinol (Oxf)*. (2010) 72(5):648–53. doi: 10.1111/j.1365-2265.2009.03673.x

19. Romano A, Chibbaro S, Marsella M, Oretti G, Spiriev T, Iaccarino C, et al. Combined endoscopic transsphenoidal-transventricular approach for resection of a giant pituitary macroadenoma. *World Neurosurg*. (2010) 74(1):161–4. doi: 10.1016/j.wneu.2010.02.024

20. Nagata Y, Watanabe T, Nagatani T, Takeuchi K, Chu J, Wakabayashi T. Fully endoscopic combined transsphenoidal and supraorbital keyhole approach for parasellar lesions. *J Neurosurg*. (2018) 128(3):685–94. doi: 10.3171/2016.11.jns161833

21. D'Ambrosio AL, Syed ON, Grobelny BT, Freda PU, Wardlaw S, Bruce JN. Surgical strategies and long-term follow-up. *Pituitary*. (2009) 12(3):217–25. doi: 10.1007/s11102-009-0171-5

22. Zhang X, Fei Z, Zhang W, Zhang JN, Liu WP, Fu LA, et al. Endoscopic endonasal transsphenoidal surgery for invasive pituitary adenoma. *J Clin Neurosci*. (2008) 15(3):241–5. doi: 10.1016/j.jocn.2007.03.008

23. Tao C, Cheng G, Chen Y, Gu P, Hu W. Early outcomes of endoscopic endonasal approach pituitary adenomas resection with minimal nasal injury. *Medicine (Baltimore*. (2021) 100(46):e27843. doi: 10.1097/md.0000000000027843

24. Fallah N, Taghvaei M, Sadaghiani S, Sadrhosseini SM, Esfahanian F, Zeinalizadeh M. Surgical outcome of endoscopic endonasal surgery of large and giant pituitary adenomas: an institutional experience from the Middle East. *World Neurosurg*. (2019) 132:e802–11. doi: 10.1016/j.wneu.2019.08.004

25. Erkan B, Barut O, Akbas A, Akpinar E, Akdeniz YS, Tanriverdi O, et al. Results of endoscopic surgery in patients with pituitary adenomas: association of tumor classification grades with resection, remission, and complication rates. *J Korean Neurosurg Soc*. (2021) 64(4):608–18. doi: 10.3340/jkns.2020.0207

26. Zhu H, Li C, Gui S, Wang X, Zong X, Zhao P, et al. Experience of endoscopic endonasal approach for 803 pituitary tumors with cavernous Sinus invasion. *J Craniofac Surg*. (2022) 33(2):e118–22. doi: 10.1097/scs.0000000000008049

27. Castaño-Leon AM, Paredes I, Munarriz PM, Jiménez-Roldán L, Hilario A, Calatayud M, et al. Endoscopic transnasal trans-sphenoidal approach for pituitary adenomas: a comparison to the microscopic approach cohort by propensity score analysis. *Neurosurgery*. (2020) 86(3):348–56. doi: 10.1093/neuros/nyz201

28. Li C, Zhu H, Zong X, Wang X, Gui S, Zhao P, et al. Experience of trans-nasal endoscopic surgery for pituitary tumors in a single center in China: surgical results in a cohort of 2032 patients, operated between 2006 and 2018. *Clin Neurol Neurosurg*. (2020) 197:106176. doi: 10.1016/j.clineuro.2020.106176

29. Pablo A, Sofia B, Maximiliano T, Patricia FD, Alvaro C, Claudio Y, et al. Endoscopic versus microscopic pituitary adenoma surgery: a single-center study. *Neurol India*. (2019) 67(4):1015–21. doi: 10.4103/0028-3886.266241

30. Lobatto DJ, de Vries F, Zamanipoor Najafabadi AH, Pereira AM, Peul WC, Vliet Vlieland TPM, et al. Preoperative risk factors for postoperative complications in endoscopic pituitary surgery: a systematic review. *Pituitary*. (2018) 21(1):84–97. doi: 10.1007/s11102-017-0839-1

31. do Amaral LC, Reis BL, Ribeiro-Oliveira A Jr, da Silva Santos TM, Giannetti AV. Comparative study of complications after primary and revision transsphenoidal endoscopic surgeries. *Neurosurg Rev*. (2021) 44(3):1687–702. doi: 10.1007/s10143-020-01360-w

32. Parikh A, Adapa A, Sullivan SE, McKean EL. Predictive factors, 30-day clinical outcomes, and costs associated with cerebrospinal fluid leak in pituitary adenoma resection. *J Neurol Surg B Skull Base*. (2020) 81(1):43–55. doi: 10.1055/s-0039-1679896

33. Cheng H, Chen BP, Soleas IM, Ferko NC, Cameron CG, Hinoul P. Prolonged operative duration increases risk of surgical site infections: a systematic review. *Surg Infect (Larchmt*. (2017) 18(6):722–35. doi: 10.1089/sur.2017.089

34. Nayak P, Montaser AS, Hu J, Prevedello DM, Kirschner LS, Ghalib L. Predictors of postoperative diabetes insipidus following endoscopic resection of pituitary adenomas. *J Endocr Soc*. (2018) 2(9):1010–9. doi: 10.1210/js.2018-00121

35. Chapman PR, Singhal A, Gaddamanugu S, Prattipati V. Neuroimaging of the pituitary gland: practical anatomy and pathology. *Radiol Clin North Am*. (2020) 58(6):1115–33. doi: 10.1016/j.rcl.2020.07.009

36. Lucas JW, Bodach ME, Tumialan LM, Oyesiku NM, Patil CG, Litvack Z, et al. Congress of neurological surgeons systematic review and evidence-based guideline on primary management of patients with nonfunctioning pituitary adenomas. *Neurosurgery*. (2016) 79(4):E533–5. doi: 10.1227/neu.0000000000001389

37. Esposito D, Olsson DS, Ragnarsson O, Buchfelder M, Skoglund T, Johannsson G. Non-functioning pituitary adenomas: indications for pituitary surgery and post-surgical management. *Pituitary*. (2019) 22(4):422–34. doi: 10.1007/s11102-019-00960-0

38. Sanmillán JL, Torres-Diaz A, Sanchez-Fernández JJ, Lau R, Ciller C, Puyalto P, et al. Radiologic predictors for extent of resection in pituitary adenoma surgery. A single-center study. *World Neurosurg*. (2017) 108:436–46. doi: 10.1016/j.wneu.2017.09.017

frontiers | Frontiers in Surgery

TYPE Original Research
PUBLISHED 31 August 2022
DOI 10.3389/fsurg.2022.979940

OPEN ACCESS

EDITED BY
Luigi Maria Cavallo,
Università di Napoli Federico II, Italy

REVIEWED BY
Yazhuo Zhang,
Beijing Tiantan Hospital, Capital Medical University, China
Narayan Jayashankar,
Dr. Balabhai Nanavati Hospital, India

*CORRESPONDENCE
Haijun Wang
whj11260@163.com
Xiaobing Jiang
xbingjiang@163.com

†These authors have contributed equally to this work and share first authorship

SPECIALTY SECTION
This article was submitted to Neurosurgery, a section of the journal Frontiers in Surgery

RECEIVED 28 June 2022
ACCEPTED 01 August 2022
PUBLISHED 31 August 2022

CITATION
Qian K, Nie C, Zhu W, Zhao H, Zhang F, Wang H and Jiang X (2022) Surgical management of tuberculum sellae meningioma: Transcranial approach or endoscopic endonasal approach? Front. Surg. 9:979940.
doi: 10.3389/fsurg.2022.979940

Surgical management of tuberculum sellae meningioma: Transcranial approach or endoscopic endonasal approach?

Kang Qian†, Chuansheng Nie†, Wende Zhu, Hongyang Zhao, Fangcheng Zhang, Haijun Wang* and Xiaobing Jiang*

Department of Neurosurgery, Union Hospital, Tongji Medical College, Huazhong University of Science and Technology, Wuhan, China

Background: Tuberculum sellae meningioma (TSM), a common benign tumor in the sellae region, usually causes neurological deficits, such as vision impairment, by squeezing the peripheral neurovascular structures. Surgical management is recommended as the optimal strategy for TSM treatment and vision restoration. However, it remains challenging to resect TSM in the traditional transcranial approach (TCA). Recently, the endoscopic endonasal approach (EEA) has emerged as an effective option in skull base surgeries. Besides the effectivity, the advantages and limitations of EEA in TSM surgery remain controversial.

Object: We compared the surgical outcomes and complications between TCA and EEA surgeries to identify the principles in TSM surgical management.

Methods: Retrospective analysis was performed on the patients, who underwent TSM surgery in Wuhan Union Hospital between January 2017 and December 2021. The patients were assigned to TCA or EEA group according to the surgery they experienced. All patients were analyzed with the extent of tumor resection, vision outcome, postoperative complications, and follow-up results.

Results: A total of 112 patients were enrolled in this study, including 78 in TCA group and 34 in EEA group. The mean follow-up was 20.5 months (range 3–36 months). There were no statistically significant differences in patient demographic data, preoperative symptoms, and tumor characteristics between TCA and EEA groups. Both TCA and EEA surgeries are effective in TSM resection with relatively high gross total resection rates (85.9% in TCA vs. 91.2% in EEA, $p > .05$). Meanwhile, EEA surgery has a better outcome in vision restoration or stabilization than TCA surgery (74.6% in TCA vs. 93.1% in EEA, $p < .05$). Whereas EEA surgery causes more occurrences of cerebrospinal fluid (CSF) leakage than TCA surgery (0% in TCA vs. 11.8% in EEA, $p < .05$).

Conclusion: Both TCA and EEA surgeries are effective in TSM resection. EEA surgery has a better outcome in vision restoration or stabilization than TCA

Abbreviations
ACA, anterior cerebral artery; CSF, cerebrospinal fluid; CT, computed tomography; EEA, endoscopic endonasal approach; GTR, gross total resection; ICA, internal carotid artery; MRI, magnetic resonance imaging; OA, ophthalmic artery; TCA, transcranial approach; TSM, tuberculum sellae meningioma.

surgery, but induces higher risk of CSF leakage. As each approach has unique advantages and limitations, we must take all aspects into consideration, including approach feathers, tumor characteristics, and clinical requirements, to make the optimal choice in TSM surgical management.

KEYWORDS

tuberculum sellae meningioma, transcranial approach, endoscopic endonasal approach, gross total resection, cerebrospinal fluid leakage

Introduction

Tuberculum sellae meningioma (TSM) is a special type of meningioma located in the suprasellar region and accounts for approximately 5%–10% of all intracranial meningiomas (1). Generally, TSM comprises meningioma arising from tuberculum sellae, limbus sphenoidale, chiasmatic sulcus, and diaphragm sellae (2). Seungjoo et al. demonstrated that 85% of TSMs tend to grow in the midline and usually cause optic nerve/chiasm lateral or superior displacement (3). It was also reported that about 56%–77% of TSMs invade the optic canal, resulting in optic nerve compression (4, 5). Therefore, the most common clinical manifestation of TSM patients is progressive vision impairment. Other clinical manifestations of TSM patient comprise headache, anosmia, seizures, and pituitary dysfunction (6).

The primary goals of TSM surgical management are tumor gross total resection (GTR) and vision restoration. However, it remains challenges in TSM surgical management, since TSMs are anatomical proximity to the vital neurovascular structures, such as optic nerve/chiasm, internal carotid artery (ICA) and its branches, pituitary stalk and hypothalamus (7). When TSM is small, the neurosurgeons can easily separate the tumor from the neurovascular structures along the well-preserved arachnoid interfaces. With TSM growing up, the arachnoid interfaces are broken down and the surrounding neurovascular structures are encased by the tumor. Moreover, the vision impairment and visual field defect are progressively exacerbated, resulting in GTR of TSM and vision restoration becoming much more difficult.

Traditional transcranial approaches (TCAs), including pterional, subfrontal, interhemispheric, and supraorbital craniotomy, are familiar to most neurosurgeons. Nevertheless, in the past decade, endoscopic endonasal approach (EEA) emerged as an effective option for neurosurgeons in skull base surgery (6, 8). Both TCA and EEA have been described in literatures with successful surgical outcome and minimum complication in TSM surgery (9, 10). But there are few studies comparing the surgical outcome and postoperative complication between TCA and EEA in TSM surgical management directly. What are their advantages and limitations? Which principles should be followed in surgical management? These controversies remain to be figured out.

In this study, we retrospectively analyzed the surgical outcome and complication of 112 TSM patients, who experienced TCA or EEA surgery in Wuhan Union Hospital. We also presented our experience in TSM surgical management.

Methods

This retrospective study enrolled all patients of TSM, who experienced TCA or EEA surgery in Wuhan Union Hospital between January 2017 and December 2021. All of these cases were pathologically confirmed as meningioma (WHO grade I). Meningiomas arising from the clinoid processes, olfactory groove and planum sphenoidale were excluded. The surgical indications included progressive headache, intracranial hypertension sign, and vision impairment. All tumors with base diameter or lateral extension over 3.0 cm were managed with TCA surgery. EEA surgery was performed in the cases of midline tumor with base diameter less than 3.0 cm. Preoperative and postoperative clinical reports of these patients were evaluated, including demographics, clinical manifestations, image data, endocrine functions, ophthalmological assessments, operative records, and complications. Endocrine functions were evaluated in 2–4 weeks postoperatively. Image data, including computed tomography (CT) and magnetic resonance imaging (MRI), was used for preoperative evaluation, surgery assessment, and postoperative outcome analysis. During the follow-up, MRI was performed in 48 h and 3–6 months postoperatively. The tumor size was presented as the largest diameters in all three dimensions (length, width, and height), depending on the preoperative MRI. The volume of tumor was calculated by the formula that tumor volume in cubic centimeters (cm^3) = (anteroposterior × coronal × craniocaudal)/2. In this formula, the tumor configuration was assumed as a rough sphere. The extent of tumor resection was evaluated according to the operation records and postoperative MRI. We defined GTR as no tumor or capsule remnant on postoperative MRI examination, and subtotal resection (STR) as tumor or capsule remnant.

Traditional TCA surgeries, including pterional, subfrontal, interhemispheric and supraorbital craniotomy, and extended EEA surgery were provided to remove the tumor in this

study. All surgeries were performed by senior neurosurgeons in our department.

Statistical analysis

The data were analyzed by SPSS 26.0. Descriptive statistics were presented as tables and used to analyze patient demographics. Continuous variables were presented as mean values with SDs. Categorical variables were described as percentages. Group comparisons were evaluated by the Student's *t*-test or Chi-square test. The value of $p < .05$ was regarded as statistically significant difference.

Results

Clinical characteristics

A total of 112 TSM patients were enrolled in this study. Among these patients, 78 were performed TCA surgery and assigned to the TCA group, 34 were performed EEA surgery and assigned to the EEA group. The mean follow-up period was 20.5 months (range 3–36 months).

The TCA group is comprised of 30 (38.5%) males and 48 (61.5%) females with a mean age of 50.5 ± 11.7 years. The EEA group is comprised of 12 (35.3%) males and 22 (64.7%) females with a mean age of 52.2 ± 10.1 years. The most common symptom was vision impairment, which was observed in 92 (82.1%) patients, including 63 (80.8%) in TCA group and 29 (85.3%) in EEA group. Headache was presented in 46 (41.1%) patients, including 33 (42.3%) in TCA group and 13 (38.2%) in EEA group. According to the imaging findings, dura tail sign was found in 77 (68.8%) patients, with 55 (70.5%) in TCA group and 22 (64.7%) in EEA group. We also listed the main optic nerve-related vessels and evaluated their relationship with tumor. The results showed 71 (63.4%) patients, including 52 (66.7%) in TCA group and 19 (55.9%) in EEA group, exhibited ICA involvement; 43 (38.4%) patients, including 29 (37.2%) in TCA group and 14 (41.2%) in EEA group, exhibited ophthalmic artery (OA) involvement; 52 (46.4%) patients, including 37 (47.4%) in TCA group and 15 (44.1%) in EEA group, exhibited anterior cerebral artery (ACA) involvement (**Supplementary Table S1**). Vascular encasement (>180°) was identified in 24 (21.4%) patients, with 18 (23.1%) in TCA group and 6 (17.6%) in EEA group. Optic canal invasion was diagnosed in 67 (59.8%) patients, with 45 (57.7%) in TCA group and 22 (64.7%) in EEA group. Moreover, we compared the degree of optic nerve compression between TCA and EEA groups. The results showed 95 (84.8%) patients, including 65 (83.3%) in TCA group and 30 (88.2%) in EEA group, exhibited optic nerve compression; 61 (54.5%) patients, including 43 (55.1%) in TCA group and 18 (52.9%) in EEA group, exhibited optic nerve displacement; 98 (87.5%) patients, including 68 (87.2%) in TCA group and 30 (88.2%) in EEA group, exhibited optic nerve adhesion; 29 (25.9%) patients, including 22 (28.2%) in TCA group and 7 (20.6%) in EEA group, exhibited optic nerve wrapped by the tumor (**Supplementary Table S1**). The mean volume of tumor was 11.2 ± 4.8 cm^3, with 11.5 ± 4.6 cm^3 in TCA group and 10.7 ± 5.2 cm^3 in EEA group. There were no statistically significant differences between TCA and EEA groups regarding sex, mean age, preoperative symptom, imaging finding, optic nerve-related vessels involvement, degree of optic nerve compression, and mean tumor volume ($p > .05$) (**Table 1**).

Extent of tumor resection

GTR of tumor was achieved in 98 (87.5%) patients, with 67 (85.9%) in TCA group and 31 (91.2%) in EEA group. In addition, we analyzed the removal of tumors invading the optic canal separately. Among the patients of optic canal invaded, 56 (83.6%) patients, including 36 (80.0%) in TCA group and 20 (90.9%) in EEA group, experienced GTR of tumors (**Supplementary Table S1**). Both TCA and EEA surgeries are effective in TSM resection with relatively high GTR rates. Although there were no statistically significant differences of GTR rates ($p > .05$) between TCA and EEA surgeries in the current study (**Table 2**). EEA surgery can provide a close and high-definition surgical view for neurosurgeons, which contributes to the identification of anatomical structures and ensures the surgical safety (5, 11, 12).

TABLE 1 Main clinical manifestations of all patients.

	Total (%)	TCA (%)	EEA (%)	*p*-value
No. of patients	112 (100)	78 (69.6)	34 (30.4)	
Mean age (SD)	51.0 (11.2)	50.5 (11.7)	52.2 (10.1)	0.467
Male sex	42 (37.5)	30 (38.5)	12 (35.3)	0.750
Symptoms				
Visual impairment	92 (82.1)	63 (80.8)	29 (85.3)	0.565
Headache	46 (41.1)	33 (42.3)	13 (38.2)	0.687
Image characteristic				
Dural tail sign	77 (68.8)	55 (70.5)	22 (64.7)	0.542
Vascular encasement (>180°)	24 (21.4)	18 (23.1)	6 (17.6)	0.520
Optic canal involvement	67 (59.8)	45 (57.7)	22 (64.7)	0.486
Mean tumor vol. (SD)	11.2 (4.8)	11.5 (4.6)	10.7 (5.2)	0.426

EEA, endoscopic endonasal approach; TCA, transcranial approach; SD, standard deviation.

TABLE 2 Postoperative outcomes and complications.

	Total	TCA (%)	EEA (%)	*p*-value
Gross total resection	98 (87.5)	67 (85.9)	31 (91.2)	0.437
Vision improved or stable	74 (80.4)	47 (74.6)	27 (93.1)	.038
Worsened	18 (19.6)	16 (25.4)	2 (6.9)	.038
CSF leakage	4 (3.6)	0 (0)	4 (11.8)	.002
Meningitis	5 (4.5)	2 (2.6)	3 (8.8)	0.140
Hypopituitarism	15 (13.4)	10 (12.8)	5 (14.7)	0.788
Diabetes insipidus	7 (6.3)	5 (6.4)	2 (5.9)	0.915
Hemorrhage	3 (2.7)	2 (2.6)	1 (2.9)	0.910
Seizures	7 (6.3)	7 (9.0)	0 (0)	.071
Death	0	0	0	

EEA, endoscopic endonasal approach; TCA, transcranial approach; CSF, cerebrospinal fluid.

Visual outcome

Among the 92 patients with vision impairment, vision restoration or stabilization was reported in 74 (80.4%) patients, including 47 (74.6%) in TCA group and 27 (93.1%) in EEA group. There were statistically significant differences ($p < .05$) between TCA and EEA groups in vision restoration or stabilization rates. On the other hand, 18 (19.6%) patients got worsening vision postoperatively, including 16 (25.4%) in TCA group and 2 (6.9%) in EEA group (**Table 2**). Overall, EEA surgery has advantages over TCA surgery in vision restoration or stabilization in TSM resection.

Postoperative complications

In our study, there were 4 (11.8%) patients experienced postoperative cerebrospinal fluid (CSF) leakage in EEA group and 2 (5.9%) of them required a secondary surgery to reconstruct the skull base. Whereas, none of the 78 patients in TCA group experienced CSF leakage. There were statistically significant differences ($p < .05$) between TCA and EEA groups in CSF leakage rates (**Table 2**). In other words, compared with TCA surgery, EEA surgery may induce a higher risk of CSF leakage in TSM surgical management.

We also observed other complications in the current study, including meningitis (2 in TCA, 3 in EEA), hypopituitarism (10 in TCA, 5 in EEA), diabetes insipidus (5 in TCA, 2 in EEA), hemorrhage (2 in TCA, 1 in EEA), and seizures (7 in TCA, 0 in EEA). No surgery-related death occurred. However, there were no statistically significant differences in these postoperative complications between TCA and EEA groups ($p > .05$) (**Table 2**).

Discussion

TSM is a common benign tumor in the sellae region (1). Generally, TSM grows slowly and does not cause any clinical symptoms in early period. With the tumor growing up, TSM squeezes the peripheral anatomical structures, including optic nerve/chiasm, ICA and its branches, pituitary stalk and hypothalamus, causing neurological dysfunctions (13, 14). Impaired visual acuity and visual field are the most common clinical manifestations of TSM. Surgical management is recommended as the optimal strategy for TSM treatment and vision restoration. However, it remains challenge in TSM surgeries, due to the anatomical proximity with vital neurovascular structures in skull base. Traditional TCA surgeries, including pterional, subfrontal, interhemispheric, and supraorbital craniotomy, have been widely applied in TSM resection (9, 10, 14–17). Likewise, with advance in optical technology and improvement in surgical technique, EEA surgery has emerged as an effective option for properly selected TSM patients in the past decade (18, 19).

Extent of tumor resection

Generally, the extent of tumor resection is an independent predictor of TSM recurrence and has an impact on the surgical outcome. The GTR rate of TSM is about 60%–100% in literatures reviewed (5–7, 20). However, it is difficult to compare the surgical outcomes between different studies directly, due to the lack of uniform criteria (6). In the current study, we use standard criteria to evaluate the degree of tumor resection in 112 patients, with a result of GTR rate 85.9% in TCA group and 91.2% in EEA group.

In line with recent literatures, multiple tumor characteristics, such as tumor size, optic canal involvement, vascular encasement, intracranial extension, surgery, and radiation history, have an impact on the GTR rate of TSM (5, 13, 20–24). EEA surgery is a better choice for small (<3.0 cm) and midline TSMs, as it provides a close, high-definition surgical view and minimizes the invasion. Herein displays a case of TSM that achieves GTR by EEA surgery (**Figures 1**, **2**). As to the large (>3.0 cm), laterally extensive, firm, or fibrous TSMs, TCA surgery is recommended to perform (9, 10, 13–15, 17, 23, 25, 26). Actually, neurosurgeons prefer to achieve GTR if possible. While in some cases, it may be extremely difficult or even dangerous to achieve that goal. In these cases, STR combined with radiotherapy is advocated to ensure safety and prevent tumor recurrence (27). In addition, the technique of neurosurgeon has a marked impact on the extent of tumor resection (28).

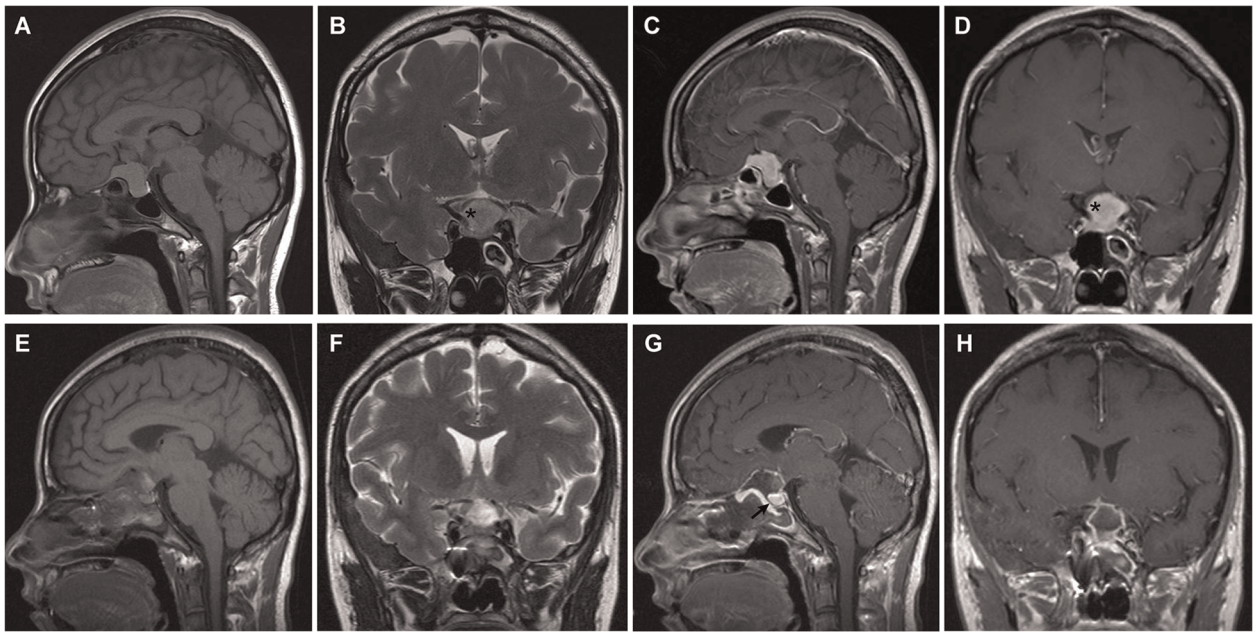

FIGURE 1
Tuberculum sellae meningioma (WHO grade I). (**A–D**) Preoperative MRI shows an intrasellar and suprasellar tumor with internal carotid artery encasement (>180°) (asterisk). (**E–H**) Postoperative MRI demonstrates gross total resection of the tumor and skull base reconstruction. The optic nerve and pituitary (arrow) were decompressed. Visual acuity and visual field were restored rapidly and pituitary function was preserved after surgery.

Visual outcome

Vision impairment is the most common clinical manifestation in the patients harboring TSM (6, 7, 9). Generally, surgical management remains to be the most effective treatment for TSM and contributes to restoring the vision (6). In the current study, there were 92 (82.1%) patients of TSM suffering from vision impairment. Among these cases, 74 (80.4%) patients displayed improved or stable vision postoperatively, including 47 (74.6%) in TCA group and 27 (93.1%) in EEA group. These results reveal that EEA surgery may have tremendous advantages on vision restoration or stabilization in TSM surgical management.

Actually, visual outcomes mainly depend on several factors, including tumor size, degree, and duration of the optic nerves compressed, optic canal involvement, perforating artery protection, and the optic nerve manipulation during tumor removal (29). For instance, subchiasmatic perforating arteries, which play important roles in the optic nerve and chiasm blood supply, are hardly to be identified in the surgical field from above in TCA surgery (24, 30, 31). Conversely, EEA surgery provides a surgical field from below, where the perforating arteries can be observed directly and preserved effectively. EEA surgery causes less disturbances in the blood supply of perforating arteries and minimizes the optic nerve manipulations compared with TCA surgery. These advantages of EEA surgery may contribute to restoring the vision in TSM surgery.

CSF leakage

CSF leakage is one of the most common postoperative complications in EEA surgery. Abrasion of the skull base and incision of the dura from below make EEA surgery more prone to CSF leakage than TCA surgery (1, 7, 32–34). In our study, 4 (11.8%) cases in EEA group experienced CSF leakage. Meanwhile, the meningitis risk was increased in line with CSF leakage. The CSF leakage and meningitis may prolong the time of hospitalization, enhance the cost of patients, or even lead to death. Autologous thigh broad fascia and vascularized nasoseptal flap are recommended to reconstruct the skull base (31, 35) (**Figures 2K, L**). Moreover, it is necessary to perform continuous lumbar drainage and apply antibiotics, if CSF leakage occurs (36). Recently, with the surgical technique progressing, the occurrence of CSF leakage keeps decreasing (6).

Conclusion

Both TCA and EEA surgeries are effective in TSM resection. Meanwhile, EEA surgery acquires a better outcome in vision restoration or stabilization than TCA surgery. Although EEA surgery induces higher risk of CSF leakage, the adverse effect is declining with the surgical technique progressing.

EEA surgery has been recommended as an effective option for properly selected TSM patients, since it offers several advantages in

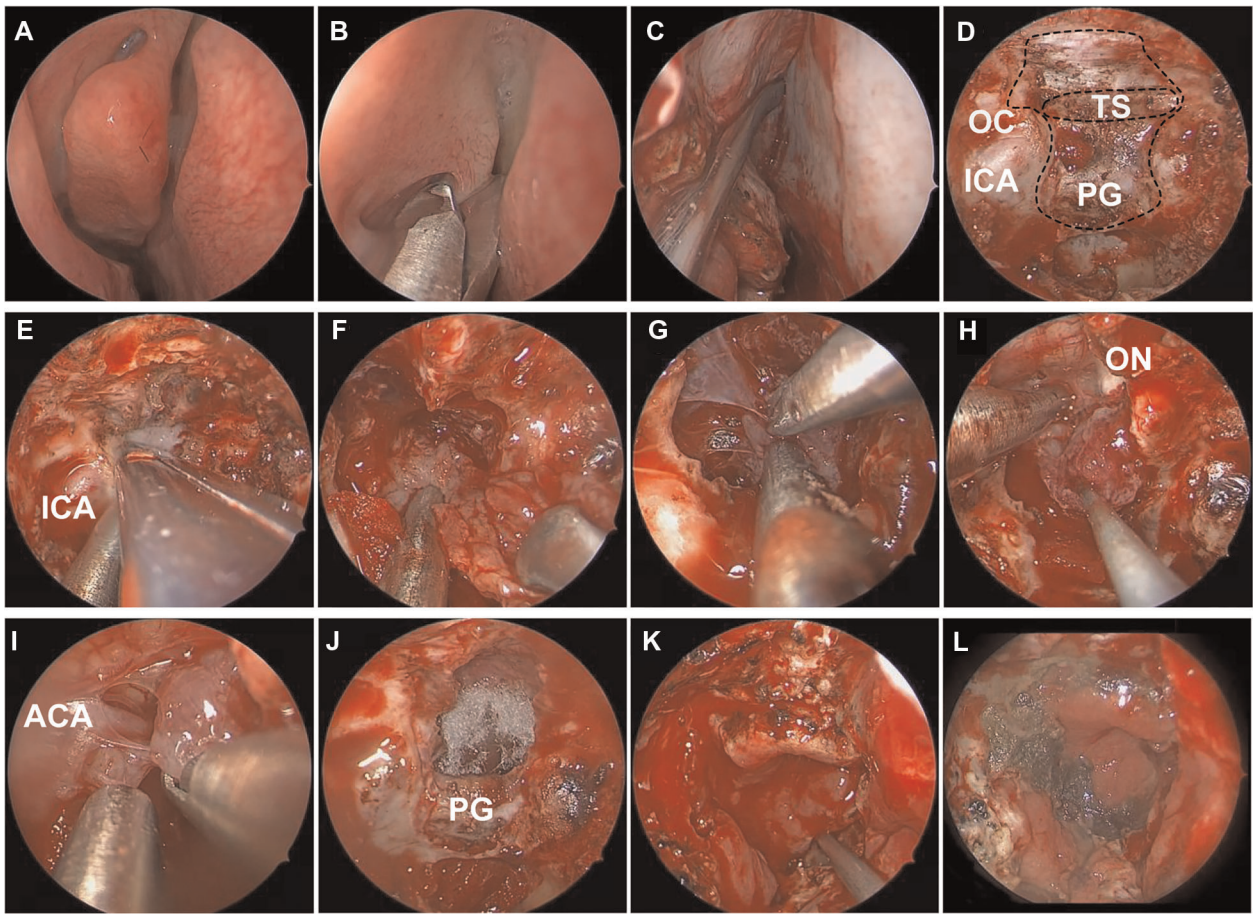

FIGURE 2
Intraoperative photos of endoscopic endonasal surgery for tuberculum sellae meningioma. (A) Nasal mucosa constriction. (B) Remove the middle turbinate. (C) Vascularized nasoseptal flap separation. (D) Expose the anterior fossa dura. (E) Enlarge the skull base exposure. (F) Intratumor decompression. (G) Dissociate the tumor boundary. (H) Resect the main part of tumor. (I) Dissect the adherent tumor from the anterior cerebral artery complex. (J) Gross total resection of tumor. (K) Reconstruct the skull base by vascularized nasoseptal flap. (L) Probe the nasal 10 days after surgery. ICA, internal carotid artery; PG, pituitary gland; TS, tuberculum sellae; OC, optic canal; ON, optic nerve; ACA, anterior cerebral artery.

TSM surgical management, including (i) EEA surgery offers a close and high-definition surgical view, which contributes to identifying the anatomical structures clearly and ensures surgical safety. (ii) EEA surgery provides better protection for the small perforating arteries, which supply the optic apparatus from below. (iii) EEA surgery reduces the retraction of brain and cranial nerves, preserves the neurological functions better. (iv) EEA surgery is more effective to perform tumor devascularization before resection. (v) EEA surgery leads to less invasion, faster recovery, and better cosmetic results. However, EEA surgery also has limitations compared to TCA surgery, such as (i) EEA surgery is unavailable to resect large tumors, especially those extend laterally. (ii) EEA surgery is difficult to remove firm or fibrous tumors. (iii) EEA surgery induces higher risk of CSF leakage than TCA surgery.

As each approach has unique advantages and limitations, we must take all aspects into consideration, including approach feathers, tumor characteristics and clinical requirements, to make the optimal choice in TSM surgical management.

Data availability statement

The original contributions presented in the study are included in the article/**Supplementary Material**, further inquiries can be directed to the corresponding author/s.

Author contributions

KQ contributed substantially to the conception and design of the study, acquisition and interpretation of the data, drafted and revised the manuscript. CN contributed substantially to the conception and design of the study. WZ, HZ, and FZ contributed to the collection

and interpretation of the data. HW and XJ designed and supervised the study, performed surgery and revised the manuscript. All authors contributed to the article and approved the submitted version.

Funding

This work was supported by Free Innovation Fund of Wuhan Union Hospital (grant numbers 2021xhyn108).

Conflict of interest

The authors declare that the research was conducted in the absence of any commercial or financial relationships that could be construed as a potential conflict of interest.

Publisher's note

Supplementary material

The Supplementary Material for this article can be found online at: https://www.frontiersin.org/articles/10.3389/fsurg.2022.979940/full#supplementary-material.

References

1. De Divitiis E, Esposito F, Cappabianca P, Cavallo LM, de Divitiis O. Tuberculum sellae meningiomas high route or low route A series of 51 consecutive cases. *Neurosurgery*. (2008) 62(3):556–63; discussion 556–63. doi: 10.1227/01.NEU.0000297113.72625.D1

2. Harsh G, Hwang P, Choudhri O, Ajlan A. Meningiomas of the tuberculum and diaphragma sellae. *J Neurol Surg B: Skull Base*. (2014) 76(01):074–9. doi: 10.1055/s-0034-1390400

3. Lee S, Hong SH, Cho YH, Kim JH, Kim CJ. Anatomical origin of tuberculum sellae meningioma: off-midline location and its clinical implications. *World Neurosurg*. (2016) 89:552–61. doi: 10.1016/j.wneu.2016.02.016

4. Nimmannitya P, Goto T, Terakawa Y, Sato H, Kawashima T, Morisako H, et al. Characteristic of optic canal invasion in 31 consecutive cases with tuberculum sellae meningioma. *Neurosurg Rev*. (2016) 39(4):691–7. doi: 10.1007/s10143-016-0735-6

5. Schick U. Surgical management of tuberculum sellae meningiomas: involvement of the optic canal and visual outcome. *J Neurol Neurosurg Psychiatry*. (2005) 76(7):977–83. doi: 10.1136/jnnp.2004.039974

6. Sankhla S, Jayashankar N, Khan M, Khan G. Surgical management of tuberculum sellae meningioma: our experience and review of the literature. *Neurol India*. (2021) 69(6):1592. doi: 10.4103/0028-3886.333529

7. Mahmoud M, Nader R, Al-Mefty O. Optic canal involvement in tuberculum sellae meningiomas: influence on approach, recurrence, and visual recovery. *Operative Neurosurgery*. (2010) 67(3):ons108–19. doi: 10.1227/01.neu.0000383153.75695.24

8. Zhang C, Ding J, Liu Y, Tuoheti M, Yang X, Wang J, et al. Endoscopic endonasal approach for resection of tuberculum sellae meningioma: a promising surgical approach. *J Craniofac Surg*. (2020) 31(6):1815–18. doi: 10.1097/scs.0000000000006413

9. Samii M, Vorkapic P, Struck M, Roser F, Nakamura M. Tuberculum sellae meningiomas: clinical outcome considering different surgical approaches. *Neurosurgery*. (2006) 59(5):1019–29. doi: 10.1227/01.neu.0000245600.92322.06

10. Koutourousiou M, Fernandez-Miranda JC, Stefko ST, Wang EW, Snyderman CH, Gardner PA. Endoscopic endonasal surgery for suprasellar meningiomas experience with 75 patients. *J Neurosurg*. (2014) 120(6):1326–39. doi: 10.3171/2014.2.JNS13767

11. Liu JK, Christiano LD, Patel SK, Tubbs RS, Eloy JA. Surgical nuances for removal of tuberculum sellae meningiomas with optic canal involvement using the endoscopic endonasal extended transsphenoidal transplanum transtuberculum approach. *Neurosurg Focus*. (2011) 30(5):E2. doi: 10.3171/2011.3.focus115

12. Kulwin C, Schwartz TH, Cohen-Gadol AA. Endoscopic extended transsphenoidal resection of tuberculum sellae meningiomas: nuances of neurosurgical technique. *Neurosurg Focus*. (2013) 35(6):E6. doi: 10.3171/2013.8.focus13338

13. Jallo GI, Benjamin V. Tuberculum sellae meningiomas: microsurgical anatomy and surgical technique. *Neurosurgery*. (2002) 51(6):1432–39; discussion 1439–40. doi: 10.1097/00006123-200212000-00013

14. Chi JH, McDermott MW. Tuberculum sellae meningiomas. *Neurosurg Focus*. (2003) 14(6):1–6. doi: 103171/foc20031466

15. Fahlbusch R, Schott W. Pterional surgery of meningiomas of the tuberculum sellae and planum sphenoidale surgical results with special consideration of ophthalmological and endocrinological outcomes. *J Neurosurg*. (2002) 96 (2):235–43. doi: 103171/jns20029620235

16. Ganna A, Dehdashti AR, Karabatsou K, Gentili F. Fronto-basal interhemispheric approach for tuberculum sellae meningiomas; long-term visual outcome. *Br J Neurosurg*. (2009) 23(4):422–30. doi: 10.1080/02688690902968836

17. Chokyu I, Goto T, Ishibashi K, Nagata T, Ohata K. Bilateral subfrontal approach for tuberculum sellae meningiomas in long-term postoperative visual outcome. *J Neurosurg*. (2011) 115(4):802–10. doi: 10.3171/2011.5.jns101812

18. Bander ED, Singh H, Ogilvie CB, Cusic RC, Pisapia DJ, Tsiouris AJ, et al. Endoscopic endonasal versus transcranial approach to tuberculum sellae and planum sphenoidale meningiomas in a similar cohort of patients. *J Neurosurg*. (2018) 128(1):40–8. doi: 10.3171/2016.9.jns16823

19. Komotar RJ, Starke RM, Raper DM, Anand VK, Schwartz TH. Endoscopic endonasal versus open transcranial resection of anterior midline skull base meningiomas. *World Neurosurg*. (2012) 77(5–6):713–24. doi: 10.1016/j.wneu.2011.08.025

20. Makarenko S, Carreras EM, Akagami R. Craniotomy for perisellar meningiomas: comparison of simple (appropriate for endoscopic approach) versus complex anatomy and surgical outcomes. *J Neurosurg*. (2017) 126 (4):1191–200. doi: 10.3171/2016.3.jns152307

21. Goel A, Muzumdar D, Desai KI. Tuberculum sellae meningioma: a report on management on the basis of a surgical experience with 70 patients. *Neurosurgery*. (2002) 51(6):1358–63; discussion 1363–4. doi: 10.1097/00006123-200212000-00005

22. Linsler S, Fischer G, Skliarenko V, Stadie A, Oertel J. Endoscopic assisted supraorbital keyhole approach or endoscopic endonasal approach in cases of tuberculum sellae meningioma: which surgical route should be favored? *World Neurosurg*. (2017) 104:601–11. doi: 10.1016/j.wneu.2017.05.023

23. Bowers CA, Altay T, Couldwell WT. Surgical decision-making strategies in tuberculum sellae meningioma resection. *Neurosurg Focus*. (2011) 30(5):E1. doi: 10.3171/2011.2.focus1115

24. Magill ST, Morshed RA, Lucas CG, Aghi MK, Theodosopoulos PV, Berger MS, et al. Tuberculum sellae meningiomas: grading scale to assess surgical outcomes using the transcranial versus transsphenoidal approach. *Neurosurg Focus*. (2018) 44(4):E9. doi: 10.3171/2018.1.focus17753

25. Maiuri F, Iaconetta G, de Divitiis O, Cirillo S, Di Salle F, De Caro ML. Intracranial meningiomas: correlations between MR imaging and histology. *Eur J Radiol*. (1999) 31(1):69–75. doi: 10.1016/s0720-048x(98)00083-7

26. Kashimura H, Inoue T, Ogasawara K, Arai H, Otawara Y, Kanbara Y, et al. Prediction of meningioma consistency using fractional anisotropy value measured

by magnetic resonance imaging. *J Neurosurg*. (2007) 107(4):784–7. doi: 10.3171/jns-07/10/0784

27. Samanci Y, Ardor GD, Peker S. Gamma knife radiosurgery for tuberculum sellae meningiomas: a series of 78 consecutive patients. *Neurosurg Rev*. (2022) 45:2315–22. doi: 10.1007/s10143-022-01753-z

28. Younus I, Gerges MM, Uribe-Cardenas R, Morgenstern PF, Eljalby M, Tabaee A, et al. How long is the tail end of the learning curve? Results from 1000 consecutive endoscopic endonasal skull base cases following the initial 200 cases. *J Neurosurg*. (2020) 134(3):750–60. doi: 10.3171/2019.12.jns192600

29. Raco A, Bristot R, Domenicucci M, Cantore G. Meningiomas of the tuberculum sellae. Our experience in 69 cases surgically treated between 1973 and 1993. *J Neurosurg Sci*. (1999) 43(4):253–60; discussion 260–2. https://pubmed.ncbi.nlm.nih.gov/10864387/

30. Wang Q, Lu XJ, Li B, Ji WY, Chen KL. Extended endoscopic endonasal transsphenoidal removal of tuberculum sellae meningiomas: a preliminary report. *J Clin Neurosci*. (2009) 16(7):889–93. doi: 10.1016/j.jocn.2008.10.003

31. Gardner PA, Kassam AB, Thomas A, Snyderman CH, Carrau RL, Mintz AH, et al. Endoscopic endonasal resection of anterior cranial base meningiomas. *Neurosurgery*. (2008) 63(1):36–52; discussion 52–4. doi: 10.1227/01.neu.0000335069.30319.1e

32. Laufer I, Anand VK, Schwartz TH. Endoscopic, endonasal extended transsphenoidal, transplanum transtuberculum approach for resection of suprasellar lesions. *J Neurosurg*. (2007) 106(3):400–6. doi: 10.3171/jns.2007.106.3.400

33. de Divitiis E, Cavallo LM, Esposito F, Stella L, Messina A. Extended endoscopic transsphenoidal approach for tuberculum sellae meningiomas. *Neurosurgery*. (2007) 61(5 Suppl 2):229–37; discussion 237–8. doi: 10.1227/01.neu.0000303221.63016.f2

34. Fatemi N, Dusick JR, de Paiva Neto MA, Malkasian D, Kelly DF. Endonasal versus supraorbital keyhole removal of craniopharyngiomas and tuberculum sellae meningiomas. *Neurosurgery*. (2009) 64(5 Suppl 2):269–84; discussion 284–6. doi: 10.1227/01.neu.0000327857.22221.53

35. Kassam A, Snyderman CH, Mintz A, Gardner P, Carrau RL. Expanded endonasal approach: the rostrocaudal axis. Part I. Crista galli to the sella turcica. *Neurosurg Focus*. (2005) 19(1):E3. https://pubmed.ncbi.nlm.nih.gov/16078817/

36. Nie C, Ye Y, Wu J, Zhao H, Jiang X, Wang H. Clinical outcomes of transcranial and endoscopic endonasal surgery for craniopharyngiomas: a single-institution experience. *Front Oncol*. (2022) 12. doi: 10.3389/fonc.2022.755342.

frontiers | Frontiers in Surgery

TYPE Original Research
PUBLISHED 01 September 2022
DOI 10.3389/fsurg.2022.962709

OPEN ACCESS

EDITED BY
Peng Zhao,
Capital Medical University, China

REVIEWED BY
Senlin Yin,
Sichuan University, China
Sabino Luzzi,
University of Pavia, Italy

*CORRESPONDENCE
Mahmoud Messerer
mahmoud.messerer@chuv.ch

†These authors have contributed equally to this work and share first authorship.

SPECIALTY SECTION
This article was submitted to Neurosurgery, a section of the journal Frontiers in Surgery

RECEIVED 06 June 2022
ACCEPTED 25 July 2022
PUBLISHED 01 September 2022

CITATION
Harel E, Cossu G, Daniel RT and Messerer M (2022) Relationship with the diaphragm to predict the surgical outcome in large and giant pituitary adenomas.
Front. Surg. 9:962709.
doi: 10.3389/fsurg.2022.962709

Relationship with the diaphragm to predict the surgical outcome in large and giant pituitary adenomas

Ethan Harel†, Giulia Cossu†, Roy Thomas Daniel and Mahmoud Messerer*

Department of Neurosurgery, University Hospital of Lausanne and University of Lausanne, Lausanne, Switzerland

Objective: Large and giant pituitary adenomas (L- and G-PAs) continue to remain a surgical challenge. The diaphragm may have a role in determining the shape of the tumor and therefore influencing the extent of resection. Our study aims to analyze our surgical series of L- and G-PAs according to their relationship with the diaphragm and invasion of cavernous sinus (CS).
Material and methods: We performed a retrospective analysis of our surgical series of patients operated for L- and G-PAs. We categorized the tumors into four grades according to their relationship with the diaphragm: grade 1 (supradiaphragmatic component with a wide incompetent diaphragm), grade 2 (purely infra-diaphragmatic tumor with a competent diaphragm), grade 3 (dumbbell-shape tumors), and grade 4 (multilobulated tumor with invasion of the subarachnoid space).
Results: A total of 37 patients were included in our analysis. According to our classification, 43.3% of patients had grade 1 tumors, 27% had grade 2, 5.4% had grade 3, and 24.3% had grade 4 tumors. CS invasion was confirmed intraoperatively in 17 out of 37 patients (46%). The gross total resection (GTR) was obtained in 19% of the cases, near-total resection in 46%, and subtotal resection in 35%. All the patients who achieved GTR had grade 1 tumors and the lowest rate of CS invasion ($p < 0.01$).
Conclusion: Radiological evaluation of the tumor relationship with the diaphragm, invasion of CS, and invasion of the subarachnoid space are crucial to plan the surgical strategy and maximize the possibilities of achieving GTR in L- and G-PAs.

KEYWORDS
cavernous sinus invasion, diaphragm, endoscopy, pituitary adenoma, surgery

Introduction

Pituitary adenomas (PAs) account for approximately 10% of intracranial neoplasms, are the third most common tumor, and account for more than 90% of pituitary tumors (1–4).

Tumor size and invasion of surrounding structures remain the important factors in the prediction of the extent of resection. Large PAs (L-PAs) are defined as tumors with a maximal diameter of ≥30 mm, while giant PAs (G-PAs) are tumors with a maximal

diameter of ≥40 mm (5–7). These tumors account for 6%–10% of PAs in recent surgical series (3, 8). In most cases, L-PAs and G-PAs are non-functional tumors (6, 9) and are diagnosed because of their mass effect on the optic pathways, the normal pituitary gland, or more rarely, their invasion of the cavernous sinus. In these situations, besides prolactin-secreting adenomas, surgery remains the first choice of treatment.

The main factors that will influence the extent of resection with large and giant lesions are the invasion of the cavernous sinus (7, 18, 19), the invasion of the subarachnoid space with encasement of the arteries of Willis circle, the optic/oculomotor nerves in their cisternal portion, and last but not the least, the consistency of the adenoma (10, 17, 20, 21). Although intuitive, tumor shape plays an important role, as tumors with a multicompartmental morphology and invasion of neurovascular with structures still represent a surgical challenge when compared with tumors of similar size but with a more regular shape. The former is associated with a more limited extent of resection and a higher risk of complications (5, 17).

The diaphragm is the dural sheath that separates the sella turcica from the chiasmatic cistern, leaving just an opening for the pituitary stalk (22, 23). The size and configuration of this opening may vary remarkably from 3 mm to 13 mm antero-posteriorly and from 3 mm to 15 mm on the lateral axis, physiologically (22–24). These variations in length and width might be the factors in determining the shape of the PA, and we can hypothesize that the competency of the diaphragm may influence the shape of the tumor and consequently the extent of resection.

Our study aims to analyze our surgical series of L-PAs and G-PAs according to their relationship with the diaphragm and invasion of CS and describe if the extent of resection can be predicted based on these factors.

Materials and methods

We performed a retrospective analysis of our consecutive surgical series on patients operated for PA between June 2011 and April 2020, and we extracted all tumors with a maximal diameter of ≥30 mm. They were classified into two types: large (30–39 mm, L-PAs) and giant (≥40 mm, G-PAs) tumors. Other tumors besides PAs arising from the sellar region or the pituitary stalk were excluded.

All patients were evaluated in the preoperative period using cerebral 1.5 or 3T MRI scanners (all Siemens, Erlangen, Germany) with 1.5-mm thick slices (or 2 mm on 1.5T scanners) with unenhanced sagittal T1-weighted spin-echo, coronal T2-weighted, dynamic coronal T1-weighted spin echo, and enhanced sagittal and coronal T1-weighted spin-echo sequences after gadolinium injection. An MRI with similar sequences was performed again 3 months after surgery.

We measured the size of the adenomas' cranio-caudal, medio-lateral, and antero-posterior diameters and defined the presence or absence of an invasion of the cavernous sinus through the application of Knosp classification. Tumors were classified as invading the cavernous sinus when the Knosp grade was >2, and the invasion of the medial wall of the cavernous sinus was confirmed during surgery. After the analysis of the preoperative MRI, we categorized the tumors according to their relationship with the diaphragm as follows (**Figure 1**):

- Grade 1: the adenoma extends to the suprasellar compartment through a wide incompetent diaphragm.
- Grade 2: the adenoma extends to the suprasellar compartment but stays infra-diaphragmatic due to a competent diaphragm.
- Grade 3: the adenoma extends to the suprasellar compartment despite a competent diaphragm through a small diaphragmatic opening resulting in a supra-diaphragmatic fragment (the typical dumbbell shape).
- Grade 4: the adenoma extends to the suprasellar compartment through a wide, incompetent diaphragm, invades the subarachnoid space, and becomes multilobulated with or without encasement of neurovascular structures.

In our surgical series, a classic endoscopic transsphenoidal surgery was performed using a uninostril approach. A medial transcavernous approach was performed to address the portion of the tumor invading the cavernous sinus. The transtubercular approach was performed for grade 3 or 4 tumors, to address the supradiaphragmatic portion and perform an extracapsular resection. When a transtubercular approach was planned, closure with a nasoseptal flap was performed to limit the risk of postoperative CSF leak. Transcranial surgeries were used in particular cases to complement the endonasal procedures in order to address extensions lateral to the internal carotid artery or when an invasion of the subarachnoid space was present, with encasement of neurovascular structures.

The surgical results were analyzed, and the extent of resection was classified as gross total resection (GTR) when no residual tumor was visible at 3-months postoperative MRI, near-total resection (NTR) when less than 5% of the initial tumor was left in place, and subtotal resection (STR) when a larger residual tumor was in place. Localization of postoperative residual tumor was also clearly defined.

All analyses were performed using the statistical software package STATA version 15 (College Station, TX, StataCorp LP). For categorical variables, $\chi^2$and Fisher's exact tests were performed. The significance level value was at $p < 0.05$.

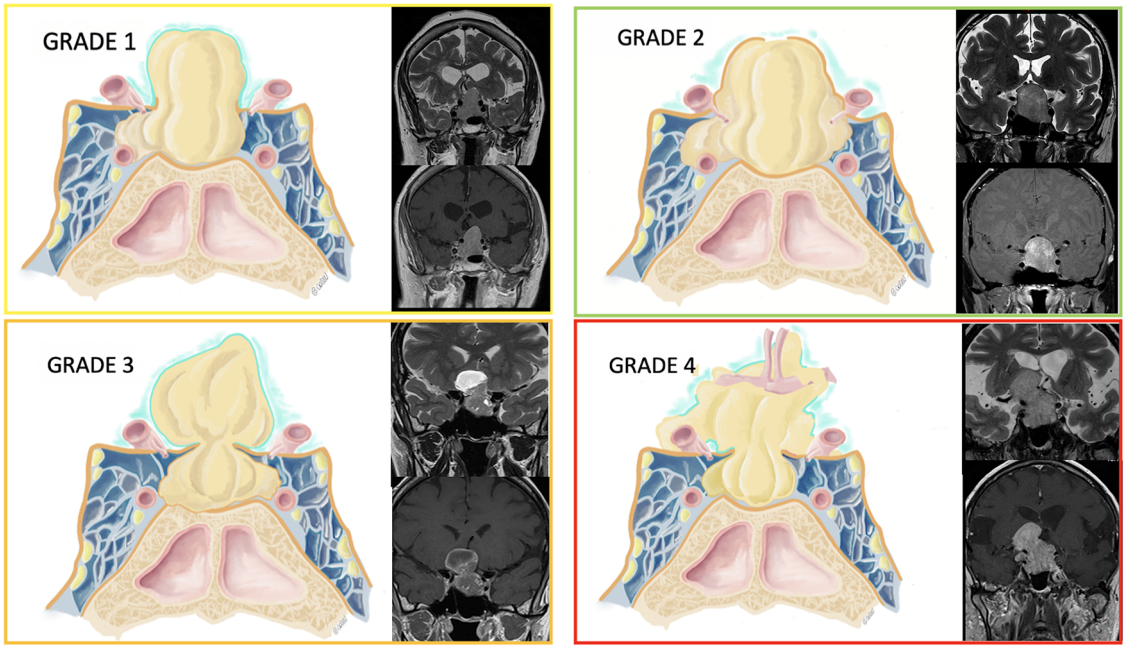

FIGURE 1
Tumors were classified according to their relationship with the diaphragm. A graphical representation is provided along with some examples of patients' MRI on the coronal plane (T2- and T1-weighted sequences after gadolinium injection).

Results

A total of 37 patients with L-PAs or G-PAs were operated by one of our senior authors (MM and RTD) during the aforementioned period. There were 20 male patients (54%) and 17 female patients (46%). The median age at the time of surgery was 57 years (range 29–88).

There were 23 out of 37 patients who presented G-PAs (62%) while 14 had L-PAs (38%). In 34 out of 37 patients, a non-functional adenoma was identified (91.9%), in two cases a prolactinoma (5.4%), and in another case an ACTH-releasing macro-adenoma (2.7%).

The clinical and radiological data of our cohort are detailed in Table 1. Preoperative MRI image analysis revealed that the mean maximal diameter was 38.3 mm (±5.9 mm) (range 30 mm–50 mm). The invasion of the cavernous sinus was assessed during surgery. Patients with Knosp 3a showed no invasion of the cavernous sinus and only a lateral displacement of the medial wall of the cavernous sinus, which remained intact. Thus, invasion of the cavernous sinus occurred in 17 out of 37 patients (46%), while there was no invasion in 20 cases (54%). Sixteen cases were suprasellar with a supradiaphragmatic component and a large opening of the diaphragm (grade 1, 43.3%), ten cases were only infra-diaphragmatic (grade 2, 27%), and only two were supradiaphragmatic tumors with a narrow diaphragmatic opening (grade 3, 5.4%). Nine patients presented had a multi-lobular morphology with the invasion of the subarachnoid space (grade 4, 24.3%) (Table 1).

GTR was obtained in 7 patients (19%), NTR in 17 (46%), and STR in 13 (35%). All patients with GTR required no further surgery. Twelve patients underwent multiple surgeries to improve the extent of the resection, but none of them obtained GTR. Nine patients underwent a second endoscopic procedure where a classic transsphenoidal approach was performed when the residual tumor descended into the sella, while an extended endoscopic approach was performed to address the intracavernous part in the medial portion of the cavernous sinus or to address the suprasellar component through a transtubercular approach. Three cases underwent a transcranial approach: one for apoplexy of the residual tumor after endoscopic surgery and two for a lateral extension into the middle cranial fossa.

Invasion of the cavernous sinus had a significant impact on the extent of resection, as GTR was significantly higher in the cohort of patients with no invasion (7/20 patients with no CS invasion vs. 0/17 patients with CS invasion, $p < 0.01$). Table 2 summarizes the location of residual tumors in our cohort of 30 patients.

All of the patients where GTR was possible belonged to grade 1, that is, they had supradiaphragmatic extension with a large opening of the diaphragm (Figure 2). When the GTR rate was compared across the different grades, the difference was statistically significant (Figure 3).

10.3389/fsurg.2022.962709

TABLE 1 Detailed clinical, pathological, and radiological data.

Mean age	57 years	29–88 years
Sex	Women	17 (46%)
	Men	20 (54%)
Clinical presentation	Visual disturbances	32 (86.5%)
	Headaches	12 (32.4%)
	Partial hypopituitarism	11 (29.8%)
	Total hypopituitarism	8 (22%)
	Secretory syndromes	3 (8.1%)
	Apoplexy	2 (5.4%)
	Incidental finding	1 (2.7%)
	Diabetes insipidus	0
Adenoma size	Large PAs	14 (38%)
	Giant PAs	23 (62%)
Immunohistochemistry	Non-functioning PA	34 (91.9%)
	• Gonadotroph	19
	• Silent	8
	• Null cell	7
	Functioning PA	3 (8.1%)
	• PRL secreting	2
	• ACTH secreting	1
Knosp grade	Knosp 0	1 (2.7%)
	Knosp 1	3 (8.1%)
	Knosp 2	5 (13.5%)
	Knosp 3a	11 (29.7%)
	Knosp 3b	6 (16.3%)
	Knosp 4	11 (29.7%)
Relationship with the diaphragm	Grade 1	16 (43.3%)
	Grade 2	10 (27%)
	Grade 3	2 (5.4%)
	Grade 4	9 (24.3%)

PA, pituitary adenoma.
Silent: non-functioning pituitary adenomas showing staining for a pituitary hormone at immunohistochemistry.

GTR was not achieved in any of the patients with grade 2 tumor. This could be attributed to the fact that when the diaphragm is competent, large and giant tumors have a tendency to develop towards the weaker area, which is the medial wall of the cavernous sinus. This was confirmed by our analysis, where grade 2 tumors presented a higher rate of cavernous sinus invasion when compared with grade 1 (70% vs. 12.5% respectively, $p < 0.01$). As expected, for grades 3 and 4, where only STR or NTR were obtained, cavernous sinus invasiveness was high (8/11 cases, $p = 0.003$). The distribution of the invasion of the cavernous sinus, according to the different grades that we propose, is summarized in **Table 3** and shown in **Figure 4**.

An example of the utility of a combined approach for a grade 4 tumor is reported in **Figure 5**.

The rate of surgical complications in this series was low. One patient had postoperative rhinorrhea and was treated with a second surgery (2.7%). Two patients had postoperative apoplexy and required trans-cranial surgery (5.4%). No new optic/oculomotor nerve palsies occurred following surgery in this series.

TABLE 2 Detailed surgical results.

Extent of resection	GTR	7 (19%)
	NTR	17 (46%)
	STR	13 (35%)
Second surgery		**TOT 12 pts**
	Endonasal endoscopic approach	9 (24%)
	Transcranial approach	3 (8%)
Localization of residual tumor		**TOT 30 pts**
	Middle cranial fossa	8 (27%)
	Cavernous sinus invasion	15 (50%)
	Posterior cranial fossa	1 (3%)
	Anterior cranial fossa	6 (20%)

GTR, gross total resection; NTR, near total resection; STR, subtotal resection.

Discussion

Surgical series dealing with L-PAs and G-PAs reported GTR in less than 50% of cases after a single surgical procedure (3, 11, 12, 17, 25). The dimensions of the tumor are not the main limiting factor in the performance of GTR; the shape seems to play an important role, as dumbbell-shaped and multilobulated PAs are respectively associated with decreased GTR, varying from 82% for round and oval PA to 0% for multilobulated PA (17, 20). Rather, it is universally accepted that the factors that preclude a complete resection are the hard consistency of the tumor, the invasion of the cavernous sinus. and the the invasion of the subarachnoid space (10, 11, 17, 21, 26).

Few classifications focused on G-PAs. One of the first was Goel's classification, which divided tumors into four grades according to the invasion and elevation of the roof of the cavernous sinus and the neurovascular encasement in the subarachnoid space (5). According to this vision, the diaphragm is in general stretched and elevated on the dome of the tumor. Recently, another classification was proposed, based on the antero-posterior, infero-superior, and lateral extensions (27). These classifications are based on tumor extension, and we agree with Micko et al. (28) that one important limiting factor for tumor resection is the neck to dome ratio, determining the feasibility of an endonasal approach for these tumors and the surgical nuances of the approach necessary to achieve a maximal resection, such as the section of the diaphragm. For tumors with large suprasellar extensions, it is well known that the diaphragm can be distended and displaced markedly in a superior direction above the tumors, even up to the third ventricle (5), but true dumbbell shape tumors are caused by a low diaphragm with a narrow opening. The anatomy of the diaphragm determines the manner in which the endonasal surgery is performed, and it dictates when a transtubercular

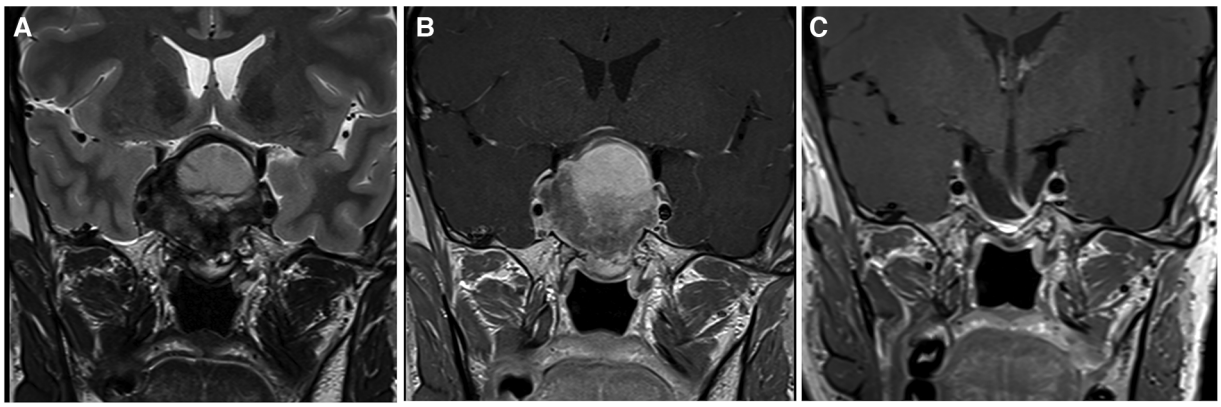

FIGURE 2
This large pituitary adenoma was classified as Knosp 3a and grade 1 according to the relationship with the diaphragm (Pictures A and B showing a coronal T2- and T1-weighted MRI after gadolinium administration, respectively). The diaphragm was wide open and the adenomas presented an oval shape. A gross total resection was possible through a classic endoscopic endonasal approach (Picture C), and no recurrent tumor is evident at 2 years of follow-up.

approach is necessary to access the large supradiaphragmatic component or when the incision of the diaphragm is required to have trans-diaphragmatic access.

Not much has been published about the conditions associated with a competent or incompetent diaphragm (22, 30), and some authors highlighted the role of intracranial hypertension and CSF dynamics (34–37). Campero et al. performed an anatomical study and classified their specimens into three groups according to the diaphragm opening: group A (<4 mm), group B (4–8 mm), and group C (>8 mm), assuming that the anatomic variability of the diaphragm opening, along with the morphology of the medial wall of the cavernous sinus, may explain the pattern of growth of pituitary tumors (22).

Thus, we studied the role of the diaphragm in determining the shape of Pas, as well as the relationship between the classification we proposed and the extent of resection performed. In group 1, when the diaphragm is large offering a natural passage to adenoma growth, the best results in terms of the extent of resection were achieved. All the tumors where GTR was possible in one single procedure could be categorized in group 1. This result was statistically significant compared with the other morphologies. Indeed, when the diaphragm is wide open, tumor resection through an endoscopic endonasal approach may be safely performed as a large working corridor is present, and the pulsating effect of CSF during surgery or specific maneuvers to increase the

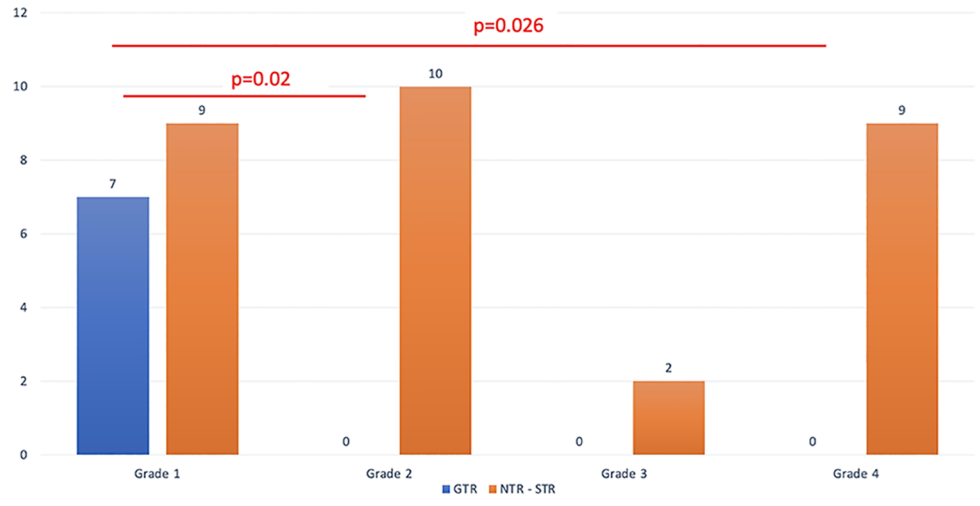

FIGURE 3
The extent of resection is detailed based on the relationship between the tumor and the diaphragm.

TABLE 3 The distribution of the different Knosp grades was detailed according to the relationship between the tumor and the diaphragm.

	Relationship with the diaphragm			
	1	2	3	4
Knosp grade				
Knosp 0	1	0	0	0
Knosp 1	3	0	0	0
Knosp 2	4	1	0	0
Knosp 3a	6	2	2	1
Knosp 3b	2	3	0	1
Knosp 4	0	4	0	7

intracranial pressure may help in the descent of residual tumor (28, 29). The value of endoscopic procedures to address these tumors was also addressed by Jin et al., and the authors reported an elevated rate of GTR (90%) (30).

At the same time, the absence of cavernous sinus invasion was associated with a higher rate of GTR, suggesting that the GTR observed in group 1 is dependent on parasellar extension and Knosp grade. Cavernous sinus invasion is a well-described limiting factor in the resection of sellar lesions, in particular when it extends lateral to the cavernous portion of the carotid artery (31, 32). We therefore could say that a higher rate of GTR can be associated with the morphology in group 1 for L-PAs and G-Pas and that this is higher when CS invasion is absent.

To summarize, three factors must be considered when planning the surgical procedure: the shape and tumor relationship to the diaphragm (proposed classification), the invasion of the cavernous sinus, and the hormonal secretion of the adenoma.

For grades 1 and 2, we performed a classic endoscopic approach. GTR was obtained as expected in a high proportion of patients with grade 1 tumors. However, in group 2, GTR was not achieved in any of the patients. This was related to the fact that when a large adenoma expands, it remains restricted superiorly by a competent diaphragm, and therefore, the tumor expands towards a zone of relatively less resistance called the infrasellar or parasellar space, through the medial wall of the cavernous sinus. In these cases, the limiting factor in obtaining GTR is the cavernous sinus invasion, and extended transcavernous approaches may be advised to obtain a greater resection.

In grade 3, the driving force of tumor growth pushes the adenoma through a small opening in a competent diaphragm, creating the typical dumbbell-shaped tumor. With this morphology, the supradiaphragmatic portion of the adenoma can be more difficult to access through a classic transsphenoidal endoscopic approach, as previously described. To obtain a greater extent of resection, a transtubercular extended transsphenoidal approach or a trans-diaphragmatic approach with incision of the diaphragm can be chosen (11). This procedure however requires a careful reconstruction of the skull base.

For multilobulated adenoma invading the subarachnoid space or the middle or anterior cranial fossae (grade 4), GTR through one single approach is extremely challenging (13–15). The complexity of surgery is secondary to the encasement of neurovascular structure in their cisternal portion and the lack of a well-defined tumor capsule (13, 14). A combination of

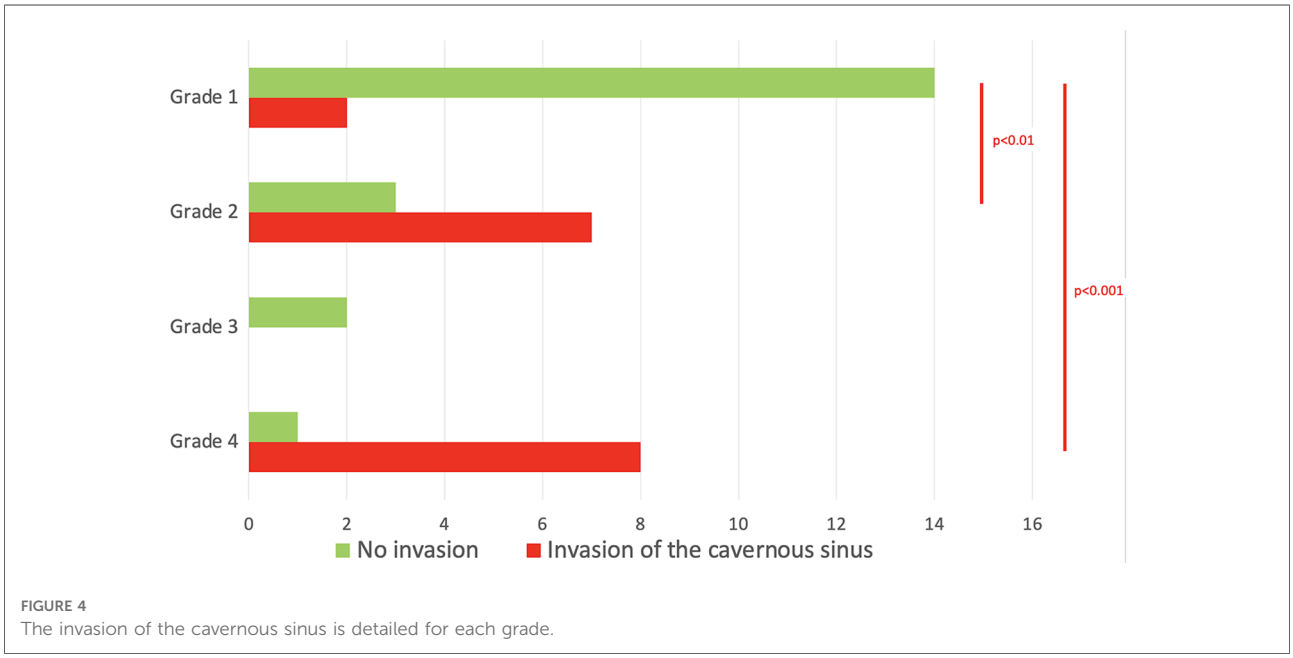

FIGURE 4
The invasion of the cavernous sinus is detailed for each grade.

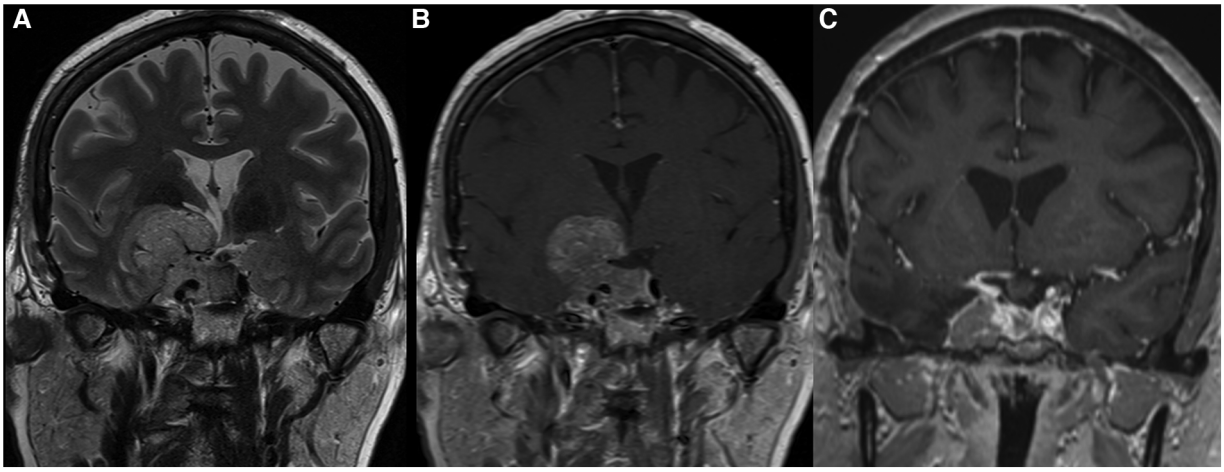

FIGURE 5
A giant macroadenoma showed invasion of the right cavernous sinus (Knosp 4), and it was classified as grade 4 according to the relationship with the diaphragm (Pictures A and B showing a coronal T2- and T1-weighted MRI after gadolinium administration, respectively). A combined approach through the use of a pterional approach and an endoscopic endonasal approach allowed to obtain a partial resection after addressing respectively the portion in the subarachnoid space and the sellar and suprasellar portion. The residual tumor in the right cavernous sinus (Picture C) was treated through Gamma Knife irradiation, and the tumor remained stable at 5 years of follow-up.

transcranial and endoscopic endonasal techniques should thus be considered (13, 16, 33). The timing between the two approaches depends on the size of the suprasellar extension.

Besides our classification and the invasion of the cavernous sinus, the hormonal secretion of the adenoma should be taken into consideration, as more aggressive approaches should be performed to obtain a biological remission with secreting tumors.

Experienced skull base surgeons and expertise in a tertiary care center are necessary when dealing with large, giant, invasive tumors, and a careful analysis of the relationship existing between the tumor and the diaphragm is mandatory to plan the surgery and predict the extent of resection after the procedure.

Limitations

Because this is a retrospective analysis of a tertiary care pituitary center about a rare pathology, we report a small surgical cohort, and the power of our statistical analysis may be limited, with no multivariate analysis possible. We were unable to determine the role of tumor consistency in predicting the extent of resection because, in order to perform a proper analysis of this factor, we need to exclude all the adenomas with CS invasion. Unfortunately, in our series, the power of our analysis was strongly reduced by the limited number of L- and G-PAs with no CS invasion.

Another limitation is represented by the fact that this proposed classification is based on subjective careful preoperative analysis rather than specific morphometric criteria.

Larger multicentric studies are mandatory to have an external validation and confirmation of the clinical and surgical relevance of our proposed grading system.

Conclusion

L-PAs and G-PAs are rare diseases in which GTR remains challenging. Careful radiological evaluation of the relationship between the tumor and the sellar diaphragm, and invasion of the cavernous sinus or the subarachnoid space are crucial factors in determining the surgical strategy and the possibilities of achieving gross total resection. When a wide opening of an incompetent diaphragm is present without invasion of the cavernous sinus, GTR is commonly achieved. In all other morphologies, GTR is more difficult to obtain, so extended endoscopic or combined approaches need to be considered.

In the drawings, the diaphragm is represented in orange, while the arachnoid is represented as a teal thinner layer.

- Grade 1: The adenoma is extending in the suprasellar compartment, and the diaphragm is wide open. As shown in the MRI, the diaphragm is not visualized on the dome of the tumor, which is only covered by a thin layer of arachnoid.
- Grade 2: The pituitary adenoma is extending in the suprasellar compartment, but stays infra-diaphragmatic (the diaphragm is competent). The diaphragm is visible as a thin hypointense line on T2-weighted sequences, and it delimitates the dome of the tumor.
- Grade 3: The adenoma is extending in the suprasellar and supradiaphragmatic compartment with a competent

diaphragm, giving a typical dumbbell shape to the tumor. The MRI shows a pituitary adenoma with a component in the suprasellar space. The opening of the diaphragm is narrow, thus limiting the access to the suprasellar component during a standard transsphenoidal approach.

- Grade 4: The adenoma is extending to the suprasellar compartment, it is multilobulated and invades the subarachnoid space, with a rupture of the arachnoid membrane (thin teal layer in the drawing) and a possible encasement of nervous and vascular structures (such as the anterior communicating complex as shown in the picture). The pituitary MRI shows a tumor with complex morphology, and the hypersignal of the mesial temporal lobe is evident on T2-sequences, witnessing an invasion of the subarachnoid space.

Data availability statement

The raw data supporting the conclusions of this article will be made available by the authors, without undue reservation.

Ethics statement

The studies involving human participants were reviewed and approved by CER-VD 2020-01338. Written informed consent for participation was not required for this study in accordance with the national legislation and the institutional requirements.

Author contributions

EH and GC analyzed the data and wrote the paper. MM conceived the paper and revised the radiology of all the cases. DRT critically revised the paper. All authors contributed to the article and approved the submitted version.

Funding

Open access funding was provided by the University of Lausanne.

Conflict of interest

The authors declare that the research was conducted in the absence of any commercial or financial relationships that could be construed as a potential conflict of interest.

Publisher's note

References

1. Gsponer J, De Tribolet N, Deruaz JP, Janzer R, Uske A, Mirimanoff RO, et al. Diagnosis, treatment, and outcome of pituitary tumors and other abnormal intrasellar masses. Retrospective analysis of 353 patients. *Medicine*. (1999) 78 (4):236–69. doi: 10.1097/00005792-199907000-00004

2. Saeger W, Ludecke DK, Buchfelder M, Fahlbusch R, Quabbe HJ, Petersenn S. Pathohistological classification of pituitary tumors: 10 years of experience with the German pituitary tumor registry. *Eur J Endocrinol*. (2007) 156(2):203–16. doi: 10.1530/eje.1.02326

3. Peto I, Abou-Al-Shaar H, White TG, Abunimer AM, Kwan K, Zavadskiy G, et al. Sources of residuals after endoscopic transsphenoidal surgery for large and giant pituitary adenomas. *Acta Neurochir*. (2020) 162 (10):2341–51. doi: 10.1007/s00701-020-04497-1

4. Ezzat S, Asa SL, Couldwell WT, Barr CE, Dodge WE, Vance ML, et al. The prevalence of pituitary adenomas: a systematic review. *Cancer*. (2004) 101 (3):613–9. doi: 10.1002/cncr.20412

5. Goel A, Nadkarni T, Muzumdar D, Desai K, Phalke U, Sharma P. Giant pituitary tumors: a study based on surgical treatment of 118 cases. *Surg Neurol*. (2004) 61(5):436–45; discussion 445–6. doi: 10.1016/j.surneu.2003.08.036

6. Iglesias P, Rodriguez Berrocal V, Diez JJ. Giant pituitary adenoma: histological types, clinical features and therapeutic approaches. *Endocrine*. (2018) 61(3):407–21. doi: 10.1007/s12020-018-1645-x

7. Cossu G, Jouanneau E, Cavallo LM, Froelichd S, Starnonia D, Giammatteia L, et al. Surgical management of giant pituitary neuroendocrine tumors: meta-analysis and consensus statement on behalf of the EANS skull base section. *Brain and Spine*. (2022) 2:100878. doi: 10.1016/j.bas.2022.100878

8. Trouillas J, Roy P, Sturm N, Dantony E, Cortet-Rudelli C, Viennet G, et al. A new prognostic clinicopathological classification of pituitary adenomas: a multicentric case-control study of 410 patients with 8 years post-operative follow-up. *Acta Neuropathol*. (2013) 126(1):123–35. doi: 10.1007/s00401-013-1084-y

9. Iglesias P, Arcano K, Trivino V, Guerrero-Perez F, Rodriguez Berrocal V, Vior C, et al. Giant non-functioning pituitary adenoma: clinical characteristics and therapeutic outcomes. *Exp Clin Endocrinol Diabetes*. (2021) 129(4):309–13. doi: 10.1055/a-1017-3288

10. Cappabianca P, Cavallo LM, Solari D, de Divitiis O, Chiaramonte C, Esposito F. Size does not matter. The intrigue of giant adenomas: a true surgical challenge. *Acta Neurochir*. (2014) 156(12):2217–20. doi: 10.1007/s00701-014-2213-7

11. Cappabianca P, Cavallo LM, de Divitiis O, de Angelis M, Chiaramonte C, Solari D. Endoscopic endonasal extended approaches for the management of large pituitary adenomas. *Neurosurg Clin N Am*. (2015) 26(3):323–31. doi: 10.1016/j.nec.2015.03.007

12. Komotar RJ, Starke RM, Raper DM, Anand VK, Schwartz TH. Endoscopic endonasal compared with microscopic transsphenoidal and open transcranial resection of giant pituitary adenomas. *Pituitary*. (2012) 15(2):150–9. doi: 10.1007/s11102-011-0359-3

13. Han S, Gao W, Jing Z, Wang Y, Wu A. How to deal with giant pituitary adenomas: transsphenoidal or transcranial, simultaneous or two-staged? *J Neurooncol*. (2017) 132(2):313–21. doi: 10.1007/s11060-017-2371-6

14. Nishioka H, Hara T, Usui M, Fukuhara N, Yamada S. Simultaneous combined supra-infrasellar approach for giant/large multilobulated pituitary

adenomas. *World Neurosurg*. (2012) 77(3–4):533–9. doi: 10.1016/j.wneu.2011.07.013

15. Honegger J, Ernemann U, Psaras T, Will B. Objective criteria for successful transsphenoidal removal of suprasellar nonfunctioning pituitary adenomas. *A prospective study. Acta Neurochir*. (2007) 149(1):21–9; discussion 29. doi: 10.1007/s00701-006-1044-6

16. Youssef AS, Agazzi S, van Loveren HR. Transcranial surgery for pituitary adenomas. *Neurosurgery*. (2005) 57(Suppl 1):168–75; discussion 168–75. doi: 10.1227/01.neu.0000163602.05663.86

17. Koutourousiou M, Gardner PA, Fernandez-Miranda JC, Paluzzi A, Wang EW, Snyderman CH. Endoscopic endonasal surgery for giant pituitary adenomas: advantages and limitations. *J Neurosurg*. (2013) 118(3):621–31. doi: 10.3171/2012.11.JNS121190

18. Messerer M, De Battista JC, Raverot G, Kassis S, Dubourg J, Lapras V, et al. Evidence of improved surgical outcome following endoscopy for nonfunctioning pituitary adenoma removal. *Neurosurg Focus*. (2011) 30(4):E11. doi: 10.3171/2011.1.FOCUS10308

19. Dehdashti AR, Ganna A, Witterick I, Gentili F. Expanded endoscopic endonasal approach for anterior cranial base and suprasellar lesions: indications and limitations. *Neurosurgery*. (2009) 64(4):677–87; discussion 687–9. doi: 10.1227/01.NEU.0000339121.20101.85

20. Berkmann S, Lattmann J, Schuetz P, Diepers M, Remonda L, Fandino J, et al. The shape grading system: a classification for growth patterns of pituitary adenomas. *Acta Neurochir*. (2021) 163(11):3181–9. doi: 10.1007/s00701-021-04912-1

21. Rutkowski MJ, Chang KE, Cardinal T, Du R, Tafreshi AR, Donoho DA, et al. Development and clinical validation of a grading system for pituitary adenoma consistency. *J Neurosurg*. (2020) 134(6):1800–7. doi: 10.3171/2020.4.JNS193288

22. Campero A, Martins C, Yasuda A, Rhoton Jr AL. Microsurgical anatomy of the diaphragma sellae and its role in directing the pattern of growth of pituitary adenomas. *Neurosurgery*. (2008) 62(3):717–23; discussion 717–23. doi: 10.1227/01.neu.0000317321.79106.37

23. Renn WH, Rhoton Jr AL. Microsurgical anatomy of the sellar region. *J Neurosurg*. (1975) 43(3):288–98. doi: 10.3171/jns.1975.43.3.0288

24. Rhoton AL J, Harris FS, Renn WH. Microsurgical anatomy of the sellar region and cavernous sinus. *Clin Neurosurg*. (1977) 24:54–85. doi: 10.1093/neurosurgery/24.cn_suppl_1.54

25. Juraschka K, Khan OH, Godoy BL, et al. Endoscopic endonasal transsphenoidal approach to large and giant pituitary adenomas: institutional experience and predictors of extent of resection. *J Neurosurg*. (2014) 121(1):75–83. doi: 10.3171/2014.3.JNS131679

26. Messerer M, Daniel RT, Cossu G. No doubt: the invasion of the cavernous sinus is the limiting factor for complete resection in pituitary adenomas. *Acta Neurochir*. (2019) 161(4):717–8. doi: 10.1007/s00701-018-03784-2

27. Shukla D, Konar S, Kulkarni A, Bhat DI, Sadashiva N, Devi BI, et al. A new comprehensive grading for giant pituitary adenomas: SLAP grading. *Br J Neurosurg*. (2022):1–8. doi: 10.1080/02688697.2022.2057432

28. Micko ASG, Keritam O, Marik W, Strickland BA, Briggs RG, Shahrestani S, et al. Dumbbell-shaped pituitary adenomas: prognostic factors for prediction of tumor nondescent of the supradiaphragmal component from a multicenter series. *J Neurosurg*. (2021):1–9. doi: 10.3171/2021.9.JNS211689

29. Jho HD, Carrau RL. Endoscopy assisted transsphenoidal surgery for pituitary adenoma. Technical note. *Acta Neurochir*. (1996) 138(12):1416–25. doi: 10.1007/BF01411120

30. Jin Z, Wu X, Wang Y. Clinical study of endoscopic treatment of a sellar pituitary adenomas with sellar diaphragm defect. *BMC Neurol*. (2020) 20(1):129. doi: 10.1186/s12883-020-01690-8

31. Fernandez-Miranda JC, Zwagerman NT, Abhinav K, Lieber S, Wang EW, Snyderman CH, et al. Cavernous sinus compartments from the endoscopic endonasal approach: anatomical considerations and surgical relevance to adenoma surgery. *J Neurosurg*. (2018) 129(2):430–41. doi: 10.3171/2017.2.JNS162214

32. Koutourousiou M, Vaz Guimaraes Filho F, Fernandez-Miranda JC, et al. Endoscopic endonasal surgery for tumors of the cavernous sinus: aseries of 234 patients. *World Neurosurg*. (2017) 103:713–32. doi: 10.1016/j.wneu.2017.04.096

33. Leung GK, Law HY, Hung KN, Fan YW, Lui WM. Combined simultaneous transcranial and transsphenoidal resection of large-to-giant pituitary adenomas. *Acta Neurochir*. (2011) 153(7):1401–8; discussion 1408. doi: 10.1007/s00701-011-1029-y

34. Ferreri AJ, Garrido SA, Markarian MG, Yanez A. Relationship between the development of diaphragma sellae and the morphology of the sella turcica and its content. *Surg Radiol Anat*. (1992) 14(3):233–9. doi: 10.1007/BF01794946

35. Maira G, Anile C, Mangiola A. Primary empty sella syndrome in a series of 142 patients. *J Neurosurg*. (2005) 103(5):831–6. doi: 10.3171/jns.2005.103.5.0831

36. Foley KM, Posner JB. Does pseudotumor cerebri cause the empty sella syndrome? *Neurology*. (1975) 25(6):565–9. doi: 10.1212/wnl.25.6.565

37. Brismar K, Bergstrand G. CSF Circulation in subjects with the empty sella syndrome. *Neuroradiology*. (1981) 21(4):167–75. doi: 10.1007/BF00367338

frontiers | Frontiers in Surgery

TYPE Original Research
PUBLISHED 05 September 2022
DOI 10.3389/fsurg.2022.990646

OPEN ACCESS

EDITED BY
Peng Zhao,
Capital Medical University, China

REVIEWED BY
Zhenxing Li,
Jinling Hospital, China
Zujue Cheng,
Second Affiliated Hospital of Nanchang University, China

*CORRESPONDENCE
Qing Liu
liuqingdr@csu.edu.cn

†ORCID
Qing Liu
orcid.org/0000-0001-7594-6798

SPECIALTY SECTION
This article was submitted to Neurosurgery, a section of the journal Frontiers in Surgery

RECEIVED 10 July 2022
ACCEPTED 03 August 2022
PUBLISHED 05 September 2022

CITATION
Li Y, Zhang C, Su J, Qin C, Wang X, Li Y and Liu Q (2022) Individualized surgical treatment of giant tuberculum sellae meningioma: Unilateral subfrontal approach vs. endoscopic transsphenoidal approach.
Front. Surg. 9:990646.
doi: 10.3389/fsurg.2022.990646

Individualized surgical treatment of giant tuberculum sellae meningioma: Unilateral subfrontal approach vs. endoscopic transsphenoidal approach

Yang Li[1], Chao Zhang[2], Jun Su[3], Chaoying Qin[1], Xiangyu Wang[1], Yue Li[1] and Qing Liu[1*†]

[1]Department of Neurosurgery in Xiangya Hospital, Central South University, Changsha, China, [2]Department of Neurosurgery, The First Affiliated Hospital of Zhejiang University, Hangzhou, China, [3]Department of Neurosurgery, Hunan Children's Hospital, Changsha, China

Objective: Giant tuberculum sellae meningiomas (TSMs) are deeply located in the suprasellar region and extensively compressed or encased in the surrounding neurovascular structures, making gross total resection (GTR) without postoperative visual impairment challenging. The authors presented individualized unilateral subfrontal approach and endoscopic transsphenoidal approach (ETSA) in a series of patients and elaborated on their advantages and indications in resecting giant TSMs.

Methods: A total of 38 patients with giant TSMs operated by a single surgeon between March 2012 and November 2021 were retrospectively reviewed. Patients underwent unilateral subfrontal approach and ETSA according to preoperative imaging characteristics. Tumor characteristics, surgical details, preoperative symptoms, and neurological outcomes of TSMs patients were collected and analyzed.

Results: In 31 patients operated with the unilateral subfrontal approach, total resection (Simpson grade I or II) was achieved in 27 patients (87.0%), while 6 patients (85.7%) achieved GTR in 7 patients using ETSA. The postoperative visual improvement was maintained in 22 (81.5%) and 5 patients (83.3%). Recurrence or progression was only observed in 2 (7.4%) patients operated with the unilateral subfrontal approach. There was no mortality in our series.

Conclusions: Preoperative imaging and visual function are important for surgical approach selection. Maximum tumor resection and optic nerve protection can be achieved concurrently by taking advantage of these surgical approaches. The cerebral artery protection strategies and individualized surgical techniques provide great utility in improving a patient's quality of life.

KEYWORDS

tuberculum sellae meningioma, endoscopic transsphenoidal approach, unilateral subfrontal approach, skull base surgery, visual function

Introduction

As one of the most common meningioma in the skull base, tuberculum sellae meningiomas (TSMs) account for 5%–10% of intracranial meningiomas (1). TSMs originate from the dura of the tuberculum sellae, chiasmatic sulcus, and limbus sphenoidale (2). These tumors were located in the suprasellar space and tend to compress the optic chiasm and optic nerves. Most of the patients were presented with progressive vision loss and visual field defects (3, 4). Except for nerves/chiasm, giant TSMs (maximum diameters ≥3 cm) usually encase vital neurovascular structures, including the carotid artery, forebrain arteries, and pituitary gland–making gross total resection (GTR) of the tumor while preserving neurological functions challenging (5, 6). The postoperative visual deterioration rates from 2.1% to 44%, and GTR rates range from 65% to 90% (7–10). However, due to the limitation of stereotactic radiotherapy, three-dimensional conformal radiotherapy, and modulated radiation therapy (10, 11), microsurgical resection is still the primary treatment for TSMs.

The primary goal of the TSMs surgery was achieving gross total resection while preserving optic nerve functions during the past few decades. Multiple transcranial microsurgical approaches have been developed to achieve this goal, including the frontolateral approach, pterional approach, lateral supraorbital approach, and unilateral approach (9, 12–15). However, with advances in endoscopy and the development of innovative strategies in the expanded endonasal approach (16, 17), the endoscopic transsphenoidal approach (ETSA) seems to have gained more acceptance in the surgical treatment of TSMs (18–20). ETSA offered a better visualization, minimized the additional surgical damage, and avoided the contraction of the optic nerve during TSM surgery (21, 22). However, there have been many controversies over indications for ETSA, especially in the surgical resection of giant TSMs.

According to recent reports and our experiences, giant TSMs were defined as meningiomas larger than 3 cm in at least one of the three-dimensional planes and extended laterally on either side of the internal carotid arteries or optic nerves (7). Giant TSMs tend to invade the adventitia of the anterior cerebral artery (ACA), extended laterally to the internal carotid artery (ICA), eroded the bone of the skull base, and calcified central tumor zone. These characteristics make gross total resection of TSMs *via* ETSA challenging and entail greater risk of artery and nerve injury. Thus, transcranial approaches became the preferred method for surgical treatment giant TSMs.

In this research, we reviewed the characteristics and outcomes of 38 consecutive patients with giant TSMs operated by the senior author (Qing Liu). We described our experience in selecting unilateral subfrontal approach or ETSA for the surgical treatment of giant TSMs. We specifically evaluated the advantages of the two approaches and proved that individualized surgical strategies provide a better prognosis for patients.

Materials and methods

Study design

Between March 2012 to November 2021, 38 consecutive patients diagnosed with TSMs were retrospectively analyzed. The patients who participated in this study were operated on by the senior author (Qing Liu) using the unilateral subfrontal approach and ETSA at the Department of Neurosurgery, Xiangya Hospital, Central South University. Only meningiomas not less than 3 cm in at least one of the three-dimensional planes and originated from the tuberculum sellae were included in this study. Neuroimaging, intraoperative video, and neurofunctions were recorded and analyzed. Meningiomas originating from the diaphragm sellae, anterior clinoid, cavernous sinus, and anterior skull base with secondary involvement of the parasellar region were excluded.

Evaluation of tumor characteristics

Tumor characteristics, including tumor dimension, depth of the sella turcica (ST), the angle between the planum sphenoidale (PS) and ST, and tumor extension were evaluated by preoperative contrast-enhanced magnetic resonance imaging (MRI) and computed tomography angiography (CTA), which were confirmed by intraoperative observation. To evaluate the relationship between tumor and surrounding vascular structures, patients underwent contrast-enhanced MRI and CTA before surgery. Visual functions were evaluated at the ophthalmology department of our institute.

Unilateral subfrontal approach

The unilateral subfrontal approach provides a larger field of vision to resect large TSMs than ETSA and the indications for the approach include: (1) the preoperative images indicated that the tumor extended to the optic canal; (2) the tumor was calcified and resulted in stenosis of cranial arteries; (3) tumor extended laterally to the ICA; (4) the ICA, ACA and their perforating branches were encased extensively by the tumor; and (5) the extensive calcification of the skull base (tuberculum sella, anterior clinoid, and anterior skull base), which need to drill the involved bone and skull base reconstruction. Patients were positioned supine, and their heads were rotated 20°–30° to the contralateral side and retroflexed 10°–20° to reduce frontal lobe retraction. The

incision of the unilateral subfrontal approach was initiated above the palpated zygoma and continued superiorly behind the hairline toward the limit of the contralateral hairline. To avoid injury to the frontal branch of the facial nerve, the subgaleal scalp along with the temporal muscle is split and retracted toward the zygomatic arch. The bone flap was made by using the craniotome, and the superciliary arch can be identified and act as the baseline of the bone flap (**Figure 1A**). A temporal craniotomy was added when the tumor extended laterally. Under microscopic view, the dura mater was cut, followed by elevating the frontal lobe using a self-retaining brain retractor (**Figure 1B**). Tumor debulking was performed after identification of ICA, an optic nerve encased by the tumor. Dissection proceeded from the ICA to the ACA and anterior communicating artery (AComA). The arachnoid plane between the tumor and the optic nerve or artery should be maintained carefully because it can act as a barrier to protect the perforating branches and blood supply of the optic nerve. The residual portion of the tumor was removed in a piecemeal fashion using a microscissor and bipolar forceps. Only when the tumor was too hard for resection using an ultrasonic surgical aspirator or invade the adventitia of the ICA, we must leave the residual tumor in this area and then perform postoperative stereotactic radiotherapy. All hyperostotic bone was removed with a high-speed drill. The dural attachment of the tumor was resected and coagulated. The tuberculum sellae, planum sphenoidale, and frontal sinus were then tamponaded with bone wax and covered with part of the subgaleal scalp and the temporal muscle in case of cerebrospinal fluid leakage. The extent of tumor resection was evaluated according to the Simpson grading scale (23).

Endoscopic transsphenoidal approach

ETSA was also applied to the patients with giant TMSs, significantly when the tumor extended superiorly to the anterior skull base or inferiorly to the sellar region but was limited to the medial of the optic nerve. The indications for ETSA were as follows: (1) extension of the tumor limited in the sella or suprasellar region; (2) tumor growth in the medial and inferior sides of the optic nerve; (3) tumor was soft and loosely adherent to the arteries or optic nerve; (4) tumor base centered around tuberculum sella without extensive extension; (5) The angle between PS and the ST was smaller than 90° (**Supplementary Figure S1**); and (6) The depth of the ST was larger than 1 cm (**Supplementary Figure S1**). The patients were positioned supine and their heads were fixed by a Mayfield headrest. Under the endoscopic vision, the sphenoid sinus and the sphenoid ostia were identified (**Figure 1C**). The nasoseptal flap should be dissected and preserved carefully. Then, the middle and superior turbinate were exposed and resected. Drilling of the bone started from the sella, followed by the planum sphenoidale, and finally the tuberculum sellae. Before opening the dura, the position of the ICA must be confirmed again by endoscopic visualization. The dura below and above the diaphragma sellae was cut and coagulated. Extensive coagulation was performed to reduce the extradural blood supply of the tumor. To reduce tumor volume, the tumor base was debulked and removed in small pieces by dissection. The arachnoidal dissection plane between the tumor and the optic nerve or ACA should be established and maintained, as the plane was necessary for efficient total resection. In particular, the pituitary gland and stalk which can be found at the posterior margin of the tumor should be

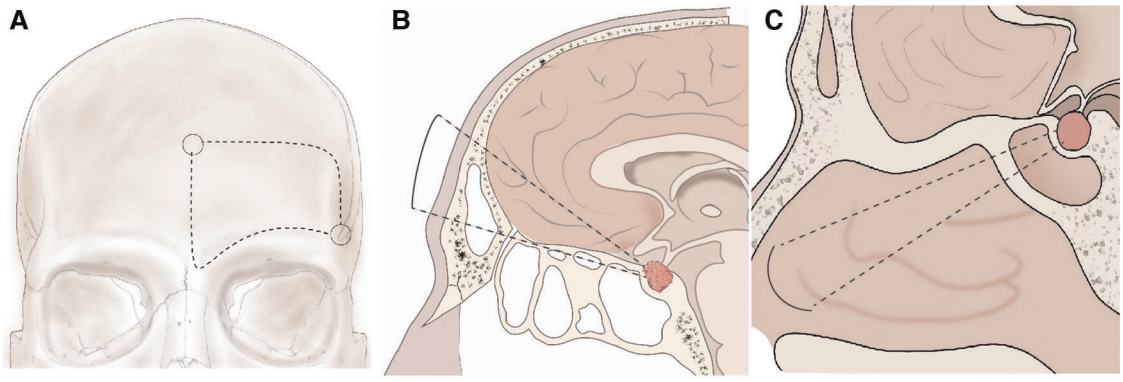

FIGURE 1
Schema of the unilateral subfrontal approach and ETSA. (**A**) The bone flap using in the unilateral subfrontal approach. One key burr hole (arrow) was placed behind the frontozygomatic process and below the superior temporal line. The other was placed in the midline above the nasion. (**B**) After unilateral subfrontal craniotomy, extradural dissection was performed in the central portion of the anterior cranial fossa around the cribriform plate. Elevation of the subfrontal dura from the planum sphenoidale can access tumor extension superior to the suprasellar region. (**C**) After drilling the bone of the sella, planum sphenoidale, and the tuberculum sellae, the dura was exposed and coagulated. The tumor in the sellar and suprasellar can be removed under endoscopic vision.

preserved and dissected carefully. A 30° view angle endoscope was used to find and remove residual tumors extended beyond the surgical field. After the tumor was removed completely, the skull base defect was firstly repaired with an artificial dura mater, then covered by a vascularized nasoseptal flap, and the nasal cavity was packed with Vaseline gauze finally.

Vascular protection strategies

Preoperative CTA indicated that giant TSMs tend to compress, dislocate, or even encase multiple intracranial arteries, including ICA, ACA, AcomA, middle cerebral artery (MCA), and basilar artery (BA). In most cases, the ICA and MCA were dislocated posterolaterally, and the AcomA and BA were dislocated posteriorly. With the help of preoperative imaging, the localization of the dislocated or encased arteries can be identified easier. Furthermore, cranial artery stenosis proved by preoperative CTA usually indicated that the adventitia was invaded by the tumor, making gross total tumor resection entail a huge risk of artery injury.

After opening the dura mater, the ipsilateral ICA should be identified first. Then, the arachnoidal dissection plane between ICA and the tumor should be followed and maintained. The plane can act as a physical barrier to protect ICA against operative injury. The arterial supply of the chiasm and optic nerve mainly arises from the superior hypophyseal arteries, which course through the inferior surface of the optic nerves. Thus, dissection of the tumor beneath the optic nerve entails a greater risk of superior hypophyseal artery injury. Superior hypophysial artery (SHA) arising from the ICA trunk and pushed backward by the tumor. Efforts must be made to dissect the artery from the tumor to prevent pituitary disorder. When the tumor invaded the adventitia of intracranial arteries, the arachnoidal plane between the tumor and artery was interrupted. Under this circumstance, aggressive tumor resection might injure the artery. The residual tumor was left in this area and treated with postoperative stereotactic radiotherapy.

Management of the optic nerve

TSMs impair vision acuity or visual field by directly compressing optic nerves and optic chiasm or decreasing the vascular supply of the optic nerves and optic chiasm. Thus, vulnerable optic nerves and optic chiasm entail a higher risk of intraoperative injury. Preoperative MRI images were used to estimate the relationship between tumor and optic nerve. Through the images, we can also find TSMs usually located in the suprasellar region with extending to the ipsilateral optic canal, dislocating the optic chiasm posteriorly and the optic nerves laterally. Thus, we can easily confirm the localization of neurovascular structures, such as optic nerves and chiasm. When tumors invade into the optic canal extensively, we sectioned the falciform ligament and drilled the roof of the optic canal at the very beginning of the surgery. Because the sharp margin of the falciform ligament may result in severer intraoperative injury of the optic nerve. Furthermore, opening the optic canal enlarged the space for resection of the tumor invading into the optic canal.

To improve the visual acuity of TSMs patients, the blood supply of the optic nerve and optic chiasm should be protected carefully. However, giant TSMs commonly extend inferomedially to the optic nerve or even encase it. The arterial supply of the chiasm and optic nerve mainly distally along the inferior surface of the optic nerves, dissection of the tumor must remain in the arachnoid plane intact and proceed on the superior surface of the optic nerve. Ophthalmic artery arising from the ICA trunk and coursing on the superior surface of the canalicular segment of the optic nerve. To avoid injury, all perforating arteries in the optic canal and orbit must be preserved. In conclusion, optic canal unroofing, preservation of the blood supply, and dissection along the arachnoid plane increase the rate of improved postoperative optic nerve function.

Result

Patient population

A total of 38 consecutive patients (15 males and 23 females) diagnosed with giant TSMs (maximal diameter $\geq$3 cm) were retrospectively analyzed. The median age was 47.7 years for all patients. The unilateral subfrontal approach was used in 31 patients, while the ETSA was applied in seven patients. The average length of surgery was longer for ETSA (6.3 h) compared with the unilateral subfrontal approach (4.2 h). However, the length of hospital stays in patients performed with the ETSA (4.7 days) was shorter than the unilateral subfrontal approach (7.3 days). The most common presenting symptoms were visual impairment (89.2%), visual field defect (65.8%), and headache (52.6%). The Karnofsky Performance Scale (KPS) was used to assess the life quality of the patients, and the mean KPS was 71.4 ± 7.4 preoperatively. All the removed meningiomas were confirmed by pathological examination.

Tumor characteristics

TSMs originate from the dura of the tuberculum sellae, chiasmatic sulcus, limbus sphenoidale, and growing upward in the suprasellar region were included. Through preoperative imaging and intraoperative observation, we found that giant

TSMs often compress or encase the neurovascular structures of the sellar, suprasellar, and parasellar region extensively, including the optic nerve, optic canal, pituitary gland, anterior clinoid, cavernous sinus and so on (Table 1). Optic nerve and optic chiasm compression were exhibited in almost all patients (31 and 29 patients) with giant TSMs. By contrast, the number of tumors that extend laterally to the sphenoid ridge or cavernous sinus lateral wall was only observed in nine patients. Similarly, tumor calcification and edema were only found in 12 and 6 patients (Table 1). We can conclude that in patients operated with the unilateral subfrontal approach, TSMs usually invaded extensively the planum sphenoidal, suprasellar and parasellar region, and optic canal, and the angle between PS and ST was larger than 90°. However, in patients operated with ETSA, the tumor growth was limited in the suprasellar and sellar region and the consistency was softer, but the depth of the ST was larger. In conclusion, we were able to choose which surgical approaches could be performed by evaluating the above characteristics.

Cranial artery involvement

The preoperative imaging and intraoperative observation indicated the involvement of the tumor with the ICA, ACA, AcomA, and MCA. According to Romani's classification (15), we classified the relationship between tumor and arteries into attachment, dislocation, and encasement based on preoperative imaging and operative observation. Giant TSMs mainly involve ICA, ACA, AcomA, and its perforating branches (SHA), whereas MCA was only involved in a few large TSMs which extend laterally (Table 2). We can also conclude that when the tumor was extended laterally and involved in the MCA, only the unilateral subfrontal approach can be applied to achieve total resection.

TABLE 1 Clinical characteristics of patients with giant TSMs.

Characteristics	No. of patients	
	Subfrontal approach	ETSA
Tumor dimension, median (cm)	3.7	3.1
Depth of the sella turcica (cm)	1.2	1.9
The angle between PS and ST (°)	101.1	88.5
Planum sphenoidal extension	29	3
Tuberculum sellae hyperostosis	10	3
Sellar region extension	25	7
Pituitary gland involvement	30	6
Optic nerve compression	31	7
Optic chiasm compression	29	6
Optic canal involvement	9	0
Intraorbital extension	6	0
Cavernous sinus involvement	9	0
Sphenoid ridge extension	9	0
Tumor calcification	12	0
Tumor Consistency (hard)[a]	13	1
Brain edema	6	0

ETSA, endoscopic transsphenoidal approach; ST, sella turcica.
[a]Tumor consistency was defined as hard when the tumor could not be aspirated even with an ultrasonic surgical aspirator.

Surgical results

The extent of tumor resection was evaluated by the Simpson grading scale. Total resection (Simpson grades I and II) was achieved in 33 patients. Subtotal resection (Simpson grade III) and partial resection (Simpson grade IV) were achieved in 3 and 2 patients, respectively (Table 3). We found there was no significant difference in total removal of the tumor when compared with the unilateral subfrontal approach and the ETSA ($p > 0.99$), but this result still needed to be proven in a multicenter study. In patients performed with the unilateral subfrontal approach, two patients achieved Simpson III grade resection because of adventitia invasion, and two achieved Simpson IV owing to the tumor calcification and densely adherent to the ICA and ACA. In patients performed with ETSA, Simpson III grade resection was achieved in 1 patient because the tumor grew laterally over the optic nerve, but the preoperative MRI missed it.

Neuroophthalmological outcome

Visual deficit was present in 32 patients preoperatively (Table 4). Among all 38 patients, 31 patients were treated with the unilateral subfrontal approach, the rest 7 patients were treated by ETSA. The visual function of most patients (25 patients) improved or remained stable after the surgery. Only a few patients (6 patients) suffered from postoperative visual deterioration. There was no difference in visual improvement between the subfrontal approach and the ETSA in our series ($p = 0.984$), which was different from other studies that have shown more visual improvement with the ETSA.

Tumor recurrence and follow up

All 38 patients were followed up regularly by the first author at 6-month intervals for the first year, and annually thereafter. Follow-up was performed with contrast-enhanced MRI and clinical status. The actual follow-up time ranges from 6 to 120 months (mean, 66.1 months). The mean KPS evaluated in patients at follow-up was 86± 7.7 months. Five patients with

TABLE 2 The relationship between the giant TSMs and cerebral arteries.

Artery	Classification	Subfrontal approach		ETSA		Total No. (%)
		Unilateral	Bilateral	Unilateral	Bilateral	
ICA	Attachment	5	10	1	3	19 (50)
	Dislocation	13	5	3	1	22 (57.9)
	Encasement	8	2	0	0	10 (26.3)
ACA	Attachment	7	3	1	1	12 (31.6)
	Dislocation	5	12	2	3	22 (57.9)
	Encasement	2	9	1	1	13 (34.2)
AcomA	Attachment	5		2		7 (18.4)
	Dislocation	17		3		20 (52.6)
	Encasement	9		2		11 (28.9)
MCA	Attachment	2	3	0	0	5 (13.2)
	Dislocation	5	7	0	0	12 (31.6)
	Encasement	3	2	0	0	5 (13.2)
SHA	Attachment	4	2	1	1	8 (21.1)
	Dislocation	8	13	1	3	25 (65.8)
	Encasement	4	8	0	2	14 (36.8)

ICA, internal carotid artery; ACA, anterior cerebral artery; AcomA, anterior communicating artery; MCA, middle cerebral artery; SHA, superior hypophysial artery.

TABLE 3 The extent of resection in patients using different surgical approaches.

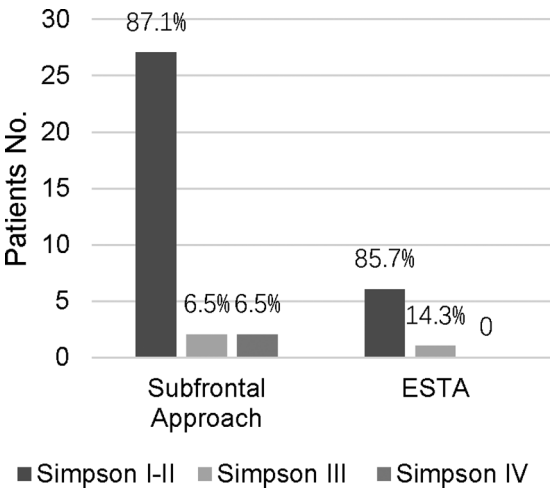

TABLE 4 Results of visual acuity in relation to tumor size.

Visual symptoms	No. of patients		*p*-value
	Subfrontal approach	ETSA	
Preop			
Yes	27	5	0.302
No	4	2	
Postop			
Improved	15	4	0.984
Worsened	6	0	
Stable	10	3	

ETSA, endoscopic transsphenoidal approach.

residual tumors received stereotactic radiotherapy 3 months after the surgery. There was no recurrence at the follow-up.

Discussion

In this study, we have elaborated the surgical techniques of the unilateral subfrontal approach and ETSA, which can be applied to the individualized surgical treatment of giant TSMs. Preoperative imaging was performed routinely to guide individualized surgical strategy making. Instead of being limited to one single surgical approach, we applied the unilateral subfrontal approach and the ETSA to 38 patients with giant TSMs according to their tumor characteristics. Owing to making full use of the advantages of the subfrontal approach and the ETSA, the GTR of giant TSMs was up to 86.8%, while the postoperative optic nerve dysfunction rate was only 15.8%.

In 1916, Cushing performed the first total surgical resection of TSM (1) and operated on 24 cases of tuberculum sellae meningiomas within 20 years. Since then, the transcranial approach has been the primary treatment for TSM. Nowadays, multiple transcranial approaches have been developed and applied to the surgery of TSM, such as the pterional approach (1, 14, 24), lateral supraorbital approach (15), subfrontal approach (6, 25), and interhemispheric approach (26). However, there were still many controversies about which approaches can be applied to achieve GTR better while improving the optic nerve function. For example, the pterional approach can visualize the ICA and minimize the retraction of the frontal lobe easily, but with narrow space and angle and a higher risk of profuse bleeding (14). In most of our surgical series, the

unilateral subfrontal approach was the primary surgical approach applied to resect giant TSMs (Figure 2). Compared with other traditional surgical approaches, the unilateral subfrontal approach provides a better medial view of the suprasellar region and is more flexible to achieve GTR when the tumor extends laterally or upward. For instance, when the tumor is extended laterally, the unilateral subfrontal approach combined with the pterional approach allowed us access to the sellar, suprasellar, and parasellar region to achieve GTR easily.

With the advancement of endoscopic technology, which provides better visualization and less invasion during operation, it is now possible to safely resect TSMs by ETSA. Hae-Dong Jho performed the first total surgical resection of TSM by a pure endoscopic approach in 2001 (27). Since then, the ETSA has been developed and widely applied to the surgical treatment of TSMs (28–30). In theory, ETSA avoids some surgical complications by approaching the TSM through the dura base, thereby minimizing the contraction of the frontal lobe, olfactory

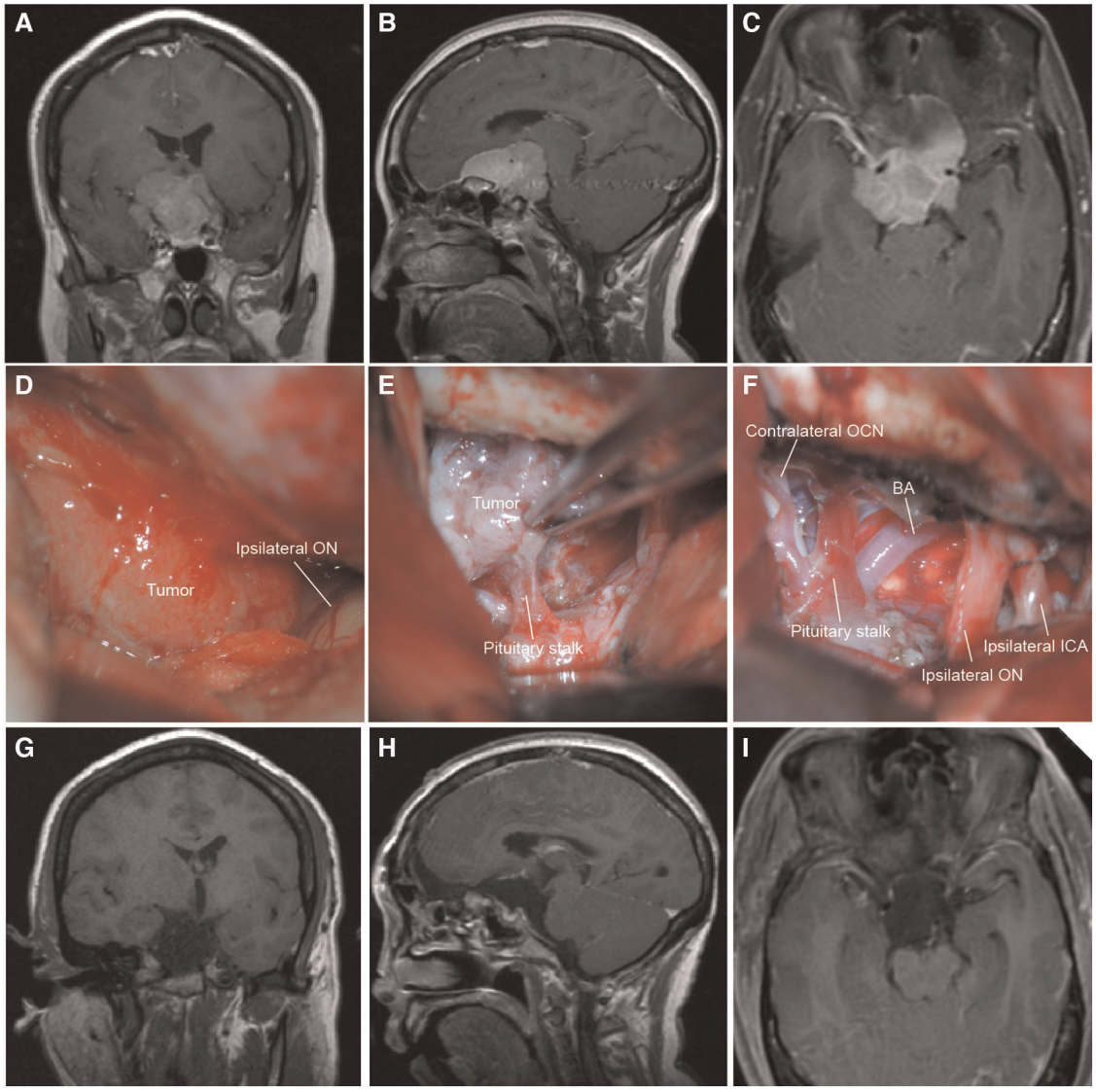

FIGURE 2
The MRI and intraoperative view of a patient operated with the unilateral subfrontal approach. (**A–C**) Preoperative T1-weighted MRI scan showing the giant TSM (maximal diameter = 4.4 cm) extended lateral to the ICA and encased neurovascular structures of the suprasellar region. (**D,E**) Intraoperative microscopic view showing the tumor through the right bilateral subfrontal approach. The ipsilateral optic nerve was displaced laterally and the pituitary was encased by the tumor. (**F**) Intraoperative microscopic view after total tumor resection. The ipsilateral ICA and optic nerve were preserved. (**G–I**) Postoperative T1-weighted MRI scan confirming total tumor removal. BA, basilar artery; OCN, oculomotor nerve; ICA, internal carotid artery.

nerve, and optic nerve. Therefore, the postoperative visual loss rate in patients with ETSA was only 1.3%, compared with 9.2% in patients operated transcranially (31). For patients, the ETSA was minimally invasive, more comfortable, and hospital stay were often shorter (32, 33). The ETSA also provided a clear visualization of perforators of the optic nerve and pituitary stalk, making preservation of the blood supply of the optic nerve and pituitary gland possible (34). In conclusion, ETSA has multiple advantages in the surgical treatment of TSMs (maximal diameters <3 cm). However, multiple problems still need to be solved when applying the ETSA to the treatment of giant TSMs (maximal diameters ≥3 cm). For example (1) giant TSMs extend over the optic nerve to the optic canal or above and lateral to the anterior clinoid process cannot be resected; (2) the incidence of cerebrospinal fluid leakage was high as 20%–30% (28); (3) tumor grow laterally and densely adherent or invade the cavernous; (4) patients have critical basic diseases and cannot bear long time operation.

To achieve maximal tumor resection and preservation of visual function Indications, we applied individualized surgical approach for patients with TSM based on preoperative

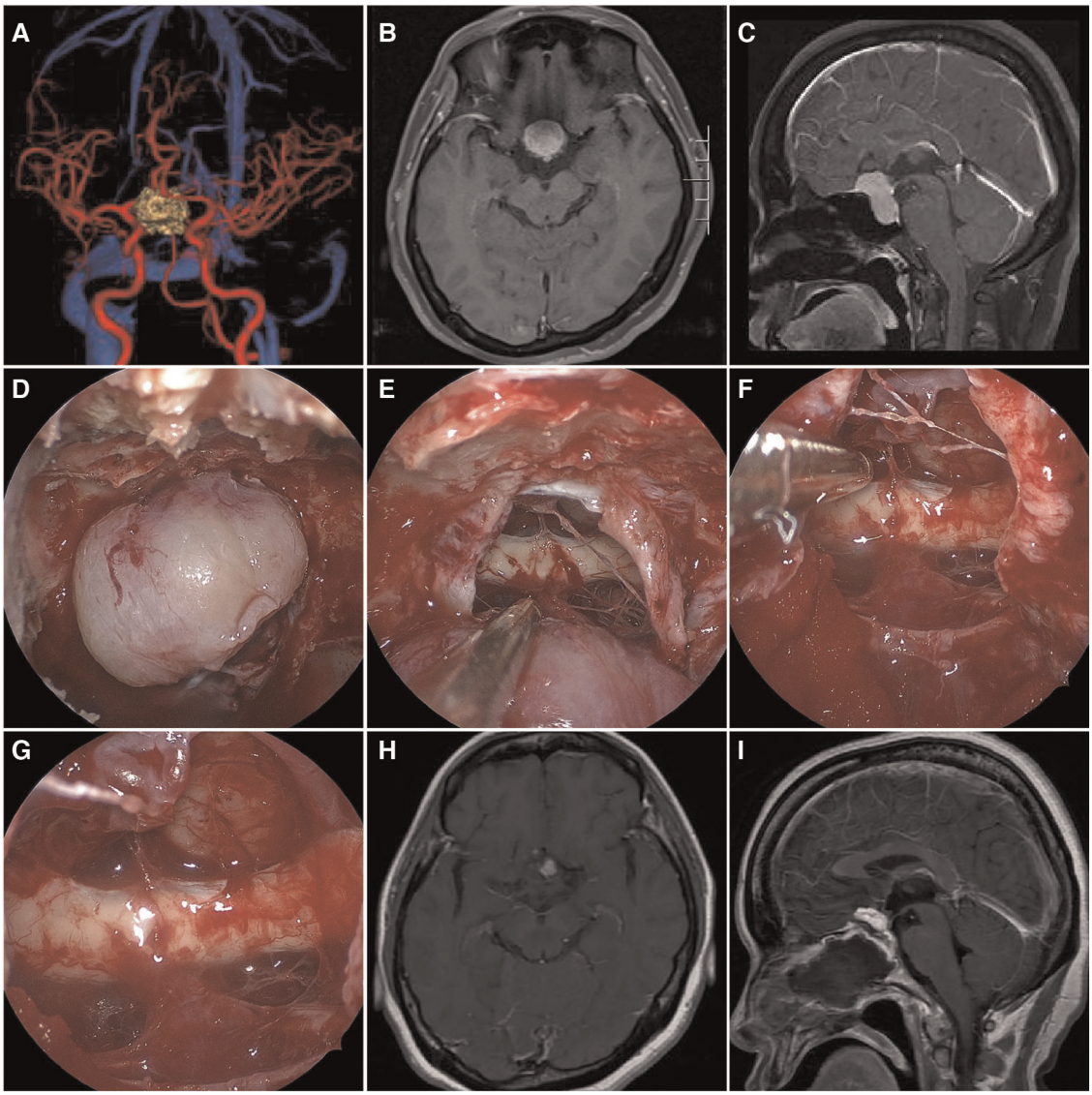

FIGURE 3
The MRI and intraoperative view of a patient operated with the ETSA. (**A**) Preoperative CTA has shown the bilateral ICA and ACA were compressed by the tumor. (**B**,**C**) Preoperative T1-weighted MRI scan showing the giant TSM (maximal diameter = 3.1 cm) growth limited in the bilateral ICA. (**D**,**E**) Intraoperative microscopic view showing the tumor and the optic chiasm after opening the dura. (**F**,**G**) The tumor was totally removed, while the bilateral optic nerve and pituitary stalk were preserved. (**H**,**I**) Postoperative T1-weighted MRI scan confirming tumor removal.

imaging characteristics. For example, when the angle between the PS and ST was less than 90° or the depth of the sella turcica larger than 1 cm, the unilateral subfrontal approach was difficult to remove the tumor invaded into the sellar region and making total resection impossible, we would choose the ETSA for tumor resection. However, when we found the tumor extended extensively and invaded into the arteries, the unilateral subfrontal approach was the primary approach for tumor removal. In 31 giant TSMs patients operated through the subfrontal approach, total tumor removal (Simpson grades I and II) was achieved in 27 patients. Only five patients suffered from postoperative brain edema, and six from visual acuity deterioration. In our series, ETSA only applied to seven giant TSMs (**Figure 3**). Among seven patients who underwent ETSA, total tumor resection (Simpson grades I and II) was achieved in six patients. The postoperative visual improvement was observed in four cases. The mean in-hospital day was only 4.7 days, compared with 7.3 days for patients who underwent the subfrontal approach. However, the risk of pituitary dysfunction and cerebrospinal fluid leakage may be higher in patients undergoing ETSA. These complications may result from excessive manipulation of the pituitary gland during sphenoidal bone removal and injury of the blood supply of the pituitary gland.

Postoperative visual deficits were both found in patients who underwent the subfrontal approach and the ETSA, but the visual deficits of the two approaches were not statistically significant. According to large-scale reports, the ETAS seems to be the primary approach to achieving better visual outcomes in the surgical treatment of TSMs (27–29). The vision improvement rate ranged from 59% to 87% in patients who underwent the ETSA, but the rate was only 25%–61% in patients who underwent the transcranial approach (27–29). However, the vision improvement rate was not statistically different in our series. This difference may be attributed to tumor size, as we only included the giant TSMs (maximum diameters ≥3 cm) in our research. In our experience, giant TSMs tend to densely compress the optic nerve and interrupt the blood supply of the optic nerve, making the deterioration of visual function irreversible. Similarly, Rosenstein and Symon proved that tumors smaller than 3 cm had a better visual outcome compared with those larger than 3 cm (30). The same results were found in other series with tumors larger than 3 or 4 cm in diameter (15, 31). In general, only six patients (15.8%) suffered from postoperative deterioration, while the visual functions were improved or stable in most of the patients (84.2%). We attribute these to vascular protection strategies. In conclusion, maximal tumor GTR and visual function improvement can be achieved by taking full advantage of the benefits of the unilateral subfrontal approach and the ETAS.

Conclusion

There was no significant difference in GTR rate and vision outcome between the unilateral subfrontal approach and the ETAS for resection of giant TSMs. By making individualized surgical approaches, surgical complications and hospital stays of patients were reduced. Furthermore, maximal resection and preservation of visual function can be achieved by performing individualized surgical strategies.

Limitation of the study

The patients involved in this study were operated on by a single surgeon and institution. Prospective studies and multi-organizational research with larger sample sizes are still needed to demonstrate the feasibility of the surgical techniques mentioned in this study.

Data availability statement

The original contributions presented in the study are included in the article/**Supplementary Material**, further inquiries can be directed to the corresponding author/s.

Ethics statement

The studies involving human participants were reviewed and approved by the Ethics Committee of Xiangya Hospital. The patients/participants provided their written informed consent to participate in this study.

Author contributions

YL analyzed and interpreted the surgical data and drafted the article. CZ and YL collected and recorded the data. CQ and JS provided revised the manuscript. XW drafted the figures. QL performed the surgeries and supervised the study. All authors contributed to the article and approved the submitted version.

Acknowledgments

All contributors to this study are included in the list of authors.

Conflict of interest

The authors declare that the research was conducted in the absence of any commercial or financial relationships that could be construed as a potential conflict of interest.

Publisher's note

All claims expressed in this article are solely those of the authors and do not necessarily represent those of their affiliated organizations, or those of the publisher, the editors and the reviewers. Any product that may be evaluated in this article, or claim that may be made by its manufacturer, is not guaranteed or endorsed by the publisher.

Supplementary material

The Supplementary Material for this article can be found online at: https://www.frontiersin.org/articles/10.3389/fsurg.2022.990646/full#supplementary-material.

SUPPLEMENTARY FIGURE 1
Evaluation the angle between the panum sphenoidal and the depth of the sella turcica in a TSM patient. Red line: angle between the panum sphenoidal and the sella turcica; blue dotted line: the line between the planum sphenoidal clivus; blue line: the depth of the sella turcica.

References

1. Jallo GI, Benjamin V. Tuberculum sellae meningiomas: microsurgical anatomy and surgical technique. *Neurosurgery*. (2002) 51(6):1432–39; discussion 9–40. doi: 10.1097/00006123-200212000-00013

2. Ajlan AM, Choudhri O, Hwang P, Harsh G. Meningiomas of the tuberculum and diaphragma sellae. *J Neurol Surg B Skull Base*. (2015) 76(1):74–9. doi: 10.1055/s-0034-1390400.

3. Hayhurst C, Teo C. Tuberculum sella meningioma. *Otolaryngol Clin North Am*. (2011) 44(4):953–63; viii–ix. doi: 10.1016/j.otc.2011.06.012

4. Sade B, Lee JH. High incidence of optic canal involvement in tuberculum sellae meningiomas: rationale for aggressive skull base approach. *Surg Neurol*. (2009) 72(2):118–23; discussion 23. doi: 10.1016/j.surneu.2008.08.007

5. Mahmoud M, Nader R, Al-Mefty O. Optic canal involvement in tuberculum sellae meningiomas: influence on approach, recurrence, and visual recovery. *Neurosurgery*. (2010) 67(3 Suppl Operative):ons108–18; discussion ons18–9. doi: 10.1227/01.NEU.0000383153.75695.24

6. Xiao F, Shen J, Zhang L, Yang J, Weng Y, Fang Z, et al. Unilateral subfrontal approach for giant tuberculum sellae meningioma: single center experience and review of the literature. *Front Oncol*. (2021) 11:708235. doi: 10.3389/fonc.2021.708235

7. Magill ST, Morshed RA, Lucas CG, Aghi MK, Theodosopoulos PV, Berger MS, et al. Tuberculum sellae meningiomas: grading scale to assess surgical outcomes using the transcranial versus transsphenoidal approach. *Neurosurg Focus*. (2018) 44(4):E9. doi: 10.3171/2018.1.FOCUS17753

8. Engelhardt J, Namaki H, Mollier O, Monteil P, Penchet G, Cuny E, et al. Contralateral transcranial approach to tuberculum sellae meningiomas: long-term visual outcomes and recurrence rates. *World Neurosurg*. (2018) 116:e1066–74. doi: 10.1016/j.wneu.2018.05.166

9. Voznyak O, Lytvynenko A, Maydannyk O, Ilyuk R, Zinkevych Y, Hryniv N. Tuberculum sellae meningioma surgery: visual outcomes and surgical aspects of contralateral approach. *Neurosurg Rev*. (2021) 44(2):995–1001. doi: 10.1007/s10143-020-01278-3

10. Bander ED, Singh H, Ogilvie CB, Cusic RC, Pisapia DJ, Tsiouris AJ, et al. Endoscopic endonasal versus transcranial approach to tuberculum sellae and planum sphenoidale meningiomas in a similar cohort of patients. *J Neurosurg*. (2018) 128(1):40–8. doi: 10.3171/2016.9.JNS16823

11. Kondziolka D, Mathieu D, Lunsford LD, Martin JJ, Madhok R, Niranjan A, et al. Radiosurgery as definitive management of intracranial meningiomas. *Neurosurgery*. (2008) 62(1):53–8; discussion 8–60. doi: 10.1227/01.NEU.0000311061.72626.0D

12. Li-Hua C, Ling C, Li-Xu L. Microsurgical management of tuberculum sellae meningiomas by the frontolateral approach: surgical technique and visual outcome. *Clin Neurol Neurosurg*. (2011) 113(1):39–47. doi: 10.1016/j.clineuro.2010.08.019

13. Karsy M, Raheja A, Eli I, Guan J, Couldwell WT. Clinical outcomes with transcranial resection of the tuberculum sellae meningioma. *World Neurosurg*. (2017) 108:748–55. doi: 10.1016/j.wneu.2017.09.090

14. Arifin MZ, Mardjono I, Sidabutar R, Wirjomartani BA, Faried A. Pterional approach versus unilateral frontal approach on tuberculum sellae meningioma: single centre experiences. *Asian J Neurosurg*. (2012) 7(1):21–4. doi: 10.4103/1793-5482.95691

15. Romani R, Laakso A, Kangasniemi M, Niemela M, Hernesniemi J. Lateral supraorbital approach applied to tuberculum sellae meningiomas: experience with 52 consecutive patients. *Neurosurgery*. (2012) 70(6):1504–18; discussion 18–9. doi: 10.1227/NEU.0b013e31824a36e8

16. Couldwell WT, Weiss MH, Rabb C, Liu JK, Apfelbaum RI, Fukushima T. Variations on the standard transsphenoidal approach to the sellar region, with emphasis on the extended approaches and parasellar approaches: surgical experience in 105 cases. *Neurosurgery*. (2004) 55(3):539–47; discussion 47–50. doi: 10.1227/01.NEU.0000134287.19377.A2

17. de Divitiis E, Esposito F, Cappabianca P, Cavallo LM, de Divitiis O, Esposito I. Endoscopic transnasal resection of anterior cranial fossa meningiomas. *Neurosurg Focus*. (2008) 25(6):E8. doi: 10.3171/FOC.2008.25.12.E8

18. Fernandez-Miranda JC, Pinheiro-Nieto C, Gardner PA, Snyderman CH. Endoscopic endonasal approach for a tuberculum sellae meningioma. *J Neurosurg*. (2012) 32(Suppl):E8. doi: 10.1227/01.NEU.0000311061.72626.0D

19. Montgomery KL, Kim JS, Franklin C. Acceptance and commitment therapy for psychological and physiological illnesses: a systematic review for social workers. *Health Soc Work*. (2011) 36(3):169–81. doi: 10.1093/hsw/36.3.169

20. Prevedello DM, Thomas A, Gardner P, Snyderman CH, Carrau RL, Kassam AB. Endoscopic endonasal resection of a synchronous pituitary adenoma and a tuberculum sellae meningioma: technical case report. *Neurosurgery*. (2007) 60(4 Suppl 2):E401; discussion E. doi: 10.1227/01.NEU.0000255359.94571.91

21. Munoz-Munoz JL, Garcia-Molina F, Molina-Alarcon M, Tudela J, Garcia-Canovas F, Rodriguez-Lopez JN. Kinetic characterization of the enzymatic and chemical oxidation of the catechins in green tea. *J Agric Food Chem*. (2008) 56(19):9215–24. doi: 10.1021/jf8012162

22. Bowers CA, Altay T, Couldwell WT. Surgical decision-making strategies in tuberculum sellae meningioma resection. *Neurosurg Focus*. (2011) 30(5):E1. doi: 10.3171/2011.2.FOCUS1115

23. Adegbite AB, Khan MI, Paine KW, Tan LK. The recurrence of intracranial meningiomas after surgical treatment. *J Neurosurg*. (1983) 58(1):51–6. doi: 10.3171/jns.1983.58.1.0051

24. Nakamura M, Roser F, Struck M, Vorkapic P, Samii M. Tuberculum sellae meningiomas: clinical outcome considering different surgical approaches. *Neurosurgery*. (2006) 59(5):1019–28; discussion 28–9. doi: 10.1227/01.NEU.0000245600.92322.06

25. Symon L, Rosenstein J. Surgical management of suprasellar meningioma. Part 1: the influence of tumor size, duration of symptoms, and microsurgery on surgical outcome in 101 consecutive cases. *J Neurosurg*. (1984) 61(4):633–41. doi: 10.3171/jns.1984.61.4.0633

26. Curey S, Derrey S, Hannequin P, Hannequin D, Freger P, Muraine M, et al. Validation of the superior interhemispheric approach for tuberculum sellae

meningioma: clinical article. *J Neurosurg*. (2012) 117(6):1013–21. doi: 10.3171/2012.9.JNS12167

27. Graffeo CS, Dietrich AR, Grobelny B, Zhang M, Goldberg JD, Golfinos JG, et al. A panoramic view of the skull base: systematic review of open and endoscopic endonasal approaches to four tumors. *Pituitary*. (2014) 17 (4):349–56. doi: 10.1007/s11102-013-0508-y

28. Kitano M, Taneda M, Nakao Y. Postoperative improvement in visual function in patients with tuberculum sellae meningiomas: results of the extended transsphenoidal and transcranial approaches. *J Neurosurg*. (2007) 107 (2):337–46. doi: 10.3171/JNS-07/08/0337

29. Komotar RJ, Starke RM, Raper DM, Anand VK, Schwartz TH. Endoscopic endonasal versus open transcranial resection of anterior midline skull base meningiomas. *World Neurosurg*. (2012) 77(5–6):713–24. doi: 10.1016/j.wneu.2011.08.025

30. Rosenstein J, Symon L. Surgical management of suprasellar meningioma. Part 2: prognosis for visual function following craniotomy. *J Neurosurg*. (1984) 61(4):642–8. doi: 10.3171/jns.1984.61.4.0642

31. Kadis GN, Mount LA, Ganti SR. The importance of early diagnosis and treatment of the meningiomas of the planum sphenoidale and tuberculum sellae: a retrospective study of 105 cases. *Surg Neurol*. (1979) 12(5):367–71. doi: 10.1007/s10143-020-01278-3

32. Zhang C, Ding J, Liu Y, Tuoheti M, Yang X, Wang J, et al. Endoscopic endonasal approach for resection of tuberculum sellae meningioma: a promising surgical approach. *J Craniofac Surg*. (2020) 31(6):1815-8. doi: 10.1097/SCS.0000000000006413

33. Marx S, Schroeder HWS. Transcranial versus endonasal approaches in tuberculum sellae meningioma surgery. *J Neurosurg*. (2018) 129(2):558-60. doi: 10.3171/2018.2.JNS18282

34. Wiedmann M, Lashkarivand A, Berg-Johnsen J, Dahlberg D. How i do it: endoscopic endonasal resection of tuberculum sellae meningioma. *Acta Neurochir. (Wien)* (2021) 163(8):2193-7. doi: 10.1007/s00701-021-04784-5

frontiers | Frontiers in Surgery

TYPE Original Research
PUBLISHED 07 September 2022
DOI 10.3389/fsurg.2022.973834

OPEN ACCESS

EDITED BY
Mario Ganau,
Oxford University Hospitals NHS Trust,
United Kingdom

REVIEWED BY
Francesco Zenga,
University Hospital of the City of Health and Science of Turin, Italy
Michel Roethlisberger,
University Hospital of Basel, Switzerland
Nikolaos CH. Syrmos,
Aristotle University of Thessaloniki, Greece

*CORRESPONDENCE
Yazhuo zhang
zyz2004520@yeah.net
Peng Zhao
kosinmed@163.com

†ORCID
Yazhuo zhang
0000-0002-8583-2580
Peng Zhao
0000-0003-4753-4889

SPECIALTY SECTION
This article was submitted to Neurosurgery, a section of the journal Frontiers in Surgery

RECEIVED 20 June 2022
ACCEPTED 22 August 2022
PUBLISHED 07 September 2022

CITATION
Li B, Zhao S, Fang Q, Nie D, Cheng J, Zhu H, Li C, Gui S, Zhang Y and Zhao P (2022) Risk factors and management associated with postoperative cerebrospinal fluid leak after endoscopic endonasal surgery for pituitary adenoma.
Front. Surg. 9:973834.
doi: 10.3389/fsurg.2022.973834

Risk factors and management associated with postoperative cerebrospinal fluid leak after endoscopic endonasal surgery for pituitary adenoma

Bin Li[1], Sida Zhao[1], Qiuyue Fang[1], Ding Nie[1], Jianhua Cheng[1], Haibo Zhu[2], Chuzhong Li[1], Songbai Gui[2], Yazhuo Zhang[1*†] and Peng Zhao[2*†]

[1]Beijing Neurosurgical Institute, Capital Medical University, Beijing, China, [2]Department of Neurosurgery, Beijing Tiantan Hospital, Capital Medical University, Beijing, China

Objective: To determine risk factors and management for the development of a postoperative cerebrospinal fluid (CSF) leak after an endoscopic endonasal surgery (EES) for pituitary adenomas.

Methods: The clinical data of 400 patients who underwent EES for resection of pituitary adenomas from December 2018 to November 2019 in the Department of Neurosurgery of Beijing Tiantan Hospital were retrospectively reviewed. Age, gender, body mass index (BMI), tumor size, Knosp grade, suprasellar extension grade, sellar floor erosion grade, repeated transsphenoidal surgery, intraoperative CSF leak, use of pedicled nasoseptal flap and lumbar drain were collected and analyzed.

Results: Postoperative CSF leak occurred in 14 of 400 patients (3.5%). Age, gender, BMI, tumor size, Knosp grade and repeated transsphenoidal surgery were not risk factors for CSF leak. Suprasellar extension grade (≥B 6.0% vs. <B 1.4%; $p = 0.024$), sellar floor erosion grade (≥III 5.7% vs. <III 0.6%; $p = 0.020$) and intraoperative CSF leak (Yes 7.5% vs. No 2.0%; $p = 0.009$) were factors associated with an increased postoperative CSF leak rate.

Conclusions: Higher suprasellar extension grade, higher sellar floor erosion grade and intraoperative CSF leak were risk factors for postoperative CSF leak after endoscopic treatment of pituitary adenoma. Strict skull base reconstruction including use of a pedicled nasoseptal flap and perioperative lumbar drainage may avoid postoperative CSF leak.

KEYWORDS

cerebrospinal fluid leak, endoscopic endonasal surgery, pituitary adenoma, risk factor, management

Abbreviations

CSF, cerebrospinal fluid; EES, endoscopic endonasal surgery; BMI, body mass index; PA, pituitary adenoma; LD, lumbar drainage; OR, odds ratio; CI, confidence interval.

Introduction

Pituitary adenoma (PA) is one of the common primary neoplasms of the central nervous system. It makes up approximately 10%–15% of all intracranial tumors (1, 2). Endoscopic endonasal surgery (EES) has become the best way to remove pituitary adenomas, with the development of neuroendoscopy equipment and technology. Postoperative cerebrospinal fluid (CSF) leak is the most important complication of EES. Postoperative CSF leak can increase the risk of intracranial infection, hospitalization time and costs (3). It is important to determine risk factors and management for the development of a postoperative CSF leak after the EES for resection of pituitary adenomas. According to previous studies, potential risk factors for CSF leak after EES include tumor size, body mass index (BMI), multiple EES and vascularized nasoseptal flap (4–6). However, there are many potential risk factors such as Knosp grade, suprasellar extension grade, sellar floor erosion grade and intraoperative CSF leak. These potential risk factors are rarely reported.

The management to prevent CSF leak after EES of pituitary adenomas is gradually improving. In 2006, the use of a vascular pedicled flap from the nasal septum mucoperiosteum was introduced, which has significantly optimized the skull base reconstruction technique (7). It reduces the incidence of CSF leak in the postoperative period after endonasal skull base surgery, because vascularized flaps promote faster and more complete healing by restoring the local blood (8). In addition, perioperative LD reduced the rate of postoperative CSF leak (6).

In our study, we comprehensively analyzed the risk factors of CSF leak after EES for pituitary tumor surgery. Based on these risk factors, we initially formulated a scheme to prevent CSF leak after EES for the resection of pituitary tumors. These risk factors include age, gender, BMI, tumor size, Knosp grade, suprasellar extension grade, sellar floor erosion grade, lumbar drain, repeated transsphenoidal surgery and intraoperative CSF leak.

Materials and methods

Study design

To determine risk factors and management for the development of a postoperative cerebrospinal fluid (CSF) leak after an endoscopic endonasal surgery (EES) for pituitary adenomas.

Participants

Patients with pituitary adenoma who underwent EES between December 2018 and November 2019 in the Department of Neurosurgery of Beijing Tiantan Hospital affiliated to Capital Medical University were selected as the research subjects. All patients were treated by the same team, Neurosurgery Oncology 3 Ward. All patients' medical records and operative notes were reviewed in detail. All patients were followed up for at least 3 months.

Variables

Accurately recorded the following information about the patients: age, gender, body mass index (BMI), tumor size, Knosp grade, suprasellar extension grade, sellar floor erosion grade, repeated transsphenoidal surgery, intraoperative CSF leak, use of pedicled nasoseptal flap and lumbar drain. Postoperative CSF leak was defined as a definite CSF leak within one month after EES. Laboratory tests indicated that fluid from the nose contained cerebrospinal fluid components (a definite CSF leak).

Quantitative variables

Tumor size is represented by the longest distance of anteroposterior, transverse and vertical diameters. The determination of the Knosp grade of the cases is based on the 0-IV grade classification proposed by Professor Knosp (9) (**Figure 1**). Knosp grade can reflect parasellar extension of the tumor. The Hardy–Wilson classification (10) was used for the assessment of suprasellar extension grades and sellar floor erosion grades (**Figures 2**, **3**). It is important to point out that since Hardy D and E grades reflect parasellar extension, we only used Hardy 0–C grades for the evaluation of suprasellar extension grade. The choice of a BMI of 24 kg/m^2 as the cutoff for our analysis was based on the definition of overweight by the National Health, Family Planning Commission of the People's Republic of China. In this study, lumbar drain refers to the placement of a drainage tube before postoperative CSF leakage occurs. Lumbar drain is usually placed immediately after surgery or the day after surgery.

Statistical analysis

To measurement variables, independent t-tests were used to compare the two groups of patients with and without CSF leaks. Chi-square tests were used to categorical variables. All independent variables that showed a significant correlation with dependent variables were placed in a multiple logistic forward stepwise regression. Multivariate logistic regression for predictors of postoperative CSF leak was conducted finally. The analyses were performed using SPSS (version 25, IBM Corp., USA), and a p value <0.05 was considered statistically significant.

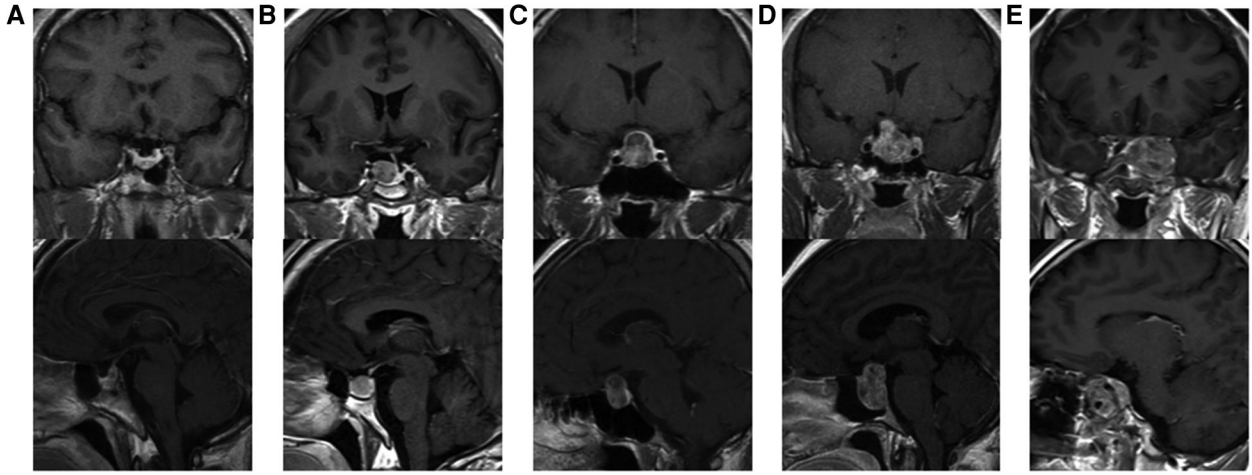

FIGURE 1
Knosp grades of patients. (A) Knosp 0, tumor is medial to medial tangent. (B) Knosp I, tumor extends to the space between the medial tangent and the intercarotid line. (C) Knosp II, tumor extends to the space between the intercarotid line and the lateral tangent. (D) Knosp III, tumor extends lateral to the lateral tangent. (E) Knosp IV, tumor with a complete encasement of intracavernous internal carotid artery.

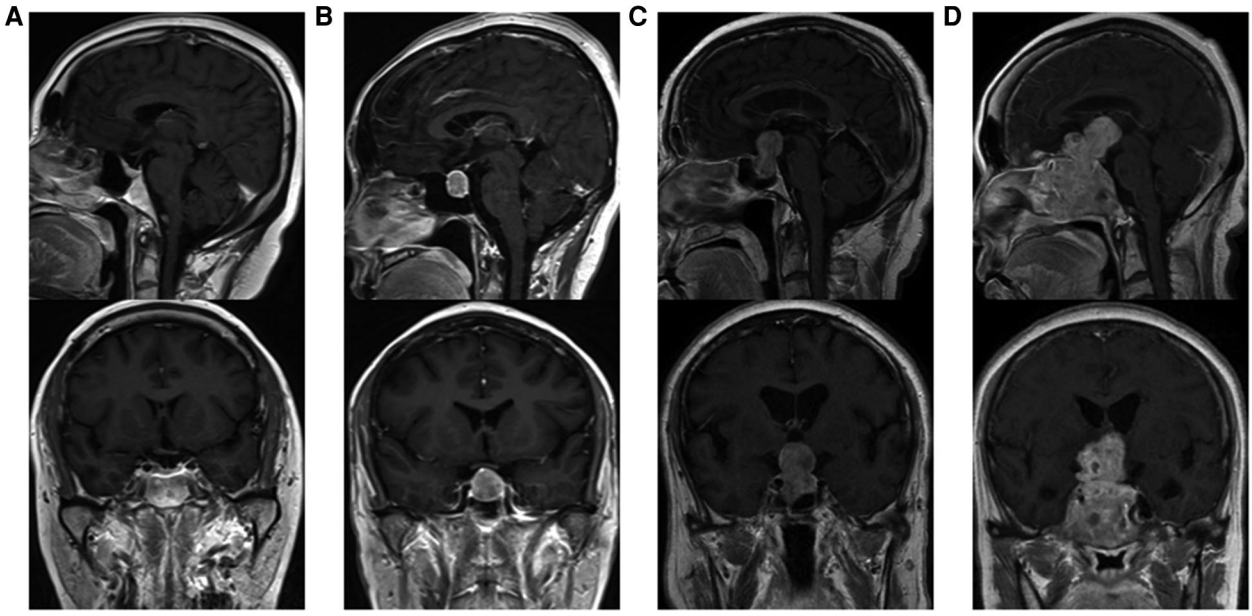

FIGURE 2
Suprasellar extension grades of patients. (A) Grade 0, no suprasellar extension. (B) Grade A, expanding into the suprasellar cistern. (C) Grade B, anterior recesses of the third ventricle obliterated. (D) Grade C, the floor of the third ventricle grossly displaced.

Results

A total of 421 pituitary adenoma patients who underwent EES were screened for inclusion in our study. 20 patients were excluded due to missing data and 1 patient was excluded for a serious complication (rupture of the left internal-carotid-artery during surgery). Finally, 400 patients were included for analysis. The clinical characteristics of patients are detailed in Table 1.

There were 191 female patients and 209 male patients. The average patient age at surgery was 48.5 years (11–82 years). The average patient BMI was 25.6 kg/m^2 (17.2–42.5 kg/m^2). Among those patients, 257 (64.25%) were overweight or obese (BMI $\geq$ 24), 143 (35.75%) of healthy weight (BMI < 24). There were 326

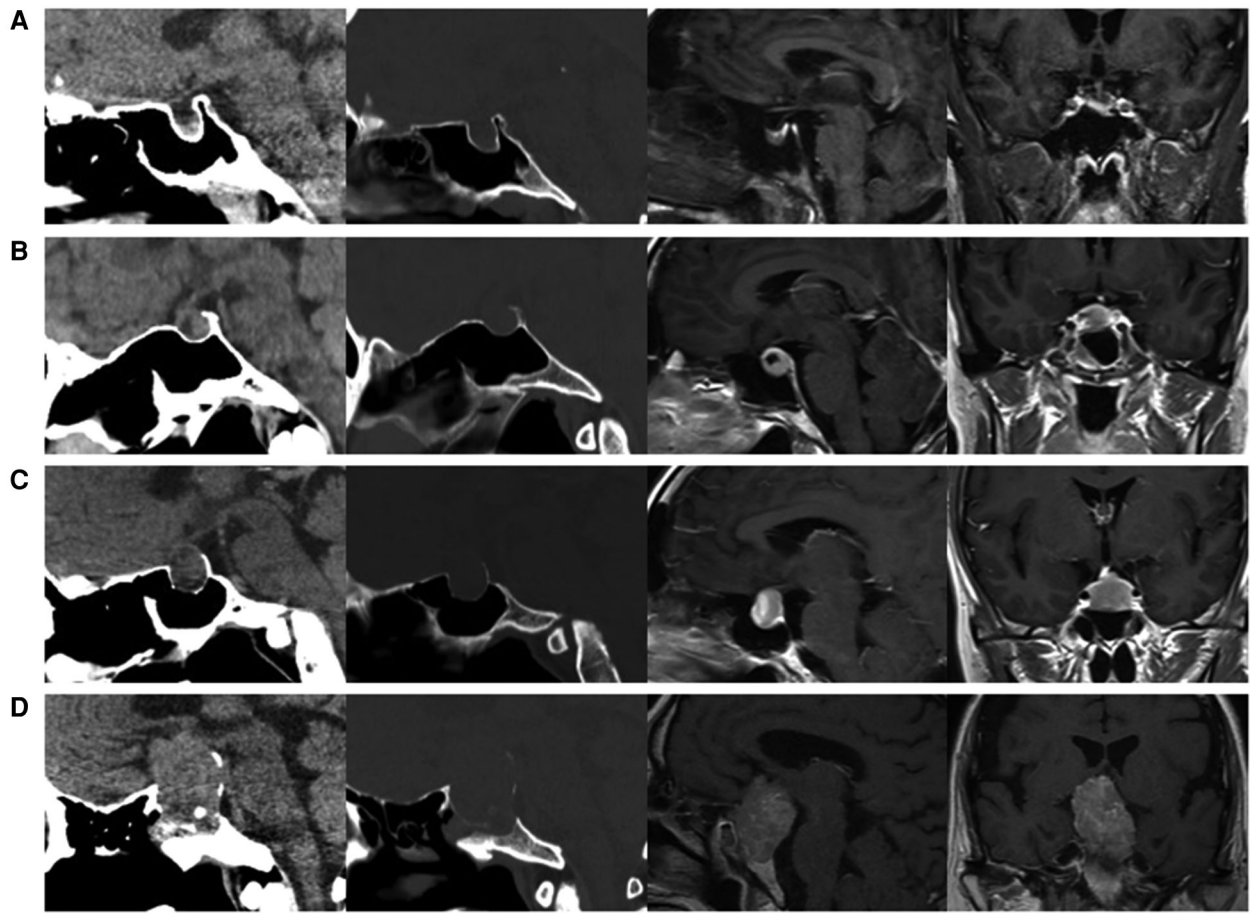

FIGURE 3
Sellar floor erosion grades of patients. (A) Grade I, sella normal or focally expanded; tumor <10 mm. (B) Grade II, sella enlarged; tumor ≥ 10 mm. (C) Grade III, localized sellar perforation. (D) Grade IV, diffuse destruction of the sellar floor.

(81.5%) patients underwent EES for the first time and 74 (18.5%) patients underwent EES again.

Of the 400 patients enrolled for analysis, fourteen patients occurred postoperative CSF leak (3.5%). Figure 4 shows that the effect of risk factors on rate of postoperative CDF leak. There was no significant difference in age, gender, BMI, Knosp grade, repeated EES and use of pedicled nasoseptal flap between those with and without postoperative CSF leaks according univariate analysis (Table 1). Although there was no statistically significant difference, patients with postoperative CSF leakage had larger tumor sizes than those without postoperative leakage (Anteroposterior diameter 28.6 ± 15.8 mm vs. 23.0 ± 10.2 mm; $p = 0.204$) (Transverse diameter 29.6 ± 12.9 mm vs. 22.8 ± 9.8 mm; $p = 0.071$) (Vertical diameter 29.1 ± 12.9 mm vs. 24.0 ± 11.8 mm; $p = 0.119$).

There were 107 patients with CSF leakage during the operation. Patients with intraoperative CSF lake were more likely to develop postoperative CSF lake (with intraoperative CSF lake 7.5% [8/107] vs. without intraoperative CSF lake 2.0% [6/293]; $p = 0.009$).

Patients with higher grades of suprasellar extension ($p = 0.015$) and sellar floor erosion ($p = 0.042$) were more likely to develop postoperative CSF leak (Tables 1, 2). Patients with suprasellar extension grades B and C had a significantly higher leakage rate than those with less than B grades (6.0% [11/182] vs. 1.4% [3/218]; $p = 0.024$). Patients with sellar floor erosion grades III and IV had a significantly higher leakage rate than those with less than III grades (5.7% [9/159] vs. 0.6% [1/167]; $p = 0.020$). Patients with Knosp less than grade 3 appeared to have a lower rate of CSF leak, but this was not statistically significant (≥III 4.7% [8/170] vs. <III 2.6% [6/230]; $p = 0.259$) (Table 3).

In 57 of 400 patients, pedicled nasoseptal flap was used for skull base reconstruction. Of these 57 patients, 4 (7.0%) patients developed postoperative CSF leakage. Leakage rates were relatively low in patients who did not use a nasoseptal flap

TABLE 1 Patient demographics.

Variable	No CSF Leak ($n = 386$)	CSF Leak ($n = 14$)	p Value
Age (years)	48.5 ± 12.9	49.3 ± 12.5	0.821
Gender (no.)			0.864
Male	202	7	
Female	184	7	
BMI (kg/m^2)	25.7 ± 3.9	23.8 ± 1.9	0.058
Tumor size (mm)			
Anteroposterior diameter	23.0 ± 10.2	28.6 ± 15.8	0.204
Transverse diameter	22.8 ± 9.8	29.6 ± 12.9	0.071
Vertical diameter	24.0 ± 11.8	29.1 ± 12.9	0.119
Knosp grade (no.)			0.564
0	19	0	
I	109	2	
II	96	4	
III	76	5	
IV	86	3	
Suprasellar extension grade (no.)			0.015
0	32	0	
A	183	3	
B	95	3	
C	76	8	
First transsphenoidal surgery (no.)			0.524
Yes	316	10	
No	70	4	
Intraoperative CSF leak (no.)			0.009
Yes	99	8	
No	287	6	
Use of pedicled nasoseptal flap (no.)			0.119
Yes	53	4	
No	333	10	
Lumbar drain (no.)			0.000
Yes	34	7	
No	352	7	

(2.9% [10/343]). But there is no statistically significant difference ($p = 0.119$).

A total of 41 patients had a lumbar drain placed after operation (10.3%). Patients who underwent postoperative lumbar drain had a higher rate of CSF leakage compared with did not underwent postoperative lumbar drain (17.1% [7/41] vs. 1.9% [7/359]; $p < 0.0001$).

Multiple logistic regression analysis showed that intraoperative CSF leak and high grade of suprasellar extension were significantly associated with postoperative CSF leak ($p < 0.05$). Patients with intraoperative CSF leak were 3.75 times more likely to have a CSF lake when compared with those without intraoperative CSF leak. Patients with a suprasellar extension grade ≥ B were 4.29 times more likely to have a postoperative CSF leak when compared with those with a suprasellar extension grade < B (**Table 4**).

Discussion

EES is the preferred first-line treatment for pituitary adenomas as skull base tumors. CSF leak is one of the most common postoperative complications after EES for pituitary adenomas. According to literature reports, the incidence of CSF leak after EES for pituitary adenomas ranges from 2.6% to 12.1% (4, 11–17). In the current study, 3.5% of patients with pituitary adenomas developed cerebrospinal fluid leakage after EES. Similar to other studies (4, 13), there was no statistically significant difference in age, gender, and Knosp grade between those with and without postoperative CSF leaks in the present study.

It is reported that increased intracranial pressure in overweight and obese patients can place additional strain on skull base reconstruction, leading to increase the risk of postoperative CSF leak (4). It is proved that BMI can be a risk factor for postoperative CSF leak in EES for pituitary adenomas (5). But based on our data, there was no statistically significant difference in BMI between those with and without postoperative CSF leaks. The reason for this difference may be racial differences. The BMI of Asians is generally lower than that of Europeans and Americans. The difference in BMI may have little effect between the two groups of patients with and without CSF leak.

Consistent with reports in the literature (13, 18), our study showed that intraoperative CSF leak increases postoperative CSF leak rate. In this study, 107 (26.8%) patients developed intraoperative CSF leak. Eight patients with intraoperative CSF leak eventually developed postoperative CSF leak. In our experience, we perform rigorous skull base reconstruction and lumbar drainage in patients with intraoperative CSF leakage. Even so, these patients had a relatively high risk of postoperative CSF leak. Of these 8 patients with postoperative CSF leak, 5 patients underwent postoperative lumbar drainage, and 4 patients used nasoseptal flaps in skull base reconstruction. Intraoperative CSF leakage, especially high-flow leakage, can increase the difficulty of skull base reconstruction and increase the risk of postoperative CSF leak. Univariate and multivariate statistical analysis showed that intraoperative CSF leak can be used as a risk factor for postoperative CSF leak in this study.

Intraoperative CSF leak flow strongly affects postoperative CSF leak rate, as reported by Di Perna et al (19). High flow CSF leak (IHFL) was defined as large dural defect and basal cisterns or ventricular opening, while small dural defect and

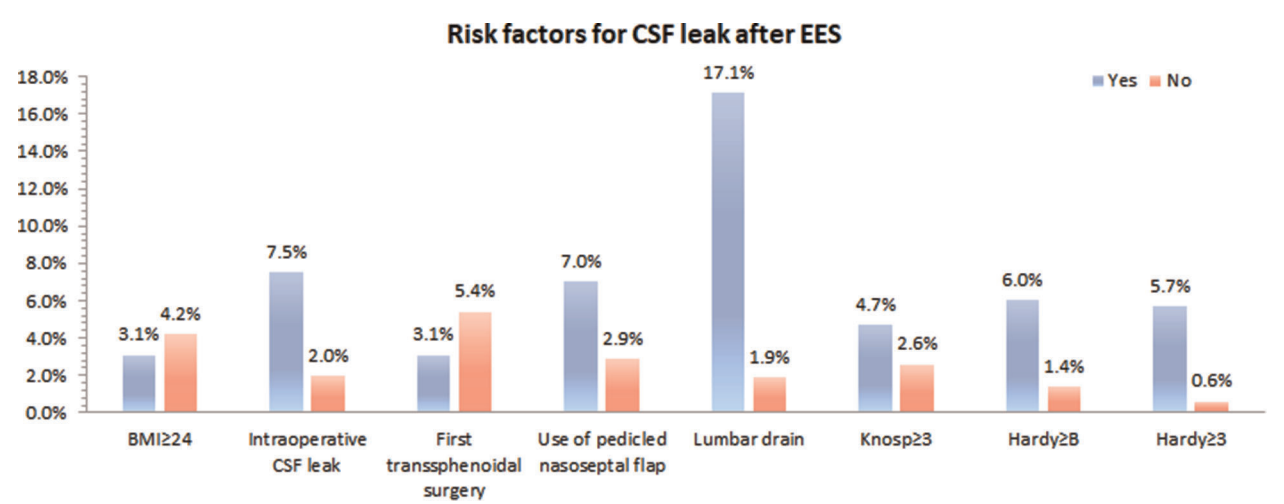

FIGURE 4
Effect of risk factors on rate of postoperative CSF leak.

TABLE 2 Sellar floor erosion grades of patients.

Variable	No CSF Leak ($n = 316$)	CSF Leak ($n = 10$)	p Value
Sellar floor erosion grade (no.)			0.042
I	10	0	
II	156	1	
III	81	5	
IV	69	4	

TABLE 3 Univariate analysis for predictors of postoperative CSF leak.

Variable	No CSF Leak	CSF Leak	p Value
BMI (kg/m^2) (no.)	$n = 386$	$n = 14$	0.572
<24	137	6	
≥24	249	8	
Knosp grade (no.)	$n = 386$	$n = 14$	0.259
<III	224	6	
≥III	162	8	
Suprasellar extension grade (no.)	$n = 386$	$n = 14$	0.024
<B	215	3	
≥B	171	11	
Sellar floor erosion grade (no.)	$n = 316$	$n = 10$	0.020
<III	166	1	
≥III	150	9	

moderate CSF leak defined the low flow leak (ILFL) (20). In the study of Perna et al, Postoperative CSF leak rate, resulted higher in the IHFL group (25.5%) than in the ILFL group (10.5%) (19). In addition, the flow of intraoperative CSF leak determines different reconstruction strategies. Research has shown that,

TABLE 4 Multivariate logistic regression for predictors of postoperative CSF leak.

Variable	p Value	OR (95% CI)
BMI ≥ 24 kg/m^2	0.618	0.758 (0.255–2.254)
Not first transsphenoidal surgery	0.500	1.516 (0.452–5.080)
Intraoperative CSF leak	0.019	3.688 (1.238–10.987)
Suprasellar extension grade ≥ B	0.020	4.610 (1.266–16.786)
Anteroposterior diameter	0.688	1.013 (0.951–1.079)
Transverse diameter	0.202	1.040 (0.979–1.105)
Vertical diameter	0.445	0.975 (0.913–1.041)

mucosal flap and inlay for high flow intraoperative CSF leak improved the postoperative CSF leak rate (21). Unfortunately, the intraoperative CSF leak flow was not recorded in our surgical records.

For the first time, we introduced the effect of suprasellar extension grades and sellar floor erosion grades on CSF leak after EES. The Hardy–Wilson classification was used for the assessment of suprasellar extension grades and sellar floor erosion grades (Figures 2, 3). Based on our data, suprasellar extension grades and sellar floor erosion grades can be used as risk factors for postoperative CSF leak after EES. Patients with higher grades of suprasellar extension and sellar floor erosion were more likely to develop postoperative CSF leak (Tables 1, 2). Patients with a higher grade of suprasellar invasion, especially those with tumor expansion into the ventricular system, have an increased risk of intraoperative CSF leakage, resulting in a relatively increased incidence of postoperative CSF leakage. Patients with a higher level of sellar floor erosion have an increased degree of dura destruction and increase difficulty in skull base reconstruction, thereby increasing the incidence of postoperative cerebrospinal fluid leakage.

With advances in the development of vascularized flaps in EES, pedicled nasoseptal flaps have been increasingly employed for skull base reconstruction. A systematic review found that vascularized flaps were associated with a lower rate of postoperative CSF leaks (22). Especially in the case of high-flow intraoperative CSF leakage, the pedicled vascularized flap has a more significant effect. In our study, although there was no statistically significant difference, use of a pedicled nasoseptal flap was associated with a higher rate of postoperative CSF leak. This association may be due to selection bias. As mentioned earlier, the vascularized flap plays an important role in reducing the incidence of postoperative CSF leakage. Currently, in our group, we routinely use pedicled nasoseptal flaps for skull base reconstruction in patients with a high risk of postoperative CSF leakage.

Lumbar drainage is often used in the perioperative period to reduce intracranial pressure and prevent postoperative CSF leaks following EES for skull base lesions (23, 24). A prospective, randomized controlled trial confirmed that perioperative lumbar drainage reduced the rate of postoperative CSF leaks after EES (6). Our study indicates that patients who underwent postoperative lumbar drain had a higher rate of CSF leakage compared with did not underwent postoperative lumbar drain. This situation is the same as the intraoperative pedicled nasoseptal flaps, which is caused by selection bias. In our study, lumbar drainage was typically placed in patients with high risk of postoperative CSF leakage. Therefore, the results of statistical analysis showed that patients with lumbar drainage were more prone to CSF leakage.

Free tissue grafts, vascularized flaps, gasket sealing and lumbar drains are most commonly used to prevent postoperative CSF leaks (25). Based on our data and the surgical experience of our team, for patients with high risk of postoperative CSF leakage, rigorous skull base reconstruction and perioperative lumbar drainage are beneficial to reduce the occurrence of postoperative CSF leakage. Rigorous skull base reconstruction includes various combinations of biomaterials, free tissue grafts (fat grafts and fascia lata grafts) and vascularized regional flaps. **Figure 5** shows a rigorous skull base reconstruction procedure in a patient with high-risk postoperative CSF leak.

Conclusions

Higher suprasellar extension grade, higher sellar floor erosion grade and intraoperative CSF leak were risk factors for postoperative CSF leak after endoscopic treatment of pituitary adenoma. Rigorous skull base reconstruction

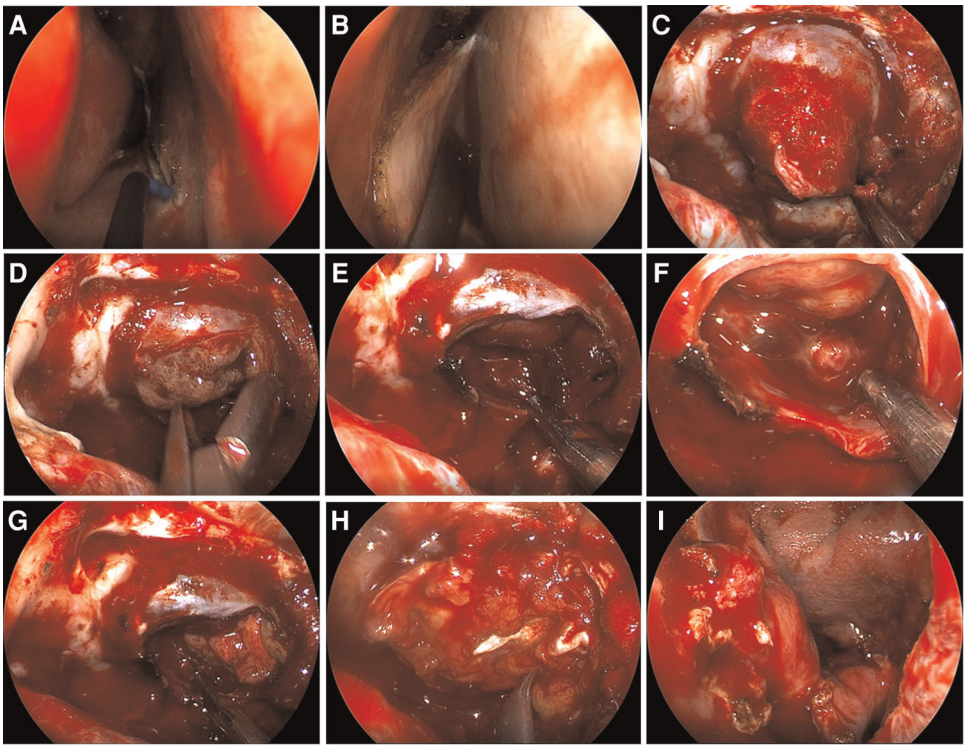

FIGURE 5
Rigorous skull base reconstruction procedure. (A,B) A pedicled nasoseptal flap was prepared in advance. (C) The tumor eroded the dura mater and protruded into the sphenoid sinus. (D) The tumor is removed in steps. (E,F) Pituitary adenoma has been completely removed and intraoperative CSF leakage occurred. (G) The fat graft was placed. (H) The fascia lata graft was placed. (I) The pedicled nasoseptal flap was placed over the fascia lata graft.

including use of a pedicled nasoseptal flap and perioperative lumbar drainage may avoid postoperative CSF leak.

Limitation

This study is a retrospective study, and there is obvious selection bias in the two risk factors of nasoseptal flap and lumbar drainage. These two risk factors require further prospective studies to clarify their impact on postoperative CSF leakage. In addition, to avoid the impact of surgeons' experience on the study due to years of operation, we only counted cases for one year. Therefore, the number of cases is relatively small. Finally, factors such as reconstruction technique, intraoperative CSF leak flow, and history of previous radiation treatment were not accounted for in our analysis.

Data availability statement

The original contributions presented in the study are included in the article/Supplementary Material, further inquiries can be directed to the corresponding author/s.

Ethics statement

The studies involving human participants were reviewed and approved by Beijing Tiantan Hospital Ethics Committee. The patients/participants provided their written informed consent to participate in this study.

Written informed consent was obtained from the individual(s) for the publication of any potentially identifiable images or data included in this article.

Author contributions

YZZ and PZ conceived the study and edited the final manuscript. BL collected the clinical data and produced the draft manuscript. SDZ performed analysis and interpretation of data. QYF and DN performed a literature review. JHC and HBZ reviewed the clinical notes. CZL and SBG helped with the writing of the manuscript and collected the clinical data. All authors contributed to the article and approved the submitted version.

Funding

This work was supported by grants from the National Natural Science Foundation of China (82103048, 82072804, 82071559).

Conflict of interest

The authors declare that the research was conducted in the absence of any commercial or financial relationships that could be construed as a potential conflict of interest.

Publisher's note

References

1. Moreno CS, Evans CO, Zhan XQ, Okor M, Desiderio DM, Oyesiku NM. Novel molecular signaling and classification of human clinically nonfunctional pituitary adenomas identified by gene expression profiling and proteomic analyses. *Cancer Res.* (2005) 65(22):10214–22. doi: 10.1158/0008-5472.CAN-05-0884

2. Loyo-Varela M, Herrada-Pineda T, Revilla-Pacheco F, Manrique-Guzman S. Pituitary tumor surgery: review of 3004 cases. *World Neurosurg.* (2013) 79 (2):331–6. doi: 10.1016/j.wneu.2012.06.024

3. Parikh A, Adapa A, Sullivan SE, McKean EL. Predictive factors, 30-day clinical outcomes, and costs associated with cerebrospinal fluid leak in pituitary adenoma resection. *J Neurol Surg Part B.* (2020) 81(1):43–55. doi: 10.1055/s-0039-1679896

4. Fraser S, Gardner PA, Koutourousiou M, Kubik M, Fernandez-Miranda JC, Snyderman CH, et al. Risk factors associated with postoperative cerebrospinal fluid leak after endoscopic endonasal skull base surgery. *J Neurosurg.* (2018) 128(4):1066–71. doi: 10.3171/2016.12.JNS1694

5. Dlouhy BJ, Madhavan K, Clinger JD, Reddy A, Dawson JD, O'Brien EK, et al. Elevated body mass index and risk of postoperative CSF leak following transsphenoidal surgery. *J Neurosurg.* (2012) 116(6):1311–7. doi: 10.3171/2012.2.JNS111837

6. Zwagerman NT, Wang EW, Shin SS, Chang YF, Fernandez-Miranda JC, Snyderman CH, et al. Does lumbar drainage reduce postoperative cerebrospinal fluid leak after endoscopic endonasal skull base surgery? A prospective, randomized controlled trial. *J Neurosurg.* (2019) 131(4):1172–8. doi: 10.3171/2018.4.JNS172447

7. Hadad G, Bassagasteguy L, Carrau RL, Mataza JC, Kassam A, Snyderman CH, et al. A novel reconstructive technique after endoscopic expanded endonasal approaches: vascular pedicle nasoseptal flap. *Laryngoscope.* (2006) 116 (10):1882–6. doi: 10.1097/01.mlg.0000234933.37779.e4

8. Moon JH, Kim EH, Kim SH. Various modifications of a vascularized nasoseptal flap for repair of extensive skull base dural defects. *J Neurosurg.* (2020) 132(2):371–9. doi: 10.3171/2018.10.JNS181556

9. Knosp E, Steiner E, Kitz K, Matula C. Pituitary adenomas with invasion of the cavernous sinus space: a magnetic resonance imaging classification compared with surgical findings. *Neurosurgery.* (1993) 33(4):610–7. discussion 7-8. doi: 10.1227/00006123-199310000-00008

10. Araujo-Castro M, Acitores Cancela A, Vior C, Pascual-Corrales E, Rodriguez Berrocal V. Radiological knosp, revised-knosp, and Hardy-Wilson classifications for the prediction of surgical outcomes in the endoscopic endonasal surgery of pituitary adenomas: study of 228 cases. *Front Oncol.* (2021) 11:807040. doi: 10.3389/fonc.2021.807040

11. Parasher AK, Lerner DK, Glicksman JT, Miranda SP, Dimentberg R, Ebesutani D, et al. Drivers of in-hospital costs following endoscopic transphenoidal pituitary surgery. *Laryngoscope*. (2021) 131(4):760–4. doi: 10.1002/lary.29041

12. Taghvaei M, Fallah S, Sadaghiani S, Sadrhosseini SM, Tabari A, Fathi M, et al. Surgical complications of endoscopic approach to skull base: analysis of 584 consecutive patients. *Eur Arch Otorhinolaryngol*. (2022) 279(6):3189–99. doi: 10.1007/s00405-022-07256-3

13. Wang M, Cai Y, Jiang Y, Peng Y. Risk factors impacting intra- and postoperative cerebrospinal fluid rhinorrhea on the endoscopic treatment of pituitary adenomas: a retrospective study of 250 patients. *Medicine*. (2021) 100 (49):e27781. doi: 10.1097/MD.0000000000027781

14. Song S, Wang L, Qi Q, Wang H, Feng L. Endoscopic vs. microscopic transsphenoidal surgery outcomes in 514 nonfunctioning pituitary adenoma cases. *Neurosurg Rev*. (2022) 45(3):2375–83. doi: 10.1007/s10143-022-01732-4

15. Zhang J, Wang Y, Xu X, Gu Y, Huang F, Zhang M. Postoperative complications and quality of life in patients with pituitary adenoma. *Gland Surg*. (2020) 9(5):1521–9. doi: 10.21037/gs-20-690

16. Huang X, Zhang X, Zhou J, Li G, Zheng G, Peng L, et al. Analysis of risk factors and preventive strategies for intracranial infection after neuroendoscopic transnasal pituitary adenoma resection. *BMC Neurosci*. (2022) 23(1):1. doi: 10.1186/s12868-021-00688-3

17. Chibbaro S, Signorelli F, Milani D, Cebula H, Scibilia A, Bozzi MT, et al. Primary endoscopic endonasal management of giant pituitary adenomas: outcome and pitfalls from a large prospective multicenter experience. *Cancers (Basel)*. (2021) 13(14):3603. doi: 10.3390/cancers13143603

18. Magro E, Graillon T, Lassave J, Castinetti F, Boissonneau S, Tabouret E, et al. Complications related to the endoscopic endonasal transsphenoidal approach for nonfunctioning pituitary macroadenomas in 300 consecutive patients. *World Neurosurg*. (2016) 89:442–53. doi: 10.1016/j.wneu.2016.02.059

19. Di Perna G, Penner F, Cofano F, De Marco R, Baldassarre BM, Portonero I, et al. Skull base reconstruction: a question of flow? A critical analysis of 521 endoscopic endonasal surgeries. *PLoS One*. (2021) 16(3):e0245119. doi: 10.1371/journal.pone.0245119

20. Conger A, Zhao F, Wang X, Eisenberg A, Griffiths C, Esposito F, et al. Evolution of the graded repair of CSF leaks and skull base defects in endonasal endoscopic tumor surgery: trends in repair failure and meningitis rates in 509 patients. *J Neurosurg*. (2018) 130(3):861–75. doi: 10.3171/2017.11.JNS172141

21. Cai X, Yang J, Zhu J, Tang C, Cong Z, Liu Y, et al. Reconstruction strategies for intraoperative CSF leak in endoscopic endonasal skull base surgery: systematic review and meta-analysis. *Br J Neurosurg*. (2021):1–11. doi: 10.1080/02688697.2020.1849548

22. Soudry E, Turner JH, Nayak JV, Hwang PH. Endoscopic reconstruction of surgically created skull base defects: a systematic review. *Otolaryngol Head Neck Surg*. (2014) 150(5):730–8. doi: 10.1177/0194599814520685

23. Cohen S, Jones SH, Dhandapani S, Negm HM, Anand VK, Schwartz TH. Lumbar drains decrease the risk of postoperative cerebrospinal fluid leak following endonasal endoscopic surgery for suprasellar meningiomas in patients with high body mass Index. *Oper Neurosurg (Hagerstown)*. (2018) 14(1):66–71. doi: 10.1093/ons/opx070

24. Allen KP, Isaacson B, Purcell P, Kutz Jr. JW, Roland PS. Lumbar subarachnoid drainage in cerebrospinal fluid leaks after lateral skull base surgery. *Otol Neurotol*. (2011) 32(9):1522–4. doi: 10.1097/MAO.0b013e318232e387

25. Khan DZ, Ali AMS, Koh CH, Dorward NL, Grieve J, Layard Horsfall H, et al. Skull base repair following endonasal pituitary and skull base tumour resection: a systematic review. *Pituitary*. (2021) 24(5):698–713. doi: 10.1007/s11102-021-01145-4

frontiers | Frontiers in Surgery

TYPE Original Research
PUBLISHED 07 September 2022
DOI 10.3389/fsurg.2022.971063

OPEN ACCESS

EDITED BY
Yazhuo Zhang,
Capital Medical University, China

REVIEWED BY
Giulia Cossu,
Centre Hospitalier Universitaire Vaudois (CHUV), Switzerland
Zhong Wang,
Soochow University, China

*CORRESPONDENCE
Zhiquan Jiang
bbjiangzhq@163.com

†These authors have contributed equally to this work

SPECIALTY SECTION
This article was submitted to Neurosurgery, a section of the journal Frontiers in Surgery

RECEIVED 16 June 2022
ACCEPTED 19 August 2022
PUBLISHED 07 September 2022

CITATION
Zheng X, Shao D, Li Y, Cai L, Xie S, Sun Z and Jiang Z (2022) Keyhole supraorbital eyebrow approach for fully endoscopic resection of tuberculum sellae meningioma.
Front. Surg. 9:971063.
doi: 10.3389/fsurg.2022.971063

Keyhole supraorbital eyebrow approach for fully endoscopic resection of tuberculum sellae meningioma

Xialin Zheng[1,2†], Dongqi Shao[2†], Yu Li[2], Longjie Cai[2], Shan Xie[2], Zhixiang Sun[2] and Zhiquan Jiang[1,2*]

[1]School of Continuing Education, Anhui Medical University, Hefei, China, [2]Department of Neurosurgery, The First Affliated Hospital of Bengbu Medical College, Bengbu, China

Background: The fully endoscopic supraorbital trans-eyebrow keyhole approach is a technique utilized for the transcranial resection of tuberculum sellae meningioma (TSM). Surgery is the first choice for TSM treatment. This study aimed to summarize and analyze the safety, feasibility, limitations, and technical requirements of the fully endoscopic supraorbital trans-eyebrow keyhole approach for TSM resection.

Methods: Data of 19 TSM fully endoscopic supraorbital trans-eyebrow keyhole approach resections cases (six and 13 on the left and right eyebrows, respectively) were retrospectively analyzed at the Neurosurgery Department of the First Affiliated Hospital of Bengbu Medical College (Bengbu, China) from August 2015 to March 2022.

Results: All 19 patients were diagnosed with meningioma (World Health Organization grade I), and according to the scope of tumor resection (EOR), 18 patients (94.7%) had gross total resection (GTR), and one patient (5.3%) had near-total resection (NTR). Preoperative chief complaints were symptomatic visual dysfunction ($n = 12$), headache and dizziness ($n = 6$), and accidental discovery ($n = 1$). Postoperative visual function improved in 83.3% of cases (10/12), and headache and dizziness were relieved in 83.3% of cases (5/6 patients). Postoperative intracranial infection occurred in one case and was cured by external drainage of the lumbar cistern and anti-infective treatment. Two cases of frontal lobe injury were discharged after conservative treatment. There was no postoperative olfactory dysfunction, eyelid ptosis, cerebrospinal fluid leakage, or death. There were no reports of disease recurrence or death during the 3-month follow-up at an outpatient clinic or by telephone.

Conclusion: Fully endoscopic TSM resection through the keyhole approach is safe and feasible. It can be used to explore angles that cannot be seen under a microscope and show the true value of endoscopy technology. The endoscopic equipment and technical skills of the surgeon and surgical team are important in this technique.

KEYWORDS

tuberculum sellae meningioma, keyhole supraorbital eyebrow approach, endoscopic resection, transcranial resection, endoscope

Introduction

Although surgical resection is the first choice for the treatment of tuberculum sellae meningioma (TSM), the degree of tumor resection and visual function pose challenges (1–3). With the improvement of microscopy, the transcranial approach (TCA) (e.g., pteral point and subfrontal approaches) has been established as the standard method for surgical TSM resection. Nevertheless, limitations still exist regardless of transcranial microsurgery type (1). In recent years, the use of the endoscopic endonasal approach (EEA) has become increasingly common owing to the rapid advancement of neuroendoscopy (4). Compared with TCA, the main advantage of EEA is the early treatment of the tumor base and Simpson grade I resection. However, cerebrospinal rhinorrhea, sellar floor reconstruction, anosmia, and nasal symptoms limit further EEA development.

The supraorbital approach has been shown as the most suitable method for TSM treatment, offering the advantages of less trauma and faster recovery compared with other TCAs (5, 6). Some scholars have proposed that there are blind areas in the microscopical approach through the eyebrow arch, and the use of angle neuroendoscopy can effectively solve this problem (7). Berhouma et al. (8) first suggested the feasibility of total endoscopic resection of anterior middle skull base lesions through the keyhole of the eyebrow arch approach. Arnaout et al. (9) performed eight dissections through the supraorbital approach on four cadaver heads using a microscope and an endoscope and compared the visibility and accessibility of the anterior cranial fossa. They concluded that both approaches provide similar visibility and accessibility for the surgeon. Based on this evidence, we evaluated the surgical techniques, clinical efficacy, and technical requirements for the resection of TSM by the supraorbital approach at the First Affiliated Hospital of Bengbu Medical College (Bengbu, China). This case series analysis and suggested algorithm aim to guide neurosurgeons in managing TSMs.

TABLE 1 Characteristics of patients with tuberculum sellae meningioma (TSM).

General information		
female	14 (73.7%)	
age	32–70, 56	
Manifestations	Headache	6 (31.6%)
	Hypopsia	12 (63.2%)
	Physical examination findings	1 (5.3%)
Eyebrow arch approach (Left/Right)	Left	6 (31.6%)
	Right	13 (68.4%)
Mean tumor volume, cm^3	3.6 ± 2.5	

TABLE 2 Intraoperative conditions of TSM patients.

Extent of Resection	GTR	17 (94.4%)
	STR	1 (5.6%)
Kuga grade	I	3 (15.8%)
	II	5 (26.3%)
	III	11 (57.9%)
Magill Grading Scale	2	4 (21.1%)
	3	5 (26.3%)
	4	5 (26.3%)
	5	5 (26.3%)
Operation time,h	2.61 ± 0.85	
The length of the incision, cm	4.81 ± 0.15	
Size of bone flap, mm^2	8.31 ± 0.65	
Optic canal invasion	yes	6 (31.6%)
	no	13 (68.4%)
Relationship with anterior cerebral communicating artery complex	Fully surrounded	3 (15.8%)
	Partially surrounded	2 (10.5%)
	Contact	12 (63.2%)

Methods

Patient selection

We reviewed the clinical outcomes and imaging data of 19 patients with TSM who underwent pure neuroendoscopic transeyebrow approach surgery at our hospital from August 2015 to March 2022. The baseline characteristics of patients are shown in **Table 1**. Computed tomography scan, magnetic resonance imaging (MRI) scan with enhancement, computed tomography angiography (CTA), visual field assessment, and examination of hormone levels in venous blood were preoperatively performed (**Figure 1**). The postoperative pathological analysis confirmed the presence of World Health Organization (WHO) grade I meningioma. All procedures were performed by a single surgical team. All patients underwent surgery for the first time.

Patients with meningiomas that did not have tumor epicenter at the tuberculum sella/posterior planum region and had invasive parasellar meningiomas arising from the cavernous sinus and/or Meckel's cave and clinoidal meningiomas were excluded from this analysis. Collected data included demographics, MRI characteristics, preoperative and postoperative clinical status, vision/visual field assessment, and complications. Differences in the skills of surgeons during tumor resection procedures were recorded. All patients were followed up for at least 3 months with MRI analysis and

pituitary hormone testing. This study was approved by the Research Ethics Committee of Bengbu Medical College. The need for informed consent was waived due to the retrospective nature of the study. Nevertheless, the confidentiality of patient data was protected according to the tenets of the Declaration of Helsinki.

Surgical method

General anesthesia was performed following orotracheal intubation. A patient was in the supine position, and the head was rotated 10°–30° to the opposite side of the approach to the eyebrow arch (i.e., if the procedure was performed on the right eyebrow arch, the head was turned to the left), and the head was tilted back 10°–15°. The DORO head brace (Germany) was used to pin the patient's head. The whole upper edge of the eyebrow (Figures 2A–C) was taken, and a skin incision was made. The skin and subcutaneous tissues were cut with a blade (an electric knife was not and should not be used in this step of the procedure). The upper edge was retracted upward using two "fishhook-morphous" retractors, and the lower edge was untied downward with sutures to untie the wound while avoiding the use of a spreader (Figure 2D). This method reduces the incidence of upper eyelid swelling after surgery. A burr drill was used to drill behind the anterior temporal line, and the small free bone flap was removed with a milling blade (Figure 2E). The anterior boundary was flattened against the superior margin of the supraorbital nerve foramen (Figure 2F). If the frontal sinus was open, the mucous membrane in the sinus cavity was first removed, followed by electric cauterization with an electric knife and repeated flushing with hydrogen peroxide and diluted iodophor. Subsequently, the inner plate of the frontal sinus was removed by drilling, and the outer plate was retained (Figures 2G,H). A gentamicin-containing gelatin sponge was filled and sealed with bone wax. In this study, there were three cases of frontal sinus opening, and there was no occurrence of cerebrospinal fluid leakage or intracranial infection after the operation. A U-shaped cut of the dura was made, and it was turned to the eye side and suspended. Intravenous administration of mannitol, hyperventilation, and release of cerebrospinal fluid from the lateral fissure

TABLE 3 Postoperative conditions of TSM patients.

Postoperative Complication	Intracranial infection	1 (5.6%)
	The frontal lobe damage	2 (10.5%)
	New vision loss	0
	Stroke	0
	Hematoma	0
	CSF leak	0
	New hypopituitarism	0
	New anosmia	0
Visual outcome	Improved	10 (83.3%)
	Unchanged	2 (16.7%)
	Worsened	0
headache outcome	Improved	5 (83.3%)
	Unchanged	1 (16.7%)
	Worsened	0
Recurrence/Mortality		0

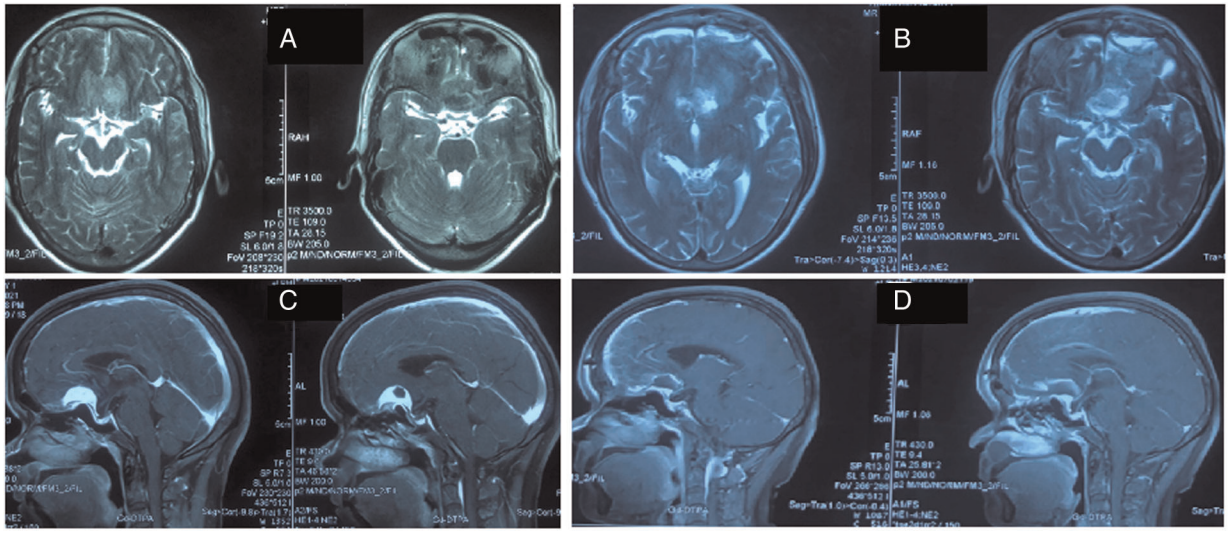

FIGURE 1
Magnetic resonance imaging of the patients (A,C) Preoperative (B,D) postoperative.

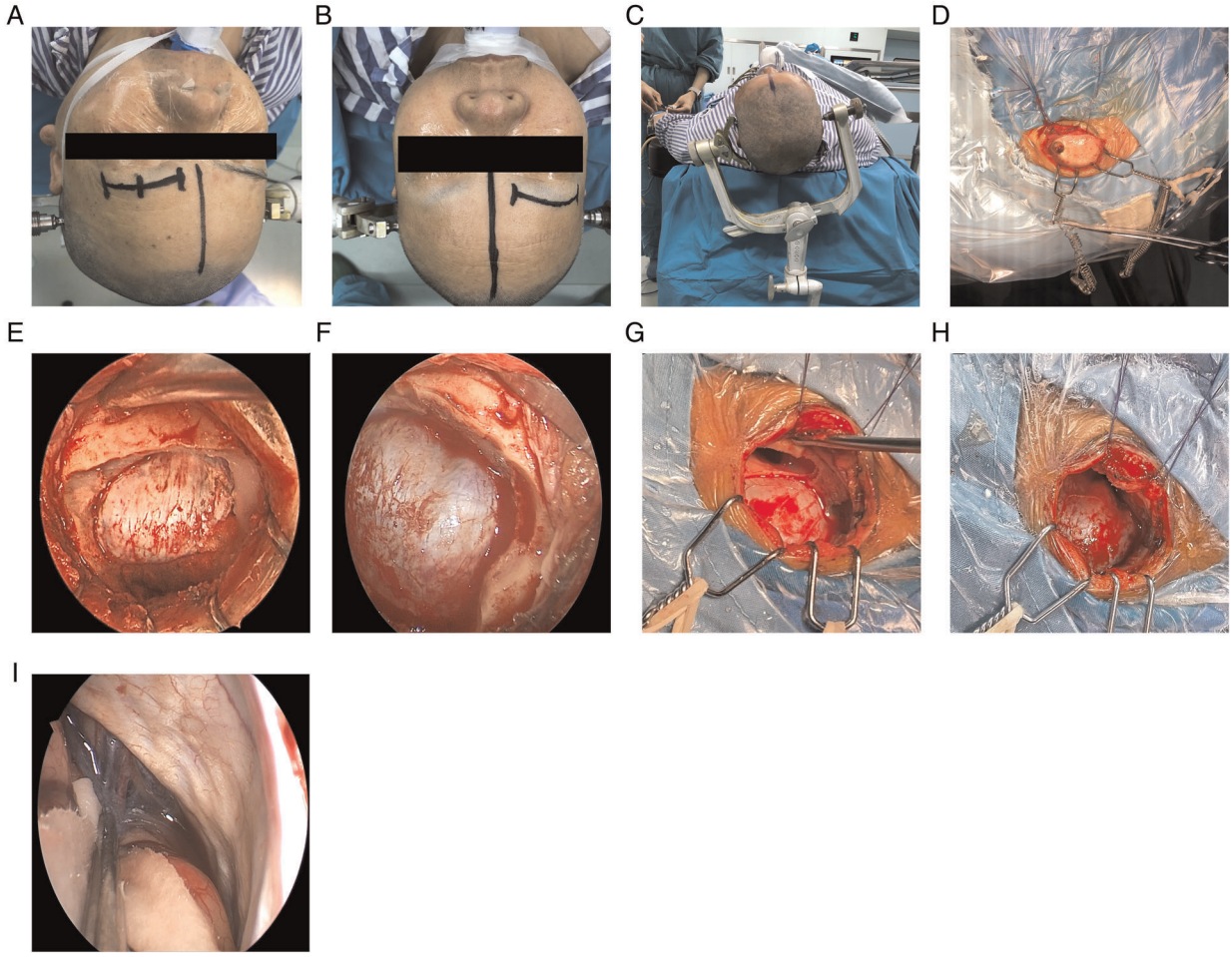

FIGURE 2
Operating procedure. (A,B) Location of the surgical approach. (C) The DORO head brace was used to fix the head of the patient. (D) Upward retraction using two "fishhook-morphous" retractors. (E) Removal of the small free bone flap. (F) Supraorbital nerve. (G,H) Opening of the frontal sinus: before and after. (I) Release of cerebrospinal fluid.

(Figure 2I) were performed to reduce the intracranial pressure. The use of an indwelling lumbar cistern external drainage tube was unnecessary. In this operation, the assistant held the endoscope, and the operator performed the microoperation (i.e., one hand was holding the suction apparatus while the other hand was holding bipolar coagulation, microscissors, forceps, etc.). The distribution of surgical instruments was triangular, with the endoscope at the apex and the remaining instruments at the base points on both sides (Figures 3A,B). The endoscope holder was on the left side of the operator, the display screen of the endoscope was on the opposite side to the operator, the hand-washing nurse was on the right side of the patient, and the anesthesiologist was behind the operator (Figure 3C). A STORZ 30° rigid endoscope was used. The endoscope gradually penetrated the anterior skull base using the supraorbital margin as the fulcrum. The instruments operated by the surgeon were located on both sides of the endoscope. The endoscope and instruments simultaneously entered and exited, and the instruments were constantly within the field of vision at the front of the endoscope.

For tumor resection, the tumor basilar part was initially removed under endoscopy. For tumors growing toward the pituitary fossa, the direction of the endoscope was adjusted, and a bending curette was applied to remove the tumor. Subsequently, piecemeal resection was performed for the tumor body.

Finally, *in-situ* interlocking or artificial repair suturing of the dura mater was performed. The sutured area was sealed with biological glue, a free bone flap was fixed with two peptide chain fixation, bone foramen and bone suture were filled with bone cubic, subcutaneous alignment was achieved by suturing, and the wound was closed with intradermal suturing (Figure 3D).

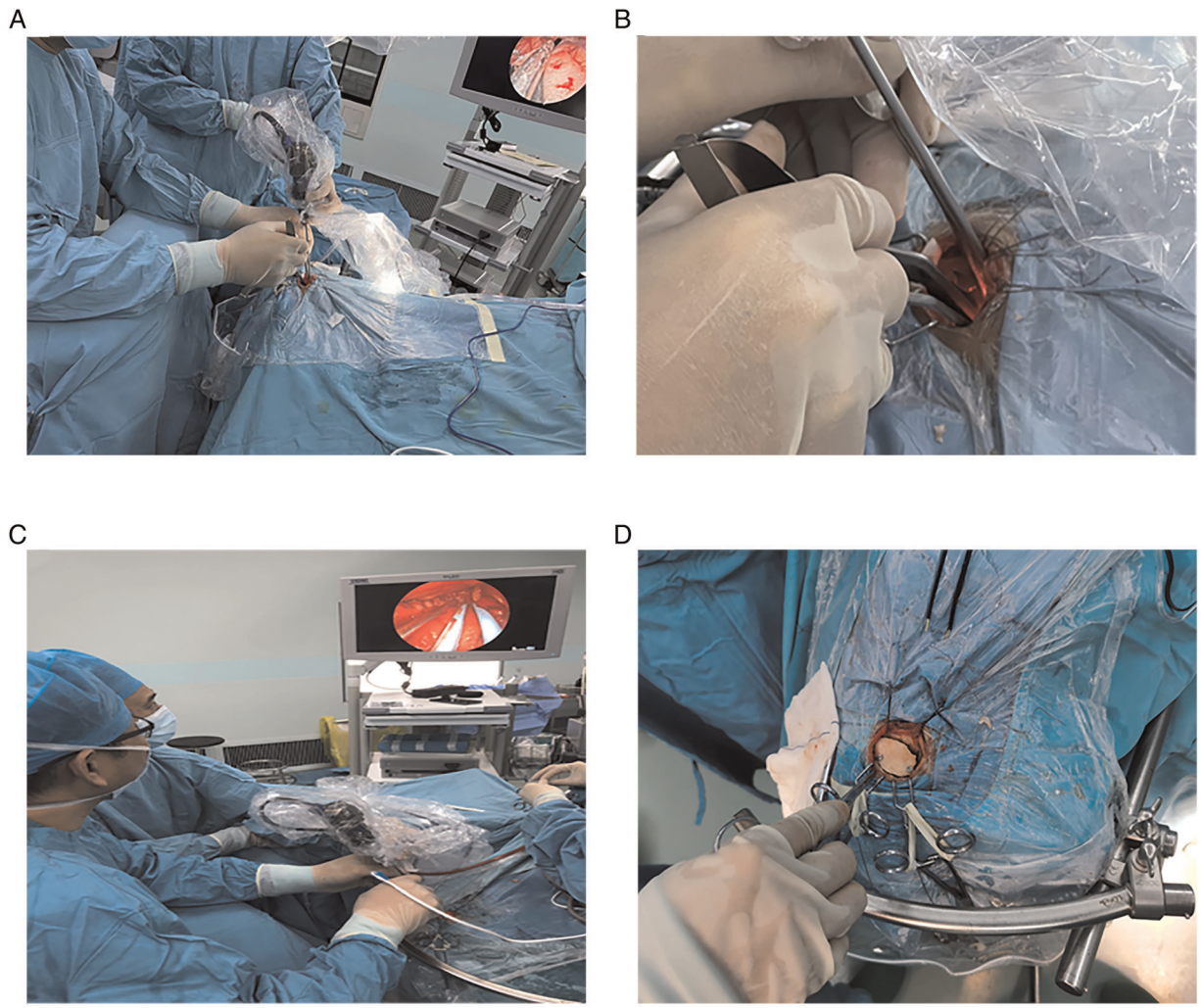

FIGURE 3
Subdural endoscopic operation. (A–C) Location of the endoscope, instrument, and operators. (D) Resetting of the bone flap.

Statistical analysis

Data are expressed as the mean ± standard deviation of the normal distribution for continuous variables and frequency or percentage for categorical variables. All statistical analyses were performed using the SPSS 23.0 (IBM Corp., Armonk, NY, USA) software. A *P*-value of <0.05 denoted a statistically significant difference.

Results

Nineteen patients (mean age: 56 ± 13 years; 73.7% females) underwent supraorbital craniotomy. The main preoperative symptoms comprised visual dysfunction ($n = 12$) and headache and dizziness ($n = 6$), while one case was inadvertently found by physical examination. Preoperative olfactory testing and analysis of hormone levels in venous blood were normal.

MRI plain scan, enhanced scan, and CTA were performed before surgery. In 12 cases, the tumor was closely related to the internal carotid artery and/or anterior cerebral traffic artery complex. Among them, two cases were partially wrapped, and three cases were completely wrapped

All patients were pathologically diagnosed with WHO grade I meningioma. According to Kuga et al. (10), tumors are classified into three types according to the imaging relationship between TSM and chiasma: type I, tumors with an intact optic apparatus; type II, tumors in which the optic chiasm is pushed superiorly by the tumor from the ventral aspect; and type III, tumors in which the optic chiasm is

pushed posteriorly by the tumor from the rostral aspect. Among 19 cases, 3, 5, and 11 cases were of types I, II, and III, respectively. The TSM grading scale proposed by Magill et al. (11) was used: tumor diameter (<17 mm: 1 point; ≥17 mm: 2 points), optic canal invasion (≤3 mm: 0 point; invades one canal and is >3 mm: 1 point; invades two canals and is >3 mm: 2 points), and arterial encapsulation (<180°: 1 point; ≥180°: 2 points). The score distribution in these 19 cases is shown in Table 1.6 patients had surgery on the left side, 13 on the right side,The mean operation time was 2.61 ± 0.85 h, and the mean tumor size was 3.6 ± 2.5 cm

The extent of resection was divided into gross total resection (GTR), near-total resection (NTR; 95%–99%), or subtotal resection (<95%) (12, 13). Of 19 patients in this group, 18 had GTR, and one had NTR. In this group, six cases had tumors that invaded the optic canal, two cases had tumors that pushed the optic nerve upward, and four cases had tumors that pushed the optic nerve laterally from the first space (**Figure 4**) (**Table 2**).

Postoperative visual function improved in 10/12 cases (83.3%), and dizziness was relieved in 5/6 cases (83.3%). Postoperative intracranial infection occurred in one case, which recovered after external drainage of the lumbar cistern and anti-infective treatment. Two cases of frontal lobe injury were discharged after conservative treatment. There was no occurrence of postoperative anosmia, eyelid ptosis, endocrine dysfunction, cerebrospinal fluid leakage, or death. There was no recurrence in total resection cases, no progress in subtotal resection cases, and no death cases during the follow-up of 7 months (**Table 3**).

Discussion

TSM accounts for 5%–10% of all meningiomas (14–16). These tumors originate from the planum sphenoidale, optic sulcus, and sphenoid margin and can extend to nearby areas, such as the sphenoid plateau, saddle area, posterior clinoid process, and cavernous sinus (16). Owing to the complex anatomical structure of this region, which includes important blood vessels and nerves (optic nerve, optic chiasm, internal carotid artery, anterior cerebral artery complex, cavernous sinus, pituitary stalk, etc.), it is difficult to achieve Simpson I level TSM resection (14, 15).

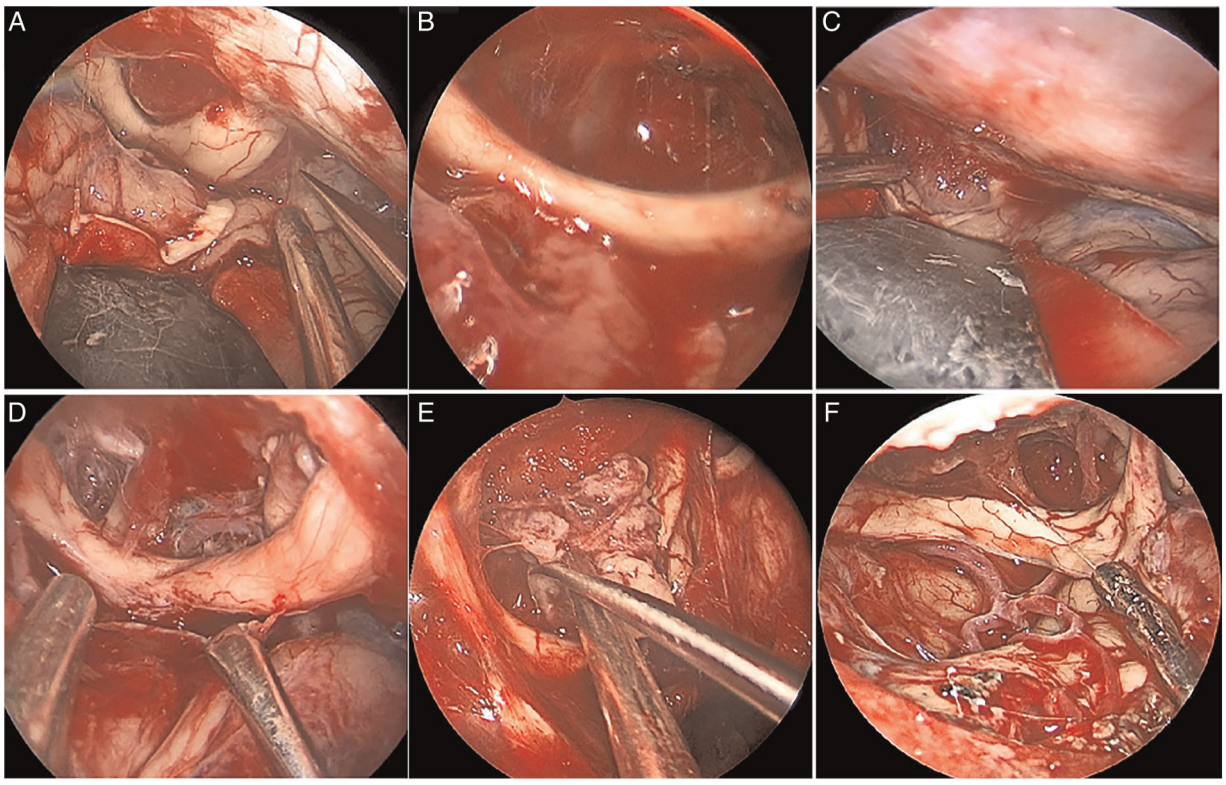

FIGURE 4
Intraoperative optic neural tube invasion (A) Under the optic nerve on the right side of the tumor and in the first space, push the optic nerve upward; (B) After total resection of the tumor (C) the main body of the tumor is located in the first space, and the right optic nerve is pushed upward and outward; (D) After total resection of the tumor.

Surgical resection, the preferred treatment for TSM, can be divided into TCA and nasal approaches according to the employed surgical method. The former includes the pterional approach, unilateral subfrontal approach, and bilateral interfrontal hemispheric approach and has been established as the standard method for surgical TSM resection for decades (2). In recent decades, significant progress has been achieved in EEA for TSM treatment with the rapid development of endoscopic technology (4). Its main advantages are a limited disturbance to brain tissue and optic nerve optic chiasma, effective treatment of the tumor base, and eventual removal of the involved dura mater and skull, rendering Simpson I resection possible. Furthermore, limitations of the EEA for TSM treatment also exist. First, the indications are limited; for example, the EEA is not applicable to vascular wrapping and laterally growing tumors or those with a size of >2–2.5 cm (17). Second, skull base reconstruction and cerebrospinal fluid (CSF) rhinorrhea are important problems limiting the development of EEA (18, 19). Studies have suggested that the incidence of CSF rhinorrhea after the treatment with TSM by EEA is 23%–40% (20). Although the technique for skull base reconstruction has improved, the incidence of CSF rhinorrhea remains at 5%–10%. This rate is significantly higher than that associated with transcranial surgery. Finally, the conchal sphenoid sinus and operative side accessory sinus inflammation are also key factors affecting the efficacy of EEA (7). There is an ongoing debate regarding the most appropriate surgical approach (i.e., TCA or EEA) in this setting (18). In a meta-analysis, Yang et al. (4) compared TCA and EEA regarding the tumor resection rate, recurrence rate, vision improvement, and CSF leakage. They concluded that there was no difference in tumor resection and recurrence rates. In their study, EEA was superior to TCA in terms of vision improvement; however, the rate of CSF leakage has been higher with EEA vs. TCA. Studies have suggested that there is no difference in postoperative recurrence rate between the two methods (21). Notably, there is also disagreement regarding the selection of EEA and endoscopic TCA (22, 23). Recently, a more effective approach has been proposed, namely, the supraorbital approach (6, 24, 25). Linsler et al. (26) suggested using the supraorbital approach for the treatment of larger TSM tumors growing to the far lateral side of the saddle region or those wrapped with blood vessels. Using a microscope, endoscope, and neural navigation, Arnaout et al. (9) performed eight operations through the supraorbital approach on four cadaver heads. They compared the visibility and accessibility of the anterior and middle cranial fossa regions. The results have demonstrated that both endoscopic and microscopic images provided the surgeon with nearly identical visibility and accessibility and that the supraorbital keyhole approach was preferable to endoscopy alone. Berhouma et al. (8) also demonstrated the feasibility of endoscopic resection of anterior middle skull base lesions through the supraorbital keyhole approach.

In this study of 19 cases of TSM, the tumors were removed by pure neuroendoscopy *via* the eyebrow arch approach, achieving good clinical results. We selected the extent of resection as the standard for tumor resection instead of the Simpson score. This decision was based on studies that suggested the absence of difference in postoperative recurrence rate and recurrence-free survival rate between Simpson grade I–III meningiomas (13) and that total tumor resection could lead to good outcomes. Oya et al. (24) have also confirmed no correlation between the resection of Simpson grade I–III WHO meningioma and recurrence-free survival. According to the tumor grades of Kuga D (10) and Magill (11), all cases in this group were covered. According to EOR grading, 18 of 19 patients in this group had GTR, and 1 had NTR. In a case of the tumor with preoperative Kuga grade III, Magill score of 5, and tumor size of 4 cm × 5 cm × 5 cm, intraoperatively, it was closely adhered to the right anterior cerebral artery and the initial part of the middle cerebral artery without clear boundaries and could not be removed even by using a microscope (**Figure 4**). Bernat et al. (21) indicated that bone dysplasia, ICA, invasion of the anterior cerebral artery and middle cerebral artery, and maximum dural tail sign in the transverse section are all considered independent factors for incomplete resection of anterior skull base tumor. No serious complications, such as second operation, cerebrospinal fluid leakage, or death, occurred. There was one case of postoperative intracranial infection in which the frontal sinus was not opened. Considering that the cause of infection might be related to the large tumor and long operation time (4 h 23 min), it has been reported in the literature that the operation time of >4 h (27) and a large benign tumor of the skull base (28) are the risk factors of intracranial infection after craniotomy. Postoperative visual function was improved in 6/7 cases (85.7%). Additionally, there was one case where the postoperative visual function was not improved, and the patient was blind in his right eye before surgery. It has been pointed out in the literature (1) that postoperative improvement might be lower in patients with poor preoperative visual acuity. In this group, postoperative follow-up lasted at least 3 months, and no recurrence was found. However, due to the short follow-up, postoperative recurrence could not be accurately reflected, and further follow-up is required. It has been reported that the optimal follow-up time after TSM is 5–10 years (2). In this group, six cases had tumors that invaded the optic nerve canal, two cases had tumors that pushed the optic nerve upward (**Figures 5A–D**), and four cases had tumors that pushed the optic nerve outwardly from the first space (**Figures 5E–F**). During the operation, the optic nerve canal was not opened by 30°-endoscope and angular curettage.

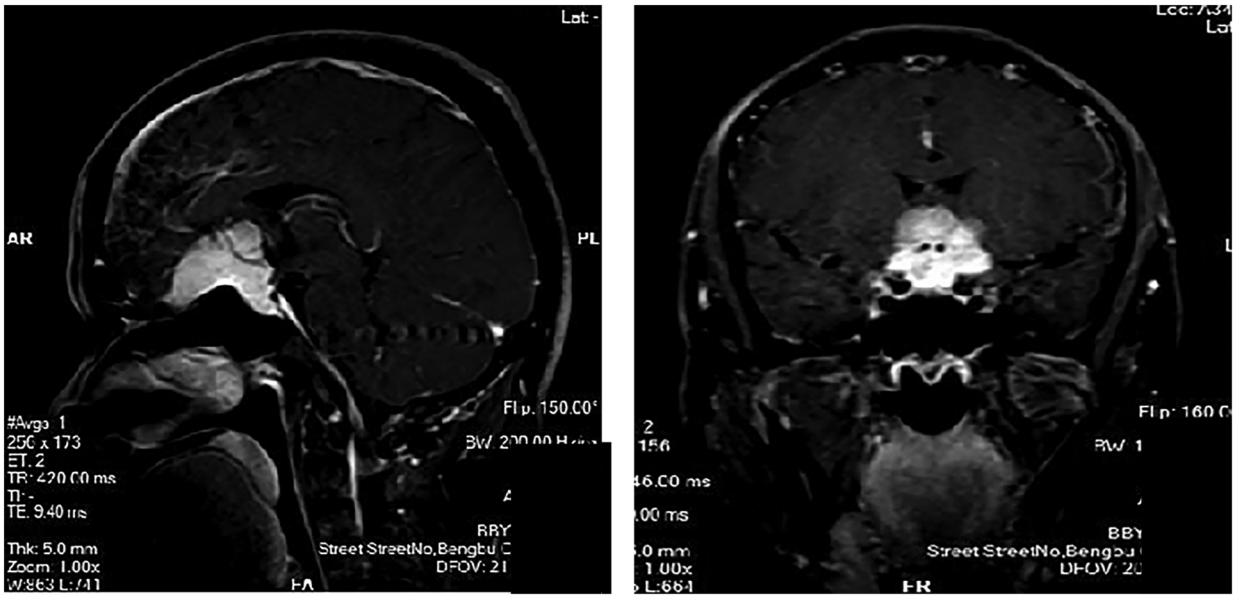

FIGURE 5
The tumor completely surrounded bilateral anterior cerebral arteries.

Summary of technical requirements and surgical techniques

Robinow et al. (4) indicated that the supraorbital approach is most suitable for anterior skull base tumors, such as TSM, and can replace the previous pterotomy. Louis et al. (6) pointed out that there were four blind areas in the microscopical approach through the brow arch: the anterior part of the olfactory groove, the sellar bottom, the inferior part of the ipsilateral optic nerve, and the anterior part of the middle cranial fossa under the sphenoid crest. Arnaout (8), such as using the microscope and endoscope and neural navigation, has performed on the eight to four cadaver head anatomy of the supraorbital superciliary arch into the road, the front, middle cranial fossa region of visibility and accessibility, conclusion endoscopy and microscopic image can provide the surgeon with almost the same visibility and accessible area so the orbital lock hole can adopt pure endoscopic approach into the road. Berhouma et al. (7) also demonstrated that total endoscopic resection of anterior middle skull base lesions through eyebrow arch keyhole is feasible. Therefore, we believe that the fully endoscopic supraorbital trans-eyebrow keyhole approach is feasible.

Endoscopic TSM resection through the supraorbital keyhole approach offers the following advantages. First, there are four blind areas in the supraorbital approach using a microscope: the anterior part of the olfactory groove, the sellar floor, the part inferior to the ipsilateral optic nerve, and the anterior part of the middle cranial fossa below the sphenoid crest (7). This problem can be overcome through the use of an angle lens in neuroendoscopy. Second, most scholars use neuroendoscopy only as the auxiliary lighting of the microscope. Therefore, two sets of equipment need to be prepared, and continuous switching between the two sets is necessary during the operation. The use of total endoscopy is effective in avoiding this process. Giammattei et al. (29) showed that EEA could be a better approach in cases of tumors that tend to extend deep in the sella turcica, suggesting evaluating the angle from the frontobasal line to the sella. These authors also found that optic canal invasion is a good indication of EEA due to the possibility of performing an early decompression of the medial part of the canal.

Due to the saddle nodules, meningioma often invades the optic canal and optic nerve or pushes it laterally, and the optic microscope below the eyebrow bending into the road is one of the four blind areas (7). The other three are the front of the olfactory groove, the bottom of the saddle, and the sphenoid ridge of the cranial fossa in the front; thus, surgeons often need to grind the optic nerve tube wall to cut the tumor. In this study, we used 30° endoscopy and angled curettage to remove residual tumors without opening the optic canal wall. However, due to the small number of cases in this study, tumor invasion of the optic canal was not too serious; hence, a large number of cases needs to be further summarized.

Below, we outline our experience during the fully endoscopic supraorbital trans-eyebrow keyhole

approach. 1. When the surgery is performed, the first choice is the side with severe visual impairment before surgery, followed by the side with frontal sinus occlusion or smaller; when the two conditions are similar, the side of the nondominant hemisphere is selected. 2. Open frontal sinus will increase the rate of postoperative infection rate; thus, appropriate disinfection measures and simultaneous strict closure of the frontal sinus are essential. 3. In addition to conventional epidural grinding of the anterior skull base bone ridge, the inner plate of the frontal sinus needs to be burnished to provide sufficient operating space and a stable fulcrum for subsequent endoscopic operation. 4. The supraorbital nerve must be preserved, and damage should be avoided. 5. We used the assistant to handle the endoscope with both hands for microscopic operation. This method can adjust the depth and angle of the endoscope as the surgeon operates, and the assistant can achieve a better endoscope flexibly by handling the endoscope with both hands compared to the mechanical arm (30, 31). Moreover, unlike the fixation arm, endoscopy can achieve "dynamic magnification" (32, 33). The fulcrum of the assistant handling the endoscope. Usually, TSM tumors are located in deep sites; hence, a stable and reliable fulcrum is needed after in-depth endoscopy. In the absence of a fulcrum, the assistant handling the endoscope is prone to shaking and fatigue. There are two fulcrums: the endoscopic fulcrum (i.e., the superior orbital margin of the bone window) and the arm fulcrum (i.e., the right hand dragging the left elbow joint). 6. Endoscopy has a proximal visual blind area; hence, endoscopy and other surgical instruments (suction, microscissors, etc.) into the easy loss after normal blood vessels or nerves, causing serious complications (8). Based on our experience, the assistant holds the endoscope, places it in the middle, and gradually penetrates along the anterior skull base. The surgeon enters through both sides of the endoscope, with both hands holding instruments. At the same time, the assistant holding the endoscope should ensure that the instrument is located at the front end of the endoscope and simultaneous entry and exit. In every operation, the surgeon should ensure that the instrument is under the vision field of the endoscope.

Limitations and generalizability

The main limitation of this study was its short follow-up period. The shortest follow-up period was only 3 months, which does not accurately assess the risk of postoperative recurrence. Furthermore, the number of cases included in this study was relatively small. Therefore, further multicenter studies with larger sample sizes are warranted to validate the presented findings.

Conclusion

Neuroendoscopic TSM resection through the supraorbital approach is safe and feasible. It can be used to explore angles that cannot be seen under a microscope and show the true value of endoscopy technology. However, it requires a high level of endoscopic competence by the surgeon and assistant, which is acquired through long-term and repeated practice. Once this technique is mastered, it becomes a simple and time-saving surgical option.

Data availability statement

The raw data supporting the conclusions of this article will be made available by the authors, without undue reservation.

Ethics statement

The studies involving human participants were reviewed and approved by the Research Ethics Committee of Bengbu Medical College. The patients/participants provided their written informed consent to participate in this study.

Written informed consent was obtained from the individual(s) for the publication of any potentially identifiable images or data included in this article.

Author contributions

XZ DS, and LC designed the study. XZ, SX, and ZS analyzed the data. XZ, ZJ, and YL wrote the manuscript. ZJ and HC revised the manuscript and supervised the study. All authors approved the final version of the manuscript for publication. All authors contributed to the article and approved the submitted version.

Funding

This study was supported by grants from the Natural Science Foundation of Anhui Province (no. KJ2021ZD0078) and 512 Talent Program of Bengbu Medical College (by51202206)

Conflict of interest

The authors declare that the research was conducted in the absence of any commercial or financial relationships that could be construed as a potential conflict of interest.

Publisher's note

References

1. Sankhla SK, Jayashankar N, Khan MA, Khan GM. Surgical management of tuberculum sellae meningioma: our experience and review of the literature. *Neurol India*. (2021) 69:1592–600. doi: 10.4103/0028-3886.333529

2. Magill ST, McDermott MW. Tuberculum sellae meningiomas. *Handb Clin Neurol*. (2020) 170:13–23. doi: 10.1016/B978-0-12-822198-3.00024-0

3. Leclerc A, Gaberel T, Laville MA, Derrey S, Quintyn JC, Emery E. Predictive factors of favorable visual outcomes after surgery of tuberculum sellae meningiomas: a multicenter retrospective cohort study. *World Neurosurg*. (2022) 164:e557–67. doi: 10.1016/j.wneu.2022.05.015.

4. Yang C, Fan Y, Shen Z, Wang R, Bao X. Transsphenoidal versus transcranial approach for treatment of tuberculum sellae meningiomas: a systematic review and meta-analysis of comparative studies. *Sci Rep*. (2019) 9:4882. doi: 10.1038/s41598-019-41292-0

5. Robinow ZM, Peterson C, Waldau B, Shahlaie K. Supraorbital keyhole craniotomy via eyebrow incision: a systematic review and meta-analysis. *World Neurosurg*. (2021) 158:e509–42. doi: 10.1016/j.wneu.2021.11.015

6. Hayhurst C, Teo C. Tuberculum sella meningioma. *Otolaryngol Clin North Am*. (2011) 44:953–63, viii-ix. doi: 10.1016/j.otc.2011.06.012

7. Louis RG, Eisenberg A, Barkhoudarian G, Griffiths C, Kelly DF. Evolution of minimally invasive approaches to the sella and parasellar region. *Int Arch Otorhinolaryngol*. (2014) 18:S136–48. doi: 10.1055/s-0034-1395265

8. Berhouma M, Jacquesson T, Jouanneau E. The fully endoscopic supraorbital trans-eyebrow keyhole approach to the anterior and middle skull base. *Acta Neurochir (Wien)*. (2011) 153:1949–54. doi: 10.1007/s00701-011-1089-z

9. Arnaout MM, Luzzi S, Galzio R, Aziz K. Supraorbital keyhole approach: pure endoscopic and endoscope-assisted perspective. *Clin Neurol Neurosurg*. (2020) 189:105623. doi: 10.1016/j.clineuro.2019.105623

10. Kuga D, Toda M, Yoshida K. Treatment strategy for tuberculum sellae meningiomas based on a preoperative radiological assessment. *World Neurosurg*. (2018) 120:e1279–88. doi: 10.1016/j.wneu.2018.09.054

11. Magill ST, Morshed RA, Lucas CG, Aghi MK, Theodosopoulos PV, Berger MS, et al. Tuberculum sellae meningiomas: grading scale to assess surgical outcomes using the transcranial versus transsphenoidal approach. *Neurosurg Focus*. (2018) 44:E9. doi: 10.3171/2018.1.FOCUS17753

12. Youngerman BE, Shtayer L, Gerges MM, Larsen AG, Tomasiewicz HC, Schwartz TH. Eyebrow supraorbital keyhole craniotomy for olfactory groove meningiomas with endoscope assistance: case series and systematic review of extent of resection, quantification of postoperative frontal lobe injury, anosmia, and recurrence. *Acta Neurochir (Wien)*. (2021) 163:101–12. doi: 10.1007/s00701-020-04552-x

13. Ansari SF, Eisenberg A, Rodriguez A, Barkhoudarian G, Kelly DF. The supraorbital eyebrow craniotomy for intra- and extra-axial brain tumors: a single-center series and technique modification. *Oper Neurosurg (Hagerstown)*. (2020) 19:667–77. doi: 10.1093/ons/opaa217

14. Mortazavi MM, Brito da Silva H, Ferreira Jr M., Barber JK, Pridgeon JS, Sekhar LN. Planum sphenoidale and tuberculum sellae meningiomas: operative nuances of a modern surgical technique with outcome and proposal of a new classification system. *World Neurosurg*. (2016) 86:270–86. doi: 10.1016/j.wneu.2015.09.043

15. Elshazly K, Kshettry VR, Farrell CJ, Nyquist G, Rosen M, Evans JJ. Clinical outcome after endoscopic endonasal resection of tuberculum sella meningiomas. *Oper Neurosurg (Hagerstown)*. (2018) 14:494–502. doi: 10.1093/ons/opx165

16. Xiao F, Shen J, Zhang L, Yang J, Weng Y, Fang Z, et al. Unilateral subfrontal approach for giant tuberculum sellae meningioma: single center experience and review of the literature. *Front Oncol*. (2021) 11:708235. doi: 10.3389/fonc.2021.708235

17. de Divitiis E, Cavallo LM, Esposito F, Stella L, Messina A. Extended endoscopic transsphenoidal approach for tuberculum sellae meningiomas. *Neurosurgery*. (2007) 61:229–37. discussion 237-8. doi: 10.1227/01.neu.0000306128.54281.7d

18. Song SW, Kim YH, Kim JW, Park CK, Kim JE, Kim DG, et al. Outcomes after transcranial and endoscopic endonasal approach for tuberculum meningiomas-a retrospective comparison. *World Neurosurg*. (2018) 109:e434–45. doi: 10.1016/j.wneu.2017.09.202

19. Ishikawa T, Takeuchi K, Nagata Y, Choo J, Kawabata T, Ishizaki T, et al. Three types of dural suturing for closure of CSF leak after endoscopic transsphenoidal surgery. *J Neurosurg*. (2018) 1–7. doi: 10.3171/2018.4.jns18366

20. Lucas JW, Zada G. Endoscopic endonasal and keyhole surgery for the management of skull base meningiomas. *Neurosurg Clin N Am*. (2016) 27:207–14. doi: 10.1016/j.nec.2015.11.008

21. Bernat AL, Priola SM, Elsawy A, Farrash F, Pasarikovski CR, Almeida JP, et al. Recurrence of anterior skull base meningiomas after endoscopic endonasal resection: 10 years' experience in a series of 52 endoscopic and transcranial cases. *World Neurosurg*. (2018) 120:e107–13. doi: 10.1016/j.wneu.2018.07.210

22. Muskens IS, Briceno V, Ouwehand TL, Castlen JP, Gormley WB, Aglio LS, et al. The endoscopic endonasal approach is not superior to the microscopic transcranial approach for anterior skull base meningiomas-a meta-analysis. *Acta Neurochir (Wien)*. (2018) 160:59–75. doi: 10.1007/s00701-017-3390-y

23. Komotar RJ, Starke RM, Raper DM, Anand VK, Schwartz TH. Endoscopic skull base surgery: a comprehensive comparison with open transcranial approaches. *Br J Neurosurg*. (2012) 26:637–48. doi: 10.3109/02688697.2012.654837

24. Otero-Rodriguez A, Tabernero MD, Munoz-Martin MC, Sousa P, Orfao A, Pascual-Argente D, et al. Re-evaluating simpson grade I, II, and III resections in neurosurgical treatment of world health organization grade I meningiomas. *World Neurosurg*. (2016) 96:483–8. doi: 10.1016/j.wneu.2016.09.007

25. Oya S, Kawai K, Nakatomi H, Saito N. Significance of Simpson grading system in modern meningioma surgery: integration of the grade with MIB-1 labeling index as a key to predict the recurrence of WHO Grade I meningiomas. *J Neurosurg*. (2012) 117:121–8. doi: 10.3171/2012.3.JNS111945

26. Linsler S, Fischer G, Skliarenko V, Stadie A, Oertel J. Endoscopic assisted supraorbital keyhole approach or endoscopic endonasal approach in cases of tuberculum ellae meningioma: which surgical route should be favored? *World Neurosurg*. (2017) 104:601–11. doi: 10.1016/j.wneu.2017.05.023

27. Fang C, Zhu T, Zhang P, Xia L, Sun C. Risk factors of neurosurgical site infection after craniotomy: a systematic review and meta-analysis. *Am J Infect Control*. (2017) 45:e123–34. doi: 10.1016/j.ajic.2017.06.009

28. Lepski G, Reis B, de Oliveira A, Neville I. Recursive partitioning analysis of factors determining infection after intracranial tumor surgery. *Clin Neurol Neurosurg*. (2021) 205:106599. doi: 10.1016/j.clineuro.2021.106599

29. Giammattei L, Starnoni D, Cossu G, Bruneau M, Cavallo LM, Cappabianca P, et al. Surgical management of tuberculum sellae meningiomas: myths, facts, and controversies. *Acta Neurochir (Wien)*. (2020) 162:631–40. doi: 10.1007/s00701-019-04114-w

30. Seaman SC, Ali MS, Marincovich A, Li L, Walsh JE, Greenlee JDW. Minimally invasive approaches to anterior skull base meningiomas. *J Neurol Surg B Skull Base*. (2022) 83:254–64. doi: 10.1055/s-0040-1716671

31. Feng BH, Zhong WX, Li ST, Wang XH. Fully endoscopic microvascular decompression of the hemifacial spasm: our experience. (2020) 162(5):1081–7. doi: 10.1007/s00701-020-04245-5

32. Caballero-García J, Morales-Pérez I, Michel-Giol-Álvarez A, Aparicio-García C, López-Sánchez M, Huanca-Amaru J. Endoscopic retrosigmoid keyhole approach in cerebellopontine angle tumors. *A Surgical Cohort. Neurocirugia (English Edition)*. (2021) 32:268–77. doi: 10.1016/j.neucie.2021.02.001

33. Sun Z, Wang Y, Cai X, Xie S. Endoscopic vascular decompression for the treatment of trigeminal neuralgia: clinical outcomes and technical note. (2020) 13:2205–11. doi: 10.2147/jpr.s268441

frontiers | Frontiers in Surgery

TYPE Original Research
PUBLISHED 08 September 2022
DOI 10.3389/fsurg.2022.934721

OPEN ACCESS

EDITED BY
Peng Zhao,
Capital Medical University, China

REVIEWED BY
Narayan Jayashankar,
Dr. Balabhai Nanavati Hospital, India
Calvin Mak,
Queen Elizabeth Hospital (QEH), Hong Kong, SAR China
Mehdi Zeinalizadeh,
Tehran University of Medical Sciences, Iran

*CORRESPONDENCE
J. F. Villalonga
jfvillalonga@gmail.com

SPECIALTY SECTION
This article was submitted to Neurosurgery, a section of the journal Frontiers in Surgery

RECEIVED 03 May 2022
ACCEPTED 08 August 2022
PUBLISHED 08 September 2022

CITATION
Villalonga J. F., Solari D., Cuocolo R., De Lucia V., Ugga L., Gragnaniello C., Pailler J. I., Cervio A., Campero A., Cavallo L. M. and Cappabianca P. (2022) Clinical application of the "sellar barrier's concept" for predicting intraoperative CSF leak in endoscopic endonasal surgery for pituitary adenomas with a machine learning analysis.
Front. Surg. 9:934721.
doi: 10.3389/fsurg.2022.934721

Clinical application of the "sellar barrier's concept" for predicting intraoperative CSF leak in endoscopic endonasal surgery for pituitary adenomas with a machine learning analysis

J. F. Villalonga[1,2]*, D. Solari[1], R. Cuocolo[3], V. De Lucia[1], L. Ugga[3], C. Gragnaniello[1,4], J. I. Pailler[2], A. Cervio[5], A. Campero[2], L. M. Cavallo[1] and P. Cappabianca[1]

[1]Division of Neurosurgery, Department of Neurosciences, Reproductive and Odontostomatological Sciences, Universita' degli Studi di Napoli Federico II, Naples, Italy, [2]LINT, Facultad de Medicina, Universidad Nacional de Tucumán, Tucumán, Argentina, [3]Department of Advanced Biomedical Sciences, Universita' degli Studi di Napoli Federico II, Naples, Italy, [4]Department of Neurological Surgery, Swedish Neuroscience Institute, Seattle, WA, United States, [5]Departamento de Neurocirugía, FLENI, Buenos Aires, Argentina

Background: Recently, it was defined that the *sellar barrier* entity could be identified as a predictor of cerebrospinal fluid (CSF) intraoperative leakage. The aim of this study is to validate the application of the sellar barrier concept for predicting intraoperative CSF leak in endoscopic endonasal surgery for pituitary adenomas with a machine learning approach.
Methods: We conducted a prospective cohort study, from June 2019 to September 2020: data from 155 patients with pituitary subdiaphragmatic adenoma operated through endoscopic approach at the Division of Neurosurgery, Università degli Studi di Napoli "Federico II," were included. Preoperative magnetic resonance images (MRI) and intraoperative findings were analyzed. After processing patient data, the experiment was conducted as a novelty detection problem, splitting outliers (i.e., patients with intraoperative fistula, $n = 11/155$) and inliers into separate datasets, the latter further separated into training ($n = 115/144$) and inlier test ($n = 29/144$) datasets. The machine learning analysis was performed using different novelty detection algorithms [isolation forest, local outlier factor, one-class support vector machine (oSVM)], whose performance was assessed separately and as an ensemble on the inlier and outlier test sets.
Results: According to the type of sellar barrier, patients were classified into two groups, i.e., strong and weak barrier; a third category of mixed barrier was defined when a case was neither weak nor strong. Significant differences between the three datasets were found for Knosp classification score ($p = 0.0015$), MRI barrier: strong ($p = 1.405 \times 10^{-6}$), MRI barrier: weak ($p = 4.487 \times 10^{-8}$), intraoperative barrier: strong ($p = 2.788 \times 10^{-7}$), and intraoperative barrier: weak ($p = 2.191 \times 10^{-10}$). We recorded 11 cases of intraoperative leakage that occurred in the majority of patients presenting a *weak sellar barrier* ($p = 4.487 \times 10^{-8}$) at preoperative MRI. Accuracy, sensitivity, and specificity for outlier detection were 0.70, 0.64, and 0.72 for IF; 0.85, 0.45, and 1.00 for LOF; 0.83, 0.64, and 0.90 for oSVM; and 0.83, 0.55, and 0.93 for the ensemble, respectively.

Conclusions: There is a true correlation between the type of *sellar barrier* at MRI and its *in vivo* features as observed during endoscopic endonasal surgery. The novelty detection models highlighted differences between patients who developed an intraoperative CSF leak and those who did not.

KEYWORDS

sellar barrier, pituitary adenoma, CSF leak, machine learning, skull base surgery

Introduction

Endoscopic endonasal approach, representing the most suitable technique (1), is indicated for the removal of lesions upon the endocrinological status and eventual neurological defects.

Pituitary macroadenomas present a predominantly vertical growth pattern and, albeit being round and soft, displace and compress pituitary gland tissue: the latter gets to be a part along with arachnoid and sellar diaphragm of the interface between the tumor and the supradiaphragmatic area (2). According to its anatomical features, it has been possible to define three categories of the "so-called sellar barrier" as seen at the preoperative MRI i.e., weak, mixed, and strong.

Rarely, pituitary adenomas may present inner features, such as hard/rubbery consistency, which might make lesion removal *via* standard endoscopic corridor more troublesome, leading to an increased risk of CSF leak (3–5).

Although postoperative CSF fistula in transsphenoidal pituitary surgery appears to be notably low as compared to extended skull base surgery, peculiar care and efforts have been given to this issue (6, 7). However, there are only few reports concerning the possible risk factors that can be detected preoperatively to predict an intraoperative CSF leakage (8–11). The *sellar barrier concept* and its role in predicting the risk of intraoperative CSF leakage has been recently introduced (12, 13) and confirmed in a clinical multicentric study (14). Radiomics, consisting of conversion of images into mineable data and subsequent analysis for decision support, has been gaining attention (15) in association with data mining and machine learning (ML) algorithms, aiding in the interpretation of a large amount of information produced. ML is a branch of artificial intelligence that includes algorithms capable of modeling themselves and improving accuracy by analyzing datasets, without prior explicit programming (16), thus leading to the creation of predictive models (17–21).

The aim of this study is to validate the application of the sellar barrier concept for predicting intraoperative CSF leak in endoscopic endonasal surgery for pituitary adenomas with a quantitative approach. MRI features of the sellar barrier were defined, with machine learning, as a predictor of CSF leakage in a series of patients with intra-suprasellar pituitary adenoma undergoing endoscopic endonasal surgery.

Materials and methods

Patients with intra-suprasellar subdiaphragmatic pituitary adenoma scheduled for tumor resection *via* endoscopic endonasal approach at the Division of Neurosurgery, Università degli Studi di Napoli "Federico II," from June 2019 to September 2020 were included in the study. Those who had a history of treatment for pituitary adenoma (radiation or medical therapy) or significant artifacts on the images used for the analysis were excluded.

Preoperative MRI

All patients underwent radiological preoperative assessment with a specific MRI protocol for the sellar region that included sagittal and coronal slices in T1-weighted volumetric sequences, with and without contrast; with axial and sagittal slices of the sealing region in T2-weighted, fluid-attenuated inversion recovery (FLAIR), and Echo Spin gradient sequences (1.5 and 3.0 T resonator).

Considering the T1-weighted volumetric sequences, the evaluations of the *sellar barrier* were made with the Horos for Mac-OSX (Apple, California, USA). The measurements were made as explained in previous publications (2, 12–14). In each case, a neurosurgery resident classified the sellar barrier based on the MRI into three subtypes: strong barrier (greater than 1 mm), weak barrier (less than 1 mm), and mixed barrier (in the cases of coexistence of the two previous subtypes) (**Figures 1–3**, parts A,B).

Intraoperative management and findings

The surgeries were performed by the Senior authors of the Naples team (PC, LMC, DS) *via* an endoscopic endonasal standard approach (22–24). A Karl Storz & Co (Tuttlingen, Germany) endoscope with 0° lens was used as the sole visualizing tool; the four hands technique was adopted from the sphenoid phase. During each surgery, the Senior surgeon pointed out the sellar barrier type upon the intraoperative observation of gland and/or dura mater (strong barrier), only arachnoid tissue (weak barrier), and mixed components (mixed barrier). The eventual presence of intraoperative CSF leak was recorded according to the classification of Esposito et al. (7).

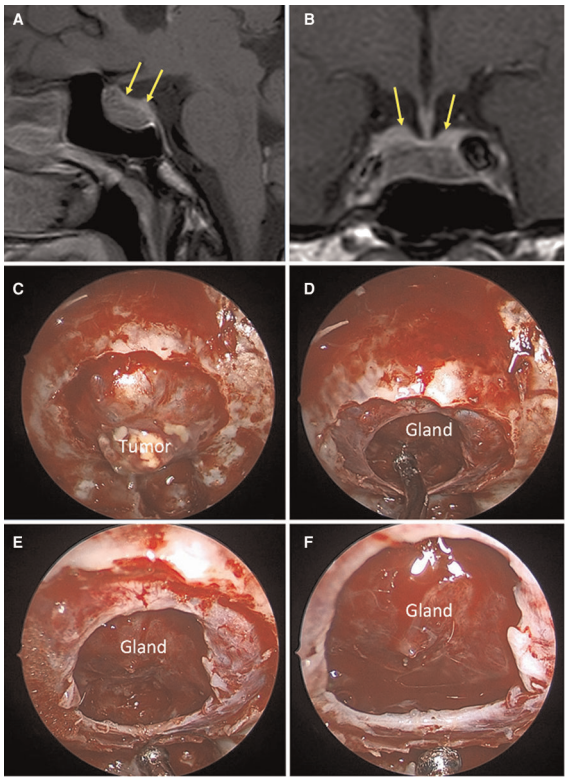

FIGURE 1
Strong sellar barrier. A 42-year-old male patient, with GH produce macroadenoma. (A,B) Preoperative MRI: the yellow arrows indicate the barrier that captures contrast with a thickness greater than 1 mm. (C–F) Intraoperative images: the barrier constituted by the gland can be seen.

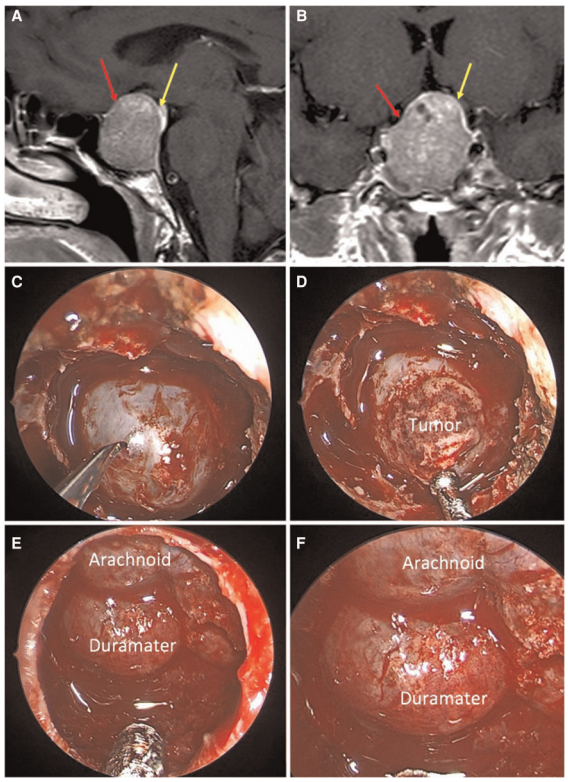

FIGURE 2
Mixed sellar barrier. A 59-year-old female patient, with a PRL produced macroadenoma. (A,B) Preoperative MRI: the yellow arrows indicate the barrier that captures contrast with a thickness greater than 1 mm and the red arrows indicate the barrier that captures contrast with a thickness less than 1 mm. (C–F) Intraoperative images: the barrier constituted by duramater and arachnoid can be seen.

Feature engineering and preprocessing

Patient data were processed based on their nature using the pandas, numpy, and scikit-learn Python packages (25). Ordinal data (modified Knosp classification score) (26) were treated as a continuous variable to avoid loss of information. The presence of presurgical treatment was dichotomized. Then, categorical data were one-hot encoded using the pandas "get_dummy" function, converting k categories to $k-1$ indicator variables. The final feature set comprised the following:

1. Age
2. Knosp classification score
3. Gender
4. Status: Growth hormone (GH) secreting
5. Status: GH Prl secreting
6. Status: Prl secreting
7. Status: Nonfunctioning
8. Size: Microadenoma
9. MRI barrier: Strong
10. MRI barrier: Weak
11. Intraoperative barrier: Strong
12. Intraoperative barrier: Weak
13. Presurgical treatment

Given the distribution of classes within the datasets, the experiment was treated as a novelty detection problem. Therefore, outliers (i.e., patients with intraoperative fistula) and inliers were split into separate datasets. Then, the latter was further separated with an 80%/20% proportion into training and inlier test datasets. The only variable with missing values within all datasets was the modified Knosp classification score (25 missing values in the training set, 5 missing values in the inlier training set, and no missing values in the outlier test set). An imputer based on the mode of this parameter was fit on the training set (mode = 2) and used to transform all datasets to remove the missing values. Then, continuous variables were normalized using a min–max scaler (range = 0–1), also fit exclusively on the training data and used to transform all datasets. Finally, principal component analysis was used to reduce the dimensionality of the data to two vectors, again by fitting only on the training set features and transforming all datasets.

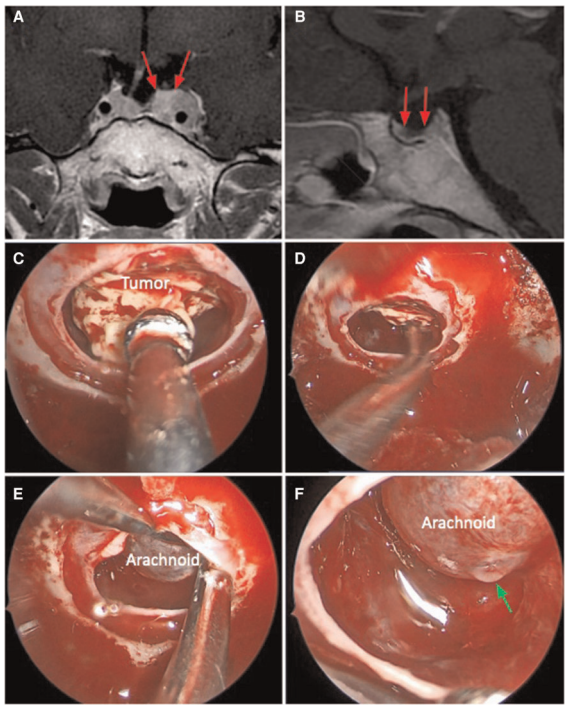

FIGURE 3
Weak sellar barrier. A 31-year-old female patient, with an ACTH produced macroadenoma. (A,B) Preoperative MRI: the red arrows indicate the barrier that captures contrast with a thickness less than 1 mm. (C–F) Intraoperative images: the barrier constituted only with arachnoid can be seen. The green arrow marks the CSF leak.

Machine learning analysis

The machine learning analysis was performed using the scikit-learn Python package (25). Different novelty detection algorithms were employed for the analysis, both independently and with a majority voting the ensemble approach: isolation forest (IF), local outlier factor (LOF), and one-class SVM (oSVM). These were fit on the inlier training dataset in an unsupervised fashion. Then, their performance was assessed separately on the inlier and outlier test sets. The predictions made on each test set case were then recorded and combined, together with the ground truths, to build confusion matrices and obtain accuracy metrics.

Statistical analysis

All statistical tests were conducted in R (R for Unix/Linux, version 3.4.4, the R Foundation for Statistical Computing, 2014). Continuous data are presented as mean and standard deviation. Categorical and ordinal data are presented as value counts and proportions. The Shapiro–Wilk test was used to assess the normality of distribution of continuous data. Analysis of variance and Fisher exact tests were used to assess for differences in variable distribution among the training and test groups. Precision (i.e., positive predictive value), recall (i.e., sensitivity), accuracy (n correct predictions/all cases), and f-score (i.e., harmonic average of precision and recall) were calculated as accuracy metrics.

Results

One hundred and fifty-five patients were enrolled in the study (M:F = 81:74 = 1.1; median age = 48.7 years; range = 18–78 years). Regarding the pituitary adenomas' features, 129 (83%) were macroadenomas and 26 (17%) were microadenomas; 81 were nonfunctioning tumors (52%), while 43 (27%) were GH secreting, 15 (9.6%) were adrenocorticotropic hormone (ACTH) producing, 12 (0.6%) were prolactinomas, and finally 3 (0.2%) were GH/prolactin (PRL)-secreting adenomas. According to Micko grading scale, i.e. modified Knosp classification (26), we found that 22 (14.2%) were grade 0, 22 (14.2%) were grade 1, 44 (28.4%) were grade 2, 27 (17.4%) were grade 3A, and 10 (0.6%) were grade 4. Among functioning tumors, we noted that 36 (23.2%) had received prior medical treatment (**Table 1**).

The distribution according to the sellar barrier subtype on MRI was as follows: 108 (69.7%) adenomas had a strong barrier, 13 a weak barrier (0.8%) (**Figures 1–3**), and finally 34 (28.1%) had a mixed barrier; as per the intraoperative findings, we observed that 111 (71.9%) had a strong barrier, 17 (12.5%) had weak barrier, and 27 (15.6%) had mixed barrier (**Figures 1–3** and **Table 1**).

The training dataset included 115 (74%) patients without intraoperative fistula, while the inlier and outlier test sets included 29 (19%) and 11 (7%) patients, respectively. Patient clinical and demographic data are presented in **Table 1**. Significant differences between the three datasets were found for Knosp classification score ($p = 0.0015$), MRI barrier: strong ($p = 1.405 \times 10^{-6}$), MRI barrier: weak ($p = 4.487 \times 10^{-8}$), intraoperative barrier: strong ($p = 2.788 \times 10^{-7}$), and intraoperative barrier: Weak ($p = 2.191 \times 10^{-10}$). Accuracy, sensitivity, and specificity for outlier detection were 0.70, 0.64, and 0.72 for IF, 0.85, 0.45, and 1.00 for LOF; 0.83, 0.64, and 0.90 for oSVM; and 0.83, 0.55, and 0.93 for the ensemble. Confusion matrices and accuracy metrics are presented in **Table 2**. **Figure 4** shows a plot of each model's decision function in relation to the distribution of inlier and outlier test set patients (**Figure 4**).

Discussion

The possibility to predict outcomes is critical to ensure the highest standards of surgical care, above all to satisfy patient inquiries with regard to the pros and cons of the procedure they are about to undergo.

TABLE 1 Patient characteristics.

		Training set	Inlier test set	Outlier test set	*p*-value
Age (years)		47.91 (±13.79)	47.69 (±15.92)	50.62 (±15.18)	0.6650
Sex	M	59	17	5	0.7256
	F	56	12	6	
Knosp	0	15	6	1	0.0015
	1	20	2	0	
	2	29	11	4	
	3	23	3	1	
	4	3	2	5	
Status	Nonfunctioning	55	17	9	0.0733
	Functioning	60	12	2	
Status PRL	0	102	29	11	0.1058
	1	13	0	0	
Status GH	0	82	19	11	0.0663
	1	33	10	9	
Status GH-PRL	0	112	29	11	1.0000
	1	3	0	0	
Size	micro	21	4	1	0.8063
	macro	94	25	10	
Preoperative treatment	0	84	24	11	0.0790
	1	31	5	0	
MRI barrier: strong	0	30	6	11	1.405×10^{-6}
	1	85	23	0	
MRI barrier: weak	0	111	28	3	4.487×10^{-8}
	1	4	1	8	
Intraoperative barrier: strong	0	29	4	11	2.788×10^{-7}
	1	86	25	0	
Intraoperative barrier: weak	0	109	28	1	2.191×10^{-10}
	1	6	1	10	

TABLE 2 Accuracy metrics.

Isolation forest
Accuracy: 0.7

		ML	
		1	0
Class	1	7	4
	0	8	21

	Precision	Recall	F1	Number
Outliers	0.47	0.64	0.54	11
Inliers	0.84	0.72	0.78	29
Macro average	0.65	0.68	0.66	40
Weighted average	0.74	0.70	0.71	40

Local outlier factor
Accuracy: 0.850

		ML	
		1	0
Class	1	5	6
	0	0	29

	Precision	Recall	F1	Number
Outliers	1.00	0.45	0.62	11
Inliers	0.83	1.00	0.91	29
Macro average	0.91	0.73	0.77	40
Weighted average	0.88	0.85	0.83	40

One-class SVM
Accuracy: 0.825

		ML	
		1	0
Class	1	7	4
	0	3	26

	Precision	Recall	F1	Number
Outliers	0.70	0.64	0.67	11
Inliers	0.87	0.90	0.88	29
Macro average	0.78	0.77	0.77	40
Weighted average	0.82	0.82	0.82	40

Ensemble
Accuracy: 0.825

		ML	
		1	0
Class	1	6	5
	0	2	27

	Precision	Recall	F1	Number
Outliers	0.75	0.55	0.63	11
Inliers	0.84	0.93	0.89	29
Macro average	0.80	0.74	0.76	40
Weighted average	0.82	0.82	0.82	40

CSF leak is one of the most threatening complications of transsphenoidal pituitary surgery, and also per its related potential complications, such as meningitis (27) or tension pneumocephalus (28).

Years of peculiar care and efforts, in terms of materials and reconstruction techniques, have been given to this issue (5, 6, 29–35), which nowadays has been reported as low as 2% among experienced groups (36–39).

It is crucial to highlight that albeit intraoperative CSF leak rates are reported as high as 10.3%–69%, postoperative CSF leak rates lower down to 1.3%–8% (38, 40–54).

In the present case series, we found a rate of intraoperative CSF leak of 7.1% and postoperative CSF leak of 0%, which are similar to those reported in the literature for this kind of surgery. These findings suggest that the rate of patients with intraoperative CSF leak who finally developed a postoperative CSF leak is negligible; this is mostly because of the improvement of reconstruction techniques over the years and the refinement of surgical skills in skull base surgeons (12).

However, there are only few reports concerning the possible risk factors that can be detected preoperatively to predict an intraoperative CSF leakage, but univocal consensus has not

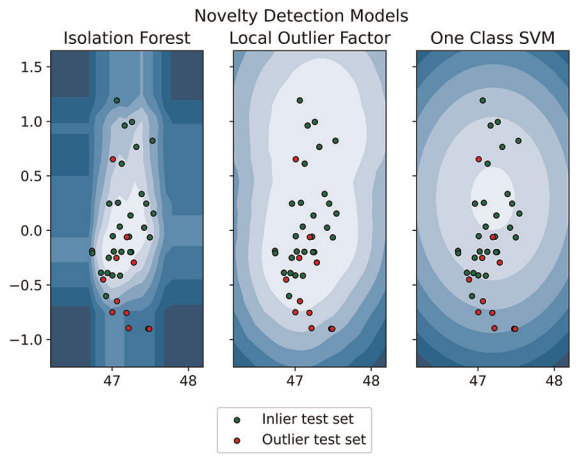

FIGURE 4
Model's decision function in relation to the distribution of inlier and outlier test set patients.

achieved yet: different groups claimed an increased risk of postoperative fistula upon the opening of the third ventricle, or in cases of patients with higher BMI (8–11).

The *sellar barrier concept* and its role in predicting the risk of intraoperative CSF leakage was recently introduced (12, 13) and confirmed in a clinical multicentric study (14).

Predictive factors of intraoperative CSF leak

In the present study, none of the patients presented intraventricular invasion, CSF leak occurred indifferently in patients with high or low/normal BMI, and all procedures were performed by expert neurosurgeons familiar with pituitary surgery, *via* a standard corridor.

The authors consider crucial the ability of predicting an intraoperative CSF leak though the sellar barrier concept is effective. The sellar barrier concept fills an empty space for contemporary literature on this topic.

We provided an analysis of the risk of postoperative CSF leak in three different classes of patients undergoing endoscopic endonasal removal of pituitary adenomas, by means of an ML model; classes were defined according to the MRI appearance of the so-called "sellar barrier."

Sellar barrier as predictor of CSF leak in endoscopic pituitary surgery

In our initial publication, we demonstrated the correlation between the intraoperative classification of the sellar barrier and the presence of intraoperative CSF leak (12). Later, in a second publication, we found a correlation between the MRI classification of the sellar barrier and the presence of CSF leak (13). In a recent multicentric study (14), this relation has been confirmed: albeit without ML analysis, patients assessed as at higher risk of intraoperative CSF leakage would benefit most from a gentle dissection of the most superior aspects of the tumor, paying attention to preserve as much as possible the layer of the gland to cover the diaphragm.

In the present study, we found that the preoperative MRI classification could predict the risk of intraoperative CSF fistula, as confirmed also by ML analysis.

Our ML model identified with outstanding accuracy that there is a cogent correlation between the weak barrier type and the intraoperative CSF leakage MRI barrier: strong ($p = 1.405 \times 10^{-6}$), MRI barrier: weak ($p = 4.487 \times 10^{-8}$), intraoperative barrier: strong ($p = 2.788 \times 10^{-7}$), and intraoperative barrier: weak ($p = 2.191 \times 10^{-10}$).

These findings are relatively new and might provide further issue to be considered when defining the surgical planning. Hence, also per intraoperative observation, a weak barrier represents a "*locus minoris resistentiae*," whose careless manipulation during tumor removal can expose the increased risk of intraoperative CSF leakage.

In the near future, this computer-aided decision-making tool might improve surgical quality by regularly identifying those patients at higher risk of developing intraoperative CSF leakage and related complications; validated machine learning tools might change routine surgical practice if properly setup: the creation of a computerized predictive algorithm can be a crucial step to further refine modern neurosurgery.

Clinical–surgical application

Our teams are working on a risk classification of intraoperative CSF leak to refine the most appropriate surgical strategy and adequately inform the patient about its postoperative course.

Claude Bernard used to say, "who doesn't know what he's looking for, doesn't understand what he finds." The clinical application of the sellar barrier concept will allow the skull base surgery team to predict the scenario they will encounter. Thanks to this, you will be able to carefully select the method to be used in the reconstructive phase.

During preoperative consultation, the use of imaging software allows the surgeon to show the sellar barrier to the patient and explain with a graphic support about their risk of CSF leakage. Thanks to this, the surgeon can speak clearly and precisely with the patient. It allows the surgeon to inform the patient about his/her possible postoperative evolution: postoperative nasal symptoms, surgery time, and the risk of postoperative CSF fistulae, among others. This type of

information would have legal implications in the postoperative period (12–14).

Limitations

The concept of the sellar barrier cannot be considered as a totally independent predictor factor of CSF leakage.

This is a prospective cohort study with a small series of patients. A multicenter study with more extensive patient series is required to validate this concept and its clinical applicability.

Finally, it is worth reminding that the downside of the ML model can be its troublesome application to a clinical context: the interpretation of this model conceives the human–machine interaction as its highest moment.

Conclusions

The sellar barrier is a new parameter to be considered in the risk assessment of intraoperative CSF leak. The present study demonstrates the efficacy of the sellar barrier concept in patients operated for endoscopic endonasal pituitary removal and strengthens its clinical applicability.

There is a true correlation between the type of *sellar barrier* at MRI and its *in vivo* features as observed during endoscopic endonasal surgery. The novelty detection models highlighted differences between patients who developed an intraoperative CSF leak and those who did not.

Data availability statement

The original contributions presented in the study are included in the article/Supplementary Material, further inquiries can be directed to the corresponding author.

Author contributions

All authors contributed to the article and approved the submitted version.

Conflict of interest

The authors declare that the research was conducted in the absence of any commercial or financial relationships that could be construed as a potential conflict of interest.

Publisher's note

References

1. Solari D, Pivonello R, Caggiano C, Guadagno E, Chiaramonte C, Miccoli G, et al. Pituitary adenomas: what are the key features? What are the current treatments? Where is the future taking US? *World Neurosurg.* (2019) 127:695–709. doi: 10.1016/j.wneu.2019.03.049

2. Villalonga JF, Fuchssteiner C, Solari D, Campero A, Cavallo LM, Cappabianca P, et al. Endoscopic anatomy of the sellar barrier: from the anatomical model to the operating room. *Clin Anat.* (2020) 33(3):468–74. doi: 10.1002/ca.23566

3. Jho H, Carrau R. Endoscopy assisted transsphenoidal surgery for pituitary adenoma. *Acta Neurochir (Wien).* (1996) 138:1416–25. doi: 10.1007/BF01411120

4. Jho H, Carrau R. Endoscopic endonasal transsphenoidal surgery: experience with fifty patients. *J Neurosurg.* (1997) 87:44–51. doi: 10.3171/jns.1997.87.1.0044

5. Patel MR, Stadler ME, Snyderman CH, Carrau RL, Kassam AB, Germanwala AV, et al. How to choose? Endoscopic skull base reconstructive options and limitations. *J Neurol Surg B Skull Base.* (2010) 20(6):397–402. doi: 10.1055/s-0030-1253573

6. Rivera-Serrano CM, Snyderman CH, Gardner P, Prevedello D, Wheless S, Kassam AB, et al. Nasoseptal "rescue" flap: a novel modification of the nasoseptal flap technique for pituitary surgery. *Laryngoscope.* (2011) 121 (5):990–3. doi: 10.1002/lary.21419

7. Esposito F, Dusick JR, Fatemi N, Kelly DF. Graded repair of cranial base defects and cerebrospinal fluid leaks in transsphenoidal surgery. *Oper Neurosurg.* (2007) 60(4):295–9. doi: 10.1227/01.NEU.0000255354.64077.66

8. Lobatto DJ, de Vries F, Zamanipoor Najafabadi AH, Pereira AM, Peul WC, Vliet Vlieland TPM, et al. Preoperative risk factors for postoperative complications in endoscopic pituitary surgery: a systematic review. *Pituitary.* (2018) 21(1):84–97. doi: 10.1007/s11102-017-0839-1

9. Dlouhy BJ, Madhavan K, Clinger JD, Reddy A, Dawson JD, O'Brien EK, et al. Elevated body mass index and risk of postoperative CSF leak following transsphenoidal surgery. *J Neurosurg.* (2012) 116(6):1311–7. doi: 10.3171/2012.2.JNS111837

10. Shikary T, Andaluz N, Meinzen-Derr J, Edwards C, Theodosopoulos P, Zimmer LA. Operative learning curve after transition to endoscopic transsphenoidal pituitary surgery. *World Neurosurg.* (2017) 102:608–12. doi: 10.1016/j.wneu.2017.03.008

11. Zhou Q, Yang Z, Wang X, Wang Z, Zhao C, Zhang S, et al. Risk factors and management of intraoperative cerebrospinal fluid leaks in endoscopic treatment of pituitary adenoma: analysis of 492 patients. *World Neurosurg.* (2017) 101:390–5. doi: 10.1016/j.wneu.2017.01.119

12. Campero A, Villalonga JF, Basso A. Anatomical risk factors for intraoperative cerebrospinal fluid leaks in transsphenoidal surgery for pituitary adenomas. *World Neurosurg.* (2019) 50(18):1878–87. doi: 10.1016/j.wneu.2018.12.094

13. Villalonga JF, Ries-Centeno T, Sáenz A, Solari D, Cervio A, Campero A. The mixed sellar barrier: a new subtype of this novel concept. *World Neurosurg.* (2019) 132(1):5–13. doi: 10.1016/j.wneu.2019.09.027

14. Villalonga JF, Solari D, Cavallo LM, Cappabianca P, Prevedello DM, Carrau R, et al. The sellar barrier on preoperative imaging predicts intraoperative cerebrospinal fluid leak: a prospective multicentric cohort study. *Pituitary.* (2021) 24(1):27–37. doi: 10.1007/s11102-020-01082-8

15. Gillies RJ, Kinahan PE, Hricak H. Radiomics: images are more than pictures, they are data. *Radiology*. (2016) 278(2):563–77. doi: 10.1148/radiol.2015151169

16. Senders JT, Zaki MM, Karhade AV, Chang B, Gormley WB, Broekman ML, et al. An introduction and overview of machine learning in neurosurgical care. *Acta Neurochir (Wien)*. (2018) 160(1):29–38. doi: 10.1007/s00701-017-3385-8

17. Cuocolo R, Stanzione A, Ponsiglione A, Romeo V, Verde F, Creta M, et al. Clinically significant prostate cancer detection on MRI: a radiomic shape features study. *Eur J Radiol*. (2019) 116:144–9. doi: 10.1016/j.ejrad.2019.05.006

18. Cuocolo R, Cipullo MB, Stanzione A, Ugga L, Romeo V, Radice L, et al. Machine learning applications in prostate cancer magnetic resonance imaging. *Eur Radiol Exp*. (2019) 3:35. doi: 10.1186/s41747-019-0109-2

19. Imbriaco M, Cuocolo R. Does texture analysis of MR images of breast tumors help predict response to treatment? *Radiology*. (2018) 286:421–3. doi: 10.1148/radiol.2017172454

20. Mokrane FZ, Lu L, Vavasseur A, Otal P, Peron JM, Luk L, et al. Radiomics machine-learning signature for diagnosis of hepatocellular carcinoma in cirrhotic patients with indeterminate liver nodules. *Eur Radiol*. (2020) 30:558–70. doi: 10.1007/s00330-019-06347-w

21. Lotan E, Jain R, Razavian N, Fatterpekar GM, Lui YW. State of the art: machine learning applications in glioma imaging. *Am J Roentgenol*. (2019) 212:26–37. doi: 10.2214/AJR.18.20218

22. Cavallo LM, Solari D, Esposito F, Cappabianca P. Endoscopic endonasal approach for pituitary adenomas. *Acta Neurochir (Wien)*. (2012) 154:2251–6. doi: 10.1007/s00701-012-1493-z

23. Solari D, Cavallo LM, Cappabianca P. Surgical approach to pituitary tumors. *Handb Clin Neurol*. (2014) 124:291–301. doi: 10.1016/B978-0-444-59602-4.00019-8

24. Cappabianca P, Cavallo LM, Solari D, Stagno V, Esposito F, de Angelis M. Endoscopic endonasal surgery for pituitary adenomas. *World Neurosurg*. (2014) 82(6):3–11. doi: 10.1016/j.wneu.2014.07.019

25. Pedregosa F, Varoquaux G, Gramfort A, Michel V, Thirion B, Grisel O, Blondel M, et al. Machine learning in python. *J Mach Learn Res*. (2011) 12:2825–30. doi: 10.5555/1953048.2078195

26. Micko AS, Wöhrer A, Wolfsberger S, Knosp E. Invasion of the cavernous sinus space in pituitary adenomas: endoscopic verification and its correlation with an MRI-based classification. *J Neurosurg*. (2015) 122(4):803–11. doi: 10.3171/2014.12.JNS141083

27. Nix P, Tyagi A, Phillips N. Retrospective analysis of anterior skull base CSF leaks and endoscopic repairs at Leeds. *Br J Neurosurg*. (2016) 30(4):422–6. doi: 10.3109/02688697.2016.1161176

28. Banu MA, Szentirmai O, Mascarenhas L, Salek AA, Anand VK, Schwartz TH. Pneumocephalus patterns following endonasal endoscopic skull base surgery as predictors of postoperative CSF leaks. *J Neurosurg*. (2014) 121(4):961–75. doi: 10.3171/2014.5.JNS132028

29. Hadad G, Bassagasteguy L, Carrau RL, Mataza JC, Kassam A, Snyderman CH, et al. A novel reconstructive technique following endoscopic expanded endonasal approaches: vascular pedicle nasoseptal flap. *Laryngoscope*. (2006) 116:1881–5. doi: 10.1097/01.mlg.0000234933.37779.e4

30. Bergsneider M, Xue K, Suh JD, Wang MB. Barrier-limited multimodality closure for reconstruction of wide sellar openings. *Oper Neurosurg*. (2011) 71(1):68–76. doi: 10.1227/NEU.0b013e318241af25

31. Cappabianca P, Esposito F, Magro F, Cavallo LM, Solari D, Stella L, et al. Natura abhorret a vacuo—use of fibrin glue as a filler and sealant in neurosurgical "dead spaces". Technical note. *Acta Neurochir (Wien)*. (2010) 152(5):897–904. doi: 10.1007/s00701-009-0580-2

32. Cavallo LM, Solari D, Somma T, Cappabianca P. The 3F (fat, flap, and flash) technique for skull base reconstruction after endoscopic endonasal suprasellar approach. *World Neurosurg*. (2019) 126:439–46. doi: 10.1016/j.wneu.2019.03.125

33. Duntze J, Litré CF, Graillon T, Maduri R, Pech-gourg G, Rakotozanany P, et al. Rhinorrhée cérébrospinale après chirurgie hypophysaire endoscopique trans-sphénoïdale: réflexions après 337 patients. *Neurochirurgie*. (2012) 58(4):241–5. doi: 10.1016/j.neuchi.2012.02.005

34. Luginbuhl AJ, Campbell PG, Evans J, Rosen M. Endoscopic repair of high-flow cranial base defects using a bilayer button. *Laryngoscope*. (2010) 120(5):876–80. doi: 10.1002/lary.20861

35. Nishioka H, Izawa H, Ikeda Y, Namatame H, Fukami S, Haraoka J. Dural suturing for repair of cerebrospinal fluid leak in transnasal transsphenoidal surgery. *Acta Neurochir (Wien)*. (2009) 151(11):1427–31. doi: 10.1007/s00701-009-0406-2

36. Berker M, Hazer DB, Yücel T, Gürlek A, Cila A, Aldur M, et al. Complications of endoscopic surgery of the pituitary adenomas: analysis of 570 patients and review of the literature. *Pituitary*. (2012) 15(3):288–300. doi: 10.1007/s11102-011-0368-2

37. Gondim JA, Almeida JP, de Albuquerque LA, Gomes E, Schops M, Mota JI. Endoscopic endonasal transsphenoidal surgery in elderly patients with pituitary adenomas. *J Neurosurg*. (2015) 123(1):31–8. doi: 10.3171/2014.10.JNS14372

38. Gondim JA, Almeida JP, Albuquerque LA, Schops M, Gomes E, Ferraz T, et al. Endoscopic endonasal approach for pituitary adenoma: surgical complications in 301 patients. *Pituitary*. (2011) 14(2):174–83. doi: 10.1007/s11102-010-0280-1

39. Sanders-Taylor C, Anaizi A, Kosty J, Zimmer LA, Theodosopoulos PV. Sellar reconstruction and rates of delayed cerebrospinal fluid leak after endoscopic pituitary surgery. *J Neurol Surg B Skull Base*. (2015) 76(4):281–5. doi: 10.1055/s-0034-1544118

40. Ajlan A, Achrol AS, Albakr A, Feroze AH, Westbroek EM, Hwang P, et al. Cavernous sinus involvement by pituitary adenomas: clinical implications and outcomes of endoscopic endonasal resection. *J Neurol Surg B Skull Base*. (2017) 78:273–82. doi: 10.1055/s-0036-1598022

41. Bokhari AR, Davies MA, Diamond T. Endoscopic transsphenoidal pituitary surgery: a single surgeon experience and the learning curve. *Br J Neurosurg*. (2013) 27:44–9. doi: 10.3109/02688697.2012.709554

42. Boling CC, Karnezis TT, Baker AB, Lawrence LA, Soler ZM, Vandergrift WA 3rd, et al. Multi-institutional study of risk factors for perioperative morbidity following transnasal endoscopic pituitary adenoma surgery. *Int Forum Allergy Rhinol*. (2016) 6:101–7. doi: 10.1002/alr.21622

43. Cerina V, Kruljac I, Radosevic JM, Kirigin LS, Stipic D, Pecina HI, et al. Diagnostic accuracy of perioperative measurement of basal anterior pituitary and target gland hormones in predicting adrenal insufficiency after pituitary surgery. *Medicine*. (2016) 95:2898–906. doi: 10.1097/MD.0000000000002898

44. Chabot JD, Chakraborty S, Imbarrato G, Dehdashti AR. Evaluation of outcomes after endoscopic endonasal surgery for large and giant pituitary macroadenoma: a retrospective review of 39 consecutive patients. *World Neurosurg*. (2015) 84:978–88. doi: 10.1016/j.wneu.2015.06.007

45. Chi F, Wang Y, Lin Y, Ge J, Qiu Y, Guo L. A learning curve of endoscopic transsphenoidal surgery for pituitary adenoma. *J Craniofac Surg*. (2013) 24:2064–7. doi: 10.1097/SCS.0b013e3182a24328

46. Chohan MO, Levin AM, Singh R, Zhou Z, Green CL, Kazam JJ, et al. Three-dimensional volumetric measurements in defining endoscope-guided giant adenoma surgery outcomes. *Pituitary*. (2016) 19:311–21. doi: 10.1007/s11102-016-0709-2

47. Chohan MO, Levin AM, Singh R, Zhou Z, Green CL, Kazam JJ, et al. Retrospective analysis of a concurrent series of microscopic versus endoscopic transsphenoidal surgeries for Knosp Grades 0-2 nonfunctioning pituitary macroadenomas at a single institution. *J Neurosurg*. (2014) 121:511–7. doi: 10.3171/2014.6.JNS131321

48. Hofstetter CP, Nanaszko MJ, Mubita LL, Tsiouris J, Anand VK, Schwartz TH. Volumetric classification of pituitary macroadenomas predicts outcome and morbidity following endoscopic endonasal transsphenoidal surgery. *Pituitary*. (2012) 15:450–63. doi: 10.1007/s11102-011-0350-z

49. Jakimovski D, Bonci G, Attia M, Shao H, Hofstetter C, Tsiouris AJ, et al. Incidence and significance of intraoperative cerebrospinal fluid leak in endoscopic pituitary surgery using intrathecal fluorescein. *World Neurosurg*. (2014) 82:513–23. doi: 10.1016/j.wneu.2013.06.005

50. Jang JH, Kim KH, Lee YM, Kim JS, Kim YZ. Surgical results of pure endoscopic endonasal transsphenoidal surgery for 331 pituitary adenomas: a 15-year experience from a single institution. *World Neurosurg*. (2016) 96:545–55. doi: 10.1016/j.wneu.2016.09.051

51. Qureshi T, Chaus F, Fogg L, Dasgupta M, Straus D, Byrne RW. Learning curve for the transsphenoidal endoscopic endonasal approach to pituitary tumors. *Br J Neurosurg*. (2016) 30:637–42. doi: 10.1080/02688697.2016.1199786

52. Robins JMW, Alavi SA, Tyagi AK, Nix PA, Wilson TM, Phillips NI. The learning curve for endoscopic trans-sphenoidal resection of pituitary macroadenomas. A single institution experience, Leeds, UK. *Acta Neurochir (Wien)*. (2018) 160:39–47. doi: 10.1007/s00701-017-3355-1

53. Thawani JP, Ramayya AG, Pisapia JM, Abdullah KG, Lee JY, Grady MS. Operative strategies to minimize complications following resection of pituitary macroadenomas. *J Neurol Surg B Skull Base*. (2017) 78:184–90. doi: 10.1055/s-0036-1597276

54. Zhan R, Ma Z, Wang D, Li X. Pure endoscopic endonasal transsphenoidal approach for nonfunctioning pituitary adenomas in the elderly: surgical outcomes and complications in 158 patients. *World Neurosurg*. (2015) 84:1572–8. doi: 10.1016/j.wneu.2015.08.035

frontiers | Frontiers in Surgery

TYPE Original Research
PUBLISHED 13 September 2022
DOI 10.3389/fsurg.2022.981669

OPEN ACCESS

EDITED BY
Peng Zhao,
Capital Medical University, China

REVIEWED BY
Zixiang Cong,
Nanjing University, China
Brandon Peter Lucke-Wold,
University of Florida, United States

*CORRESPONDENCE
Bin Tang
tonytang19850815@sina.com

†These authors have contributed equally to this work.

SPECIALTY SECTION
This article was submitted to Neurosurgery, a section of the journal Frontiers in Surgery

RECEIVED 29 June 2022
ACCEPTED 22 August 2022
PUBLISHED 13 September 2022

CITATION
Xiong Y, Liu Y, Xin G, Xie S, Luo H, Xiao L, Wu X, Hong T and Tang B (2022) Exploration of the causes of cerebrospinal fluid leakage after endoscopic endonasal surgery for sellar and suprasellar lesions and analysis of risk factors. Front. Surg. 9:981669.
doi: 10.3389/fsurg.2022.981669

Exploration of the causes of cerebrospinal fluid leakage after endoscopic endonasal surgery for sellar and suprasellar lesions and analysis of risk factors

Yicheng Xiong[1†], Yajing Liu[2†], Guo Xin[1], Shenhao Xie[1], Hai Luo[1], Liming Xiao[1], Xiao Wu[1], Tao Hong[1] and Bin Tang[1*]

[1]Department of Neurosurgery, The First Affiliated Hospital of Nanchang University, Nanchang, China, [2]Operating Theater, The First Affiliated Hospital of Nanchang University, Nanchang, China

Objective: Postoperative cerebrospinal fluid (CSF) leakage following endoscopic endonasal surgery (EES) is a frequent complication. This study aims to identify potential risk factors of postoperative CSF leakage.
Methods: A retrospective review of 360 patients who underwent EES was included. The associations between postoperative CSF leakage and patient demographics, medical history, tumor characteristics, and intraoperative repair techniques were analyzed; the diagnosis and repair of postoperative CSF leakage were also introduced.
Results: Postoperative CSF leakage occurred in 14 patients (3.9%), 2 of them cured by lumbar cistern drainage, 12 underwent endoscopic repair. Among these 12 cases, 3 were repaired twice, and the rest were cured the first time. During the repair surgery, insufficient embedded fat was detected in one case detected, seven with breached inner artificial dura, three had vascularized pedicle nasoseptal flap (VP-NSF) displacement, two with VP-NSF perforation, two with VP-NSF inactivation, and one with imperfect adherence to VP-NSF to the skull base. Eight cases had intracranial infections. Excluding one case who died of severe intracranial infection, the rest were cured and discharged without obvious sequelae. Multivariate analysis revealed that the suprasellar lesion, subarachnoid invasion, and intraoperative grade 3 flow CSF leakage were the risk factors of CSF leakage after operation, while the bone flap was a protective factor.
Conclusion: Bone flap combined with VP-NSF and iodoform gauze for skull base reconstruction is recommended in high-risk patients, while postoperative lumbar cistern drain remains dispensable.

KEYWORDS
endoscopic endonasal surgery, risk factors, cerebrospinal fluid leakage, postoperative leakage, skull base reconstruction, bony reconstruction

Introduction

Cerebrospinal fluid (CSF) leakage is a pathologic condition where CSF flows out from defects of the dural and skull base, and it can be caused by a multitude of different factors, mainly including trauma (1) and endoscopic endonasal surgery (EES). Although with the recent development of neuroendoscopic equipment,

intraoperative hemostatic materials, and the concept of skull base reconstruction, EES has been employed in various types of skull base tumors. EES (including expend EES) allows tumor removal at anterior skull base, parasellar, suprasellar, and petroclival regions from the midline access. Noteworthy, as one of the most common complications in EES (2–4), CSF leakage after operation not only increases the duration of hospital stay (5) and readmission rates but also increases the risk of postoperative intracranial infection and seriously affects the prognosis (6). It has been reported that postoperative CSF leakage ranges from 7.2% to 25.4% (7–11), making EES questionable.

While several studies have reported the factors affecting postoperative CSF leakage, discussion related to the reconstruction defects is really rare. Here, we investigated the risk factors of postoperative CSF leakage through systematic analysis and discussed the defects in reconstruction technique. We hope our research could serve as a reference for the progression of EES.

Materials and methods

Data collection

A total of 360 patients who underwent EES were selected from the Department of Neurosurgery, the First Affiliated Hospital of Nanchang University, including 184 males and 176 females. Ages ranged from 4–81 years, with an average of (46 ± 14) years, including craniopharyngiomas ($n = 57$), pituitary adenomas ($n = 264$), tuberculum sellae meningioma ($n = 32$), and Rathke's cysts ($n = 7$).

Surgical procedure

Two-person/three-hand or the two-person/four-hand technique was used in EES. Decision of harvesting a vascularized pedicle nasoseptal flap (VP-NSF) or a free mucosal flap was made according to the surgery approach (classic EES or expend EES). After harvesting the NSF, the posterior nasal tract was opened and the nasal septum bone flap was made; the details are described in our previous article (12). Wide opening of the sphenoid sinus after the nasal procedure, exposing the posterior and lateral walls of the sphenoid sinus, with the sellar floor at the center, the sphenoethmoid planum above, and the clival indentation below. For creating a bone flap *in situ* (ISBF), the details are described in the article by Jin et al. (13) with intraoperative CSF leakage after lesion removal. The classification of intraoperative flow CSF leakage was defined as follows: grade 0:absence of CSF leakage, with intact sellar diaphragma; grade 1: small "weeping" leak, with only tiny diaphragmatic defect; grade 2: obvious defect of sellar diaphragma or skull base dura mater with moderate CSF exudation; grade 3: high-flow CSF leak, large sellar diaphragmatic or skull base dura defect with the total opening of the suprasellar arachnoid cistern and/or opening of the floor of the third ventricle (14). See **Figure 1** for details. Meanwhile, we performed multilayer skull base reconstruction according to intraoperative flow of CSF leakage. As for the reconstruction steps of intraoperative grade 3 flow CSF leakage, we changed before and after September 2018 as shown in **Table 1**. The details of bone flap placement are as follows: (1) After artificial dural embedding, the nasal septum bone flap was trimmed based on the shape and size of the skull base bone window to repair the bone defect, placement not inside or outside but just at the same plane with the skull base for the optimized simulation of the inherent anatomical structure. (2) After artificial dural embedding, the ISBF was gently countersunk into the bone defect; then, several points of the edge of the ISBF were wedged between the dura and bone for fixation (13).

Diagnosis and management of postoperative CSF leakage

For all patients, CT scan was typically performed within 6 h postoperatively. MRI of the sellar region was reexamined within

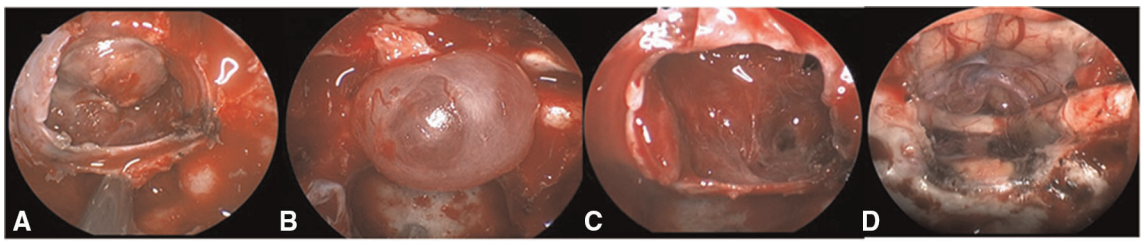

FIGURE 1
Grading of CSF leakage during operation. (A) Grade 0: the sellar diaphragm was intact and no CSF leakage after tumor resection. Postoperative pathology showed that one case had no functional pituitary adenoma. (B) Grade 1: the sellar diaphragm was intact and a small vesicle with CSF accumulation was formed around it after tumor resection. Postoperative pathology showed one case of nonfunctional pituitary adenoma. (C) Grade 2: the sellar diaphragm defect and moderate CSF leakage can be observed after tumor resection. Pathology showed one case of nonfunctional pituitary adenoma. (D) Grade 3; postoperative pathology showed one case craniopharyngioma of with extensive suprasellar arachnoid cistern opening during operation. CSF, cerebrospinal fluid.

TABLE 1 Cerebrospinal fluid leak repair protocol.

January 2018–August 2018	
Grade of leakage	Repair method
0	Collagen sponge + free mucosal graft + iodoform gauze support
1	Collagen sponge + artificial dura + VP-NSF + iodoform gauze support
2	Autologous fat graft + artificial dura + VP-NSF + balloon support
3	Autologous fat graft + artificial dura mater + fascia lata + VP-NSF + balloon support + lumbar cistern drainage for 72 h (Figure 2)
September 2018–December 2020	
Grade of leakage	Repair method
0	The same as above
1	Collagen sponge + artificial dura + *in situ* bone flap or nasal septum bone flap + VP-NSF + iodoform gauze support
2	Autologous fat graft + artificial dura + *in situ* bone flap or nasal septum bone flap + VP-NSF + iodoform gauze support
3	Autologous fat graft + artificial dura + *in situ* bone flap or nasal septum bone flap + VP-NSF + iodoform gauze support (Figures 3, 4)

VP-NSF, vascularized pedicle nasoseptal flap.

3 days. The nasal packing was removed at about 5–7 days postoperatively for patients with grade 0 and 1 CSF leakage during operation and at 12–14 days postoperatively for those with grade 2 and 3. Endoscopic nasal cleaning was performed 2, 4, and 6 weeks after nasal packing removal. CT examination was conducted first to determine the presence of neurocranium if patients were suspected of postoperative CSF leakage and then endoscopic re-exploration was done as soon as possible. The diagnosis of postoperative CSF leakage is as follows: (1) Patients with clear liquid flow out from the nasal cavity after operation. CSF routine test, biochemical parameters (15), β-2 transferrin (16), and β-trace protein (17) examination of the liquid sample should be performed immediately, and CT scan should be performed to exclude intracranial pneumatosis. (2) Patients with no clear fluid flow from the nasal cavity after operation; patients complaining of itching in the throat, a foreign body sensation, and salty water flowing down the posterior pharynx should be suspected of CSF leakage. In addition, patients with recurrent postoperative fever, uncontrollable pulmonary infection, and clinical features of intracranial infection should also be suspected. Early endoscopic exploration for CSF leakage suspects is absolutely advocated, and prompt endoscopic repair after clear diagnosis is necessary.

Statistical analysis

All statistical analyses were performed using SPSS version 26 (IBM Corporation, USA). The continuous variables conforming to the normal distribution were expressed by mean ± standard deviation (M ± SD). An independent-sample *t*-test was used for comparison between the two groups. The number of cases or percentages is expressed in the classified data. Chi-square tests were used for comparison between groups, and group comparisons were made with chi-square or Fisher's exact test in cases with a small number of expected outcomes. All independent variables thought to be of clinical significance *a priori* were placed into a logistic multiple regression model. P value <0.05 was considered statistically significant for all statistical tests.

The statistical steps were mainly divided into two steps: first, age, gender, and tumor type were included as influencing factors in the univariate and multifactor analysis, and then the univariate and multifactor analysis were done separately for different types of tumors.

Results

Results and causes of postoperative CSF leakage

Of the cases, 3.9% had postoperative CSF leakage (14/360), including four cases of craniopharyngioma, eight cases of pituitary adenoma, and two cases of sellar tubercle meningioma. Intraoperative CSF leakage of grade 3 was found in 10 cases, grade 2 in 3 cases, and grade 1 in 1 case. Among these, nine cases of postoperative CSF leakage occurred within 14 days, five cases occurred within 15–30 days, and the average time was (13 ± 5) days. Among all, 2 cases were cured by lumbar drainage, and the other 12 cases were explored under endoscopy. We found that the leading cause of postoperative CSF leakage was inadequate reconstruction, including one case with insufficient embedded fat (Figure 5A), seven cases with breached inner artificial dura, three cases with VP-NSF displacement, two cases with VP-NSF inactivation (Figure 5B), two cases with VP-NSF perforation, and one case with imperfect adherence of VP-NSF to the skull base (Table 2).

Treatment of postoperative CSF leakage

Two of the 14 patients with postoperative CSF leakage were cured by lumbar cistern drainage (LD). Twelve patients underwent endoscopic exploration and repair. The principle of repair was to determine the causes and then repair. When the cause was determined to be insufficient embedded fat, refilling the subdural leak with fat is necessary (Figure 6). When faced with the breached inner artificial dura, the artificial dura was reinserted between cellulite and dura mater. In case of VP-NSF inactivation, fascia lata was used instead

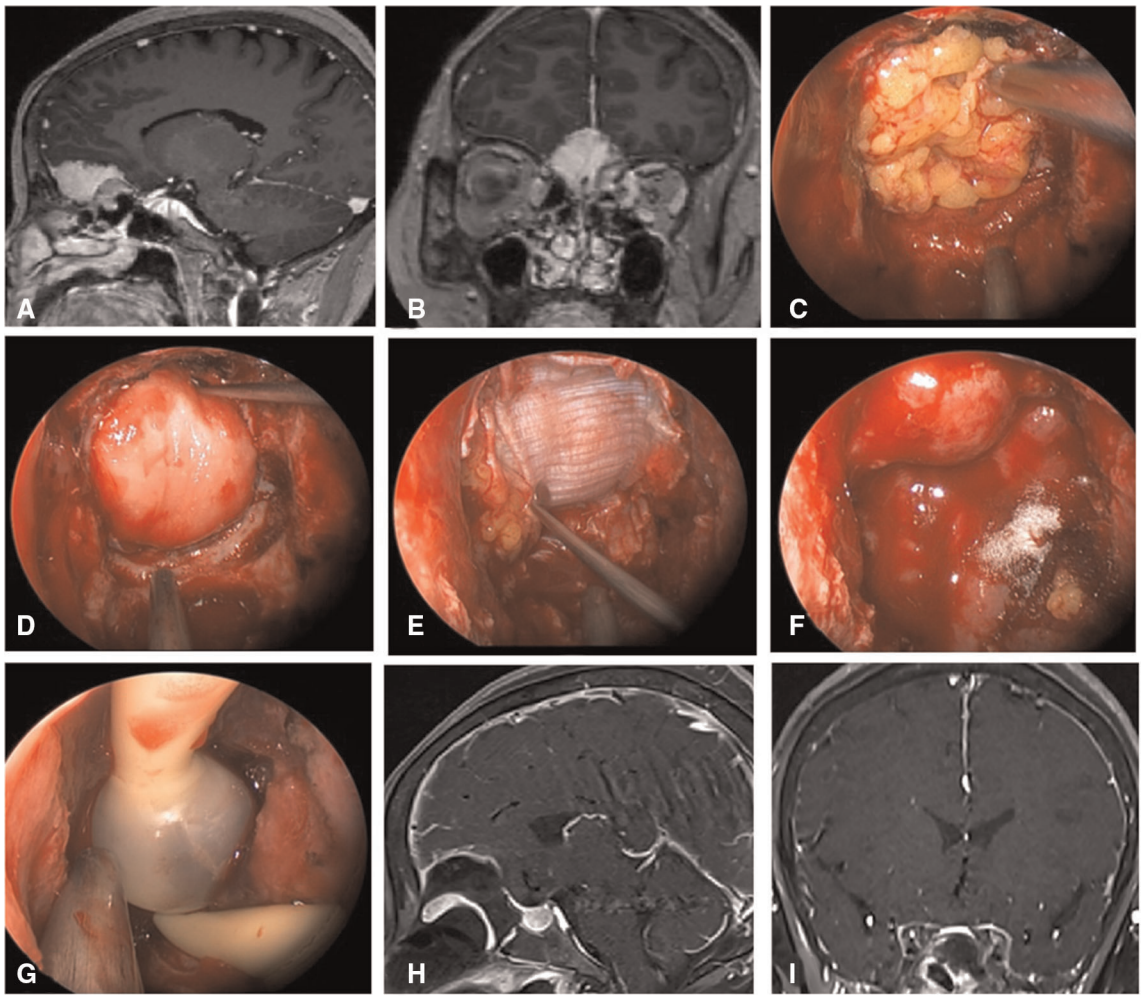

FIGURE 2
Changes in reconstruction strategy/(before). (A,B) Sagittal and coronal enhanced MRI in sellar region before operation, and olfactory groove meningioma was considered. (C) Subdural fat packing. (D) Artificial dura mater embedded between cellulite and dura mater. (E) Cover the fascia lata on the artificial dura mater. (F) Cover the VP-NSF on the fascia lata. (G) Balloon support. (H,I) Sagittal and coronal enhanced MRI in sellar region after operation, and postoperative pathology showed meningioma.

(Figure 7). Necessity of LD was based on the flow of CSF leakage during the repair. Three patients were repaired twice to resolve the postoperative CSF leakage, while the others were cured after the first time. Eight cases were complicated with intracranial infection; except for one case who died of severe intracranial infection, the rest were cured and discharged without obvious sequelae.

Univariate and multivariate analysis of postoperative CSF leakage

The univariate analysis described that craniopharyngioma, pituitary adenoma, lesions in the sellar or suprasellar region, subarachnoid invasion, intraoperative CSF leakage, bony reconstruction, balloon support, and postoperative LD were significantly correlated with postoperative CSF leakage. In addition, age, sex, hypertension, diabetes, radiotherapy, revision surgery, and maximum tumor diameter were not significantly associated with postoperative CSF leakage (Table 3). Further multivariate logistic regression analysis confirmed that the lesion was located on the suprasellar [odds ratio (OR) = 3.690, 95% CI: 1.029–5.783, $P = 0.003$] or subarachnoid space invasion (OR = 4.879, 95% CI: 1.243–12.820, $P = 0.007$); intraoperative grade 3 CSF leakage flow was the risk factor CSF leakage after EES (OR = 7.392, 95% CI: 2.458–19.736, $P = 0.012$), while bony reconstruction (OR = 0.313, 95% CI: 0.099–0.694, $P = 0.019$) was the protective factor. Tumor types, balloon support, postoperative LD, and sellar lesion were not significantly correlated with CSF leakage after the operation (Table 4).

10.3389/fsurg.2022.981669

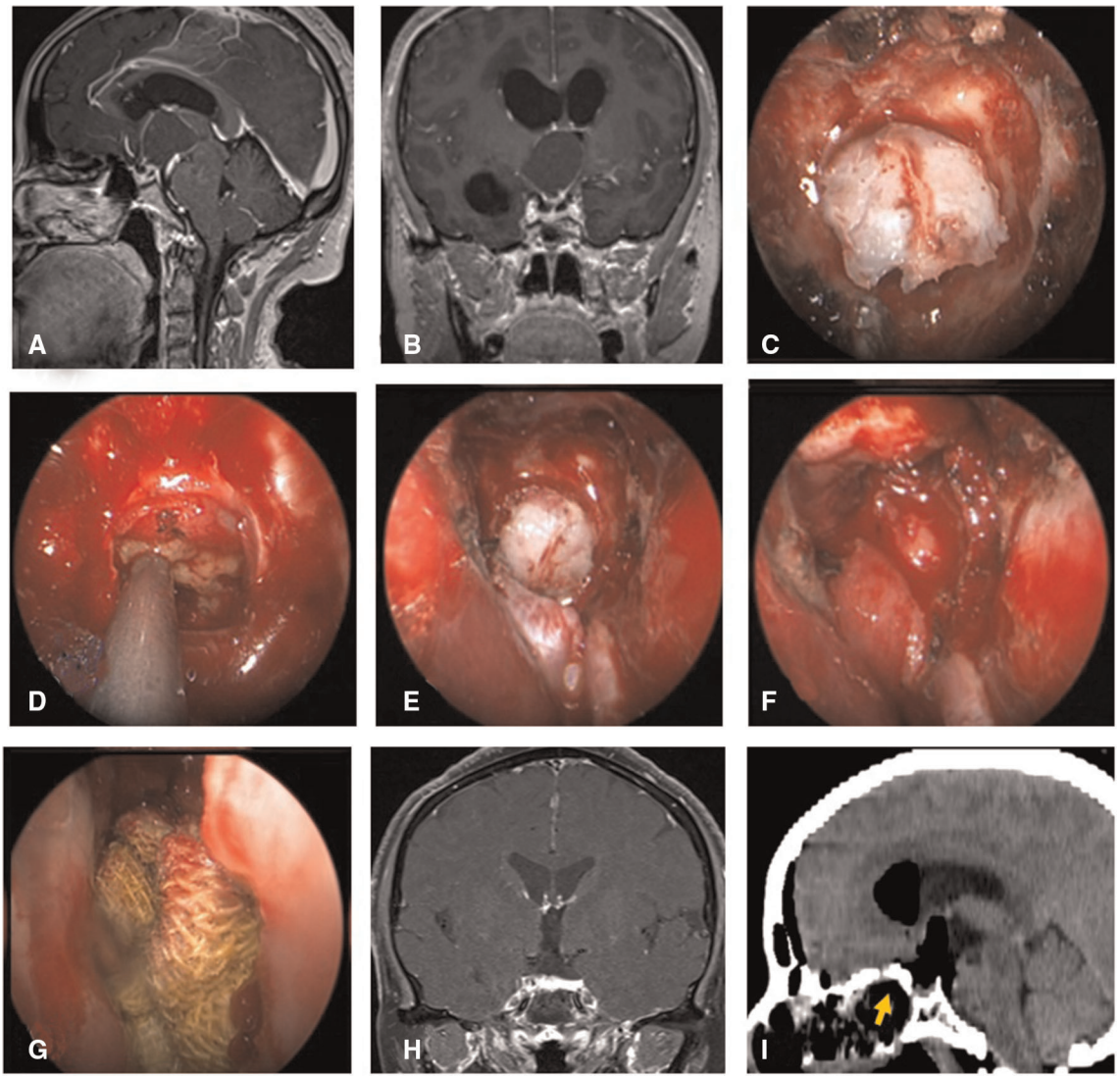

FIGURE 3
Changes in reconstruction strategy/(after) [(**C**) ISBF harvesting; (**D**–**G**) process of reconstruction]. (**A**,**B**) MRI enhanced in sellar region before operation, and craniopharyngioma was considered; .**C**) Osteoclastic craniectomy to creating a bone flap *in situ*. (**D**) Subdural fat packing. (**E**) Repair of skull base bone window with ISBF. (**F**) Cover the VP-NSF on the ISBF. (**G**) Gauze support. (**H**) Coronal enhanced MRI in sellar after operation and postoperative pathology showed craniopharyngioma. (**I**) CT bone window showing ISBF was in place. VP-NSF, vascularized pedicle nasoseptal flap, ISBF, *in situ* bone flap.

Discussion

Although the incidence of postoperative CSF leakage was significantly reduced by 5%–10% with reconstruction using the VP-NSF multilayer reconstruction technique (8, 12–14), the complications still remained unacceptable. Thus, it is imperative to explore the causes of postoperative CSF leakage and potential influencing factors.

Endoscopic exploration of patients with postoperative CSF leakage

In this study, we found that postoperative CSF leakage was more common in patients with intraoperative grade 3 flow CSF leakage (10/14), and the leading causes of postoperative CSF leakage were insufficient subdural and epidural reconstruction in multilayer skull base reconstruction. The details are as follows: (1) Insufficient subdural

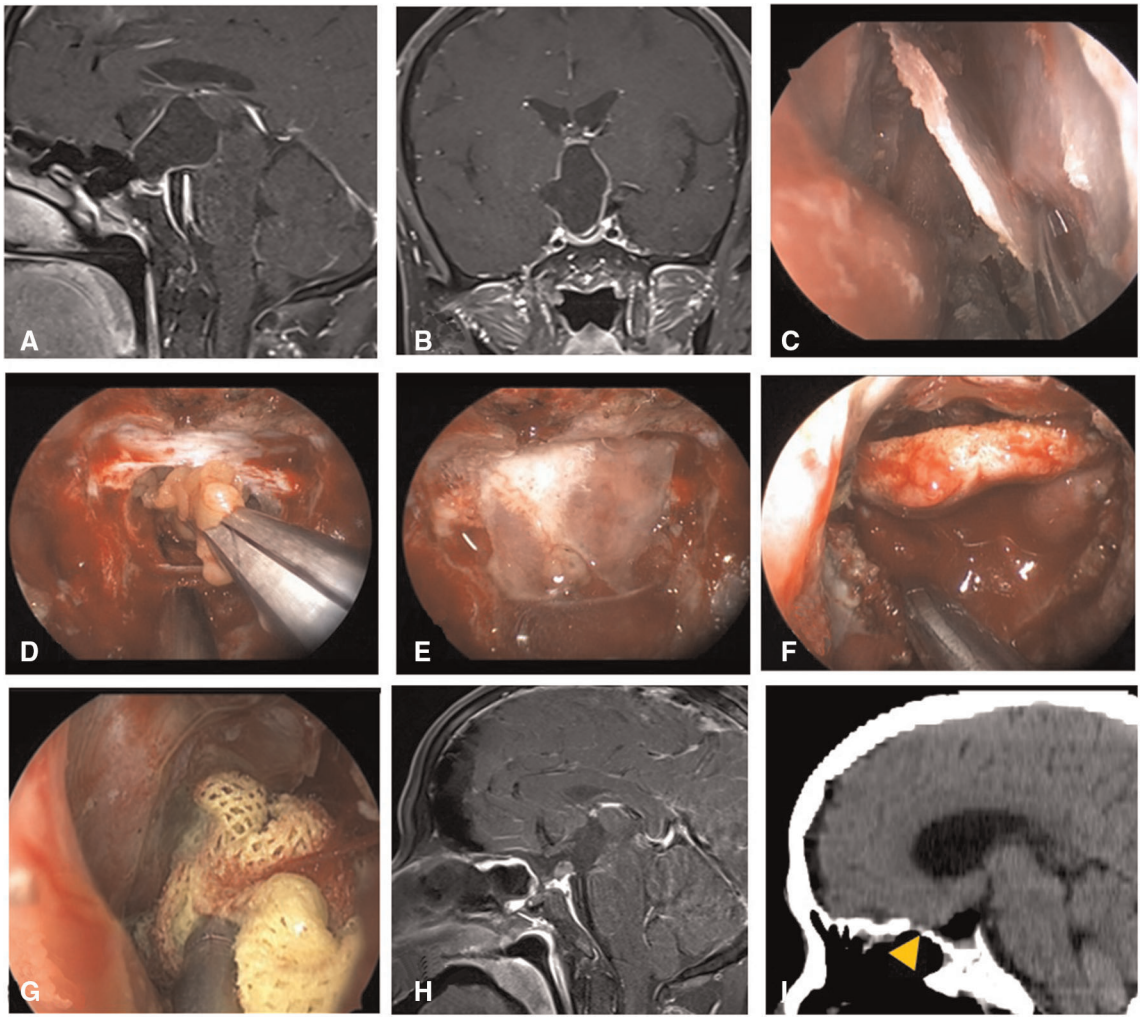

FIGURE 4
Changes in reconstruction strategy/(after) [(**C**) harvest of nasal septum bone flap; (**D–G**) process of reconstruction]. (**A,B**) MRI enhanced in sellar region before operation, and craniopharyngioma was considered before operation. (**C**) Separation of nasal septum bone flap. (**D**) Subdural fat packing. (**E**) Repair of skull base bone window with trimmed nasal septum bone flap. (**F**) Cover the VP-NSF on the nasal septum bone flap. (**G**) Gauze support. (**H**) MRI enhanced in sellar after operation and postoperative pathology showed craniopharyngioma. (**I**) CT bone window showing nasal septum bone flap was in place. VP-NSF, vascularized pedicle nasoseptal flap.

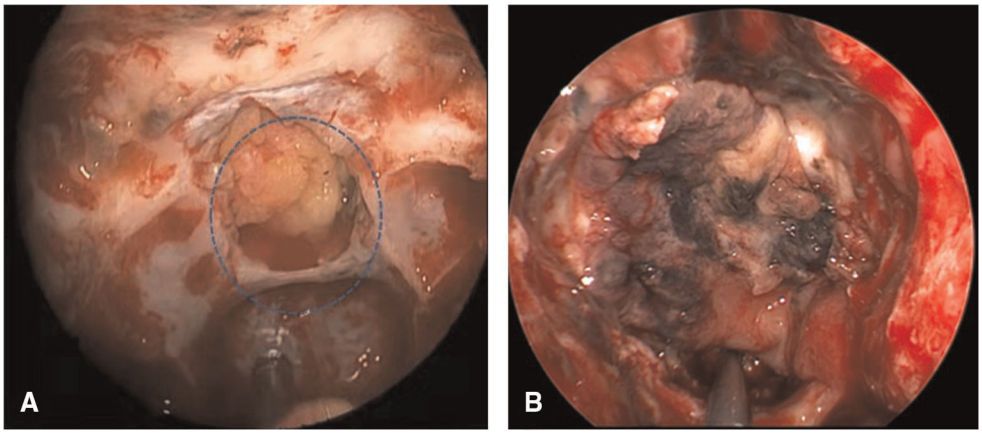

FIGURE 5
(**A**) Insufficient embedded fat (**circle**). (**B**) VP-NSF inactivation. VP-NSF, vascularized pedicle nasoseptal flap.

TABLE 2 Causes of CSF after endoscopic endonasal surgery.

ID	Sex /age	Pathology	ICSF leakage flow grading	Causes	Time	Repair times	Nasal packing	Complication
1	M/29	Pituitary adenoma	Grade 3	Insufficient embedded fat	14	1	B	Intracranial infection
2	F/52	Meningioma	Grade 3	Inner artificial dura breach	15	1	G	—
3	F/50	Pituitary adenoma	Grade 2	VP-NSF perforation	23	1	B	—
4	M/45	Pituitary adenoma	Grade 3	VP-NSF Perforation	20	2	B	—
5	M/19	Craniopharyngioma	Grade 3	Inner artificial dura breach + Not firm adherence of VP-NSF to the skull base	19	2	B	Intracranial infection
6	F/57	Craniopharyngioma	Grade 3	Inner artificial dura breach	12	1	B	Intracranial infection
7	F/48	Pituitary adenoma	Grade 3	VP-NSF displacement + Inner artificial dura breach	5	1	B	—
8	M/53	Pituitary adenoma	Grade 2	Inner artificial dura breach	9	1	B	—
9	M/58	Pituitary adenoma	Grade 3		10	1	G	Intracranial infection
10	F/63	Craniopharyngioma	Grade 3	Inner artificial dura breach + VP-NSF displacement	14	2	B	Intracranial infection
11	F/61	Pituitary adenoma	Grade 3	VP-NSF inactivation + VP-NSF displacement	13	1	G	Intracranial infection
12	M/42	Meningioma	Grade 3	Inner artificial dura breach	15	1	B	Intracranial infection
13	M/22	Craniopharyngioma	Grade 2	LD < 72 h	3	0	G	Intracranial infection
14	F/43	Pituitary adenoma	Grade 1	LD < 72 h	14	0	B	/

Grade 1 = small "weeping" leak, without obvious or with only small diaphragmatic defect; grade 2 = obvious defect of sellar diaphragma or skull base dura mater with moderate CSF exudation; grade 3 = large CSF leak, large sellar diaphragmatic or skull base dural defect with extensive opening of suprasellar arachnoid cistern and/or opening of the floor of the third ventricle.
B, balloon; G, gauze; LD, lumbar cistern drainage; VP-NSF, vascularized pedicle nasoseptal flap; CSF, cerebrospinal fluid; ICSF, intraoperative cerebrospinal fluid.

reconstruction due to the inadequate embedded fat and inlaid artificial dura. Inlaid artificial dura is easily washed away in grade 3 CSF leakage flow from the suprasellar arachnoid cistern and even the third ventricle. (2) Insufficient epidural reconstruction, including displacement, necrosis, perforation of the VP-NSF, and imperfect adherence of VP-NSF to the skull base. Displacement of VP-NSF is always caused by improper support of the balloon and inadvertent removal of nasal packing. VP-NSF necrosis usually resulting from impaired vascular pedicle, including irregular nasoseptal flap (NSF) harvesting, high-pressure nasal packing, and sharp bone protuberances of the sphenoid sinus.

Predictors of postoperative CSF leakage

Suprasellar lesion

Multivariate analysis revealed suprasellar lesion as a risk factor for postoperative CSF leakage. The possible reason is that the suprasellar lesion invades the suprasellar arachnoid cistern or even the floor of the third ventricle; tumor removal might result in opening of the floor of the three ventricles and the suprasellar arachnoid cistern while causing a large skull base defect, which in turn leads to intraoperative grade 3 flow CSF leakage, which leads to the occurrence of postoperative CSF leakage.

Subarachnoid space invasion

Skull base tumors sometimes invade the bone, dura mater, subarachnoid space, arachnoid cistern, and even protrude into the third ventricle. During the operation of pituitary adenoma, we observed a barrier composed of dura mater, with or without pituitary gland tissue, or arachnoid between tumors and CSF. Tumor invasion to the arachnoid might weaken the anti-CSF barrier and leads to postoperative CSF leakage. It is reported that Villalonga et al. (18) developed a model for predicting intraoperative and postoperative CSF leakage; the results confirmed a significant correlation between subarachnoid space invasion and postoperative CSF leakage (OR = 4.879, 95% CI: 1.243–12.820, $P = 0.007$), and revealed a significantly increased risk of postoperative CSF leakage in patients with incomplete arachnoid structures. In our data, only 4 out of 14 cases of CSF leakage did not develop subarachnoid invasion. Suprasellar tumors, especially tuberculum sellae meningiomas, were difficult to keep the arachnoid intact after lesion removal because of the tumor consistency, and even accompanied with injury to the brain tissue and perforating vessels (19, 20), the risk of CSF

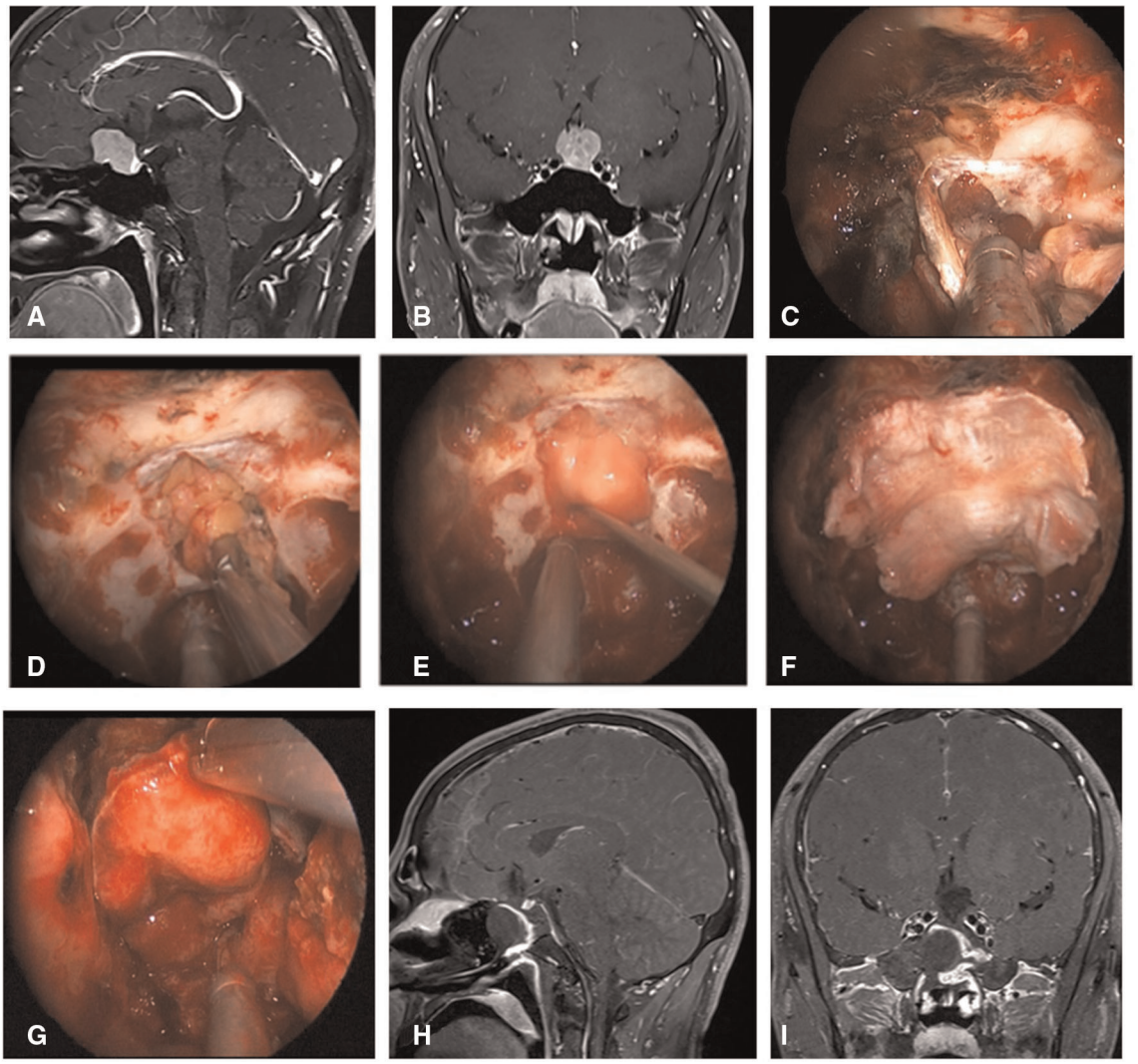

FIGURE 6
Repair process of patient with insufficient embedded fat. (A,B) MRI enhanced in sellar region before operation and was considered pituitary adenoma. (C) Uncover the VP-NSF to see the subdural leakage. (D) Subdural fat packing. (E) Artificial dura mater embedded between cellulite and dura mate. (F) Cover fascia lata on the artificial inlay dura (arrow). (E) Cover the VP-NSF on the fascia lata. (H,I) Sagittal and coronal enhanced MRI in sellar region after operation, and postoperative pathology showed pituitary adenoma. VP-NSF, vascularized pedicle nasoseptal flap.

leakage is relatively high in these cases. Therefore, we point out that the integrity of the arachnoid is a more influencing factor than the tumor size or suprasellar extension in postoperative CSF leakage, which is consistent with findings of Campero et al. described previously (21).

Intraoperative grade 3 flow CSF leakage

Several studies reported that intraoperative CSF leakage was an independent factor of postoperative CSF leakage (11, 22). However, a few literature studies analyzed the postoperative CSF leakage by classifying intraoperative CSF leakage flow. Here, we showed that the incidence of postoperative CSF leakage in patients with intraoperative CSF leakage was 7.1%, which is in accord with the range of 6%–53.2% reported in literature studies (10, 14, 22). The risk of postoperative CSF leakage was significantly higher than that of patients without intraoperative CSF leakage (7.1% vs. 0%). The result suggests that patients with intraoperative CSF leakage are more needed aggressive treatment to prevent postoperative CSF leakage. In addition, some cases in which sellar diaphragm remains intact after tumor removal still developed postoperative CSF leakage, which might be attributed to inadequate postoperative skull base reconstruction or low-flow CSF leakage omitted intraoperatively (23).

Further study of intraoperative flow CSF leakage showed that not all intraoperative CSF leakages were associated with

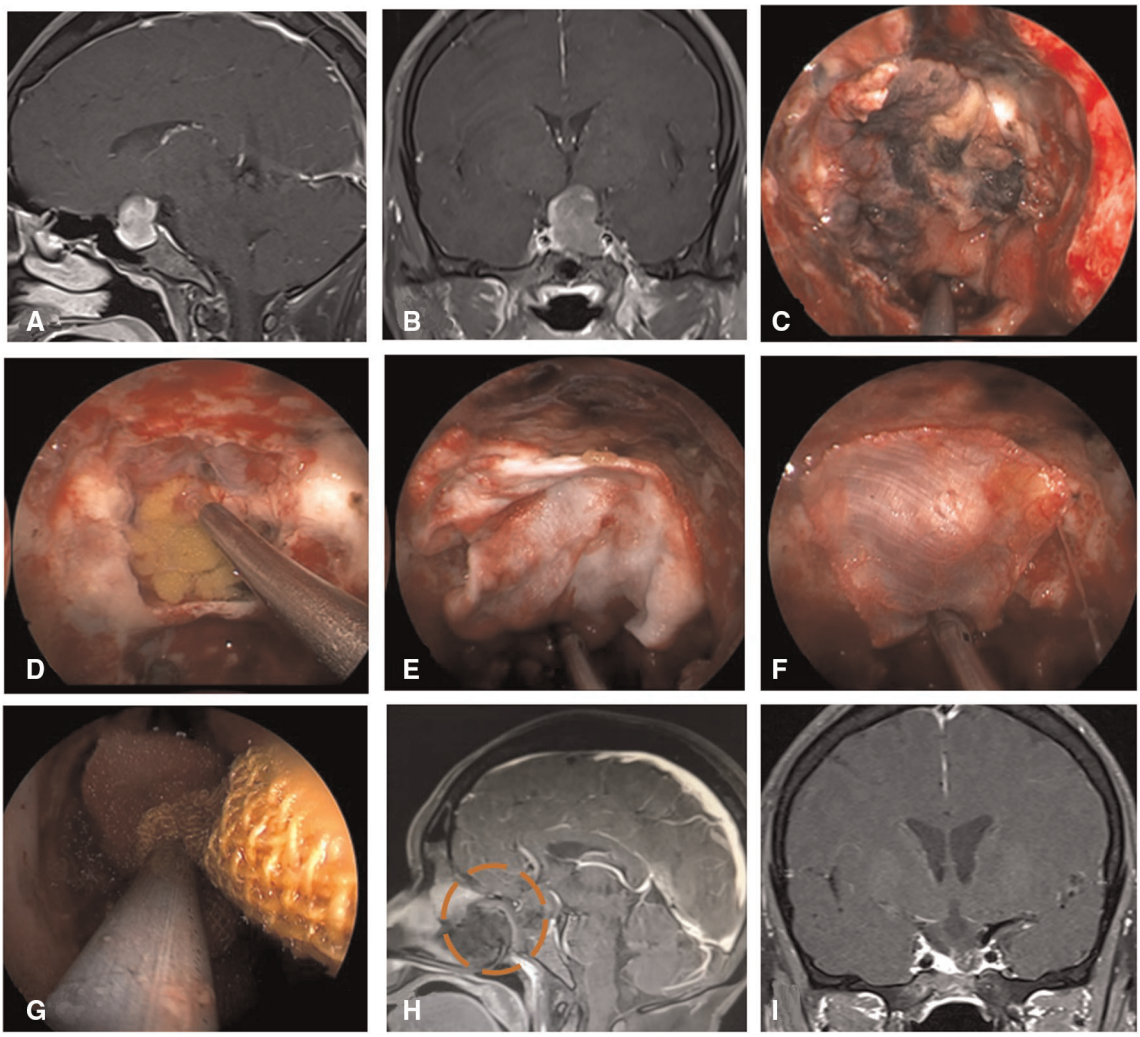

FIGURE 7
Repair process of patient with VP-NSF inactivation. (A,B) MRI enhanced in sellar region before operation and was considered pituitary adenoma. (C) VP-NSF inactivation observed on the endoscopy (black area). (D) Unraveling the artificial inner dura. (E) Artificial dura mater embedded between cellulite and dura mater. (F) Replacement of inactivated nasal septal mucosal flap using fascia lata. (G) Collagen sponge and biological protein glue was fixed and then supported with iodoform gauze. (H) MRI enhancement at postoperative week 2 showed no significant enhancement of VP-NSF (circle). (I) Postoperative MRI enhancement in sellar region. VP-NSF, vascularized pedicle nasoseptal flap.

postoperative CSF leakage. Intraoperative grade 1 or grade 2 flow CSF leakage was not statistically correlated with CSF leakage after the operation. It might be related to the fact that the tumor did not invade the suprasellar region, the sellar diaphragm was intact intraoperatively, and CSF was compressed less on the reconstructed structures.

Grade 3 flow CSF leakage was the risk factor ($P < 0.05$) possibly due to a larger defect in the sellar diaphragm in patients with intraoperative grade 3 flow CSF leakage and the intraoperative opening of the suprasellar cistern. Therefore, once extensive leakage was determined, a more aggressive treatment is required to prevent postoperative CSF leakage.

Bony reconstruction

In situ bone flap or nasal septum bone flap + VP-NSF were used to repair the bony structure of the skull base after September 2018 (Table 5). Among the 104 patients who used bone reconstruction combined with membranous reconstruction, 1 case developed postoperative CSF leakage (0.9%, 1/104) and 4 cases developed intracranial infection (3.8%, 4/104), consistent with previous studies (12), suggesting the reconstruction effect is reliable. Furthermore, the univariate and multivariate analyses results confirmed that bone flap reconstruction was the protective factor of postoperative CSF leakage (OR = 0.313, 95% CI: 0.099–0.694, *P*

TABLE 3 Univariate analysis of factors affecting occurrence of postoperative CSF leakage.

Patient/tumor characteristics	CSF leakage ($n = 14$)	No CSF leakage ($n = 346$)	χ^2/t	P value
Sex, M/F	7/7	177/169	0.013	0.908
Age, years	44 ± 15	45 ± 14	0.365	0.809
Hypertension	0 (0)	43 (12)	Fisher	0.688
Diabetes	2 (14.3)	16 (4.6)	Fisher	0.162
Radiotherapy	0 (0)	6 (1.7)	Fisher	1.000
Revision surgery	1 (7.1)	47 (13.6)	Fisher	0.704
Pathology				
Craniopharyngioma	4 (29)	53 (15.3)	Fisher	0.003
Pituitary adenoma	8 (57.1)	256 (74.0)	7.038	0.015
Meningioma	2 (18.8)	30 (8.7)	Fisher	0.634
Rathke's cleft cyst	0 (0)	7 (2.0)	Fisher	1.000
Location				
Sellar	1 (7.1)	192 (55.5)	11.349	<0.001
Suprasellar	13 (81.2)	154 (44.5)	20.204	<0.001
Subarachnoid space invasion	10 (71.4)	100 (28.9)	12.474	<0.001
Maximal tumor diameter, cm	3.0 ± 0.6	2.9 ± 1.2	0.577	0.068
ICSF leakage	14 (100)	182 (52.6)	9.458	0.002
Grade 1	1 (6.3)	34 (9.8)		
Grade 2	3 (21.4)	94 (27.2)		
Grade 3	10 (71.4)	54 (15.6)		
Foley balloon support	10 (71.4)	73 (21.0)	Fisher	0.002
Bony reconstruction	1 (7.1)	103 (29.7)	Fisher	0.013
Postoperative lumbar drainage	9 (64.3)	41 (11.8)	Fisher	<0.001

Bold indicates significance.
Sellar lesions include lesions in the intrasellar and cavernous sinus.
Grade 1 = small "weeping" leak, without obvious or with only small diaphragmatic defect; grade 2 = obvious defect of sellar diaphragma or skull base dura mater with moderate CSF exudation; grade 3 = large CSF leak, large sellar diaphragmatic or skull base dural defect with extensive opening of suprasellar arachnoid cistern and / or opening of the floor of the third ventricle.
F, female; M, male; CSF, cerebrospinal fluid; ICSF, Intraoperative cerebrospinal fluid.

= 0.019). For patients without CSF leakage during operation, whether to use sellar bone defect reconstruction still remained uncertain. The need for bony reconstruction in patients without intraoperative CSF leakage was still inconclusive, and many surgeons did not consider bony reconstruction as a necessary step when without intraoperative CSF leakage (24). However, for patients with intraoperative CSF leakage, we recommend the use of a bone flap combined with VP-NSF for skull base reconstruction for the following reasons: first, for reconstruction of the outer mucosal layer, the bone flap can theoretically provide mechanical support against the pressure of CSF on the reconstructed site and maintain the original

TABLE 4 Multivariate analysis for postoperative CSF leakage.

Factors	OR	95% CI	P
Subarachnoid invasion	4.879	1.243–12.820	0.007
Suprasellar lesion	3.690	1.029–5.783	0.003
Intraoperative flow CSF leakage			
Grade 1	2.387	1.085–4.783	0.128
Grade 2	5.442	1.781–14.021	0.111
Grade 3	7.392	2.458–19.736	0.012
Bony reconstruction	0.313	0.099–0.694	0.019

[a]Bold indicates significance.
CI, confidence interval; CSF, cerebrospinal fluid; OR, odds ratio.
Grade 1 = small "weeping" leak, without obvious or with only small diaphragmatic defect; grade 2 = obvious defect of sellar diaphragma or skull base dura mater with moderate CSF exudation; grade 3 = large CSF leak, large sellar diaphragmatic or skull base dural defect with extensive opening of suprasellar arachnoid cistern and/or opening of the floor of the third ventricle.

TABLE 5 Frequency of postoperative CSF leakage among tumor pathologies.

Tumor pathology	Cases (proportion %)
Pituitary adenoma	8/264 (3.0%)
Craniopharyngioma	4/57 (7.0%)
Meningioma	2/32 (6.3%)

CSF, cerebrospinal fluid.

structure of the skull base (13). In addition, bony reconstruction avoids the need for routine postoperative placement of LD, reducing the incidence of retrograde infection, facilitating early postoperative activity, and decreasing the occurrence of venous thrombosis. As to the comparison between *in situ* bone flap and nasal septal bone flap reconstruction in terms of the difference in reconstructive efficacy, there is still no relevant literature report.

Pathology, tumor size, and other factors

Univariate analysis shows that craniopharyngioma, pituitary adenoma, and meningioma were associated with postoperative CSF leakage. However, this difference was not significant. Pathology did not appear to be correlated with postoperative CSF leakage after multivariate analysis. Furthermore, due to the small sample size, we were unable to compare whether there was a difference in postoperative CSF leakage between pathological types by $R \times C$ chi-square test. However, the frequency of postoperative CSF leakage is lower in pituitary adenoma than in craniopharyngiomas and meningioma according to data (Table 5). In addition, larger tumors would theoretically increase the likelihood of invasion of the sellar diaphragm, increasing the postoperative CSF leak rate (7, 25). However, except that the maximum diameter of tumor growth can be located in any axis, tumor does not always

invade the arachnoid. Therefore, there was no significant correlation between tumor size and postoperative CSF leakage.

As for other factors including sex, age, diabetes, and hypertension, none of the above was significantly associated with postoperative CSF leakage on adjusted analysis ($P > 0.05$).

Changes of reconstruction strategy

Nasal packing

The main nasal packing support used before was a foley balloon catheter. The multivariate statistical results proved that its usage did not significantly reduce the occurrence of postoperative CSF leakage. Balloon support can significantly reduce the incidence of postoperative CSF leakage for patients with grade 3 flow CSF leakage during operation (26). However, Raza and Schwartz (27) did not suggest using the balloon since it might increase the risk of flap ischemia and cause patient discomfort. However, the author still insists on improving the way of external support. The main reasons are as follows: first, VP-NSF displacement might happen when the foley balloon is placed or extracted. Second, iodoform gauze has uniform pressure distribution and a longer retention time than balloon (14D vs. 7D), which can avoid pulling out the external support when the reconstructed tissue is not completely fibrotic. Finally, it has a certain analgesic effect.

Postoperative lumbar drainage

Postoperative LD was used to prevent postoperative CSF leakage based on our experience that a multilayered skull base reconstruction approach with VP-NSF and fascia lata repair alone is inadequate for patients of intraoperative grade 3 flow CSF leakage. However, the statistical results showed that LD was not associated with postoperative CSF leakage. The literature remains unclear on the benefits and risk of postoperative LD as an adjunct in repairing grade 3 flow CSF leakage. Hu et al. (28) advocated routine LD after the operation. Conger et al (29) suggest that LD will cause retrograde infection, low intracranial pressure, and tension pneumocephalus. Others suggest that postoperative LD should be used selectively depending on the location of the skull base defect and the risk factors of CSF leakage (30, 31). In the meantime, a recent meta-analysis revealed that the overall incidence of postoperative CSF leakage in patients who received LD was 7.5%, and the overall incidence of postoperative CSF leakage in patients who did not receive LD was 3.4% (32). All these results suggest that postoperative LD does not reduce the incidence of postoperative CSF leakage. Our data suggest that the bone flap combined with the mucosal flap is sufficient to resist intraoperative grade 3 flow CSF leakage without the need for postoperative LD (12). However, we do not deny the role of postoperative LD in reconstruction strategy. If there is CSF leakage during the repair, we will place LD according to the grade of CSF leakage postoperatively. Thus, we recommend using bone flap combined with VP-NSF for skull base reconstruction in high-risk patients, avoiding routine postoperative using LD.

Limitations of this study

This study still has some limitations. Preoperative BMI values (33), postoperative intracranial pneumatosis (34), hydrocephalus (35), and intracranial hypertension (36) might be postoperative CSF leakage risk factors. Lucke-Wold et al. (37) suggest that the CSF leakage was associated with multiorganism meningitis. These possible influencing factors were not included in this study. Therefore, the potential factors relate to CSF leakage still need to be studied.

Conclusion

To summarize, tumor invasion of the subarachnoid space, suprasellar extension, intraoperative grade 3 flow CSF leakage risk factors for postoperative CSF leakage, and bony reconstruction was a protective factor for postoperative CSF leakage. Attention should be paid to patients with high-risk factors. Meanwhile, skull base reconstruction should be given great importance after tumor resection. We recommend using bone flap combined with VP-NSF and iodoform gauze for skull base reconstruction in high-risk patients, avoiding routine postoperative using LD. Patients with suspected postoperative CSF leakage should be explored and repaired promptly.

Data availability statement

The raw data supporting the conclusions of this article will be made available by the authors, without undue reservation.

Ethics statement

The studies involving human participants were reviewed and approved by Ethical Committee of the First Affiliated Hospital of Nanchang University review board. Written informed consent to participate in this study was provided by the participants' legal guardian/next of kin.

Author contributions

BT contributed to the conception and design of the article. SX, HL, and LX acquired the data and analyzed the results. YX,

YL, and GX designed the study and drafted the article. XW and TH revised the manuscript. All authors contributed to the article and approved the submitted version.

Funding

This work was supported by the National Natural Science Foundation of China (grant no. 81460381), the Key research and invention plan of Jiangxi Science and Technology Department (20192BBG70026), and the Ganpo555 Engineering Excellence of Jiangxi Science and Technology Department (2013).

Conflict of interest

The authors declare that the research was conducted in the absence of any commercial or financial relationships that could be construed as a potential conflict of interest.

Acknowledgments

We express our sincere appreciation to Dr. Le Yang (Department of Neurosurgery, Nanfang Hospital, Southern Medical University, Guangzhou, China) for the review, revision, and language editing the paper.

Publisher's note

References

1. Eisinger RS, Sorrentino ZA, Cutler C, Azab M, Pierre K, Lucke-Wold B, et al. Clinical risk factors associated with cerebrospinal fluid leak in facial trauma: a retrospective analysis. *Clin Neurol Neurosurg.* (2022) 217:107276. doi: 10.1016/j.clineuro.2022.107276

2. Naunheim MR, Sedaghat AR, Lin DT, Bleier BS, Holbrook EH, Curry WT, et al. Immediate and delayed complications following endoscopic skull base surgery. *J Neurol Surg B Skull Base.* (2015) 76:390–6. doi: 10.1055/s-0035-1549308

3. Lee JA, Cooper RL, Nguyen SA, Schlosser RJ, Gudis DA. Endonasal endoscopic surgery for pediatric sellar and suprasellar lesions: a systematic review and meta-analysis. *Otolaryngol Head Neck Surg.* (2020) 163:284–92. doi: 10.1177/0194599820913637

4. Kassam AB, Prevedello DM, Carrau RL, Snyderman CH, Thomas A, Gardner P, et al. Endoscopic endonasal skull base surgery: analysis of complications in the authors' initial 800 patients. *J Neurosurg.* (2011) 114:1544–68. doi: 10.3171/2010.10.Jns09406

5. Grotenhuis JA. Costs of postoperative cerebrospinal fluid leakage: 1-year, retrospective analysis of 412 consecutive nontrauma cases. *Surg Neurol.* (2005) 64:490–3. doi: 10.1016/j.surneu.2005.03.041

6. Guo K, Heng L, Zhang H, Ma L, Zhang H, Jia D. Risk factors for postoperative intracranial infections in patients with pituitary adenoma after endoscopic endonasal transsphenoidal surgery: pneumocephalus deserves further study. *Neurosurg Focus.* (2019) 47:E5. doi: 10.3171/2019.5.Focus19269

7. Jakimovski D, Bonci G, Attia M, Shao H, Hofstetter C, Tsiouris AJ, et al. Incidence and significance of intraoperative cerebrospinal fluid leak in endoscopic pituitary surgery using intrathecal fluorescein. *World Neurosurg.* (2014) 82:e513–523. doi: 10.1016/j.wneu.2013.06.005

8. Soudry E, Turner JH, Nayak JV, Hwang PH. Endoscopic reconstruction of surgically created skull base defects: a systematic review. *Otolaryngol Head Neck Surg.* (2014) 150:730–8. doi: 10.1177/0194599814520685

9. Kim JS, Hong SD. Risk factors for postoperative CSF leakage after endonasal endoscopic skull base surgery: a meta-analysis and systematic review. *Rhinology.* (2021) 59:10–20. doi: 10.4193/Rhin20.145

10. Paluzzi A, Fernandez-Miranda JC, Tonya Stefko S, Challinor S, Snyderman CH, Gardner PA. Endoscopic endonasal approach for pituitary adenomas: a series of 555 patients. *Pituitary.* (2014) 17:307–19. doi: 10.1007/s11102-013-0502-4

11. Ozawa H, Sekimizu M, Saito S, Nakamura S, Mikoshiba T, Watanabe Y, et al. Risk factor for cerebrospinal fluid leak after endoscopic endonasal skull base surgery: a single-center experience. *Acta Otolaryngol.* (2021) 141:621–5. doi: 10.1080/00016489.2021.1900600

12. Luo C, Liu X, Xie S, Hong T, Tang B. Experience and modification of skull base reconstruction results in lower complications rates. *Acta Neurochir.* (2022) 164:1127–33. doi: 10.1007/s00701-021-05082-w

13. Jin B, Wang XS, Huo G, Mou JM, Yang G. Reconstruction of skull base bone defects using an in situ bone flap after endoscopic endonasal transplanum-transtuberculum approaches. *Eur Arch Otorhinolaryngol.* (2020) 277:2071–80. doi: 10.1007/s00405-020-05911-1

14. Esposito F, Dusick JR, Fatemi N, Kelly DF. Graded repair of cranial base defects and cerebrospinal fluid leaks in transsphenoidal surgery. *Oper Neurosurg.* (2007) 60:295–303. doi: 10.1227/01.Neu.0000255354.64077.66

15. Oakley GM, Alt JA, Schlosser RJ, Harvey RJ, Orlandi RR. Diagnosis of cerebrospinal fluid rhinorrhea: an evidence-based review with recommendations. *Int Forum Allergy Rhinol.* (2016) 6:8–16. doi: 10.1002/alr.21637

16. Abuabara A. Cerebrospinal fluid rhinorrhoea: diagnosis and management. *Med Oral Patol Oral Cir Bucal.* (2007) 12:E397–400. PMID: 17767107.

17. Lund VJ. Endoscopic management of cerebrospinal fluid leaks. *Am J Rhinol.* (2002) 16:17–23. doi: 10.1177/194589240201600104

18. Villalonga JF, Solari D, Cavallo LM, Cappabianca P, Prevedello DM, Carrau R, et al. The sellar barrier on preoperative imaging predicts intraoperative cerebrospinal fluid leak: a prospective multicenter cohort study. *Pituitary.* (2021) 24:27–37. doi: 10.1007/s11102-020-01082-8

19. Ditzel Filho LF, Prevedello DM, Jamshidi AO, Dolci RL, Kerr EE, Campbell R, et al. Endoscopic endonasal approach for removal of tuberculum sellae meningiomas. *Neurosurg Clin N Am.* (2015) 26:349–61. doi: 10.1016/j.nec.2015.03.005

20. Al-Mefty O, Smith RR. *Tuberculum sellae meningiomas*. New York: Raven Press (1991).

21. Campero A, Villalonga JF, Basso A. Anatomical risk factors for intraoperative cerebrospinal fluid leaks during transsphenoidal surgery for pituitary adenomas. *World Neurosurg.* (2019) 124:e346–355. doi: 10.1016/j.wneu.2018.12.094

22. Seiler RW, Mariani L. Sellar reconstruction with resorbable vicryl patches, gelatin foam, and fibrin glue in transsphenoidal surgery: a 10-year experience with 376 patients. *J Neurosurg.* (2000) 93:762–5. doi: 10.3171/jns.2000.93.5.0762

23. Patel PN, Stafford AM, Patrinely JR, Smith DK, Turner JH, Russell PT, et al. Risk factors for intraoperative and postoperative cerebrospinal fluid leaks in endoscopic transsphenoidal sellar surgery. *Otolaryngol Head Neck Surg.* (2018) 158:952–60. doi: 10.1177/0194599818756272

24. Cong Z, Liu K, Wen G, Qiao L, Wang H, Ma C. Universal sellar anatomical reconstruction using the sellar floor flap after endoscopic pituitary adenoma surgery. *Otolaryngol Head Neck Surg*. (2018) 158:774–6. doi: 10.1177/0194599818756861

25. Zhou Q, Yang Z, Wang X, Wang Z, Zhao C, Zhang S, et al. Risk factors and management of intraoperative cerebrospinal fluid leaks in endoscopic treatment of pituitary adenoma: analysis of 492 patients. *World Neurosurg*. (2017) 101:390–5. doi: 10.1016/j.wneu.2017.01.119

26. Cai X, Yang J, Zhu J, Tang C, Cong Z, Liu Y, et al. Reconstruction strategies for intraoperative CSF leak in endoscopic endonasal skull base surgery: systematic review and meta-analysis. *Br J Neurosurg*. (2021) 21:1–11. doi: 10.1080/02688697.2020.1849548

27. Raza SM, Schwartz TH. Multi-layer reconstruction during endoscopic endonasal surgery: how much is necessary? *World Neurosurg*. (2015) 83:138–9. doi: 10.1016/j.wneu.2014.07.004

28. Hu F, Gu Y, Zhang X, Xie T, Yu Y, Sun C, et al. Combined use of a gasket seal closure and a vascularized pedicle nasoseptal flap multilayered reconstruction technique for high-flow cerebrospinal fluid leaks after endonasal endoscopic skull base surgery. *World Neurosurg*. (2015) 83:181–7. doi: 10.1016/j.wneu.2014.06.004

29. Conger A, Zhao F, Wang X, Eisenberg A, Griffiths C, Esposito F, et al. Evolution of the graded repair of CSF leaks and skull base defects in endonasal endoscopic tumor surgery: trends in repair failure and meningitis rates in 509 patients. *J Neurosurg*. (2018) 130:861–75. doi: 10.3171/2017.11.Jns172141

30. Zwagerman NT, Wang EW, Shin SS, Chang YF, Fernandez-Miranda JC, Snyderman CH, et al. Does lumbar drainage reduce postoperative cerebrospinal fluid leak after endoscopic endonasal skull base surgery? A prospective, randomized controlled trial. *J Neurosurg*. (2018) 131:1172–78. doi: 10.3171/2018.4.Jns172447

31. Tien DA, Stokken JK, Recinos PF, Woodard TD, Sindwani R. Cerebrospinal fluid diversion in endoscopic skull base reconstruction: an evidence-based approach to the use of lumbar drains. *Otolaryngol Clin North Am*. (2016) 49:119–29. doi: 10.1016/j.otc.2015.09.007

32. Ahmed OH, Marcus S, Tauber JR, Wang B, Fang Y, Lebowitz RA. Efficacy of perioperative lumbar drainage following endonasal endoscopic cerebrospinal fluid leak repair. *Otolaryngol Head Neck Surg*. (2017) 156:52–60. doi: 10.1177/0194599816670370

33. Sun I, Lim JX, Goh CP, Low SW, Kirollos RW, Tan CS, et al. Body mass index and the risk of postoperative cerebrospinal fluid leak following transsphenoidal surgery in an Asian population. *Singapore Med J*. (2018) 59:257–63. doi: 10.11622/smedj.2016159

34. Banu MA, Szentirmai O, Mascarenhas L, Salek AA, Anand VK, Schwartz TH. Pneumocephalus patterns following endonasal endoscopic skull base surgery as predictors of postoperative CSF leaks. *J Neurosurg*. (2014) 121:961–75. doi: 10.3171/2014.5.Jns132028

35. Fraser S, Gardner PA, Koutourousiou M, Kubik M, Fernandez-Miranda JC, Snyderman CH, et al. Risk factors associated with postoperative cerebrospinal fluid leak after endoscopic endonasal skull base surgery. *J Neurosurg*. (2018) 128:1066–71. doi: 10.3171/2016.12.Jns1694

36. Snyderman CH, Kassam AB, Carrau R, Mintz A. Endoscopic reconstruction of cranial base defects following endonasal skull base surgery. *Skull Base*. (2007) 17:73–8. doi: 10.1055/s-2006-959337

37. Lucke-Wold B, Mendez G, Cua D, Akins P, Gillham H, Ciporen J. Combined endoscopic transorbital and endonasal repair of high flow orbital apex/middle fossa cerebrospinal fluid leak with a nasoseptal flap. *J Neuroinflamm Neurodegener Dis*. (2018) 2:100005. PMID: 29676403

frontiers | Frontiers in Surgery

TYPE Original Research
PUBLISHED 23 September 2022
DOI 10.3389/fsurg.2022.996290

OPEN ACCESS

EDITED BY
Songbai Gui,
Capital Medical University, China

REVIEWED BY
Delia Cannizzaro,
Humanitas Research Hospital, Italy
Adolfo De La Lama,
Servicio Gallego de Salud, Spain

*CORRESPONDENCE
Bin Tang
tonytang19850815@sina.com

†These authors have contributed equally to this work

SPECIALTY SECTION
This article was submitted to Neurosurgery, a section of the journal Frontiers in Surgery

RECEIVED 17 July 2022
ACCEPTED 05 September 2022
PUBLISHED 23 September 2022

CITATION
Xin G, Liu Y, Xiong Y, Xie S, Luo H, Xiao L, Wu X, Hong T and Tang B (2022) The use of three-dimensional endoscope in transnasal skull base surgery: A single-center experience from China.
Front. Surg. 9:996290.
doi: 10.3389/fsurg.2022.996290

The use of three-dimensional endoscope in transnasal skull base surgery: A single-center experience from China

Guo Xin[1†], Yajing Liu[2†], Yicheng Xiong[1], Shenhao Xie[1], Hai Luo[1], Liming Xiao[1], Xiao Wu[1], Tao Hong[1] and Bin Tang[1*]

[1]Department of Neurosurgery, The First Affiliated Hospital of Nanchang University, Nanchang, China, [2]Operating Theater, The First Affiliated Hospital of Nanchang University, Nanchang, China

Objective: The development of skull base surgery in the past decade has been influenced by advances in visualization techniques; recently, due to such improvements, 3D endoscopes have been widely used. Herein, we address its effect for transnasal endoscopic skull base surgery.
Methods: A total of 63 patients who under endoscopic endonasal surgery (EES) with 3-D endoscope were retrospectively reviewed, including pituitary adenomas, craniopharyngiomas, meningiomas, Rathke's cleft cysts, and chordomas. According to different lesions, transsellar approach (24 cases), transsphenoidal–transtuberculum approach (14 cases), transclival approach (6 cases), and transpterygoid approach (19 cases) were selected.
Results: Total removal of tumors was achieved in 56 patients (88.9%) and subtotal removal in 7 cases (11.1%). Complications included diabetes insipidus in seven patients (11.1%), cerebrospinal fluid (CSF) leakage in two patients (3.2%), major vascular injury occurred in one patient (1.6%), cranial nerve injury in nine patients (14.3%), and meningitis in two patients (3.2%). There was no mortality in the series. All patients recovered and were back to normal daily life, and no tumor recurrence or delayed CSF leakage was detected during the follow-up (2–13 months, mean 7.59 months).
Conclusions: Via 3D EES, it improved depth perception and preserved important neurovascular tissue when tumors were removed, which is important for improving the operative prognosis.

KEYWORDS
three-dimensional endoscope, endoscopic endonasal surgery, skull base surgery, depth perception, stereo vision

Introduction

One of the most challenging areas in neurosurgery is the skull base, which is surrounded by a vast number of crucial neurovascular structures. Furthermore, a tumor's oncological size, aggressiveness, and irregular expansion make surgical resection of this area highly challenging (1–3). Technical advancements in microscopic development such as the transition from microscopic to endoscopic surgery since the late 1990s benefit from increased efficiency and sufficient surgical field of view that allows more effective surgical treatment of tumors (4–7).

For instance, transnasal techniques and technological advances in the last decade allowed treatments of several skull base lesions through the expanded transsphenoidal approach to the skull base, providing a new approach for treating deep skull base lesions (8). Moreover, neuroendoscopic techniques are widely used in endoscopic endonasal surgery (EES) and are crucial in neurosurgery, otorhinolaryngology, and disorders in the skull base area (9).

Although two-dimensional (2D) high-definition (HD) or ultrahigh-definition (UHD) neuroendoscopes are mostly used nowadays, the lack of depth perception remains an issue. On the other hand, only experienced surgeons can get three-dimensional (3D) depth perception with visual and haptic cues, dynamic movements of the scope, light, shadow, and adequate anatomical knowledge (10, 11). In other words, a relatively steep learning curve is required to overcome such limitations. Nevertheless, following the development and application of 3D camera technology, EES procedures have gradually involved 3D neuroendoscopes with 3D perception in presenting neurovascular tissues (12).

While the use of 3D neuroendoscopes has been reported (13–17), such reports are rare in China. This study presents a retrospective analysis of the results of using 3D EES to treat 63 patients with skull base disorders. A gap in the literature with respect to 3D neuroendoscopic techniques in China, including preliminary experience of the application and advantages of 3D neuroendoscopes, is described.

Patients and methods

Patient population

Clinical data of 63 patients who underwent 3D EES from February 2021 to January 2022 were retrospectively analyzed at the Department of Neurosurgery, the First Affiliated Hospital of Nanchang University, China. The cases included 24 males and 39 females with ages ranging from 4 to 72 years (median, 44 years). Clinical data were collected from the patients' medical records. Among them, 15 cases underwent reoperation. The study conformed to the World Medical Association Declaration of Helsinki ethical principles for medical research involving human subjects. At the same time, each patient involved provided informed consent by signing an informed consent for surgery form.

Clinical presentation

Pre- and postsurgery evaluations were conducted on the serum levels of free triiodothyronine, free thyroxine, thyroid-stimulating hormone, luteinizing hormone, follicle-stimulating hormone, prolactin, growth hormone, cortisol, and adrenocorticotropic hormone. The preoperative endocrinological evaluation identified 11 patients with hypothyroidism, 5 with decreased adrenocorticotropic hormone, 7 with low testosterone, 4 with hyperprolactinemia, 5 with high-growth hormone, and 8 with low cortisol, while 38 patients showed normal preoperative pituitary hormone function. Furthermore, all patients underwent ophthalmologic examinations (visual acuity and computerized visual field examinations) before and after surgery.

Neuroradiological evaluation

Preoperative imaging examinations included magnetic resonance imaging (MRI) + enhancement in the sellar area and thin section computed tomography (CT) examination of paranasal sinuses. Preoperative MRI was used to evaluate tumor volume, maximum tumor diameter, and tumor type.

TABLE 1 Clinical manifestation and characteristics of patients before surgery.

Variable	No. of cases	%
Total	63	100
Age (years old)	42.6 ± 16.8	
Gender		
Male	24	38.1
Female	39	61.9
Operative history		
Primary	48	76.2
Recurrent	15	23.8
Headache	27	42.9
Visual impairment	35	55.5
Diabetes insipidus	4	6.3
Amenorrhea	10	15.9
Cranial nerve injury		
Abducens nerve	1	1.6
Oculomotor nerve	1	1.6
Hypopituitarism		
Partial hypopituitarism	18	28.6
Panhypopituitarism	5	7.9
Consistency		
Cystic	9	14.3
Solid	44	69.8
Mixed	10	15.9
Maximum diameter		
<3 cm	46	73.0
≥3 cm	17	27.0
Tumor type		
Noninvasive pituitary adenomas	20	31.7
Invasive pituitary adenomas	21	33.3
Craniopharyngiomas	11	17.5
Meningiomas	4	6.3
Rathke's cleft cyst	4	6.3
Clival chordoma	3	4.8

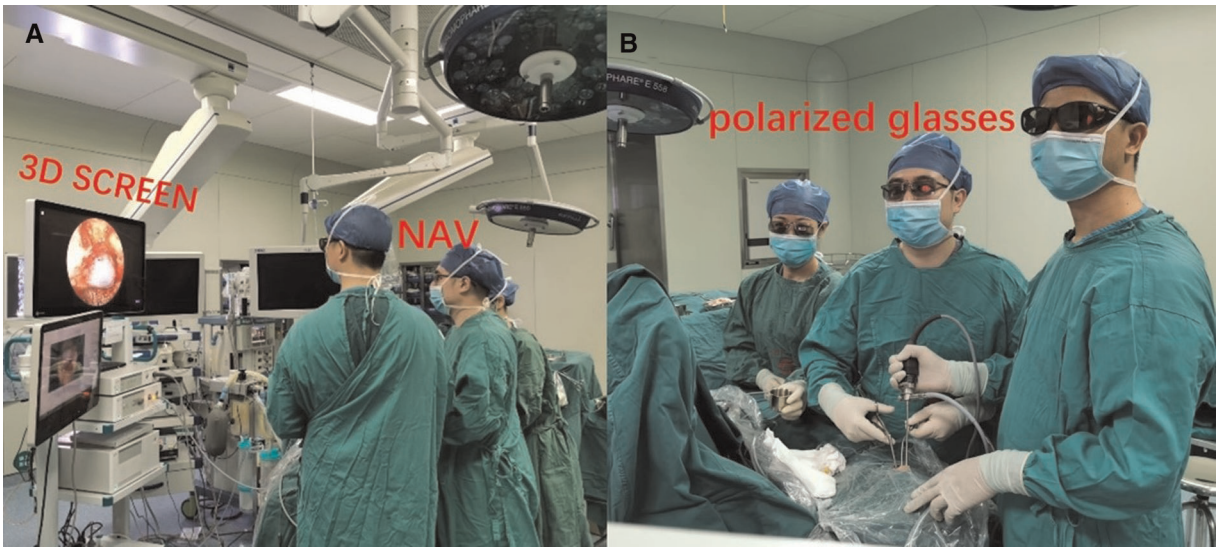

FIGURE 1
Operating room ergonomics. Position of the device in a comfortable position for surgeon, assistant, and surgical nurses (wearing polarized 3D glasses) to see the 3D video screen directly. (A) Placement of the 3D screen (3D SCREEN), neuronavigation (NAV). Note the distance between the surgeon and the 3D screen (at least 2 m), which is necessary for the perception of the 3D image. (B) Positioning of surgeon and assistant to have a direct view of the display screen. Operate using the two-person/three-hand technique.

TABLE 2 Major postoperative complications and tumor categories.

Complication	Number and type of tumors
CSF leakage	2 (2 CP)
Transient diabetes insipidus	7 (1 TB sellar meningiomas, 6 CP)
Meningitis	2 (2 CP)
Cranial nerve injury	9 (2 chordoma, 7 cavernous sinus pituitary adenoma)
Epistaxis	2 (2 cavernous sinus pituitary adenoma)
Vascular injury	1 (1 cavernous sinus pituitary adenoma)

CSF, cerebrospinal fluid; TB, tuberculum; CP, craniopharyngioma.

Tumor volume was approximated by a modified ellipsoid volume, that is, $(A \times B \times C) \times \pi/6$, where A–C represent the maximum tumor diameters in each of the three dimensions. Tumor consistency was obtained from preoperative MRI and intraoperative video (Table 1).

Endoscopic equipment

The equipment included a 3D rigid endoscope with 4.0 mm, 0° and 30° (XION, Germany), which is equipped with real 3D and a full-HD monitor. The 3D stereoscopic endoscope with the standard resolution was used on 63 patients. Images were displayed on a 32-inch stereo (dual flat-screen) mirror, 3D,

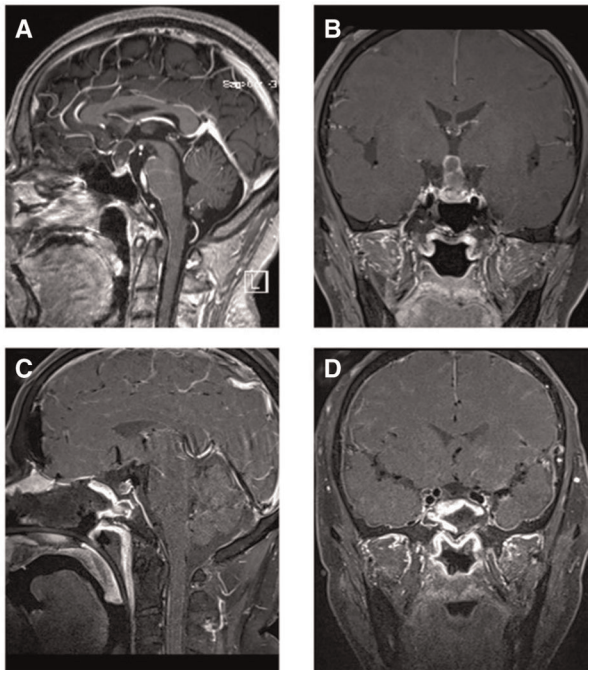

FIGURE 2
T1-weighted MRI image with contrast enhancement of a suprasellar craniopharyngioma. (A) Preoperative sagittal view. (B) Preoperative coronal view. (C) Postoperative sagittal view. (D) Postoperative coronal view. Note in (C) and (D) the autologous fat employed intradurally to fill the empty space within the suprasellar after tumor removal.

and a full HD monitor (MATRIX *P* Spectar) system that uses a double-coated polarized mirror to overlay right and left images. Polarizing glasses were worn for 3D visualization. All the procedures were performed under the guidance of the Ultrasound Navigation System (BRAINLAB) using MRI or CT data and, in selected cases, utilized the intraoperative portable CT scanner that allowed noncontrast angiography and contrast perfusion scans (**Figure 1**).

Surgical procedure

After the application of general anesthesia, all patients were placed in the supine position. The head was slightly extended and rotated 10°–15° to the right and fixed on a rigid, 3-pin Mayfield–Kees skull brace by using image guidance. A rigid 0° endoscope, 18 cm in length and 4 mm in diameter (XION, Germany), was used during the procedure.

All cases were managed using the two-person/three-hand or two-person/four-hand technique. According to different lesions, transsellar approach (24 cases), transsphenoidal–transtuberculum approach (14 cases), transclival approach (6 cases), and transpterygoid approach (19 cases) were selected. During surgery, electrophysiological monitoring, neuronavigation, ultrasound Doppler, and other techniques were applied to the tumor, which enclosed the internal carotid artery or severely damaged the surrounding anatomical structures.

Finally, multilayer skull base reconstruction methods without postoperative lumbar drainage were performed according to intraoperative flow of CSF leakage. Throughout the reconstruction, an iodoform gauze containing aureomycin is used for 7–14 days as a support to prevent graft migration.

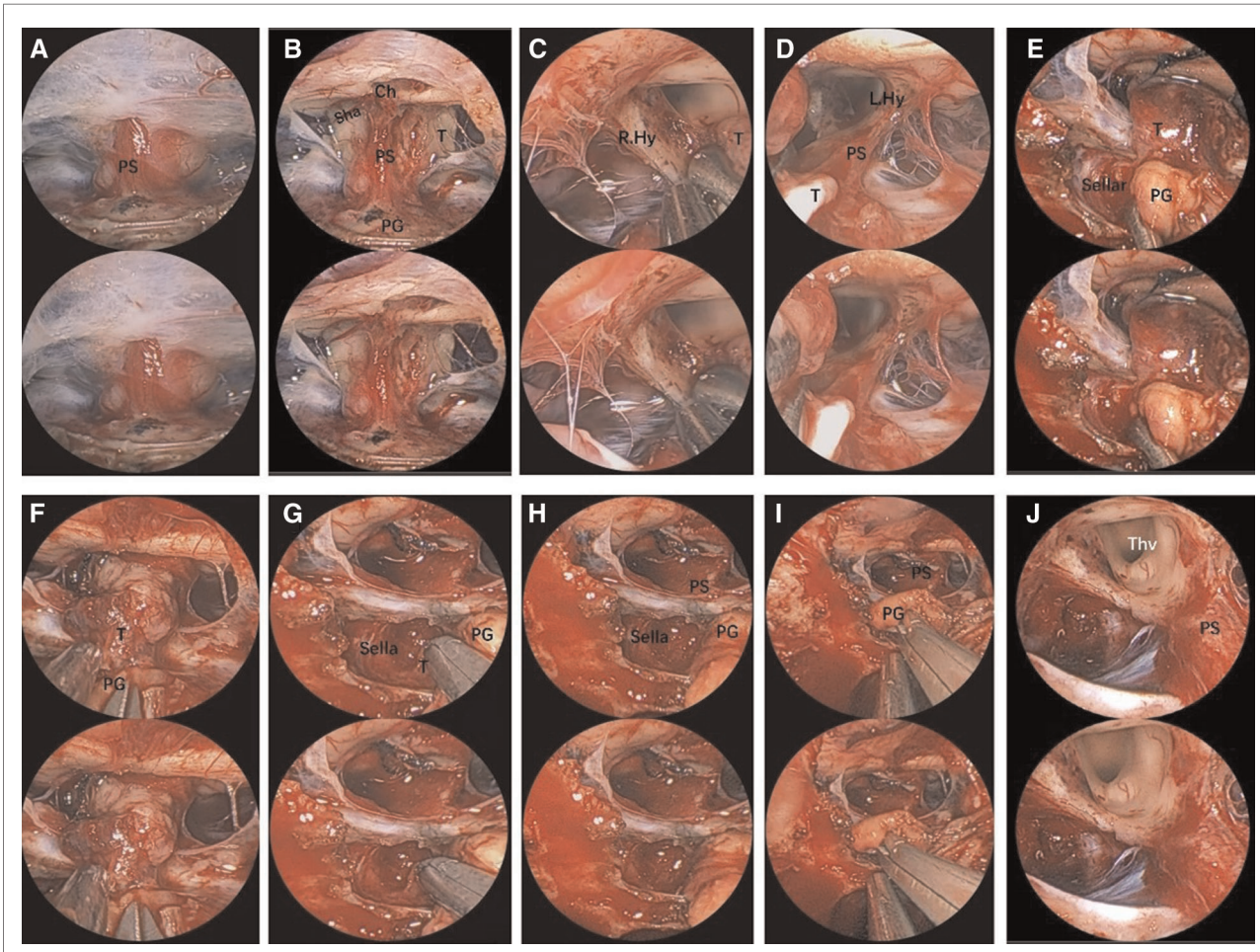

FIGURE 3
Endoscopic visualization of a suprasellar craniopharyngioma. (**A**) View of the pituitary stalk. (**B**) View of optic nerves, the chiasm, and the anterior complex during extracapsular dissection of tumor. (**C**,**D**) Close-up view of the pituitary stalk and optic nerves, crucial for tumor dissection. (**E**,**F**) Anatomical view of the main body of the suprasellar craniopharyngioma. (**G**) A view showing a small part of tumor in the sellar. (**H**,**I**) View of the PG was pulled and not in placed after surgery. (**J**) Final view of the third ventricle and pituitary stalk after craniopharyngioma removal. The 3D image can be obtained with cross-viewing method. PS, pituitary stalk; PG, pituitary gland; OC, optic chiasm; ON, optic nerve; sha, superior hypophyseal artery; T, tumor; ThV, third ventricle.

Postoperative management and follow-up

All patients were provided routine prophylactic antibiotics with 100 ml of 0.9% normal saline containing 1.5 g cefuroxime sodium 3 days before surgery within 30–45 min and levofloxacin eye drops (5 mg/ml) in the nose for anti-inflammatory treatment. Patients were asked to undergo a head CT scan within 6 h and MRI enhancement of the sellar area or head within 3 days after surgery to determine the degree of tumor resection and skull base reconstruction. The removal rate for skull base tumors was determined according to intraoperative findings and confirmed by the 3-month follow-up imaging. The gross total resection (GTR) was defined as 100% for tumor resection, 80%–99% subtotal resection (STR), and <80% for partial resection. Postsurgery patients were closely monitored for vital signs, water electrolytes, and hypothalamic-pituitary functions.

Moreover, transnasal neuroendoscopic exploration was performed at 2, 4, and 8 weeks postoperatively to clean the nasal cavity and monitor healing in the nasal mucosa. Finally, after patients are discharged, a regular MRI review method was used to determine the recurrence of primary pathology. Then, postsurgery patients undergo 3-month, 6-month, and annual follow-up imaging and visual assessments; Examinations were further repeated when clinically appropriate.

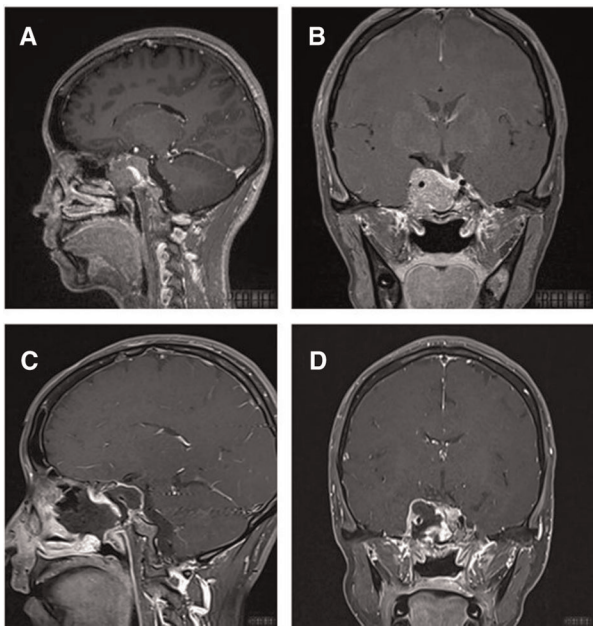

FIGURE 4
T1-weighted MRI image with contrast enhancement of a cavernous sinus pituitary tumor. (A) Preoperative sagittal view. (B) Preoperative coronal view. (C) Postoperative sagittal view. (D) Postoperative coronal view. Note in (C) and (D) the autologous fat employed intradurally to fill empty space within the sellar after tumor removal.

Result

GTR was achieved in 56 patients (88.9%), while STR was achieved in 7 (11.1%) patients. Mean tumor volume was 8.18 cm^3 (range: 0.09–36.65 cm^3).

The STR patients included one case with pituitary macroadenoma with suprasellar lateral fissure invasion, resulting in a little residue; one case with craniopharyngioma (CP) on the saddle pituitary stalk, resulting in a small residual cyst wall due to thin cyst wall and adhesion of the hypothalamus that could not be separated; one case with cavernous sinus (CS) meningioma where the proximal end of the internal carotid artery at the CS could not be fully exposed; and one case where a hypothalamic-pituitary CP stalk showed residual parts due to the difficult separation of giant calcified plaques from close adhesions on the optic nerve and Circle of Willis. Two cases of recurrent pituitary adenomas (RPA) invading the CS showed a little residual due to significant scar adhesions. One case of a pituitary tumor with invasion of the CS showed a little residue and a small daughter tumor in the direction of the optic nerve.

Preoperative visual impairment was present in 35 cases, improved in 33 cases, and worsened in 2 cases after surgery, including one case of tuberculum sellae meningioma and one case of giant pituitary adenoma. At least 27 cases of preoperative headaches were relieved after an operation, of which 10 cases were from amenorrhea and recovered menstruation. At least five cases of diabetes insipidus (DI) were not significantly relieved through operative therapy. Preoperative oculomotor nerve palsy occurred in one case, relieved considerably after the surgery. One patient showed preoperative symptoms of abducens nerve injury, which was not alleviated after surgery.

The seven cases of postoperative DI include one case of tuberculum sellar meningioma and six cases of CP, all of which were transient DI and improved after drug treatment. Two patients with CS pituitary tumors showed postsurgery epistaxis and recovered by treatment. Two cases of chordoma and two cases of CS RPA developed abducens nerve palsy. Three recurrent cases and one initial case of CS pituitary tumor developed oculomotor nerve palsy. One cases of CS RPA developed trigeminal palsy after surgery. One case of CS RPA developed internal carotid artery injury after surgery, which was treated by electrocoagulation. Two cases of postoperative CP developed CSF leakage and intracranial infection, which were cured by lumbar drainage, CSF leakage repair surgery, and antibiotic treatment. There were no procedure-related deaths.

We collected data on tumor types and postoperative complications (shown in Table 2). All cases showed complete healing of nasal mucosa, with rosy color observed by transnasal neuroendoscopic exploration (the important and typical cases are shown in Figures 2–7).

All patients received 2–13 months of follow-up examinations (mean: 7.59 months) and MRI reviews that showed no tumor recurrence in all patients. Patients with operative complications during the follow-up period include four cases with abducens nerve palsy, four cases with oculomotor nerve palsy, and one case with trigeminal nerve palsy complications, which completely recovered after rehabilitation treatment and left no relevant sequelae. One case with internal carotid artery injury recovered without developing pseudoaneurysm. One case with vision loss showed no continuing aggravation. Seven DI cases recovered to normal status after medication. One case with preoperative symptoms of oculomotor nerve palsy recovered normal function.

Finally, all patients maintained normal endocrine levels and returned to normal life. Moreover, there were no cases of deaths or delayed CSF leakage during the follow-up period (Table 3).

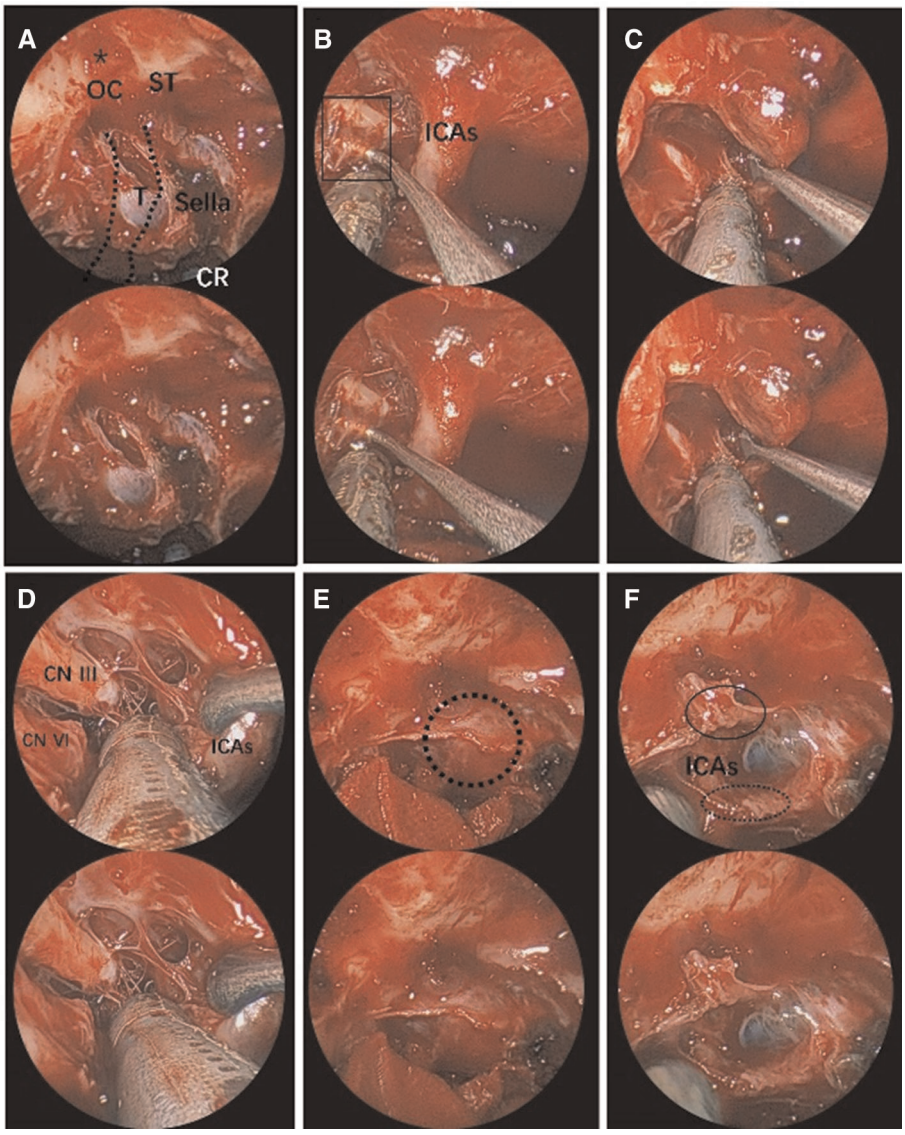

FIGURE 5
Endoscopic visualization of CS pituitary tumor. (A) Exposure of the planum sphenoidale and supraoptic recess (black asterisk). The route of the internal carotid artery. The black asterisk represents the supraoptic recess. (B) View of the fiber texture in CS. (C,D) Close-up view of the ICAs and nerves, crucial for tumor dissection. (E) View of the proximal and distal dural rings of the internal carotid artery (black dotted circle). (F) This is the proximal and distal dural ring of the internal carotid artery after resection of the tumor. The black ellipse represents the distal dural ring. The black dotted line ellipse represents the proximal dural ring. The 3D image can be obtained with cross-viewing method. ICAs, intracavernous segment of internal carotid artery; CR, clival recess; CN III, oculomotor nerve; CN VI, abducens nerve; T, tumor; CS, cavernous sinus.

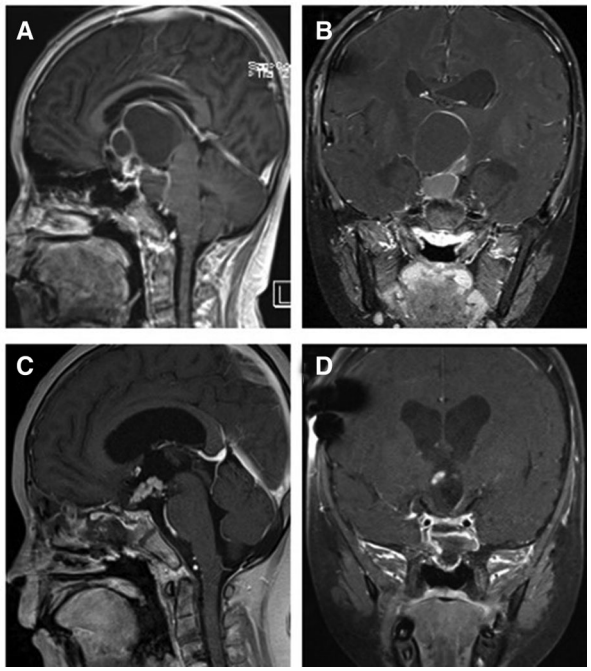

FIGURE 6
T1-weighted MRI image with contrast enhancement of suprasellar craniopharyngioma. (A) Preoperative sagittal view. (B) Preoperative coronal view. (C) Postoperative sagittal view. (D) Postoperative coronal view. Note in (C) and (D) the autologous fat employed intradurally to fill empty space within the sellar after tumor removal.

Discussion

The most challenging types of skull base surgery involve pituitary tumors, one of the most common tumors in the sellar region and include invasive and noninvasive pituitary tumors. Moreover, CS invasion is associated with high surgical risks and recurrence rates, STR and endocrine remission, and the need for adjuvant therapy (18, 19). To address these issues, Cushing suggested a transsphenoidal surgical approach in 1907 (20). Through the exploration of surgeons and the development of endoscopic techniques, EES has become one of the primary approaches for treating skull base tumors (21–23). As surgeons gained EES experience and development, they advanced into novel territories such as complex, skull base tumors (e.g., CS invasion tumor), which were once considered inoperable.

Due to the increasing use and difficulty of EES cases, the 2D neuroendoscopes became insufficient to meet surgical demands. Further development of new devices and instruments for EES, from the initial single-chip endoscopic camera with bright and dark, single-color displays to the three-chip, HD, and UHD 2D neuroendoscopes, can help in enhancing neurosurgery technology.

Because of the 3D nature of human anatomy, depth perception is essential to all surgical procedures. Since the widely used 2D neuroendoscopes cannot meet surgical requirements, developing 3D neuroendoscopes with 3D visibility is significant (24).

With its 3D visualization advantages, the 3D endoscope was first applied in laparoscopic surgery, then developed (14–16, 25) and gradually applied to other surgical fields. However, its development in neurosurgery was not ideal due to the large size of the early 3D endoscope, which had a 4.9 mm tip diameter.

With developments in 3D and small-aperture camera technology, the new generation of 4.0 mm 3D HD neuroendoscope provides advantages such as better depth perception and improved hand–eye coordination for surgeons, and is widely used in skull base surgery, particularly in the treatment of deep brain lesions. In addition, this new neuroendoscope provides better resolution of tiny neurovascular structures so that surgeons can assess more accurately the tissue structure and the distances between lesions and critical neurovascular structures (13, 26–28). Due to these advantages, the 3D neuroendoscope has been increasingly used in EES. Moreover, research studies confirm its practical clinical value in different treating skull base lesions.

Although studies have shown that 3D endoscopic techniques have been developed earlier in other countries, it has not been used as widely as 2D endoscopic devices due to the high cost of 3D endoscopic devices when they were initially developed, the high cost of the procedure, the lack of user experience, and adverse visual effects such as visual fatigue and lack of 3D depth perception (6, 29, 30).

However, our 3D technology exploration is relatively late. Now, fairly well-developed 3D equipment is available, along with surgeons experienced in endoscopic techniques. Moreover, the lower procedural cost and surgeons with more experience in endoscopic techniques can help reduce or avoid the adverse effects associated with 3D endoscopes, such as visual fatigue and imperfect depth perception. In other words, the use of 3D EES can be promoted. Although this study found complications such as cranial nerve injury and DI, cranial nerve palsy and endocrine levels recovered to normal due to rehabilitation. In particular, the depth perception obtained by 3D endoscopes allowed precise dissection, thus protecting the neurovascular tissue during CS pituitary tumors and CP surgery.

This report describes the use of 3D neuroendoscopes (XION, Germany) in EES as follows: (1) The layout of the endoscopic surgery room is consistent with previous EES use of a 2D neuroendoscope. However, the correct distance of the surgeons should be at least 2 m from the 3D screen or at least 1 m farther than when using a 2D neuroendoscope. This distance is crucial for viewing the 3D image and reducing visual fatigue to avoid the effects of long-term 3D use on the

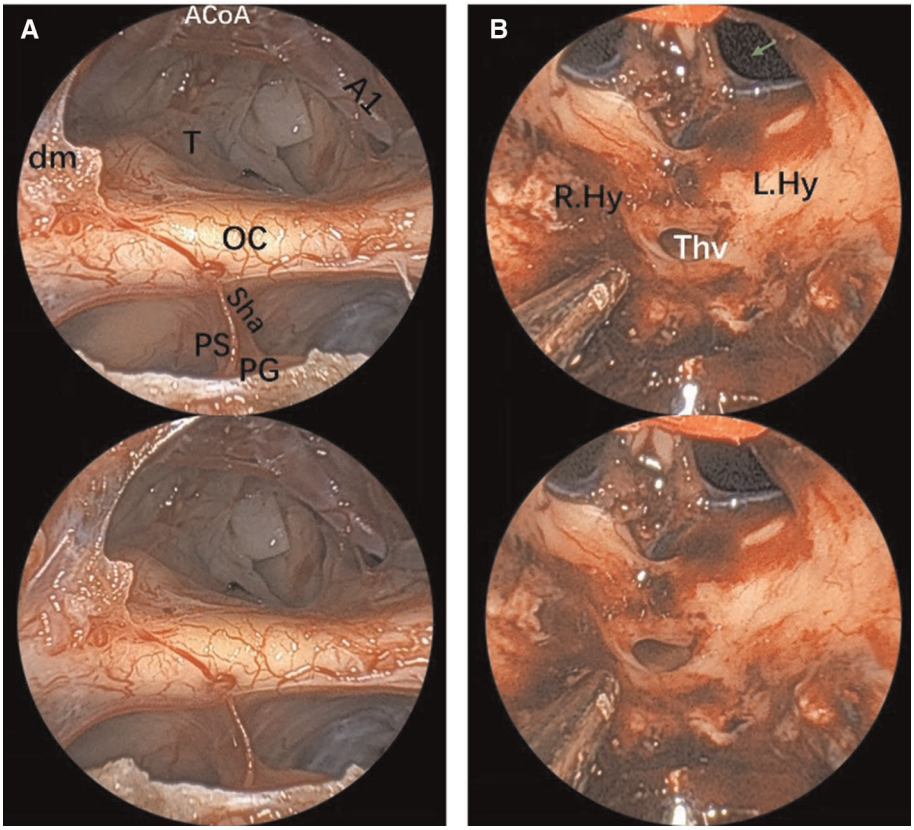

FIGURE 7
Endoscopic visualization of a suprasellar craniopharyngioma. (**A**) View of optic nerves, the chiasm and the anterior complex during extracapsular dissection of a large suprasellar craniopharyngioma. The tiny vessels adherent to the tumor are clearly demonstrated, which helps perform meticulous dissection maneuver. (**B**) Final view of the third ventricle after craniopharyngioma removal. The 3D image can be obtained with cross-viewing method. PS, pituitary stalk; PG, pituitary gland; OC, optic chiasm; sha, superior hypophyseal artery; T, tumor; dm, dura mater; ThV, third ventricle; green arrow, foramen of Monro; A1, segment of anterior cerebral artery; ACoA, anterior communicating artery, Hy, hypothalamus.

TABLE 3 Preoperative, postoperative, and follow-up statuses in all patients.

Statuses	Total	Preoperative	Postoperative			Follow-up Normalized
			Improved	Unchanged	Worsened	
Endocrinological						
Normal pituitary function	38	38	—	35 (92.1%)	3 (7.9%)	38 (100%)
Partial hypopituitarism	18	18	13 (72.2%)	4 (22.2%)	1 (5.5%)	18 (100%)
Panhypopituitarism	5	5	5 (100%)	0 (0%)	0 (0%)	5 (100%)
Preop DI	5	5	0 (0%)	5 (100%)	0 (0%)	0 (0%)
New cases of DI	7	—	—	—	—	7 (100%)
Hyperprolactinemia	4	4	4 (100%)	0 (0%)	0 (0%)	4 (100%)
High GH	5	5	5 (100%)	0 (0%)	0 (0%)	5 (100%)
Clinical symptoms						
Headache	27	27	27 (100%)	0 (0%)	0 (0%)	27 (100%)
Visual impairment	35	35	33 (94.3%)	0 (0%)	2 (5.7%)	33 (94.3%)
Visual normal	28	28	0 (0%)	28 (100%)	0 (0%)	28 (100%)
Amenorrhea	4	4	4 (100%)	0 (0%)	0 (0%)	4 (100%)
Preop CN palsy	2	2	1 (50%)	1 (50%)	0 (0%)	2 (50%)
New cases of CN palsy	9	—	—	—	—	9 (100%)

DI, diabetes insipidus; GH, growth hormone; CN, cranial nerve.

surgeon's vision (31). (2) The 3D system can overcome the major drawbacks of lens contamination and visual degradation when operating in a narrow nasal cavity (32). During the tumor dissection, 3D endoscopy is most helpful in understanding the surgical anatomy (33). Therefore, better knowledge of the 3D transnasal skull base anatomy allows a more selective dissection of the structure of the skull base, even in the CS, during EES. (3) After completing the surgical approach, removing lesion in the open field of vision can best display the 3D visual effect and the lens is seldom polluted. In other words, the 3D depth perception is effective in reducing the incidence of complications. The HD resolution clearly differentiates a neural subdural lesion from adjoining blood vessels and diseased vs. healthy peripheral nerve blood vessels (17, 31, 34). (4) Although the 3D neuroendoscope has only 0° and 30° endoscopes and no 45° and 70° endoscopes, in most cases, a 30° 3D endoscope allows surgeons to see skull base corners and perform surgical procedures under direct vision. (5) Surgeons with rich EES experience and long-term use of the 2D neuroendoscope will only need a very short time to fully adapt to the stereoscopic effect of the 3D neuroendoscope. Moreover, junior doctors who have just started with EES do not need a long learning curve (35, 36).

The total resection rate was 88.9% (56/63) in this study, similar to the data reported in the literature. Moreover, the surgical results are reasonable when compared with data retrieved from recent literature reports (**Table 4**) (27, 29, 30, 37–40).

The preceding literature review and this study conclude that the advantages of 3D neuroendoscope in EES include improved depth perception, identification of deep anatomical structures, and enhanced surgery safety. Patient complications, such as DI, nerve injury, and CSF leakage, were related to lesions but not to the 3D neuroendoscopic technique or the surgical instruments. While the significant effects of 3D vision are evident, further controlled studies with more patients are necessary to assess the objective significance of 3D visualization in EES.

Limitations of this study

One limitation of this study is the lack of a controlled study on 2D and 3D endoscopic surgical outcomes. The potential value of 3D stereoscopic visualization is evident, explaining why the next research focus should be on assessing the objective significance of 3D visualization techniques in transnasal skull base surgery through a controlled study with an appropriate sample.

Conclusions

The 3D endoscope can overcome the principal limit of the 2D endoscope: the lack of depth perception. Using the advantages of 3D neuroendoscope, it is indeed conducive to more stereoscopic and subtle perception of deep anatomical structures by the physician during EES, overcoming the major drawbacks of traditional 2D neuroendoscope, facilitating hand–eye coordination, discerning the important peripheral neurovascular structures during tumor resection, and

TABLE 4 Literature review of complications of 3D EES.

Authors (year)	No. of patient	GTR (N/%)	Cerebrospinal fluid leakage (N/%)	Meningitis (N/%)	Vascular injury (N/%)	Epistaxis (N/%)	Diabetes insipidus (N/%)	Hypopituitarism (N/%)
Pennacchietti et al. (2016) (37)	104	73 (70.1)	5 (4.8)	N P	2 (1.9)	1 (1.9)	6 (5.7)	17 (16.3)
Tabaee et al. (2009) (38)	13	10 (76.9)	0	0	0	0	N P	N P
Kari et al. (2010) (27)	26	N P	1 (3.8)	N P	N P	N P	5 (19.2)	1 (3.8)
Felisati et al. (2013) (29)	10	6 (60)	2 (20)	2 (20)	N P	N P	2 (20)	5 (50)
Haidari et al. (2018) (39)	116	87 (75)	11 (9.5)	4 (3.4)	N P	7 (6.0)	N P	11 (9.5)
Barkhoudarian et al. (2013) (40)	65	N P	1 (1.6)	N P	N P	2 (3.1)	1 (1.6)	N P
Catapano et al. (2016) (30)	70	50 (71.4)	5 (7.1)	1 (1.4)	N P	N P	9 (12.9)	9 (12.9)
Present study	63	56 (88.9)	2 (3.2)	2 (3.2)	1 (1.6)	2 (3.2)	7 (11.1)	4 (6.3)

EES, endoscopic endonasal surgery; GTR, gross total resection; N P, Not Reported.

improving the safety and efficacy of surgery. We point out that the 3D endoscope is a concrete and promising development tool for EES.

Data availability statement

The original contributions presented in the study are included in the article/Supplementary Material, further inquiries can be directed to the corresponding author.

Ethics statement

The survey was approved by the Ethical Committee of the First Affiliated Hospital of Nanchang University review board. The informed consent was provided by all the patients, and this study was conducted in accordance with the relevant guidelines. Patients were informed that they had the opportunity to opt out if they were not willing to participate.

Author contributions

BT made contributions to conception and design. SX, HL, and LX acquired the data and analyzed the consequence. GX, YL, and YX designed the study and drafting the article. XW and TH revised the manuscript. All authors contributed to the article and approved the submitted version.

Funding

This work was supported by the Key Research and Invention Plan of Jiangxi Science and Technology Department (20192BBG70026).

Acknowledgments

We express our sincere appreciation to Le Yang (Department of Neurosurgery, Nanfang Hospital, Southern Medical University, Guangzhou, China) for reviewing, revising, and language editing the paper.

Conflict of interest

The authors declare that the research was conducted in the absence of any commercial or financial relationships that could be construed as a potential conflict of interest.

Publisher's note

References

1. Abu-Ghanem S, Shilo S, Yehuda M, Abergel A, Safadi A, Fliss DM. Anterior skull base surgery in the 21st century: the role of open approaches. *Adv Otorhinolaryngol.* (2020) 84:56–67. doi: 10.1159/000457925

2. Castelnuovo P, Battaglia P, Bignami M, Ferreli F, Turri-Zanoni M, Bernardini E, et al. Endoscopic transnasal resection of anterior skull base malignancy with a novel 3D endoscope and neuronavigation. *Acta Otorhinolaryngol Ital.* (2012) 32 (3):189–91.

3. Cavallo LM, Somma T, Solari D, Iannuzzo G, Frio F, Baiano C, et al. Endoscopic endonasal transsphenoidal surgery: history and evolution. *World Neurosurg.* (2019) 127:686–94. doi: 10.1016/j.wneu.2019.03.048

4. Emanuelli E, Zanotti C, Munari S, Baldovin M, Schiavo G, Denaro L. Sellar and parasellar lesions: multidisciplinary management. *Acta Otorhinolaryngol Ital.* (2021) 41(Suppl. 1):S30–41. doi: 10.14639/0392-100X-suppl.1-41-2021-03

5. Fletcher AM, Marentette L. Anterior skull-base surgery: current opinion. *Curr Opin Otolaryngol Head Neck Surg.* (2014) 22(4):322–5. doi: 10.1097/MOO.0000000000000073

6. Vasudevan K, Saad H, Oyesiku NM. The role of three-dimensional endoscopy in pituitary adenoma surgery. *Neurosurg Clin N Am.* (2019) 30(4):421–32. doi: 10.1016/j.nec.2019.05.012

7. Wagenmann M, Scheckenbach K, Kraus B, Stenin I. [Complications of anterior skull base surgery]. *HNO.* (2018) 66(6):438–46. doi: 10.1007/s00106-018-0508-3

8. Roth JA, Seljeskog EL, Duvall 3rd AJ, Long DM. Transnasal transsphenoidal approach to the sella. *Laryngoscope.* (1977) 87(1):47–57. doi: 10.1288/00005537-197701000-00006

9. Maroon JC. Skull base surgery: past, present, and future trends. *Neurosurg Focus.* (2005) 19(1):E1. doi: 10.3171/foc.2005.19.1.2

10. Baussart B, Declerck A, Gaillard S. Mononostril endoscopic endonasal approach for pituitary surgery. *Acta Neurochir (Wien).* (2021) 163(3):655–9. doi: 10.1007/s00701-020-04542-z

11. Al Kadah B, Bumm K, Charalampaki P, Schick B. [First experience in endonasal surgery using a new 3D-chipendoscope]. *Laryngorhinootologie.* (2012) 91(7):428–33. doi: 10.1055/s-0032-1309051

12. Wang AJ, Zaidi HA, Laws Jr ED. History of endonasal skull base surgery. *J Neurosurg Sci.* (2016) 60(4):441–53.

13. Abarca-Olivas J, Monjas-Canovas I, Lopez-Alvarez B, Lloret-Garcia J, Sanchez-del Campo J, Gras-Albert JR, et al. [Three-dimensional endoscopic endonasal study of skull base anatomy]. *Neurocirugia (Astur).* (2014) 25(1):1–7. doi: 10.1016/j.neucir.2013.02.009

14. Inoue D, Yoshimoto K, Uemura M, Yoshida M, Ohuchida K, Kenmotsu H, et al. Three-dimensional high-definition neuroendoscopic surgery: a controlled comparative laboratory study with two-dimensional endoscopy and clinical application. *J Neurol Surg A Cent Eur Neurosurg.* (2013) 74(6):357–65. doi: 10.1055/s-0033-1345100

15. Kawanishi Y, Fujimoto Y, Kumagai N, Takemura M, Nonaka M, Nakai E, et al. Evaluation of two- and three-dimensional visualization for endoscopic endonasal surgery using a novel stereoendoscopic system in a novice: a comparison on a dry laboratory model. *Acta Neurochir (Wien)*. (2013) 155 (9):1621–7. doi: 10.1007/s00701-013-1757-2

16. Liang H, Liang W, Lei Z, Liu Z, Wang W, He J, et al. Three-dimensional versus two-dimensional video-assisted endoscopic surgery: a meta-analysis of clinical data. *World J Surg*. (2018) 42(11):3658–68. doi: 10.1007/s00268-018-4681-z

17. Marcus HJ, Hughes-Hallett A, Cundy TP, Di Marco A, Pratt P, Nandi D, et al. Comparative effectiveness of 3-dimensional vs 2-dimensional and high-definition vs standard-definition neuroendoscopy: a preclinical randomized crossover study. *Neurosurgery*. (2014) 74(4):375–80, discussion 380–1. doi: 10.1227/NEU.0000000000000249

18. Wu X, Xie SH, Tang B, Yang YQ, Yang L, Ding H, et al. Pituitary adenoma with posterior area invasion of cavernous sinus: surgical anatomy, approach, and outcomes. *Neurosurg Rev*. (2021) 44(4):2229–37. doi: 10.1007/s10143-020-01404-1

19. Doglietto F, Lauretti L, Frank G, Pasquini E, Fernandez E, Tschabitscher M, et al. Microscopic and endoscopic extracranial approaches to the cavernous sinus: anatomic study. *Neurosurgery*. (2009) 64(5 Suppl 2):413–21, discussion 421–2. doi: 10.1227/01.NEU.0000338943.08985.73

20. Cushing III H. Partial hypophysectomy for acromegaly: with remarks on the function of the hypophysis. *Ann Surg*. (1909) 50(6):1002–17. doi: 10.1097/00000658-190912000-00003

21. Verillaud B, Bresson D, Sauvaget E, Mandonnet E, Georges B, Kania R, et al. Endoscopic endonasal skull base surgery. *Eur Ann Otorhinolaryngol Head Neck Dis*. (2012) 129(4):190–6. doi: 10.1016/j.anorl.2011.09.004

22. Schwartz TH, Morgenstern PF, Anand VK. Lessons learned in the evolution of endoscopic skull base surgery. *J Neurosurg*. (2019) 130(2):337–46. doi: 10.3171/2018.10.JNS182154

23. Munson PD, Moore EJ. Pediatric endoscopic skull base surgery. *Curr Opin Otolaryngol Head Neck Surg*. (2010) 18(6):571–6. doi: 10.1097/MOO.0b013e3283401fdc

24. Fraser JF, Allen B, Anand VK, Schwartz TH. Three-dimensional neurostereoendoscopy: subjective and objective comparison to 2d. *Minim Invasive Neurosurg*. (2009) 52(1):25–31. doi: 10.1055/s-0028-1104567

25. Sinha RY, Raje SR, Rao GA. Three-dimensional laparoscopy: principles and practice. *J Minim Access Surg*. (2017) 13(3):165–9. doi: 10.4103/0972-9941.181761

26. Stokken JK, Halderman A, Recinos PF, Woodard TD, Sindwani R. Strategies for improving visualization during endoscopic skull base surgery. *Otolaryngol Clin North Am*. (2016) 49(1):131–40. doi: 10.1016/j.otc.2015.09.008

27. Kari E, Oyesiku NM, Dadashev V, Wise SK. Comparison of traditional 2-dimensional endoscopic pituitary surgery with new 3-dimensional endoscopic technology: intraoperative and early postoperative factors. *Int Forum Allergy Rhinol*. (2012) 2(1):2–8. doi: 10.1002/alr.20036

28. Patel SK, Kashyrina O, Duru S, Miyabe M, Lim FY, Peiro JL, et al. Comparison of two- and three-dimensional endoscopic visualization for fetal myelomeningocele repair: a pilot study using a fetoscopic surgical simulator. *Childs Nerv Syst*. (2021) 37(5):1613–21. doi: 10.1007/s00381-020-04999-4

29. Felisati G, Lenzi R, Pipolo C, Maccari A, Messina F, Revay M, et al. Endoscopic expanded endonasal approach: preliminary experience with the new 3d endoscope. *Acta Otorhinolaryngol Ital*. (2013) 33(2):102–6.

30. Catapano G, de Notaris M, Di Maria D, Fernandez LA, Di Nuzzo G, Seneca V, et al. The use of a three-dimensional endoscope for different skull base tumors: results of a preliminary extended endonasal surgical series. *Acta Neurochir (Wien)*. (2016) 158(8):1605–16. doi: 10.1007/s00701-016-2847-8

31. Kikuchi D, Kaise M, Nomura K, Toba T, Kuribayashi Y, Tanaka M, et al. Feasibility study of the three-dimensional flexible endoscope in endoscopic submucosal dissection: an ex vivo animal study. *Digestion*. (2017) 95(3):237–41. doi: 10.1159/000468924

32. Bickerton R, Ahmed S, Kholief A, Nassimizadeh AK. Breadth and depth: three-dimensional endoscopic field of view: two-dimensional versus three-dimensional endoscopic field of view. *World Neurosurg*. (2019) 127:e717–21. doi: 10.1016/j.wneu.2019.03.247

33. Ogino-Nishimura E, Nakagawa T, Sakamoto T, Ito J. Efficacy of three-dimensional endoscopy in endonasal surgery. *Auris Nasus Larynx*. (2015) 42 (3):203–7. doi: 10.1016/j.anl.2014.10.004

34. Wasserzug O, Margalit N, Weizman N, Fliss DM, Gil Z. Utility of a three-dimensional endoscopic system in skull base surgery. *Skull Base*. (2010) 20 (4):223–8. doi: 10.1055/s-0030-1247630

35. Egi H, Hattori M, Suzuki T, Sawada H, Kurita Y, Ohdan H. The usefulness of 3-dimensional endoscope systems in endoscopic surgery. *Surg Endosc*. (2016) 30(10):4562–8. doi: 10.1007/s00464-016-4793-1

36. Roth J, Singh A, Nyquist G, Fraser JF, Bernardo A, Anand VK, et al. Three-dimensional and 2-dimensional endoscopic exposure of midline cranial base targets using expanded endonasal and transcranial approaches. *Neurosurgery*. (2009) 65 (6):1116–28, discussion 1128–30. doi: 10.1227/01.NEU.0000360340.85186.7A

37. Pennacchietti V, Garzaro M, Grottoli S, Pacca P, Garbossa D, Ducati A, et al. Three-dimensional endoscopic endonasal approach and outcomes in sellar lesions: a single-center experience of 104 cases. *World Neurosurg*. (2016) 89:121–5. doi: 10.1016/j.wneu.2016.01.049

38. Tabaee A, Anand VK, Fraser JF, Brown SM, Singh A, Schwartz TH. Three-dimensional endoscopic pituitary surgery. *Neurosurgery*. (2009) 64(5 Suppl 2):288–93, discussion 294–5. doi: 10.1227/01.NEU.0000338069.51023.3C

39. Hajdari S, Kellner G, Meyer A, Rosahl S, Gerlach R. Endoscopic endonasal surgery for removal of pituitary adenomas: a surgical case series of treatment results using different 2- and 3-dimensional visualization systems. *World Neurosurg*. (2018) 119:e80–6. doi: 10.1016/j.wneu.2018.07.018

40. Barkhoudarian G, Del Carmen Becerra Romero A, Laws ER. Evaluation of the 3-dimensional endoscope in transsphenoidal surgery. *Neurosurgery*. (2013) 73: ons74–ons79. doi: 10.1227/NEU.0b013e31828ba962

frontiers | Frontiers in Surgery

TYPE Clinical Trial
PUBLISHED 23 September 2022
DOI 10.3389/fsurg.2022.1007883

OPEN ACCESS

EDITED BY
Peng Zhao,
Capital Medical University, China

REVIEWED BY
Mendel Castle-Kirszbaum,
Monash University, Australia
Sheng Han,
The First Affiliated Hospital of China Medical University, China

*CORRESPONDENCE
Chiyuan Ma
machiyuan_nju@126.com

†These authors have contributed equally to this work

SPECIALTY SECTION
This article was submitted to Neurosurgery, a section of the journal Frontiers in Surgery

RECEIVED 31 July 2022
ACCEPTED 05 September 2022
PUBLISHED 23 September 2022

CITATION
Zhu J, Wen G, Tang C, Cong Z, Cai X, Yang J and Ma C (2022) One-and-a-half nostril versus binostril endoscopic transsphenoidal approach to the pituitary adenomas: A prospective randomized controlled trial.
Front. Surg. 9:1007883.
doi: 10.3389/fsurg.2022.1007883

One-and-a-half nostril versus binostril endoscopic transsphenoidal approach to the pituitary adenomas: A prospective randomized controlled trial

Junhao Zhu[1†], Guodao Wen[2†], Chao Tang[1], Zixiang Cong[1], Xiangming Cai[3,4], Jin Yang[1] and Chiyuan Ma[1,3*]

[1]Department of Neurosurgery, Affiliated Jinling Hospital, Medical School of Nanjing University, Nanjing, China, [2]Department of Neurosurgery, DongGuan SongShan Lake Tungwah Hospital, Dongguan, China, [3]School of Medicine, Southeast University, Nanjing, China, [4]Department of Molecular Cell Biology and Immunology, Amsterdam UMC, Vrije Universiteit Amsterdam, Amsterdam, Netherlands

Background: Binostril endoscopic transsphenoidal approach (BETA) is the most used approach for sellar lesions nowadays, while its damage to the nasal structures may cause nasal discomfort and affect nasal functions including respiration and olfaction. With the purpose to improve the post-operative sinonasal quality of life (QoL), we introduced the one-and-a-half nostril endoscopic transsphenoidal approach (OETA) in 2016 which preserved more natural structures and registered a prospective randomized controlled trial (ChiCTR-IOR-16008222) to compare the two approaches regarding the surgical outcomes and complications.

Methods: Sixty patients with pituitary adenomas were recruited and randomly assigned to the OETA group and the BETA group between April 2016 and May 2017 in Jinling Hospital. The tumor resection rate, endocrinal and visual outcomes, and surgical complications between the OETA and BETA groups were analyzed. Besides, the questionnaire Anterior Skull Base Nasal Inventory-12 (ASK Nasal-12) was used to evaluate patients' sinonasal QoL at seven time points (pre-operative; 2-weeks, 1-month, 3-months, 6-months, 12-months, and long-term post-operatively). The Sniffin' Sticks were used to assess patients' olfactory function objectively in a long term. Each patient was followed for at least 12 months post-operatively.

Results: There was no significant difference in tumor resection rate, hormonal and visual outcomes, and surgical complications between the two groups. Regarding the ASK Nasal-12, patients in the OETA group complained less about dried nasal material at 2 weeks after surgery ($P = 0.017$). One month after surgery, the OETA group had better olfaction function ($P = 0.019$) compared with the BETA group. However, there was no significant difference in early and long-term postoperative sinonasal QoL between the two approaches according to the entire ASK Nasal-12 metric. The results of the Sniffin' Sticks showed that the two groups had a similar olfactory performance at long-time follow-up.

Conclusion: In this single tertiary center trial, the results showed that the OETA achieved the same surgical outcomes and post-operative sinonasal QoL as the BETA.

Clinical Trial Registration: http://www.chictr.org.cn/showproj.aspx?proj=13852, identifier: ChiCTR-IOR-16008222

KEYWORDS

endoscopic surgery, pituitary adenoma, skull base, quality of life, olfaction

Introduction

Pituitary adenomas (PAs) are the most common sellar lesions and account for approximately 15% of intracranial tumors (1). Its prevalence ranges from 77 to 115 cases per 100,000 individuals and is increasing over the past decades (2, 3). Patients with PAs may have symptoms including decreased visual acuity, visual field defect, headache, and tumor-associated endocrinopathies. Since fully endoscopic approaches to the sellar region were reported in the mid-1990s, the endoscopic endonasal transsphenoidal approach (EETA) has become the mainstay of treatment for PAs requiring surgical intervention (4).

The EETA is mostly operated through both nostrils (binostril endoscopic transsphenoidal approach, BETA), which requires the removal of the posterior nasal septum. Although it provides a wide view of the surgical field, its damage to the nasal structures may result in poor sinonasal quality of life (QoL) and anosmia (5–7). Another more minimally invasive approach, the mononostril technique, was also used in EETA. However, its working space was limited to one nostril (8).

In 2016, we introduced the one-and-a-half nostril endoscopic transsphenoidal approach (OETA) with the expectation of combining the advantages of the binostril and mononostril approaches (9). This approach provided superior exposure and surgical freedom and caused less damage to the nasal septum (10).

In this study, we reported the results of this prospective randomized controlled trial which was conducted to compare OETA with BETA in terms of surgical outcomes and complications.

Methods

Design of the clinical trial

The study was a prospective, randomized and controlled trial. This clinical trial (flowchart shown in **Figure 1**) was approved by the Ethics Committee of Jinling Hospital and registered in 2016 (ChiCTR-IOR-16008222). The study was carried out under the principles of the Declaration of Helsinki, local laws, and regulations. All patients gave informed consent to participate in this trial. Patient recruitment began in April 2016 and finished in May 2017.

The patients were eligible for enrollment if they were diagnosed as PAs by MRI and serum hormone assays, and surgical intervention was considered necessary by multidisciplinary experts. The patients with the following conditions were excluded from this study: (1) patients who have undergone endonasal surgery before; (2) patients with significant septal deviation which narrows the view and compromises the approach from the right side; (3) patients with other intracranial tumors; (4) patients with central nervous system infection or severe systematic infection; (5) patients with a history of chronic obstructive pulmonary disease, coronary heart disease, chronic kidney disease [GFR < 60 ml/(min * 1.73 m^2)] and blood disorders; (6) women in the gestational or lactational period.

The primary outcome was the gross total resection (GTR) rate. The second outcomes include endocrine outcome, visual outcome, surgical complications, sinonasal QoL, and olfactory function. The trial was designed to show the non-inferiority of OETA to BETA regarding the primary outcome with a non-inferiority margin of −0.3. Accounting for a potential dropout rate, 64 patients (32 in each group) are needed to be enrolled, which ensured a power of 80%.

Sixty-four patients were enrolled and randomly (Simple Randomization) assigned to the two groups: the OETA group (OETA, $n = 32$) and the BETA group ($n = 32$). Four patients harboring PAs with significant lateral suprasellar extension that could not be adequately removed transsphenoidally were operated through EETA after randomization followed by craniotomy and excluded from this trial. At last, there were 29 patients in the OETA group and 31 in the BETA group.

The surgical procedures were described in detail in the following section. The patients were asked to return to the hospital for radiologic examinations and hormone level checks at 1, 3, 6, 12 months, and long-term points (more than 16 months) post-operatively for assessment of tumor resection rate and hormonal outcomes.

The criteria for the determination of hormonal remission vary depending on the tumor type. For prolactinoma, the criterion is a normal serum prolactin level. For growth hormone-secreting adenoma, the criteria are a normal value of IGF-1 and a suppression of GH excretion of less than 1.0 ng/ml during an oral glucose tolerance test.

The questionnaire Anterior Skull Base Nasal Inventory-12 [ASK Nasal-12 (11), shown in supplemental **Table 1**] was used to evaluate their sinonasal QoL at 7 time points (preoperative; 2-weeks, 1-month, 3-months, 6-months, 12-

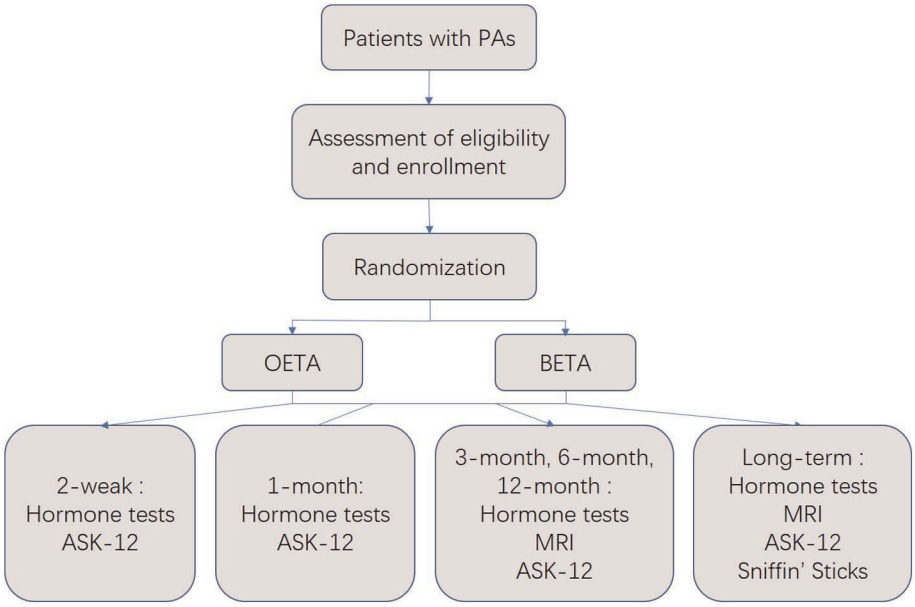

FIGURE 1
Flowchart of the trial. Anterior Skull Base Nasal Inventory-12, ASK Nasal-12; binostril endoscopic transsphenoidal approach, BETA; one-and-a-half nostril endoscopic transsphenoidal approach, OETA; pituitary adenomas, PAs.

TABLE 1 Patient basic characteristics and pre-op symptoms.

	OETA ($n = 29$)	BETA ($n = 31$)	*P* value
Age	49.38 ± 13.98	50.90 ± 10.43	0.633
Male/Female	15/14	16/15	0.993
The course of the disease (month)	29.98 ± 33.64	16.49 ± 31.08	0.112
Duration of follow-up (month)	20.45 ± 4.86	21.03 ± 4.02	0.613
Maximum diameter (cm)	2.37 ± 1.10	2.43 ± 1.10	0.953
Knosp grade, *n* (%)			0.678
0	2 (6.90%)	1 (3.23%)	
1	5 (17.24%)	10 (32.26%)	
2	6 (20.69%)	5 (16.13%)	
3	11 (37.93%)	9 (29.03%)	
4	5 (17.24%)	6 (19.35%)	
Hardy grade, *n* (%)			0.821
0–2, A–B	16 (55.17%)	18 (58.06%)	
3–4, C–E	13 (44.83%)	13 (41.93%)	
Functioning adenoma, *n* (%)	7 (24.14%): 4 GH-secreting adenoma, 3 prolactinoma	4 (12.90%): 2 GH-secreting adenoma, 2 prolactinoma	0.261
Hypopituitarism, *n* (%)	4 (13.79%)	5 (16.13%)	0.800
Visual defect, *n* (%), *n* (%)	8 (27.59%)	12 (38.71%)	0.361
Headache, *n* (%)	14 (48.27%)	11 (35.48%)	0.260

months, and long-term post-operatively). We also used Sniffin' Sticks to assess patients' olfactory function objectively at long-term points. Sniffin' Sticks is an objective test of olfactory performance based on pen-like odor-dispensing devices (12). We did the odor identification test which is composed of sixteen multiple forced choices from a list of four descriptors (13). It has been validated and used in endoscopic skull base surgery to evaluate patients' olfaction (14–16).

The tumor resection rate, hormonal and visual outcomes, and surgical complications were confirmed at the latest follow-up and analyzed between the OETA and BETA groups.

Blinding

The patients were not blinded while the data collection and statistical analysis were blinded for objective assessment.

Surgical procedures

OETA

We performed OETA as we described before (9). Briefly speaking, the patient was under general anesthesia and in a supine position with 10 degrees of extension. The bilateral nasal cavities were packed with cottonoids containing 0.01% epinephrine for vasoconstriction and irrigated with iodine for

disinfection. The operation started from the right nostril under a 0° endoscope (Karl Storz, Tuttlingen, Germany). The right inferior and middle turbinates were out-fractured for access to the sphenoethmoidal recess. Then, the right rescue flap was made with caution to protect the olfactory epithelium (17). The next operation was to dissect the bony nasal septum and expose the sphenoid rostrum. The left nasal septum mucosa was then pushed towards the left cavity to make the left sphenoid ostium visible. The main difference between the BETA and OETA was that the two approaches followed different methods of resecting the posterior nasal septum mucosa (**Figure 2**). For the BETA, a part of bilateral posterior septal mucosa was necessarily resected for bilateral access to the sellar pathology. For the OETA, the left mucosa of the posterior nasal septum was intact. As to the left nasal septal mucosa, only a 2 cm vertical incision was needed at the anterior level of the middle turbinate. The sphenoid ostium was enlarged with a low-speed drill and rongeur. After the enlargement of the sphenoid sinus and removal of the intra-sphenoid septum, the following procedures were the same as the BETA.

BETA

The nasal preparation and creation of the rescue flap were identical to the OETA. Sphenoidotomy was performed on both sides. A posterior septal window was created by removing the posterior part of the bony nasal septum to allow bilateral access. The optic nerve canal and the carotid prominence were identified as landmarks. The sellar floor was then flattened with a drill and opened with the rongeur. After opening the dura with scissors, the tumor was removed with curettes and a suction cannula. The 30°-angled endoscope was introduced into the sella for inspection of tumor remnants. If an intraoperative cerebrospinal fluid (CSF) leak occurred, the rescue flap was then fashioned to ensure a vascularized repair. Gelfoam and Tabotamp fibrillar (Johnson & Johnson Medical GmbH) were routinely used for skull base reconstruction. Nasal packing was not used routinely.

Statistic analysis

The SPASS (IBM SPASS Statistics 26) was used for statistical calculation. Descriptive statistics were used to summarize patients' demographic, clinical, and other outcomes. Continuous variables were assessed for normality and equality of variances between groups. Discrete variables were summarized by frequencies/proportions. For continuous variables, analysis of variance will be used, where appropriate. The comparison of the two groups concerning frequencies/proportions will be performed using the χ^2 test and, if necessary, Fisher's test. The ranked data of the two groups will be compared using the Wilcoxon rank sum test.

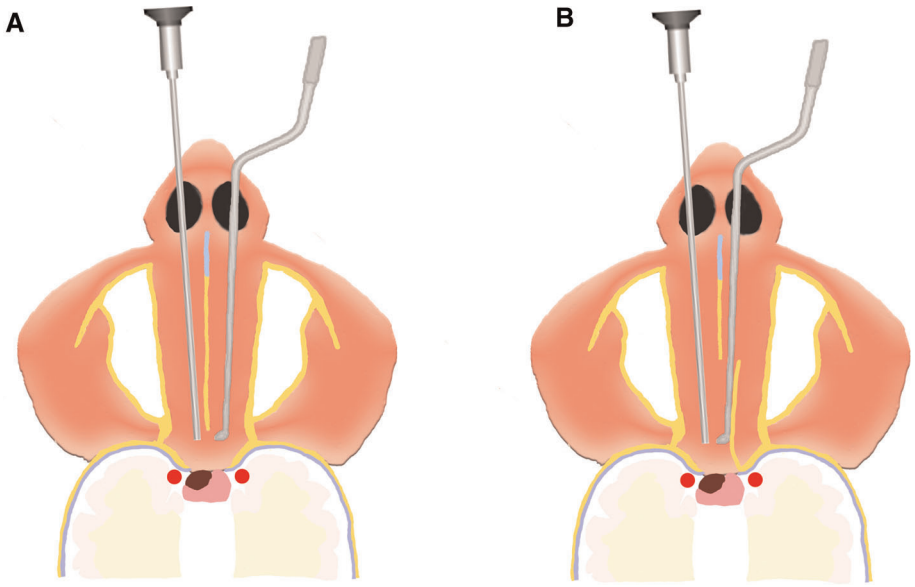

FIGURE 2
The difference between the OETA and BETA. (**A**) For BETA: a part of bilateral posterior septal mucosa was necessarily resected. (**B**) For OETA, the left mucosa of the posterior nasal septum was intact. As to the left nasal septal mucosa, only a 2 cm vertical incision was needed at the anterior level of the middle turbinate.

Results

Patient characteristics

A total of 60 patients were included in the trial (OETA: $n = 29$; BETA: $n = 31$). The average age of the OETA group was 49.38 (range 12–74) and for BETA it was 50.90 (range 20–69). All patients who participated in the trial received at least 12 months of follow-up and 51 of them received a longer observation which lasted for at least 16 months. The mean duration of follow-up was 20.45 months (range 12–31 months) in the OETA group and 21.03 months (range 12–28 months) in the BETA group.

All the PAs in the two groups were macroadenomas (maximum tumor diameter >10 mm), except for 2 microadenomas in the OETA group and 1 microadenoma in the BETA group. The mean maximum diameter was 2.37 cm for the OETA group and 2.43 cm for the BETA group. The invasive PAs (Knosp grade 3 and 4) accounted for 55.17% (16/29) in the OETA group and 48.38% (15/31) in the BETA group.

Concerning the endocrinological symptoms, 7 patients (3 prolactinomas and 4 growth hormone-secreting adenomas) in the OETA group and 4 patients (2 prolactinomas and 2 growth hormone-secreting adenomas) in the BETA group presented a hypersecretion-related syndrome, whereas a single axis defect or multiple axes defect were disclosed in 4 patients in the OETA group and 5 patients in the BETA group.

Preoperative visual examination revealed 8 patients in the OETA group and 12 patients in the BETA group with the visual defect.

The details of the basic characteristics and clinical symptoms of the patients were shown in **Table 1**. No significant difference was found between the two groups in these characteristics.

Tumor removal

The GTR rate was 68.97% (20/29) for the OETA group and 67.74% (21/31) for the BETA group (determined by MRI which focused on the sellar region, including coronal and sagittal views —with native and contrast-enhanced sequences postoperatively).

The GTR was achieved in all PAs with Knosp grade 0–2 in the OETA group and 97.37% (15/16) in the BETA group. In the OETA group, subtotal resection (>70%) was achieved in 9 patients (Knosp grade 3: $n = 4$; Knosp grade 4: $n = 5$). In the BETA group, 9 patients received subtotal resection (Knosp grade 3: $n = 3$; Knosp grade 4: $n = 6$).

No significant difference was found between the two groups regarding the tumor resection rate. The details of the tumor removal results were shown in **Figure 3** and **Supplementary Table S2**.

Post-operative endocrinal outcome

The hormonal remission rate of the functioning adenomas in the OETA group was 57.14% (4/7) and 75.00% (3/4) in the BETA group.

In the OETA group, of the 4 patients presenting pre-operative hypopituitarism, 3 patients improved while one patient remained unchanged. One patient developed new-onset hypocortisolism and two patients developed new-onset hypothyroidism post-operatively.

In the BETA group, of 5 patients presenting pre-operative hypopituitarism, 2 patients improved while 3 patients remained unchanged. One patient developed new-onset hypocortisolism and two patients developed new-onset hypothyroidism post-operatively.

No significant difference was found between the two groups regarding the endocrinal outcomes. The details of the

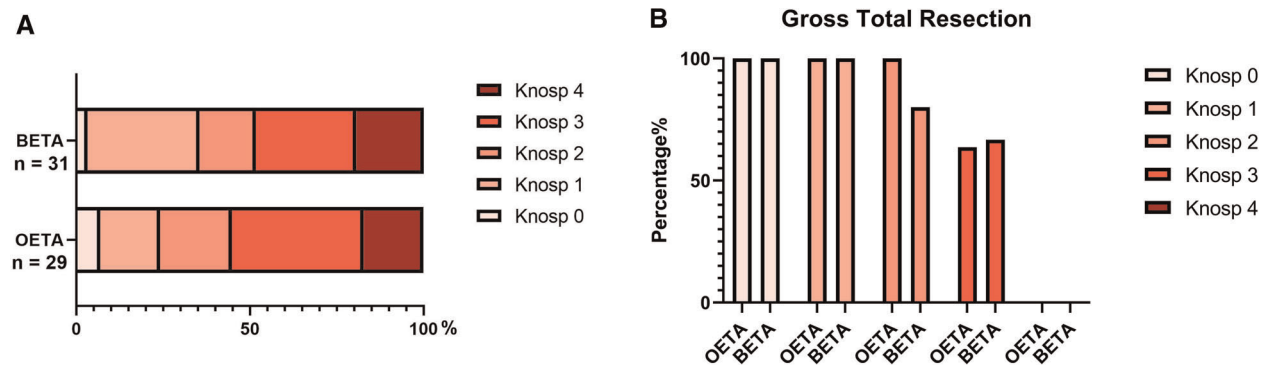

FIGURE 3
The tumor removal of the patients. (**A**) The constituent of patients with different Knosp grades in the two groups. (**B**) The gross total resection rate of tumors with different Konsp scores. binostril endoscopic transsphenoidal approach, BETA; one-and-a-half nostril endoscopic transsphenoidal approach, OETA.

TABLE 2 Post-op endocrinal outcomes.

		OETA	BETA
Hormone remission, *n*/*N* = Functioning adenoma		4/7 (57.14%)	3/4 (75.00%)
Patient with pre-op hypopituitarism, *n*/*N* = pre-op hypopituitarism	Improved	3/4 (75.00%)	2/5 (40.00%)
	Unchanged	1/4 (25.00%)	3/5 (60.00%)
New onset hypopituitarism, *n*	Hypocortisolism	1	1
	Hypothyroidism	2	2

endocrinal outcome were shown in Table 2 and Supplementary Table S2.

Post-operative visual outcome

Visual defect improved in 5 cases (5/8, 62.50%) in the OETA group and 7 cases (7/12, 58.33%) in the BETA group. None of the patients of both groups with a normal preoperative visual assessment experienced any postoperative worsening.

No significant difference was found between the two groups regarding the visual outcomes. The details of the visual outcome were shown in Table 3 and Supplementary Table S2.

Surgical complications

The most common surgical complication was temporary diabetes insipidus in this series, which occurred in 6 patients in OETA and 5 patients in BETA. All these patients with temporary diabetes insipidus recovered after three months. Concerning the postoperative CSF leakage, the number was 2 in OETA and 3 in BETA. Of the 5 patients, intracranial infection (2 in OETA and 2 in BETA) occurred in 4 of them. After antibiotic treatment and lumbar drainage, all of them recovered with no sequela. Two patients reported in BETA while none occurred in OETA.

No carotid injury or cranial nerve injury was observed. There was no death related to the procedure.

No significant difference was found between the two groups regarding the surgical complication. The details of the surgical complication were shown in Table 4 and Supplementary Table S2.

TABLE 3 Post-op visual outcomes.

		OETA	BETA
Patient with pre-op visual defect, *n*/*N* = pre-op visual defect	Improved	5/8 (62.50%)	7/12 (58.33%)
	Unchanged	3/8 (37.50%)	5/12 (41.67%)
	Worsened	0/8 (0%)	0/12 (0%)
Patient with normal pre-op visual function, *n*/*N* = normal pre-op visual function	Unchanged	21/21 (100%)	19/19 (100%)
	Worsened	0/21 (0%)	0/21 (0%)

TABLE 4 Postoperative complication.

Postoperative complication, *n*	OETA (*n* = 29)	BETA (*n* = 31)
Carotid injury	0 (0%)	0 (0%)
CSF leakage	2 (6.90%)	3 (9.68%)
Intracranial infection	2 (6.90%)	2 (6.45%)
Cranial nerve injury	0 (0%)	0 (0%)
Temporary diabetes insipidus	6 (20.69%)	5 (16.13%)
Nasal bleeding	0 (0%)	2 (6.45%)

Sinonasal quality of life

We compared the results of ASK Nasal-12 between the OETA group and the BETA group pre-operatively and post-operatively. The results were shown in Table 5. We found that patients in the OETA group complained less about dried nasal material at the 2-week point ($P = 0.017$) and reported better olfactory function at the 1-month point ($P = 0.019$) compared with the BETA group. However, there was no significant difference in early and long-term post-operative sinonasal QoL between the two approaches according to the entire ASK Nasal-12 metric.

Olfactory outcomes

The mean score of the Sniffin' Sticks odor identification test was 11.58 ± 1.69 in the OETA group and 11.70 ± 1.20 in the BETA group. There was no significant difference between the two groups (Figure 4).

Discussion

The endonasal transsphenoidal approach was developed in the 1910s under the leadership of Oskar Hirsch, who never stopped advocating for this approach in the pre-antibiotic era (18). However, with the drawbacks of poor illumination and limited visualization, it was not until the introduction of the microscope in the 1960s that the microscopic transsphenoidal approach regained widespread favor (19). In the mid-1990s, a fully endoscopic endonasal transsphenoidal approach was reported and underwent dramatic evolution in the last two decades (20). Compared with microscopic surgery, endoscopic surgery provides a wider visual field and better illumination for sellar regions (21).

Some neurosurgeons are used to reach the sphenoid sinus through one nostril (the mononostril approach) with the help of a nasal speculum (21). However, the speculum restricts the bimanual handling of instruments (22). Another surgical technique, the binostril approach, typically does not require a

TABLE 5 Comparison of ASK nasal-12 between OETA and BETA.

	preoperative	2-week postoperative	1-month postoperative	3-month postoperative	6-month postoperative	12-month postoperative	Long term postoperative
Sense of smell	0.45 ± 0.99 0.55 ± 1.06	3.10 ± 0.31 3.10 ± 0.30	2.55 ± 0.78* 2.97 ± 0.48*	0.34 ± 1.05 0.39 ± 1.20	0.31 ± 0.93 0.32 ± 1.01	0.31 ± 0.93 0.26 ± 0.82	0.25 ± 0.74 0.30 ± 0.67
Sense of taste	0.24 ± 0.83 0.45 ± 0.85	1.14 ± 0.58 1.06 ± 0.36	1.07 ± 0.59 1.00 ± 0.00	0.14 ± 0.74 0.00 ± 0.00	0.10 ± 0.56 0.00 ± 0.00	0.10 ± 0.56 0.00 ± 0.00	0.13 ± 0.61 0.00 ± 0.00
Urge to blow nose	0.55 ± 1.15 0.48 ± 0.89	1.10 ± 0.41 1.00 ± 0.00	1.03 ± 0.19 0.97 ± 0.18	0.00 ± 0.00 0.00 ± 0.00	0.00 ± 0.00 0.00 ± 0.00	0.00 ± 0.00 0.00 ± 0.00	0.08 ± 0.28 0.07 ± 0.27
Postnasal discharge	0.21 ± 0.56 0.35 ± 0.76	1.48 ± 0.95 1.23 ± 0.72	0.39 ± 0.79 0.19 ± 0.60	0.00 ± 0.00 0.00 ± 0.00	0.00 ± 0.00 0.00 ± 0.00	0.00 ± 0.00 0.00 ± 0.00	0.00 ± 0.00 0.07 ± 0.27
Thick nasal discharge	0.21 ± 0.49 0.26 ± 0.68	1.10 ± 0.49 1.13 ± 0.43	0.10 ± 0.31 0.00 ± 0.00	0.00 ± 0.00 0.00 ± 0.00	0.00 ± 0.00 0.00 ± **0**.00	0.00 ± 0.00 0.00 ± **0**.00	0.00 ± 0.00 0.11 ± **0**.42
Headache	1.17 ± 1.63 1.03 ± 1.40	1.31 ± 0.89 1.13 ± 0.67	0.41 ± 1.09 0.16 ± 0.58	0.21 ± 0.77 0.16 ± 0.58	0.17 ± 0.66 0.10 ± 0.40	0.34 ± 0.61 0.13 ± 0.43	0.33 ± 0.48 0.30 ± 0.72
Nose whistling	0.55 ± 1.24 0.58 ± 0.89	3.21 ± 0.49 3.03 ± 0.18	0.24 ± 0.91 0.10 ± 0.54	0.10 ± 0.56 0.03 ± 0.18	0.03 ± 0.19 0.03 ± 0.18	0.07 ± 0.26 0.03 ± 0.18	0.04 ± 0.20 0.00 ± 0.00
Dried nasal material	0.00 ± 0.00 0.00 ± 0.00	1.69 ± 1.31* 2.48 ± 0.77*	0.76 ± 0.91 0.84 ± 0.93	0.00 ± 0.00 0.00 ± 0.00	0.00 ± 0.00 0.00 ± 0.00	0.00 ± 0.00 0.03 ± 0.18	0.08 ± 0.28 0.00 ± 0.00
Trouble breathing: day	0.31 ± 0.71 0.52 ± 0.93	3.03 ± 0.19 3.06 ± 0.25	1.31 ± 0.60 1.16 ± 0.64	0.28 ± 0.65 0.06 ± 0.25	0.10 ± 0.56 0.10 ± 0.40	0.10 ± 0.41 0.13 ± 0.43	0.08 ± 0.41 0.15 ± 0.36
Trouble breathing: night	0.59 ± 1.15 0.87 ± 1.18	3.10 ± 0.31 3.06 ± 0.25	0.48 ± 1.24 0.19 ± 0.79	0.31 ± 0.81 0.06 ± 0.25	0.34 ± 0.94 0.06 ± 0.25	0.34 ± 0.86 0.03 ± 0.18	0.21 ± 0.59 0.04 ± 0.19
Trouble breathing	0.34 ± 0.94 0.35 ± 0.71	3.00 ± 0.00 3.03 ± 0.18	0.17 ± 0.60 0.16 ± 0.64	0.00 ± 0.00 0.10 ± 0.54	0.00 ± 0.00 0.10 ± 0.54	0.00 ± 0.00 0.13 ± 0.56	0.00 ± 0.00 0.00 ± 0.00

The upper line of the cell represents OETA and the lower line represents BETA.
*$P < 0.05$.

nasal speculum and offers better maneuverability of instruments than the mononostril approach (21). In our meta-analysis comparing the mononostril approach and binostril approach for PAs, the binostril approach had a shorter length of hospital stay and fewer surgical complications (diabetes insipidus and hypopituitarism) than the mononostril approach while patients undergone the binostril approach tended to have a higher rate of epistaxis than the mononostril group (23).

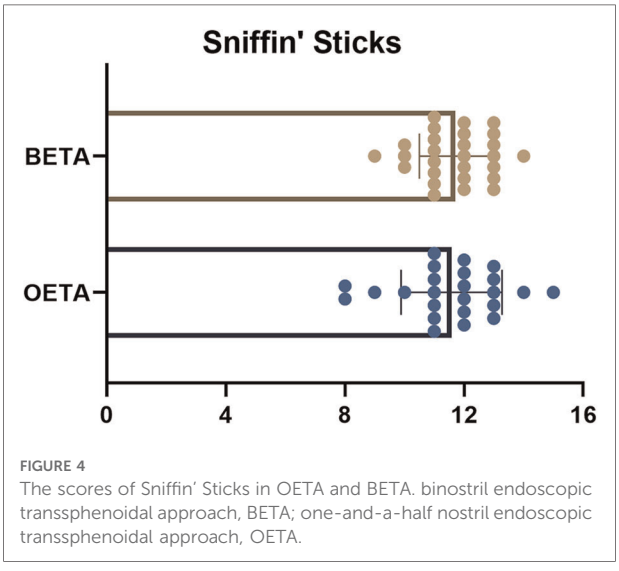

FIGURE 4
The scores of Sniffin' Sticks in OETA and BETA. binostril endoscopic transsphenoidal approach, BETA; one-and-a-half nostril endoscopic transsphenoidal approach, OETA.

With the use of the nasal flap for skull base reconstruction (24), the most common complication of EETA, the CSF leakage, has been controlled at a low rate. However, harvesting of this vascularized flap involves cutting the mucosa and is associated with an increased risk of postoperative nasal crusting, raising concern about worsening postoperative sinonasal quality of life (25). Among the nasal symptoms, the loss of olfaction was a major concern for surgeons and patients. In our previous review, the incidence of postoperative decreased olfactory function was 18.48% for the patients after endonasal skull base surgery (7). More attention should be paid to patients' sinonasal QoL and olfaction.

To improve patients' post-operative sinonasal QoL, we introduced OETA in 2016 (9). This technique provides not only a sufficient surgical corridor for a 2-surgeon/4-hands operation but also ensures minimal invasion to the nasal cavity, which combines the advantages of the binostril approach and the mononostril approach. In the technical report, we describe the procedures of OETA in detail and analyzed the clinical outcomes of 57 consecutive patients who underwent OETA between March 2014 and June 2015 at Jinling hospital (9). The GTR rate was 79% (9) for all the PAs. Post-operative hormone remission was achieved in 77.8% (14/18) of patients with

functioning Pas (9). Concerning the sinonasal QoL, the most frequent complaint at the 2-week point was thick nasal discharge (36%), followed by loss of smell (28%) and trouble breathing during the day (18%) (9). Other symptoms, including post nasal discharge (8%), dried nasal material (6%), headache (6%), and decrease in sense of taste (4%) were also reported (9). Three months after surgery, most of the symptoms disappeared or were significantly relieved (9). The above results showed that the OETA was a simple and reliable technique.

We also compared surgical freedom and working angles between OETA and BETA in cadaveric dissection (10). The results showed that the OETA had similar surgical freedom and working angles to the BETA for most anatomic targets in the sellar or parasellar region.

A prospective randomized controlled trial was then registered to provide high-quality evidence for this approach. After two years of enrollment and several years of follow-up, the results confirmed that the two approaches had similar GTR rates (OETA: 68.97%; BETA: 67.74%). As to the invasive PAs, the GTR rates were also similar between the two groups (OETA: 43.75%; BETA: 40.00%).

Three patients with prolactinomas (2 in OETA and 1 in BETA) did not reach hormone remission after surgery, with 2 Knosp grade 4 PAs and 1 Knosp grade 3 PA. Dopamine receptor agonist therapy was taken for them to control the serum prolactin level. With regards to the 6 patients with acromegaly, we luckily achieved GTR in all of them and the patients reached hormone remission post-operatively, probably because there was no Knosp grade 4 PA in these 6 patients. New-onset Hypopituitarism occurred in 6 patients (OETA: $n = 3$; BETA: $n = 3$) and they were transferred to endocrinologists for hormone replacement therapy.

There was also no significant difference regarding the surgical complications between OETA and BETA. Eleven patients (OETA: $n = 6$; BETA: $n = 5$) suffered from temporary diabetes insipidus post-operatively and all recovered three months after surgery. The most worrisome complication, postoperative CSF leakage, occurred in five patients (OETA: $n = 2$; BETA: $n = 3$) and consequent intracranial infection occurred in four of them (OETA: $n = 2$; BETA: $n = 2$). After antibiotic treatment and lumbar drainage, all of them recovered with no sequela. It's also worth noting that two patients reported epistaxis in BETA while none reported in OETA. No carotid injury or cranial nerve injury was observed in these patients.

As for the sinonasal quality of life, the patients in the two groups had the same recovery course. Although OETA seemed to have potential benefits in two components of ASK Nasal-12 at early postoperative time points (dried nasal material at the 2-week point, $P = 0.017$; olfaction at the 1-month point, $P = 0.019$), there was no significant difference in early and long-term post-operative sinonasal QoL between the two approaches according to the entire ASK Nasal-12 metric.

Many factors may affect sinonasal outcomes after endoscopic endonasal surgery, including the intraoperative protection of nasal mucosa, harvesting nasoseptal flaps, nasal packing, and postoperative nasal care. The harvest of the nasoseptal flap is an important factor that is associated with worse sinonasal QoL within the early postoperative period (26). In our series, 9 patients received nasoseptal flaps in skull base reconstruction (4 in OETA and 5 in BETA).

More preservation of the nasal natural structures is a feasible way to improve the sinonasal QoL. Several groups have reported alternative closure of the skull base to the nasoseptal flap with the local sphenoidal mucosa or the sellar floor flap (27, 28), which could help improve sinonasal outcomes.

The reason why this trial failed to find a difference between the two approaches in sinonasal outcomes may lie in the small numbers of the trial and the relatively small difference between the two approaches.

We assessed patients' olfactory performance objectively with the Sniffin' Sticks. Both two groups had satisfactory results from objective olfactory examinations (OETA: 11.58 ± 1.69; BETA: 11.70 ± 1.20). 54.17% (13/24) of patients in OETA had a great olfactory assessment score (>11) and the rate in BETA was 55.56% (15/27).

Conclusion

In this single tertiary center trial, the results proved that the OETA achieved the same surgical outcomes and post-operative sinonasal QoL as the BETAL.

Data availability statement

The original contributions presented in the study are included in the article/**Supplementary Material**, further inquiries can be directed to the corresponding author/s.

Ethics statement

The studies involving human participants were reviewed and approved by the Ethics Committee of Jinling Hospital. The patients/participants provided their written informed consent to participate in this study.

Author contributions

ZJ and MC designed the protocol. CX and ZJ were responsible for data management and statistical analyses. CZ, YJ, and CX were responsible for data collection and quality control. ZJ and WG drafted the manuscript. MC and TC were responsible for revising and finalizing this paper. All authors contributed to the article and approved the submitted version.

Conflict of interest

The authors declare that the research was conducted in the absence of any commercial or financial relationships that could be construed as a potential conflict of interest.

Publisher's note

All claims expressed in this article are solely those of the authors and do not necessarily represent those of their affiliated organizations, or those of the publisher, the editors and the reviewers. Any product that may be evaluated in this article, or claim that may be made by its manufacturer, is not guaranteed or endorsed by the publisher.

Supplementary material

The Supplementary Material for this article can be found online at: https://www.frontiersin.org/articles/10.3389/fsurg.2022.1007883/full#supplementary-material.

References

1. Melmed S. Pituitary-tumor endocrinopathies. *N Engl J Med*. (2020) 382 (10):937–50. doi: 10.1056/NEJMra1810772

2. Fernandez A, Karavitaki N, Wass JA. Prevalence of pituitary adenomas: a community-based, cross-sectional study in banbury (Oxfordshire, UK). *Clin Endocrinol*. (2010) 72(3):377–82. doi: 10.1111/j.1365-2265.2009.03667.x

3. Agustsson TT, Baldvinsdottir T, Jonasson JG, Olafsdottir E, Steinthorsdottir V, Sigurdsson G, et al. The epidemiology of pituitary adenomas in Iceland, 1955–2012: a nationwide population-based study. *Eur J Endocrinol*. (2015) 173 (5):655–64. doi: 10.1530/EJE-15-0189

4. Agam MS, Wedemeyer MA, Wrobel B, Weiss MH, Carmichael JD, Zada G. Complications associated with microscopic and endoscopic transsphenoidal pituitary surgery: experience of 1153 consecutive cases treated at a single tertiary care pituitary center. *J Neurosurg*. (2018) 130(5):1576–83. doi: 10.3171/2017.12.JNS172318

5. Molteni G, Sacchetto A, Saccardo T, Gulino A, Marchioni D. Quality of life evaluation after trans-nasal endoscopic surgery for skull base tumors. *Am J Rhinol Allergy*. (2021) 35(4):507–15. doi: 10.1177/1945892420972045

6. Pledger CL, Elzoghby MA, Oldfield EH, Payne SC, Jane Jr JA. Prospective comparison of sinonasal outcomes after microscopic sublabial or endoscopic endonasal transsphenoidal surgery for nonfunctioning pituitary adenomas. *J Neurosurg*. (2016) 125(2):323–33. doi: 10.3171/2015.6.JNS142695

7. Zhu J, Feng K, Tang C, Yang J, Cai X, Zhong C, et al. Olfactory outcomes after endonasal skull base surgery: a systematic review. *Neurosurg Rev*. (2020) 44 (4):1805–14. doi: 10.1007/s10143-020-01385-1

8. Linsler S, Gaab MR, Oertel J. Endoscopic endonasal transsphenoidal approach to sellar lesions: a detailed account of our mononostril technique. *J Neurol Surg B Skull Base*. (2013) 74(3):146–54. doi: 10.1055/s-0033-1338258

9. Wen G, Tang C, Zhong C, Li J, Cong Z, Zhou Y, et al. One-and-a-half nostril endoscopic transsphenoidal approach for pituitary adenomas-a technical report. *J Otolaryngol Head Neck Surg*. (2016) 45(1):60. doi: 10.1186/s40463-016-0174-y

10. Yang J, Wen G, Tang C, Zhong C, Zhu J, Cong Z, et al. Evaluation of surgical freedom for one-and-a-half nostril, mononostril, and binostril endoscopic endonasal transsphenoidal approaches. *J Neurol Surg B Skull Base*. (2021) 82 (04):383–91. doi: 10.1055/s-0040-1701526

11. Little AS, Kelly D, Milligan J, Griffiths C, Rosseau G, Prevedello DM, et al. Prospective validation of a patient-reported nasal quality-of-life tool for endonasal skull base surgery: the anterior skull base nasal inventory-12. *J Neurosurg*. (2013) 119(4):1068–74. doi: 10.3171/2013.3.JNS122032

12. Kobal G, Hummel T, Sekinger B, Barz S, Roscher S, Wolf S. "Sniffin' sticks": screening of olfactory performance. *Rhinology*. (1996) 34(4):222–6. doi: https://www.rhinologyjournal.com/Abstract.php?id=283

13. Hummel T, Sekinger B, Wolf SR, Pauli E, Kobal G. 'Sniffin' sticks': olfactory performance assessed by the combined testing of odor identification, odor discrimination and olfactory threshold. *Chem Senses*. (1997) 22(1):39–52. doi: 10.1093/chemse/22.1.39

14. Netuka D, Masopust V, Fundova P, Astl J, Skoloudik D, Majovsky M, et al. Olfactory results of endoscopic endonasal surgery for pituitary adenoma: a prospective study of 143 patients. *World Neurosurg*. (2019) 129:e907–14. doi: 10.1016/j.wneu.2019.05.061

15. Gong SW, Ahmadi S, Blackburn SL, Ulin L, Citardi MJ, Luong A, et al. Sniffin' sticks to measure olfactory function and recovery following bilateral superior turbinate resection as part of endoscopic transsphenoidal approach. *Ann Otol Rhinol Laryngol*. (2021) 130(6):636–42. doi: 10.1177/0003489420965621

16. Cingoz ID, Kizmazoglu C, Guvenc G, Sayin M, Imre A, Yuceer N. Evaluation of the olfactory function with the "sniffin' sticks" test after endoscopic transsphenoidal pituitary surgery. *J Craniofac Surg*. (2018) 29 (4):1002–5. doi: 10.1097/SCS.0000000000004398

17. Rivera-Serrano CM, Snyderman CH, Gardner P, Prevedello D, Wheless S, Kassam AB, et al. Nasoseptal "rescue" flap: a novel modification of the nasoseptal flap technique for pituitary surgery. *Laryngoscope*. (2011) 121 (5):990–3. doi: 10.1002/lary.21419

18. Liu JK, Cohen-Gadol AA, Laws Jr. ER, Cole CD, Kan P, Couldwell WT. Harvey cushing and oskar hirsch: early forefathers of modern transsphenoidal surgery. *J Neurosurg*. (2005) 103(6):1096–104. doi: 10.3171/jns.2005.103.6.1096

19. Hardy J. Excision of pituitary adenomas by trans-sphenoidal approach. *Union Med Can*. (1962) 91:933–45. doi: http://europepmc.org/article/MED/13952789

20. van Furth WR, de Vries F, Lobatto DJ, Kleijwegt MC, Schutte PJ, Pereira AM, et al. Endoscopic surgery for pituitary tumors. *Endocrinol Metab Clin North Am*. (2020) 49(3):487–503. doi: 10.1016/j.ecl.2020.05.011

21. Conrad J, Ayyad A, Wuster C, Omran W, Weber MM, Konerding MA, et al. Binostril versus mononostril approaches in endoscopic transsphenoidal pituitary surgery: clinical evaluation and cadaver study. *J Neurosurg*. (2016) 125 (2):334–45. doi: 10.3171/2015.6.JNS142637

22. Oertel J, Gaab MR, Tschan CA, Linsler S. Mononostril endoscopic transsphenoidal approach to sellar and peri-sellar lesions: personal experience and literature review. *Br J Neurosurg*. (2015) 29(4):532–7. doi: 10.3109/02688697.2015.1014997

23. Wen G, Tang C, Zhong C, Li X, Li J, Li L, et al. Mononostril versus binostril endoscopic transsphenoidal approach for pituitary adenomas: a systematic review and meta-analysis. *PLoS One*. (2016) 11(4):e0153397. doi: 10.1371/journal.pone.0153397

24. Hadad G, Bassagasteguy L, Carrau RL, Mataza JC, Kassam A, Snyderman CH, et al. A novel reconstructive technique after endoscopic expanded endonasal approaches: vascular pedicle nasoseptal flap. *Laryngoscope*. (2006) 116(10):1882–6. doi: 10.1097/01.mlg.0000234933.37779.e4

25. Kim BY, Son HL, Kang SG, Kim SW, Hong YK, Jeun SS, et al. Postoperative nasal symptoms associated with an endoscopic endonasal transsphenoidal approach. *Eur Arch Otorhinolaryngol*. (2013) 270(4):1355–9. doi: 10.1007/s00405-012-2226-x

26. Castle-Kirszbaum M, Wang YY, King J, Uren B, Dixon B, Zhao YC, et al. Patient wellbeing and quality of life after nasoseptal flap closure for endoscopic skull base reconstruction. *J Clin Neurosci*. (2020) 74:87–92. doi: 10.1016/j.jocn.2020.01.072

27. Cong Z, Liu K, Wen G, Qiao L, Wang H, Ma C. Universal sellar anatomical reconstruction using the sellar floor flap after endoscopic pituitary adenoma surgery. *Otolaryngol Head Neck Surg*. (2018) 158(4):774–6. doi: 10.1177/0194599818756861

28. Castle-Kirszbaum M, Wang YY, Uren B, Dixon B, Rimmer J, King J, et al. Closure of skull base defects after endoscopic endonasal transsphenoidal surgery: the role of the local sphenoid mucosal flap for low flow leaks. *Neurosurg Rev*. (2022) 45(1):429–37. doi: 10.1007/s10143-021-01547-9

frontiers | Frontiers in Surgery

TYPE Original Research
PUBLISHED 23 September 2022
DOI 10.3389/fsurg.2022.1011845

OPEN ACCESS

EDITED BY
Luigi Maria Cavallo,
Università di Napoli Federico II, Italy

REVIEWED BY
Zongmao Zhao,
Second Hospital of Hebei Medical University, China
Fuxing Zuo,
National Cancer Center, Chinese Academy of Medical Sciences, China

*CORRESPONDENCE
Liang Wang
saintage7@126.com
Zhen Wu
wuzhen1966@aliyun.com

SPECIALTY SECTION
This article was submitted to Neurosurgery, a section of the journal Frontiers in Surgery

RECEIVED 04 August 2022
ACCEPTED 31 August 2022
PUBLISHED 23 September 2022

CITATION
Tian K, Ma J, Wang K, Li D, Zhang J, Wang L and Wu Z (2022) PTEN is recognized as a prognostic-related biomarker and inhibits proliferation and invasiveness of skull base chordoma cells.
Front. Surg. 9:1011845.
doi: 10.3389/fsurg.2022.1011845

PTEN is recognized as a prognostic-related biomarker and inhibits proliferation and invasiveness of skull base chordoma cells

Kaibing Tian, Junpeng Ma, Ke Wang, Da Li, Junting Zhang, Liang Wang* and Zhen Wu*

Department of Neurosurgery, Beijing Tiantan Hospital, Capital Medical University, Beijing, China

Objective: This work aimed to examine the function of phosphatase and tensin homologue deleted on chromosome 10 (PTEN) in skull base chordoma (SBC) at the clinical and cellular levels.

Methods: Totally 65 paraffin-embedded and 86 frozen specimens from 96 patients administered surgery were analyzed. Immunohistochemical staining and quantitative real-time polymerase chain reaction were performed, and the associations of PTEN expression with clinical features were assessed. At the cellular level, PTEN was knocked down by the siRNA approach in the UCH-1 cell line, and cell proliferation and invasion were detected by the CCK-8 and migration assays, respectively.

Results: At the protein level, PTEN expression was increased in non-bone-invasive tumor samples in comparison with bone-invasive specimens ($p = 0.025$), and elevated in soft SBCs in comparison with hard tumors ($p = 0.017$). Increased PTEN protein expression was associated with decreased risk of tumor progression ($p = 0.002$; hazard ratio = 0.981, 95% confidence interval: 0.969–0.993). At the gene expression level, the cut-off value was set at 10.5 after ROC curve analysis, and SBC specimens were divided into two groups: PTEN high group, ΔCt value below 10.5; PTEN low group, ΔCt value above 10.5. In multivariate regression analysis of PFS, the risk of tumor progression was increased in PTEN low group tumors in comparison with PTEN high group SBCs ($p = 0.006$). In the CCK-8 assay, in comparison with control cells, PTEN knockdown cells had increased absorbance, suggesting elevated cell proliferation rate. In the invasion assay, the number of tumor cells penetrating into the lower chamber was significantly increased in the PTEN knockdown group compared with control cells.

Conclusions: Decreased PTEN expression in SBC, at the protein and gene levels, is associated with reduced PFS. PTEN knockdown in chordoma cells led to enhanced proliferation and invasiveness.

Abbreviations

SBC, skull base chordoma; PTEN, phosphatase and tensin homologue deleted on chromosome 10; KPS, Karnofsky Performance Status; qRT-PCR, quantitative real-time polymerase chain reaction; ROC, Receiver operating characteristic; K-M, Kaplan-Meier; OS, overall survival; PFS, progression-free survival; PI3K, phosphatidylinositol 3-kinase; mTOR, the mammalian target of rapamycin; Akt, protein kinase B.

KEYWORDS
Pten, skull base, chordoma, progression, invasion, p-AKT, p-mTOR

Introduction

Chordoma represents a low-grade malignancy originating from notochord remnants (1, 2) that mostly occurs in the sacrococcygeal (29.2%) and skull base regions (32%–42%) (1, 3, 4). This malignant disease affects 0.08–0.089/100,000 individuals, with a male predominance (morbidity rates of 0.1–0.16/100,000 and 0.06–0.066/100,000 in men and women, respectively) (4). Chordoma tumors can affect neighboring soft tissues and destroy surrounding bones. Skull base chordoma (SBC) is generally near critical blood vessels, cranial nerves and other major structures, and SBC patients often exhibit symptoms of cranial nerve dysfunction, including headache, paralysis, diplopia, decreased visual acuity, visual field defect, dysphagia, facial paralysis and numbness. Entire resection of cranial chordoma is hard to achieve and may result in serious complications, while chemotherapy generally has low efficacy. Currently applied treatments comprise radical resection and postsurgical radiation therapy, resulting in median patient survival in SBC of 151 months (5, 6). Postsurgical tumor progression represents an important challenge faced by patients as well as neurosurgeons. In recent years, despite revolutionizing advances in SBC treatment, the disease remains poorly understood at the molecular level (3, 7, 8).

Previously, brachyury and additional biomarkers were detected in chordoma (9, 10); however, molecular markers related to tumor features are rare. Phosphatase and tensin homologue deleted on chromosome 10 (PTEN) represents an important tumor suppressor protein that is poorly expressed in many malignant tumors (11–13). We recently demonstrated PTEN is involved in tumor invasion (14). The present study aims to further examine the function of PTEN in SBC at the clinical and cellular levels.

Materials and methods

Overview

Tumor specimens were obtained from SBC cases surgically treated between January 2008 and November 2015, and diagnosed as chordoma. Cases with paraffin-embedded samples assessable by immunohistochemistry or frozen samples usable for mRNA extraction were included. Exclusion criteria were: clinical data unavailability; other tumors or genetic disorders; other serious diseases that could affect prognosis. This study conformed to the Committee on Publication Ethics (COPE) and the International Committee of Medical Journal Editors (ICMJE) recommendations for ethics and had approval from Beijing Tiantan Hospital's ethics committee. Each patient provided signed informed consent. Data collection and analysis were performed in a blinded fashion.

Clinical data

Demographic data and treatment history, including postsurgical radiation therapy, were obtained from medical records. Presurgical Karnofsky Performance Status (KPS) scores, surgical methods, blood supply and tumor texture were retrieved from the surgical records. Tumor blood supply was either abundant or poor, based on which the cases were categorized. Tumor texture was recorded as soft or hard (tumors with both soft and hard constituents were considered hard tumors). Follow-up was mostly performed on an outpatient basis, and phone calls were utilized for those unable to visit the hospital. Tumor progression was considered for recurrence or regrowth of the residual tumor.

Histological analysis was performed by 2 or more pathologists with >10 years of experience in chordoma assessment. The tumors were grouped into conventional, chondroid, poorly differentiated and dedifferentiated types, as proposed by the International Agency for Research on Cancer (15). No poorly differentiated and dedifferentiated tumors were detected in the present analysis, which only comprised conventional (**Figure 1A**) and chondroid (**Figure 1B**) tumors.

Magnetic resonance (MR) imaging scans were assessed by two experienced radiologists with the Picture Archiving and Communication System. Tumor diameter was measured separately in three mutually perpendicular dimensions, with the greatest value considered the "diameter". Invasiveness was considered for bone (**Figures 1C,D**) or non-bone (**Figures 1E, F**) invasive tumors. SBC stages were defined based on the presence of dura erosion. Tumor lobulation was reflected by unevenly lobulated borders, and the lobulation condition was recorded as with or without lobulation. The extent of resection was determined by postoperative MR imaging findings. Resection was classified as follows: (1) gross total resection, total resection of the visible tumor, with the affected bone ground for normal bone tissue exposure, and no tumor detected by postoperative MR imaging; (2) near total resection, total resection of any visible tumor with >90% of the tumor removed based on postsurgical MR imaging; (3) subtotal resection, 70%–90% of the tumor removed based on postsurgical MR imaging; (4) a partial resection and biopsy, <70% of the tumor removed. For simplification, the gross total resection and near total resection groups were considered aggressive resection (>90%), while subtotal resection, partial resection and biopsy were combined as non-aggressive resection (≤90%).

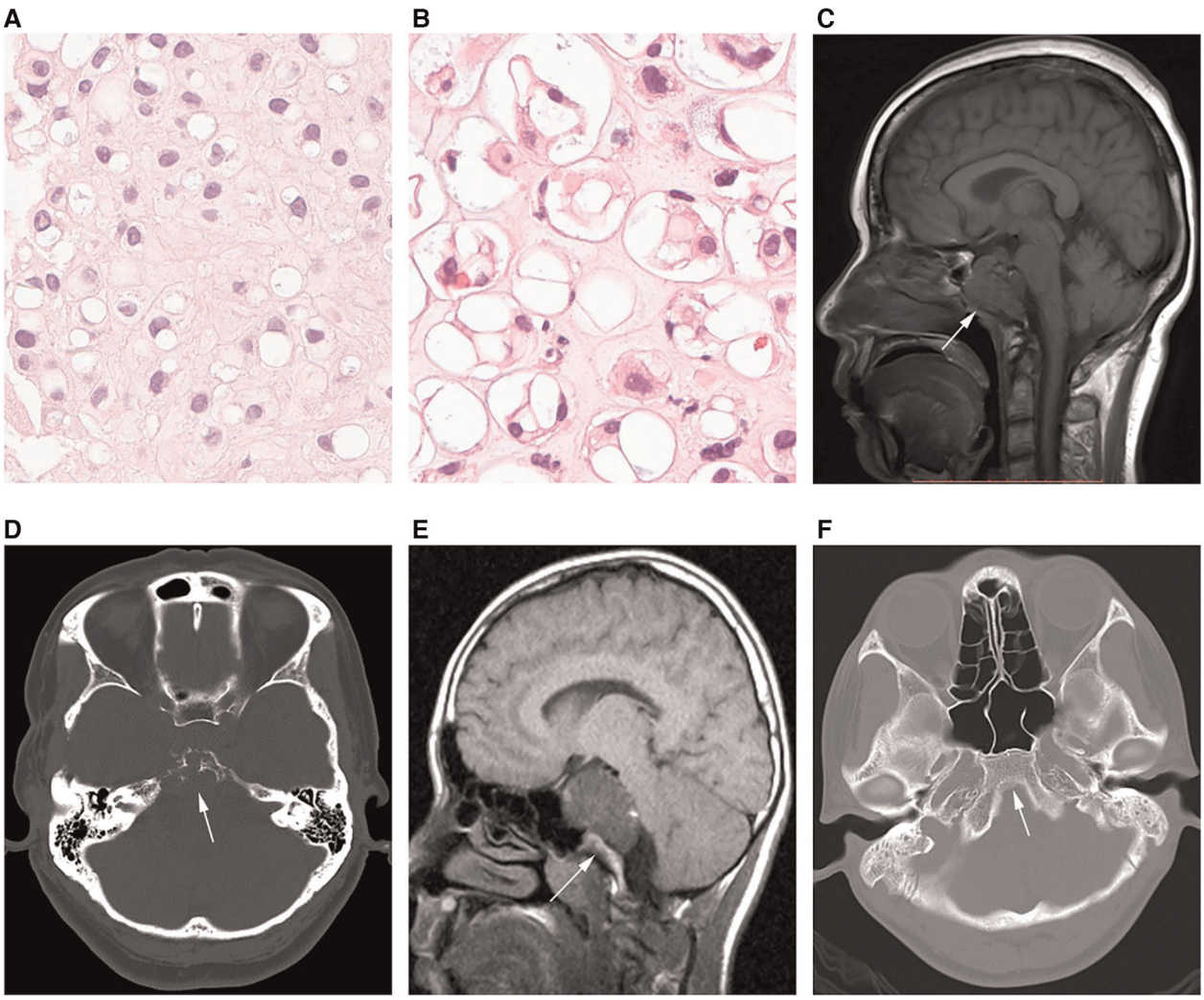

FIGURE 1
Different chordoma types. (A) Pathological image of classical chordoma showing many large cells with clear to eosinophilic cytoplasm; physalides are common in tumor cells. (B) Image of chondroid chordoma showing structures similar to the cartilage matrix between tumor cells. (C,D) MRI and CT scans in an SBC case showing that the tumor grows with the invasion of the whole clival bone (arrow). (E,F) CT image in another SBC case, with no bone invasion (arrow).

Immunohistochemistry

Tumor specimens underwent formalin fixation in the 30 min following extraction from patients, paraffin-embedding, sectioning at and 5-μm. Then, the sections were dewaxed and hydrated. After antigen retrieval, the specimens underwent incubation with endogenous peroxidase and blocking. Next, sections were submitted to successive incubations with primary (1:400, Abcam, UK; 4°C overnight) and secondary (1:250, TransGen Biotech, China; 1 h at ambient). Finally, treatment with diaminobenzidine was followed by dehydration and mounting.

Five or more high-power fields were assessed per sample at 400×, and positivity rates for various samples were determined by two pathologists independently. Consensual discussions were applied to resolve any discrepancy.

Quantitative real-time polymerase chain reaction (qRT-PCR)

Total RNA was extracted with TRIzol from tumor specimens snap frozen in liquid nitrogen in the initial 30 min following extraction from patients. In brief, 1 ml TRIzol (Thermo Fisher Scientific, Waltham, MA, USA) was mixed with 20 mg of tissue. PrimeScript RT reagent Kit with gDNA Eraser (Takara, Kusatsu, Shiga, Japan) was utilized for cDNA synthesis, as directed by the manufacturer. qRT-PCR was

performed with TaqMan probes for PTEN (Figure 2) and GAPDH (Thermo Fisher Scientific, USA). Amplification was carried out in 10-μl reactions at 95°C (10 min), followed by 40 cycles of 95°C (15 s) and 60°C (60 s). The ΔCt values were used for further analysis.

In cellar level experiments, TRIzol was used for RNA extraction, followed by reverse transcription with Reverse Transcription Kit (Takara, Kyoto, Japan). Quantitative polymerase chain reaction (PCR) was carried out with real time-PCR Recording Kit (Takara) by the SYBR Green method. The primers were as follows: PTEN, forward 5′-GCC CTG TAC CAT CCC AAG TC-3′ and reverse 5′-GAT GCT GCC GGT AAA CTC CA-3′; GAPDH, forward 5′-GGA GCG AGA TCC CTC CAA AAT-3′ and reverse 5′-GGC TGT TGT CAT ACT TCT CAT GG-3′. Amplification was performed at 95°C (30 s), followed by 40 cycles of 95°C (5 s) and 60°C (30 s); or 95°C (15 s), 60°C (30 s) and 95°C (15 s). The $2^{-\Delta\Delta CT}$ method was applied to examine transfection efficiency; transfection efficiency above 50% was considered to indicate a qualified transfection.

Cell culture

The chordoma UCH-1 cell line was acquired from Chordoma Foundation (https://www.chordomafoundation.org). Pretreatment of culture plates/flasks was carried out with gelatin (Sigma-Aldrich, Inc., St. Louis, MO, USA) to increase cell adhesion. IMDM and RPMI 1,640 (Thermo Fisher Scientific) were used as the basic medium mixture (4:1), supplemented with nonessential amino acid solution (1×) and penicillin/streptomycin (1×) (Thermo Fisher Scientific) and 10% fetal bovine serum (Hyclone, Logan, UT, USA). This cell line was subcultured every three days.

Cell proliferation assay

Cell transfection was performed by applying short interfering RNA (siRNA), the target siRNAs (Gima Genetics, Suzhou, China) were designed as follows: 5′-UGA ACC UGA UCA UUA UAG A-3′; the negative control siRNA was 5′-ATC TAG ATT AAC GAC ATT G-3′. SiRNA MATE™ was utilized as the transfection reagent (Gima Genetics), and tumor cells were grown in 6-well plates in antibiotic-free medium to approximately 6×10^4/well; the medium was changed before transfection. The transfection medium comprised 6 pmol siRNA, 200 μl Opti-MEM medium, and 15 μl siRNA MATE™, and was added to tumor cells and incubated under routine conditions. After 6 h of transfection, the medium was changed, and transfection efficiency was examined after 48 h of incubation.

Cell Counting Kit-8 (CCK-8; Dojindo Molecular Technologies, Japan) was utilized for cell proliferation assessment. Cells were inoculated in a 96-well plate, and medium containing 10% CCK-8 was replaced after transfection for 24, 48 and 72 h, respectively. Absorbance at 450 nm was measured on a microtiter plate reader.

Cell invasion assay

The 24-well transwell chambers (Corning, NY, USA) were applied for cell invasion experiments. The chambers were pretreated witt Matrigel (Corning), followed by addition of serum-free cell suspension and 20% serum-containing medium into the upper and lower chambers, respectively. Staining was performed after 12 h of incubation.

Statistical analysis

SPSS (v. 20.0; IBM Corp., Armonk, NY, USA) was utilized for data analysis. Differences in PTEN expression between the SBC types were assessed by the t test or rank sum test. Receiver operating characteristic (ROC) curve analysis was carried out to set a cutoff value. The Kaplan-Meier (K-M) method was employed for examining survival and progression risks between different PTEN expression groups. In overall survival (OS) and progression-free survival (PFS) Cox regression models, each parameter was firstly included in univariable analysis; parameters with $p < 0.05$ were further assessed by multivariable analysis. $P < 0.05$ indicated statistical significance.

Results

Analysis of epidemiological data

Ninety-eight patients were included in this study. Only cases administered their first surgery in our hospital were assessed. Paraffin-embedded and frozen specimens were obtained from 65 to 86 cases, respectively. Both sample types were available for 53 cases. The patients were 11–64 years old (median, 39 ± 13.7 years), including 51 women and 47 men. Following the first surgical procedure in our hospital, 33 cases underwent another surgery for tumor progression, 2 had two further surgeries each, 3 had three further surgeries each, and 1 had four more surgeries for multiple postsurgical tumor progression events. Eighteen patients received postsurgical radiation therapy, 3 only had conventional radiation therapy, 12 only underwent stereotactic radiation therapy, 2 only had proton radiation therapy, and 1 had stereotactic and proton radiotherapies. In the present study, 26 cases died and 58 had tumor progression. Three-year OS was 70%. PFS rates at 3 and 5 years were 37% and 18%, respectively, and median PFS was 30.5 months. (More data in Table 1)

Association between PTEN protein expression and patients' clinical characteristics

The 65 patients with paraffin-embedded specimens were 11 to 63 years old (median, 39 ± 14.1 years), including 38 women and 27 men. Age ($p = 0.619$) and sex ($p = 0.420$) were similar between this subgroup and the overall population. Table 1 lists all patient features. PTEN was mostly detected in the matrix, cytosol and nucleus. The positivity rates for all tumors were 20%–100% (median, 85%). PTEN protein expression significantly differed between SBC tumors of divergent invasive types or textures. PTEN was upregulated in non-bone-invasive tumor samples in comparison with bone-invasive tumor specimens ($p = 0.025$) (Figures 3A–C), and PTEN expression was increased in soft tumors in comparison with hard ones ($p = 0.017$) (Figures 3D–F). In univariable cox regression analysis of PFS, higher PTEN expression was correlated with reduced tumor progression risk ($p = 0.002$; hazard ratio [HR] = 0.981, 95% confidence interval [CI] 0.969–0.993).

TABLE 1 Categorical variables for skull base chordoma patients.

	All patients	Patients with paraffin embedded samples	Patients with frozen samples
Sex			
Women	51	38	45
Men	47	27	41
Treatment history			
Yes	32	20	28
No	66	45	58
Invasion condition			
Bone invasion	88	58	77
Non-bone invasion	10	7	9
Stage			
Dura erosion	40	28	37
No dura erosion	58	37	49
Lobulation			
With lobulation	54	35	49
Without lobulation	44	30	37
PTEN expression			
High group			35
Low group			51
Texture			
Soft	42	27	38
Hard	56	38	48
Resection grade			
Aggressive resection	53	37	43
Non-aggressive resection	45	28	43
Pathology			
Conventional	66	48	59
Chondroid	32	17	27
Post radiotherapy			
Yes	18	11	17
No	80	54	69
Tumor progression			
Yes	58	40	54
No	40	25	32
Sum	98	65	86

Number of patients represent raw data.

Association between PTEN gene expression and patients' clinical characteristics

The 86 cases with frozen specimens were 11–62 years old (median, 39 ± 13.8 years). In total, 45 women and 41 men were included. Age ($p = 0.986$) and sex ($p = 0.846$) were comparable between this subgroup and the overall population (Tables 1, 2). In univariable cox regression analysis of PFS, the ΔCt value of PTEN was a significant variable; a cut-off value was set at 10.5 after ROC curve analysis (Figure 4A), and SBCs were divided into two groups: PTEN high group, tumors with ΔCt value below 10.5 (higher PTEN expression); PTEN low group, ΔCt value above 10.5 (lower PTEN expression). After statistical analysis, patients' age, tumor diameter and presurgical KPS score were not significantly different between PTEN high and low groups, and no significant differences were found between PTEN high and low groups in patients with different sex, treatment history, pathological types, invasiveness status, stages and lobulation status ($p < 0.05$). In K-M curve analysis, PFS was increased in PTEN high group compared with PTEN low group ($p = 0.014$) (Figure 4B). After inclusion of presurgical KPS score, PTEN expression groups, patient sex and age, tumor diameter, treatment history, pathological type, invasiveness status, disease stage, lobulation status, resection grade and postsurgical radiation therapy in univariable cox regression analysis of PFS, treatment history, pathological type, PTEN expression groups, presurgical KPS score, tumor texture and resection grade were significantly associated with decreased PFS. The latter 5 parameters were further examined by multivariate regression analysis, which showed treatment history, pathological type and PTEN expression group independently predicted reduced PFS, and higher tumor progression risk was detected for PTEN low group compared with PTEN high group SBCs ($p = 0.006$), consistent with protein level data (Table 3).

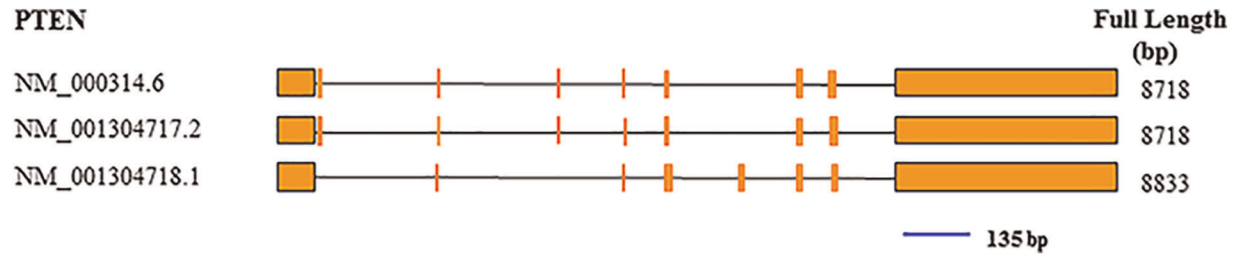

FIGURE 2
Exon composition of the PTEN gene, and position of the qRT-PCR amplicon (blue line). The amplicon was 135 bp.

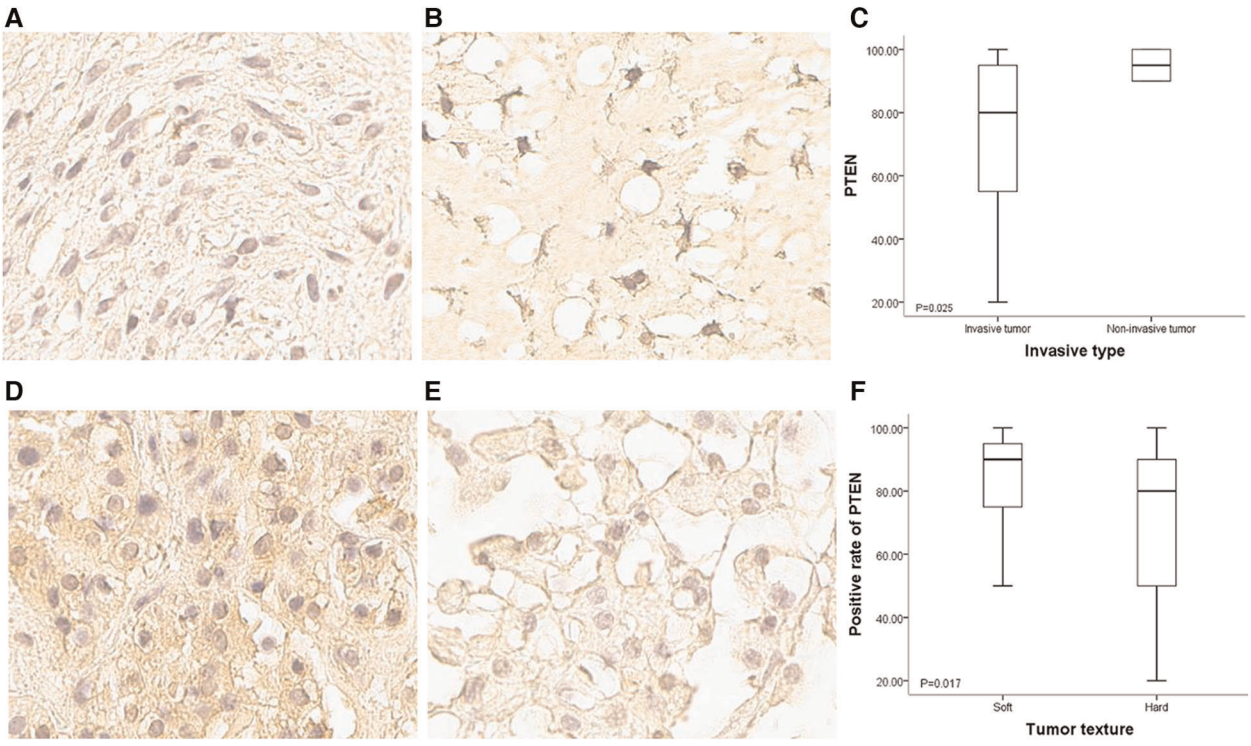

FIGURE 3
PTEN expression in SBCs of different invasiveness and texture conditions. (**A**) Immunohistochemical staining of PTEN for a bone invasive SBC (400×); staining signals were light, and mainly located in the cytoplasm and intercellular matrix. (**B**) Immunohistochemical staining of PTEN for a non-bone invasive SBC (400×); staining signals were strong, and the nucleus was positive. (**C**) Positivity rate for PTEN expression was higher in non-bone invasive tumors compared with bone invasive ones ($p = 0.025$). (**D**) Immunohistochemical staining of PTEN for a soft SBC (400×); staining signals were strong in the cytoplasm and intercellular matrix. (**E**) Immunohistochemical staining of PTEN for a hard SBC (400×); staining signals were weak, and the positivity rate was very low. (**F**) Positivity rate for PTEN was higher in soft tumors than in hard tumors ($p = 0.017$).

Effects of PTEN at the cellular level

UCH-1 cells were transfected with siRNA to knockdown PTEN, and the knockdown rate was 64.1% after transfection (Figure 5A). Absorbance in cells treated with the CCK-8 reagent was measured by a microtiter plate reader. It was found that in comparison with control cells, absorbance in PTEN knockdown cells was increased, suggesting elevated cell proliferation rate (Figure 5B). In invasion assays, the number of tumor cells migrating into the lower chamber was significantly increased in the PTEN knockdown group in comparison with control cells, indicating an enhanced invasive ability for tumor cells in the PTEN knockdown group (Figures 5C,D).

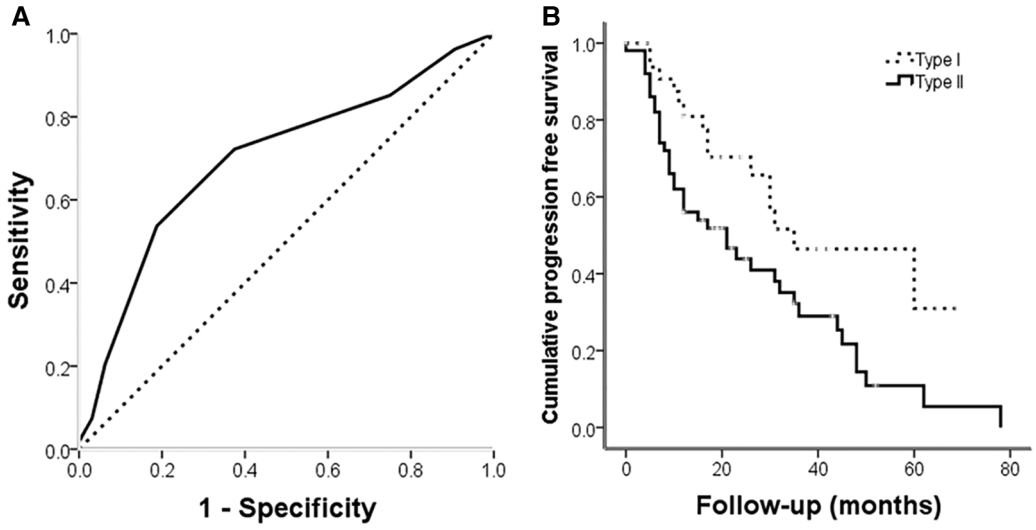

FIGURE 4
(A) ROC curve for PTEN expression at the gene level for tumor progression; the area under the curve was 0.699 (p = 0.002). (B) Kaplan-Meier analysis illustrating progression free survival for different PTEN expression groups. Progression free survival was longer in PTEN high expression group cases than in PTEN low expression group patients ((log rank = 6.1, p = 0.014).

TABLE 2 Continuous variables for skull base chordoma cases with frozen samples.

	Minimum	Maximum	Mean	Median	SD
Age (y)	11	62	36.6	39	13.8
Preoperative KPS	40	100	76.1	80	12.7
Diameter (mm)	15	85	44.6	44.9	14.1
ΔCt	8	16	11	11	1.6

Minimum and maximum values are based on raw data.

Discussion

In the present study, the protein and mRNA amounts of PTEN were assessed, and its functions and preliminary mechanism were further examined at the cellular level. The results indicated that decreased PTEN expression in SBCs had associations with tumor invasion, hard tumor texture and decreased PFS, and PTEN knockdown in tumor cells led to enhanced cell proliferation and invasion.

PTEN is encoded by a tumor suppressor gene commonly deleted in malignant diseases. PTEN protein is located in the cytoplasm and nucleus, and often secreted into the extracellular space (16). PTEN plays a role in dephosphorylating the cellular lipid signal phosphatidylinositol 3,4,5-trisphosphate, which acts antagonistically to phosphatidylinositol 3-kinase (PI3K) signaling to affect multiple cell processes, including growth, proliferation and polarization (17–18). In addition, PTEN inhibits other pathways, including the mammalian target of rapamycin protein (mTOR) pathway that controls cell growth, in part by regulating PI3K activity (19, 20). PTEN loss was noted in numerous tumors, including prostate cancers, breast cancers and gliomas (21–23). In recent years, PTEN loss has also been reported in chordomas (24–26).

Decreased PTEN expression was associated with reduced PFS and inhibit cell proliferation

PTEN loss is associated with cell growth and tumor progression. Park et al. found the mTOR pathway is activated after PTEN deletion in adult retinal ganglion cells, which robustly induces axon regeneration upon optic nerve damage (27). Penninger et al. reported that PTEN deficiency results in increased proliferation of neural stem cells (28). Le and collaborators found PTEN deficiency is not associated with patient survival but associated with protein kinase B (Akt)/mTOR activation, which may lead to tumor progression (29). PTEN disruption was also correlated with elevated Ki-67 proliferation index, which is a well-known biomarker of tumor progression in chordoma (30). Consistent with former studies, in the present study, decreased PTEN expression in SBC was proved to be associated with reduced PFS, and led to increased tumor cell proliferation. These findings indicate decreased levels of PTEN suppress its inhibitory effect on PI3K/AKT/mTOR signaling, which might lead to increased chordoma cell proliferation.

TABLE 3 Progression free survival analysis for skull base chordoma patients with frozen samples.

Parameter	Univariate analysis			Multivariate analysis		
	x ± sd	95% CI	*p*-value	HR	95% CI	*p*-value
Age			0.096			
Diameter			0.239			
Preoperative KPS			0.005*	0.992	0.967–1.017	0.508
Sex			0.173			
Men	36.7 ± 5.0	26.9–46.6				
Women	27.6 ± 3.4	21.0–34.3				
Treatment history			<0.001*	3.875	2.094–7.170	<0.001*
With	16.1 ± 3.2	9.9–22.3				
Without	39.0 ± 3.8	31.5–46.4				
Invasion condition			0.699			
Invasion	32.8 ± 3.3	26.2–39.3				
Non-invasion	25.1 ± 5.7	14.0–36.3				
Stage			0.717			
Dura erosion	33.1 ± 4.6	24.0–42.2				
No dura erosion	30.6 ± 3.7	23.3–37.9				
Lobulation condition			0.675			
No lobulation	33.0 ± 4.4	24.3–41.7				
Lobulation	31.2 ± 4.0	23.4–39.1				
Resection grade			0.025*	1.362	0.752–2.464	0.308
Aggressive resection	37.4 ± 3.8	30.0–45.0				
Non-aggressive resection	26.1 ± 4.2	17.9–34.4				
Texture			0.054			
Soft	39.6 ± 5.3	29.2–50.1				
Hard	26.7 ± 3.3	20.2–33.1				
Pathology			0.004*	0.485	0.248–0.948	0.034*
Conventional	26.3 ± 3.5	19.5–33.0				
Chondroid	43.5 ± 4.8	34.1–53.0				
Radiotherapy			0.902			
Without	32.0 ± 3.4	25.3–38.6				
With	30.4 ± 6.5	17.6–43.1				
PTEN expression			0.014*	2.425	1.282–4.588	0.006*
High	41.3 ± 4.9	31.8–50.8				
Low	26.4 ± 3.4	19.8–33.1				

HR, hazard ratio.
*$p < 0.05$.

PTEN in inhibit invasion and migration in SBC

PTEN deficiency is associated with tumor invasion and migration. Studies demonstrated PTEN deletion might lead to metastatic invasive prostate cancer (31, 32). Masahito et al. demonstrated that overexpression of PTEN inhibits cell migration, growth and focal adhesion (33). In our previous report about factors involved in chordoma with bone invasion, PTEN expression was significantly reduced (14). In the present study, consistent results were obtained. PTEN expression was significantly decreased in SBCs with bone invasion, and its knockdown in tumor cells led to elevated proliferation and invasion. Regarding the mechanism of PTEN in inhibiting tumor invasion and migration, different explanations have been provided. Raftopoulou et al. demonstrated PTEN suppresses cell migration and invasion through its C2 domain but not the PI3K pathway, with the C2 domain activated by phosphorylation at its Thr383 site (18). Wang and collaborators found PI3K/AKT signaling is activated in PTEN-reduced breast cancer with axillary lymph node metastasis. These researchers proposed PI3k/AKT

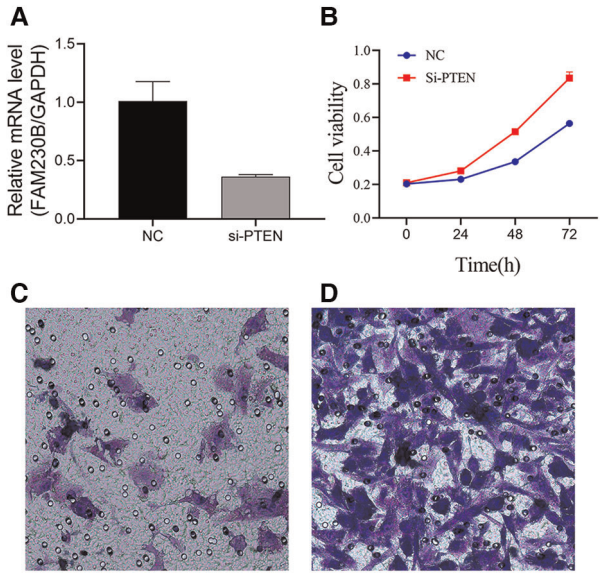

FIGURE 5
Effects of PTEN at the cellular level. (A) Histogram of PTEN knockdown efficiency. PTEN gene expression was significantly higher in the control group than in the knockdown group, with a knockdown efficiency of 64.1%. (B) Line graph of UCH-1 cell proliferation. Cell proliferation was higher after PTEN knockdown compared with control cells at 24 h, 48 h and 72 h, respectively. (C,D) Migrating cells observed at 200×. (C,D) are normal UCH-1 cells and PTEN knockdown cells, respectively. Cell migration was significantly increased in the PTEN knockdown group compared with the control group.

pathway induction is involved in tumor invasion and migration (34). Puzio-Kuter et al. reported mTOR signaling has an important function in prostate cancer invasiveness (32). Thus, this issue requires further investigation.

Decreased PTEN expression was associated with hard tumor texture

Although the relationship between PTEN expression and tumor texture is rarely described in the literature, PTEN expression was associated with tumor texture in SBCs. PTEN expression level in soft SBCs was increased compared with hard tumors. We learn from **Table 3** that the tumor progression rates between soft and hard SBCs were potentially significant ($p = 0.054$, hazard ratio: 1.712, 95% confidence level: 0.974–3.008). Specifically, hard tumors exhibited higher progression rates than soft tumors, indicating that hard tumors grow faster than soft tumors. This difference may be caused by reduced PTEN expression in tumors with hard components. Another explanation is that tumors with reduced PTEN expression are more invasive to surrounding bone, and the bone component makes the tumors harder compared with soft tumors with increased PTEN expression.

The present study included 96 SBC cases with 86 frozen and 65 paraffin-embedded specimens, with available clinical information. the relationship between PTEN and patients' prognosis and clinical characteristics were investigated at protein and gene level respectively, the function of PTEN in chordoma at the cellular level was further verified. This is the largest study to date about PTEN in skull base chordoma, and this is also the first study to demonstrate the role of PTEN in skull base chordoma at protein, genet, and cellular levels. The results indicated that PTEN in SBCs control tumor invasion and tumor progression. These findings provide novel insights into the development of tools for SBC treatment.

Nevertheless, this study had shortcomings. Firstly, not all the patients included contributed both frozen and paraffin-embedded specimens. Secondly, the present study was mainly exploratory, and the mechanism was not adequately studied. Additionally, only one cell line was used *in vitro* experiments caused by the slow growth of other chordoma cell lines, we will repeat the experiment involved in this study in other cell lines in the future.

Conclusion

PTEN expression in SBCs was assessed at the protein and mRNA levels. In addition, the associations of PTEN expression with patient features were analyzed, and its functions and preliminary mechanism were further verified at the cellular level. The results indicated that PTEN protein expression in SBC was correlated with tumor invasiveness and tumor texture, and decreased PTEN protein and gene expression levels in SBC were associated with reduced PFS. Finally, knockdown of PTEN in tumor cells led to higher proliferation and invasion.

Contribution to the field statement

Skull base chordoma represents a rarely diagnosed low-grade malignancy. With invasive growth, this tumor damages the surrounding bone seriously and is prone to recurrence after surgery; its long-term prognosis is poor, and there is no effective chemotherapy. Relevant factors and mechanisms involved in skull base chordoma are urgently needed. This study focused on PTEN expression in this tumor. In this study, 96 patients with skull base chordoma were included, including 65 with paraffin-embedded specimens and 86 with frozen specimens. Immunohistochemical staining and qRT-PCR were performed to detect PTEN expression at the protein and mRNA levels, respectively. PTEN expression and the clinical characteristics of SBC patients were next analyzed. Further, the PTEN gene in the chordoma cell line UCH-1 was knocked down using an siRNA, and cell function changes

after knockdown were analyzed. Finally, our results revealed decreased PTEN expression in SBC was associated with shorter progression free survival, and PTEN silencing in chordoma cells led to higher cell proliferation and invasiveness.

Data availability statement

The original contributions presented in the study are included in the article/Supplementary Material, further inquiries can be directed to the corresponding author/s.

Ethics statement

The studies involving human participants were reviewed and approved by Beijing Tiantan Hospital Ethics Committee. Written informed consent to participate in this study was provided by the participants' legal guardian/next of kin.

Written informed consent was obtained from the individual(s) for the publication of any potentially identifiable images or data included in this article.

Author contributions

KT: experiment implementation, data collection, data analysis, and article writing. JM: experiment implementation, data collection and manuscript editing. KW, DL and JZ: pathological diagnosis, immunohistochemical data collection, data analysis and manuscript revision. LW and ZW: conception and design of the study, and quality control. All authors contributed to manuscript revision, agreed to be accountable for all aspects of the work, and read and approved the submitted version. All authors contributed to the article and approved the submitted version.

Funding

The study was funded by the National Natural Science Foundation of China (81802683 and 82141113).

Acknowledgments

Special thanks to Li Qi of Clinical Medical Research Laboratory, Beijing Tiantan Hospital, for guidance.

Conflict of interest

The authors declare that the research was conducted in the absence of any commercial or financial relationships that could be construed as a potential conflict of interest.

Publisher's note

References

1. Ulici V, Hart J. Chordoma. *Arch Pathol Lab Med*. (2022) 146(3):386–95. doi: 10.5858/arpa.2020-0258-RA

2. Salisbury JR. The pathology of the human notochord. *J Pathol*. (1993) 171 (4):253–5. doi: 10.1002/path.1711710404

3. Wedekind MF, Widemannm BC, Cote G. Chordoma: current status, problems, and future directions. *Curr Prob Cancer*. (2021) 45(4):100771. doi: 10.1016/j.currproblcancer.2021.100771

4. Frezza AM, Botta L, Trama A, Dei TA, Stacchiotti S. Chordoma: update on disease, epidemiology, biology and medical therapies. *Curr Opin Oncol*. (2019) 31(2):114–20. doi: 10.1097/CCO.0000000000000502

5. Bohman L, Koch M, Bailey RL, Alonso-Basanta M, Lee JYK. Skull base chordoma and chondrosarcoma: influence of clinical and demographic factors on prognosis: a SEER analysis. *World Neurosurg*. (2014) 82(5):806–14. doi: 10.1016/j.wneu.2014.07.005

6. Jones PS, Aghi MK, Muzikansky A, Shih HA, Barker FG, Curry WT. Outcomes and patterns of care in adult skull base chordomas from the Surveillance, Epidemiology, and End Results (SEER) database. *J Clin Neurosci*. (2014) 21(9):1490–6. doi: 10.1016/j.jocn.2014.02.008

7. Shinya Y, Hasegawa H, Shin M, Kawashima M, Koga T, Hanakita S, et al. High dose radiosurgery targeting the primary tumor sites contributes to survival in patients with skull base chordoma. *Int J Radiat Oncol Biol Phys*. (2022) 113(3):582–7. doi: 10.1016/j.ijrobp.2022.02.024

8. Pikis S, Mantziaris G, Peker S, Samanci Y, Nabeel AM, Reda WA, et al. Stereotactic radiosurgery for intracranial chordomas: an international multiinstitutional study. *J Neurosurg*. (2022):1–8. doi: 10.3171/2021.12.JNS212416

9. Scheipl S, Igrec J, Leithner A, Smolle M, Haybäck J, Liegl B. [Chordoma: is there a molecular basis for diagnosis and treatment?]. *Pathologe*. (2020) 41 (2):153–62. doi: 10.1007/s00292-020-00761-4

10. Barresi V, Ieni A, Branca G, Tuccari G. Brachyury: a diagnostic marker for the differential diagnosis of chordoma and hemangioblastoma versus neoplastic histological mimickers. *Dis Markers*. (2014) 2014:514753. doi: 10.1155/2014/514753

11. Chen CY, Chen J, He L, Stiles BL. PTEN: tumor suppressor and metabolic regulator. *Front Endocrinol (Lausanne)*. (2018) 9:338. doi: 10.3389/fendo.2018.00338

12. Worby CA, Dixon JE. PTEN. *Annu Rev Biochem*. (2014) 83:641–69. doi: 10.1146/annurev-biochem-082411-113907

13. Carnero A, Blanco-Aparicio C, Renner O, Link W, Leal JF. The PTEN/PI3K/AKT signalling pathway in cancer, therapeutic implications. *Curr Cancer Drug Targets*. (2008) 8(3):187–98. doi: 10.2174/156800908784293659

14. Wu Z, Wang L, Guo Z, Wang K, Zhang Y, Tian K, et al. Experimental study on differences in clivus chordoma bone invasion: an iTRAQ-based quantitative proteomic analysis. *PLoS One*. (2015) 10(3):e119523. doi: 10.1371/journal.pone.0119523

15. Flanagan AM, Yamaguchi T. World health organization (WHO) classification of tumors of soft tissue and bone: notochordal. *Lyon: IARC Press*. (2013):328–9.

16. Li DM, Sun H. TEP1, Encoded by a candidate tumor suppressor locus, is a novel protein tyrosine phosphatase regulated by transforming growth factor beta. *Cancer Res*. (1997) 57(11):2124–9.

17. Papa A, Pandolfi PP. The PTEN–PI3K axis in cancer. *Biomolecules*. (2019) 9 (4):153. doi: 10.3390/biom9040153

18. Raftopoulou M. Regulation of cell migration by the C2 domain of the tumor suppressor PTEN. *Science*. (2004) 303(5661):1179–81. doi: 10.1126/science.1092089

19. Marquard FE, Jücker M. PI3K/AKT/mTOR Signaling as a molecular target in head and neck cancer. *Biochem Pharmacol*. (2020) 172:113729. doi: 10.1016/j.bcp.2019.113729

20. Aoki M, Fujishita T. Oncogenic roles of the PI3K/AKT/mTOR axis. *Curr Top Microbiol Immunol*. (2017) 407:153–89. doi: 10.1007/82_2017_6

21. Turnham DJ, Bullock N, Dass MS, Staffurth JN, Pearson HB. The PTEN conundrum: how to target PTEN-deficient prostate cancer. *Cells-Basel*. (2020) 9 (11):2342. doi: 10.3390/cells9112342

22. Csolle MP, Ooms LM, Papa A, Mitchell CA. PTEN And other PtdIns(3,4,5) P(3) lipid phosphatases in breast cancer. *Int J Mol Sci*. (2020) 21(23):9189. doi: 10.3390/ijms21239189

23. Cohen AL, Colman H. Glioma biology and molecular markers. *Cancer Treat Res*. (2015) 163:15–30. doi: 10.1007/978-3-319-12048-5_2

24. Xu Z, Zhang L, Wen L, Chao H, Wang Q, Sun M, et al. Clinical and molecular features of sacrum chordoma in Chinese patients. *Ann Transl Med*. (2022) 10(2):61. doi: 10.21037/atm-21-6617

25. Yang C, Sun J, Yong L, Liang C, Liu T, Xu Y, et al. Deficiency of PTEN and CDKN2A tumor-suppressor genes in conventional and chondroid chordomas: molecular characteristics and clinical relevance. *Onco Targets Ther*. (2020) 13:4649–63. doi: 10.2147/OTT.S252990

26. Chen K, Mo J, Zhou M, Wang G, Wu G, Chen H, et al. Expression of PTEN and mTOR in sacral chordoma and association with poor prognosis. *Med Oncol*. (2014) 31(4):886. doi: 10.1007/s12032-014-0886-7

27. Park KK, Liu K, Hu Y, Smith PD, Wang C, Cai B, et al. Promoting axon regeneration in the adult CNS by modulation of the PTEN/mTOR pathway. *Science*. (2008) 322(5903):963–6. doi: 10.1126/science.1161566

28. Penninger JM. STEM CELLS: PTEN–coupling tumor suppression to stem cells? *Science*. (2001) 294(5549):2116–8. doi: 10.1126/science.1067931

29. Le LP, Nielsen GP, Rosenberg AE, Thomas D, Batten JM, Deshpande V, et al. Recurrent chromosomal copy number alterations in sporadic chordomas. *PLoS One*. (2011) 6(5):e18846. doi: 10.1371/journal.pone.0018846

30. Lee DH, Zhang Y, Kassam AB, Park MJ, Gardner P, Prevedello D, et al. Combined PDGFR and HDAC inhibition overcomes PTEN disruption in chordoma. *PLoS One*. (2015) 10(8):e134426. doi: 10.1371/journal.pone.0134426

31. Wang S, Gao J, Lei Q, Rozengurt N, Pritchard C, Jiao J, et al. Prostate-specific deletion of the murine Pten tumor suppressor gene leads to metastatic prostate cancer. *Cancer Cell*. (2003) 4(3):209–21. doi: 10.1016/S1535-6108(03)00215-0

32. Puzio-Kuter AM, Castillo-Martin M, Kinkade CW, Wang X, Shen TH, Matos T, et al. Inactivation of p53 and Pten promotes invasive bladder cancer. *Gene Dev*. (2009) 23(6):675–80. doi: 10.1101/gad.1772909

33. Tamura M, Gu J, Matsumoto K, Aota S, Parsons R, Yamada KM. Inhibition of cell migration, spreading, and focal adhesions by tumor suppressor PTEN. *Science*. (1998) 280(5369):1614–7. doi: 10.1126/science.280.5369.1614

34. Wang LL, Hao S, Zhang S, Guo LJ, Hu CY, Zhang G, et al. PTEN/PI3K/AKT protein expression is related to clinicopathological features and prognosis in breast cancer with axillary lymph node metastases. *Hum Pathol*. (2017) 61:49–57. doi: 10.1016/j.humpath.2016.07.040

frontiers | Frontiers in Surgery

TYPE Original Research
PUBLISHED 29 September 2022
DOI 10.3389/fsurg.2022.983958

OPEN ACCESS

EDITED BY
Peng Zhao,
Capital Medical University, China

REVIEWED BY
Mian Guo,
The Second Affiliated Hospital of Harbin Medical University, China
Zhiyu Ding,
Central South University, China

*CORRESPONDENCE
Changchen Hu
hucc88@163.com
Fake Lu
fakelu@binghamton.edu

†These authors have contributed equally to this work and share first authorship

SPECIALTY SECTION
This article was submitted to Neurosurgery, a section of the journal Frontiers in Surgery

RECEIVED 01 July 2022
ACCEPTED 13 September 2022
PUBLISHED 29 September 2022

CITATION
Liu J, Wang K, Ji H, Zhang G, Chen S, Zhang S, Lu F and Hu C (2022) Integrated analysis of competitive endogenous ribose nucleic acids (ceRNAs)-related regulatory networks in invasive and non-invasive non-functioning pituitary adenomas (NFPAs).
Front. Surg. 9:983958.
doi: 10.3389/fsurg.2022.983958

Integrated analysis of competitive endogenous ribose nucleic acids (ceRNAs)-related regulatory networks in invasive and non-invasive non-functioning pituitary adenomas (NFPAs)

Jiangtao Liu[1†], Kaixuan Wang[1†], Hongming Ji[1], Gangli Zhang[1], Shengli Chen[1], Shiyuan Zhang[1], Fake Lu[2*] and Changchen Hu[1,3*]

[1]Department of Neurosurgery, Shanxi Provincial People's Hospital, Shanxi Medical University, Taiyuan, China, [2]Department of Biomedical Engineering, Binghamton University, State University of New York, Binghamton, United States, [3]Department of Neurosurgery, Shuozhou People's Hospital, Shuozhou, China

Background: This study aims to identify the differentially expressed (DE) non-coding ribose nucleic acids (ncRNAs), messenger RNA (mRNA) expression profiles, and competitive endogenous RNA (ceRNA)-related regulatory networks in invasive and non-invasive nonfunctioning pituitary adenomas (NFPAs).
Methods: A full-transcriptome sequencing of invasive and non-invasive NFPAs is carried out to evaluate the expression profiles of circular RNAs (circRNAs), long non-coding RNAs (lncRNAs), microRNAs (miRNAs), and mRNA expression profiles.
Results: The screening criteria resulted in 118 DEcircRNAs (88 up-regulated and 30 down-regulated), 105 DElncRNAs (68 up-regulated and 37 down-regulated), 43 DEmiRNAs (22 up-regulated and 21 down-regulated), and 268 DEmRNAs (194 up-regulated and 74 down-regulated). Accordingly, a ceRNA regulatory network related to invasive NFPA is constructed. Further, the Gene Ontology and Kyoto Encylopedia of Genes and Genomes analyses showed that circRNAs and lncRNAs in the network are related to chromatin remodeling, participating in the Janus kinase/signal transducer and activator of transcription (JAK-STAT) and calcium signaling pathways. Hsa-miR-1248 showed exceptional connectivity in the ceRNA regulatory network, which could be closely related to the invasiveness of NFPAs.
Conclusions: Together, these findings clarified the regulatory mechanisms of invasive and non-invasive NFPAs, providing innovative research avenues and therapeutic targets for invasive NFPAs.

KEYWORDS

pituitary adenomas, competitive endogenous RNA, regulatory networks, nonfunctional adenoma, invasiveness, non-coding RNA

Background

Pituitary adenoma (PA) is one of the most common benign intracranial tumors on the pituitary gland. This rare pathological condition often results from excessive secretion of growth hormone. The PA condition can be classified into functioning pituitary adenomas (FPAs) with characteristic symptoms of acromegaly or Cushing's disease and non-functioning pituitary adenomas (NFPAs). The NFPAs are usually caused by gonadotropin-secreting cells, resulting in the reduced secretion of pituitary hormone. Moreover, NFPAs can be accessibly diagnosed at a specific tumor size as it begins to oppress the intracranial nerve and surrounding brain tissues. Although most PAs are biologically benign, some PAs can migrate to the important structures around the cavernous sinus, internal carotid artery, and optic chiasma. In rare cases, PAs are accompanied by severe metastasis, leading to challenges in their complete surgical resection and a high risk of recurrences even being removed entirely. Hitherto, the precise mechanism related to the invasiveness of NFPA is yet to be explored, requiring the discovery of various vital biomarkers. In addition, it is required to investigate specific genetic changes to explore invasive NFPA further and provide evidence to support the molecular theranostics of the disease.

In recent times, tremendous advancements have resulted in the development of high-throughput sequencing technology to investigate the expression profiles of non-coding ribose nucleic acids (ncRNAs), including circular RNA (circRNA), long non-coding RNA (lncRNA), and micro RNA (miRNA). Initially, these ncRNAs were regarded as "junk molecules" regarding gene expression, which have been further identified as biomarkers for disease prognosis and regulators of various cellular processes. In this context, several transcriptome studies confirmed a significant correlation between ncRNA and human diseases, including oncological, neurological, and developmental diseases (1, 2). Recently, a study indicated that different RNAs could interact and regulate the expression of genes at the post-transcriptional level through complex molecular mechanisms, in which competitive endogenous RNA (ceRNA) networks played essential roles in various physiological processes (3). CeRNAs, a general term representing different transcripts, possess similar miRNA response elements (MREs) and constitute a competitive relationship, including circRNAs, lncRNAs, mRNAs, and pseudogenes. Notably, ceRNAs bind to similar miRNAs, forming a complex RNA regulatory network. These RNA regulatory networks not only regulate the ceRNA expression levels but also influence each other, eventually affecting the biological process of cells. Consequently, a potential ceRNA network, namely the lncRNA-circRNA-miRNA-mRNA network, can be established based on the same miRNAs. For instance, the integrated analysis of the ceRNA network confirmed that the ceRNA network played an important role in the progression of brain tumors (4, 5).

Despite the success in establishing the ceRNA network, the characteristic comprehensive expression profiles of circRNAs, lncRNAs, miRNAs, and mRNAs related to invasive NFPA, as well as the mechanism of ceRNA-related regulatory networks, remain unclear. Motivated by these considerations, this study aims to construct a gene regulatory network model of invasive NFPA by ceRNAs. Further, we analyze and provide new ideas and methods for further understanding the disease. Finally, the regulatory mechanisms of invasive and non-invasive NFPAs are clarified, providing innovative research avenues and therapeutic targets for invasive NFPAs.

Materials and methods

Patients and tissue collection

The tissue samples were collected from the selected patients with invasive and non-invasive NPFA ($n = 6$ each) who underwent transsphenoidal surgery at the Shanxi Provincial People's Hospital, Shanxi, PR China, from 2020 to 2021. It should be noted that the patients had not received radiotherapy or chemotherapy before surgery. Further, the diagnosis of NFPA was confirmed by the histopathological analysis. The tumor invasion was defined as Knosp grade 3 or 4 (**Figure 1**), or sphenoid sinus invasion was detected during surgery. The resected tumor specimens were preserved in liquid nitrogen for 2 h and then stored in a freezer at −80°C. Further, the high-throughput sequencing was performed to analyze ncRNA and mRNA expression profiles in all invasive and non-invasive NPFA ($n = 12$) samples and validated by quantitative reverse transcription polymerase chain reaction (qRT-PCR) analysis. The experimental protocols were approved by the ethical committee of the Shanxi Provincial People's Hospital. The informed consent was obtained from all patients.

Library building and sequencing

Initially, the total RNA extracted from tissues or cells was purified using 1% agarose gel electrophoresis to detect RNA degradation and contamination. Then, the preliminary NanoPhotometer® spectrophotometer (IMPLEN, Westlake Village, CA, USA) was employed to check the RNA purity. Further, the Qubit® RNA Assay Kit in Qubit® 2.0 Fluorometer (Life Technologies, Carlsbad, CA, USA) was applied to quantify the RNA concentration. Finally, the RNA Nano 6000 Assay Kit of the Agilent Bioanalyzer 2,100 system (Agilent Technologies, CA, USA) was utilized to confirm RNA integrity.

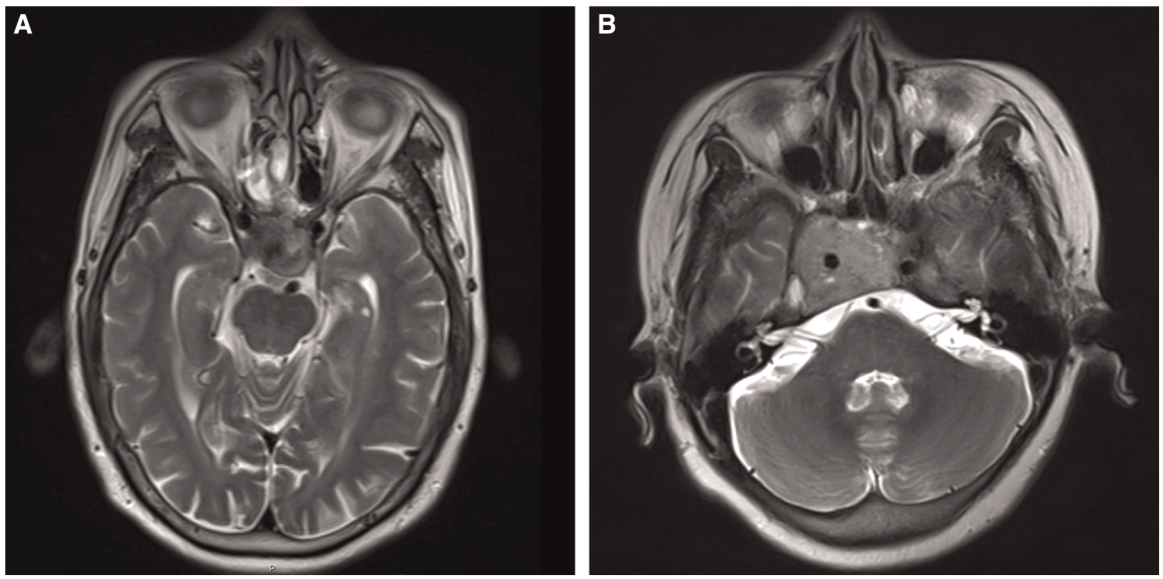

FIGURE 1
(A,B) T2-weighted images of nonfunctional pituitary adenomas with Knosp grades 3 and 4, respectively.

The miRNA library was initially constructed using NEBNext® Multiplex Small RNA Library Prep Set for Illumina® (NEB, USA). Further, lncRNA, mRNA, and circRNA libraries were fabricated by NEBNext® Ultra™ Directional RNA Library Prep Kit for Illumina® (NEB, USA) (6). The fabricated libraries were preliminarily quantified using Qubit2.0, and the insert size of the library was then detected using an Agilent 2,100 Bioanalyzer. After the insert size met the expectations, the effective concentration of the library was then quantified precisely by the qRT-PCR analysis to substantially ensure the quality of RNA libraries. Further, the sequencing was executed using an IlluminaHiSeq™2500/MiSeq Illumina Hiseq platform, based on the effective concentration of the RNA library and the demand for data output pooling. In this study, the library construction and RNA sequencing were accomplished with the support of Nuohe Zhiyuan Technology Co., Ltd. (Beijing, China).

Data filtering

Typically, the original sequencing data often contain a small number of reads with sequencing connectors or low sequencing quality. To overcome this aspect, the sequencing data were filtered to ensure the quality and reliability of the data analysis. In the cases of lncRNA, circRNA, and mRNA, the purified data (clean reads) were obtained by eliminating the reads containing adapter, reads containing ploy-N, and low-quality reads from raw data. For miRNA, the raw data were purified by removing reads containing ploy-N, with 5′ adapter contaminants, without 3′ adapter or the insert tag, containing ploy A or T or G or C, and low-quality reads. Simultaneously, Q20, Q30, and GC content of the clean data were calculated. It should be noted that all the downstream analyses were based on clean data with high quality.

Data analysis

The differentially expressed (DE) ncRNAs (including DElncRNAs, DEcircRNAs, and DEmiRNAs), as well as DEmRNAs, were screened using the DESeq2 R package (1.8.3) (7). The default threshold for differential expression, i.e., the adjusted p-value (p_{adj}), was obtained by the multiple test correction of p-values using the Benjamini-Hochberg method at the high false positive rate. Notably, a smaller p_{adj} value would indicate a more significant result. Therefore, $p_{adj} < 0.05$ was considered a defined level of statistically significant difference. If $p_{adj} < 0.05$ with no difference, $p < 0.05$ was then used for differential screening in subsequent analysis. Further, Ggplot2 and pheatmap packages were applied to draw volcano and heat maps of the expression profiles of DElncRNAs, DEmiRNAs, and DEmRNAs, respectively.

Construction of miRNA regulatory network

According to the DEmiRNA target genes (mRNA), miRNA target genes were analyzed to predict the intersection of

miRanda and RNAhybrid softwares (8–10). Further, the target mRNAs corresponding to DEmiRNAs and mRNAs-overlapped DEmRNAs were analyzed. Considering the inhibitory effect of miRNAs on mRNAs, the combinations of significantly down-regulated miRNAs, and significantly up-regulated mRNAs, as well as significantly up-regulated miRNAs, and significantly down-regulated mRNAs were selected as target gene pairs to generate the miRNA-mRNA regulatory network.

Construction of ceRNA regulatory network

Notably, lncRNAs and circRNAs possess several miRNA-binding sites that can act as miRNA sponges to competitively constrain the regulatory effects of miRNAs on their target genes, thus indirectly regulating gene expression. According to the ceRNA theory, circRNA/lncRNA target gene pairs were identified with the same miRNA-binding sites. Then, the circRNA-miRNA-mRNA regulatory relationship was constructed with lncRNAs and circRNAs as decoys, miRNA as the core, as well as mRNAs as the target to create a ceRNA regulatory network.

Functional analyses

The Gene Ontology (GO) and Kyoto Encyclopedia of Genes and Genomes (KEGG) pathway analyses were carried out based on the results of the screened target gene (mRNA). In addition, the functions of lncRNAs and circRNAs were predicted using the Cytoscape software (version 6.7) to predict mRNAs in the invasive NFPA-related ceRNA networks (11).

Results

Differential expression analysis

Based on the screening criteria, various RNAs and their altered expressions were identified, such as 118 DEcircRNAs (88 up-regulated and 30 down-regulated), 105 DElncRNAs (68 up-regulated and 37 down-regulated), 43 DEmiRNAs (22 up-regulated and 21 down-regulated), as well as 268 DEmRNAs (194 up-regulated and 74 down-regulated). **Figure 2** shows the distribution of DElncRNAs, DElncRNAs, and DEmRNAs as cluster heat maps and volcano maps. It was observed from the results that the invasive and non-invasive NFPA could be significantly separated, indicating reliable differential expression analysis. Further, the enrichment of DEcircRNAs and DElncRNAs by GO and

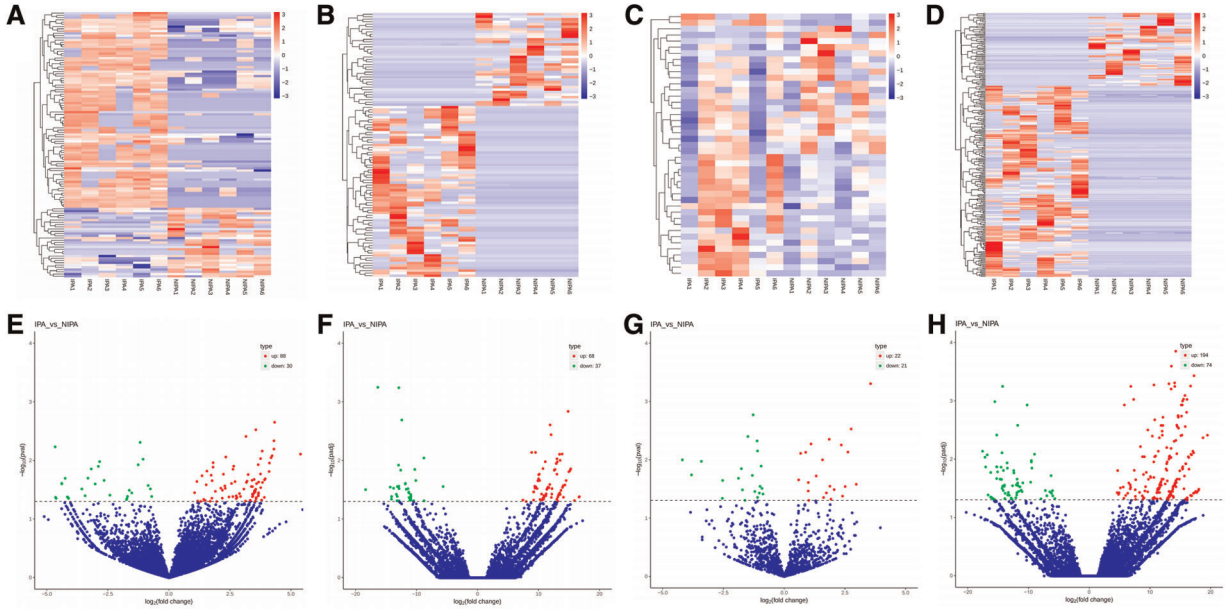

FIGURE 2
(A–D) Cluster heat map of DEcircRNAs, DElncRNAs, DEmiRNAs, and DEmRNAs. Red indicates up-regulation and blue indicates down-regulation. (E–H) Volcano map of DEcircRNAs, DElncRNAs, DEmiRNAs, and DEmRNAs. Red indicates up-regulation and green indicates down-regulation. DE, differential expression; circRNA, circular RNA; lncRNA, long chain non-coding RNA; IPA, invasive nonfunctional pituitary adenomas; NIPA, non-invasive nonfunctional pituitary adenomas.

KEGG analyses were analyzed, representing that DEcircRNAs were significantly related to the cellular composition, tissue or biogenesis, cellular protein metabolism, and tight junctions, as well as axonal orientation (Figure 3). In this context, DElncRNAs were substantially associated with the cell surface receptor signaling pathways, cell responses to chemical stimuli, and cytokine–cytokine receptor interactions (Figure 4).

Construction of miRNA regulatory network

To construct the miRNA regulatory network, the combinations of differentially expressed miRNAs and mRNAs were identified, in which 15 significantly down-regulated miRNAs, and 24 significantly up-regulated mRNAs, as well as 17 significantly up-regulated miRNAs, and 6 significantly

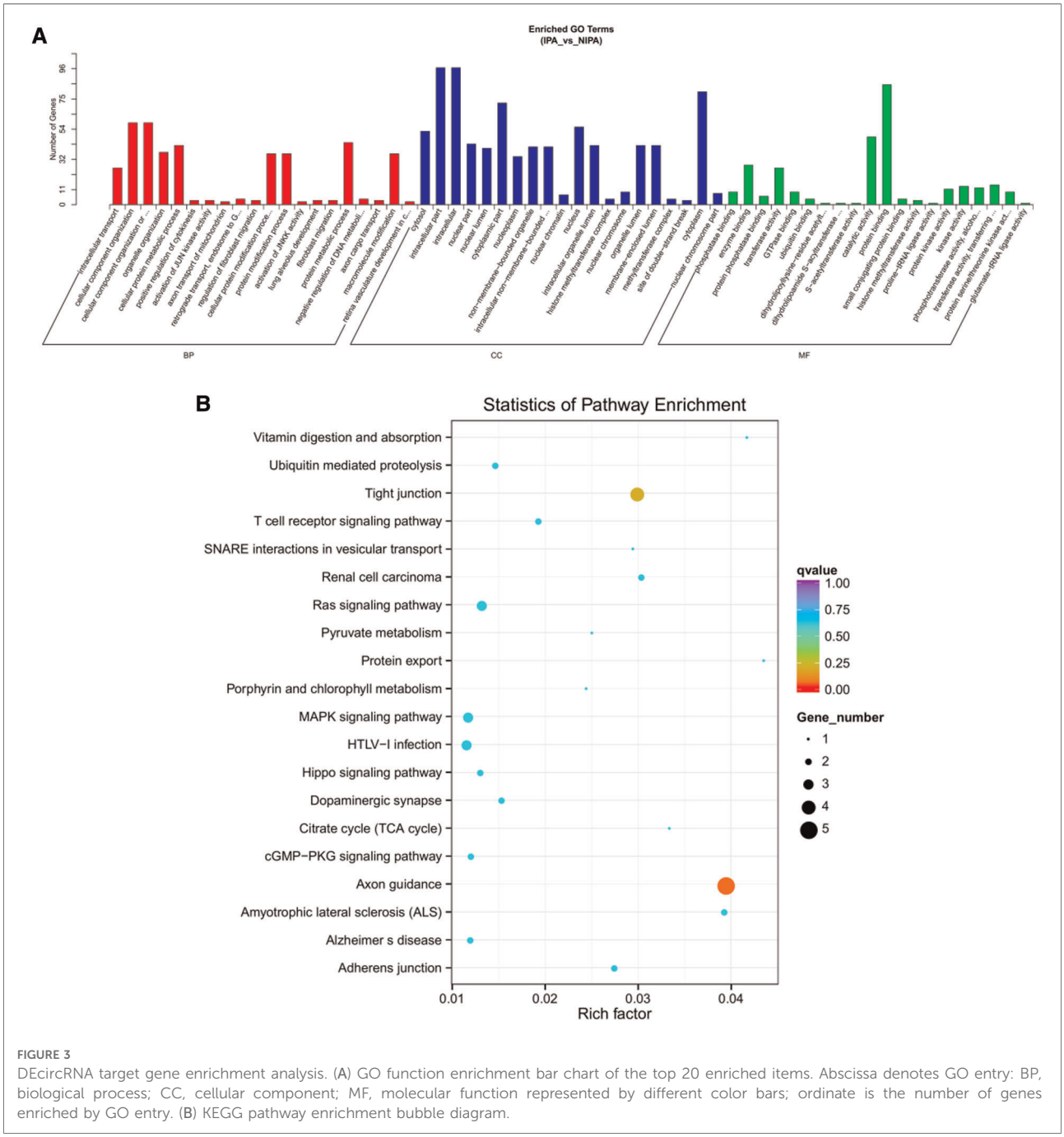

FIGURE 3
DEcircRNA target gene enrichment analysis. (A) GO function enrichment bar chart of the top 20 enriched items. Abscissa denotes GO entry: BP, biological process; CC, cellular component; MF, molecular function represented by different color bars; ordinate is the number of genes enriched by GO entry. (B) KEGG pathway enrichment bubble diagram.

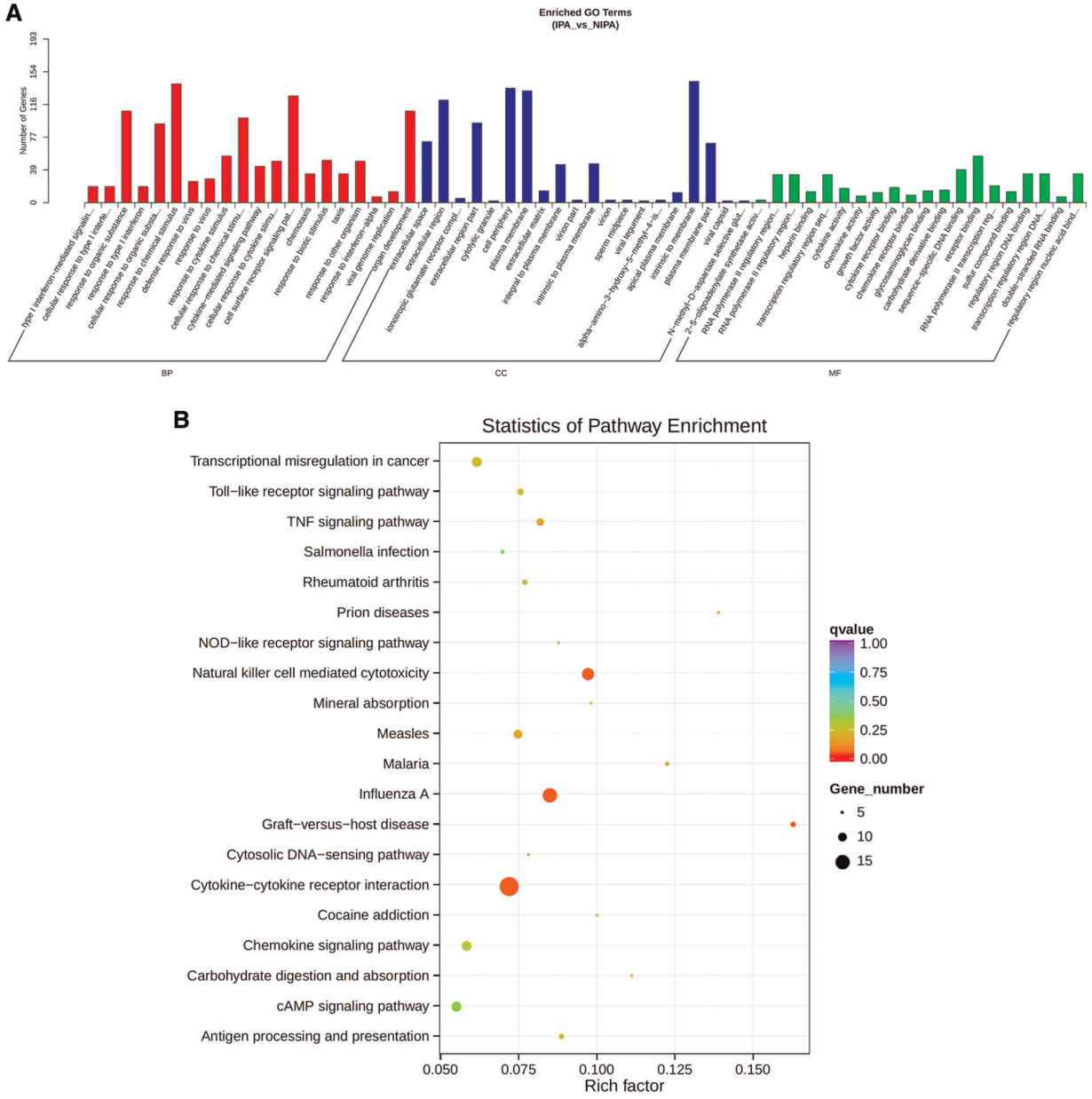

FIGURE 4
DElncRNA target gene GO and KEGG enrichment analyses. (**A**) Top 20 GO-BP, CC, and MF entries. BP, biological process; CC, cell components; MF, molecular function. (**B**) Top 20 enrichment pathways.

down-regulated mRNAs were selected as target gene pairs. These selected target genes were then entered into Cytoscape to obtain a total of 62 sides of a DEmiRNA–DEmRNA regulatory network (Figure 5). Further, the target genes corresponding to the DEmiRNA–DEmRNA regulatory network were examined by the GO functional enrichment (Figures 2, 3) and KEGG enrichment analyses (Figure 6). On the one hand, the GO functional enrichment analysis showed that the target genes of DEmiRNAs were substantially related to the sequence-specific deoxyribonucleic acid (DNA) binding of the transcriptional regulatory region, sequence-specific DNA binding of the RNA polymerase II regulatory region, and structure-specific DNA binding. On the other hand, the KEGG pathway analysis showed that DEmRNAs might be involved in the O-glycan synthesis, adenosine 5′-monophosphate (AMP)-activated protein kinase (AMPK) signaling pathway, osteoclast differentiation, and viral carcinogenesis.

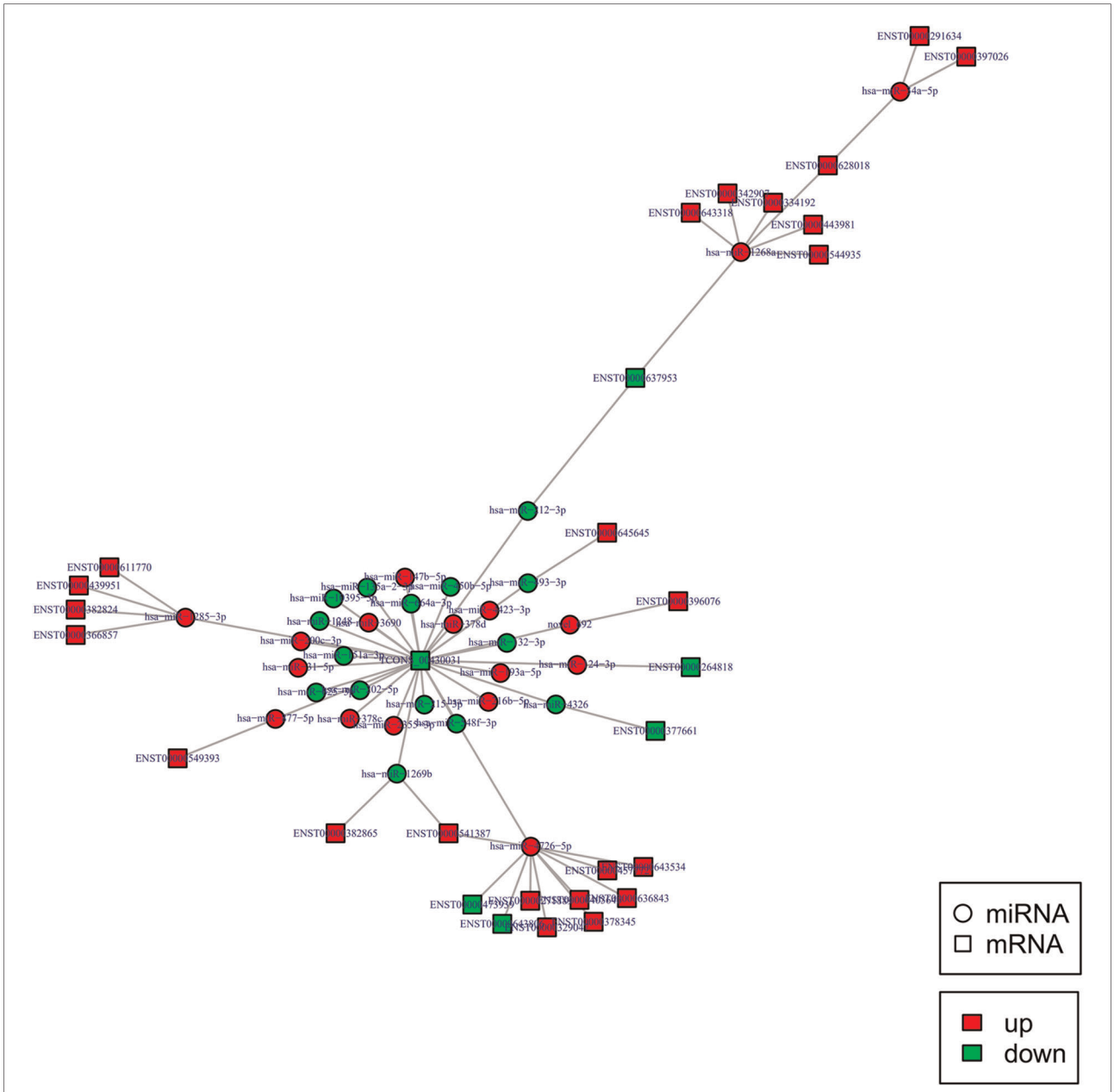

FIGURE 5
DEmiRNA and targeted DEmRNA regulatory network. Circle: miRNA, square: lncRNA. Red: up-regulation, green: down-regulation.

Construction of the circRNA-lncRNA coregulatory ceRNA network

Indeed, circRNAs and lncRNAs can bind to MRE and participate in the regulation of post-transcriptional expression. Considering this aspect, a circRNA–lncRNA co-regulatory ceRNA network was constructed to explore whether circRNAs and lncRNAs could share the same miRNA-mRNA relationship pair (same competing MRE). This regulatory ceRNA network included 242 nodes (61 up-regulated and 22 down-regulated circRNAs, 62 up-regulated and 35 down-regulated lncRNAs) and 654 edges (**Figure 7**). The network subsequently revealed that most circRNAs and lncRNAs functioned by jointly regulating miRNAs. For instance, it was predicted that the circRNA, hsa_circ_0005558, and lncRNA, CCDC144NL-AS1 displayed the same target, i.e., hsa-miR-1268a, as ceRNA could up-regulate SWI/SNF related, matrix-associated, actin-dependent regulator of chromatin, subfamily e, member 1(SMARCE1) to mediate chromatin remodeling.

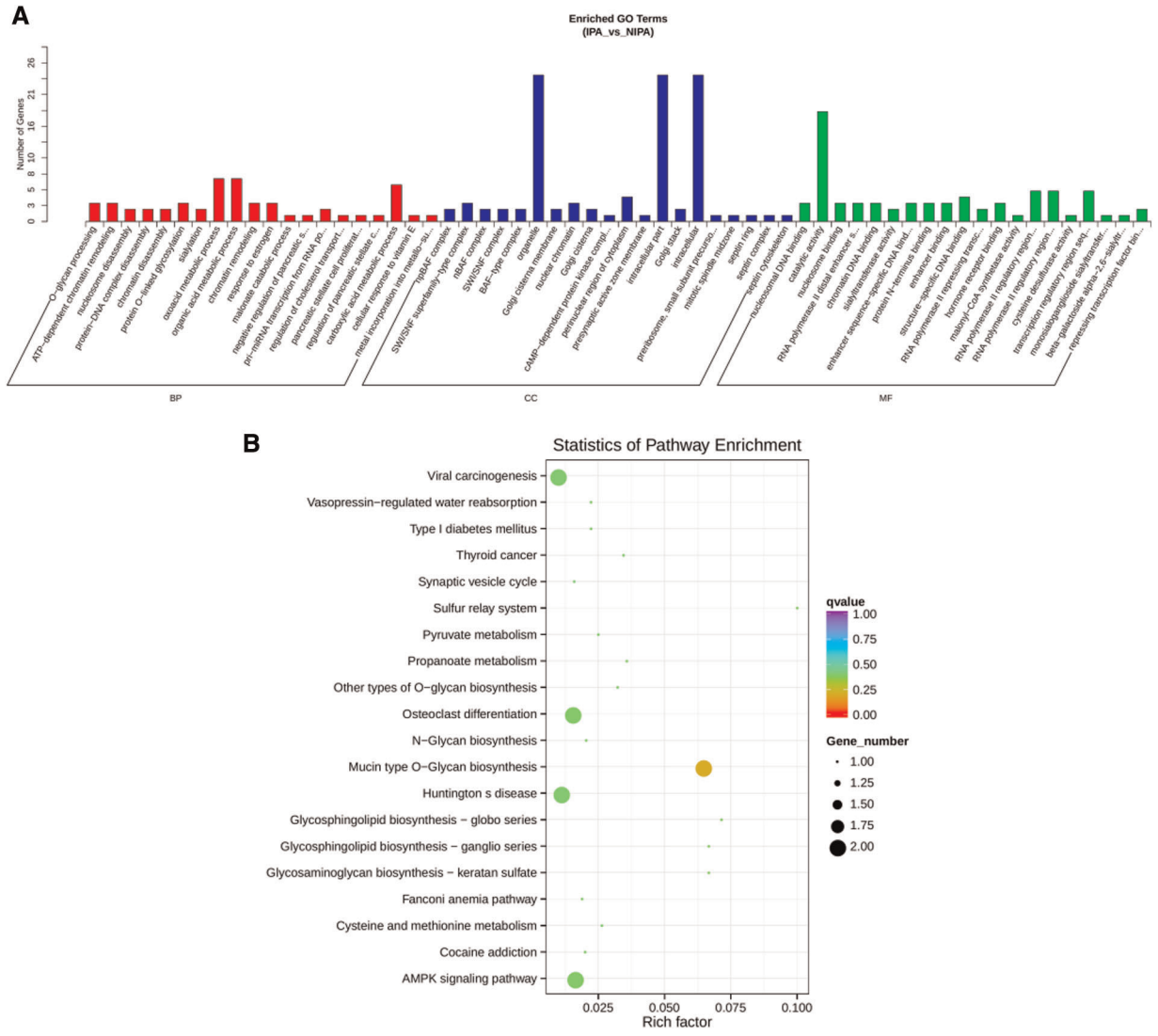

FIGURE 6
miRNA regulatory network target gene enrichment analysis. (A) GO function enrichment bar chart of the top 20 enriched items. Abscissa denotes GO entry, BP, biological process; CC, cellular component; MF, molecular function are represented by different color bars; ordinate is the number of genes enriched by GO entry. (B) KEGG pathway enrichment bubble diagram of top 20 enriched pathway entries.

Notably, hsa-miR-1248 possessed the highest connectivity in the co-regulatory ceRNA network and the most number of node interactions, suggesting its potential role in invasive NFPA. To clarify the potential functions of lncRNAs and circRNAs in invasive NFPA, the GO and KEGG pathway enrichment analyses were further used to detect the critical functionalities of the abnormally expressed mRNAs in the lncRNA-circRNA co-regulated ceRNA network. It was observed that the lncRNAs and circRNAs in this regulatory network were mainly related to various biological processes, such as chromatin remodeling, closely related to tumor formation (Figure 7). In addition, the KEGG pathway analysis indicated that the Janus kinase/signal transducer and activator of transcription (JAK-STAT), as well as calcium signaling pathways, were enriched in the ceRNA regulatory network (Figure 8). Together, it could be concluded that these pathways involved in many intracellular metabolic processes could substantially play critical roles in the occurrence and development of invasive NFPA.

Discussions

This study is aimed at identifying various DE ncRNAs and mRNA expression profiles, as well as ceRNA-related regulatory networks in invasive and non-invasive NFPAs. Accordingly, the

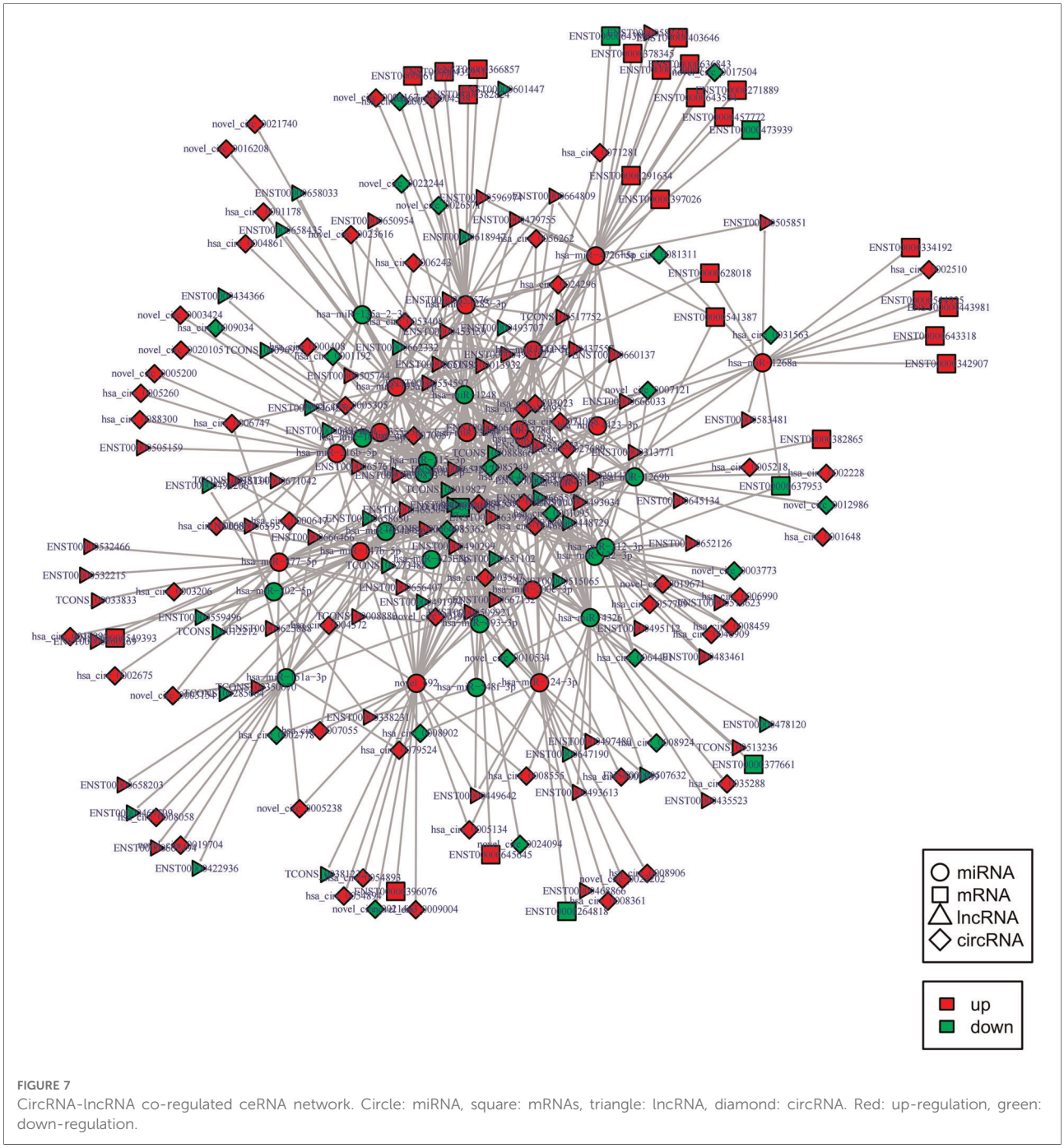

FIGURE 7
CircRNA-lncRNA co-regulated ceRNA network. Circle: miRNA, square: mRNAs, triangle: lncRNA, diamond: circRNA. Red: up-regulation, green: down-regulation.

full-transcriptome sequencing of invasive and non-invasive NFPA tissue samples resulted in various DE RNAs, including 118 DEcircRNAs (88 up-regulated and 30 down-regulated), 105 DElncRNAs (68 up-regulated and 37 down-regulated), 43 DEmiRNAs (22 up-regulated and 21 down-regulated), and 268 DEmRNAs (194 up-regulated and 74 down-regulated). Further, the GO and KEGG-based enrichment analyses of lncRNAs and circRNAs indicated that their target genes were associated with cell composition, tissue or biogenesis, cell protein metabolism, cell surface receptor signaling pathways, and cytokine-cytokine receptor interactions.

Considering the inhibitory effect of miRNAs on mRNAs, the abnormally expressed miRNAs and mRNAs were screened significantly to establish a cooperative regulatory network. The functional enrichment analysis of DEmRNAs in the miRNA regulatory network presented that the sequence-specific DNA binding of the transcriptional regulatory region, sequence-specific DNA binding of the RNA polymerase II regulatory

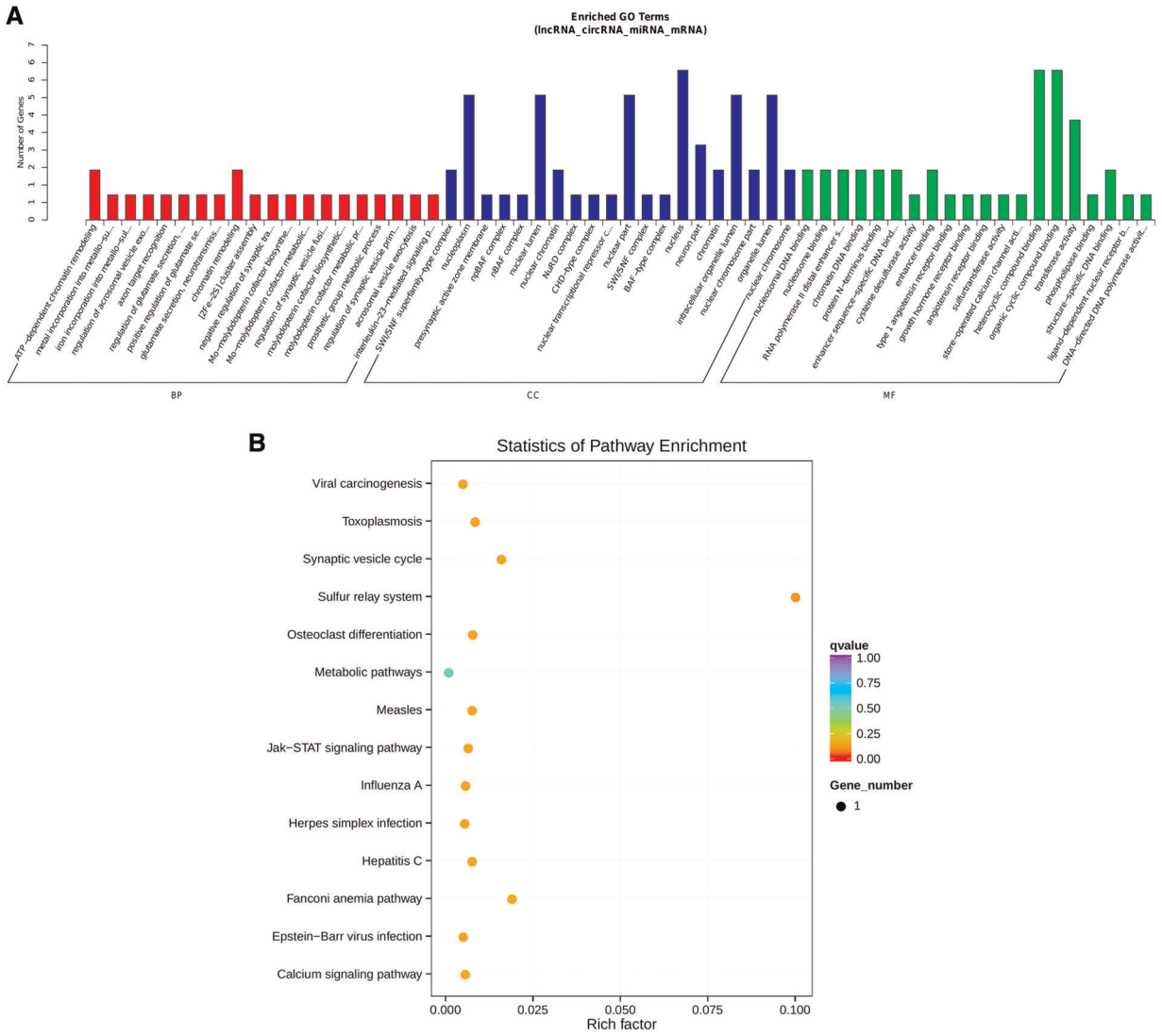

FIGURE 8
ceRNA regulatory network target gene enrichment analysis. (**A**) GO function enrichment bar chart of the top 20 enriched items. Abscissa denotes GO entry, BP, biological process; CC, cellular component; MF, molecular function represented by different color bars; ordinate is the number of genes enriched by GO entry. (**B**) KEGG pathway enrichment bubble diagram.

region, and structure-specific DNA binding were closely associated with the invasive NFPA. In this context, previous studies indicated that the oncoprotein Ras instigated the transcriptional silencing of Fas and other tumor suppressor genes by substantially binding to ZFP354B (a sequence-specific DNA-binding protein) (12). In addition, several recent reports presented that the tumor suppressor p53 was a sequence-specific DNA-binding protein that significantly activated the gene transcription to regulate the survival and proliferation of cells (13). These results suggested that the role of mRNAs in growth hormone-secreting pituitary adenomas (GHPA) might be significantly related to the sequence-specific DNA binding. In addition, the KEGG pathway analysis displayed that O-glycan synthesis, AMPK signaling pathway, osteoclast differentiation, and viral carcinogenesis were the most abundant pathways of the target genes. Specifically, AMPK is a heterotrimeric protein composed of α, β, and γ subunits, which can be activated by cellular stress, increasing the AMP levels by allosteric binding of AMP to the γ subunit and phosphorylation of Thr172 in the h subunit by serine/threonine kinase 11, calcium/calmodulin-dependent protein kinase, and transforming growth factor-b activated kinase (14–16). Notably, in a case, it was demonstrated that inhibiting AMPK signaling could reduce gonadotropin secretion in NFPA (17). To this end, O-polysaccharides also play critical roles in the malignant progression of tumors,

including promoting the migration, invasion, and metastasis of pancreatic cancer cells (18). Hence, mRNAs associated with invasive NFPA may play key roles through sequence-specific DNA binding and the AMPK signaling pathway.

Indeed, lncRNAs and circRNAs are considered molecular sponges of miRNAs due to the same miRNA-binding sites. In this regard, lncRNAs and circRNAs bind to the miRNAs and indirectly regulate the expressions of their downstream target genes through inhibition, representing a new relationship between ncRNAs and invasive NFPA. Therefore, a circRNA–lncRNA co-regulatory ceRNA network was constructed in this study. Specifically, miRNAs located between circRNAs/lncRNAs and mRNAs occupied the central position in the circRNA/lncRNA-miRNA-mRNA gene axis, indicating that these could significantly play essential roles in the treatment and diagnosis of diseases (19). In the present study, the down-regulated hsa-miR-1248 showed the highest degree of connectivity in the ceRNA regulatory network associated with invasive NFPA. Previous studies indicated that overexpression of thymidylate synthetase (TYMS) could suppress DNA synthesis and affect DNA methylation patterns, thus supporting cell proliferation, invasion, and tumor progression. In another case, it was demonstrated that hsa-miR-1248 bound to the 3′-untranslated region of the TYMS rs2790G allele and inhibited its expression in non-small cell lung cancer *in vitro* (20, 21), indirectly demonstrating a close relationship between hsa-miR-1248 and migration of tumors.

In this study, it was observed that hsa-miR-1285-3p, hsa-miR-4326, hsa-miR-4726-5p, hsa-miR-147b-5p, and hsa-miR-34a-5p showed high connectivity in the ceRNA regulatory network related to invasive NFPA. These miRNAs could regulate the expressions of various genes involved in many biological processes, including tumor cell proliferation, differentiation, migration, and invasion. Since the functionalities of these RNAs have been moderately confirmed, we believe that our results were in agreement with the findings of the previous studies indicating their potential roles in the invasive NFPA (22, 23). In this context, a report indicated that hsa-miR-1285-3p could directly inhibit the expression of the JUN oncogene in hepatocellular carcinoma (24). Further, it was validated and implied that hsa-miR-1285-3p could act as a potential tumor suppressor. In this study, the GO and KEGG analysis confirmed that the co-expressed mRNAs in circRNA-lncRNA co-regulated ceRNA network were closely related to the chromatin remodeling, as well as JAK-STAT signaling and calcium signaling pathways, involving in tumor cell proliferation, metastasis, invasion and immune regulation (25, 26). Together, these results confirmed that most circRNAs and lncRNAs in the ceRNA regulatory network were associated with tumor invasiveness.

Despite the success in constructing and analyzing the regulatory networks, the current study showcased some limitations in various aspects, as stated below. Firstly, the theoretical and experimental data for RNAs were insufficient, requiring further experiments to obtain more detailed information about the gene pathways and functions of the network. Secondly, the results were obtained from considerable a small sample size, requiring validation with larger sample size. Thirdly, more information about the mechanism of tumor invasion could be obtained by comparing NFPA with normal pituitary tissue. Finally, this study has just analyzed the invasiveness of NFPA with no exploration of details of tumor recurrence. Considerably, in addition to the above-notified investigations, addressing these limitations may provide new directions for further research.

Conclusions

In summary, we have systematically analyzed the correlation between ncRNAs and invasive NFPA by full-transcriptome sequencing. In addition, a ceRNA regulatory network characterized by abnormally expressed circRNAs/lncRNAs/miRNAs and mRNAs were established. It was observed that various genes, including SMARCE1, chromodomain helicase DNA binding protein 4 (CHD4), tyrosine kinase 2 (TYK2), and calcium release-activated calcium modulator 2 (ORAI2), were involved in the chromatin remodeling, JAK-STAT signaling, and calcium signaling pathways. These pathways might substantially play important roles in the pathogenesis of invasive NFPA. Together, these findings validated the complexity of the genome networks in the invasive NFPA, suggesting potential new therapeutic targets for patients with invasive NFPA.

Data availability statement

The authors acknowledge that the data presented in this study must be deposited and made publicly available in an acceptable repository, prior to publication. Frontiers cannot accept a manuscript that does not adhere to our open data policies.

Ethics statement

The studies involving human participants were reviewed and approved by Ethics Committee of Shanxi Provincial People's Hospital. The patients/participants provided their written informed consent to participate in this study.

Author contributions

JL, FL and CH conceived and designed the work and drafted the manuscript. HJ, GZ, SC, SZ and FL conceived and designed the work and revised the manuscript. KW acquired the data and participated the operation. CH performed the operation and approved the final version. All authors contributed to the article and approved the submitted version.

Funding

National Science Foundation of China (30901774); Natural Science Foundation of Shanxi Province (2014011038-2); Shanxi Province Science and Technology Development Plan (Social Development Section) (20140313011-5); Key R & D Plan of Shanxi Province (International Cooperation Project) (201803D421055); Shanxi Province Overseas Students Science and Technology Activities Selection Funding Project (2018014); Scientific Research Projects with Provincial Special Funds in Shanxi Provincial people's Hospital (sj20019003); Fundamental Research Program of Shanxi Province (20210302123352); Shanxi Province Health Commission Scientific Research Project (2022052), Research Project Supported by Shanxi Scholarship Council of China (2022-205), Four "Batches" Innovation Project of Invigorating Medical through Science and Technology of Shanxi Province (2022XM21).

Conflict of interest

The authors declare that the research was conducted in the absence of any commercial or financial relationships that could be construed as a potential conflict of interest.

Publisher's note

All claims expressed in this article are solely those of the authors and do not necessarily represent those of their affiliated organizations, or those of the publisher, the editors and the reviewers. Any product that may be evaluated in this article, or claim that may be made by its manufacturer, is not guaranteed or endorsed by the publisher.

References

1. Lekka E, Hall J. Noncoding RNAs in disease. *FEBS Lett*. (2018) 592:2884–900. doi: 10.1002/1873-3468.13182

2. Esteller M. Non-coding RNAs in human disease. *Nat Rev Genet*. (2011) 12:861–74. doi: 10.1038/nrg3074

3. Tay Y, Rinn J, Pandolfi PP. The multilayered complexity of ceRNA crosstalk and competition. *Nature*. (2014) 505:344–52. doi: 10.1038/nature12986

4. Wang Q, Cai J, Fang C, Yang C, Zhou J, Tan Y, et al. Mesenchymal glioblastoma constitutes a major ceRNA signature in the TGF-β pathway. *Theranostics*. (2018) 8:4733–49. doi: 10.7150/thno.26550

5. Wang Y, Liu X, Guan G, Xiao Z, Zhao W, Zhuang M. Identification of a five-pseudogene signature for predicting survival and its ceRNA network in glioma. *Front Oncol*. (2019) 9:1059. doi: 10.3389/fonc.2019.01059

6. Parkhomchuk D, Borodina T, Amstislavskiy V, Banaru M, Hallen L, Krobitsch S, et al. Transcriptome analysis by strand-specific sequencing of complementary DNA. *Nucleic Acids Res*. (2009) 37:e123. doi: 10.1093/nar/gkp596

7. Love MI, Huber W, Anders S. Moderated estimation of fold change and dispersion for RNA-seq data with DESeq2. *Genome Biol*. (2014) 15:550. doi: 10.1186/s13059-014-0550-8

8. Krüger J, Rehmsmeier M. RNAhybrid: microRNA target prediction easy, fast and flexible. *Nucleic Acids Res*. (2006) 34:W451–4. doi: 10.1093/nar/gkl243

9. Bo X, Wang S. Targetfinder: a software for antisense oligonucleotide target site selection based on MAST and secondary structures of target mRNA. *Bioinformatics*. (2005) 21:1401–2. doi: 10.1093/bioinformatics/bti211

10. John B, Enright AJ, Aravin A, Tuschl T, Sander C, Marks DS, et al. Human microRNA targets. *PLoS Biol*. (2004) 2:e363. doi: 10.1371/journal.pbio.0020363

11. Huang DW, Sherman BT, Lempicki RA. Systematic and integrative analysis of large gene lists using DAVID bioinformatics resources. *Nat Protoc*. (2009) 4:44–57. doi: 10.1038/nprot.2008.211

12. Wajapeyee N, Malonia SK, Palakurthy RK, Green MR. Oncogenic RAS directs silencing of tumor suppressor genes through ordered recruitment of transcriptional repressors. *Genes Dev*. (2013) 27:2221–6. doi: 10.1101/gad.227413.113

13. He F, Borcherds W, Song T, Wei X, Das M, Chen L, et al. Interaction between p53 N terminus and core domain regulates specific and nonspecific DNA binding. *Proc Natl Acad Sci U S A*. (2019) 116:8859–68. doi: 10.1073/pnas.1903077116

14. Carling D, Sanders MJ, Woods A. The regulation of AMP-activated protein kinase by upstream kinases. *Int J Obes*. (2008) 32(Suppl 4):S55–9. doi: 10.1038/ijo.2008.124

15. Kola B, Boscaro M, Rutter GA, Grossman AB, Korbonits M. Expanding role of AMPK in endocrinology. *Trends Endocrinol Metab*. (2006) 17:205–15. doi: 10.1016/j.tem.2006.05.006

16. Xie M, Zhang D, Dyck JR, Li Y, Zhang H, Morishima M, et al. A pivotal role for endogenous TGF-beta-activated kinase-1 in the LKB1/AMP-activated protein kinase energy-sensor pathway. *Proc Natl Acad Sci U S A*. (2006) 103:17378–83. doi: 10.1073/pnas.0604708103

17. Tosca L, Froment P, Rame C, McNeilly JR, McNeilly AS, Maillard V, et al. Metformin decreases GnRH- and activin-induced gonadotropin secretion in rat pituitary cells: potential involvement of adenosine 5′ monophosphate-activated protein kinase (PRKA). *Biol Reprod*. (2011) 84:351–62. doi: 10.1095/biolreprod.110.087023

18. Oliveira-Ferrer L, Legler K, Milde-Langosch K. Role of protein glycosylation in cancer metastasis. *Semin Cancer Biol*. (2017) 44:141–52. doi: 10.1016/j.semcancer.2017.03.002

19. Shoeibi S. Diagnostic and theranostic microRNAs in the pathogenesis of atherosclerosis. *Acta Physiol*. (2020) 228:e13353. doi: 10.1111/apha.13353

20. Chen M, Rahman L, Voeller D, Kastanos E, Yang SX, Feigenbaum L, et al. Transgenic expression of human thymidylate synthase accelerates the development of hyperplasia and tumors in the endocrine pancreas. *Oncogene*. (2007) 26:4817–24. doi: 10.1038/sj.onc.1210273

21. Xu J, Tian S, Yin Z, Wu S, Liu L, Qian Y, et al. MicroRNA-binding site SNPs in deregulated genes are associated with clinical outcome of non-small cell lung cancer. *Lung Cancer*. (2014) 85:442–8. doi: 10.1016/j.lungcan.2014.06.010

22. Xu H, Zhang Y, Qi L, Ding L, Jiang H, Yu H, et al. NFIX circular RNA promotes glioma progression by regulating miR-34a-5p via notch signaling pathway. *Front Mol Neurosci*. (2018) 11:225. doi: 10.3389/fnmol.2018.00225

23. Tayebi B, Abrishami F, Alizadeh S, Minayi N, Mohammadian M, Soleimani M, et al. Modulation of microRNAs expression in hematopoietic stem cells treated with sodium butyrate in inducing fetal hemoglobin expression. *Artif Cells Nanomed Biotechnol*. (2017) 45:146–56. doi: 10.3109/21691401.2016.1138487

24. Liu J, Yan J, Zhou C, Ma Q, Jin Q, Yang Z. miR-1285-3p acts as a potential tumor suppressor miRNA via downregulating JUN expression in hepatocellular carcinoma. *Tumour Biol*. (2015) 36:219–25. doi: 10.1007/s13277-014-2622-5

25. Xin P, Xu X, Deng C, Liu S, Wang Y, Zhou X, et al. The role of JAK/STAT signaling pathway and its inhibitors in diseases. *Int Immunopharmacol*. (2020) 80:106210. doi: 10.1016/j.intimp.2020.106210

26. Tateno T, Zhu X, Asa SL, Ezzat S. Chromatin remodeling and histone modifications in pituitary tumors. *Mol Cell Endocrinol*. (2010) 326:66–70. doi: 10.1016/j.mce.2009.12.028

frontiers | Frontiers in Surgery

TYPE Original Research
PUBLISHED 21 October 2022
DOI 10.3389/fsurg.2022.1007447

OPEN ACCESS

EDITED BY
Roberto Colasanti,
University Hospital of Padua, Italy

REVIEWED BY
Hamid Borghei-Razavi,
Cleveland Clinic Florida, United States
Bulent Omay,
Yale University, United States
Matteo De Notaris,
Azienda Ospedaliera San Pio di Benevento, Italy
Francesco Signorelli
The Catholic University of America,
United States

*CORRESPONDENCE
Alberto Di Somma
Albertodisomma87@gmail.com

SPECIALTY SECTION
This article was submitted to Neurosurgery, a section of the journal Frontiers in Surgery

RECEIVED 30 July 2022
ACCEPTED 21 September 2022
PUBLISHED 21 October 2022

CITATION
De Rosa A, Di Somma A, Mosteiro A, Ferrés A, Reyes LA, Roldan P, Torné R, Torales J, Solari D, Cavallo LM, Enseñat J and Prats-Galino A (2022) Superior eyelid endoscopic transorbital approach to the tentorial area: A qualitative and quantitative anatomic study.
Front. Surg. 9:1007447.
doi: 10.3389/fsurg.2022.1007447

Superior eyelid endoscopic transorbital approach to the tentorial area: A qualitative and quantitative anatomic study

Andrea De Rosa[1], Alberto Di Somma[2]*, Alejandra Mosteiro[2], Abel Ferrés[2], Luis Alberto Reyes[2], Pedro Roldan[2], Ramon Torné[2], Jorge Torales[2], Domenico Solari[1], Luigi Maria Cavallo[1], Joaquim Enseñat[2] and Alberto Prats-Galino[3,4]

[1]Division of Neurosurgery, Department of Neurosciences, Reproductive and Odontostomatological Sciences, Università degli Studi di Napoli "Federico II", Naples, Italy, [2]Department of Neurosurgery, Hospital Clinic, Barcelona, Spain, [3]Laboratory of Surgical Neuroanatomy, Faculty of Medicine, Universitat de Barcelona, Barcelona, Spain, [4]Research Group of Clinical Neurophysiology, Institut d'Investigacions Biomèdiques August Pi i Sunyer (IDIBAPS), Barcelona, Spain

Objective: Superior eyelid endoscopic transorbital approach (SETOA) is nowadays gaining progressive application in neurosurgical scenarios. Both anatomic and clinical reports have demonstrated the possibility of taking advantage of the orbital corridor as a minimally invasive route to reach anterior and middle cranial fossae and manage selected surgical lesions developing in these areas. The aim of this paper is to further shed light on other anatomic regions of the skull base as seen from a transorbital perspective, namely, the posterior cranial fossa and tentorial area, describing technical feasibility and steps in reaching this area through an extradural-transtentorial approach and providing quantitative evaluations of the "working area" obtained through this route.

Material and methods: Four cadaveric heads (eight sides) were dissected at the Laboratory of Surgical Neuroanatomy (LSNA) of the University of Barcelona, Spain. A stepwise dissection of the transorbital approach to the tentorial area was described. Qualitative anatomical descriptions and quantitative analyses of working were evaluated by using pre- and postdissections CT and MRI scans, and three-dimensional reconstructions were made using Amira software.

Results: With the endoscopic transorbital approach, posterior cranial fossa dura was reached by an extradural middle cranial fossa approach and drilling of the petrous apex. After clipping the superior petrosal sinus, the tentorium was divided and cut. An endoscope was then introduced in the posterior cranial fossa at the level of the tentorial incisura. Qualitative analysis provided a description of the tentorial and petrosal surfaces of the cerebellum, middle tentorial incisura, cerebellopontine fissures, and, after arachnoid dissection, by a 30° endoscopic visualization, the posterior aspect of the cerebellomesencephalic fissure. Quantitative analysis of the "working area" obtained after bone removal was also provided.

Conclusions: This anatomic qualitative and quantitative study sheds light on the anatomy of the posterior cranial fossa contents, such as the tentorial area and incisura, as seen through a transorbital perspective. The first aim of

the article is to enrich the anatomical knowledge as seen through this relatively new corridor and to provide quantitative details and insights into the technical feasibility of reaching these regions in a surgical scenario.

KEYWORDS

skull base, endoscopic, neurosurgery, brain tumors, basic and clinical research, transorbital approach

Introduction

The endoscopic transorbital approach is nowadays entering the neurosurgical armamentarium as a minimally invasive approach for the management of selected skull base lesions, primarily involving the orbit and the anterior and middle cranial fossae (1–3). Its application ended up in clinical settings starting from several anatomic studies investigating the feasibility of such an approach and shedding light on a different perception of the anatomy of the skull base as seen through a ventrolateral perspective. The anatomy of the posterior cranial fossa, and particularly tentorial incisura, has been initially described through a transorbital perspective by utilizing an intradural transtentorial route (4), but a quantitative evaluation of the working space obtained with this corridor has not been reported. The aim of this article is to describe further the anatomy of the posterior cranial fossa and tentorial incisura, reached by an extradural transorbital-transtentorial corridor, and to add detailed quantitative measures of the working area, expressed as the total available space that is exposed after dedicated bone removal and incision of the tentorium, achieved by this minimally invasive route.

Materials and methods

Anatomic dissections were performed at the Laboratory of Surgical NeuroAnatomy (University of Barcelona, Spain). Four specimens (eight orbits) were cleaned from blood clots, fixed with Cambridge solution, and injected with red and blue latex to highlight arterial and venous systems, respectively. Before and after dissection, all specimens underwent a multislice helical computed tomography (CT) scan (SIEMENS Somaton GoTop software version VA30A-SP03) with 0.5 mm thick axial spiral sections and a 0° gantry angle and an MRI study to obtain a 3D reconstruction of the main neurovascular structures. Endoscopic transorbital approaches were performed using a rigid endoscope of 4 mm diameter and 18 cm length, with 0° and 30° lenses (Karl Storz, Tuttlingen, Germany). The endoscope was connected to a light source through a fiber optic cable (300 W Xenon; Karl Storz) and to an HD camera (Endovision Telecam SL; Karl Storz). Data were uploaded to the Medtronic Workstation System to allow navigation guidance and point registration during dissection. A superior eyelid endoscopic transorbital approach was then performed as previously described (5–9).

Endoscopic transorbital approach

The specimen was placed in line with the position of the head during the surgical procedure, i.e., with the head in a neutral position, with a slight flexion 5°–10° toward the contralateral side of the approach, to position the lateral wall of the orbit in an optimal position for drilling during the "working space creation" phase. The dissection was accomplished with a four-hand technique in which one surgeon usually holds the endoscope and the aspirator, and the other one performs the dissection manually. This is also the technique we usually apply during surgery, without the need for pneumatic or automatic endoscope holders. The skin phase of the procedure was accomplished with the aim of an operating microscope. A curvilinear incision along an eyelid wrinkle, extended about 1.5 cm laterally, was performed. The skin, subcutaneous tissue, and orbicularis muscle were divided until the "white plane," made of the orbital septum and superior tarsus, was reached and respected (5). Dissection proceeded laterally to expose the lateral orbital rim, which was fully skeletonized. Temporalis muscle and fascia were detached from the lateral aspect of the orbital rim (**Figure 1**). Medially, the dissection was pursued in a subperiosteal fashion to detach the periorbita from the lateral wall of the orbit without violating it so that orbital fat tissue would not protrude into the surgical field. Zygomaticofacial and zygomaticotemporal arteries were identified and cut at the inferolateral border of the lateral wall of the orbit. Periorbita dissection proceeded until the inferior and superior orbital fissures were reached; at this point, the operative field was wide enough to allow the introduction of the endoscope. Drilling of the lateral wall of the orbit started until temporalis fascia was identified. Temporalis fascia and inferior and superior orbital fissures are the main anatomic landmarks in this phase, and their identification provides orientation during the drilling of the posterior portion of the lateral wall of the orbit, formed here by the greater sphenoid wing, to reach the ventral aspect of the middle cranial fossa finally. Drilling of the greater sphenoid wing proceeded until a "V"-shaped

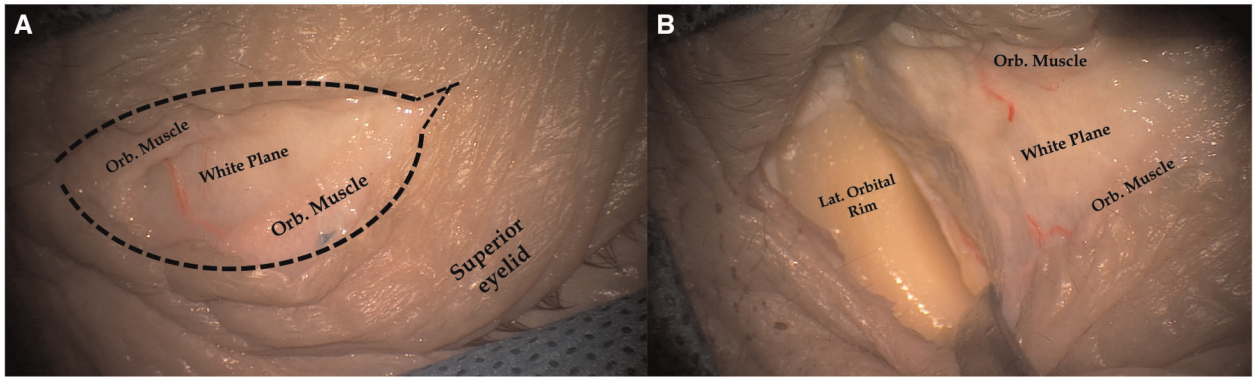

FIGURE 1
Pictures showing a skin incision for the endoscopic transorbital approach. The skin incision is run along a wrinkle of the superior eyelid. The orbicularis muscle is identified, and its fibers are separated, thus exposing the "white plane", which is formed by the orbital septum and superior tarsus and which represents the posterior limit of the dissection (**A**). Dissection proceeds laterally until the periosteum of the lateral orbital rim is reached and cut. After the lateral orbital rim is completely skeletonized, subperiosteal–subperiorbital dissection can be started (**B**). Black dotted line, skin incision; Orb. Muscle, orbitalis muscle; Lat. Orbital Rim, lateral orbital rim.

osseous wall is identified, limited medially by the sphenoid crest (10) (in the depth of the surgical field) and periorbita, laterally by the external surfaces of the greater sphenoid wing and temporal bone (in relationship with the temporalis muscle and fascia), inferiorly by the junction between the lateral wall and the floor of the orbit pointing at the inferior orbital fissure, and superiorly by the bone corresponding to the lesser sphenoid wing. Superomedially, the superior orbital fissure can be encountered.

Extradural middle cranial fossa-transtentorial approach

Once the dura mater covering the temporal pole was exposed at the center of the "V"-shaped osseous wall, bone removal proceeded medially at the level of the sagittal crest, leading to the meningo-orbital band (11), which was cut. At this point, temporal dura was peeled off the middle cranial fossa lateral wall and floor, exposing the foramen rotundum with maxillary division of the trigeminal nerve (V2), anteriorly and inferomedially, and *eminentia arcuata*, posteriorly and laterally (12). Before that, the mid-subtemporal ridge came into view. Peeling of the lateral wall of the cavernous sinus started from V2, exposing the ophthalmic division (V1) of the trigeminal nerve and the oculomotor nerve, all entering the superior orbital fissure. Peeling continued until the trigeminal ganglion (inside the Meckel cave) and petrous apex were reached (**Figure 2**).

Drilling and flattening of the floor of the middle fossa were then completed by removal of the mid-subtemporal ridge, behind which foramen spinosum and foramen *ovale* were identified. The middle meningeal artery was cut. The anterolateral surface of the petrous bone, from *eminentia arcuata* to the petrous apex, was thus exposed. After identification of the main anatomical landmarks defining the Kawase triangle, namely, V3 and trigeminal ganglion, anteriorly, the greater petrosal nerve, laterally, and the *eminentia arcuata*, posterolaterally, and after gentle medialization of trigeminal ganglion and V3, drilling of the petrous apex was started as previously described to enter posterior cranial fossa (13). Drilling of the petrous apex represents an important step during this approach to improve surgical visualization and maneuverability within the posterior cranial fossa (13). This step also facilitates superior sagittal sinus detachment and clipping and the subsequent tentorial incision. At this point, the endoscope was entered through the drilled portion of the petrous apex toward the posterior cranial fossa to identify the vestibulofacial bundle entering the internal acoustic meatus. This allows for additional bone removal at the level of the roof of the internal acoustic meatus. Dissection proceeded with isolation and cut of the superior petrosal sinus along the superior petrous ridge, in its more medial aspect.

Calculation of the working area

After the approach was completed and under endoscopic visualization, we used neuronavigation to collect coordinates delimitating the contours of the available space for surgical maneuverability within the middle and posterior cranial fossae, namely, the "working area." Such coordinates were then transferred to Amira software, where they were fused with the pre- and postdissection CT scan of the specimen. Through this software, we could then quantify and obtain a

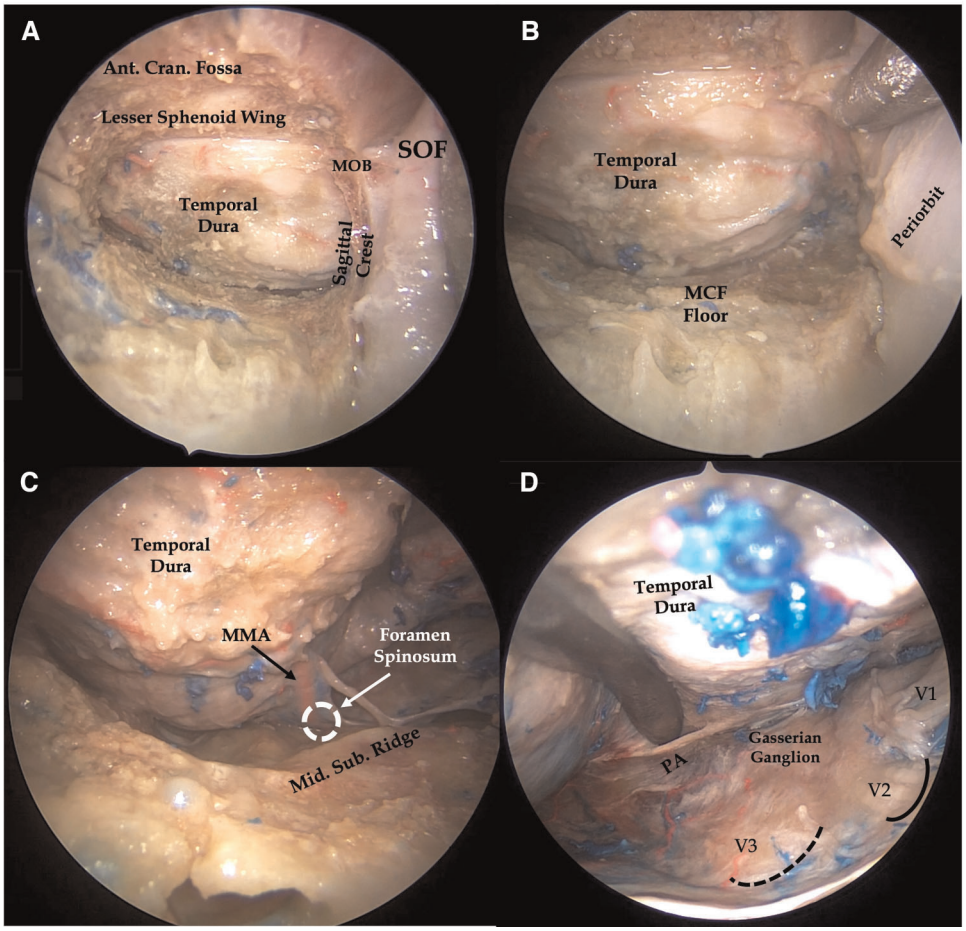

FIGURE 2
Right endoscopic transorbital approach to the middle cranial fossa. After removal of the anterior aspect of the greater sphenoid wing, the temporal dura is exposed (A) and peeled off from the middle fossa floor (B), which is further flattened. Once the foramen rotundum is exposed, peeling of the dura mater is started from V2, thus exposing the lateral wall of the cavernous sinus along with cranial nerves running within it. The middle meningeal artery, running through the foramen spinosum, is also identified and cut (C). Dura covering the middle fossa floor is then elevated posteriorly to expose the trigeminal ganglion and petrous apex (D). III, third cranial nerve; V1, ophthalmic division of trigeminal nerve; V2, maxillary division of the trigeminal nerve; V3, Mandibular division of trigeminal nerve; MCF Floor, middle cranial fossa floor; Mid. Sub. Ridge, midsubtemporal ridge; MMA, middle meningeal artery; MOB, meningo-orbital band; PA, petrous apex; black dotted line, foramen ovale; continuous black line, foramen rotundum.

3D reconstruction of the area comprised within the points collected. The procedure was applied to each side of each specimen.

Results

Qualitative analysis

Once the superior petrosal sinus was identified and dissected from the superior petrosal ridge, two surgical clips were positioned, from lateral to medial, starting from right medial to the level of the internal acoustic meatus. Tentorium was cut starting in between the two surgical clips, given that the trochlear nerve was expected to enter the free margin of the tentorium far more anteriorly. The tentorial incision was then extended in a posterior and medial direction (Figures 3, 4).

After the tentorium incision, the tentorial surface of the cerebellum, along with terminal branches of the superior cerebellar artery, came into view. At the most anterior part of the field, the superior petrosal vein, or Dandy vein, and its junction with the superior petrosal sinus could be visualized. By detaching and elevating the tentorium medially, the tentorial incisura, and particularly the middle incisural space below the free tentorial edge, corresponding to the ambient cistern, could be exposed. After arachnoid dissection, the cisternal portion of the trochlear nerve, running along the superior margin of the main trunk of the superior cerebellar

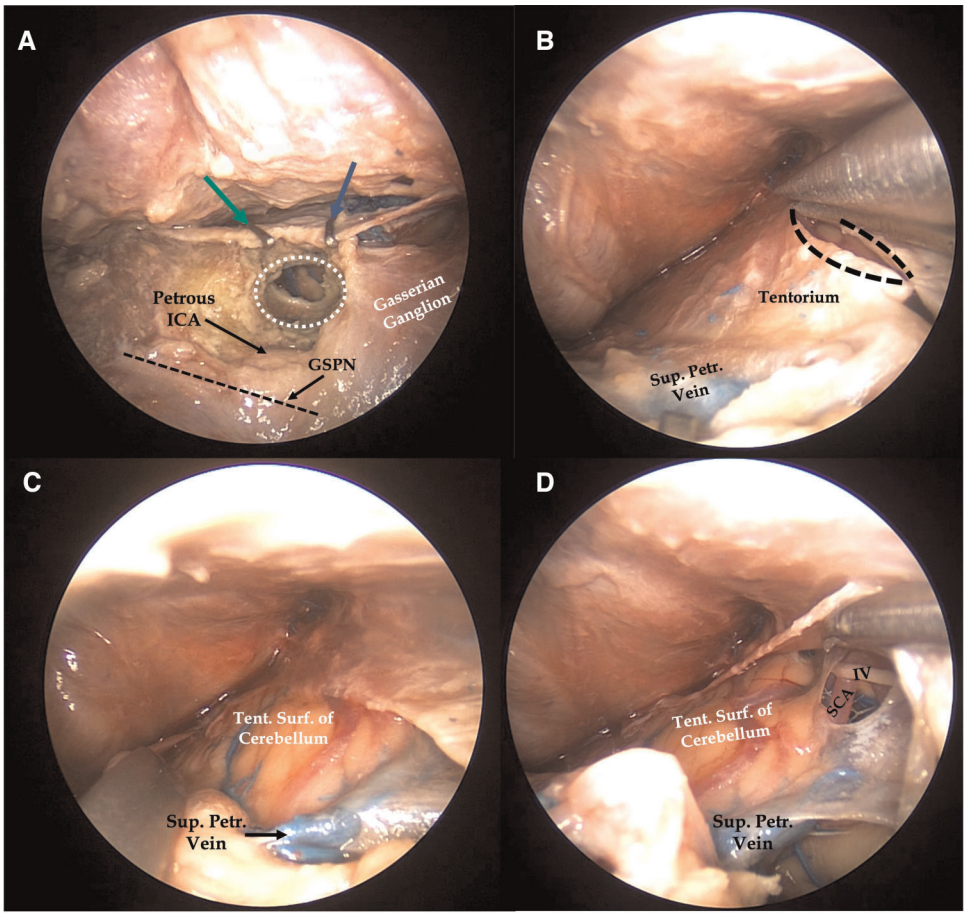

FIGURE 3
Right endoscopic transorbital approach to the tentorial incisura. After exposure of the petrous apex, two surgical clips (green and blue arrows) are positioned to the superior petrosal sinus before the tentorium cut. After identification of the anatomical landmark of Kawase's quadrilateral, the petrous apex is drilled (**A**). Tentorium cut is extended posteriorly from the area of the superior petrosal sinus closed by the surgical clips (**B**), thus exposing the tentorial surface of the cerebellum, laterally (**C**), and the middle tentorial incisura, medially (**D**). White dotted area, petrous apex removed after drilling; straight dark dotted line, course of the greater superficial petrosal nerve; curved dark dotted lines, margins of tentorium after the cut; IV, trochlear nerve; GSPN, greater superficial petrosal nerve; Petrous ICA, petrous segment of the internal carotid artery; SCA, superior cerebellar artery; Sup. Petr. Vein, superior petrosal vein; Tent. Surf. of Cerebellum, tentorial surface of the cerebellum.

artery, came into view. Below the superior cerebellar artery, the ponto-mesencephalic fissure was visualized and, at the most anterior and medial part of the field, the trigeminal root, emerging from the mid part of the pons, appeared with its superior and lateral direction, before leaning on the trigeminal impression of the petrous bone and entering the Meckel cave in the middle fossa. The transverse pontine vein, in relation to the emerging root of the trigeminal nerve, and the vein of cerebellopontine fissure were also appreciated. With a 30° endoscope, by directing the light inferomedially, the vestibulofacial bundle was highlighted (**Figure 5**).

We pushed our arachnoid dissection forward by opening the cerebellopontine cistern, limited laterally by the petrosal surface of the cerebellum and medially by the middle cerebellar peduncle. By dividing the anteromedial border of the cerebellum laterally and moving a 30° endoscope in the deep of the cistern, along the upper border of the middle cerebellar peduncle, the posterior-most aspect of the cerebellomesencephalic fissure was reached. In this space, we could evaluate the posterior margin of the fissure, limited by the lingula of the cerebellum, which lies above the superior medullary velum. This region corresponds to the cisternal (external) surface of the upper part of the roof of the fourth ventricle (**Figure 6**) (Video 1).

Quantitative analysis

The working area was defined as the available surface of surgical maneuverability after extensive bone drilling of

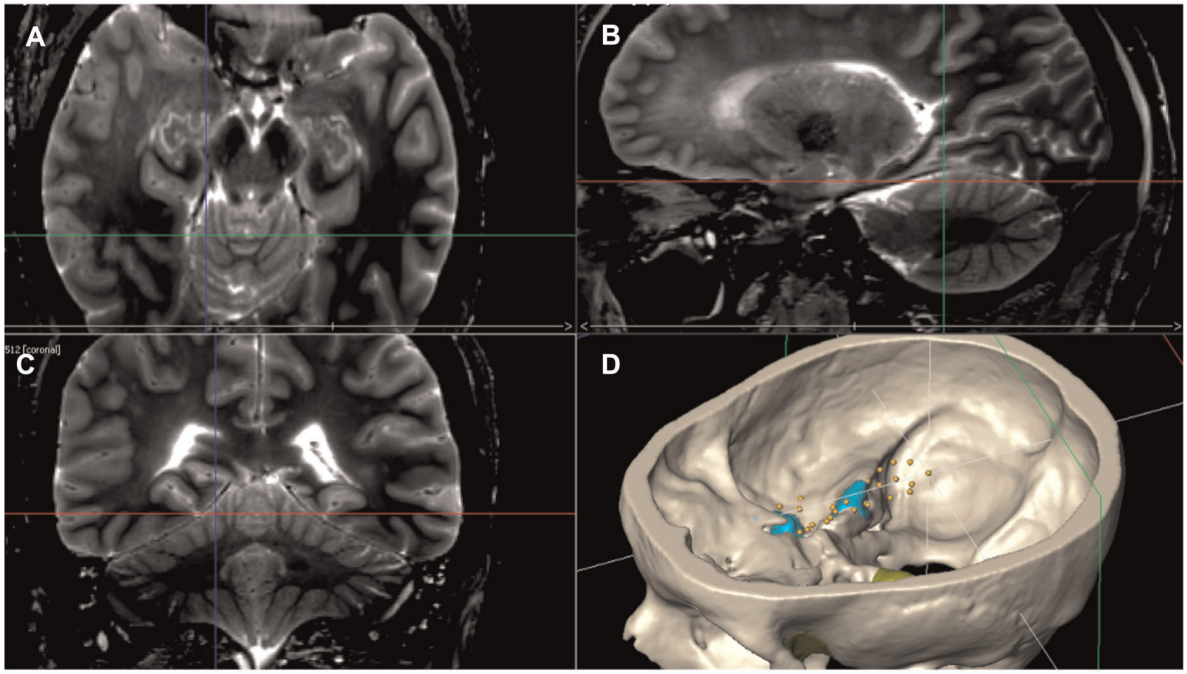

FIGURE 4
Pictures retrieved from neuronavigation axial (A), sagittal (B), and coronal (C) T2 MRI scans of one specimen and from Amira software reconstruction (D) of the same specimen indicating the posterior limit of the tentorial cut.

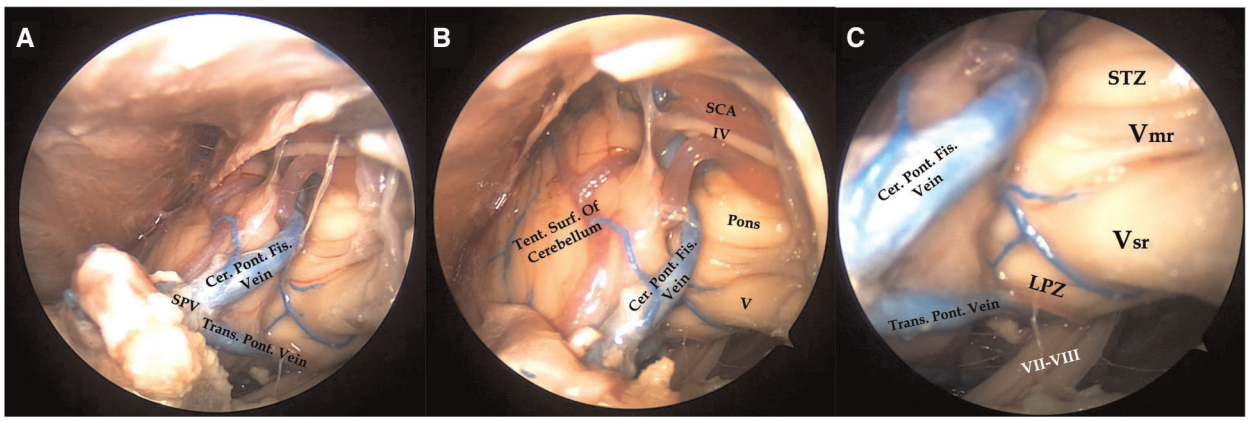

FIGURE 5
Right endoscopic transorbital approach to the tentorial incisura. After superomedial retraction of the margin of the tentorium, the contents of the middle incisural space are exposed (A). Cisternal segment of the trochlear nerve running along the superior surface of the superior cerebellar artery, lateral surface of the pons, the origin of the trigeminal root, and vein of the cerebellopontine fissure joining to the superior petrosal vein are visualized (B). By means of a 30° lens, directing the endoscope inferomedially, the vestibulofacial bundle is exposed in its course to the internal acoustic meatus, along with the transverse pontine vein joining the superior petrosal vein (C). IV, trochlear nerve; V, trigeminal nerve; Vsr, sensory root of the trigeminal nerve; Vmr, motor rootlets of the trigeminal nerve; VII–VIII, vestibulofacial bundle; Cer. Pon. Fis. Vein, Cerebellopontine fissure vein; LPZ, lateral pontine zone; SCA, superior cerebellar artery; SPV, superior petrosal vein; STZ, supratrigeminal zone; Tent. Surf. of Cerebellum, tentorial surface of the cerebellum; Trans. Pon. Vein, transverse pontine vein.

the middle cranial fossa floor and of the petrous apex, and tentorial incisions were achieved. This area includes a larger amount of the middle cranial fossa and a lesser amount of the posterior cranial fossa, which is reached out after tentorial incision and division. We obtained eight measures from our four specimens (Table 1), and the mean value was 2,800.52 mm^3 (SD ± 364.28) (Figures 7, 8).

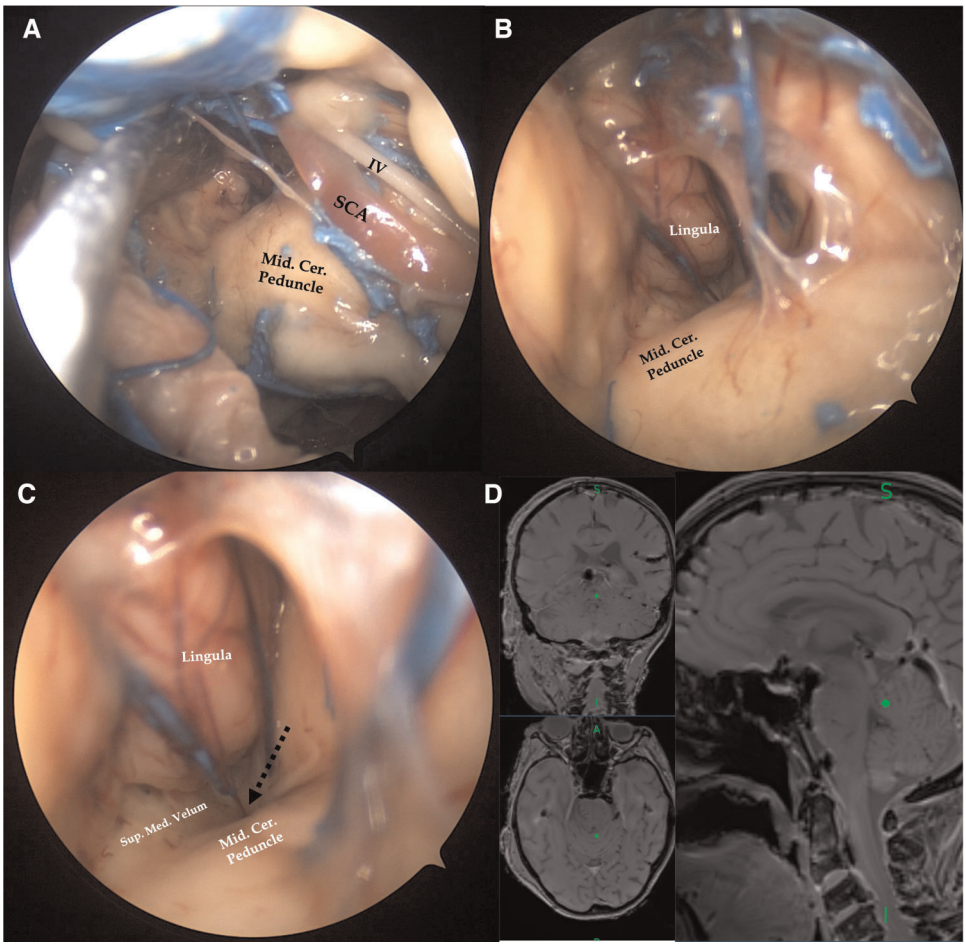

FIGURE 6
Right endoscopic transorbital exposure of the tentorial incisura and cerebellomesencephalic fissure. Extending forward arachnoid dissection of the cerebellopontine fissure, the middle cerebellar peduncle is divided from the petrosal surface of the cerebellum (**A**). By inserting a 30°endoscope along the superior margin of the middle cerebellar peduncle and directing the light inferiorly, the posterior margin of the cerebellomesencephalic fissure, represented by the lingula of the cerebellum, and the external surface of the superior part of the roof of the fourth ventricle (black dotted arrow), represented by the superior medullary velum, are visualized (**B**,**C**). We confirmed our anatomic findings by pointing the navigator (Medtronic StealthStation) at the level of the lingula (**D**). IV, cisternal portion of the trochlear nerve; Mid.Cer.Peduncle, middle cerebellar peduncle; SCA, superior cerebellar artery; Sup.Med.Velum, superior medullary velum.

Discussion

Since its introduction, in the last 10 years, transorbital endoscopic surgery has been increasingly utilized in the neurosurgical field as an alternative to standard craniotomies to manage selected lesions of the skull base (8). In its early applications, this minimally invasive corridor was proposed as an adjunct to the well-known endoscopic endonasal corridor to reach the lateral-most portion of central skull base lesions with large parasellar extension (14). Anatomic studies have helped in improving the knowledge of anatomy as seen through the ventral perspective provided by the transorbital route: anterior and middle cranial fossa compartments, along with the optocarotid region, sylvian fissure, cavernous sinus,

TABLE 1 Quantitative analysis of the available "working area" within the posterior and middle cranial fossa, obtained after complete bone removal through the endoscopic transorbital approach.

Specimen	Side	Working area (mm^3)
1	Right	3,432.64
	Left	2,296.15
2	Right	2,916.45
	Left	2,726.27
3	Right	3,009.62
	Left	2,422.02
4	Right	2,986.30
	Left	2,614.74
Mean (mm^3)		2,800.52
Standard deviation		±364.28

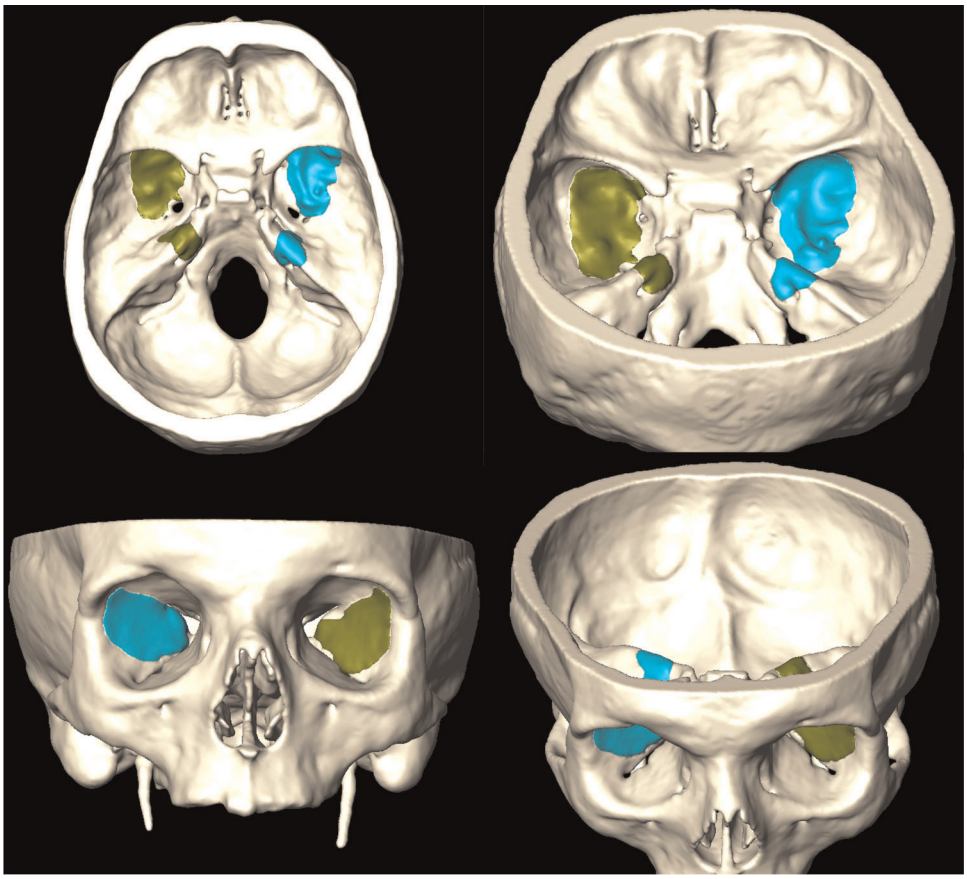

FIGURE 7
Amira software 3D reconstructions from postdissection CT scans, highlighting the amount of bone removal at the level of the middle cranial fossa and petrous apex.

Meckel cave, and petrous apex, have been extensively described (10, 11, 13, 15–20). As neurosurgeons became more familiar with this new anatomic perspective, surgical applications and indications of the endoscopic transorbital approach, alone or in combination with other minimally invasive corridors, namely, the endonasal one, extended to the removal of several skull base lesions, both intradural and extradural, such as intraorbital lesions, intraparenchymal temporal lesions, cavernous sinus meningiomas, trigeminal schwannomas, spheno-orbital meningiomas, middle cranial fossa meningiomas, and petroclival meningiomas (6, 7, 21–27). Recently, as a resume to the collected pearls and pitfalls of this approach, a classification of the levels of difficulty of the endoscopic transorbital approach for the management of different lesions has been proposed, pointing out the steps of the learning curve that the neurosurgeon must gain to minimize complications and achieve better patient outcomes (28). Tentorial incisura is one of the most challenging regions to reach, and, given the variety of its content, it could be the site of many kinds of lesions, such as trigeminal schwannomas, petroclival and tentorial meningiomas, and brainstem lesions. Many transcranial approaches are nowadays considered the gold standard to gain access to this region; among the others are the anterior and posterior petrosal, occipital-transtentorial, and supracerebellar-infratentorial approaches together with their modifications (29–36).

In a recent paper by Vasquez et al. (37), four different transcranial approaches, namely, frontotemporal transsylvian transtentorial (38, 39), subtemporal transtentorial (40, 41), posterior petrosectomy (42), and combined posterior suprainfratentorial transsinus approaches (43), addressed to the tentorial region and with the common step of splitting the tentorium to gain a wider visualization, were compared in terms of area of exposure. The transsylvian transtentorial approach provided a limited area of visualization of the most anterior portion of the tentorial incisura, with the potential complication of injury to the oculomotor nerve along its course under the tentorium. The subtemporal approach, with the addition of petrosectomy as described by Kawase, provides a wider exposure of the middle tentorial incisura, after

10.3389/fsurg.2022.1007447

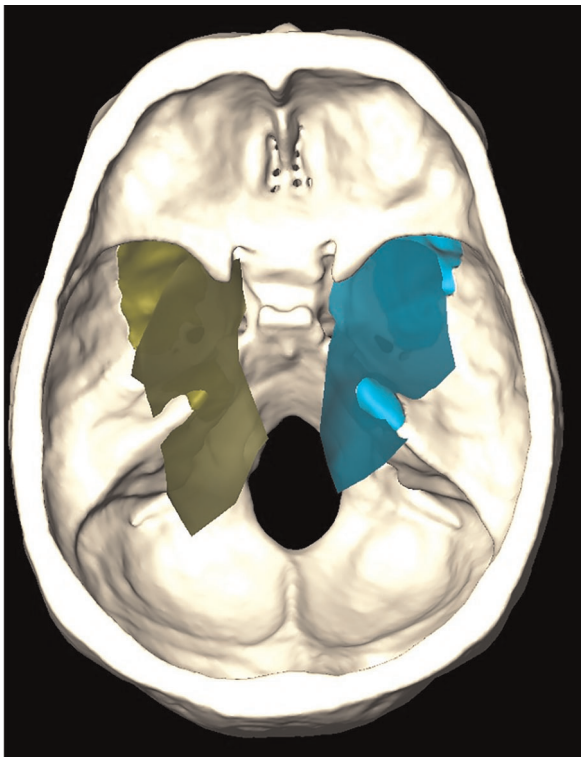

FIGURE 8
Amira software 3D reconstruction showing the working area (superimposed shaded green and blue areas) at the level of the middle and posterior cranial fossae, which can be obtained after bone removal (darker underimposed green and blue areas).

tentorium is cut, with the main disadvantages represented by the retraction of the temporal lobe. With the posterior petrosectomy, the area of visualization is further enhanced because exposure from the midbrain, superiorly, to the lower cranial nerve, inferiorly, is possible but with the risk of injury to the venous sinuses and vein of Labbé, to the labyrinth and cochlea, and still to the temporal lobe because of sustained retraction. The combined posterior supra/infratentorial-transsinus approach allows for a wide visualization of the posterior portion of the tentorial incisura and pineal region, with the main drawback being represented by the need for transecting the nondominant transverse sinus during the approach (37).

In this scenario, we aim to describe the anatomy of the tentorial incisura through an endoscopic extradural-middle cranial fossa-transtentorial transorbital approach and quantify the amount of available working area that is obtained after extensive bone work and tentorial incision. Middle tentorial incisura could be reached in a completely extradural fashion, and extensive drilling of the middle fossa floor and the petrous apex provided the surgical maneuverability to detach and clip the superior petrosal sinus and then open the tentorium. Tentorial incision and opening can be achieved away from the entry point of the trochlear nerve. With a 0°-lens endoscope, the inferior portion of the middle tentorial incisura, corresponding to the ambiens cistern, can be visualized. The surgical exposure is limited medially by the trigeminal root, superiorly by the free edge of the tentorium, which also limits the exposure of the superior compartment of the middle incisura, laterally by the tentorial surface of the cerebellum, and inferiorly by a plane parallel to the petrous bone. We observed that surgical maneuverability could be furtherly improved by drilling the superolateral aspect of the petrous apex, corresponding to the roof of the internal acoustic meatus, a procedure that must be accomplished only when vestibulocochlear and facial nerves are identified in their course to the internal acoustic meatus (suprameatal drilling). The lateral surface of the mesencephalon and pons, along with the origin of the trigeminal nerve, the superior cerebellar artery along with the trochlear nerve crossing the ambiens cistern, can be exposed. With the aim of a 30°-lens endoscope, pointing inferomedially, the prepontine cistern can also be visualized. Furthermore, arachnoid dissection between the petrosal surface of the cerebellum and pons allows for the opening of the cerebellopontine fissure, which can be entered following the superior aspect of the middle cerebellar peduncle until the dorsal aspect of the pons is reached. This region corresponds to the cerebellomesencephalic fissure, limited posteriorly by the lingula of the cerebellum, inferiorly by the superior medullary velum, and anteriorly by the posterior surface of the midbrain.

Recently, Lin et al. already described the anatomy of the middle tentorial incisura through an intradural transsylvian transorbital approach (4). In their article, the middle tentorial incisura is reached after exposure of both anterior and middle cranial fossa and resection of the anterior clinoid. Then, after the temporal dural incision, an intradural corridor between the cavernous sinus, medially, and the medial temporal lobe, laterally, is used to gain access to the tentorial incisura. We propose a different pathway to reach this region in a complete extradural fashion, thus limiting the manipulation of the temporal lobe intradurally and avoiding the dissection of the arterial vasculature around the mesial temporal lobe. However, a more anterior exposure of the crural and interpeduncular cistern, which was described by the authors, was not exposed with our corridor.

Even though our contribution is a purely anatomic description, we think that, according to the results of quantitative analysis of the working area obtained after the approach, some considerations can be made regarding the clinical applicability of the transorbital route directed at the tentorial incision. Because of the working space that can be obtained if extensive drilling of the middle fossa floor and petrous apex is achieved, tumors extending from the middle fossa and projecting into the middle tentorial incisura, such as meningiomas arising from the dura mater surrounding the region of the tentorial incisura, with a medial and inferior extension could be reached with this kind of approach

(probably in combination with the endonasal route). Furthermore, if limited, brainstem exposure also provides access to two safe entry zones of the pons (44), namely, the lateral pontine zone and supratrigeminal zone. Compared to the more conventional transcranial route, the advantages of this approach would be represented by minimal soft tissue manipulation, the absence of a visible scar (performing the skin incision in a wrinkle of the superior eyelid allows to hide the surgical wound when the patient is with opened eyes), which translates in a better aesthetic outcome for the patient, and the minimal temporal lobe retraction needed to reach the tentorial area. On the other hand, lesser surgical maneuverability provides a remarkable drawback in managing venous or arterial bleeding, a concept shared with any endoscopic skull base technique. Nevertheless, we are aware that clinical experience with the transtentorial extension of the endoscopic transorbital approach is still lacking and it would require great surgeon's expertise and specific instrumentation to be safely perfromed; endoscopic transorbital surgery in the posterior cranial fossa is indeed classified as the final step (Level 5 of difficulty) in the classification recently proposed (28). It must also be stressed that even if this corridor provides a minimally invasive alternative to standard craniotomies, thus avoiding complications related to these approaches such as brain retraction and contusion, venous infarction, soft-tissue complications related to craniotomy, the improving clinical experience suggests that ophthalmologic and visual complications remain one the main concerns of this surgical strategy, even if permanent visual alterations have been rarely described until now (45). Concerning cerebrospinal fluid leak, which is one of the main complications related to the endoscopic endonasal corridor, does not seem to be a frequent sequela of the transorbital route since, at the end of the procedure, tight closure can be achieved for all the tissue layers.

Study limitations

We are aware that, as it happens with cadaveric anatomical study, differences in tissue consistency, the absence of bleeding, which could be present, for example, during middle cranial fossa floor drilling or during tentorium cut and elevation, and the tolerance to retraction all make anatomic results difficult to translate into clinical applications. Our contribution should be interpreted as an adjunct to the available knowledge of anatomy as seen from this ventral perspective. Furthermore, the design of our article was not intended to provide a comparison between the perspectives given by the endoscopic transorbital approach and other transcranial approaches that are used to reach the tentorial area. We think that such a comparison would have added important information about the pros and cons of different surgical strategies. Future studies are already planned to address this issue.

Conclusions

In this article, we provided an anatomical description of the middle incisural space as seen through an endoscopic transorbital perspective and a quantification of the working area that can be obtained. In particular, we propose a purely extradural-middle cranial fossa approach to reach and cut the tentorium. We observed that adequate "bone work" on the middle cranial fossa floor and petrous apex provides adequate working space for surgical maneuverability in this deep-seated region of the skull base. Further anatomical contributions, comparing this corridor to the standard transcranial approaches, and clinical reports are necessary to highlight the possible advantages and indications of this technique.

Data availability statement

The raw data supporting the conclusions of this article will be made available by the authors, without undue reservation.

Author contributions

AS and AR contributed to the conception and design of the study. AR, AM, and AS performed anatomic dissections. AP-G performed data analyses and 3D reconstructions. AR wrote the first draft of the manuscript. AF, LR, PR, JT, and RT wrote sections of the manuscript. AS, DS, LC, JE, and AP-G reviewed and edited the manuscript. All authors contributed to the article and approved the submitted version.

Funding

This study has been funded by the Instituto de Salud Carlos III (ISCIII) through project PI19/00592 and cofunded by the European Union; it has also been funded by the "Fundació La Marató de TV3" (Reg. 95/210; Codi projecte 201914).

Conflict of interest

The authors declare that the research was conducted in the absence of any commercial or financial relationships that could be construed as a potential conflict of interest.

Publisher's note

All claims expressed in this article are solely those of the authors and do not necessarily represent those of

their affiliated organizations, or those of the publisher, the editors and the reviewers. Any product that may be evaluated in this article, or claim that may be made by its manufacturer, is not guaranteed or endorsed by the publisher.

Supplementary material

The Supplementary Material for this article can be found online at: https://www.frontiersin.org/articles/10.3389/fsurg.2022.1007447/full#supplementary-material.

References

1. Di Somma A, Guizzardi G, Valls Cusiné C, Hoyos J, Ferres A, Topczewski TE, et al. Combined endoscopic endonasal and transorbital approach to skull base tumors: a systematic literature review. *J Neurosurg Sci*. (2021). [Epub ahead of print]

2. Vural A, Carobbio ALC, Ferrari M, Rampinelli V, Schreiber A, Mattavelli D, et al. Transorbital endoscopic approaches to the skull base: a systematic literature review and anatomical description. *Neurosurg Rev*. (2021) 44(5):2857–78. doi: 10.1007/s10143-020-01470-5

3. Lee WJ, Hong SD, Woo KI, Seol HJ, Choi JW, Lee JI, et al. Combined endoscopic endonasal and transorbital multiportal approach for complex skull base lesions involving multiple compartments. *Acta Neurochir (Wien)*. (2022) 164(7):1911–22. doi: 10.1007/s00701-022-05203-z

4. Lin BJ, Hong KT, Chung TT, Liu WH, Hueng DY, Chen YH, et al. Endoscopic transorbital transtentorial approach to middle incisural space: preclinical cadaveric study. *Acta Neurochir (Wien)*. (2019) 161(4):831–9. doi: 10.1007/s00701-019-03831-6

5. Di Somma A, Sanchez España JC, Alobid I, Enseñat J. Endoscopic superior eyelid transorbital approach: how I do it. *Acta Neurochir (Wien)*. (2022) 164(7):1953–9. doi: 10.1007/s00701-022-05177-y

6. Almeida JP, Omay SB, Shetty SR, Chen YN, Ruiz-Treviño AS, Liang B, et al. Transorbital endoscopic eyelid approach for resection of sphenoorbital meningiomas with predominant hyperostosis: report of 2 cases. *J Neurosurg*. (2018) 128(6):1885–95. doi: 10.3171/2017.3.JNS163110

7. Dallan I, Sellari-Franceschini S, Turri-Zanoni M, de Notaris M, Fiacchini G, Fiorini FR, et al. Endoscopic transorbital superior eyelid approach for the management of selected spheno-orbital meningiomas: preliminary experience. *Oper Neurosurg (Hagerstown)*. (2018) 14(3):243–51. doi: 10.1093/ons/opx100

8. Moe KS, Bergeron CM, Ellenbogen RG. Transorbital neuroendoscopic surgery. *Neurosurgery*. (2010) 67(3 Suppl Operative):ons16–28.

9. Di Somma A, Andaluz N, Cavallo LM, de Notaris M, Dallan I, Solari D, et al. Endoscopic transorbital superior eyelid approach: anatomical study from a neurosurgical perspective. *J Neurosurg*. (2018) 129(5):1203–16. doi: 10.3171/2017.4.JNS162749

10. Corrivetti F, de Notaris M, Di Somma A, Dallan I, Enseñat J, Topczewski T, et al. "Sagittal crest": definition, stepwise dissection, and clinical implications from a transorbital perspective. *Oper Neurosurg (Hagerstown)*. (2022) 22(5):e206–12. doi: 10.1227/ons.0000000000000131

11. Dallan I, Di Somma A, Prats-Galino A, Solari D, Alobid I, Turri-Zanoni M, et al. Endoscopic transorbital route to the cavernous sinus through the meningo-orbital band: a descriptive anatomical study. *J Neurosurg*. (2017) 127(3):622–9. doi: 10.3171/2016.8.JNS16465

12. Guizzardi G, Mosteiro A, Hoyos J, Ferres A, Topczewski T, Reyes L, et al. Endoscopic transorbital approach to the middle Fossa: qualitative and quantitative anatomic study. *Oper Neurosurg*. (2022) 23(4):e267–75. doi: 10.1227/ons.0000000000000308

13. Di Somma A, Andaluz N, Cavallo LM, Topczewski TE, Frio F, Gerardi RM, et al. Endoscopic transorbital route to the petrous apex: a feasibility anatomic study. *Acta Neurochir (Wien)*. (2018) 160(4):707–20. doi: 10.1007/s00701-017-3448-x

14. Koutourousiou M, Gardner PA, Stefko ST, Paluzzi A, Fernandez-Miranda JC, Snyderman CH, et al. Combined endoscopic endonasal transorbital approach with transconjunctival-medial orbitotomy for excisional biopsy of the optic nerve: technical note. *J Neurol Surg Rep*. (2012) 73(1):52–6. doi: 10.1055/s-0032-1323156

15. Di Somma A, Cavallo LM, de Notaris M, Solari D, Topczewski TE, Bernal-Sprekelsen M, et al. Endoscopic endonasal medial-to-lateral and transorbital lateral-to-medial optic nerve decompression: an anatomical study with surgical implications. *J Neurosurg*. (2017) 127(1):199–208. doi: 10.3171/2016.8.JNS16566

16. Almeida JP, Ruiz-Treviño AS, Shetty SR, Omay SB, Anand VK, Schwartz TH. Transorbital endoscopic approach for exposure of the sylvian fissure, middle cerebral artery and crural cistern: an anatomical study. *Acta Neurochir (Wien)*. (2017) 159(10):1893–907. doi: 10.1007/s00701-017-3296-8

17. Priddy BH, Nunes CF, Beer-Furlan A, Carrau R, Dallan I, Prevedello DM-S. A side door to meckel's cave: anatomic feasibility study for the lateral transorbital approach. *Oper. Neurosurg*. (2017) 13(5):614–21. doi: 10.1093/ons/opx042

18. De Rosa A, Pineda J, Cavallo LM, Di Somma A, Romano A, Topczewski TE, et al. Endoscopic endo- and extra-orbital corridors for spheno-orbital region: anatomic study with illustrative case. *Acta Neurochir (Wien)*. (2019) 161(8):1633–46. doi: 10.1007/s00701-019-03939-9

19. Nannavecchia BA, Ganau M, Cebula H, Scibilia A, Bozzi MT, Zaed I, et al. Endoscopic transorbital approaches to anterior and middle cranial fossa: a laboratory investigation on surgical anatomy and potential routes. *J Neurol Surg B Skull Base*. (2020) 82(4):443–9. doi: 10.1055/s-0040-1713101

20. López CB, Di Somma A, Cepeda S, Arrese I, Sarabia R, Agustín JH, et al. Extradural anterior clinoidectomy through endoscopic transorbital approach: laboratory investigation for surgical perspective. *Acta Neurochir (Wien)*. (2021) 163(8):2177–88. doi: 10.1007/s00701-021-04896-y

21. Chen HI, Bohman LE, Loevner LA, Lucas TH. Transorbital endoscopic amygdalohippocampectomy: a feasibility investigation. *J Neurosurg*. (2014) 120(6):1428–36. doi: 10.3171/2014.2.JNS131060

22. Dallan I, Castelnuovo P, Locatelli D, Turri-Zanoni M, AlQahtani A, Battaglia P, et al. Multiportal combined transorbital transnasal endoscopic approach for the management of selected skull base lesions: preliminary experience. *World Neurosurg*. (2015) 84(1):97–107. doi: 10.1016/j.wneu.2015.02.034

23. Jeon C, Hong CK, Woo KI, Hong SD, Nam DH, Lee JI, et al. Endoscopic transorbital surgery for Meckel's cave and middle cranial fossa tumors: surgical technique and early results. *J Neurosurg*. (2018):1–10. doi: 10.3171/2018.6.JNS181099

24. Park HH, Hong SD, Kim YH, Hong CK, Woo KI, Yun IS, et al. Endoscopic transorbital and endonasal approach for trigeminal schwannomas: a retrospective multicenter analysis (KOSEN-005). *J Neurosurg*. (2020) 133(2):467–76. doi: 10.3171/2019.3.JNS19492

25. Di Somma A, Langdon C, de Notaris M, Reyes L, Ortiz-Perez S, Alobid I, et al. Combined and simultaneous endoscopic endonasal and transorbital surgery for a Meckel's cave schwannoma: technical nuances of a mini-invasive, multiportal approach. *J Neurosurg*. (2020) 134(6):1836–45. doi: 10.3171/2020.4.JNS20707

26. Kim EH, Yoo J, Jung IH, Oh JW, Kim JS, Yoon JS, et al. Endoscopic transorbital approach to the insular region: cadaveric feasibility study and clinical application (SevEN-005). *J Neurosurg*. (2021):1–9. doi: 10.3171/2020.8.JNS202255

27. Park HH, Roh TH, Choi S, Yoo J, Kim WH, Jung IH, et al. Endoscopic transorbital approach to mesial temporal lobe for intra-axial lesions: cadaveric study and case series (SevEN-008). *Oper Neurosurg (Hagerstown)*. (2021) 21(6):E506–E15. doi: 10.1093/ons/opab319

28. Di Somma A, Kong DS, de Notaris M, Moe KS, Sánchez España JC, Schwartz TH, et al. Endoscopic transorbital surgery levels of difficulty. *J Neurosurg*. (2022) 137(4):1187–90. doi: 10.3171/2022.3.JNS212699

29. Giammattei L, Starnoni D, Benes V, Froelich S, Cossu G, Borsotti F, et al. Extreme lateral supracerebellar infratentorial approach: surgical anatomy and review of the literature. *World Neurosurg*. (2021) 147:89–104. doi: 10.1016/j.wneu.2020.12.042

30. Alexander AY, Leonel LCPC, Agosti E, Celda MP, Lanzino G. The precuneal interhemispheric, trans-tentorial corridor to the pineal region and brainstem, surgical anatomy, and case illustration. *Acta Neurochir (Wien)*. (2022) 164(4):1095–103. doi: 10.1007/s00701-022-05167-0

31. Kalani MY, Martirosyan NL, Nakaji P, Spetzler RF. The supracerebellar infratentorial approach to the dorsal midbrain. *Neurosurg Focus*. (2016) 40 (Video Suppl 1):2016.1.FocusVid.15462. doi: 10.3171/2016.1.FocusVid.15462

32. Liyong S, Bao Y, Liang J, Li M, Ren J. Posterior interhemispheric transtentorial approach for resection of a meningioma at the posteromedial tentorial incisura. *Neurosurg Focus*. (2016) 40(Video Suppl 1):2016.1.FocusVid.15428. doi: 10.3171/2016.1.FocusVid.15428

33. Ansari SF, Young RL, Bohnstedt BN, Cohen-Gadol AA. The extended supracerebellar transtentorial approach for resection of medial tentorial meningiomas. *Surg Neurol Int*. (2014) 5:35. doi: 10.4103/2152-7806.128918

34. Sabatino G, Rigante L, Marchese E, Albanese A, Esposito G, Capone G, et al. Anterior subtemporal approach for posterolateral brainstem cavernomas: report of ten cases. *Acta Neurochir (Wien)*. (2012) 154(11):2009–16. doi: 10.1007/s00701-012-1496-9

35. Fava A, di Russo P, Passeri T, Camara B, Paglia F, Matano F, et al. The mini-combined transpetrosal approach: an anatomical study and comparison with the combined transpetrosal approach. *Acta Neurochir (Wien)*. (2022) 164(4):1079–93. doi: 10.1007/s00701-022-05124-x

36. Morisako H, Ohata H, Shinde B, Nagahama A, Watanabe Y, Goto T. Minimal anterior and posterior combined transpetrosal approach for large petroclival meningiomas. *J Neurosurg*. (2021) 135(4):1180–9. doi: 10.3171/2020.8.JNS202060

37. Vasquez CA, Thompson JA, Youssef AS. The tentorial bridge to deep skull base exposure: anatomic morphometric study. *World Neurosurg*. (2018) 114: e588–e96. doi: 10.1016/j.wneu.2018.03.037

38. Yasargil MG, Antic J, Laciga R, Jain KK, Hodosh RM, Smith RD. Microsurgical pterional approach to aneurysms of the basilar bifurcation. *Surg Neurol*. (1976) 6(2):83–91.

39. Gupta SK. Trans-sylvian transtentorial approach for skull base lesions extending from the middle fossa to the upper petro-clival region. *Br J Neurosurg*. (2009) 23(3):287–92. doi: 10.1080/02688690802716129

40. Kawase T, Shiobara R, Toya S. Anterior transpetrosal-transtentorial approach for sphenopetroclival meningiomas: surgical method and results in 10 patients. *Neurosurgery*. (1991) 28(6):869–75; discussion 75–6. doi: 10.1227/00006123-199106000-00014

41. Hernesniemi J, Ishii K, Niemelä M, Kivipelto L, Fujiki M, Shen H. Subtemporal approach to basilar bifurcation aneurysms: advanced technique and clinical experience. *Acta Neurochir Suppl*. (2005) 94:31–8. doi: 10.1007/3-211-27911-3_6

42. Samii M, Tatagiba M. Experience with 36 surgical cases of petroclival meningiomas. *Acta Neurochir (Wien)*. (1992) 118(1–2):27–32. doi: 10.1007/BF01400723

43. Sekhar LN, Goel A. Combined supratentorial and infratentorial approach to large pineal-region meningioma. *Surg Neurol*. (1992) 37(3):197–201. doi: 10.1016/0090-3019(92)90230-K

44. Cavalcanti DD, Preul MC, Kalani MY, Spetzler RF. Microsurgical anatomy of safe entry zones to the brainstem. *J Neurosurg*. (2016) 124(5):1359–76. doi: 10.3171/2015.4.JNS141945

45. Kim W, Moon JH, Kim EH, Hong CK, Han J, Hong JB. Optimization of orbital retraction during endoscopic transorbital approach via quantitative measurement of the intraocular pressure—[SevEN 006]. *BMC Ophthalmol*. (2021) 21(1):76. doi: 10.1186/s12886-021-01834-5

frontiers | Frontiers in Surgery

TYPE Methods
PUBLISHED 31 October 2022
DOI 10.3389/fsurg.2022.984015

OPEN ACCESS

EDITED BY
Peng Zhao,
Capital Medical University, China

REVIEWED BY
Michel Roethlisberger,
University Hospital of Basel, Switzerland
Valentina Tardivo,
San Carlo Borromeo Hospital, Italy
Matteo De Notaris,
Azienda Ospedaliera San Pio di Benevento, Italy

*CORRESPONDENCE
Changchen Hu
hucc88@163.com
Ian F. Dunn
Ian-Dunn@ouhsc.edu

†These authors have contributed equally to this work and share first authorship

SPECIALTY SECTION
This article was submitted to Neurosurgery, a section of the journal Frontiers in Surgery

RECEIVED 01 July 2022
ACCEPTED 03 October 2022
PUBLISHED 31 October 2022

CITATION
Li P, Wang K, Ji H, Zhang G, Chen S, Zhang S, Dunn IF and Hu C (2022) Endoscopy-assisted high anterior cervical approach in craniovertebral junction (CVJ).
Front. Surg. 9:984015.
doi: 10.3389/fsurg.2022.984015

Endoscopy-assisted high anterior cervical approach in craniovertebral junction (CVJ)

Pengfei Li[1†], Kaixuan Wang[1†], Hongming Ji[1], Gangli Zhang[1], Shengli Chen[1], Shiyuan Zhang[1], Ian F. Dunn[2*] and Changchen Hu[1,3*]

[1]Department of Neurosurgery, Shanxi Provincial People's Hospital, Shanxi Medical University, Taiyuan, China, [2]Department of Neurosurgery, University of Oklahoma Health Sciences Center, Oklahoma City, OK, United States, [3]Department of Neurosurgery, Shuozhou People's Hospital, Shuozhou, China

Background: Surgical procedures in the craniovertebral junction (CVJ) suffer from specific challenges due to the proximity between the cranium and spine containing the critical neurovascular structures and the brainstem, respectively. Owing to the complex transitional zone, it is highly challenging for classic surgical approaches to practically acquire the additional exposure to neurovascular structures of the CVJ. Inspired by these facts, we explore the feasibility of an endoscopy-assisted high anterior cervical approach in the CVJ.
Methods: To explore the feasibility of an endoscopy-assisted approach, we quantitatively assessed the surgical corridor and extent of exposure of the CVJ in 6 cadaveric specimens using 0° and 30° endoscopes.
Results: The applied endoscopes provided adequate exposure to neurovascular structures and the brainstem in the CVJ. Notably, the resection of the anterior arch of C1 is avoided in minimal anterior clivectomy. Further, improved exposure of the CVJ is obtained after removing the odontoid.
Conclusion: An endoscope-assisted high anterior cervical approach in the CVJ significantly preserved the cervical spine stability while minimalizing the risk of neurovascular injury within the surgical corridor.

KEYWORDS
endoscope-assisted surgery, high anterior cervical approach, craniovertebral junction, endoscopic technique, application

Background

The craniovertebral junction (CVJ) characterizes the complex transitional zone between the cranium and the spine. The surgical procedures in the CVJ present specific challenges due to the proximity of critical neurovascular structures and the brainstem. In this context, several ventral and dorsal approaches to operating CVJ have been reported for accessing a variety of pathologies. These approaches are classified into anterior, posterior, and lateral strategies. In this regard, several classic approaches, such as the midline suboccipital and the transcondylar approaches, are preferred for operating posterior and lateral lesions at the cervicomedullary junction

Abbreviations
CVJ, craniovertebral junction; BA, basilar artery; VA, vertebral artery; PICA, posterior inferior cerebellar artery; CN, cranial nerve

(1). To this end, the ventral lesions, especially extradural pathologies, could be readily accessed through the anterior corridors, including transoral and transnasal methods (2–7). Notably, it is highly challenging to apply transoral and transnasal approaches in the setting of oral or nasal cavity lesions or when the majority of the lesion extends laterally or caudally into the cervical spine. Previous reports indicated that the high anterior cervical approach provided adequate decompression of the cervicomedullary junction (8). In addition, several reports showed that anterior cervical fixation or fusion could be performed through this approach (9). Simultaneously, the oropharyngeal mucosa could be preserved with fewer pharyngeal complications. However, this approach suffers from a significant shortcoming of very long working distance under the microscope, which utilizes the posterior pharyngeal space. In addition, it is difficult to retract and gain access to the posterior pharyngeal wall soft tissue due to maxilla and muscle soft tissue constraints. Moreover, there exists only a tiny bony window through the clivus within minimal anterior clivectomy (8). Owing to these shortcomings, it is practically challenging to obtain extra exposure to neurovascular structures in the CVJ. Recently, endoscopes have garnered increasing attention from researchers as a part of the neurosurgical armamentarium. Inspired by these aspects, herein, we explored the feasibility of the endoscope-assisted high anterior cervical approach for extended exposure in the CVJ.

Methods

All anatomical dissections were executed at the Skull Base Laboratory and Minimally Invasive Neurosurgery Laboratory. The embalmed human cadaveric heads ($n = 6$) from body donations were obtained from the anatomical laboratory of Shanxi Medical University, Shanxi, China. Notably, the donors were informed and agreed that cadavers would be used for medical research. The study was approved by the Ethical Committee of the Hospital, and required permissions were obtained to utilize these samples from Shanxi medical university. The microscopic anatomical dissections were performed under 3–40x optical magnifications using an operating microscope (Global Instruments, Trenton, MO, USA). To this end, the endonasal anatomical dissections were carried out using 0° and 30° rod-lens, 4-mm diameter, 18-cm length, Hopkins II endoscopes (Karl Storz Endoscopy, Tuttlingen, Germany). These endoscopes were connected to a high-definition camera and projected onto a monitor. All the digitally recorded data were stored in a workstation for future reference (Gefen System, Petaluma, CA, USA).

Results

Surgical procedure

The high anterior cervical retropharyngeal approach to the upper cervical spine has been described in detail (10–12). In a case, Russo and colleagues applied this approach to the clivus and foramen magnum (8). In this study, this approach was executed following the series of steps discussed below. The procedure was performed with the patient positioned supine. Initially, the patient's head was extended 20°–30° and rotated 30°–45° away from the side. In addition, the mandible was displaced superiorly. Further, an incision was made approximately 3–4 cm inferior and parallel to the mandible, avoiding injury to the marginal mandibular branch of the facial nerve (**Figure 1A**). Then, the platysma was divided and retracted superiorly, thus exposing and elevating the submandibular gland (**Figure 1B**). Further, the posterior belly of the digastric muscle was brought into view under the submandibular glands. Then, the anterior belly of the digastric muscle was retracted medially, as well as the facial artery and vein laterally. The posterior belly and tendons of the digastric muscle were elevated superiorly. After dividing the posterior belly deep, the hypoglossal nerve was revealed, passing inferior to the muscle (**Figures 1C,D**). The hypoglossal nerve was carefully dissected and retracted rostrally. The external carotid artery and the facial artery branch were then retracted laterally and superiorly, and the lingual artery was retracted inferiorly (**Figures 1B,C**). The pharyngeal muscles were then retracted medially, thus opening the retropharyngeal space. The pharyngeal muscles were further separated deeply, and the anterior tubercle of C1, as well as the anterior surface of the cervical vertebrae, were exposed (**Figure 1E**). Subsequently, the prevertebral fascia and the anterior longitudinal ligament in the midline were preserved, which are important for cervical spine stability, exposing the entire arch of C1 and the body of C2. The anterior atlantooccipital membrane and the longus capitis muscles were detached from the anterior rim of the foramen magnum and midlateral portion of the clivus (**Figure 1F**). Accordingly, the upper boundary was the vomer and pterygoid process medial plate, and the petroclival fissure as the bilateral boundary.

Anatomical measurements

Further, the anatomical structures of the free clivus in the specimen were measured. The mean distance from the anterior rim of the foramen magnum to the vomer was measured as 27.1 mm (range 26–28.9 mm). The mean width of the clivus at the pterygoid process medial plate level was around 21.6 mm (range 21.0–22.3 mm). The mean width of

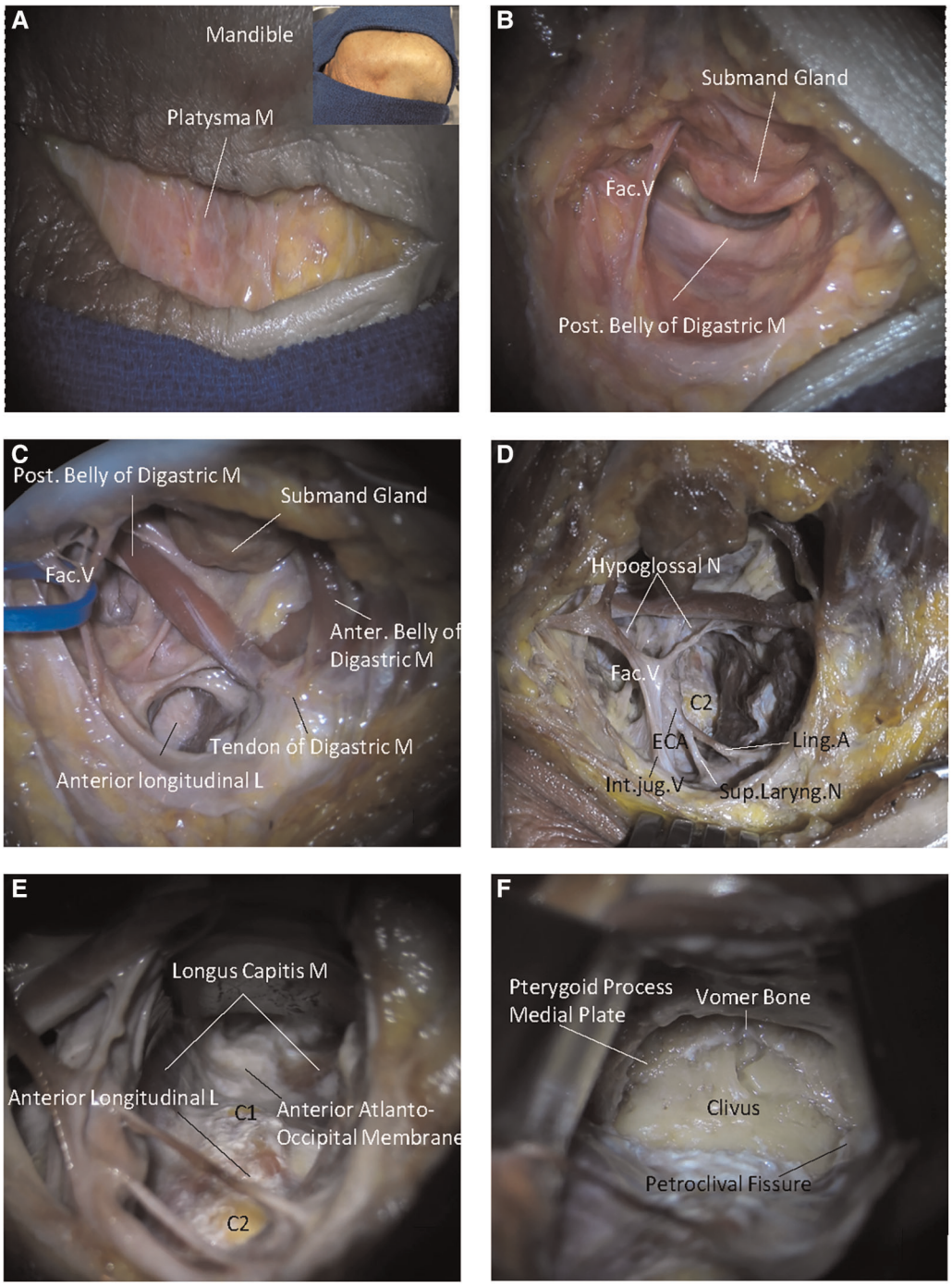

FIGURE 1
The surgical procedure of endoscope-assisted high anterior cervical approach. (**A**) A straight skin incision is made about 2 cm below and parallel to the inferior border of the mandible. (**B**) The platysma muscle is elevated. The submandibular gland and posterior belly of the digastric muscle are exposed. (**C**) The submandibular gland and posterior belly of the digastric muscle are released and retracted and the entrance of the retropharyngeal space is exposed. (**D**) The hypoglossal nerve passes and the lingual artery is divided; and the retropharyngeal space is opened. (**E**) The pharyngeal muscles are retracted medially and further separated deeply. The anterior surface of the cervical vertebrae and anterior atlantooccipital membrane are exposed. (**F**) The lower clivus is exposed, including the vomer, pterygoid precess medial plate, petroclival, and the anterior rim of the foramen magnum. The arrows indicate the direction in the space, S represents the superior part of the cadaveric heads, M represents the medial part of the cadaveric heads.

the clivus at the pharyngeal tubercle level was 27.8 mm (range 26.9–28.4 mm). The mean width of the clivus at the hypoglossal canal outside the hole midpoint level was 28.7 mm (range 27.6–29.1 mm). The mean width of the clivus at the inferior margin of the hypoglossal canal outside the hole was around 29.6 mm (range 28.7–31.1 mm, Figure 2A).

In addition, we measured the mean distance of the previous step on the heads, which showed an excellent exposure of the

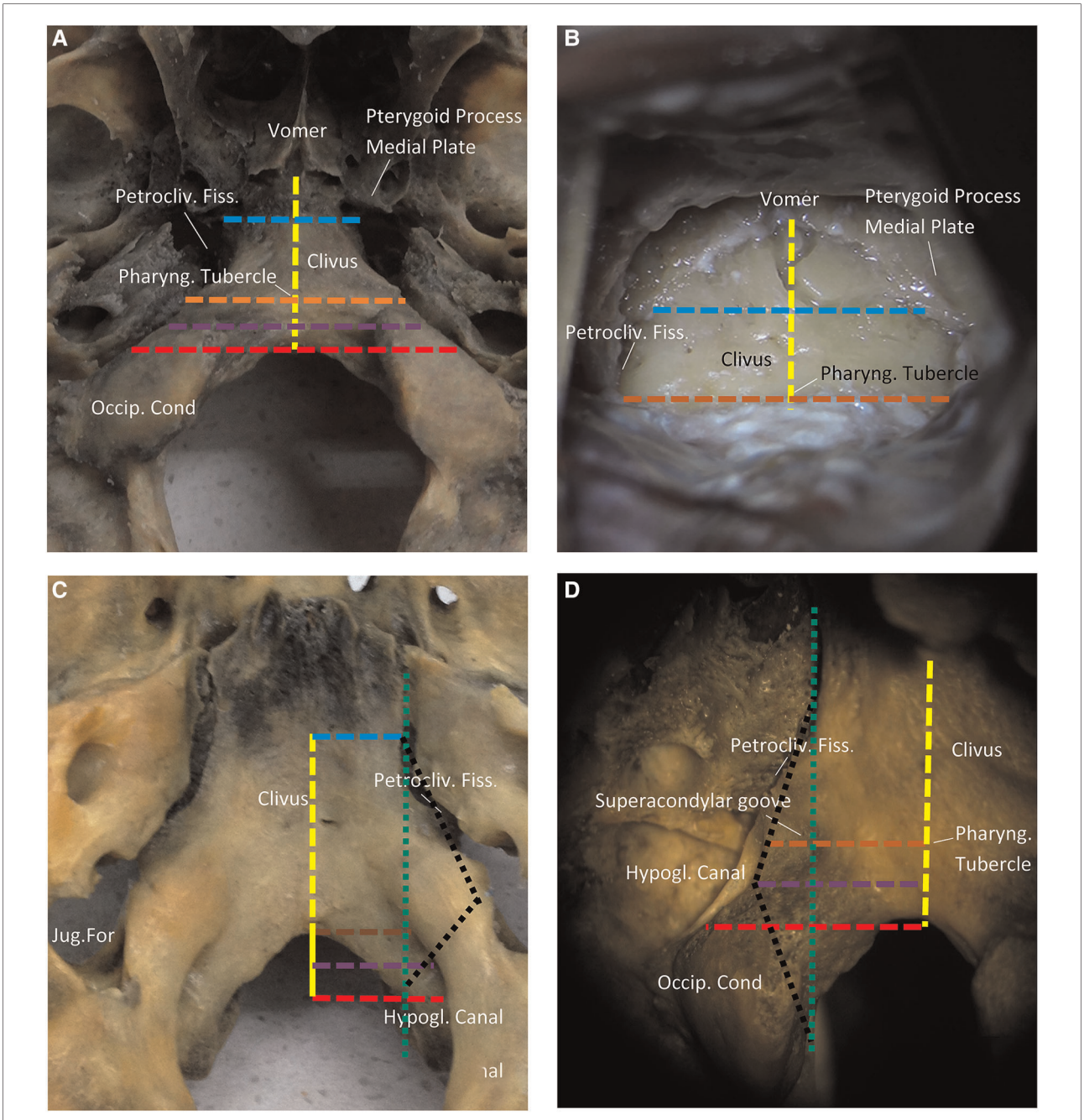

FIGURE 2
Surgical anatomy and measurements of the lower clivus and ventral foramen magnum. (A) The ventral side of the clivus. Occipital foramen-vomer (yellow line). The width of the clivus at the pharyngeal tubercle level (brown line). The width of clivus at the pterygoid process medial plate level (blue line). The width of clivus at the hypoglossal canal outside the hole midpoint (purple line). The width of the clivus at the inferior margin of the hypoglossal canal outside the hole (red line). (B) Initial exposure of the clivus. (C) The interior side of the clivus. The green line is the line from the petroclival fissure to the hypoglossal canal inside the hole. The lateral limit of the medial condylectomy is the hypoglossal canal inside the hole. (D) The hypoglossal canal outside the hole. It is directed backward and medially at a 45° angle with the sagittal plane. The pharyngeal tubercle is at the same level with the superior margin of hypoglossal canal outside the hole. The lateral limit of the medial condylectomy is defined by the dotted black line (petroclival fissure to superior margin hypoglossal canal outside the hole to the hypoglossal canal inside the hole).

clivus. The anterior rim of the foramen magnum has adhered to the longus capitis muscle, rectus capitis anterior muscle, pharyngobasilar fascia, and mucosa. It should be noted that dissecting from the anterior margin of the foramen magnum was challenging, especially the fascia on the supracondylar groove. In addition, it was challenging to dissect from the cortical bone surface of the groove, which was an essential landmark on the clivus for localizing the hypoglossal canal due to similar depths. At this stage, the mean distance from the pharyngeal tubercle to the vomer was measured as 19.1 mm (range 18.7–20.9 mm). The mean width of the clivus at the pterygoid process medial plate level was recorded as 20.1 mm (range 19.3–20.9 mm). The mean width of the clivus at the pharyngeal tubercle level was around 25.9 mm (range 24.9–26.4 mm, Figure 2B). Nevertheless, no noticeable difference was observed compared with the measurements of the free clivus, indicating the convenience of separating the mucosa of the clivus bilaterally from the petroclival fissure.

In the case of CVJ, the hypoglossal canal and nerve are essential structures. The hypoglossal canal was directed posteriorly and medially at a 45° angle with the sagittal plane, thus locating its extracranial outside hole proximately above the junction of the anterior and middle third of the occipital condyle, as well as medial to the jugular foramen. The interior view of the clivus indicated that the hypoglossal canal was positioned at the back of the free anterior rim of the foramen magnum. Thus, the medial border of the intracranial hole and the petroclival fissure possessed the same vertical line (Figure 2C). In the exterior view of the clivus, the hypoglossal canal was located at the front of the free anterior rim of the foramen magnum. It should be noted that the midpoint of the hypoglossal canal outside the hole acted as the lateral limiting point. Accordingly, a black line was dotted as the lateral limit of the medial condylectomy (petroclival fissure to the midpoint of the hypoglossal canal outside the hole to the hypoglossal canal inside the hole, Figure 2D).

Exposure of CVJ

The exposure of the CVJ was performed by disclosing the clivus and the high cervical area. Initially, the clivus resection was performed using a high-speed drill or rongeur through the midline of the inferior portion of the clivus. Indeed, the upper boundary, i.e., the sphenoidal sinus, was limited laterally by the medial border of the petroclival fissure. In

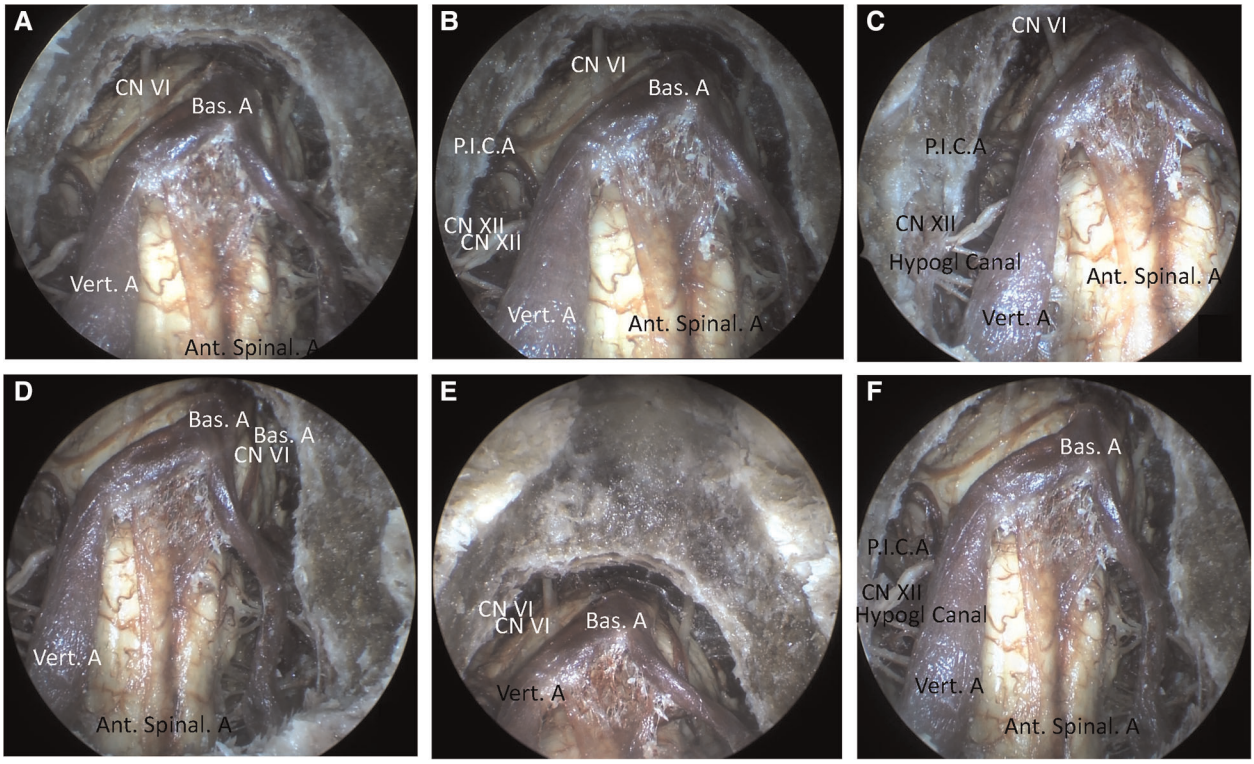

FIGURE 3
(A) The view of the resection of the clivus (0°). (B–F) The view of the resection of the clivus and the atlas. (B) The view of resection of the clivus and the atlas (0°). (C) The view of the resection of the clivus and the atlas (30°, right). (D) The view of the resection of the clivus and the atlas (30°, left). (E) The view of the resection of the clivus and the atlas (30°, cranial). (F) The view of the resection of the clivus and the atlas (30°, caudal).

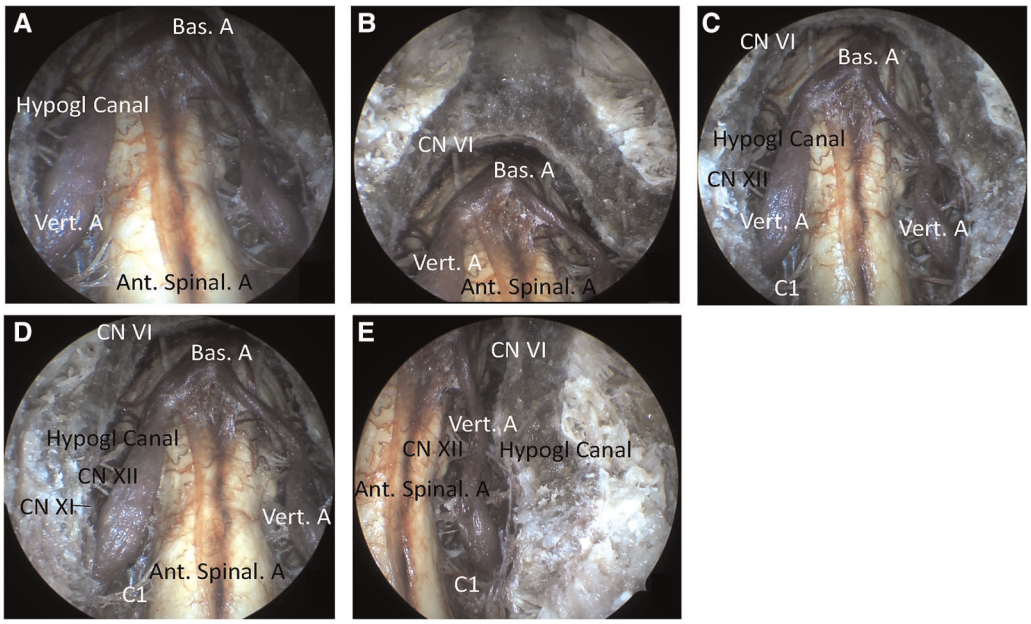

FIGURE 4
The view of the resection of the clivus, atlas, and dens. (**A**) The view of the 0° endoscope. (**B**) The view of the 30° endoscope (cranial). (**C**) The view of the 30° endoscope (caudal). (**D**) The view of the 30° endoscope (right). (**E**) The view of the 30° endoscope (left).

contrast, the lower boundary was the anterior rim of the foramen magnum. In this resection, the atlantooccipital anterior membrane, anterior longitudinal ligament, and apical ligament of the dens of C1 were preserved. However, there existed a 20 mm × 30 mm bony window through the clivus, as previously reported by Russo and colleagues (8). After opening the dura mater, the ventral aspect of the brainstem and the related vascular and neural structures could be observed (**Figure 3A**). The proximal segment of the basilar artery (BA) and bilateral vertebral artery (VA) could be initially detected. From the top view, the 6th cranial nerve (abducent nerve) could be observed from its origin. The abducent nerve is very very important when performing the approach. The abducens nerve runs in the prepontine cistern between the clivus and the pontine base, and the hypoglossal and oculomotor nerves are adjacent to the rostral and caudal ends of the clivus, respectively. The glossopharyngeal, vagus and facial auditory nerves all run lateral to the clivus. in the brain cistern. There is a potential risk of injuring the abducens nerve, when endoscopically enlarged transnasal approach for the treatment of clivus tumors. This nerve root enters and exits the brainstem zone (REZ) and cisternal segment (CS), which are particularly vulnerable to clivus resection and dura dissection *via* the clivus approach. The Eustachian tube is a constant and easily identifiable structure, and most EEA transclivi approach does not necessarily require resection of ET, so ET can be used as an anatomical landmark for CN VI in endoscopic skull base surgery *via* transclivi approach. The pontomedullary sulcus was exposed in the middle. The anterior spinal artery could be observed in the midline, while the posterior inferior cerebellar artery (PICA) and cranial nerve (CN) XII could be partly observed bilaterally.

Further, the endoscope-assisted high anterior cervical approach was executed by expanding the bone window. The anterior atlantooccipital membrane, and anterior longitudinal ligament were preserved. After drilling the medial third of the lateral mass of C1 and the anteromedial third of the occipital condyle, the CVJ vascular and neural structures were observed using 0° and 30° rod-lens endoscopes. In addition, the BA, VA, abducens nerve, and pontomedullary sulcus could be observed, increasing the exposure of the inferior field. The hypoglossal canal, CN XII, and P.I.C.A. were still bilaterally observed partially using 0° endoscopes, with an improved observation range (**Figure 3B**). However, it could be observed completely using 30° endoscopes (**Figures 3C–F**). Notably, the occipital condyle anatomic levels, in turn, were observed as cortical bone, soft cancellous bone, hard cortical bone, and hypoglossal canal. Moreover, it should be noted that the deeper layer of hard cortical bone of the occipital condyle should be carefully drilled to protect the hypoglossal nerve.

Further, drilling down to the level of the body of C2 was continued to expand the inferior field exposure. After opening the dura mater, the cervicomedullary junction was then exposed. Notably, the CVJ area was sufficiently exposed after drilling out the dens (**Figure 4A**). In addition, other

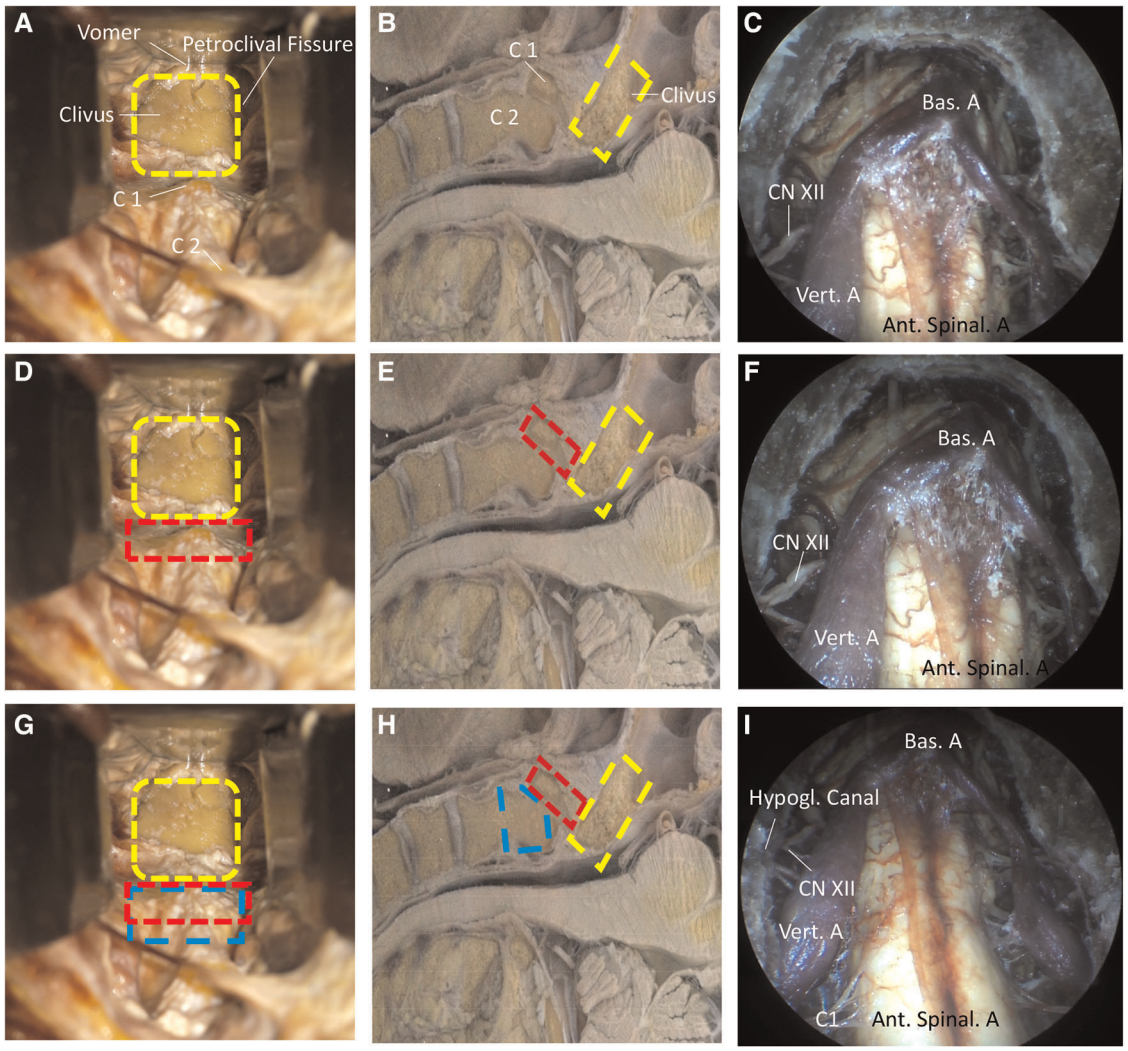

FIGURE 5
The relation of exposure degree and resection range of CVJ. (A,D,G) The different resection range of CVJ. (B,E,H) From the sagittal display, different degrees of resection of CVJ in another specimen. (C,F,I) Exposure degree under the endoscope. (A–C) The view of the resection of the clivus. The orange portion represents the resected clivus. (D–F) The view of the resection of the clivus and the atlas. The green portion represents the resected atlas. (G–I) The view of the resection of the clivus, atlas, and odontoid. The yellow portion represents the resected odontoid. It is important to resect the odontoid in order to sufficiently expose the CVJ in the anterior cervical approach to the CVJ. There is not an obvious increase in the exposure degree of the CVJ when the atlas is drilled out based on the resected clivus in the anterior cervical approach. After removing the odontoid. A greater exposure of the CVJ area is obtained. It is imperative to resect the dens in order to sufficiently expose the CVJ in the anterior cervical approach. The arrows indicate the direction in the space, S represents the superior part of the cadaveric heads, M represents the medial part of the cadaveric heads.

structures such as BA, VA, abducens nerve, pontomedullary sulcus, hypoglossal canal, CN XII, and PICA were exposed. Further, the vascular and neural structures of the expanded CVJ region were observed using a 0° endoscope along with the upper cervical spinal cord. In addition, the vertebral artery intradural segments were observed completely, specifically from their dural entrance points to the supramedial rising segment. More importantly, the spinal nerve C1 could be bilaterally observed completely using a 0° endoscope. Together, using a 30°endoscope resulted in greater exposure of the CVJ region than a 0° endoscope (Figures 4B–E).

Exposure degree and resection range of the CVJ

The relationship between the exposure degree and resection range of the CVJ is summarized in Figure 5. Figures 5A–C display the endoscopic views of the resected clivus in the endoscope-assisted high anterior cervical approach, while Figures 5D–F display endoscopic views of resectioning the clivus and atlas. It was observed from the results that there existed no apparent increase in the exposure degree of the CVJ. Figures 5G–I display the endoscopic views of the

resectioned clivus, atlas, and odontoid. The experimental results indicated that no apparent increase in the exposure degree of the CVJ was observed during drilling out the atlasbased on the resected clivus in the anterior cervical approach (**Figures 5C,F**). After removing the odontoid, greater exposure to the CVJ area was obtained (**Figures 5C,F,I**). Together, these findings indicated that it was imperative to resect the dens to sufficiently expose the CVJ in the anterior cervical approach, especially for large lesions involving the high cervical spinal region.

Discussion

Indeed, some recent studies have reported the applicability of the high anterior cervical approach. In a case, Vender and colleagues demonstrated anterior cervical fixation or fusion through the endoscopic approach (9). In another case, Park and coworkers studied the high anterior cervical approach for the upper cervical spine fixation (13). In addition, Singh et al. reviewed the high anterior cervical retropharyngeal approach in ventral surgical approaches to CVJ chordomas (14). Russo and colleagues demonstrated a microsurgical anatomy study of the high anterior cervical approach to the clivus and foramen magnum (8). Although a deep retractor and a self-retaining retractor could be employed to elevate the pharyngeal mucosa and maintain lateral displacement of the longus capitis, rectus capitis anterior, and longus colli, the working distance could remain long under the microscope through this approach. It was highly challenging to retract the posterior pharyngeal wall soft tissue due to the maxilla and muscle soft tissue constraints. In this study, the ventral surfaces of the foramen magnum, clivus, petroclival region, and CVJ were exposed under the microscope in a tubular surgical field (**Figure 6**). In addition, there was only a 20 mm × 30 mm bony window through the clivus within minimal anterior clivectomy (8). Considering these aspects, it could be challenging to obtain extra exposure to the neurovascular structures of the CVJ practically. These factors significantly limited the application of this approach in clinical practice. To this end, a fish eye effect under endoscopy could be utilized to obtain a multi-angle and close-distance observation of the operative region (**Figure 6**). This approach could substantially overcome the limitation of the tubular surgical field under the microscope. In addition, endoscope technology as part of the neurosurgical armamentarium has recently gained increasing attention from researchers. Considering these aspects, in this study, we demonstrate the development of the endoscope-assisted high anterior cervical approach.

While utilizing a deep retractor and a self-retaining retractor to expose the CVJ, the visualization of the inferior portion of the clivus and the anterior rim of the foramen magnum was

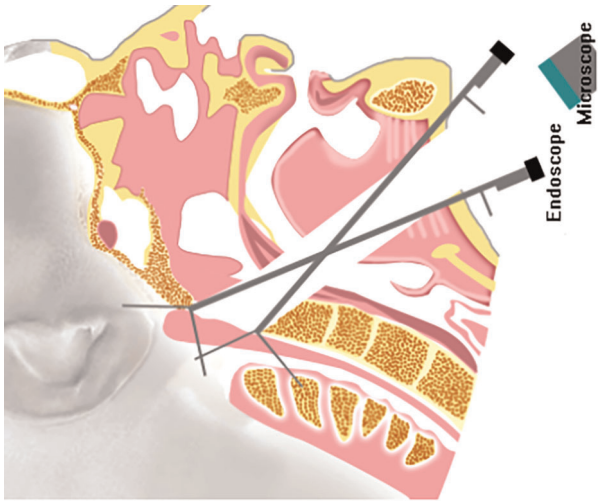

FIGURE 6
The comparison of the high anterior cervical approach to the craniovertebral junction under the endoscope and microscope.

obstructed by the anterior arch of C1 under the microscope during the high anterior cervical approach (8). At this stage, the resection of the anterior arch of C1 between the lateral masses was converted to a normal drilling or resection step, even in minimal anterior clivectomy (8). The deep retractor was repeatedly pushed towards the bilateral and upward sides to obtain greater exposure *via* the operation corridor under the microscope. Nonetheless, it should be noted that the blood vessels and nerves of the neck could be damaged easily. Utilizing the multi-angle and close distance observation of the endoscope, the inferior portion of the clivus and the anterior rim of the foramen magnum could be observed (**Figure 4**), avoiding the resection of the anterior arch of C1 and maintaining the stability of the cervical spine.

Different descriptions of the lateral limit of resection have been reported in the literature. In a case, Wang et al. designed the vertical line (from the foramen lacerum to the occipital condyle) in medial condylectomy as the lateral limit of the medial condylectomy (15). In another case, Russo et al. described the lateral limit of bone resection, the petroclival fissure, the anteromedial third of the occipital condyle, and the anterior half of the jugular tubercle (8). Notably, all these landmarks existed in the free occipital bone. In the actual operation, these landmarks were covered or embedded with other tissue, leading to challenges in judgment during the operation itself. Similarly, the same lateral limit of resection was encountered. However, we believed that the intraoperative assessment should be simple.

The petroclival fissure and the medial border of the intracranial hole represented the superolateral and inferior-lateral limits of resection. In the interior view of the clivus, the medial border of the intracranial hole and the petroclival

fissure possessed the same vertical lines (Figure 2C). The midpoint of the hypoglossal canal outside the hole acted as the limiting lateral point (Figure 2D). It was observed that the supracondylar groove and hypoglossal canal were at the same craniocaudal level, and the hypoglossal canal was deep enough. As a surface landmark on the clivus for localizing the hypoglossal canal, thus, the lateral point of the supracondylar groove could act as the lateral limit during the operation (Figures 2C,D). Therefore, we could outline the boundaries for resection (black dot line) using the petroclival fissure, vertical line, and the lateral point of the supracondylar groove during the operation. All of these landmarks were marked on the outside surface of the occipital bone.

The high anterior cervical approach is often used in the upper cervical spine, such as for chordomas of the upper cervical spine (16), fusion at the cervical spine (9), cervical pyogenic C1–2 abscess (17), and cervical spondylosis (18). On the one hand, there existed a degree of angle between the spine's long axis and the operation corridor in the high anterior cervical approach, in some instances, an acute angle, less than 45°. As shown in Figure 6, it was relatively easier to operate upper cervical spine lesions. While, in the cases of the lesions located in the lower clivus and foramen magnum, the degree between the spine's long axis and the operation corridor could be more negligible. On the other hand, it could be difficult to resect the anterior atlantooccipital membrane, occipital condyle, atlantooccipital joint, and apical and alar ligaments.

Furthermore, the upper structures in the bone windows could be observed due to the acute angle between the operation corridor and the operation bone window (Figure 7). When the atlas was drilled out (Figures 5D,E), no significant increase in the acute angle between the operation corridor and operation bone window was detected. Thus, no evident increase in exposure degree of the CVJ was observed compared with the clivectomy in the anterior cervical approach (Figures 5C,F). After removing the odontoid, greater exposure of the CVJ area was observed (Figures 5C,F,I). Together, these findings indicated that it was imperative to resect the dens to sufficiently expose the CVJ in the anterior cervical approach, especially for large lesions involving the high cervical spinal region.

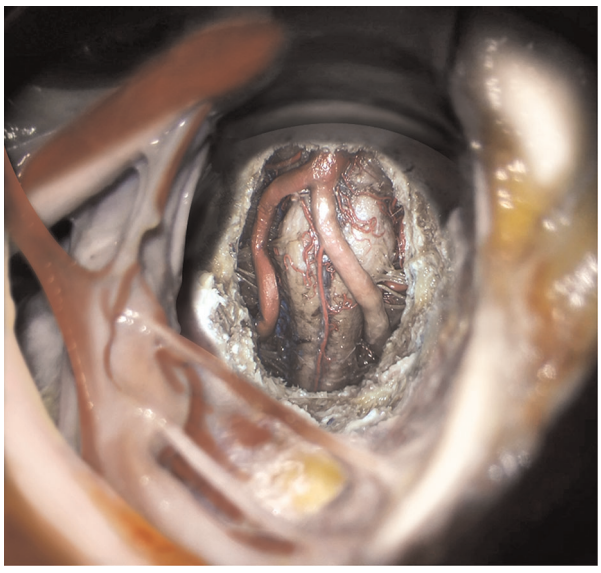

FIGURE 7
Artist's illustration of the exposure of the high anterior cervical approach to the craniovertebral junction.

Conclusion

In summary, the applicability of the endoscopy-assisted high anterior cervical approach in the CVJ has shown excellent feasibility. This approach maintained the stability of the cervical spine and minimized the chances of damage to blood vessels and nerves around the operation corridor. Together, it could be feasible to obtain maximum exposure with the least amount of resection by applying the endoscope-assisted high anterior cervical approach.

Data availability statement

The original contributions presented in the study are included in the article/Supplementary Material, further inquiries can be directed to the corresponding author/s.

Ethics statement

The studies involving human participants were reviewed and approved by Ethics Committee of Shanxi Provincial People's Hospital. The patients/participants provided their written informed consent to participate in this study. Written informed consent was not obtained from the individual(s) for the publication of any potentially identifiable images or data included in this article.

Author contributions

Conception and design: IFD and CH. Acquisition of data: PL. Analysis and interpretation of data: CH and KW. Drafting the article: all authors. Critically revising the article: all authors. Reviewed submitted version of manuscript: all authors. Approved the final version of the manuscript on behalf of all authors: IFD and CH. Statistical analysis: HJ and SZ. Administrative, technical, material support: GZ, SC, and

SZ. Study supervision: CH, HJ and SZ. All authors contributed to the article and approved the submitted version.

Funding

This research was funded by the National Science Foundation of China (30901774); Natural Science Foundation of Shanxi Province (2014011038-2); Shanxi Province Science and Technology Development Plan (Social Development Section) (20140313011-5); Key R&D Plan of Shanxi Province (International Cooperation Project) (201803D421055); Shanxi Province Overseas Students Science and Technology Activities Selection Funding Project (2018014); Scientific research projects with provincial special funds in Shanxi Provincial People's Hospital (sj20019003); Fundamental Research Program of Shanxi Province (20210302123352); Shanxi Province Health Commission Scientific Research Project (2022052), Research Project Supported by Shanxi Scholarship Council of China (2022-205), Four "Batches" Innovation Project of Invigorating Medical through Science and Technology of Shanxi Province (2022XM21).

Conflict of interest

The authors declare that the research was conducted in the absence of any commercial or financial relationships that could be construed as a potential conflict of interest.

Publisher's note

References

1. Samii M, Klekamp J, Carvalho G. Surgical results for meningiomas of the craniocervical junction. *Neurosurgery*. (1996) 39:1086–95. doi: 10.1097/00006123-199612000-00003

2. Mullan S, Naunton R, Hekmat-Panah J, Vailati G. The use of an anterior approach to ventrally placed tumors in the foramen magnum and vertebral column. *J Neurosurg*. (1966) 24:536–43. doi: 10.3171/jns.1966.24.2.0536

3. Miller E, Crockard HA. Transoral transclival removal of anteriorly placed meningiomas at the foramen magnum. *Neurosurgery*. (1987) 20:966–8. doi: 10.1227/00006123-198706000-00026

4. Crockard HA, Sen CN. The transoral approach for the management of intradural lesions at the craniovertebral junction: review of 7 cases. *Neurosurgery*. (1991) 28:88–97. doi: 10.1227/00006123-199101000-00014

5. Fernandez-Miranda JC, Morera VA, Snyderman CH, Gardner P. Endoscopic endonasal transclival approach to the jugular tubercle. *Neurosurgery*. (2012) 71:146–58. doi: 10.1227/NEU.0b013e3182592faa

6. Koutourousiou M, Gardner PA, Tormenti MJ, et al. Endoscopic endonasal approach for resection of cranial base chordomas: outcomes and learning curve. *Neurosurgery*. (2012) 71:614–24. doi: 10.1227/NEU.0b013e31825ea3e0

7. Morera VA, Fernandez-Miranda JC, Prevedello DM, Henry SL, Stefko ST, Kassam AB, et al. "Far-medial" expanded endonasal approach to the inferior third of the clivus: the transcondylar and transjugular tubercle approaches. *Neurosurgery*. (2010) 66:211–9. doi: 10.1227/01.NEU.0000369926.01891.5D

8. Russo VM, Graziano F, Russo A, Albanese E, Ulm AJ. High anterior cervical approach to the clivus and foramen Magnum: a microsurgical anatomy study. *Neurosurgery*. (2011) 69(1 Suppl Operative):ons103–14. doi: 10.1227/NEU.0b013e31821664a6

9. Vender JR, Harrison SJ, McDonnell DE. Fusion and instrumentation at C1-3 via the high anterior cervical approach. *J Neurosurg*. (2000) 92(1 Suppl):24–9. doi: 10.3171/spi.2000.92.1.0024

10. McAfee PC, Bohlman HH, Riley LH, Robinson RA, Southwick WO, Nachlas NE. The anterior retropharyngeal approach to the upper part of the cervical spine. *J Bone Joint Surg*. (1987) 69:1371–83. doi: 10.2106/00004623-198769090-00010

11. McDonnell DE. Anterolateral cervical approach to the craniovertebral junction. *Neurosurg Op Atlas*. (1991) 3:147–64.

12. McDonnell DE, Harrison SJ. High cervical retropharyngeal approach to the craniovertebral junction. *Perspect Neurol Surg*. (1996) 7:121–41.

13. Park SH, Sung JK, Lee SH, Park J, Hwang JH, Hwang SK. High anterior cervical approach to the upper cervical spine. *Surg Neurol*. (2007) 68(5):519–24. doi: 10.1016/j.surneu.2006.11.070

14. Singh H, Harrop J, Schiffmacher P, Rosen M, Evans J. Ventral surgical approaches to craniovertebral junction chordomas. *Neurosurgery*. (2010) 66(3 Suppl):96–103. doi: 10.1227/01.NEU.0000365855.12257.D1

15. Wang WH, Abhinav K, Wang E, Snyderman C, Gardner PA, Fernandez-Miranda JC. Endoscopic endonasal transclival transcondylar approach for foramen Magnum meningiomas: surgical anatomy and technical note. *Oper Neurosurg*. (2016) 12(2):153–62. doi: 10.1227/NEU.0000000000001102

16. Jiang L, Liu ZJ, Liu XG, Ma QJ, Wei F, Lv Y, et al. Upper cervical spine chordoma of C2-C3. *Eur Spine J*. (2009) 18(3):293–8. doi: 10.1007/s00586-009-0907-y

17. Aranibar RJ, Del Monaco DC, Gonzales P. Anterior microscopic transtubular (MITR) surgical approach for cervical pyogenic C1-2 abscess: a case report. *Int J Spine Surg*. (2015) 7(9):56. doi: 10.14444/2056

18. Song Y, Tharin S, Divi V, Prolo LM, Sirjani DB. Anterolateral approach to the upper cervical spine: case report and operative technique. *Head Neck*. (2015) 37(9):E115–9. doi: 10.1002/hed.23951

frontiers | Frontiers in Surgery

TYPE Original Research
PUBLISHED 04 November 2022
DOI 10.3389/fsurg.2022.994102

OPEN ACCESS

EDITED BY
Peng Zhao,
Capital Medical University, China

REVIEWED BY
Ruoran Wang,
Sichuan University, China
Han Song Sheng,
Second Affiliated Hospital & Yuying Children's Hospital of Wenzhou Medical University, China

*CORRESPONDENCE
Yuanli Zhao
zhaoyuanli@pkuih.edu.cn

†These authors have contributed equally to this work

SPECIALTY SECTION
This article was submitted to Neurosurgery, a section of the journal Frontiers in Surgery

RECEIVED 14 July 2022
ACCEPTED 13 October 2022
PUBLISHED 04 November 2022

CITATION
Yang Y, Lv C, Zhang J and Zhao Y (2022) Hyponatremia after neuroendoscopic skull base tumor surgery: Clinical characteristics and nursing management.
Front. Surg. 9:994102.
doi: 10.3389/fsurg.2022.994102

Hyponatremia after neuroendoscopic skull base tumor surgery: Clinical characteristics and nursing management

Yanjun Yang[1†], Chunmei Lv[2†], Jing Zhang[1] and Yuanli Zhao[1*]

[1]Department of Neurosurgery, Peking University International Hospital, Beijing, China, [2]Department of Outpatient, Peking University International Hospital, Beijing, China

Purpose: The current study was conducted to explore the clinical characteristics of hyponatremia after neuroendoscopic skull base tumor resection, and to summarize the nursing experience and provide insight for nursing management.
Methods: In total, we enrolled 181 patients who underwent neuroendoscopic resection of skull base tumors in the Department of Neurosurgery of our hospital from 2016 to 2021. The patients' general data and parameters, including blood sodium level, polyuria, and other symptoms in different periods after surgery, were retrospectively reviewed.
Results: Forty-four patients developed hyponatremia after Surgery. The total incidence of hyponatremia was 24.30%, including 38 cases of mild hyponatremia and 6 cases of moderate and severe hyponatremia. Most cases of moderate and severe hyponatremia occurred 6 days after surgery. The incidence of hyponatremia varied in different pathological types and periods in patients undergoing skull base tumors. After standardized sodium supplementation, water restriction, and urine volume control, hyponatremia was corrected in all patients, and no osmotic demyelination syndrome (ODS) and nursing-related events occurred.
Conclusion: Secondary hyponatremia after neuroendoscopic resection of skull base tumors can occur in various time periods after surgery. Early monitoring of manifestations and standardized intervention are thus necessary for clinical nursing practice to timely correct hyponatremia and avoid demyelination.

KEYWORDS

hyponatremia, skull base tumor, neuroendoscopy, complication, nursing management

Introduction

Skull base tumor is a life-threatening condition that originates from the skull base and its adjacent tissue structures. The disease develops from the cranial to the extracranial or from the cranial to the intracranial compartments, passing through the skull base fissure, and growing after destroying the skull base bone (1). Currently, the most effective treatment for skull base tumors is surgical resection. However, traditional craniotomy is traumatic, and the pulling or touching of the surrounding brain tissue during the surgery may cause serious complications, such as hearing loss and facial paralysis.

Neuroendoscopy can directly reach the skull base through the natural channel of the nasal cavity. Its application in skull base tumor resection has the advantages of small trauma, less bleeding, and rapid postoperative recovery. It has gradually been recognized by clinicians and patients, with wide applications in clinical practice (2, 3). Due to the complex tissue structure surrounding skull base tumors, it is still inevitable to cause damage to the pituitary gland, hypothalamus, and other critical neuroendocrine regulatory centers when the tumor is resected by neuroendoscopy. Based on previous studies, the incidence of delayed hyponatremia after the neuroendoscopic resection of skull base tumor was 15.34%–19.8% (4, 5), which is closely related to the abnormal secretion of antidiuretic hormone (6) and brain natriuretic peptide, and the sympathetic nerve function. It often causes brain edema, mental abnormalities, and even death of patients. During treatment, inappropriate correction of hyponatremia may result in complications such as water electrolyte disorder (7). Moreover, very fast correction of hyponatremia can cause osmotic demyelinating syndrome (ODS) (8). Standardized assessment of patients and detailed nursing management to control or reduce the occurrence of hyponatremia are challenging for doctors and nursing staff (7). The purpose of this study was to retrospectively analyze the characteristics of hyponatremia in patients with skull base tumors who underwent neuroendoscopic resection in our hospital and to summarize the nursing experience of hyponatremia, in an attempt to provide basic evidence and insight for the postoperative rehabilitation of patients and to improve the quality of clinical practice.

Materials and methods

Clinical background

We enrolled 181 patients who underwent neuroendoscopic resection of skull base tumors in the Department of Neurosurgery of our hospital from March 2016 to April 2021. The participants included 95 males and 86 females, with a median age of 46 years (46.8 ± 14.8). The inclusion criteria were as follows: (1) patients with skull base tumors confirmed by imaging and pathology; (2) neuroendoscopic tumor resection. The exclusion criteria were as follows: (1) patients diagnosed with co-existing tumors in other organs; (2) patients with hyponatremia before surgery. There was no statistical difference in baseline data between the two groups, as shown in Table 1.

Treatment method

Surgical intervention

All patients underwent neuroendoscopic skull base tumor resection after general anesthesia, and the specimens were timely collected for examination to determine the pathological classification. Skull base reconstruction was performed during the surgery.

Treatment of hyponatremia

Oral sodium supplementation

For sober patients, doctors guided them to eat more sodium-rich foods (such as pickled vegetables and pickled foods) or drink warm saline water (7). Oral salt has a poor taste and is irritating to the oral cavity and gastrointestinal tract, increasing the amount of drinking water, which results in poor compliance of patients. Therefore, we guided the patients to take oral salt capsules (salt into empty capsules) with meals, to reduce the stimulation of the patient's taste and sodium salt excretion caused by transient blood volume expansion following intravenous rehydration. The dosage of salt capsules was determined according to the blood sodium level of patients, generally 12 g/day, 3–4 times.

Intravenous sodium supplementation

Intravenous sodium supplementation was given according to the doctor's instructions, based on the urine osmotic pressure and actual condition of patients. The amount of sodium to be supplemented was calculated according to the formula: sodium to be supplemented (mmol) = (normal blood sodium (mmol/L) —measured blood sodium (mmol/L)) * body weight (kg) * 0.5 (female) or 0.6 (male) (9). An increase in blood sodium >10 mmol/L should be avoided in the first 24 h, and then <8 mmol/L every 24 h. The rate of sodium supplementation should not be very fast. The rising rate of blood sodium should be maintained below 0.7–1.0 mmol/(L·h), and not exceed 12 mmol/L in 24 h. According to the calculation that 17 mmol sodium is equal to 1 g sodium chloride, in the present study,

TABLE 1 Clinical data of two groups.

Group	Case	Sex		Age (year)		Tumor type		Degree of tumor resection	
		Male	Female	≤46	>46	Pituitary adenoma	others	Total resection	Subtotal resection
Hyponatremia group	44	22	22	29	15	37	7	27	17
Normonatremia group	137	73	64	63	74	129	8	103	34
X^2		0.144		5.289		4.443		3.143	
P		0.704		0.021		0.035		0.076	

60–80 ml of 10% sodium chloride was generally added to 500 ml of 0.9% sodium chloride solution; the infusion pump was used to control the drip rate at 140–145 ml/h, and the infusion was completed within 4 h. After the target level of blood sodium was reached, the sodium supplementation was continued according to the urine volume and urine sodium level. The total amount of urine sodium excreted in the last 24 h plus the physiological requirement was supplemented daily until the blood sodium level became stable (10, 11).

Control of urine volume and restricted intake

After the surgery, doctors and nurses guided and assisted the patient to accurately measure and record their urine volume, and actively asked them whether there was any increase in urine volume, especially the urine volume per hour. If the urine volume per hour is ≥200 ml for 2 consecutive hours, it is necessary to inform the doctor in time (12). According to the doctor's instructions, 0.1 mg desmopressin acetate was given until the urine volume was controlled. If necessary, urinary sodium and 24-hour urine osmotic pressure was monitors, and water restriction measures were implemented according to the doctor's advice.

Evaluation indicators and data collection

Diagnostic criteria of hyponatremia

Mild hyponatremia: 130–135 mmol/L; Moderate to severe hyponatremia: <130 mmol/L (13).

Nursing related events

Nursing related events were collected during the hospitalization, such as falling down and falling off the bed.

Statistical analysis

Excel 2007 and SPSS 23.0 were utilized for data collection and statistical analysis. Quantitative data were expressed as means and standard deviation, and qualitative data were expressed as frequency and percentage (%) and compared using the chi square test. A $p < 0.05$ indicated statistical significance.

Results

Incidence of postoperative hyponatremia in patients with different types of skull base tumors

In this study, the incidence of hyponatremia after growth hormone type pituitary adenoma surgery was the lowest, with the earliest occurrence time and fastest correction time. The incidence, occurrence, and correction time of postoperative hyponatremia in patients with different types of skull base tumors are shown in **Table 2**

Incidence of postoperative hyponatremia in patients with skull base tumors at different stages

Some studies depicted that hyponatremia occurring 3 days after surgery is late-onset hyponatremia (5), and other studies suggested that hyponatremia occurring 5–7 days after surgery is late-onset hyponatremia (14). In our study, 33 patients (75%) developed hyponatremia 3 days after surgery, including all patients with moderate to severe hyponatremia. The incidence of postoperative hyponatremia in patients with skull base tumors at different stages is shown in **Table 3**.

Urine volume control

In this study, there were 98 patients with polyuria after surgery, of which 96 were orally or intravenously treated with desmopressin acetate, and the effect of urine volume control was good.

TABLE 2 Occurrence and correction of postoperative hyponatremia in patients with different types of skull base tumors.

Tumor classification	Gonadotropic pituitary adenoma	Adrenergic pituitary adenoma	Prolactin type pituitary adenoma	Growth hormone type pituitary adenoma	Multihormone cellular pituitary adenoma	Pituitary adenoma without endocrine function	Unclassified pituitary adenoma	Other types besides pituitary adenoma
Case	39	28	14	29	24	26	6	15
Cases of hyponatremia	8	5	6	2	9	4	1	9
Incidence of hyponatremia (%)	20.5	17.9	42.9	6.9	37.5	15.4	16.7	60
Time of hyponatremia (day)	5.75 ± 4.59	4.60 ± 3.65	6.00 ± 3.10	1.50 ± 0.71	8.25 ± 5.78	7.75 ± 3.30	0	4.25 ± 3.85
Correction time (day)	4.75 ± 3.37	8.80 ± 12.03	7.50 ± 4.09	3.50 ± 2.12	7.25 ± 6.63	4.50 ± 2.38	2.00	6.50 ± 4.34

TABLE 3 Incidence of hyponatremia among patients in different periods.

Time of postoperative hyponatremia (day)	Mild hyponatremia (case)	Moderate to severe hyponatremia (case)
<3	11	0
3–6	11	1
>6	16	5

Nursing-related events

All patients had no nursing-related events such as scald, fall and bed fall during their stay in the hospital.

Discussion

The incidence of hyponatremia varied in patients with skull base tumors in different pathological types and different periods

According to some earlier studies, the incidence of delayed hyponatremia after surgery for non-secretory pituitary adenoma and adrenocorticotropic cell adenoma was higher than that of other groups. The clinical symptoms of patients with moderate to severe hyponatremia could be improved within approximately 2 days when treated with hypertonic saline and hydrocortisone (15). In this study, the incidence of hyponatremia after growth hormone type pituitary adenoma surgery was the lowest, with the earliest occurrence time and fastest correction time, which was thought to be associated with the routine hydrocortisone supplementation in the early postoperative period. Based on our study, hyponatremia occurred in all patients from 0 to 30 days after surgery, suggesting that the blood sodium level of patients should be closely monitored throughout the perioperative period and should be an important part of the follow-up after discharge.

Pay close attention to the changes in blood sodium value and select the appropriate sodium supplementation approach to correct hyponatremia

Several studies (16, 17) have shown that even mild hyponatremia can have an impact on the prognosis of patients. In nursing management, the nursing of patients with mild hyponatremia should not be neglected, but close attention should be paid to their changes. Dynamic monitoring of 24 h urinary sodium and blood electrolyte levels is an important method for observing the effect and timely adjusting the strategy of sodium supplementation. Blood samples are collected 4 h after sodium supplementation (13), and the collection should be avoided when sodium-containing drugs are infused. If the patient is receiving liquid infusion into one limb, the other limb should be selected for collection. It is prohibited to collect blood samples from Peripherally Inserted Central Catheter(PICC) catheterization or other deep vein catheterization ends and through the peripheral indwelling needle to avoid the influence of residual sealing solution in the pipeline on the test results. If it is needed to puncture the indwelling needle and collect blood at the same time, avoid passing saline through the tube before puncture. When intravenous infusion of highly concentrated saline is used, an infusion pump is applied to control the speed of sodium supplementation. This method does not only achieve a constant infusion speed, but also prevents the patients or others from adjusting the drip speed by themselves or forgetting to adjust the drip speed when changing the liquid and consequently cause adverse consequences due to rapid infusion. Different brands of equipment indeed have differences in flow rate and accuracy (18). It is therefore recommended to select an infusion pump of the same brand and use the matching infusion device to calibrate the infusion pump on time to ensure reliable quality and accurate data of the infusion pump. In this study, the patients did not have severe complications such as osmotic demyelination syndrome (ODS) due to the rapid rise of blood sodium concentration.

Control of urine volume and restriction of intake are significant steps to correct hyponatremia

Due to the special location of the skull base tumor, the pituitary stalk and hypothalamus may be interfered with during the surgery, and the secretion of antidiuretic hormone, polyuria, and disturbance of water and salt metabolism may occur, resulting in hyponatremia. Most of the symptoms are transient, which could be managed with antidiuretic analogue treatment (5). Timely supplementation of desmopressin acetate can reduce sodium loss. In this study, during the use of desmopressin acetate, the patients' urine color and urine volume were accurately assessed. Once the urine volume was controlled, the drug could be stopped. The family members were guided to use unified and standard measuring tools to measure and record the drinking water volume with a graduated measuring cup, and the water content of food was assessed and recorded by the nurses. The same graduated measuring cup was utilized to calculate the volume, especially the urine volume. On the other hand, the use of disposable drainage or urine bags as measuring tools should be avoided. Bedridden patients were assisted to discharge their urine to the urinal, and then use the measuring cup for measurement.

The entry and exit record sheet was placed beside the bed for easy recording. The patients were reminded not to directly discharge their urine into the toilet for estimation. Burke et al. reported that the incidence of hyponatremia in patients with pituitary adenomas can be significantly reduced by strictly limiting the daily water intake to 1,000 ml one week after surgery (19). Therefore, the patients were advised to avoid drinking a lot of water and to control the drinking water volume within 1,000 ml/day after surgery.

Pay attention to the bedside handover and the patient's complaints and performance, and jointly ensure the safety of patients

The clinical symptoms of hyponatremia vary according to its severity and the rate of blood sodium decline (7). The clinical manifestations of early hyponatremia lack specificity. During the critical process of shift handover, doctors and nurses should closely enquire and assess whether patients with hyponatremia have symptoms such as weakness of both lower limbs, poor appetite, dizziness, and inattention; hang high-risk tips for falls at the bedside; and instruct their families to pay attention to the patients' emotions. The patients should be accompanied by their families to timely inform abnormalities and improve safety management. Nursing-related events such as falling, scalding, and bed falling should be avoided. After sodium supplementation, blood samples should be taken on time for recheck. The results of blood sodium re-examination should be closely monitored to timely inform the doctor and adjust the sodium supplementation scheme according to the changes in blood sodium value. Oral sodium supplementation and dietary sodium supplementation are also considered important methods to supplement sodium. In our study, nurses chose the method of putting salt into capsules, which provides little stimulation on oral taste and accurate sodium supplementation. The acceptance of oral sodium supplementation was improved, reflecting the humanistic spirit of nursing.

Conclusions

In summary, we showed that patients who underwent endoscopic resection of skull base tumors were prone to hyponatremia at different times after surgery. Based on the characteristics of its occurrence and development, nurses should focus on postoperative observation, accurate assessment, and medication administration to identify the causes of hyponatremia through observation. Moreover, the principles, methods, and approaches of sodium supplementation should be mastered to complete the sodium supplementation treatment in a standardized manner, so that hyponatremia can be corrected. In clinical nursing practice, efforts are made through propaganda and education to guide the process of sodium supplementation and to evaluate the effect. Nurses should be involved in the whole management process of patients with hyponatremia and truly implement the details of nursing measures, so that patients could avoid complications, ensure safety, and recover as soon as possible.

Data availability statement

The original contributions presented in the study are included in the article/Supplementary Materials, further inquiries can be directed to the corresponding author/s.

Ethics statement

Written informed consent was not obtained from the minor(s)' legal guardian/next of kin for the publication of any potentially identifiable images or data included in this article.

Author contributions

YY and CL carried out the research. YY, CL and YZ participated in data analysis. YY and CL drafted the manuscript. YZ and YY critically reviewed the overall manuscript as well as supervised the study. All authors contributed to the article and approved the submitted version.

Conflict of interest

The authors declare that the research was conducted in the absence of any commercial or financial relationships that could be construed as a potential conflict of interest.

Publisher's note

References

1. Zhong P. History and prospect of skull base surgery. *Shanghai Med J*. (2017) 40:650–55. doi: CNKI:SUN:SHYX.0.2017-11-006

2. Rui Z, Cui L, Hongwei G, Weihong C, Tong L. Craniopharyngioma patients after endoscopic nasal minimally invasive surgery complications nursing care. *J Nurs*. (2020) 27:63–5. doi: 10.16460/j.issn1008-9969.2020.15.0063

3. Gui SB. Neuroendoscopic transnasal approach for the treatment of craniopharyngioma. *Chin Neurosurg J*. (2019) 35(4):330–33. doi: 10.3760/cma.j.issn.1001-2346.2019.04.002

4. Peng Y, Wang M, Gu H, Xiang J, Xu Y, Jiang Y. Delayed hyponatremia after neuroendoscopic transnasal transsphenoidal surgery for pituitary adenoma. *Clin Neurosurg*. (2020) 17:125–29. doi: CNKI:SUN:LCSW.0.2020-02-002

5. Zhang J, Wang Y, Xu X, Gu Y, Huang F, Zhang M. Postoperative complications and quality of life in patients with pituitary adenoma. *Gland Surg*. (2020) 9:1521–29. doi: 10.21037/gs-20-690. PMID: 33224827; PMCID: PMC7667121

6. Tan R, Shan Y, Tian C, Huang D, Shi Q, Yang F, et al. The neurological effects of the prognosis of patients with severe hyponatremia. *People's Liberation Army Med J*. (2022) 47(07):717–722. doi: 10.11855/j.issn.0577-7402.2022.07.0717

7. Yu D, Huang N, Guo Y. Glioma by hyponatremia after risk factor analysis and intervention countermeasures. *J Nurs Train J*. (2021) 4:380–83. doi: 10.16821/j.carol carrollnkiHSJX.2021.04.015

8. Fan C, Zhang Q. Interpreting the neurosurgeon guide clinical diagnosis and treatment of hyponatremia. *Int J Neurol Neurosurg*. (2010) 37(02):158–61. doi: 10.16636/j.carolcarrollnkijinn.2010.02.001

9. Spasovski G, Vanholder R, Allolio B, Annane D, Ball S, Bichet D, et al. Clinical practice guideline on diagnosis and treatment of hyponatraemia. *Intensive Care Med*. (2014) 40:320–31. doi: 10.1007/s00134-014-3210-2

10. Expert Consensus Compilation Committee on Craniopharyngioma Treatment, Pediatric Neurosurgery Group, Chinese Neurosurgery Society. Chinese Expert consensus on perioperative management of craniopharyngioma (2017). *Chin J Med*. (2018) 98:5–10. doi: 10.3760/cma.j.issn.0376-2491.2018.01.003

11. Wu Z, Xiong Z, Wang D, Li J. Diagnosis and treatment of cerebral salt depletion syndrome after craniocerebral injury. *Chin J Clin Neurosurg*. (2021) 26:945–7. doi: 10.13798/j.issn.1009-153X.2021.12.016

12. Sun J, Zhao Y. The difference and nursing measures of water and sodium disorder in patients with neurological tumor resection. *Electron J Clin Med Lit*. (2020) 7:107–8. doi: 10.16281/j.cnki.jocml.2020.10.061

13. Yu L. *Analysis of factors associated with hyponatremia after transsphenoidal pituitary adenoma resection* [*Dissertation*]. Yanji:Yanbian University (2017).

14. Lu Y. *Influencing factors and treatment of delayed hyponatremia after transsphenoidal pituitary tumor resection*. Tianjin: Tianjin Medical University (2019).

15. Wu J, Lu AD, Zhang LP, Zuo YX, Jia YP. Study of clinical outcome and prognosis in pediatric core binding factor-acute myeloid leukemia. *Zhonghua Xue Ye Xue Za Zhi*. (2019) 40:52–7. doi: 10.3760/cma.j.issn.1001-2346.2016.01.005

16. Funk GC, Lindner G, Druml W, Metnitz B, Schwarz C, Bauer P, et al. Incidence and prognosis of dysnatremias present on ICU admission. *Intensive Care Med*. (2010) 36:304–11. doi: 10.1007/s00134-009-1692-0. Epub 2009 Oct 22. PMID: 19847398

17. Lazúrová I. Syndróm neprimeranej antidiurézy (SIAD) a súčasný manažment hyponatriémie [syndrome of inappropriate antidiuresis and the current management of hyponatremia]. *Vnitr Lek*. (2017) 63:593–7. Czech. PMID: 29120656. doi: 10.36290/vnl.2017.118

18. Huang H, Feng X. Influence of different brands of syringes on the flow accuracy of syringe pump. *Chin J Med Device*. (2022) 35:26–31.

19. Burke WT, Cote DJ, Iuliano SI, Zaidi HA, Laws ER. A practical method for prevention of readmission for symptomatic hyponatremia following transsphenoidal surgery. *Pituitary*. (2018) 21:25. doi: 10.1007/s11102-017-0843-5

frontiers | Frontiers in Surgery

TYPE Original Research
PUBLISHED 06 January 2023
DOI 10.3389/fsurg.2022.1054416

OPEN ACCESS

EDITED BY
Yupeng Zhang,
Capital Medical University, China

REVIEWED BY
Wei Hua,
Fudan University, China
Zhen Zhang,
Shandong Provincial Hospital, China
Zhenyu Wang,
Peking University Third Hospital, China

*CORRESPONDENCE
Peng Zhao
zhaopeng@ccmu.edu.cn
Changyu Lu
luchangyu@pkuih.edu.cn

†These authors have contributed equally to this work and share first authorship

SPECIALTY SECTION
This article was submitted to Neurosurgery, a section of the journal Frontiers in Surgery

RECEIVED 26 September 2022
ACCEPTED 08 November 2022
PUBLISHED 06 January 2023

CITATION
Liang J, Li K, Luo B, Zhang J, Zhao P and Lu C (2023) Effect comparison of neuroendoscopic vs. craniotomy in the treatment of adult intracranial arachnoid cyst.
Front. Surg. 9:1054416.
doi: 10.3389/fsurg.2022.1054416

Effect comparison of neuroendoscopic vs. craniotomy in the treatment of adult intracranial arachnoid cyst

Jianfeng Liang[1†], Kai Li[1†], Bin Luo[1], Jun Zhang[1], Peng Zhao[2*] and Changyu Lu[1*]

[1]Department of Neurosurgery, Peking University International Hospital, Beijing, China, [2]Department of Neurosurgery, Beijing Tiantan Hospital, Capital Medical University, Beijing, China

Purpose: Intracranial arachnoid cysts are common, accounting for about 1%–2% of intracranial space-occupying lesions. There is controversy over the method of surgical intervention, and in order to provide guidance for surgical decision making, this study compares the efficacy of craniotomy vs. neuroendoscopic surgery in treating arachnoid cysts.

Methods: The adult patients with arachnoid cyst admitted to our department from October 2016 to August 2021 were retrospectively analyzed. Thirteen adult patients were recruited, and divided into two groups: neuroendoscopic group (group A) and craniotomy group (group B). We compared the gender, age, clinical symptoms, preoperative and postoperative cyst sizes, symptom improvement, complications, length of hospital stay, and hospital costs between two groups to analyze the therapeutic effects of these two surgical methods.

Results: The cost of hospitalization in group A was significantly lower than that in group B (47,292.8 vs. 65,151.8 yuan, $P < 0.05$), and there was no difference in the length of hospital stay between the two groups. The preoperative cysts in group A were significantly larger than those in group B (6.38 vs. 2.97 cm, $P < 0.05$). In groups A and B, the short-term symptom improvement rates were 100% and 75.0%, respectively. The long-term symptom improvement rates were 77.78% and 75.0% ($P > 0.05$), respectively.

Conclusion: Both neuroendoscopic and craniotomy have good curative effects for the treatment of intracranial arachnoid cysts. There was no significant difference in the outcomes between the two surgical techniques. The cost of hospitalization can be reduced with neuroendoscopic surgery. Neuroendoscopic treatment is recommended for large intracranial arachnoid cysts, and craniotomy is suitable for small intracranial arachnoid cysts.

KEYWORDS

neuroendoscopic, craniotomy, intracranial arachnoid cyst, surgery, complication

Introduction

Intracranial arachnoid cyst is a benign cyst occurring in the central nervous system, which is closely related to arachnoid. The cystic fluid is often colorless, clear, and similar to cerebrospinal fluid. Intracranial arachnoid cyst can cause neurological symptoms clinically, and the incidence rate of these legions is about 1% of intracranial space-occupying lesions (1).

In recent years, the application of head CT and/or MRI has become widespread with the development of imaging examinations. Usually, an intracranial arachnoid cyst is found by imaging examination after brain trauma (2), and most of the patients have no clinical symptoms (3). Thus, intracranial arachnoid cysts are often found by accident, and the clinical detection rate of intracranial arachnoid cysts is significantly higher than before (2).

Intracranial arachnoid cysts are usually stable; the size mostly remains unchanged, and some cysts might shrink and disappear (4, 5). Compared with pediatric intracranial arachnoid cyst patients, the adult patient's lesion is more stable (6). Thus, there are fewer adult intracranial arachnoid cyst patients with an indication for surgery. The indications for surgery for an intracranial arachnoid cyst include intracranial hypertension, seizure, dysneuria, hemorrhage, and an enlarged cyst (7, 8).

The surgical approaches to intracranial arachnoid cyst include endoscopic surgery, shunt, craniotomy, and drainage (9, 10). Craniotomy and endoscopic surgery are common approaches to intracranial arachnoid cyst, but it is still unclear which approach has better efficacy (10, 11).

In this study, we retrospectively followed up adult patients with intracranial arachnoid cysts who underwent craniotomy or endoscopic surgery in our hospital and compared the improvement of clinical symptoms, complications, treatment costs, and hospitalization days in order to provide a basis for the selection of surgical methods for the clinical treatment of intracranial arachnoid cysts.

Materials and methods

General data

The present study is a retrospective study on 13 adult patients with intracranial arachnoid cyst who were admitted to our hospital for medical treatment between October 2016 and August 2021. The patients were divided into two groups depending on the surgical approach. The patients in group A underwent endoscopic surgery ($n = 9$), and the patients in group B underwent craniotomy ($n = 4$). The patient's general data are listed in **Table 1**.

Imaging examination

All cases in the group underwent CT and/or MRI examinations before and after the operation. In group A, three patients' lesions were in the frontal lobe, three lesions were in the temporal lobe, two lesions were in the cerebellopontine angle (CPA), one lesion was in the saddle,

TABLE 1 Overview of patients.

No	Group	Sex	Age (years)	Symptoms	Follow-up (months)	MD (cm, pre)	MD (cm, post)	Complication (post)	Location
1	A	Female	26	Dizziness, giddiness, memory deterioration	64	6.29	6.17	Intracranial infection, hyponatremia	Saddle
2	A	Male	36	Headache	62	12.90	12.68	None	Left frontal and temporal lobes
3	A	Female	44	Headache	46	5.54	5.25	Hyponatremia	Prepontine cistern
4	A	Female	60	Dizziness	38	5.85	4.26	LDVT	Right frontal lobe
5	A	Female	63	Dizziness decreased muscle strength in left limb	39	6.12	3.08	None	Right temporal lobe
6	A	Male	36	Headache	26	6.65	5.27	None	Right temporal lobe
7	A	Male	19	Seizure	13	3.76	1.37	Intracranial infection, hyponatremia, hypokalemia	Right frontal lobe
8	A	Female	26	Ataxia, dysarthria,	11	6.10	4.2	None	Left CPA
9	A	Female	33	Dizziness, tinnitus, ataxia	11	4.23	2.94	None	Right CPA
10	B	Male	35	Hand tremor	69	3.69	3.65	None	Left temporal lobe
11	B	Male	35	Dizziness, headache, vomiting	61	4.45	3.58	None	Cerebellum
12	B	Female	66	Headache	38	1.54	1.04	LDVT	Left CPA
13	B	Female	55	Hand numbness, headache	20	2.21	0.83	Dysphagia, hoarseness	Left CPA

No, number; MD, maximum diameter of intracranial arachnoid cyst; Pre, preoperative; Post, postoperative; cm, centimeter; LDVT, lower extremity deep venous thrombosis; CPA, cerebellopontine angle. MD (cm, post) showed the smallest MD of the cyst which was available on MRI or CT image during the follow-up period.

and one lesion was in the prepontine cistern. In group B, two lesions were in CPA, one was in the temporal lobe, and one was in the cerebellum. Because of the irregular shape of the cyst, we measured the maximum diameter of the cyst for comparison. The maximum diameter of each intracranial arachnoid cyst was measured in before and after operation (Table 1).

Surgical approaches

Neuroendoscopic surgery

After general anesthesia, one hole was drilled with the use of a bone drill. Then, the dura was suspended and the neuroendoscope was applied. The dura was dissected to expose the arachnoid cyst wall under neuroendoscope. The cyst was cut open, and the cyst fluid was released. In order to keep the cyst from communicating with the cisterna, a cyst-ventricular cisternostomy was performed by bipolar electrocoagulation, and part of the cyst wall was resected with microshear (Figures 1A–C) (12).

Craniotomy

A craniotomy was performed under general anesthesia to expose the arachnoid cyst, and the parietal arachnoid layer was cut off to release the cystic fluid. The cyst wall was partially or extensively resected under the microscope. The cisternae adjacent to the arachnoid cyst cavity were gently pushed through so that the arachnoid cyst cavity and cisternae could communicate with each other to avoid cyst recurrence after the surgery.

Follow-up

Patient information was collected from the medical record system of our hospital and followed up by telephone and outpatient clinic (13, 14). Imaging data (CT and MRI) were obtained from the imaging system of our hospital and other communication devices.

Statistical analysis

Data with normal distribution were described by mean ± standard deviation ($x \pm s$). The difference in means between the two samples was compared using an independent sample t-test. Categorical variables were described by the number of cases and constituent ratio, and the differences between groups were tested by the χ^2 test. A $P < 0.05$ was defined as statistically significant (two tails) (13, 15).

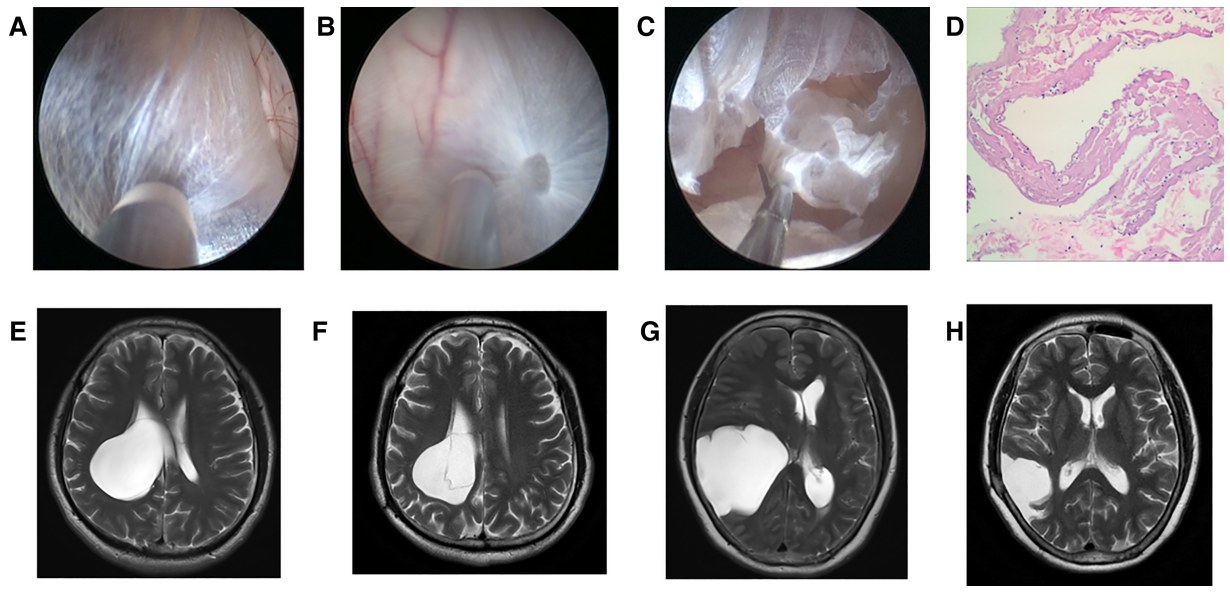

FIGURE 1
Neuroendoscopic treatment to intracranial arachnoid cyst. (A) Lateral wall of intracranial arachnoid cyst before it was incised (No. 6 patient). (B) Medial wall of intracranial arachnoid cyst after entering it with neuroendoscope (No. 6 patient). (C) Part of medial wall was resected with microshear (No. 6 patient). (D) Pathological image of the arachnoid cyst wall which was resected. (E) Preoperative T2 MRI image of No. 6 patient. (F) T2 MRI image of No. 6 patient at 2 years and 2 months after neuroendoscopic surgery. (G) Preoperative T2 MRI image of No. 5 patient. (H) T2 MRI image of No. 5 patient at 1 year after neuroendoscopic surgery.

Results

Demographic data

A total of nine patients with intracranial arachnoid cyst were included in group A: 3 (33.3%) were male and 6 (66.7%) were female. In group B, there were 2 (50%) male and 2 (50%) female. The patient age was 38.11 ± 5.04 years in group A, and 47.75 ± 7.70 years in group B. The preoperative hospital stay, postoperative in-hospital stay, and total in-hospital stay were not different between the two groups, but the hospital cost of group A was significantly lower than that of group B (47,292.8 vs. 65,151.8 yuan) (Table 2).

TABLE 2 Comparison of clinical data between group A and group B.

Item	Group A (9 cases)	Group B (4 cases)	*P*-value
Age (year, $x \pm s$)	38.11 ± 5.04	47.75 ± 7.70	0.314
Male/female (cases)	3/6	2/2	0.569
Hospitalization cost (RMB, ten thousand)	4.73 ± 0.47	6.52 ± 0.52	0.045
Total hospital stay (day)	17.11 ± 1.50	13.5 ± 0.87	0.1567
Preoperative hospital stay (day)	4.44 ± 0.55	3.75 ± 0.48	0.460
Postoperative hospital stay (day)	12.67 ± 1.61	9.75 ± 1.11	0.280

TABLE 3 Symptoms and signs in group A and group B.

Symptoms and signs	Group A (9 cases)	Group B (4 cases)
Dizziness	4 (44.4%)	2 (50.0%)
Headache	3 (33.3%)	2 (50.0%)
Ataxia	2 (22.2%)	2 (50.0%)
Seizure	1 (11.1%)	0 (0%)
Dysarthria	1 (11.1%)	0 (0%)
Tinnitus	1 (11.1%)	0 (0%)
Hand tremor	0 (0%)	1 (25.0%)
Hand numbness	0 (0%)	1 (25.0%)

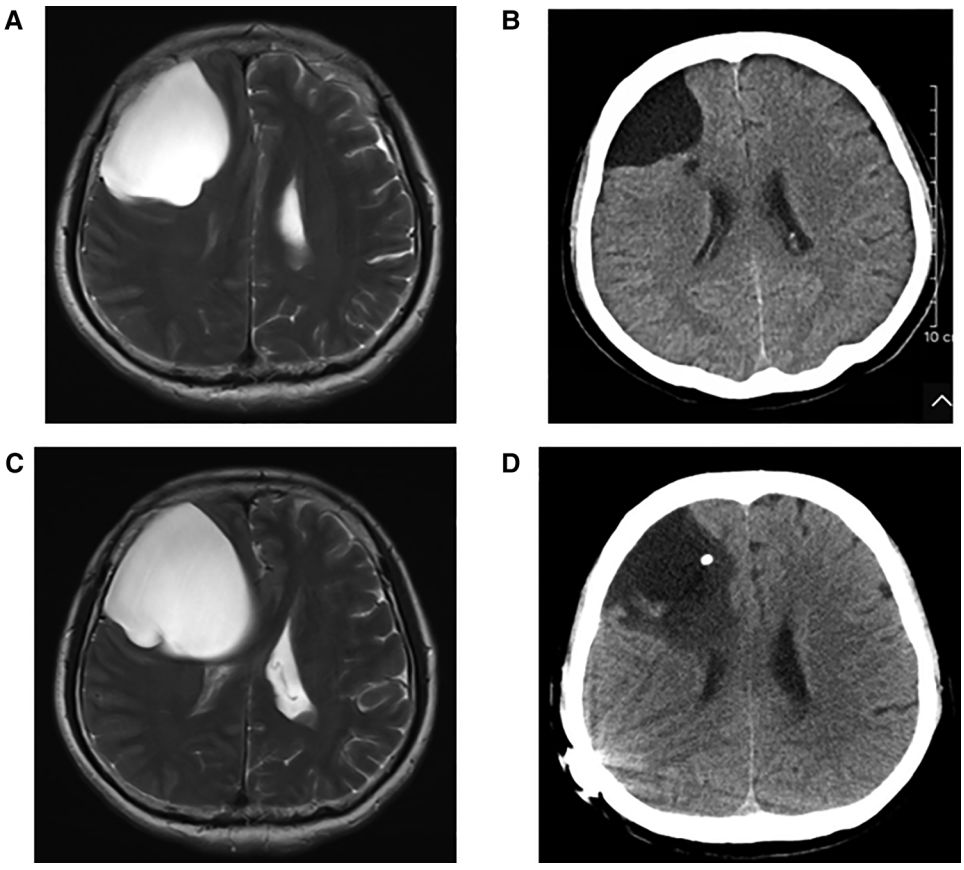

FIGURE 2
(A) Preoperative T2 MRI image of No. 4 patient. (B) CT image of No. 4 patient at 1 year and 4 months after neuroendoscopic surgery. (C) T2 MRI image of No. 4 patient at 2 years and 6 months after neuroendoscopic surgery. (D) CT image of No. 4 patient after intracranial arachnoid cyst-peritoneal shunt.

Clinical presentation and follow-up outcomes

In group A, four patients presented with dizziness in the preoperative period; three of the four patients had relief of dizziness in the postoperative period. The three patients suffered from headache before surgery, and headache symptoms improved in all of them after surgery. However, two of the three patients had an increase in headache symptoms during the follow-up period (No. 3 and No. 4 patients). Their MRI showed the intracranial arachnoid cysts had grown larger than them in the preoperative period, and they then underwent intracranial arachnoid cyst-peritoneal shunt in our department (No. 4 patient's MRI and CT images are shown in Figure 2). Two patients presented with cerebellar ataxia in the preoperative period, and their symptoms improved after surgery. One patient had epileptic symptoms before surgery, and his frequency of seizures decreased after surgery (Table 3).

In group B, three patients suffered from headache, and they had relief of headache after surgery. Two patients presented with cerebellar ataxia. After surgery, one patient's symptom was improved, but the other patient presented with symptoms related to the posterior cranial nerve. One patient had aphasia and showed progressive improvement in aphasia during the follow-up period.

TABLE 4 Outcomes in group A and group B.

Item	Group A (9 cases)	Group B (4 cases)	*P*-value
MD (cm, preoperative)	6.38 ± 0.87	2.97 ± 0.66	0.034
MD (cm, postoperative)	5.03 ± 1.07	2.28 ± 0.78	0.138
Postoperative complication	4 (44.44%)	2 (50.0%)	0.852
Follow-up period (month)	34.44 ± 6.90	47 ± 11.14	0.344
Symptom relief (short-term)	9 (100%)	3 (75.0%)	0.119
Symptom relief (long-term)	7 (77.78%)	3 (75.0%)	0.913

MD, maximum diameter of intracranial arachnoid cyst; cm, centimeter.

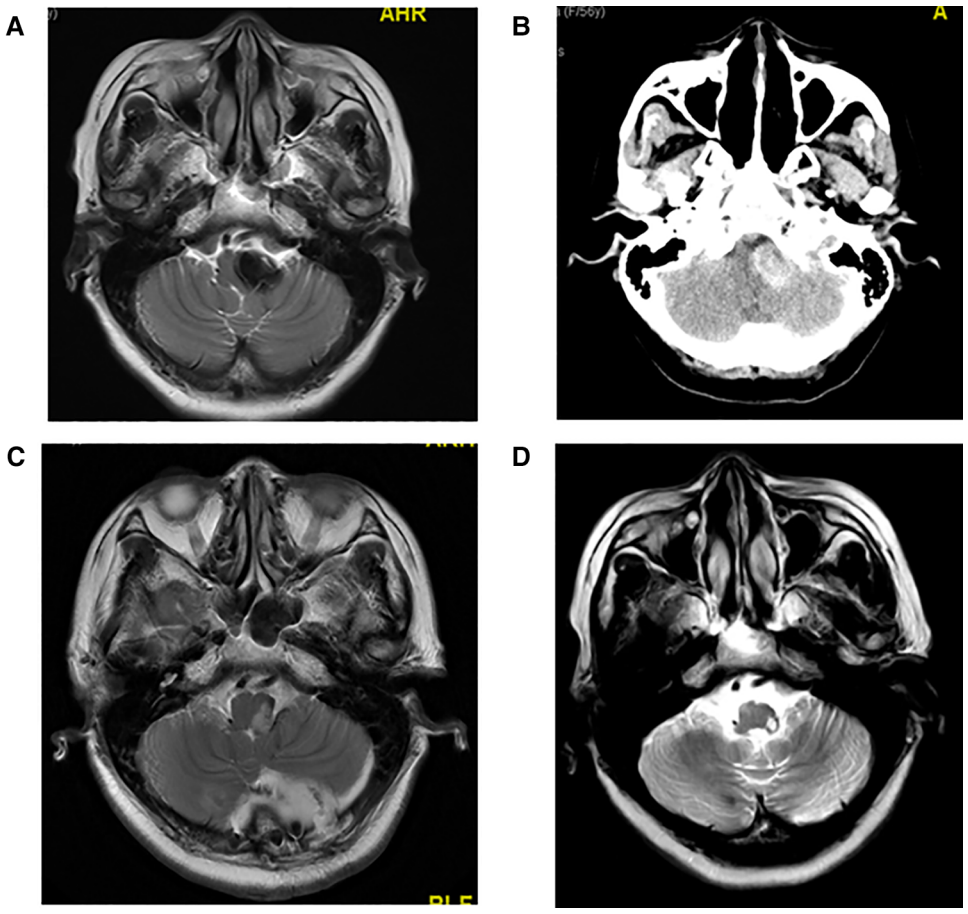

FIGURE 3
(A) Preoperative T2 MRI image of No. 13 patient. (B) Preoperative CT image of No. 13 patient with high CT signal. Hemorrhage was observed in the arachnoid cyst during craniotomy. (C) T2 MRI image of No. 13 patient at 1 week after craniotomy. (D) T2 MRI image of No. 13 patient at 1 year and 10 months after craniotomy.

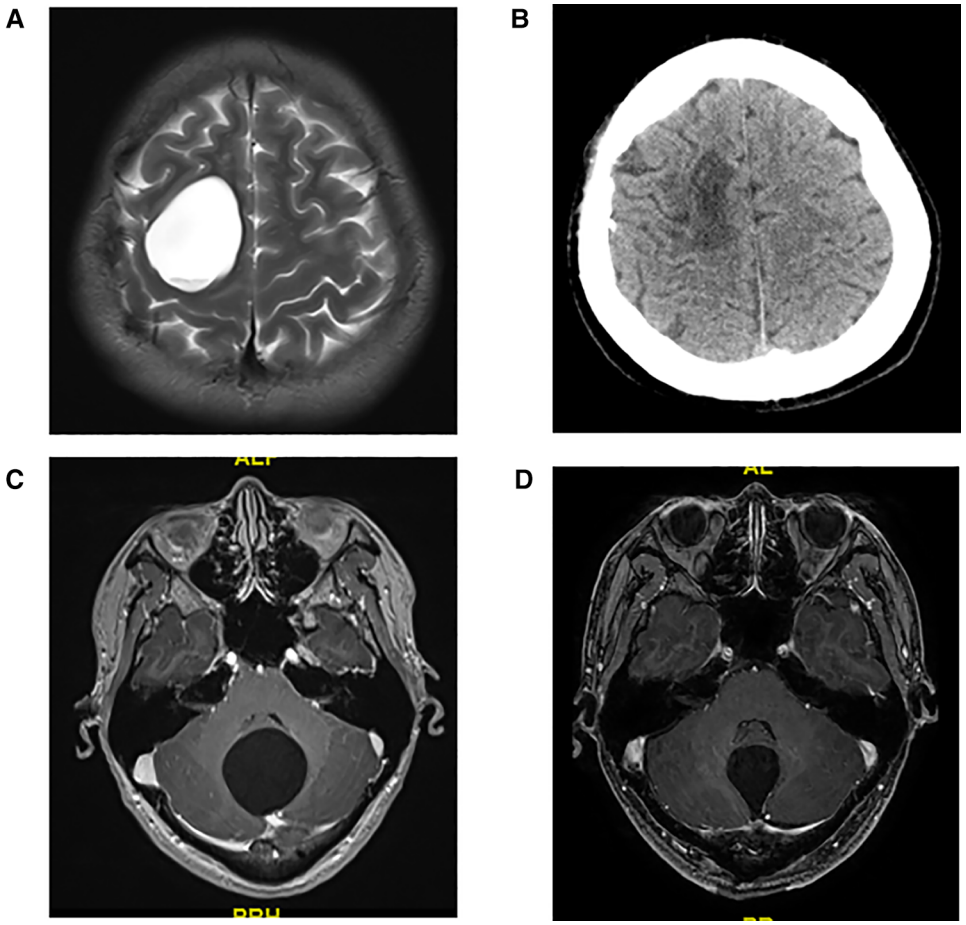

FIGURE 4
(A) Preoperative T2 MRI image of No. 7 patient. (B) CT image of No. 7 patient at 1 month after neuroendoscopic surgery. (C) Preoperative T1 MRI image of No. 11 patient. (D) T1 MRI image of No. 11 patient at 1 week after craniotomy.

The maximum diameter of intracranial arachnoid cysts in group A was 6.38 cm on average, and that in group B was 2.97 cm on average, which was significantly different between the two groups (**Tables 1**, **4**). In group A, all of the patients' intracranial arachnoid cysts showed a remarkable reduction in cyst size during the follow-up period (e.g., No. 6 and No. 5 patients' MRI images are shown in **Figures 1E–H**). However, two patients' cysts recurred, and an intracranial arachnoid cyst-peritoneal shunt was performed. In group B, patients' intracranial arachnoid cysts were resected, then the brain tissue tends to return to the normal anatomical structure (e.g., No. 13 patient's MRI and CT images are shown in **Figure 3**), and the cyst did not recur during the follow-up period.

Discussion

Intracranial arachnoid cysts are common intracranial space-occupying lesions. Previous studies reported the incidence of this cyst in males is the same as with that in females (16). Intracranial arachnoid cysts are often found in the middle cranial fossa, posterior cranial fossa, suprasellar, and quadrigeminal bodies (7, 9). Some intracranial arachnoid cyst patients present with clinical symptoms, such as headache, nausea, vomiting, dizziness, seizures, and cranial hypertension (7, 8). Although it is still controversial about the operation's indication to intracranial arachnoid cysts, patients with clinical symptoms are suggested to surgical therapy.

In this study, we demonstrated that short-term outcomes for patients who underwent endoscopic surgery in group A were the same as those in group B, and that hospital costs were significantly lower in group A than in group B. However, in group A patient No. 3, the intracranial arachnoid cysts recurred after neuroendoscopic surgery a year later, and she underwent intracranial arachnoid cyst-peritoneal shunt. No. 4 patient in group A resuffered from dizziness in 2.5 years after neuroendoscopic surgery and presented with intracranial arachnoid cyst recurrence in the right frontal lobe, and she also

underwent an intracranial arachnoid cyst-peritoneal shunt. The recurrence rate in group A is 22.2% but in group B is 0%; thus, long-term outcome in group B might be better than that in group A. After neuroendoscopic surgery, the cyst became smaller, and the defect of the arachnoid cyst may regrow and fuse, then cyst-cisterna communication was interrupted. This might be the reason for the recurrence.

Neuroendoscopic surgery is a minimally invasive technique that allows for direct visualization of intracranial area. Few previous studies compared the length of hospital stay and hospitalization costs of these two surgical methods for treating adult intracranial arachnoid cysts. In the current study, the total in-hospital stay was 17.1 days vs. 13.5 days (group A vs. group B), but the hospital cost of group A was significantly lower than that of group B (47,292.8 vs. 65,151.8 yuan). This study compared the economic burden and found that neuroendoscopic surgery could reduce hospitalization costs and the economic burden on patients.

It is still controversial which surgical approach is suitable for adult intracranial arachnoid cysts patients (9, 11). In the current study, we did not use the volume to compare the intracranial arachnoid cyst because in some cases the lesion shape was irregular and the area could not be calculated; thus, we used the maximum diameter of the lesion to compare the lesions. The maximum diameter of intracranial arachnoid cysts in group A is significantly larger than in group B. A large intracranial arachnoid cysts may have a wide range of adhesion with normal brain tissue, and resection might cause more serious postoperative complications; thus, in our study, neuroendoscopic surgery was applied to patient with larger intracranial arachnoid cysts (maximum diameter > 4.5 cm), and craniotomy was used to treat patient with small intracranial arachnoid cysts (maximum diameter < 3.0 cm). The selection of the surgical approach to the cyst with maximum diameter between 3.0 and 4.5 cm, depending on the cyst's the position, was close to the function area. For example, patient No. 7 had the lesion in motor function area, and neuroendoscopic surgery was performed to avoid motor function impairment (**Figures 4A,B**). No. 11 patient had the cyst in the dorsal part of the cerebellum, and craniotomy was used to complete resection of the lesion (**Figures 4C,D**).

Intracranial arachnoid cyst in an adult patient with surgical indication is an extremely rare case. Due to low incidence rate, this study collected only 14 cases, which may have an impact on the results of the study, and we plan to recruit more patients for a further study. In addition, prospective studies are needed to provide strong evidence, that can provide a basis for the choice of surgical methods.

Conclusion

Both neuroendoscopic and craniotomy have good curative effects for the treatment of intracranial arachnoid cysts. There was no significant difference in the outcomes between the two surgical techniques. The cost of hospitalization can be reduced with neuroendoscopic surgery. Neuroendoscopic treatment is recommended for large intracranial arachnoid cysts (maximum diameter > 4.5 cm), and craniotomy is suitable to small intracranial arachnoid cysts (maximum diameter < 3.0 cm).

Data availability statement

The original contributions presented in the study are included in the article/Supplementary Material, further inquiries can be directed to the corresponding author/s.

Author contributions

JL and KL carried out the research. JL and KL participated in data analysis. JL drafted the manuscript. CL and PZ critically reviewed the overall manuscript as well as supervised the study. All authors contributed to the article and approved the submitted version.

Funding

This study was supported by Peking University International Hospital Research Grant (No. YN2020ZD04).

Acknowledgments

The authors wish to acknowledge the help received from Lu Liu and Yimeng Ma and all the members in the Department of Neurosurgery.

Conflict of interest

The authors declare that the research was conducted in the absence of any commercial or financial relationships that could be construed as a potential conflict of interest.

Publisher's note

References

1. Wang Y, Wang F, Yu M, Wang W. Clinical and radiological outcomes of surgical treatment for symptomatic arachnoid cysts in adults. *J Clin Neurosci*. (2015) 22:1456–61. doi: 10.1016/j.jocn.2015.03.016

2. Canty KW, Shiroishi MS, Zada G, Sharma S, Jimenez MA. Bilateral arachnoid cyst-associated subdural fluid collections in an infant following TBI. *J Forensic Leg Med*. (2021) 81:102189. doi: 10.1016/j.jflm.2021.102189

3. Li L, Ali M, Menezes AH, Dlouhy BJ. Intracranial extradural arachnoid cyst in a child. *Childs Nerv Syst*. (2017) 33:2201–4. doi: 10.1007/s00381-017-3556-1

4. Adilay U, Guclu B, Tiryaki M, Hicdonmez T. Spontaneous resolution of a Sylvian arachnoid cyst in a child: a case report. *Pediatr Neurosurg*. (2017) 52:343–5. doi: 10.1159/000479328

5. Liu Z, Li J, Xu J. Teaching NeuroImages: spontaneous resolution of a giant intracranial arachnoid cyst. *Neurology*. (2016) 86:e199–200. doi: 10.1212/WNL.0000000000002639

6. Al-Holou WN, Yew AY, Boomsaad ZE, Garton HJL, Muraszko KM, Maher CO. Prevalence and natural history of arachnoid cysts in children. *J Neurosurg Pediatr*. (2010) 5:578–85. doi: 10.3171/2010.2.PEDS09464

7. Mustansir F, Bashir S, Darbar A. Management of arachnoid cysts: a comprehensive review. *Cureus*. (2018) 10:e2458. doi: 10.7759/cureus.2458

8. Al-Holou WN, Terman S, Kilburg C, Garton HJL, Muraszko KM, Maher CO. Prevalence and natural history of arachnoid cysts in adults. *J Neurosurg*. (2013) 118:222–31. doi: 10.3171/2012.10.JNS12548

9. Chen Y, Fang H-J, Li Z-F, Yu S-Y, Li C-Z, Wu Z-B, et al. Treatment of middle cranial fossa arachnoid cysts: a systematic review and meta-analysis. *World Neurosurg*. (2016) 92:480–90. doi: 10.1016/j.wneu.2016.06.046

10. Merola J, Manivannan S, Ooi S, Li Chia W, Makwana M, Lang J, et al. The efficacy of cystoperitoneal shunting for the surgical management of intracranial arachnoid cysts in the elderly: a systematic review of the literature. *Surg Neurol Int*. (2021) 12:624. doi: 10.25259/SNI_463_2021

11. Mørkve SH, Helland CA, Amus J, Lund-Johansen M, Wester KG. Surgical decompression of arachnoid cysts leads to improved quality of life: a prospective study. *Neurosurgery*. (2016) 78:613–25. doi: 10.1227/NEU.0000000000001100

12. Zhang P, Zhang L, Zhao R. Application of MRI images based on Spatial Fuzzy Clustering Algorithm guided by Neuroendoscopy in the treatment of Tumors in the Saddle Region. *Pak J Med Sci*. (2021) 37:1600–4. doi: 10.12669/pjms.37.6-WIT.4850

13. Liang J, Lv X, Lu C, Ye X, Chen X, Fu J, et al. Prognostic factors of patients with Gliomas – an analysis on 335 patients with Glioblastoma and other forms of Gliomas. *BMC Cancer*. (2020) 20:35. doi: 10.1186/s12885-019-6511-6

14. Liang J, Guo Z, Zhang L, Yu Y. Adolescent-onset idiopathic hemifacial spasm. *Neurol India*. (2014) 62:175–7. doi: 10.4103/0028-3886.132367

15. Zhao W, Liang J, Chen Z, Diao Y, Miao G. Combined analysis of circRNA and mRNA profiles and interactions in patients with Diabetic Foot and Diabetes Mellitus. *Int Wound J*. (2020) 17:1183–93. doi: 10.1111/iwj.13420

16. Rabiei K, Jaraj D, Marlow T, Jensen C, Skoog I, Wikkelsø C. Prevalence and symptoms of intracranial arachnoid cysts: a population-based study. *J Neurol*. (2016) 263:689–94. doi: 10.1007/s00415-016-8035-1

frontiers | Frontiers in Oncology

TYPE Original Research
PUBLISHED 24 July 2023
DOI 10.3389/fonc.2023.1008291

OPEN ACCESS

EDITED BY
Philipp Taussky,
Harvard Medical School, United States

REVIEWED BY
Gianluca Trevisi,
G d'Annunzio University, Italy
Fabio Cofano,
University of Turin, Italy
Sheng Han,
The First Affiliated Hospital of China Medical University, China

*CORRESPONDENCE
Peng Zhao
zhaopeng@ccmu.edu.cn

†These authors have contributed equally to this work and share first authorship

RECEIVED 31 July 2022
ACCEPTED 30 June 2023
PUBLISHED 24 July 2023

CITATION
Li K, Liang J, Niu H, Lan S, Liang X, Zhao Y and Zhao P (2023) Effect comparison of neuroendoscopy versus microsurgery in the treatment of lateral ventricular tumors. *Front. Oncol.* 13:1008291. doi: 10.3389/fonc.2023.1008291

Effect comparison of neuroendoscopy versus microsurgery in the treatment of lateral ventricular tumors

Kai Li[1†], Jianfeng Liang[1†], Hongchuan Niu[1†], Shuang Lan[2], Xiaoning Liang[3], Yuanli Zhao[1,4] and Peng Zhao[1,4*]

[1]Department of Neurosurgery, Peking University International Hospital, Beijing, China, [2]Department of Operating Theatre, Peking University International Hospital, Beijing, China, [3]Department of Neurosurgery, PKUCare Zibo Hospital, Zibo, Shandong, China, [4]Department of Neurosurgery, Beijing Tiantan Hospital, Capital Medical University, Beijing, China

Purpose: We sought to reveal the clinical characteristics of lateral ventricle tumors and to evaluate the superior surgical procedure available.

Methods: There involved a total of of 49 adult patients harboring lateral ventricle tumors in neurosurgery department of our hospital from January 2016 to March 2022. The patients enrolled were retrospectively analyzed, so are their clinical manifestations, pathological characteristics and surgical strategies. The patients were allocated into neuroendoscope group (11 cases) and microsurgery group (38 cases) according to the operation method. The two groups underwent a detailed evaluation of operation effectiveness and safety profile (operation time, intraoperative bleeding, surgical resection rate, postoperative complications) and economic indicators (postoperative hospital stay, hospital costs).

Results: The neuroendoscope group demonstrated a markedly shorter operation time than the microsurgery group ($p<0.05$), with the amount of bleeding significantly less than the microsurgery group ($p<0.01$). However, there was no significant difference in the resection rate and postoperative complications between the two groups ($p>0.05$). Significant difference was found in the economic indicators (postoperative hospital stay and hospital costs) of the patients in the neuroendoscope group ($p<0.05$).

Conclusion: Surgery intervention is regarded as the core treatment option for lateral ventricle tumors. Both microsurgery and neuroendoscopy are effective with safety profile. In the selected lateral ventricle tumor surgery, the application of neuroendoscopic surgery showed promising results, in terms of less intraoperative bleeding, and shorter operation time, postoperative hospital stays, and hospital costs. The selection of surgical approach and methods for lateral ventricle tumors is principally depended on the experience of neurosurgeon concerning the surgical approach and related neuroanatomy.

KEYWORDS

lateral ventricle tumor, Neuro-Endoport, microsurgery, surgery, neuroendoscopy

1 Introduction

Lateral ventricle tumor refers to ventricular tumor that develops in the lateral ventricle, accounting for about 0.8-1.6% of intracranial tumors (1, 2). The disease can be originally divided into primary and secondary lateral ventricle tumor. The former originates from the ventricular wall and intraventricular tissue, and the latter from adjacent brain tissue and invades the lateral ventricle. The ever-present challenge of patients with lateral ventricular tumors is that no special clinical symptoms showed in the early stage since the tumors grow in the ventricular cavity. Following the enlarging process, the tumor blocks the cerebrospinal fluid circulation pathway and invades the adjacent structures, the corresponding clinical symptoms appear (3, 4). Surgical resection is currently identified as the preferred method for patients with lateral ventricle tumors. However, Key nerves and blood vessels near the deep structure and rich blood supply to increase the risk of surgery. For most neurosurgeons, lateral ventricle tumor resection is still a challenging operation. Despite that both microsurgery and endoscopic surgery are available, how to select the appropriate surgical approaches is still an ongoing debate, such as transcortical approach and transcallosal approach. There are few comparative studies on the surgical methods of microscopic surgery or endoscopic surgery for lateral ventricle tumors in the past. From January 2016 to March 2022, we operated on 49 adult patients with lateral ventricle tumors and retrospectively analyzed their clinical manifestation, surgical plan, surgical effect, safety and economic indicators, in order to offer theoretical insight for the selection of surgical methods in clinical practice.

2 Materials and methods

2.1 General data

Clinical data of 49 eligible adult patients harboring lateral ventricle tumors in the neurosurgery department of our hospital from January 2016 to March 2022 were retrospectively analyzed. Inclusion criteria (1): tumor located completely or mainly in ventricle (2); The surgery was the first surgery without radiotherapy and/or chemotherapy (3); Complete clinical data. If the diameter of ventricular tumor is more than 5.5cm, microsurgery is selected; if the diameter is less than 5.5cm, microsurgery or neuroendoscopic surgery is selected according to the location of the tumor and the experience of the operator. The patients were allocated into neuroendoscope group (11 cases) and microsurgery group (38 cases) according to the operation method. All 49 patients signed informed consent, and this study complied with the principles of the Declaration of Helsinki. The clinical background of the patients was collected, including age, gender, initial symptoms, pathogenic site (Figures 1A–F, 2A–F), pathological type (Figures 3F, 4D), operation effectiveness and safety indicators (operation time, intraoperative bleeding, surgical resection rate, postoperative complications), and economic indicators (postoperative hospital stay, hospital costs).

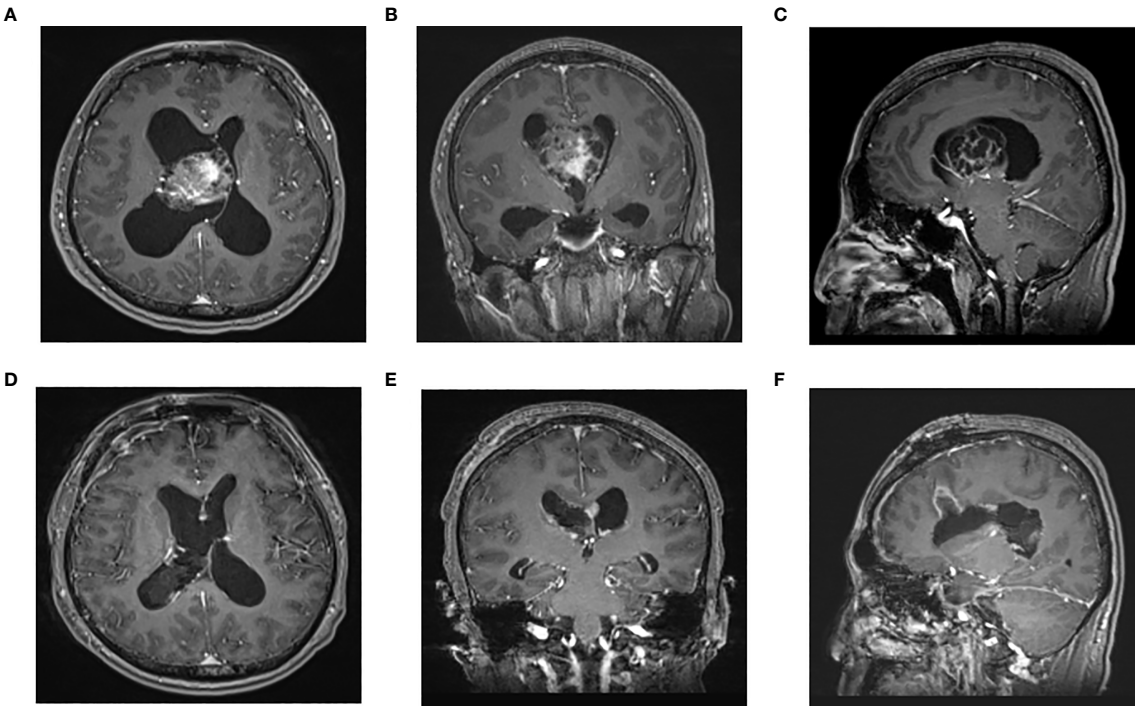

FIGURE 1
Enhanced MRI of head in one patient in endoscopic group before operation **(A–C)** and 3 days after operation **(D–F)**: The tumor was located in the right lateral ventricle. The tumor was resected satisfactorily and the brain channel recovered well after operation. **(A)** Preoperative axial **(B)** Preoperative coronal **(C)** Preoperative sagittal **(D)** Postoperative axial **(F)** Postoperative coronal F Postoperative sagittal.

10.3389/fonc.2023.1008291

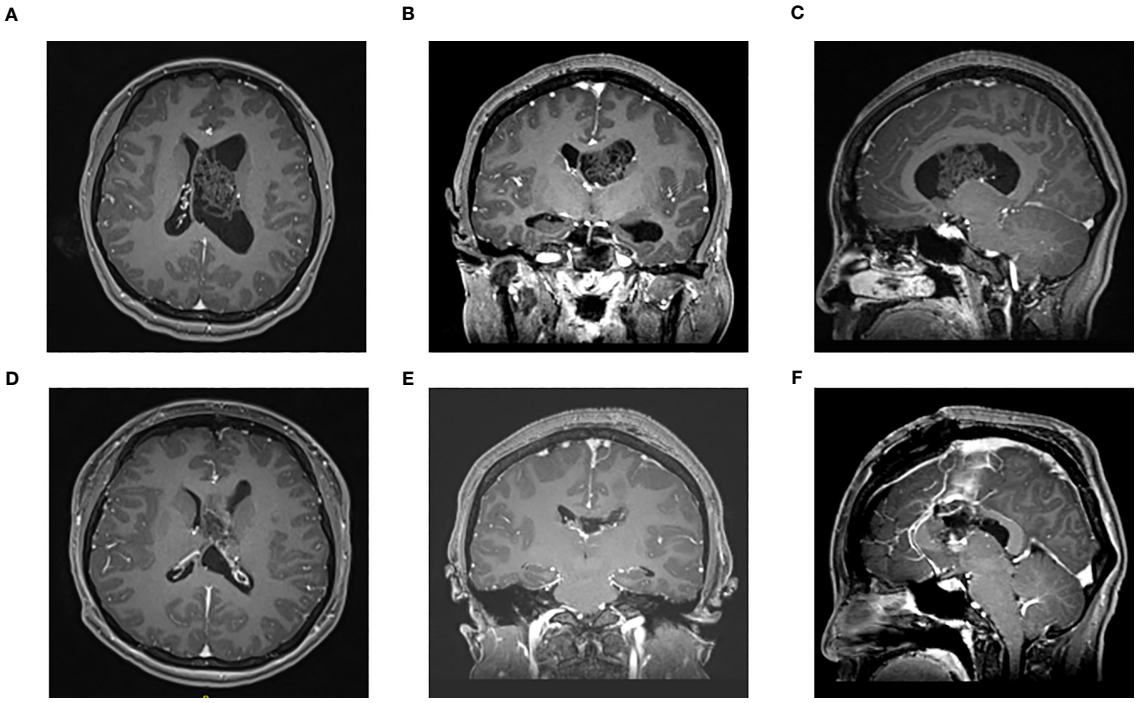

FIGURE 2
Enhanced MRI of head in one patient in the microscope group before surgery **(A–C)** and 3 days after surgery **(D–F)**: The tumor was located in the left lateral ventricle. **(A)** Preoperative axial **(B)** Preoperative coronal **(C)** Preoperative sagittal **(D)** Postoperative axial **(E)** Postoperative coronal **(F)** Postoperative sagittal.

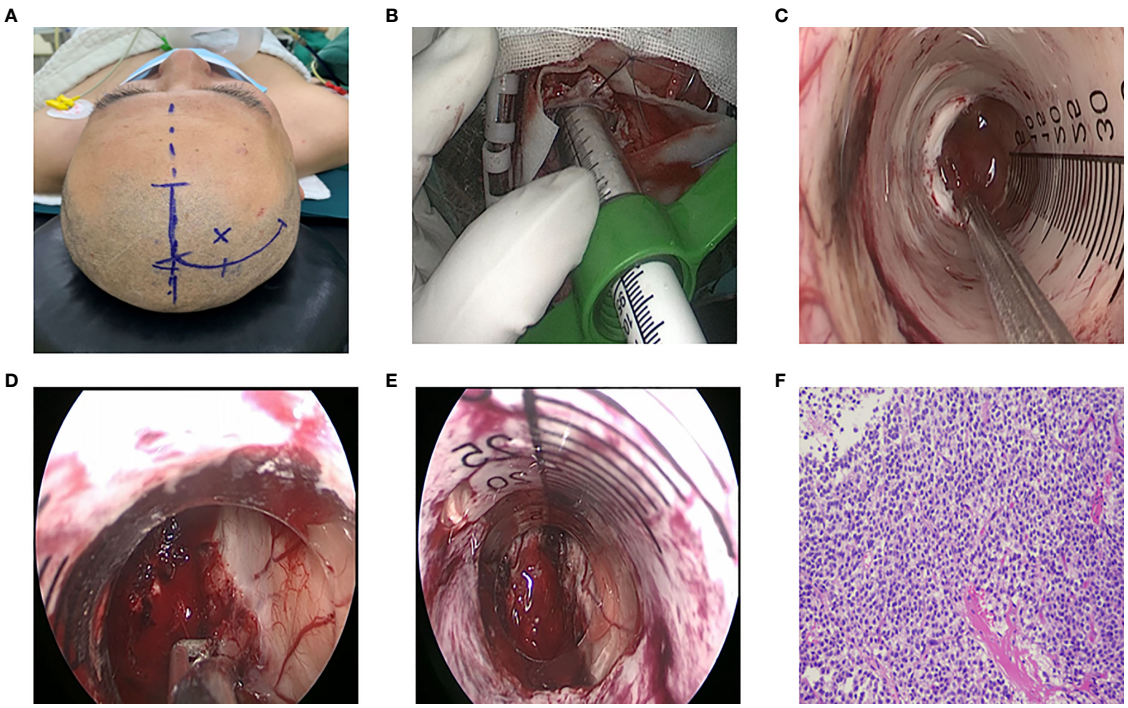

FIGURE 3
Surgical procedure of endoscopic treatment for intraventricular tumors. **(A)** Right frontal surgical incision. **(B)** Endoport retractor. **(C)** Observe the tumor boundary under endoscope. **(D)** The blood supply of tumor was coagulated by bipolar electrocoagulation, and the tumor was excised by suction. **(E)** Tumor resection, adequate hemostasis, **(F)** Postoperative pathology: central neurocytoma, WHOII grade.

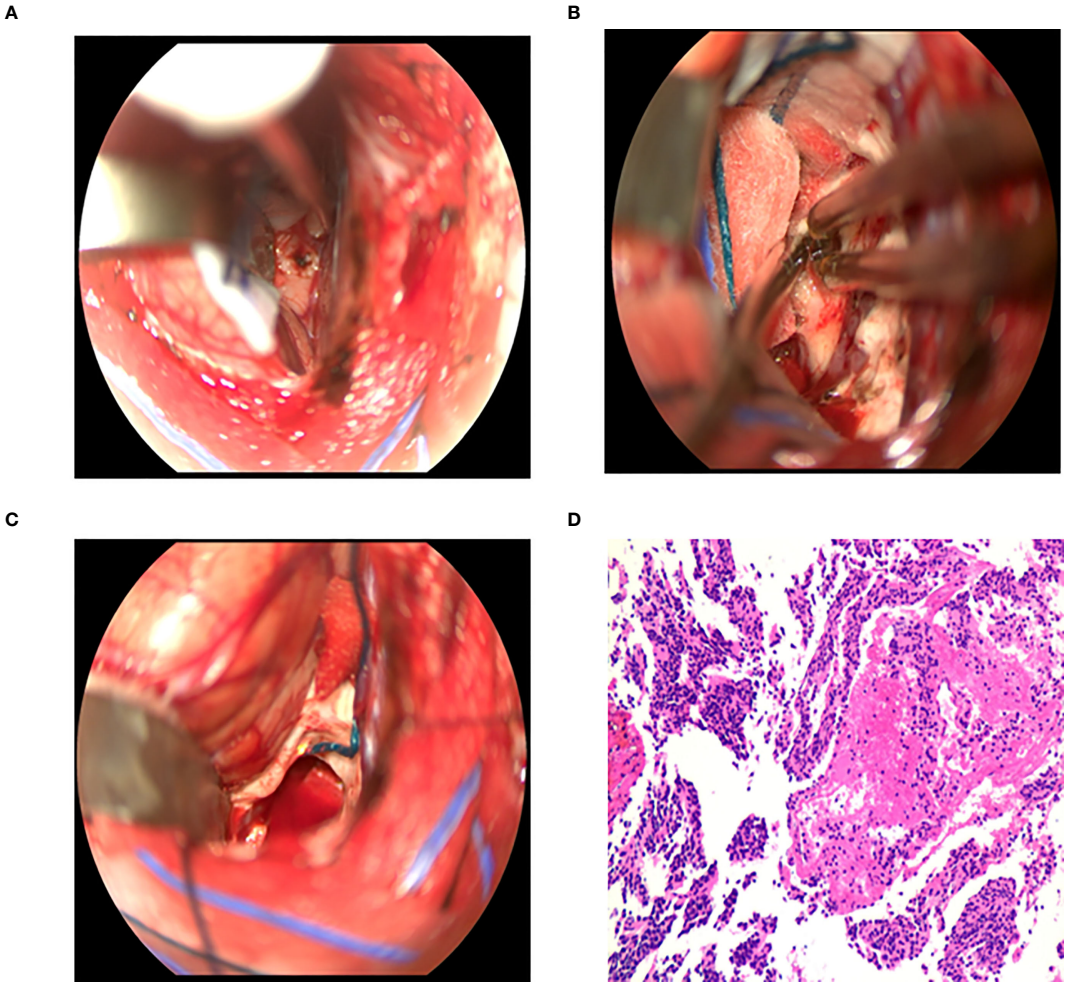

FIGURE 4
Surgical procedure of intraventricular tumors in the microscopic group. **(A)** The corpus callosum was incised 1.5 - 2 cm to expose the tumor. **(B)** The blood supply of tumor was coagulated by bipolar electrocoagulation, and the tumor was excised by suction. **(C)** Tumor resection and full hemostasis. **(D)** Postoperative pathology: central neurocytoma, WHOII grade.

2.2 Surgical methods

2.2.1 Microsurgery procedure

Behind the frontal or temporal or parietal occipital bone flap, the cerebral cortex was cut 3 to 4cm or the cortex was fistulated into the lateral ventricle, and the brain tissue was pulled away to remove the tumor. Through the anterior approach of the corpus callosum, a "U" shaped incision near the midline was performed to form a 6cm×4cm bone flap. The posterior edge of the bone flap was located in the coronal suture. And the dura mater was turned to the side of the sagittal sinus. The small reflux vein between the brain surface and the sagittal sinus was cut off by electrocoagulation, and the cut side was close to the brain surface. The right lobe of the brain was stretched to expose the corpus callosum along the longitudinal fissure, and surgeons needed to protect the pericallosal artery during exposure to avoid damage. The corpus callosum was cut about 2cm into the lateral ventricle (Figure 4A) and the tumor was removed (Figures 4B, C). During the operation, the interventricular foramen was protected to prevent blood from flowing into the contralateral ventricle or the third ventricle. At the same time, the stria colliculus vein and internal cerebral vein were strictly protected, followed by electro coagulating the choroid plexus, to reduce the secretion of cerebrospinal fluid after the operation.

2.2.2 Procedures under neuroendoscope

With the help of neuronavigation system, the approach to enter was determined. A curved incision (Figure 3A) was made around the endoscopic insertion point to free the small bone flap. The bone flap was about 3cmx3cm in size. And the dura was cut in an arc. After electrocoagulation in the avascular area on the cortical surface, the lateral ventricle was punctured with a brain needle. After successful puncture, the brain needle was withdrawn, and the ventriculoscope sheath or Endoport channel (Figure 3B) along the direction of the brain needle was placed. The tumor was removed according to the blood supply, size and origin of the tumor. The neuroendoscope was withdrawn after there had been no active

bleeding, and the guider was withdrawn slowly along the original channel (Figures 3C-E). Moreover, the dura was sutured layer by layer after there had been no bleeding, and the bone flap was reset.

2.3 Statistical analysis

SPSS 19.0 software was applied for statistical analysis. Continuous variables were tested for normal distribution using Shapiro Wilk method. Data with normal distribution was described by mean ± standard deviation (x ± s). The difference in means between the two sample was compared using independent sample t-test. Categorical variables were described by the number of cases and constituent ratio, and the differences between groups were tested by x^2 test. A $p<0.05$ was defined as statistically significant (two tails).

3 Results

3.1 Preoperative characteristics

Demographic data and clinical symptoms are shown in Table 1. Among the 49 adult patients with lateral ventricle tumors, 21 were males and 28 were females, aged from 20 to 75 years, with an average of 42.1 years. The diameter of the tumor was 1cm-8.3cm, with an average of 4.3cm. The most common symptoms included headache/dizziness in 30 cases (61.2%), nausea/vomiting in 10 cases (20.4%), unintentional discovery of the disease in 7 cases (14.3%), visual impairment in 6 cases (12.2%), limb numbness in 5 cases (10.2%), limb weakness in 2 cases (4.1%), memory impairment in 2 cases (4.1%), gait instability in 2 cases (4.1%), seizures in 1 case (2.0%), disturbance of consciousness in 1 case (2.0%) and urinary incontinence in 1 case (2.0%). The course of disease ranged from 3 days to 3 years, with an average of 4 months.

3.2 Surgical features and pathology

There were 39 cases in the microsurgery group, with 15 cases undergoing frontal transcortical approach, 4 undergoing anterior transcallosal approach, and 3 undergoing temporal transcortical approach. Transcortical approach of parietal occipital lobe was performed in 16 cases. On the other hand, there were 11 patients in the neuroendoscope group, 3 of whom were treated using ventriculoscopy and 8 with Endoport-assisted neuroendoscopy. The operative approaches were frontal cortex approach in 8 cases and parietal occipital triangle approach in 3 cases. Postoperative pathology: meningioma in 17 cases (34.7%), central neurocytoma in 13 cases (26.5%), glioma in 8 cases (16.3%) (low grade: 5 cases, high grade: 3 cases), subependymal tumor in 4 cases (8.2%), and ependymoma, epidermoid cyst, low-grade malignant mesenchymal tumor, germinoma, choroid plexus granuloma, metastasis (lung cancer metastasis) and neuroepithelial cyst in 1 case each (2.0%). Surgical approach and pathology are summarized in Table 2.

TABLE 1 Characteristics of 49 patients with lateral ventricle tumors.

Characteristics	N (%)
Demographics	
Mean age, (years) (range)	42.1 (20–75)
Sex (male/female)	21/28
Tumor features	
Mean size, (cm) (range)	4.3 (1.0-8.3)
Tumor diameter in neuroendoscope group 0-3(cm)	4 (8.2%)
Diameter 3-5(cm)	5 (10.2%)
Diameter >5(cm)	2 (4.1%)
Tumor diameter in microsurgery group 0-3(cm)	6 (12.2%)
Diameter 3-5(cm)	18 (36.7%)
Diameter >5(cm)	14 (28.6%)
Location	
Left	27 (55.1%)
Right	21 (42.9)
Both sides	1 (2.0%)
The frontal horn	6(12.2%)
The body	20 (40.8%)
The atrium	20 (40.8%)
The body, the atrium	2 (4.1%)
The body, the atrium, the temporal horn	1 (2.0%)
Symptoms	
Headache and dizziness	30 (61.2%)
Nausea and vomiting	10 (20.4%)
Unintentional discovery of the disease	7 (14.3%)
Visual impairment	6 (12.2%)
Limb numbness	5 (10.2%)
Limb weakness	2 (4.1%)
Memory impairment	2 (4.1%)
Gait instability	2 (4.1%)
Seizures	1 (2.0%)
Urinary incontinence	1 (2.0%)
Disturbance of consciousness	1 (2.0%)
Mean symptoms duration, (months)	4.0
Range	3 days-3years

3.3 Comparison of two surgical methods

Table 3 laid out the comparison of general data between the two groups. There was no significant difference in the age and gender of patients in the two groups (P=0.533, P=0.379). Based on the

TABLE 2 Surgical approach and pathology.

Surgical approach and pathology	N (%)
Neuroendoscopy Transfrontal approach	8 (16.3%)
Transparietal occipital triangle approach	3 (6.1%)
Microsurgery Frontal transcortical approach	15 (30.6%)
Anterior transcallosal approach	4(8.2%)
Transcortical approach of temporal lobe	3 (6.1%)
Transcortical approach of parietooccipital lobe	16 (32.7%)
Pathology	
Meningioma	17 (34.7%)
Central neurocytoma	13 (26.5%)
Low-grade glioma	5 (10.2%)
Subependymal tumor	4 (8.2%)
High-grade glioma	3 (6.1%)
Epidermoid cyst	1 (2.0%)
Low-grade malignant mesenchymal tumor	1 (2.0%)
Germ cell tumor	1 (2.0%)
Choroid plexus granuloma	1 (2.0%)
Ependymoma	1 (2.0%)
Metastatic tumor (brain metastasis of lung cancer)	1 (2.0%)
Neuroepithelial cyst	1 (2.0%)

comparison of economic indicators (Table 3), the length of hospital stay (P=0.039) and hospitalization cost (P=0.021) of patients in the neuroendoscopy group were lower than those in the microsurgery group. Results of comparison of efficacy and safety showed that the operation time in the neuroendoscope group was significantly shorter than that in the microsurgery group (P=0.021<0.05). The intraoperative bleeding in the neuroendoscope group was significantly less than that in the microsurgery group (P=0.001<0.01). However, there was no significant difference in resection rate (P=0.820) and postoperative complications (P=0.178) between the two groups (p>0.05). In the neuroendoscope group, 1 case had bleeding in the puncture tract and 1 case had intracranial infection. In the microsurgery group, there were 16 cases of complications, 3 of epilepsy, 3 of epidural hematoma, 2 of intracranial infection, 2 of isolated temporal angle, 2 of death, 1 of cerebral infarction, 1 of intracranial hematoma, 1 of diabetes insipidus and 1 of brain swelling.

Two groups of patients according to tumor size, to compare the operation time, intraoperative blood loss and postoperative complications When the tumor diameter was less than 5 cm, the endoscopic group had less operation time and intraoperative bleeding than the tumor group, but the postoperative complications were not significantly reduced (Table 4)

4 Discussion

4.1 Clinical presentation

The ever-present challenge of patients with lateral ventricular tumors is that no special clinical symptoms showed in the early stage since the tumors grow in the ventricular cavity. Following the enlarging process, the tumor blocks the cerebrospinal fluid circulation pathway and invades the adjacent structures, the corresponding clinical symptoms appear (3, 4). Li-Feng Chen et al. (5) reported that preoperative symptom duration ranged from 2 days to 2 years (mean, 5.5 months). The most common signs and symptoms are associated with increased intracranial pressure (ICP), including headache, nausea, vomiting, and sleepiness. Gokalp et al. (2) depicted that 42.9% of patients had papilledema, 35.7% had headache, 25% had dyskinesia, 25% had sensory disturbance, and 22.3% had nausea/vomiting. Study supported by Sherif M. Elwatidy et al. (3) showed that there included headache (29 cases, 69%), nausea/vomiting (16 cases, 38%), visual impairment (10 cases, 24%), and seizes (7 cases, 17%) in patients with lateral ventricular tumors. In our study, the average duration of preoperative symptoms was 4.0 months, and the longest was 3 years. The most common symptoms were related to increased ICP and hydrocephalus after cerebrospinal fluid circulation obstruction, including headache/dizziness in 30 cases (61.2%), nausea/vomiting in 10 cases (20.4%), visual impairment in

TABLE 3 Comparison of clinical data between neuroendoscopy group and microsurgery group.

Item	Neuroendoscopy group (11 cases)	Microsurgery group (38 cases)	P value
Age (year, x±)	45.2 ± 16.1	41.2 ± 12.3	0.533
Male/female(cases)	6/5	15/23	0.379
Postoperative hospital stay (day)	11.2 ± 4.4	16.8 ± 10.6	0.039
Hospitalization cost (RMB,ten thousands)	7.5 ± 3.3	10.4 ± 4.2	0.021
Operation time (min)	255.4 ± 168.5	315.9 ± 93.5	0.021
Intraoperative blood loss (ml)	96.3 ± 73.5	459.5 ± 455.4	0.001
Surgical resection rate (%)	99.6 ± 1.51	98.5 ± 5.2	0.820
Postoperative complications (case)	2	16	0.136

TABLE 4 Comparison of surgical effects of tumors with different diameters.

Item	Diameter (cm)	Neuroendoscopy group	Microsurgery group	P value
Operation time (min)	0<D<5 D≥5	221.8 ± 62.8 406.5 ± 443.4	305.8 ± 90.6 332.6 ± 99.5	0.016 0.531
Intraoperative blood loss (ml)	0<D<5 D≥5	84.4 ± 77.2 110.0 ± 56.6	459.5 ± 455.4 675.0 ± 671.0	0.001 0.011
Postoperative complications (case)	0<D<5 D≥5	1 1	10 6	0.097 0.849

6 cases (12.2%). And 7 cases (14.3%) were asymptomatic in the early stage and found unintentionally during physical examination. The minimum and maximum diameter of the tumor was 1cm and 8.3cm, resulting in the difficulty to early identify the tumor.

4.2 Pathology

Lateral ventricle tumors account for about 0.8-1.6% of intracranial tumors (1, 2). And benign tumors account for 64%, moderate malignant tumors 15%, and malignant tumors 21% of intraventricular tumors (2). The nature of lateral ventricular tumors is more uncertain and likely to vary by the age of onset. For instance, choroid plexus papilloma and malignant small cyanocytoma are common in children. In contrast, pilocytic astrocytoma, subependymal giant cell astrocytoma and diffuse low-grade astrocytoma mostly occur in patients aged 6-30 years. Meningiomas, metastases, and high-grade gliomas are commonly seen in patients over the age of 30. According to the study of Gokalp et al. (2), the most common pathologies were ependymoma (25%), astrocytoma (21.4%), and oligodendrocytoma (7.1%). In another study of Marvin Darkwah et al. (6), Malignancies (metastasis or WHO grade III/IV tumor) were uncommon and only diagnosed in 7 (13.5%). And in the present study, the most common tumors were 17 meningiomas (34.7%), 13 central neurocytomas (26.5%), 8 gliomas (16.3%) (5 low-grade, 3 high-grade), and 4 subependymal tumors (8.2%). Metastatic tumor (brain metastasis of lung cancer) occurred in a 75- year-old male.

4.3 Surgical methods and approaches

4.3.1 Comparison between microsurgery and neuroendoscope

Surgery for intraventricular tumors remains a controversial and evolving field (7). At present, the surgical treatment of lateral ventricle tumors depends on bone flap craniotomy under microsurgery. Open surgery continues to be the gold standard, especially in large and highly vascularized lesions in which endoscopy still has a limited role (7). Althrough craniotomy is acknowledged as the golden standard, especially in the lesions with large tumor diameter and abundant blood vessels, the role of neuroendoscopy is largely limited. Under the microsurgery, the operation not only has clear visual field exposure, complete hemostasis, high total tumor resection rate, and less complications, but can clearly identify the anatomical structure, and protect the thalamus, striated veins, basal nuclei and other important structures. However, there are several disadvantages of microsurgery. A larger stoma is usually required to better expose the tumor. The traditional brain pressure plate is often utilized during the operation. Due to uneven stress and insufficient protection of the operation channel, it is easy to cause severe brain edema after the operation, which may cause great damage to the brain tissue, and the probability of epilepsy and neurological loss after the operation may increase (8). Moreover, due to the tubular visual field of the microsurgery and the deep location of the ventricular tumor, the exposure of the operating field is limited, which affects the total resection of the tumor (9).

In recent years, as the advances of neuroendoscope instruments and neuroendoscope technology, the application of neuroendoscope in ventricular lesions has expanded from biopsy of ventricular tumors to complete resection of ventricular tumors by neuroendoscope. Advantages of neuroendoscope include (9–11): 1) compared with the microsurgery, neuroendoscope provides a visual field that can be viewed directly and from multiple angles, with good illumination. It can effectively help identify the details of the tumor and the surrounding important tissues, improve the total tumor resection rate, and help avoid nerve function damage. 2) During neuroendoscopic surgery, the surgical channel is relatively fixed, and the pulling force on the brain tissue is small. And the movement of surgical instruments is effectively limited to cause damage to the surrounding tissues, which reduces the probability of severe brain edema and epilepsy after surgery. 3) The cerebrospinal fluid circulation channel can be reconstructed while the tumor is removed. There are several disadvantages of neuroendoscope (12). Firstly, neurosurgeons need to receive specific technical training. The operation of instruments is not as convenient and skilled as that under the microsurgery, and it is difficult to deal with intraoperative bleeding (13). Secondly, it is difficult to treat tumors with large diameter or abundant blood vessels in the lateral ventricle (7). Some scholars believe that the indications for the application of neuroendoscopy are that the maximum diameter of the tumor is <2.5cm, with clear boundary, less adhesion, narrow pedicle and free in the ventricle (14). However, the maximum diameter of the tumor in this group of cases was 5.2cm. Neuro-Endoport channel was used during neuroendoscopy, and the surgeon can perform with both hands to complete the operation. On the basis of multi-angle movement of the channel, greater exposure space could be obtained the tumor could be resected in blocks (15–17).

Our experience based on the study is the following: 1) in order to avoid brain tissue injury and important tissue contusion around

the interventricular foramen, intraoperative neuronavigation and intraoperative ultrasound can be applied together to more accurately plan the surgical path, and the use of ultrasonic attractor and needle electrode can improve the surgical efficiency (15). 2) Neuro-Endoport technology provides an independent surgical channel, which is able to obtain a larger exposure space. Furthermore, endoscopes, aspirators and conventional surgical instruments are placed, hence the operator can perform with both hands. 3) The operation should be done with caution to protect the important structures around the ventricles and deep veins, especially the internal cerebral veins and the veins of the colliculus. 4) The shape, size, blood supply, pedicle and adjacent structures of the tumor should be closely observed after the neuroendoscope enters the ventricle, to firstly deal with the base and blood supply vessels of the tumor. If the tumor originates from the midline, the tumor could be removed after identifying the midline structure (such as septum pellucidum and the inner side of the interventricular foramen) to disconnect the tumor base. If it originates from the periphery of the ventricular wall, the surrounding tissues should be closely protected before tumor resection. If the tumor has abundant blood supply, identify the normal anatomical structure, electrocoagulate the blood supply vessels first, and then remove the tumor as a whole. 5) The application of endoscope support arm is conducive to simultaneous operation of both hands and the coordination of electrocoagulation, shearing, pulling and other operations. 6) During the operation, the cerebrospinal fluid passage can be closed with cotton pieces, and the bleeding enters the cerebrospinal fluid circulation. 7) When the tumor diameter was less than 5 cm, the endoscopic group had less operation time and intraoperative bleeding than the tumor group, but the postoperative complications were not significantly reduced. Our clinical experience is also that endoscopic surgery is more suitable for tumors <5 cm in diameter. If the diameter of the tumor is too large, improper pushing and pulling of the tumor will not only damage the ventricular wall and thalamostriate vein, but also cause postoperative coma. Once the blood supply vessels of the tumor are ruptured, intraventricular hemorrhage may occur before the tumor is completely removed, and the consequences are quite serious.

In this study, the economic indicators, including the postoperative hospital stay and hospital costs of patients in the neuroendoscopy group were lower than those in the microsurgery group. As for the efficacy and safety profile, the operation time of neuroendoscope group was shorter than that of microsurgery group, and the amount of intraoperative bleeding was significantly less than that of microsurgery group. The microsurgery group had 16 cases of complications, including 2 cases of death. Among the dead cases, one case received the anterior approach of the corpus callosum. After the operation, the patient suffered from coma and severe diencephaledema, and finally died. It was considered to be caused by the injury of the internal cerebral vein and the great cerebral vein. Another dead case was treated via the parieto occipital cortical approach. After the operation, the patient continued to have grand mal seizures, and finally died of severe cerebral ischemia and swelling. There was no difference in resection rate and postoperative complications between the two groups. There were no postoperative deaths in the neuroendoscope group (0/11), while 2 postoperative deaths occurred in the microsurgery group (2/38). Microsurgery and neuroendoscope are both optional methods for lateral ventricle tumor surgery, mainly based on the experience of neurosurgeon in the surgical approach and related neuroanatomy. Further technical improvement is needed to improve the application of neuroendoscopy in lateral ventricle tumor surgery (7, 18).

4.3.2 Surgical approaches

Surgical approaches for lateral ventricle tumors are mainly divided into transcortical or transcallosal approach, and the selection of appropriate approach has been the topic of debate (6). There are currently four common surgical approaches (6, 19).

4.3.2.1 Parieto occipital transverse approach

This approach is preferred for tumors situated entirely within the atrium, posterior part of the body of the lateral ventricle, Atrial tumors extending into the occipital horn can also be approached using this route. The parieto occipital or interparietal sulcus approach can be used to avoid language dysfunction in the dominant hemisphere. The longitudinal cortex fistula in the parietal lobe 4 to 5cm posterior to the central sulcus to the parieto occipital sulcus is performed. The operation is performed behind the sensory area and above the angular gyrus and supramarginal gyrus to avoid damaging the angular gyrus and supramarginal gyrus. Gerstmann's syndrome was reported in one third of patients undergoing this approach, when the dominant hemisphere is involved. Apraxia and acalculia m ay also occur (12).

4.3.2.2 Frontal transcortical approach

This approach is suitable for lesions of the frontal horn and the anterior port ion of the body of the lateral ventricle. Frontal transcortical approach is easy to expose the anterior choroidal artery. During the transfrontal approach, the cortex is usually cut along the running direction of the middle frontal gyrus at 3cm in front of the central anterior gyrus to avoid damaging the language center of the inferior frontal gyrus of the dominant hemisphere (20).

4.3.2.3 Temporal transcortical approach

Transcortical approach is used for tumors in the middle or posterior third of the temporal horn.Temporal transcortical approach is used for transverse cortical fistulation in the posterior 1/3 of the middle temporal gyrus. Parallel visual irradiation can reduce the incidence of postoperative hemianopia, facilitate the treatment of tumor blood supply, and minimize postoperative visual field defects (20).

4.3.2.4 Corpus callosum approach

This approach is used for tumors located in the anterior horn and middle part of the body of the lateral ventricles. In the absence of ventriculomegaly, this approach is easier to perform and is superior to the anterior transcortical approach when the tumor is

small, located near the midline, and does not require excessive hemispheric retraction. Compared with the transcortical approach, the transcallosal approach has the advantages of easy access to the lateral ventricle, no cortical incision, and reduced risk of postoperative seizures. Advantages of the corpus callosum approach include: 1) make full use of the natural anatomical space of the brain to approach and expose the tumor without damaging the cerebral hemisphere; 2) low incidence of postoperative epilepsy; 3) no important anatomical structure and little damage to physiological function; 4) longitudinal incision of the corpus callosum for 2cm do not greatly affect the information transmission of the bilateral hemispheres. However, the available length of the corpus callosum for incision is limited, about 2 to 2.5cm. It is difficult to reach the tumors in the triangle, posterior, occipital and temporal angle (15, 20).

Patients undergoing transcortical surgery are prone to have postoperative seizures (3, 20). However, some investigations have shown that seizures mainly occur in patients through the transcallosal approach. It is reported that the disadvantages of transcallosal approach include temporary silence and sacrifice of bridging vein in longitudinal fissure path, resulting in postoperative brain swelling and infarction (6, 21). Nevertheless, Sherif M. Elwatidy and Ulas Cikla believed that with the improvement of microscopy, the risk of epilepsy and other complications after transcortical approach and transcallosal approach may be reduced. There was no difference in postoperative cognitive function between the transcortical and transcallosal surgical approaches (22).

The first or second approach is available for neuroendoscope, and the abovementioned four approaches can be selected for microsurgery. Interhemispheric transcallosal and transcortical approaches were the best surgical access routes (20). However, whether microsurgery or endoscopic surgery, the surgical approach should be determined depending on a variety of other factors, including tumor location, cerebral ventricle and tumor size, location of arterial blood supply, pathological characteristics of the tumor, preoperative neurological deficit and experience of surgeon (19, 23).

5 Conclusion

Surgery intervention is regarded as the core treatment option for lateral ventricle tumors. Both microsurgery and neuroendoscopy are effective with safety profile. In the selected lateral ventricle tumor surgery, the application of neuroendoscopic surgery showed promising results, in terms of less intraoperative bleeding, and shorter operation time, postoperative hospital stay, and hospital costs. The selection of surgical approach and methods for lateral ventricle tumors is principally depended on the experience of neurosurgeon concerning the surgical approach and related neuroanatomy.

Neuroendoscopy can be a safe and effective tool for the resection of intraventricular tumors. Proper patient selection and a specially trained neurosurgeon are essential. Currently, the main limitation continues to be a larger size or vascularization of the lesion. In the future, endoscopic resection will become more popular.

Data availability statement

The original contributions presented in the study are included in the article/supplementary material. Further inquiries can be directed to the corresponding author.

Author contributions

KL and JL carried out the research. KL, JL and SL participated in data analysis. KL and HN drafted the manuscript. YZ and PZ critically reviewed the overall manuscript as well as supervised the study. All authors contributed to the article and approved the submitted version.

Funding

This study was supported by Peking University International Hospital Research Grant (No. YN2020ZD04).

Conflict of interest

The authors declare that the research was conducted in the absence of any commercial or financial relationships that could be construed as a potential conflict of interest.

Publisher's note

References

1. Lapras C, Deruty R, Bret PH. Tumours of the lateral ventricles. In: Symon L, editor. *Advances and technical standards in neurosurgery*, vol. 11. New York: Springer (1984). p. 103–67.

2. Gokalp HZ, Yuceer N, Arasil E, Deda H, Attar A, Erdogan A, et al. Tumors of the lateral ventricle: a retrospective review of 112 cases operated upon 1970–1997. *Neurosurg Rev* (1998) 21(2–3):126–37. doi: 10.1007/BF02389318

3. Elwatidy Sherif M, Albakr Abdulrahman A, Al Towim Abdullah A, Malik Safdar H. Tumors of the lateral and third ventricle: surgical management and outcome analysis in 42 cases. *Neurosci (Riyadh)* (2017) 22(4):274–81. doi: 10.17712/nsj.2017.4.20170149

4. Mei GH, Liu XX, Zhou P, Shen M. Clinical and imaging features of subependymal giant cell astrocytoma: report of 20 cases. *Chin Neurosurg Jl* (2017) 3:14. doi: 10.1186/s41016-017-0077-4

5. Chen L-F, Yang Y, Ma X-D, Yu X-G, Xu B-N, Zhou D-B. Operative management of intraventricular central neurocytomas: an analysis of a surgical experience with 32 cases. *Turk Neurosurg* (2016) 26(1):21–8. doi: 10.5137/1019-5149.JTN.11356-14.2

6. Darkwah Oppong M, Müller O, Jabbarli R, Dammann P, Sure U, El Hindy N. Intraventricular mass lesions: still a question of surgical approach? *J Clin Neurosci* (2017) 43:157–62. doi: 10.1016/j.jocn.2017.05.036

7. Ibáñez-Botella G, Segura M, De Miguel L, Ros B, Arráez MÁ. Purely neuroendoscopic resection of intraventricular tumors with an endoscopic ultrasonic aspirator. *Neurosurgical Rev* (2019) 42(4):973–82 doi: 10.1007/s10143-018-1011-8

8. Kutlay M, Durmaz MO, Kırık A, Yasar S, Ezgu MC, Kural C, et al. Resection of intra- and paraventricular malignant brain tumors using fluorescein sodium-guided neuroendoscopic transtubular approach. *Clin Neurol Neurosurg* (2021) 207:106812. doi: 10.1016/j.clineuro.2021.106812

9. Engh JA, Lunsford LD, Amin DV, Ochalski PG, Fernandez-Miranda J, Prevedello DM, et al. Stereotactically guided endoscopic port surgery for intraventricular tumor and colloid cyst resection. *Neurosurgery* (2013) 67(3 Suppl Operative):ons198–205. doi: 10.1227/01.NEU.0000382974.81828.F9

10. Nanda A, Bir SC, Maiti T, Konar S. Intraventricular meningioma: technical nuances in surgical management. *World Neurosurg* (2016) 88:526–37. doi: 10.1016/j.wneu.2015.10.071

11. Akiyama Y, Wanibuchi M, Mikami T, Horita Y, Komatsu K, Suzuki K, et al. Rigid endoscopic resection of deep-seated or intraventricular brain tumors. *Neurological Res* (2015) 37(3):278–82. doi: 10.1179/1743132814Y.0000000439

12. Mazher S, Imran M, Ashraf J, Ahmed A, Shah IU, Zulfiqar F. Outcome of open transcortical approach in the management of intraventricular lesions. *J Coll Physicians Surgeons–Pakistan* (2013) 23(12):857–61.

13. Mohanty A, Thompson BJ, Patterson J. Initial experience with endoscopic side cutting aspiration system in pure neuroendoscopic excision of large intraventricular tumors. *World Neurosurg* (2013) 80(5):655.e15–655.e6.55E21. doi: 10.1016/j.wneu.2012.11.070

14. Elbabaa SK. Ventricular neuroendoscopic surgery: lessons learned from the literature. *World Neurosurg* (2016) 88:646–8. doi: 10.1016/j.wneu.2015.11.019

15. Gaab MR, Schroeder HW. Neuroendoscopic approach to intraventricular lesions. *Neurosurgical Focus* (1999) 6(4):e5. doi: 10.3171/foc.1999.6.4.8

16. Qiao L, Souweidane MM. Purely endoscopic removal of intraventricular brain tumors: a consensus opinion and update. *Minimally Invasive Neurosurg* (2011) 54 (4):149–54. doi: 10.1055/s-0031-1284386

17. Eliyas JK, Glynn R, Kulwin CG, Rovin R, Young R, Alzate J, et al. Minimally invasive transsulcal resection of intraventricular and periventricular lesions through a tubular retractor system: multicentric experience and results. *World Neurosurg* (2016) 90:556–64. doi: 10.1016/j.wneu.2015.12.100

18. Najjar MW, Azzam NI, Baghdadi TS, Turkmani AH, Skaf G. Endoscopy in the management of intra-ventricular lesions: preliminary experience in the middle East. *Clin Neurol Neurosurg* (2010) 112(1):17–22. doi: 10.1016/j.clineuro.2009.08.027

19. Cikla U, Swanson KI, Tumturk A, Keser N, Uluc K, Cohen-Gadol A, et al. Microsurgical resection of tumors of the lateral and third ventricles: operative corridors for difficult-to-reach lesions. *J Neuro-oncology* (2016) 130(2):331–40. doi: 10.1007/s11060-016-2126-9

20. Dănăilă L. Primary tumors of the lateral ventricles of the brain. *Chirurgia (Bucharest Romania 1990)* (2013) 108(5):616–30.

21. Nakajo K, Uda T, Goto T, Morisako H, Nishijima S, Kawashima T, et al. Changes in cognitive function after resection of lesions in the anterior part of the lateral ventricle via an interhemispheric transcallosal approach. *J Clin Neurosci* (2020) 79:39–44. doi: 10.1016/j.jocn.2020.07.026

22. He J, Li Z, Yu Y, Lu Z, Li Z, Gong J. Cognitive function assessment and comparison on lateral ventricular tumors resection by the frontal transcortical approach and anterior transcallosal approach respectively in children. *Neurosurgical Rev* (2020) 43(2):619–32. doi: 10.1007/s10143-019-01088-2

23. Deopujari CE, Karmarkar VS, Shaikh ST, Mohanty CB, Sharma V, Tadghare J, et al. Neuroendoscopy in the surgical management of lateral and third ventricular tumors: looking beyond microneurosurgery. *Neurol India* (2021) 69(6):1571–8. doi: 10.4103/0028-3886.333458

Frontiers in Surgery

Explores and improves surgical practice and clinical patient management

A multidisciplinary journal which explores surgical practices - from fundamental principles to advances in microsurgery and minimally invasive techniques. It fosters innovation and improves the clinical management of patients.

Discover the latest Research Topics

See more →

Frontiers

Avenue du Tribunal-Fédéral 34
1005 Lausanne, Switzerland
frontiersin.org

Contact us

+41 (0)21 510 17 00
frontiersin.org/about/contact